

UC Berkeley

UC Berkeley Electronic Theses and Dissertations

Title

Chiral Acyclic Diaminocarbene Gold(I) Complexes and their Applications in Asymmetric Catalysis

Permalink

<https://escholarship.org/uc/item/7x68n1rn>

Author

Khrakovsky, Dimitri

Publication Date

2016

Peer reviewed|Thesis/dissertation

Chiral Acyclic Diaminocarbene Gold(I) Complexes and their Applications in
Asymmetric Catalysis

By Dimitri Alexander Khrakovsky

A dissertation submitted in partial satisfaction of the requirements

for the degree of Doctor of Philosophy

in

Chemistry

in the

Graduate Division

of the

University of California, Berkeley

Committee in Charge:

Professor F. Dean Toste, Chair

Professor Robert Bergman

Professor Stuart Linn

Spring 2016

Abstract

Chiral Acyclic Diaminocarbene Gold(I) Complexes and their Applications in Asymmetric Catalysis

by

Dimitri Alexander Khrakovsky

Doctor of Philosophy in Chemistry

University of California, Berkeley

Professor F. Dean Toste, Chair

In the span of three decades, asymmetric gold(I) catalysis has transformed from an esoteric curiosity to a powerful synthetic tool. The advancements in gold(I)-catalyzed enantioselective transformations have been critically enabled by a diversity of chiral phosphorus-based ligands, including axially chiral diphosphines and phosphoramidites, among others. The development of chiral carbenes has recently began to augment the library of ligands for gold(I) catalysis. This dissertation will focus on the design and synthesis of chiral acyclic diamino-carbene (ADC) gold(I) complexes, as well as their role in the optimization of a number of synthetic organic transformations.

Chapter 1. This chapter examines and summarizes the various chiral ligand frameworks employed in asymmetric gold(I) catalysis that have been previously reported in the literature. This leads into our own work on the development of new chiral ADC gold(I) complexes, with particular emphasis on the modulation and diversification of these chiral structures.

Chapter 2. The gold(I)-catalyzed enantioselective hydroazidation of arylallenes is presented herein, which represents the first such transformation employing unconjugated substrates. The superior selectivity of our ADC gold(I) complexes relative to other chiral gold(I) catalysts is demonstrated. The racemization of starting materials and products is also discussed.

Chapter 3. The ADC gold(I) complexes are also shown to be effective in the enantioselective hydroamination of arylallenes. Relative to the hydroazidation chemistry, the sense of enantioinduction is reversed, allowing access to both enantiomers of the corresponding allylic amines using the same catalyst enantiomer. Additional complementarity in reaction outcomes with various substrates are highlighted.

Chapter 4. The synthesis of chiral indenenes and cyclopentadienes is investigated with ADC gold(I) complexes. In service to these targets, efforts toward the optimization of enantioselective hydroarylation and cycloisomerization reactions are presented.

Chapter 5. Enantioselective tandem reactions give rise to highly functionalized polycyclic indoline-fused products. Initial studies on applying linear free-energy relationships (LFER) to modelling the reaction outcomes are disclosed.

Table of Contents

| | |
|---|------------|
| Chapter 1. Overview of Ligands in Asymmetric Gold(I) Catalysis, and Synthesis of Chiral Acyclic Diaminocarbene Gold(I) Complexes Derived from BINAM..... | 1 |
| Introduction..... | 2 |
| Bidentate Phosphorus Ligands..... | 2 |
| Monodentate Phosphorus Ligands..... | 5 |
| Carbenes..... | 7 |
| Results and Discussion..... | 14 |
| Experimental..... | 20 |
| References..... | 38 |
| Appendix 1 - NMR Spectra..... | 41 |
| Appendix 2 - Crystallographic Data..... | 65 |
| Chapter 2. Enantioselective Hydroazidation of Allenes..... | 82 |
| Introduction..... | 83 |
| Results and Discussion..... | 86 |
| Experimental..... | 95 |
| References..... | 112 |
| Appendix 1 - NMR Spectra..... | 114 |
| Appendix 2 - HPLC Traces..... | 154 |
| Chapter 3. Enantioselective Hydroamination of Allenes..... | 176 |
| Introduction..... | 177 |
| Results and Discussion..... | 181 |
| Experimental..... | 187 |
| References..... | 195 |
| Appendix 1 - NMR Spectra..... | 197 |
| Appendix 2 - HPLC Traces..... | 211 |
| Chapter 4. Enantioselective Hydroarylation and Cycloisomerization of Allenes: Synthesis of Chiral Indenes and Cyclopentadienes..... | 227 |
| Introduction..... | 228 |

| | |
|--|------------|
| Enantioselective Gold(I)-Catalyzed Hydroarylation..... | 228 |
| Gold(I)-Catalyzed Synthesis of Indenes and Cyclopentadienes..... | 229 |
| Indenes..... | 229 |
| Cyclopentadienes..... | 233 |
| Results and Discussion..... | 235 |
| Experimental..... | 240 |
| References..... | 244 |
| Appendix 1 - NMR Spectra..... | 246 |
| Appendix 2 - HPLC Traces..... | 250 |
| Chapter 5. Enantioselective Tandem [3,3]-Rearrangement—[2+2] Cycloaddition..... | 253 |
| Introduction..... | 254 |
| Results and Discussion..... | 257 |
| Experimental..... | 261 |
| References..... | 262 |
| Appendix 1 - HPLC Traces..... | 263 |

Abbreviations

| | | | |
|--------------------|--|-----------------------|---|
| [α] | Specific rotation | IPr | 1,3-bis(2,6-diisopropyl-phenyl)imidazol-2-ylidene |
| AAC | Acyclic aminocarbene | <i>J</i> | Coupling constant (in hertz) |
| Ac | Acetyl | <i>m</i> | Multiplet |
| ADC | Acyclic diaminocarbene | <i>M</i> | Molar |
| Ar | Aryl | Me | Methyl |
| BArF ₂₄ | Tetrakis[(3,5-trifluoro-methyl)phenyl]borate | Mes | Mesityl |
| Bn | Benzyl | MTBE | Methyl <i>tert</i> -butyl ether |
| Boc | <i>tert</i> -Butyloxycarbonyl | NAC | Nitrogen acyclic carbene |
| brs | Broad singlet | n/d | Not determined |
| Bu | Butyl | NHC | N-heterocyclic carbene |
| Bz | Benzoyl | NMR | Nuclear magnetic resonance (spectroscopy) |
| cat | Catalytic or catalyst | Ns | Nosyl |
| CatBH | Catecholborane | o/n | Overnight |
| Cbz | Carboxybenzoyl | PG | Protecting group |
| CPME | Cyclopentyl methyl ether | Ph | Phenyl |
| <i>c</i> Pr | Cyclopropyl | Phth | Phthalimide |
| δ | Chemical shift (in parts per million) | PhCF ₃ | α,α,α -Trifluorotoluene |
| d | Doublet | PhH | Benzene |
| DCE | Dichloroethane | PhMe | Toluene |
| DCM | Dichloromethane | PMB | <i>para</i> -Methoxybenzyl |
| dd | Doublet of doublets | PPh ₃ | Triphenylphosphine |
| DME | Dimethoxyethane | Pr | Propyl |
| DMF | Dimethyl formamide | q | Quartet |
| DMM | Dimethoxymethane | RT or rt | Room temperature |
| dms | Dimethylsulfide | s | Singlet |
| DMSO | Dimethyl sulfoxide | t | Triplet |
| ee | Enantiomeric excess | <i>t</i> Bu | <i>tert</i> -butyl |
| EI | Electron ionization | TCA | Trichloroethane |
| Et | Ethyl | TCE | Trichloroethylene |
| ESI | Electrospray ionization | TFA | Trifluoroacetic acid |
| EWG | Electron-withdrawing group | THF | Tetrahydrofuran |
| Fmoc | Fluorenylmethyloxycarbonyl | TLC | Thin-layer chromatography |
| HPLC | High performance liquid chromatography | TMS | Trimethylsilyl |
| HRMS | High resolution mass spectrometry | Tf | Triflate |
| Het | Heteroaryl | TOF | Turnover frequency |
| Hz | Hertz | <i>t</i> _r | Retention time |
| <i>i</i> Pr | Isopropyl | Troc | 2,2,2-Trichloroethoxycarbonyl |
| | | Ts | Tosyl |

Acknowledgements

I express my gratitude to my advisor, Professor F. Dean Toste, for his mentorship and guidance. More importantly, I thank him for allowing me to work independently and to chart the course of my graduate career. Although at times I was at wits' end in managing my research projects, I am ultimately a better scientist for developing the critical thinking and self-discipline through the challenges I faced. I also thank Professor Robert G. Bergman, who has not only devoted time and energy as a member of my qualifying exam and dissertation committees, but also taught me the fundamentals of physical organic chemistry, and helped me develop as a teacher in the context of an undergraduate research laboratory class. Additionally, I thank Stuart Linn, who graciously agreed to fill in as a replacement on my dissertation committee on very short notice.

I am grateful to the undergraduate and graduate students, postdoctoral researchers, and visiting scholars with whom I have collaborated on my research projects throughout my time in graduate school, including Dr. Miles Johnson, Dr. Christian Kuzniewski, Zachary Niemeyer, Levi Pilapil, Sophie Shevick, Amandeep Singh, Dr. Chuanzhou Tao, Richard Thornbury, Mackenzie Thorpe, and Dr. Yi-Ming Wang. Without them, my research accomplishments would not have been possible. I also thank the senior graduate students and postdoctoral researchers who were and continue to be my good friends and mentors, in particular Dr. Carolina Avila, Dr. Jörg Hehn, Dr. Aaron Lackner, Dr. David Nagib, Dr. Hosea Nelson, Dr. Matt Winston, Dr. Jeff Wu, and Dr. Chen Zhao. These people helped me with my chemistry, and also helped me stay sane. I especially thank my cohort, now Ph.D.'s one and all: Dr. Dillon Miles, Dr. Andrew Neel, Dr. Jigar Patel, and Dr. William Wolf. Back in our first year, we were told that at least one of us would drop out, statistically speaking. But we all made it! I'd like to think it was because we helped each other out along the way.

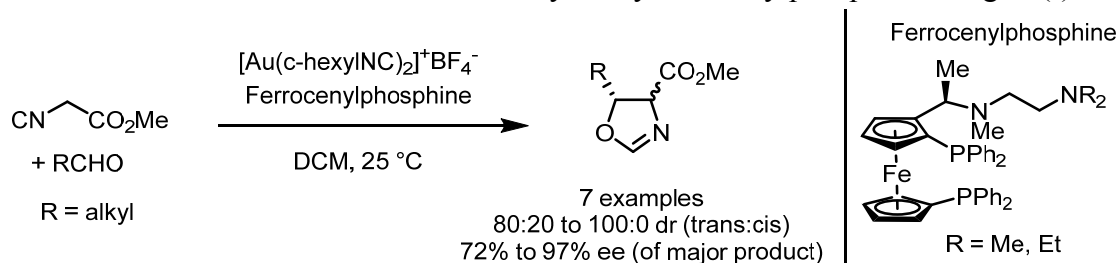
I thank my family—my parents, grandparents, and my sister—for their love, support, and emotional investment in my research, about which they justifiably know very little. Still, it helped motivate my work to know that people outside of the small, insular world of organic chemistry cared about what I was doing and the progress I was making. Finally, I am grateful for my girlfriend, Rachel Draznin-Nagy, who will soon be a (juris) doctor along with me! We have both encountered difficulties and challenges in our respective graduate programs, but we always pulled each other through, and will continue to do so. There will be plenty of new adventures awaiting us in the future, and I can't wait to take them on together.

Chapter 1. Overview of Ligands in Asymmetric Gold(I) Catalysis, and Synthesis of Chiral Acyclic Diaminocarbene Gold(I) Complexes Derived from BINAM

Introduction

Research on homogeneous gold(I) catalysis has undergone tremendous growth in the last three decades.¹ The early forays into asymmetric gold(I) catalysis were launched by the seminal work of Ito and Hayashi,² who reported the first enantioselective gold(I)-catalyzed synthetic transformation: an aldol reaction of aldehydes and isocyanoacetates employing chiral ferrocenylphosphine ligands (Figure 1.1). The asymmetric gold(I)-catalyzed aldol reaction continued to be studied extensively by Hayashi and Ito,^{3,4} Togni and Pastor,^{5,6} as well as Lin and coworkers.⁷ It was also used as an early key step in the enantioselective total synthesis of (-)- α -Kainic Acid.⁸

Figure 1.1 Enantioselective aldol reaction catalyzed by ferrocenylphosphine and gold(I)



The work of Hayashi and Ito also charted the course for many future investigations. Specifically, they borrowed the chiral ferrocenylphosphine ligand from a wholly different area of research—it was originally synthesized for use in palladium cross-coupling and hydrogenation reactions.⁹ Many other chiral ligand sets developed for use in transition metal-catalyzed transformations would prove to be competent for achieving enantioselectivity in gold(I) catalysis.

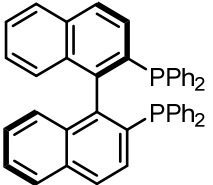
In asymmetric catalysis, the energy difference between two diastereomeric transition states is leveraged to achieve enantioselectivity. This difference can be tiny: 2 kcal/mol at room temperature, or roughly the rotation barrier in a molecule of ethane, corresponds to a selectivity of 95% ee.¹⁰ The choice of ancillary ligand is therefore of paramount importance, because the interactions between ligand and substrate largely govern the energies of the transition states. It is particularly important in regard to asymmetric gold(I) catalysis, since the gold(I) typically adopts a two-coordinate, linear geometry. Therefore, the chiral ligand is spatially removed from the catalytic open site, making it challenging to achieve efficient enantioinduction. This challenge has been met by the application of a diversity of chiral ligands, which fall into three main categories: bidentate phosphorus ligands, monodentate phosphorus ligands, and carbenes.

Bidentate Phosphorus Ligands

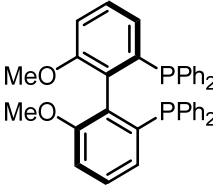
There is one privileged class of ligands borrowed from transition metal chemistry that has enjoyed widespread use in a wide variety of gold(I) transformations: axially chiral atropisomeric biaryl diphosphines. This class includes several ligand families: BINAP, MeOBIPHEP, and SEGPHOS, among others. In lieu of a lengthy discussion of the origin of these ligands, which has been covered elsewhere,¹¹ their relevant data are summarized in Table 1.1.

Table 1.1 Axially chiral atropisomeric biaryl diphosphines: key data from the literature

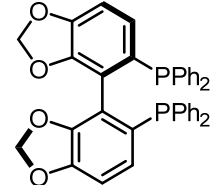
| Ligand | First report (year) | Senior Author | Asymmetric Reaction | Metal | Substrates |
|--------------------------------|---------------------|---------------|---------------------|-------|------------------------------------|
| <i>BINAP</i> ¹² | 1980 | R. Noyori | Hydrogenation | Rh | α -(acylamino)acrylic acids |
| <i>MeOBIPHEP</i> ¹³ | 1991 | R. Schmid | Isomerization | Rh | N,N-diethylnerylamine |
| <i>SEGPPOS</i> ¹⁴ | 2001 | T. Saito | Hydrogenation | Ru | various ketones |



(*R*)-BINAP



(*R*)-MeOBIPHEP



(*R*)-SEGPPOS

These diphosphines have become the benchmark ligands for enantioselective gold(I) chemistry, and they have been identified as the most enantiodiscriminating scaffolds in many, many transformations. The literature on the use of BINAP, MeOBIPHEP, SEGPPOS and their derivatives in gold(I) catalysis has proliferated to the extent that a full review is beyond the scope of this introduction. In the interest of brevity, some notable examples are summarized in Table 1.2.

Table 1.2 Select examples of atropisomeric biaryl diphosphines in asymmetric gold(I) catalysis

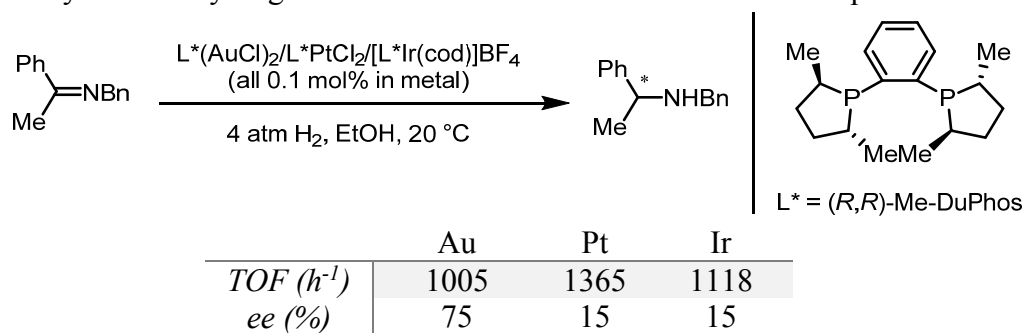
| Asymmetric Reaction | Optimal Ligand Class | Year | Senior Author | Substrates | Examples, ee range |
|---|---------------------------|------|-------------------|---|--------------------|
| <i>Cycloisomerization-Hydroalkoxylation</i> ¹⁵ | BINAP | 2005 | A. M. Echavarren | 1,6-enynes, alcohols | 5, 2-94% |
| <i>Cyclopropanation</i> ¹⁶ | SEGPPOS | 2005 | F. D. Toste | Styrenes, propargyl esters | 11, 65-94% |
| <i>Hydroalkoxylation</i> ¹⁷ | MeOBIPHEP | 2007 | R. A. Widenhoefer | Alcohol-tethered allenes | 10, 45-99% |
| <i>Hydroamination</i> ¹⁸ | BINAP, MeOBIPHEP, SEGPPOS | 2007 | F. D. Toste | Sulfonamide-tethered allenes | 16, 70-99% |
| <i>[2+2] Cycloaddition</i> ¹⁹ | SEGPPOS | 2007 | F. D. Toste | 1,6-allenenes | 7, 54-96% |
| <i>Cycloisomerization-Hydroarylation</i> ²⁰ | MeOBIPHEP | 2009 | V. Michelet | 1,6-enynes, electron-rich aromatics | 11, 72-98% |
| <i>Ring Expansion</i> ²¹ | MeOBIPHEP | 2009 | F. D. Toste | Allenyl-cyclopropanols | 13, 84-94% |
| <i>Cycloisomerization-Hydroxy- and Alkoxy cyclization</i> ²² | MeOBIPHEP | 2010 | R. Sanz | Ortho-(alkynyl)styrenes | 24, 20-92% |
| <i>Polycyclization</i> ²³ | MeOBIPHEP | 2010 | F. D. Toste | Mono-/dienynes with tethered nucleophiles | 5, 88-97% |

| Asymmetric Reaction | Optimal Ligand Class | Year | Senior Author | Substrates | Examples, ee range |
|---|----------------------|------|-----------------|---------------------------------------|--------------------|
| <i>[2+2+3]</i> Cycloaddition ²⁴ | MeOBIPHEP | 2012 | R.-S. Liu | 1,6-enynes, nitrones | 10, 84-95% |
| Cyclopropanation ²⁵ | BINAP | 2012 | H. M. L. Davies | Aryl alkynes, aryl diazoacetates | 19, 84-98% |
| Carboalkoxylation ²⁶ | MeOBIPHEP | 2013 | F. D. Toste | Acetal-tethered aryl/vinyl acetylenes | 17, 60-99% |
| Vinylogous <i>[3+2]</i> Cycloaddition ²⁷ | SEGPHOS | 2013 | H. M. L. Davies | Enol ethers, vinyl diazoacetates | 13, 88-96% |
| Allylic Substitution ²⁸ | SEGPHOS | 2014 | M. Rueping | Phenol-tethered allylic alcohols | 9, 80-88% |
| Rautenstrauch Rearrangement ²⁹ | SEGPHOS | 2015 | F. D. Toste | Indole-tethered propargyl ketals | 17, 71-97% |
| <i>[2+2]</i> Cycloaddition ³⁰ | SEGPHOS | 2015 | M. Bandini | Indoles, allenamides | 16, 81-99% |

Besides these ubiquitous diphosphine ligands, there are several other notable examples that have yet to find widespread use in any other gold(I)-catalyzed reactions.

Corma and coworkers reported the hydrogenation of alkenes and imines with a gold(I) complex derived from DuPhos.³² They found that the (*R,R*)-Me-DuPhos complexes of Au(I), Pt(II) and Ir(I) all performed with comparable catalytic efficiencies, while the Au(I) catalyzed reactions typically had the best enantioselectivities (Table 1.3). DuPhos was first synthesized as a ligand for rhodium in the asymmetric hydrogenation of enamide esters to amino acid precursors.³¹

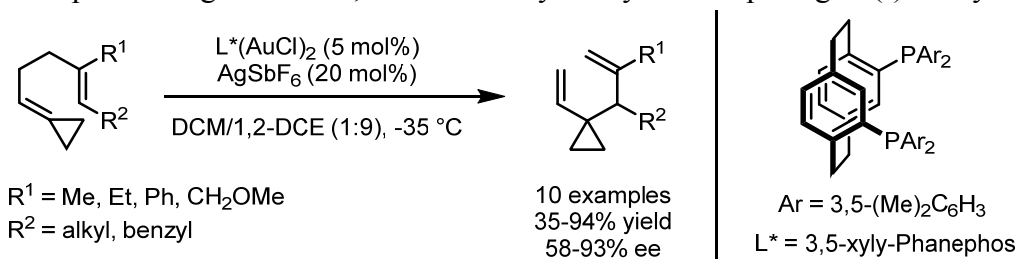
Table 1.3 Asymmetric hydrogenation of an imine with metal-DuPhos complexes



Another ligand which has been repurposed for asymmetric gold(I) catalysis is Phanephos. Developed by chemists at Merck, Phanephos was originally employed for the rhodium(I)-catalyzed asymmetric hydrogenation of dehydroamino acid methyl esters.³³ In their studies on the asymmetric gold(I)-catalyzed Cope rearrangement of 1,5-dienes, Gagné and coworkers identified a Phanephos analogue as the optimal ligand (Figure 1.2).³⁴ The use of methylenecyclopropane substrates was critical for the thermodynamics of this reaction: the relief of the ring strain provides

the driving force for the otherwise disfavored rearrangement to a product with less-substituted double bonds.

Figure 1.2 Cope rearrangement of 1,5-dienes catalyzed by a Phanephos gold(I) catalyst



Monodentate Phosphorus Ligands

As with the bidentate ligands, there is one class of monodentate phosphorus ligands that has exerted outsized influence in the development of enantioselective gold(I)-catalyzed transformations: phosphoramidites derived from axially chiral atropisomeric biaryl diols. Originally developed by Feringa and coworkers as chiral shift reagents,³⁵ chiral phosphoramidites derived from optically active BINOL were first employed as ligands in the copper-catalyzed conjugate addition of dialkylzinc reagents to α,β -unsaturated ketones.³⁶ Since that time, a variety of axially chiral diols (e.g. SPINOL, VANOL) have become commercially available, and the diversity of phosphoramidite scaffolds has consequently followed suit (Figure 1.3). A survey of notable enantioselective gold(I)-catalyzed transformations featuring phosphoramidite ligands is summarized in Table 1.4.

Figure 1.3 Phosphoramidite ligands based on chiral diols

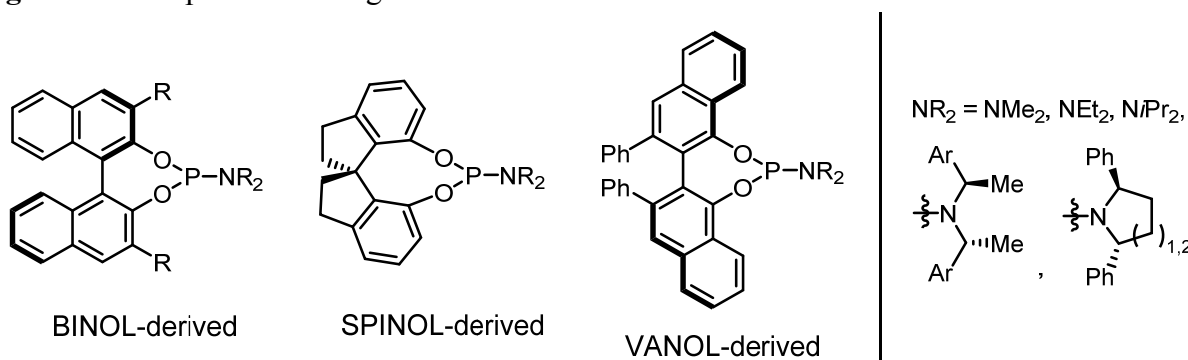


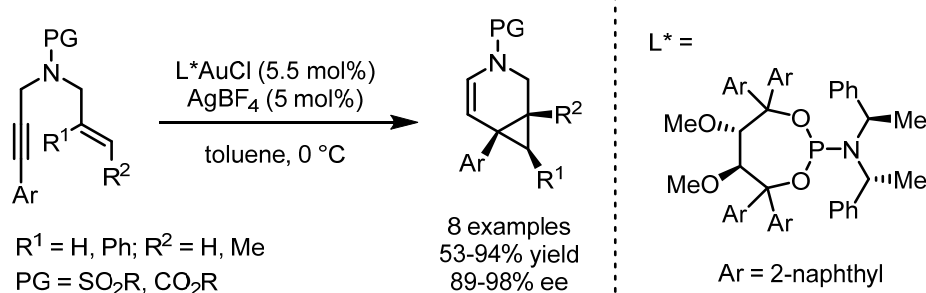
Table 1.4 Select examples of phosphoramidite ligands in asymmetric gold(I) catalysis

| Asymmetric Reaction | Optimal Ligand Class | Year | Senior Author | Substrates | Examples, ee range |
|--|--------------------------------|------|------------------|-----------------------|--------------------|
| $[4+2]$ Cycloaddition ³⁷ | BINOL-derived | 2009 | J. L. Mascareñas | Allenedienes | 4, 91-97% |
| $[2+2]$ Cycloaddition ³⁸ | BINOL-, SPINOL-derived | 2011 | F. D. Toste | 1,6-allenenes | 23, 14-97% |
| Intermolecular $[2+2]$ Cycloaddition ³⁹ | BINOL-, VANOL-, SPINOL-derived | 2012 | J. M. González | Allenamides, styrenes | 14, 70-99% |

| Asymmetric Reaction | Optimal Ligand Class | Year | Senior Author | Substrates | Examples, ee range |
|--|----------------------|------|---------------|------------------------------|--------------------|
| <i>[3+2] Dipolar Cycloaddition</i> ⁴⁰ | BINOL-derived | 2013 | Z. Chen | Allenamides, nitrones | 21, 63-99% |
| <i>Hetero-Diels-Alder</i> ⁴¹ | BINOL-derived | 2013 | L.-Z. Gong | Dienes, diazenes | 11, 86-99% |
| <i>[2+2], [4+2] Cycloadditions</i> ⁴² | BINOL-derived | 2015 | J. Zhang | Allenamides, indolylstyrenes | 25, 82-97% |

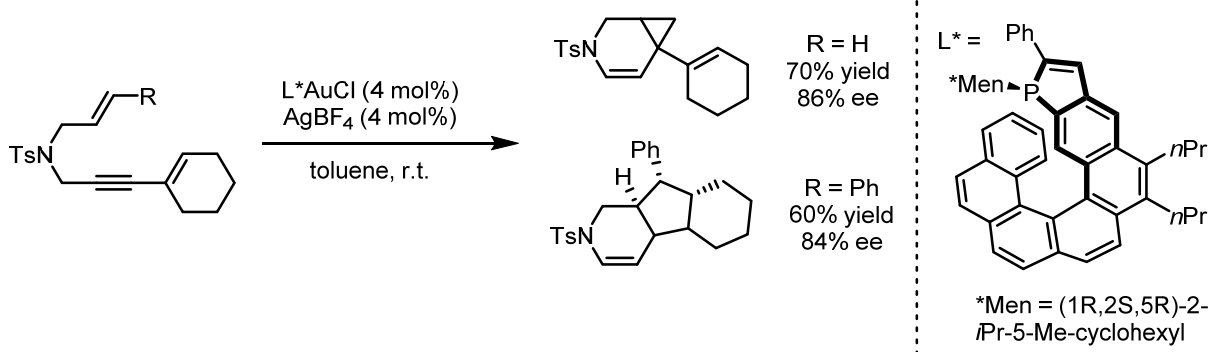
There are also several noteworthy monodentate phosphorus ligands used in asymmetric gold(I) catalysis that do not fall into this classification. Fürstner and coworkers investigated phosphoramidites based on TADDOL,⁴³ and identified variants with an acyclic backbone as excellent ligands in a number of gold(I)-catalyzed reactions.^{44,45} In one example, the cycloisomerization of N-tethered 1,6-enynes affords cyclopropyl-fused dihydropyridines in high yields and with excellent enantioselectivities (Figure 1.4).

Figure 1.4 Cycloisomerization of 1,6-enynes catalyzed by TADDOL-like gold(I) catalyst



Marinetti and coworkers reported the development of chiral helicenes with embedded P-stereogenic phosphole units.^{46,47} These unusual ligands display both helical and point chirality in a single structure. Good yields and enantioselectivities were obtained in cycloisomerization reactions using gold(I) complexes bearing these ligands (Figure 1.5).

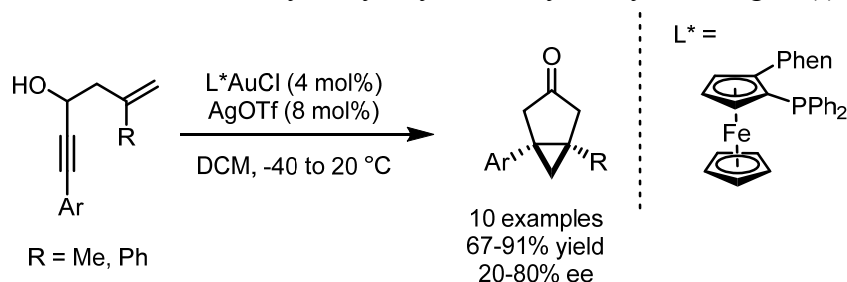
Figure 1.5 Cycloisomerization of dienynes with a helical phosphole gold(I) catalyst



Very recently, researchers in the Marinetti group also reported the asymmetric cycloisomerization of 3-hydroxy-1,5-enynes catalyzed by monophosphine ferrocene (MOPF) gold(I) complexes (Figure 1.6).⁴⁸ The MOPF ligands were first synthesized by Pedersen and Johannsen for use in palladium(II)-catalyzed hydrosilylation of styrenes.⁴⁹ In the cycloisomerization

reaction manifold, the installation of a bulky 9-phenanthryl substituent on the Cp ring adjacent to the phosphine was necessary for achieving increased enantioselectivities.

Figure 1.6 Cycloisomerization of 3-hydroxy-enynes catalyzed by MOPF gold(I) catalyst



Overall, there is an abundance of asymmetric gold(I) literature enabled by ligands containing phosphorus. And while a wide variety of ligands have been demonstrated to achieve high enantioselectivities in a diversity of synthetic transformations, there is another ligand class which warrants review.

Carbenes

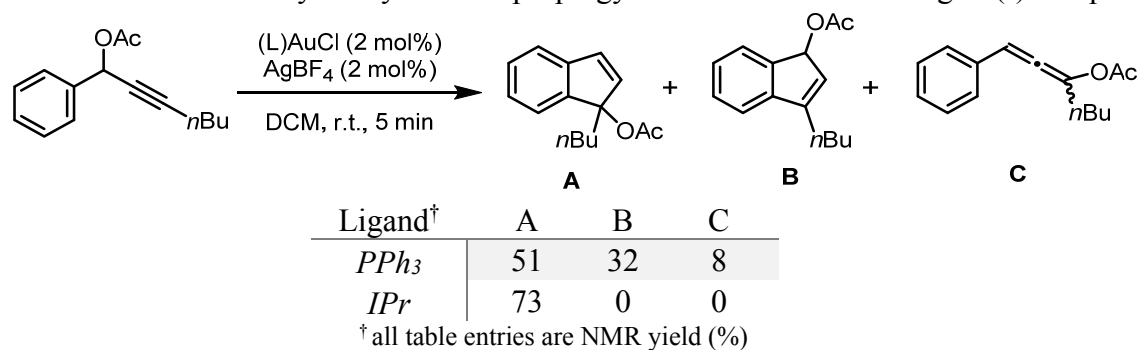
In the context of gold(I) catalysis, carbenes are an important ligand set because they may enable higher reactivity or divergent selectivity relative to phosphorus-based ligands.⁵⁰ Two examples serve well to illustrate and quantify these differences.

First, in two separate reports from Widenhoefer and coworkers on the hydroamination of alkenes with tethered nitrogen nucleophiles, the reaction outcomes with a number of ligands were examined.^{51,52} The authors found that gold(I) complexes bearing carbene ligands catalyzed this reaction most efficiently, requiring the lowest reaction temperatures and shortest reaction times, even in comparison to a very electron-rich phosphine (Table 1.5).

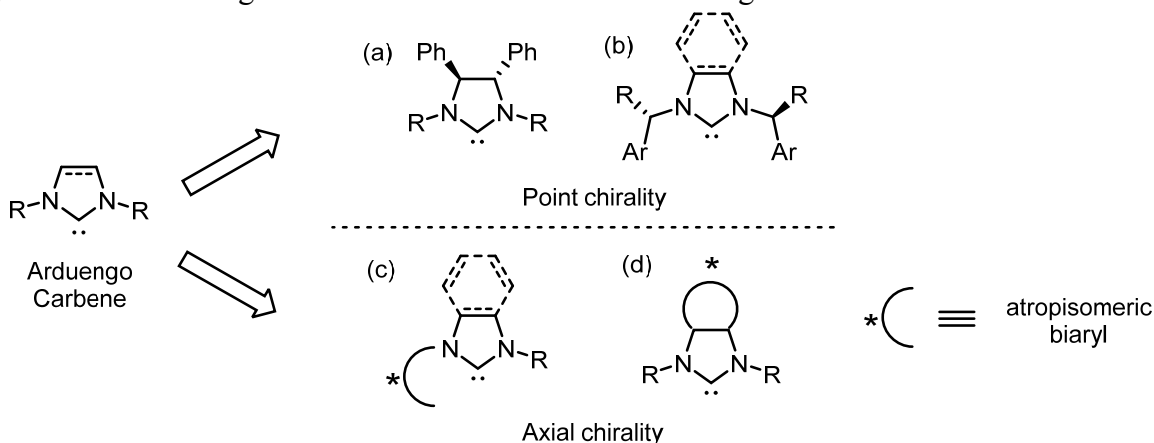
Table 1.5 Intramolecular hydroamination of alkenyl carbamates with different gold(I) complexes

| Ligand | Temp (°C) | Time (h) | Yield (%) |
|--|-----------|----------|-----------|
| <i>PPh</i> ₃ | 100 | 24 | 75 |
| <i>P</i> (<i>t</i> Bu) ₂ (<i>o</i> -biphenyl) | 60 | 18 | 97 |
| <i>IPr</i> | 45 | 15 | 96 |

Second, in a publication by Nolan and coworkers, the intramolecular hydroarylation of propargyl acetates was observed to proceed by two distinct pathways, leading to the formation of three potential products (Table 1.6).⁵³ The substrate either underwent 3,3-rearrangement to an allene intermediate (**C**) which then proceeded to indene **A** by a hydroarylation reaction, or direct hydroarylation of the starting alkyne gave indene **B** possessing different regiochemistry. While a phosphine ligand afforded a mixture of products, the carbene ligand was selective for one pathway.

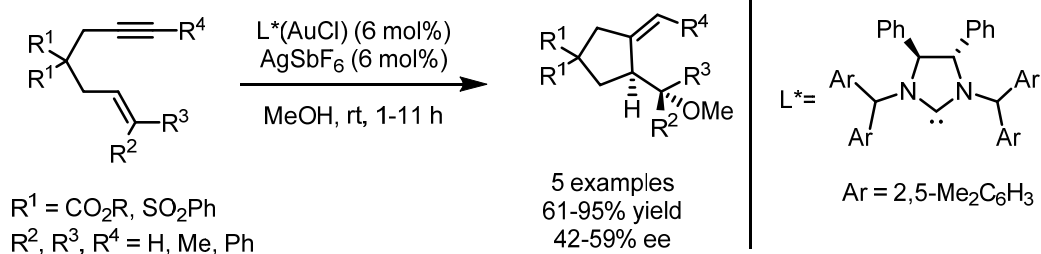
Table 1.6 Intramolecular hydroarylation of propargyl acetates with different gold(I) complexes

Despite these attractive features, chiral carbene ligands are relatively less developed than their phosphorus-containing counterparts, but they have recently started to receive greater interest from the synthetic community.⁵⁴ Many chiral carbene structures are derived from the seminal Arduengo imidazole carbene.⁵⁵ This is achieved by constructing the imidazole ring from optically active amines and diamines which display either point chirality or axial chirality (Figure 1.7).

Figure 1.7 Two strategies for chiral derivatization of Arduengo carbenes

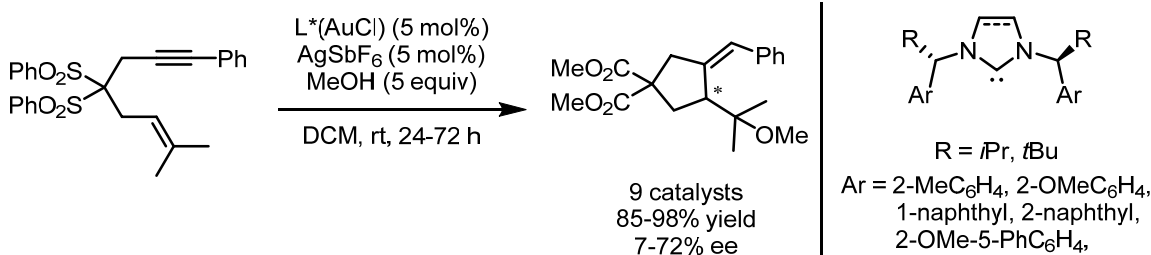
One example is the use of optically active *trans*-1,2-diphenylethylenediamine as the source of two chiral phenyl residues in the imidazole backbone (Figure 1.7a). Sterically bulky groups adjacent to the heterocyclic nitrogens transmit this stereochemical information closer to the site of metal ligation. The use of such carbenes was first reported by Grubbs and coworkers in their report on enantioselective ruthenium-catalyzed olefin metathesis.⁵⁶ In the context of asymmetric gold(I) catalysis, Tomioka and coworkers applied this ligand set to methoxycyclization of 1,6-enynes.^{57,58} Although the catalysts displayed good reactivity, the observed enantioselectivities were only moderate (Figure 1.8).

Figure 1.8 Methoxycyclization of 1,6-enynes with chiral NHC gold(I) complexes



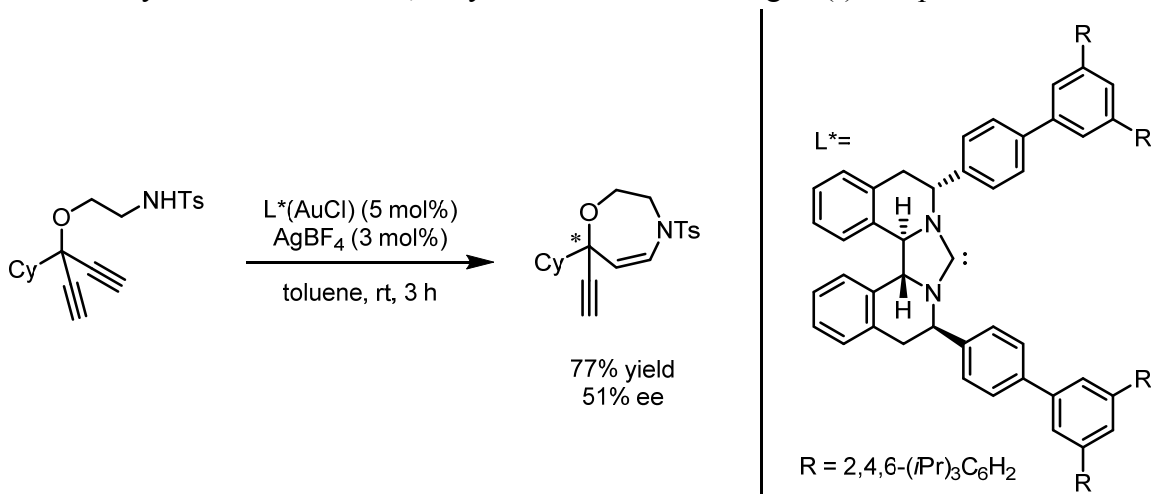
Another example is the installation of chiral centers directly adjacent to the heterocyclic nitrogens, and thereby in closer proximity to the carbene (Figure 1.7b). The groups of Gung^{59,60} and Kündig⁶¹ reported the synthesis of such gold(I) complexes, and the latter utilized them in the asymmetric methoxycyclization of 1,6-enynes (Figure 1.9). While the strategy of more proximal chirality appears to have some validity, the reported enantioselectivities leave room for further optimization.

Figure 1.9 Methoxycyclization of 1,6-enynes with chiral NHC gold(I) complexes



A final example comes from the work of Czekelius and coworkers. They reported carbene ligands for gold(I) complexes which combine the chiral elements from the previous examples, and display four chiral centers: two in the imidazole backbone and two adjacent to the heterocyclic nitrogens. They applied these catalysts to the desymmetrization of 1,4-diynes by 7-endo-dig cyclizations.^{62,63} However, even the introduction of extremely bulky substituents on the ligand scaffold failed to afford highly enantioenriched product (Figure 1.10).

Figure 1.10 Hydroamination of a 1,4-diyne with a chiral NHC gold(I) complex



Extensive investigations of gold(I) carbenes with axially chiral scaffolds appended to the heterocyclic nitrogen (Figure 1.7c) were carried out by Min Shi and coworkers.^{64–68} These ligands, obtained from 1,1'-binaphthyl-2,2'-diamine (BINAM), were extensively derivatized and functionalized (Figure 1.11). The highest enantioselectivity values obtained with this catalyst family were reported in the oxidative cycloisomerization of 1,6-enynes, up to 70% ee (Figure 1.12).⁶⁵

Figure 1.11 Chiral NHC ligands derived from BINAM developed in the Shi laboratory

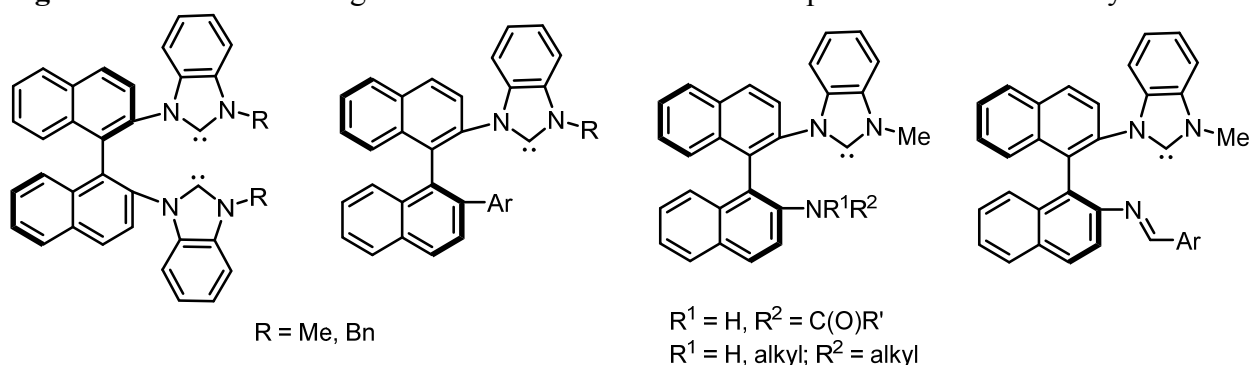
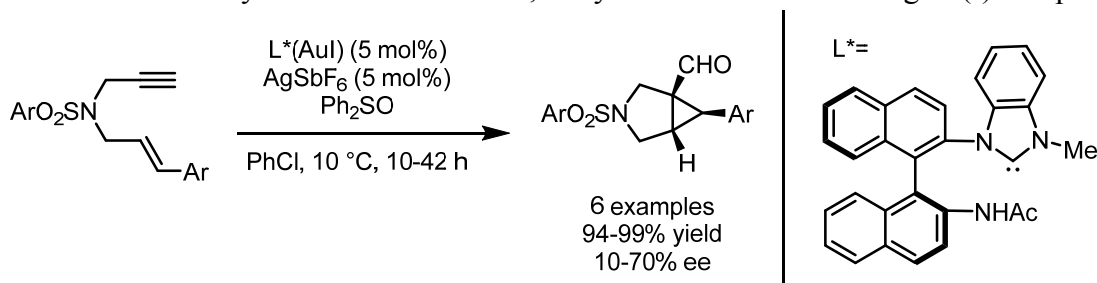
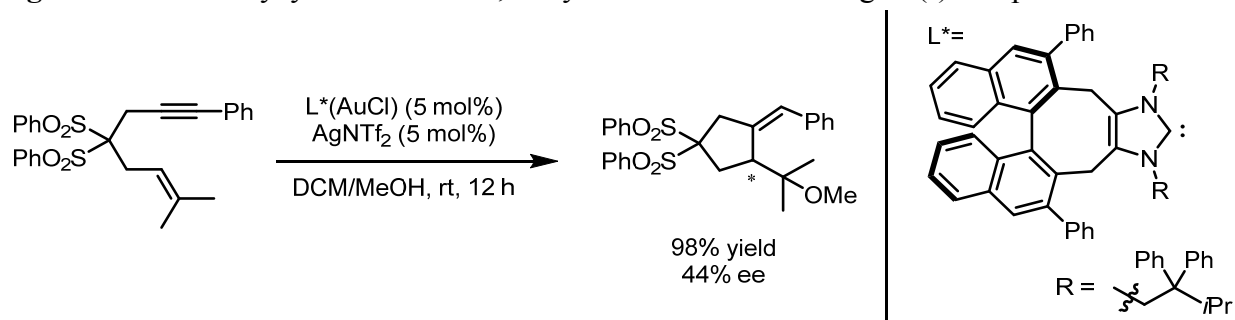


Figure 1.12 Oxidative cycloisomerization of 1,6-enynes with a chiral NHC gold(I) complex



Recently, Nakada and coworkers disclosed a related scaffold possessing axial chirality: in their design, a carbene ligand displays a BINOL-derived backbone appended to the heterocyclic backbone (Figure 1.7d). As with the Tomioka catalysts, this distal chiral information is transmitted to the active site through large substituents on the heterocyclic nitrogens. This design strategy demonstrated promising, but only moderate, levels of enantioselectivity in the cycloisomerization of 1,6-enynes (Figure 1.13).⁶⁹

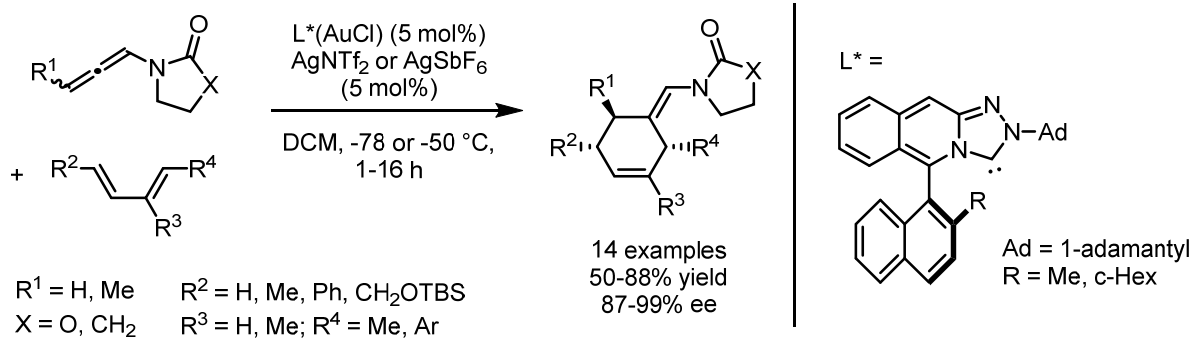
Figure 1.13 Methoxycyclization of a 1,6-enyne with a chiral NHC gold(I) complex



To date, the most highly enantioselective transformation catalyzed by a NHC gold(I) complex is a [4+2] cycloaddition reaction of allenamides and dienes reported by Mascareñas and

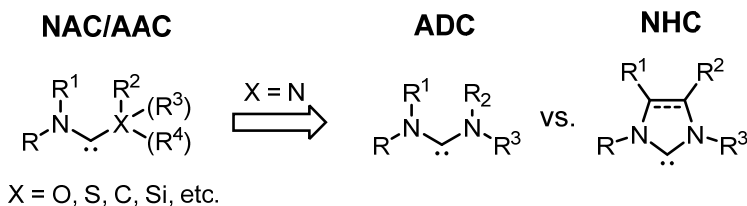
coworkers.⁷⁰ They synthesized gold(I) catalysts featuring axially chiral triazoloisoquinolin-3-ylidene ligands, wherein the carbene heterocycle is fused to the chiral residue. While the transformation features a broad substrate scope, good reactivities, and excellent enantioselectivities (Figure 1.14), the precatalyst synthesis required an eight step linear sequence and a chiral HPLC resolution, hampering the ability to rapidly diversify the ligand.

Figure 1.14 [4+2] Cycloaddition of allenamides and dienes with a chiral NHC gold(I) complex



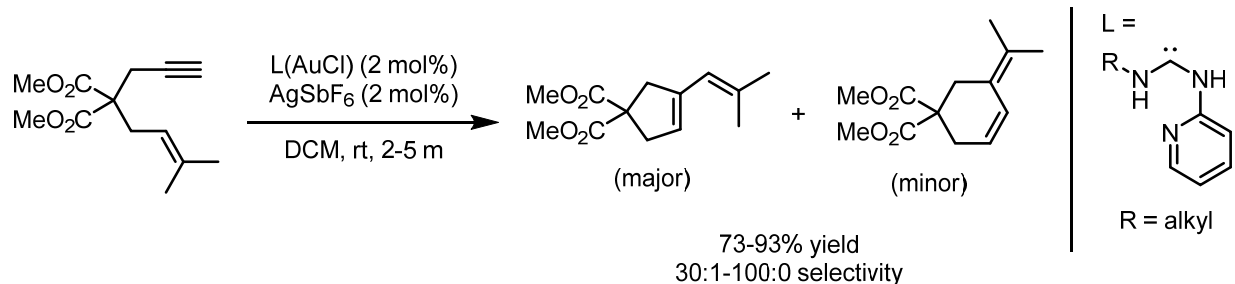
Acyclic aminocarbenes (AAC), also known as nitrogen acyclic carbenes (NAC), recently emerged as an alternative to their cyclic counterparts.⁷¹ A special subset of the AAC family are the acyclic diaminocarbenes (ADC); their structures are illustrated in Figure 1.15.

Figure 1.15 Comparison of acyclic and heterocyclic carbenes



While AAC gold(I) complexes have been known in the literature for decades,⁷² they have only recently begun to be explored as catalysts. Espinet and Echavarren reported in 2008 that ADC gold(I) complexes featuring 2-pyridyl substituents were efficient catalyst for cycloisomerization reactions of 1,6-enynes (Figure 1.16).⁷³

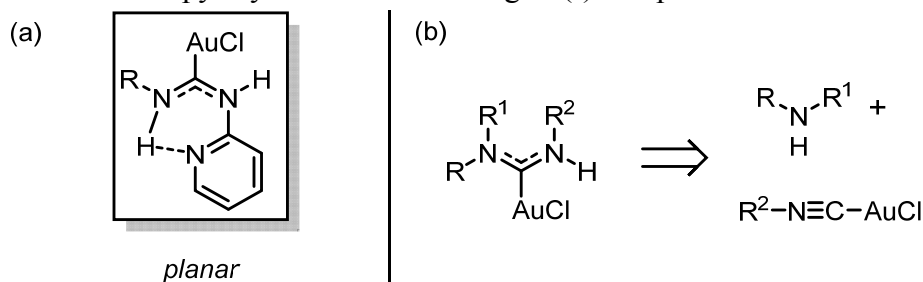
Figure 1.16 Cycloisomerization of 1,6-enynes with ADC gold(I) complexes



Two characteristics of these complexes are noteworthy. First, the intramolecular hydrogen bonding by the pyridyl residue, observable by a strong downfield shift in the ¹H NMR spectrum in all but the most polar protic solvents, enforces a planar configuration (Figure 1.17a). Second, ADC gold(I) complexes are synthesized in a convergent manner from primary or second amines and gold(I) isocyanides (Figure 1.17b). Indeed, it is this characteristic that caused the authors to

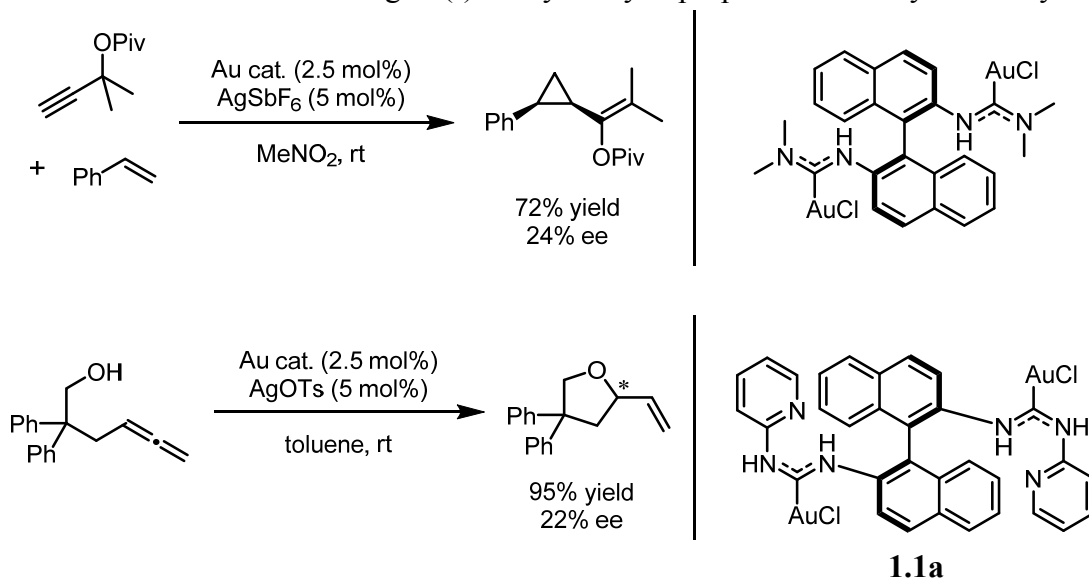
note that, “[t]he modular construction of the catalysts makes them an attractive alternative to tune the catalysis.”

Figure 1.17 Features of 2-pyridyl substituted ADC gold(I) complexes



Espinet and coworkers went on to show that ADC ligands could be rendered chiral by incorporation of optically active amines and diamines, recapitulating the strategy of the construction of chiral NHC ligands.⁷⁴ The main difference, though, was their ability to incorporate the chiral elements in the final step of the precatalyst synthesis, owing to the convergent synthesis of ADC gold(I) complexes. With a small library of chiral ADC gold(I) catalysts in hand, the authors achieved modest enantioselectivity in two transformations—cyclopropanation and hydroalkoxylation—previously rendered highly enantioselective through the application of axially chiral diposphine gold(I) complexes.^{16,17} In both cases, the best catalysts they surveyed were derived from BINAM (Figure 1.18).

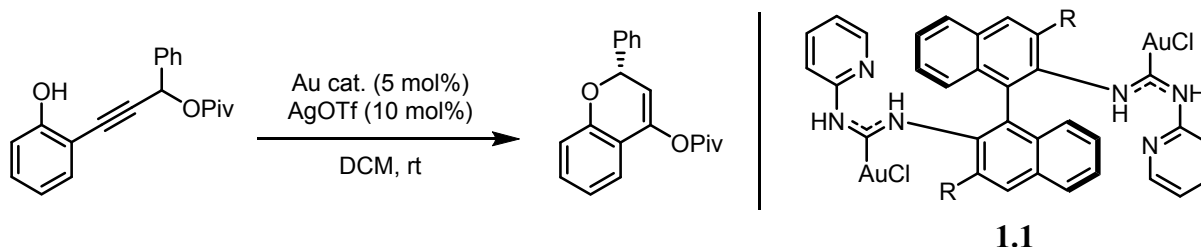
Figure 1.18 Enantioselective ADC gold(I) catalysis: cyclopropanation and hydroalkoxylation



Armed with this insight, investigators in the Toste lab attempted to apply these BINAM-derived ADC gold(I) complexes to a rearrangement reaction that afforded chiral chromenyl pivalate products.⁷⁵ While initially they observed low enantioselectivity with the BINAM-derived ADC gold(I) complex **1.1a**, they found that the introduction of aryl substituents at the 3 and 3' positions of the binaphthyl scaffold (particularly those bearing electron-withdrawing substituents, complex **1.1c**) led to a significant improvement in enantioselectivity (Table 1.7). With this catalyst modification and some optimization of the reaction conditions, the authors

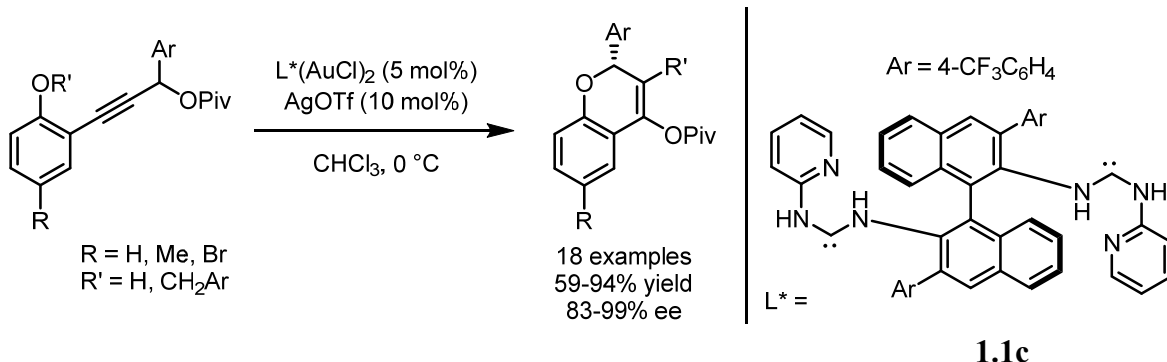
demonstrated a broad substrate scope with good yields and enantioselectivities across the board (Figure 1.19).

Table 1.7 Effect of BINAM substituents on ee in the cycloisomerization of propargyl ester



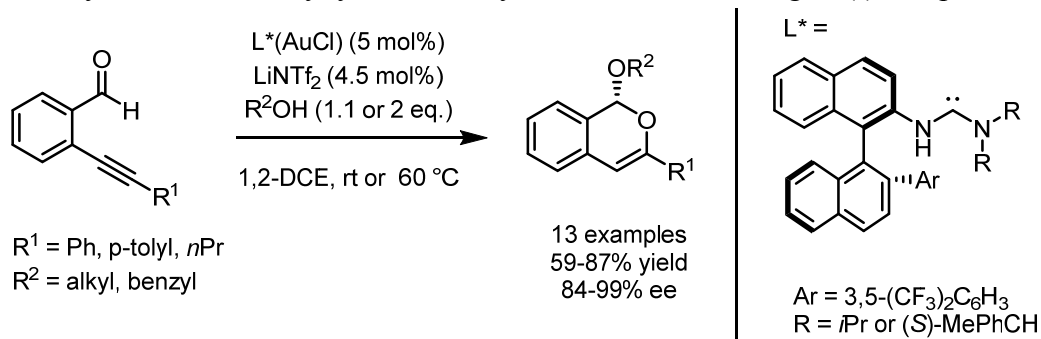
| Entry | Complex | R | ee (%) |
|-------|-------------|---|--------|
| 1 | 1.1a | H | 22 |
| 2 | 1.1b | Ph | 56 |
| 3 | 1.1c | 4-CF ₃ C ₆ H ₄ | 73 |

Figure 1.19 Cycloisomerization of propargyl esters with a chiral ADC gold(I) complex



Soon after this report, Handa and Slaughter disclosed a different gold(I)-catalyzed cyclization reaction with related mononuclear, chiral ADC gold(I) complexes.⁷⁶ As in the previous example, the best enantioselectivities in this transformation were obtained using a ligand bearing an electron-deficient aryl ring that projects into the site of reactivity. The authors attribute this enhanced steric effect to a cation- π interaction between the aromatic residue and the gold center.

Figure 1.20 Cyclizations of alkynyl benzaldehydes with chiral ADC gold(I) complexes

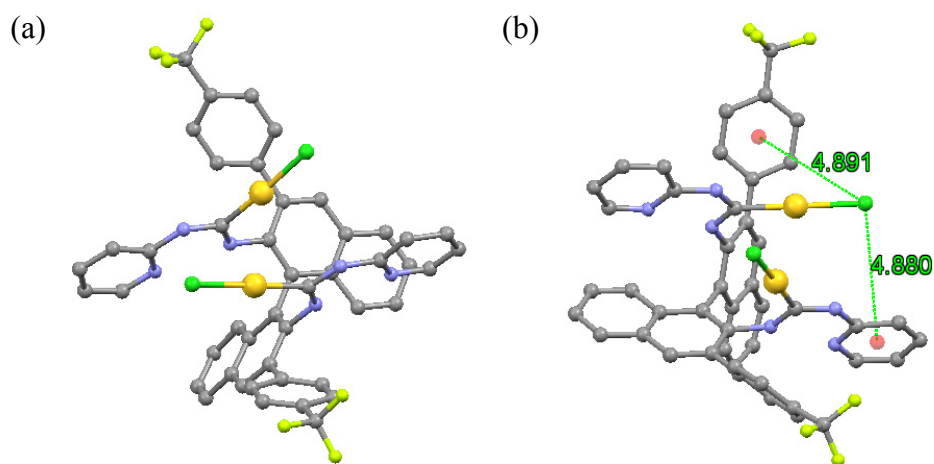


Results and Discussion

In light of these highly enantioselective examples of ADC gold(I)-catalyzed transformations, and given the relative dearth of effective chiral carbene architectures in the literature, I became interested in further exploring and expanding the library of ADC gold(I) catalysts. Specifically, I sought to diversify the ADC gold(I) complexes derived from BINAM and apply them to new reaction manifolds. Moreover, I wished to explore not only modifications to the BINAM-derived precursors, but also the isocyano-gold(I) complexes which comprise the other (achiral) portion of the ligand.

The impetus for pursuing these latter modifications arose from a hypothesis developed by careful examination of the crystal structure of the optimal BINAM-derived ADC gold(I) complex **1.1c** (Figure 1.21). The trifluoromethyl aryl groups project into the site of reactivity, as evidenced by their proximity to the chloride atoms (colored in green) which correspond to the open coordination sites of the cationic gold(I) complex. The steric influence of these substituents, acting as walls to block off one side of the chiral pocket, is presumed to enable enhanced enantioinduction compared to that observed with the parent compound (**1.1a**).

Figure 1.21 Two views of the crystal structure of BINAM-derived ADC gold(I) complex **1.1c** (hydrogens omitted for clarity)

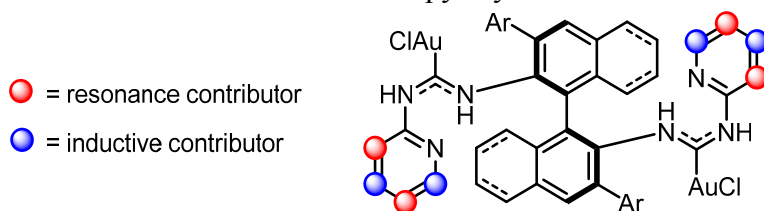


Further inspection reveals that the pyridyl residues also reside in close spatial proximity to the gold centers bound to the opposite carbene centers (compare the distances from the chloride to the centroids in Figure 1.21b). Due to the intramolecular hydrogen bonding present in these architectures, substituents introduced on the pyridyl residue are oriented in space in a rigid and predictable fashion. Therefore, I became interested in probing the effects of installing additional steric elements, especially *ortho*- to the carbene nitrogen, as a second avenue for tuning the chiral environment of the gold(I) complexes.

I quickly realized that this approach also enabled electronic modulation, given the potential for inductive and resonance effects of the pyridyl substituents on the carbene (Figure 1.22). This too represented an avenue for potentially fruitful investigations, as it had been previously shown

that modulating the electronics of a carbene gold(I) complex can beneficially affect reaction outcomes.⁷⁷

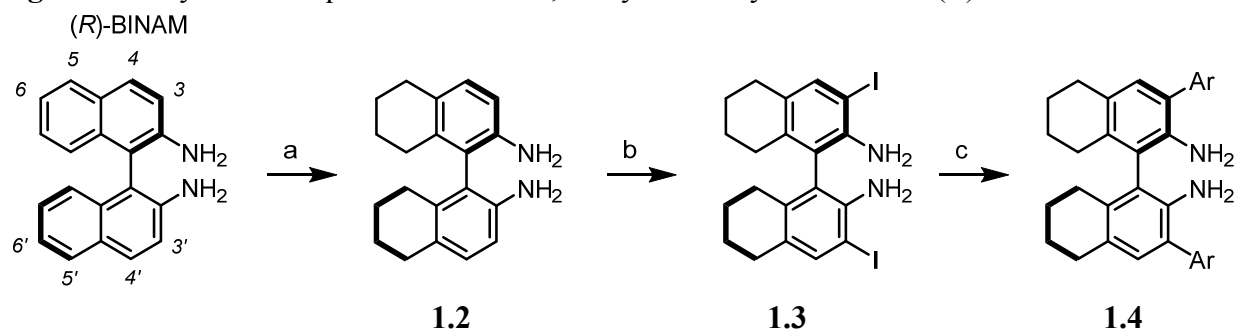
Figure 1.22 Envisioned electronic contributions of pyridyl substituents



In the remainder of this chapter, I will describe the synthesis and preparation of these novel BINAM-derived ADC gold(I) complexes (detailed procedures may be found in the Experimental section). In the chapters that follow, I will report their application in asymmetric gold(I) catalysis, targeting hydroamination, hydroazidation, hydroarylation, and tandem rearrangement-cycloaddition reactions.

The first synthetic sequence provides access to substituted analogues of the binaphthyl core. Commercially available (*R*)-BINAM was hydrogenated to afford the corresponding octahydro derivative **1.2**, and subsequent iodination gave intermediate **1.3**. The hydrogenation step was necessary to achieve selective iodination at the 3 and 3' positions (treatment of fully aromatic BINAM gives 6,6'-iodination). Next, Suzuki coupling was employed to install a diversity of aromatic substituents, furnishing intermediate **1.4**.

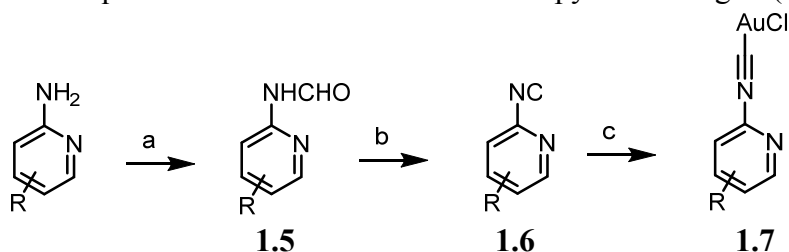
Figure 1.23 Synthetic sequence to install 3,3'-aryl diversity elements on (*R*)-BINAM



Conditions: a) H₂ (50 bar), Pd/C, EtOH, 100 °C, 2 h, 95% yield; b) [BnNMe₃]⁺[ICl₂]⁻, CaCO₃, DCM/MeOH, 0 °C to rt, 2 h; c) ArB(OH)₂ (2-3 equiv), Pd(OAc)₂, SPhos, K₃PO₄, toluene, 100 °C, o/n, 63-80% yield.

The second convergent sequence allows for incorporation of substituents on the 2-pyridyl isocyanogold(I) intermediate. Substituted 2-aminopyridines (many of which are commercially available) were converted to the corresponding formamides **1.5**, which were indefinitely bench-stable. These were then dehydrated to the respective isocyanides **1.6**, and subsequently metalated with dimethylsulfide gold(I) chloride by a ligand substitution, affording complexes **1.7**. Depending on their substituents, compounds **1.6** and **1.7** may decompose quickly, and should be used in their subsequent reactions immediately upon purification and isolation.

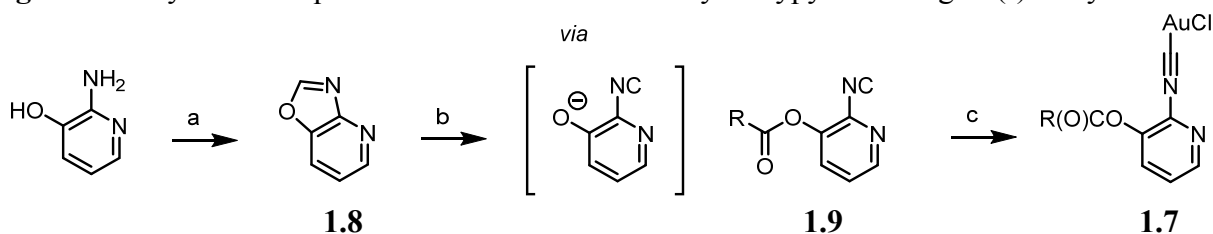
Figure 1.24 Synthetic sequence to convert substituted aminopyridines to gold(I) isocyanides



Conditions: a) formic acid, acetic anhydride, THF, 50 °C to rt, o/n, 60-97% yield; b) POCl₂X (X = Cl, OEt, or OPh), DCM/Et₃N, rt, 2-4 h, 30-65% yield; c) (dms)AuCl, acetone, rt, 20 min, >90% yield.

In certain cases, a different route was employed. Commercially available 2-amino-3-hydroxypyridine was converted to fused oxazole **1.8**, and then treatment with *n*-butyllithium led to a ring-opened intermediate which was trapped with a suitable electrophile to give isocyanide **1.9**. This was metalated to give certain gold(I) isocyanides **1.7** which were difficult to access by the previous route.

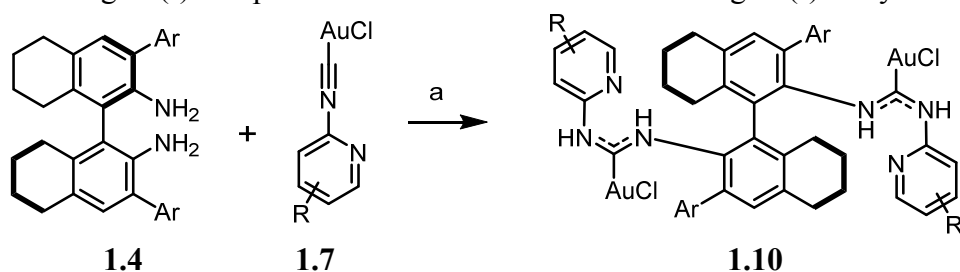
Figure 1.25 Synthetic sequence to convert 2-amino-3-hydroxypyridine to gold(I) isocyanides



Conditions: a) HC(OEt)₃, reflux, 4h, 92% yield; b) 1) *n*-BuLi, 2) acetic anhydride or benzoyl chloride, THF, -78 °C to rt, 26-46% yield; c) (dms)AuCl, acetone, rt, 20 m, >90% yield.

In the final step, the two diversified components **1.4** and **1.7** were reacted to form the ADC gold(I) complexes **1.10**. These gold(I) precatalysts were then purified by silica gel column chromatography and vapor diffusion recrystallization.

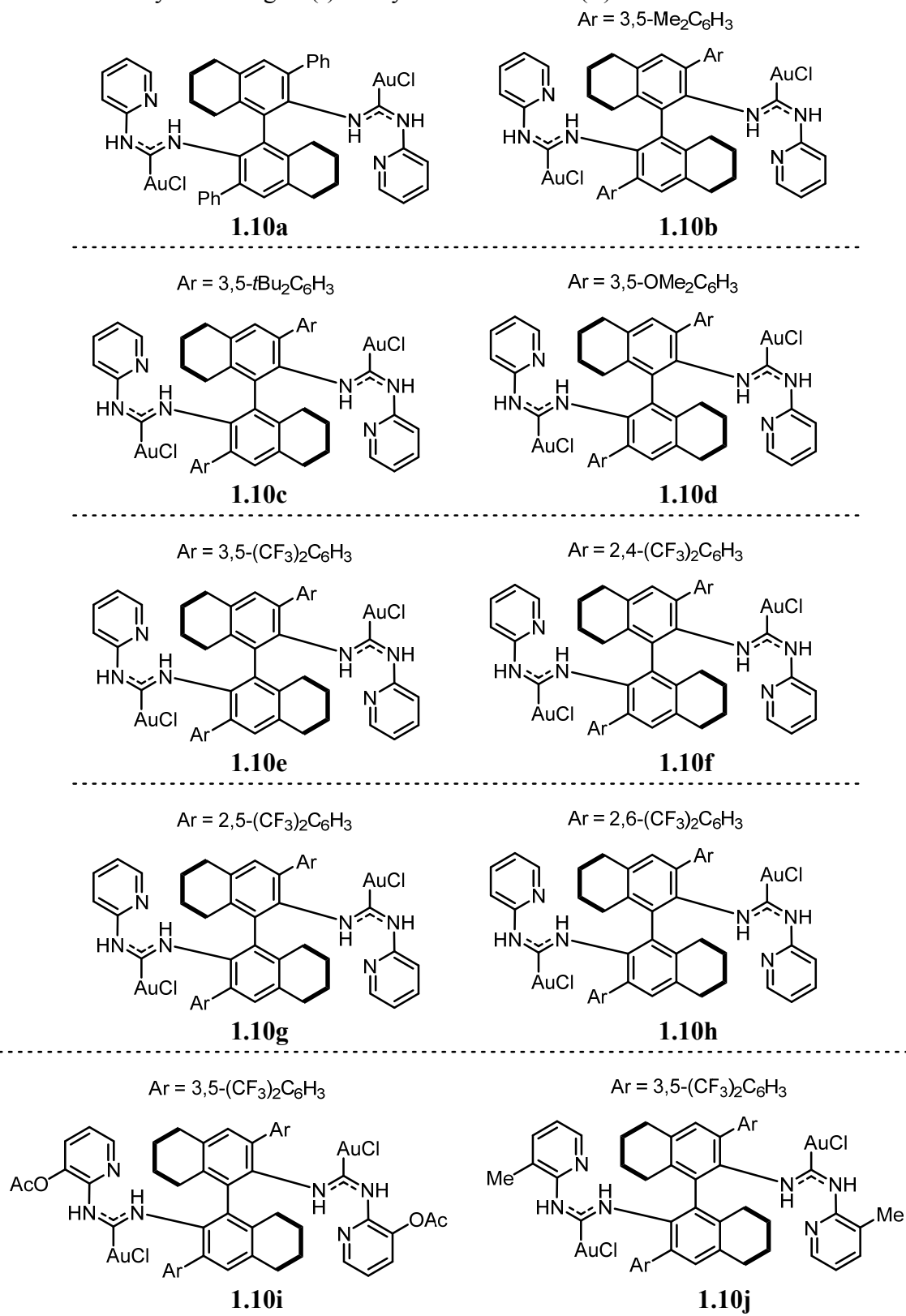
Figure 1.26 ADC gold(I) complexes from BINAM derivatives and gold(I) isocyanides

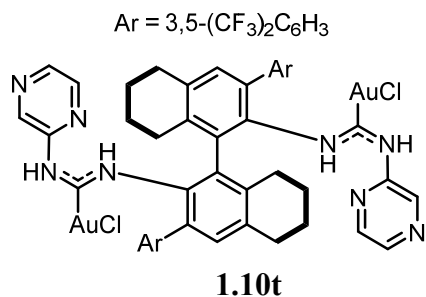
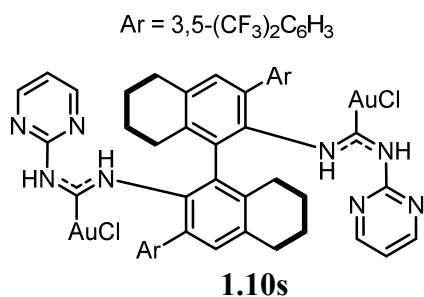
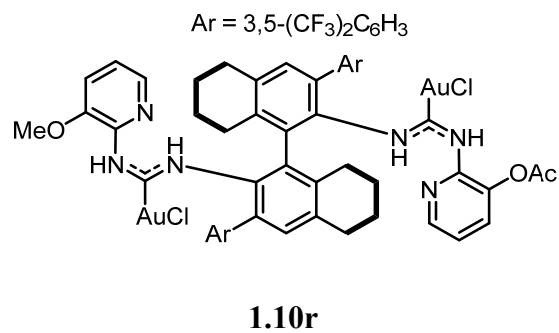
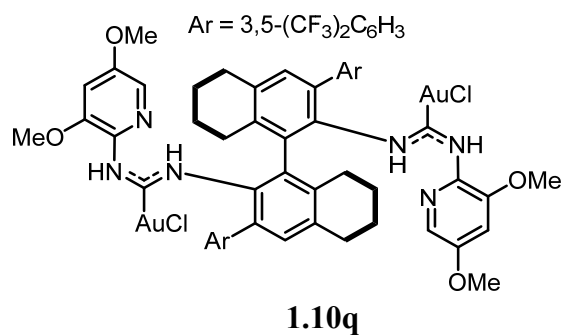
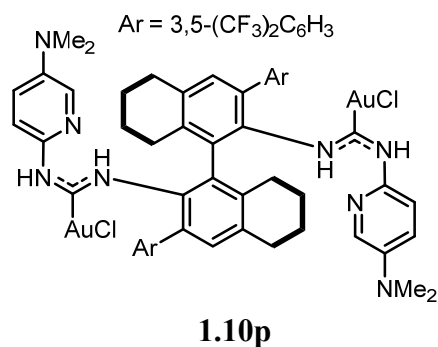
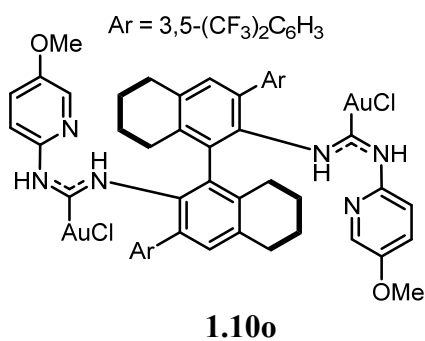
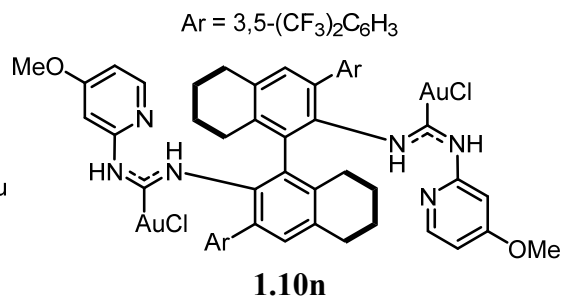
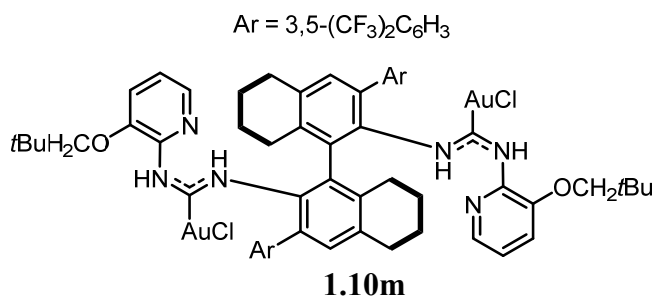
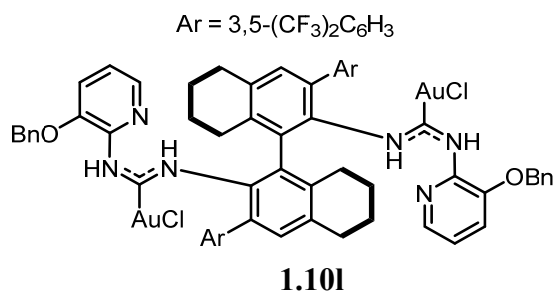
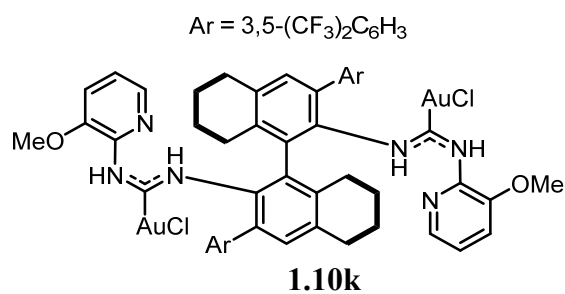


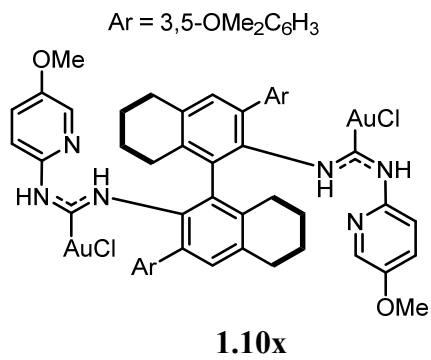
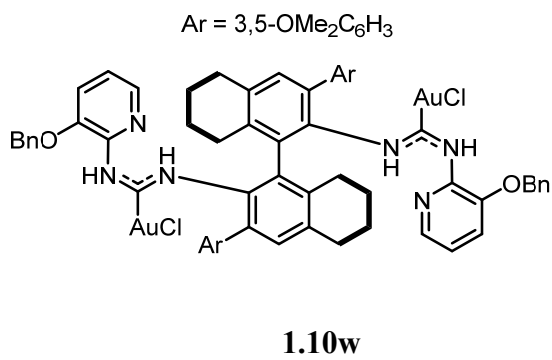
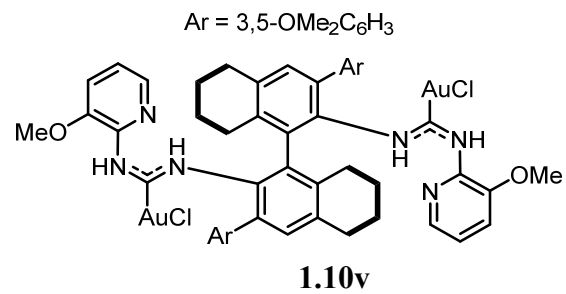
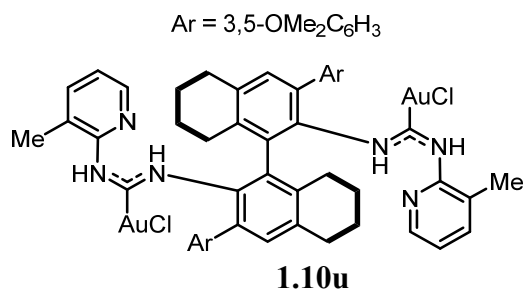
Conditions: a) **1.4** (1 equiv), **1.7** (2-3 equiv), DCM (rt) or CHCl₃ (reflux), o/n, 51- 64% yield.

Using this rapid and straightforward synthesis (7 total steps, 4 step longest linear sequence), I accessed a variety of structures, covering a range of steric and electronic parameters, and this library of ADC gold(I) precatalysts is listed in Figure 1.27. The specific applications to asymmetric catalysis in the following chapters will refer back to these numbered structures.

Figure 1.27 Library of ADC gold(I) catalysts derived from (*R*)-BINAM







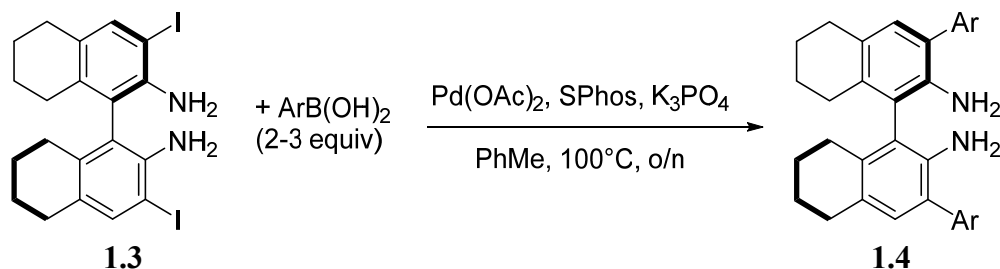
Experimental

General information

Unless otherwise noted, reagents were obtained from commercial sources and used without further purification. Dry toluene was obtained by passage through activated alumina columns under argon. All other solvents used are HPLC grade. TLC analysis of reaction mixtures was performed on Merck silica gel 60 F₂₅₄ TLC plates and visualized by ultraviolet light, iodine or potassium permanganate stain. Flash chromatography was carried out with ICN SiliTech 32-63 D 60 Å silica gel. ¹H and ¹³C NMR spectra were recorded with Bruker AV-500, DRX-500, or AV-600 spectrometers and were referenced to residual ¹H and ¹³C signals of the deuterated solvents, respectively (δ H 7.26, δ C 77.16 for chloroform-d; δ H 5.32, δ C 54.00 for dichloromethane-d₂; δ H 2.13, δ C 118.26 for acetonitrile-d₃). ¹⁹F spectra were recorded with a Bruker AVQ-400 spectrometer and were referenced to trichlorofluoromethane (CFCl₃, δ F 0.00 in chloroform-d). Mass spectral data were obtained via the Micro-Mass/Analytical Facility operated by the College of Chemistry, University of California, Berkeley using a Thermo LTQ-FT (ESI) instrument. X-ray crystallographic analysis was carried out at the College of Chemistry X-Ray Crystallographic Facility (CHEXRAY, University of California, Berkeley) using an APEX 2 Quazar diffractometer.

Preparation of ADC gold(I) complexes

5,5',6,6',7,7',8,8'-octahydro-3,3'-diido-2,2'-diamino-1,1'-binaphthyl (**1.3**) and 5,5',6,6',7,7',8,8'-octahydro-3,3'-aryl substituted 2,2'-diamino-1,1'-binaphthyls (**1.4**) were prepared in procedures modified from those reported by Maruoka and coworkers.⁷⁸ The synthesis 2-isocyanopyridines has been described previously.^{79,80} Isocyanopyridyl gold(I) complexes⁸¹ and ADC gold(I) complexes⁷⁴ were prepared in procedures modified from those reported by Espinet and coworkers. A representative synthesis is described.



Suzuki-Miyuara coupling to install 3,3'-aryl substituents

(*R*)-3,3'-bis(3,5-bis(trifluoromethyl)phenyl)-5,5',6,6',7,7',8,8'-octahydro-[1,1'-binaphthalene]-2,2'-diamine (Ar = 3,5-(CF₃)₂-C₆H₃)

A flame-dried round bottom flask equipped with a teflon-coated stir bar containing **1.3** (2.47 g, 4.54 mmol, 1.0 eq.), 3,5-bis(trifluoromethyl)-phenylboronic acid (2.98 g, 11.55 mmol, 2.5 equiv), Pd(OAc)_2 (48.3 mg, 0.215 mmol, 0.05 equiv), SPhos (179.5 mg, 0.437 mmol, 0.10 equiv), and K_3PO_4 (4.38 g, 20.62 mmol, 4.5 equiv) was evacuated and backfilled with nitrogen. Dry toluene (110 mL) was added and the mixture was stirred vigorously at 100°C overnight. The reaction

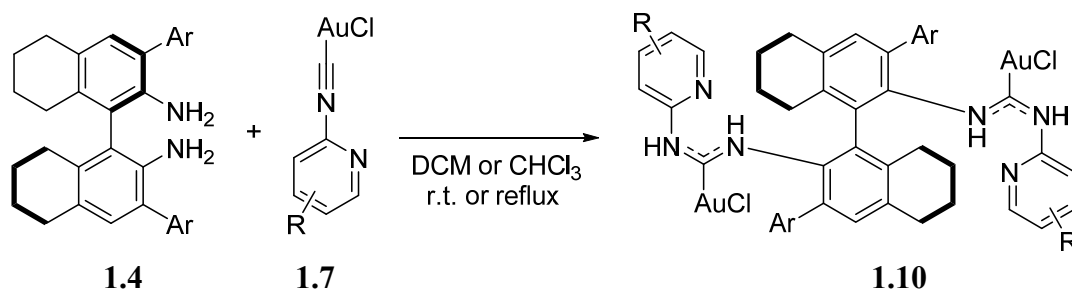
mixture was then filtered through a pad of silica gel and Celite with dichloromethane eluent and concentrated. Purification by flash column chromatography (3:1 hexanes/dichloromethane) afforded **1.4** as a yellow foam (2.37 g, 3.31 mmol, 73% yield). Other 3,3'-disubstituted H₈-BINAM derivatives were prepared analogously.

¹H NMR (600 MHz, CDCl₃) δ 7.99 (s, 4H), 7.84 (s, 2H), 6.92 (s, 2H), 3.46 (br s, 4H), 2.88 – 2.63 (m, 4H), 2.47 – 2.32 (m, 2H), 2.31 – 2.13 (m, 2H), 1.84 – 1.68 (m, 8H).

¹³C NMR (151 MHz, CDCl₃) δ 142.39, 138.70, 137.56, 132.21 (q, *J* = 33.3 Hz), 130.79, 129.58, 128.70, 123.53 (q, *J* = 273.3 Hz), 122.83, 122.56, 120.92 – 120.82 (m), 29.41, 27.31, 23.49 (d, *J* = 1.7 Hz), 23.29 (d, *J* = 1.7 Hz).

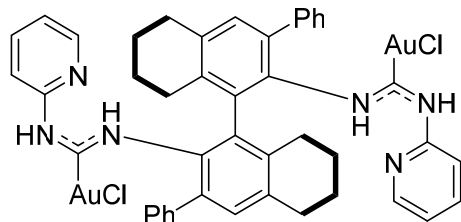
¹⁹F NMR (376 MHz, CDCl₃) δ -63.20.

HRMS (ESI+): calc'd for [C₃₆H₂₈N₂F₁₂]⁺H: 717.2134, found: 717.2129



Synthesis of ADC gold(I) complexes **1.10** (procedure for **1.10e**, Ar = 3,5-(CF₃)₂C₆H₃, R = H)

To a solution of **1.7** (369 mg, 1.10 mmol, 2.2 equiv) in dry DCM (50 mL) was added **1.4** (358 mg, 0.499 mmol, 1.0 equiv) in one portion. The mixture was stirred in the dark overnight, until TLC analysis showed complete consumption of **S2**. The mixture was then concentrated *in vacuo* and chromatographed on silica gel (DCM → 20:1 DCM/Et₂O). Decomposition of unreacted **S3** was observed as purple streaks on the column. The isolated product was further purified by vapor diffusion recrystallization from CHCl₃ and pentane, affording transparent crystals. The mother liquor was decanted, the crystals were washed with hexanes, dissolved in DCM, and filtered through a fine frit Buchner filter funnel, and dried *in vacuo* to afford the desired product **1.10y** as a white powder. The mother liquor was recrystallized by vapor diffusion again, and purified similarly to yield another crop of crystals. Other ADC gold(I) complexes were prepared analogously.



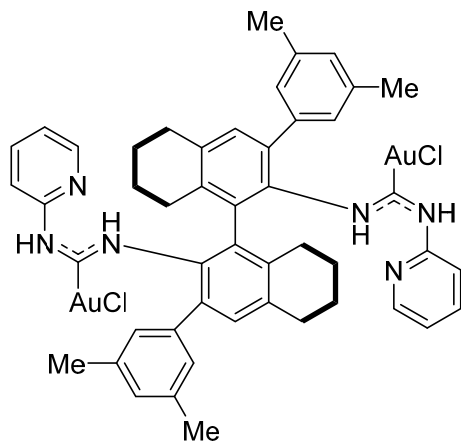
Complex 1.10a

0.0794 mmol scale, 73% yield (64.4 mg, 0.0576 mmol)

^1H NMR (500 MHz, CD_2Cl_2) δ 13.44 (s, 2H), 8.36 (s, 2H), 8.29 – 8.22 (m, 2H), 7.80 – 7.66 (m, 2H), 7.31 (d, $J = 7.5$ Hz, 4H), 7.24 (dt, $J = 14.5, 7.1$ Hz, 6H), 7.18 – 7.07 (m, 4H), 6.86 (d, $J = 8.3$ Hz, 2H), 2.83 (d, $J = 7.2$ Hz, 4H), 2.61 (dt, $J = 13.4, 6.5$ Hz, 2H), 2.52 – 2.27 (m, 2H), 2.01 (d, $J = 10.6$ Hz, 2H), 1.87 (td, $J = 14.8, 12.9, 6.6$ Hz, 6H).

^{13}C NMR (126 MHz, CD_2Cl_2) δ 195.24, 155.17, 145.88, 139.79, 139.31, 138.51, 138.31, 135.26, 134.99, 133.40, 132.65, 130.59, 128.69, 127.25, 120.12, 114.95, 30.10, 28.75, 23.87, 23.46.

HRMS (ESI⁺): calc'd for $[\text{C}_{44}\text{H}_{40}\text{N}_6\text{Au}_2\text{Cl}_2]\text{Na}$: 1139.1915, found: 1139.1934



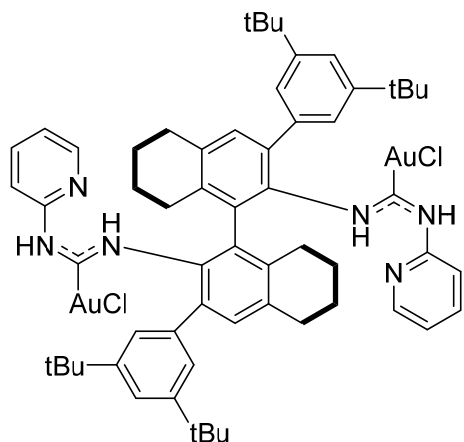
Complex 1.10b

0.287 mmol scale, 80% yield (269.5 mg, 0.230 mmol)

^1H NMR (400 MHz, CD_2Cl_2) δ 13.39 (s, 2H), 8.33 – 8.24 (m, 2H), 8.14 (s, 2H), 7.72 (ddd, $J = 8.3, 7.4, 1.9$ Hz, 2H), 7.15 (s, 2H), 7.12 (ddd, $J = 7.4, 5.1, 1.0$ Hz, 2H), 6.94 – 6.92 (m, 4H), 6.86 – 6.82 (m, 4H), 2.83 (t, $J = 6.0$ Hz, 4H), 2.72 – 2.52 (m, 2H), 2.37 (dt, $J = 16.1, 5.1$ Hz, 2H), 2.15 (s, 12H), 2.06 – 1.97 (m, 2H), 1.95 – 1.80 (m, 6H).

^{13}C NMR (126 MHz, CD_2Cl_2) δ 195.39, 155.07, 145.94, 139.43, 139.38, 138.55, 138.46, 138.13, 135.32, 134.74, 133.29, 132.29, 128.65, 128.56, 120.13, 114.64, 30.15, 28.75, 23.90, 23.49, 21.37.

HRMS (ESI⁺): calc'd for $[\text{C}_{48}\text{H}_{48}\text{N}_6\text{Au}_2\text{Cl}_2]\text{Na}$: 1195.2541, found: 1195.2546



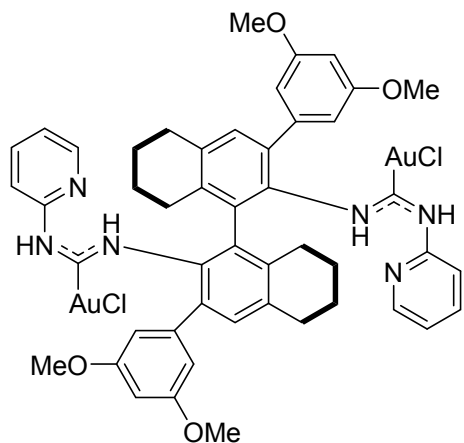
Complex 1.10c

0.156 mmol scale, 64% yield (133.6 mg, 0.0995 mmol)

^1H NMR (500 MHz, CD_2Cl_2) δ 13.44 (s, 2H), 8.27 (d, $J = 4.2$ Hz, 4H), 7.69 (t, $J = 7.9$ Hz, 2H), 7.24 (t, $J = 2.0$ Hz, 2H), 7.19 (s, 2H), 7.10 (d, $J = 1.9$ Hz, 6H), 6.79 (d, $J = 8.3$ Hz, 2H), 2.86 (t, $J = 5.8$ Hz, 4H), 2.66 (d, $J = 17.0$ Hz, 2H), 2.45 (dd, $J = 14.1, 9.0$ Hz, 2H), 2.05 (q, $J = 7.7$ Hz, 2H), 1.90 (dd, $J = 20.1, 12.5$ Hz, 6H), 1.13 (s, 36H).

^{13}C NMR (126 MHz, CD_2Cl_2) δ 195.54, 155.25, 150.99, 145.94, 139.63, 139.51, 138.69, 138.38, 135.35, 134.63, 133.52, 132.28, 125.25, 121.03, 120.12, 114.55, 35.14, 31.55, 30.24, 28.93, 23.98, 23.58.

HRMS (ESI⁺): calc'd for $[\text{C}_{60}\text{H}_{72}\text{N}_6\text{Au}_2\text{Cl}_2]\text{Na}$: 1363.4419, found: 1363.4442

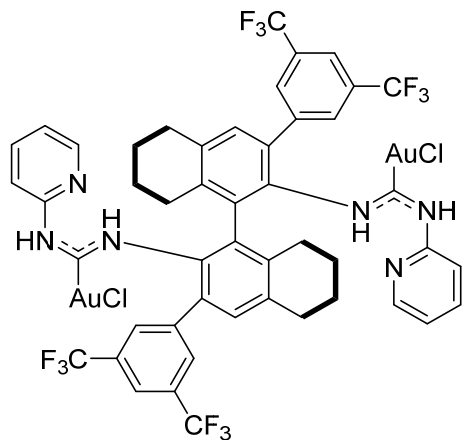


Complex 1.10d

^1H NMR (500 MHz, CD_2Cl_2) δ 13.39 (s, 2H), 8.42 (s, 2H), 8.24 (d, $J = 5.1$ Hz, 2H), 7.72 (t, $J = 7.9$ Hz, 2H), 7.16 (s, 2H), 7.15 – 7.01 (m, 2H), 6.88 (d, $J = 8.3$ Hz, 2H), 6.46 (d, $J = 2.5$ Hz, 4H), 6.30 (t, $J = 2.5$ Hz, 2H), 3.61 (s, 12H), 2.83 (s, 4H), 2.58 (d, $J = 17.1$ Hz, 2H), 2.38 (dd, $J = 13.9, 8.8$ Hz, 2H), 2.05 – 1.78 (m, 8H).

^{13}C NMR (126 MHz, CD_2Cl_2) δ 195.14, 160.96, 155.21, 145.82, 141.68, 139.41, 138.54, 138.45, 135.26, 135.13, 133.33, 132.32, 120.17, 114.96, 108.50, 100.32, 55.84, 30.12, 28.79, 23.86, 23.45.

HRMS (ESI⁺): calc'd for $[\text{C}_{48}\text{H}_{48}\text{O}_4\text{N}_6\text{Au}_2\text{Cl}_2]\text{Na}$: 1259.2338, found: 1259.2367



Complex 1.10e

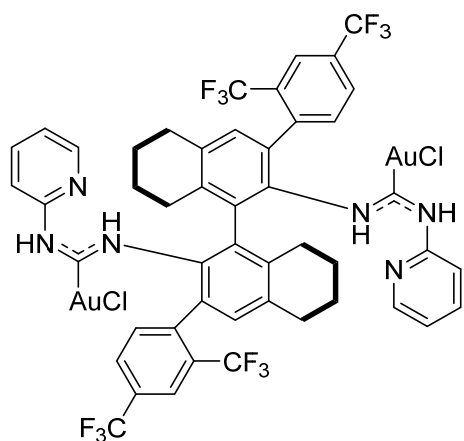
0.268 mmol scale, 77% yield (287.7 mg, 0.207 mmol)

^1H NMR (500 MHz, CD_2Cl_2) δ 13.57 (s, 2H), 8.78 (s, 2H), 8.25 (d, $J = 5.0$ Hz, 2H), 7.77 (s, 4H), 7.74 (d, $J = 10.0$ Hz, 4H), 7.25 (s, 2H), 7.19 – 7.08 (m, 2H), 6.90 (d, $J = 8.3$ Hz, 2H), 2.89 (t, $J = 5.9$ Hz, 4H), 2.70 – 2.57 (m, 2H), 2.43 (dt, $J = 17.2, 5.1$ Hz, 2H), 2.18 – 1.81 (m, 8H).

^{13}C NMR (126 MHz, CDCl_3) δ 195.16, 155.05, 144.82, 141.08, 138.94, 138.26, 135.83, 135.45, 134.95, 133.56, 131.76, 131.40 (q, $J = 33.1$ Hz), 130.63, 123.28 (q, $J = 273.4$ Hz), 120.60, 119.82, 115.07, 29.82, 28.58, 23.38, 23.00.

^{19}F NMR (376 MHz, CDCl_3) δ -63.54.

HRMS (ESI⁺): calc'd for $[\text{C}_{48}\text{H}_{36}\text{N}_6\text{Au}_2\text{Cl}_2\text{F}_{12}]\text{Na}$: 1411.1410, found: 1411.1391



Complex 1.10f

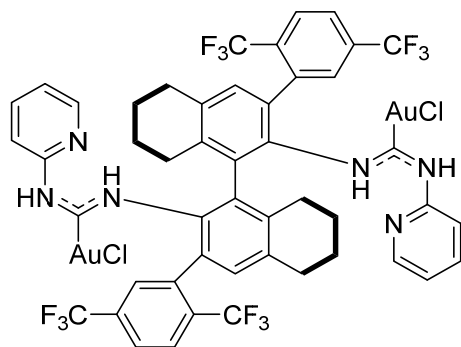
0.0996 mmol scale, 56% yield (77.0 mg, 0.0554 mmol)

^1H NMR (600 MHz, CD_2Cl_2) δ 13.50 (s, 2H), 8.40 (s, 2H), 8.19 (dd, $J = 5.2, 1.8$ Hz, 2H), 8.07 (d, $J = 8.5$ Hz, 2H), 7.81 (s, 2H), 7.80 (s, 2H), 7.71 – 7.67 (m, 2H), 7.14 – 7.06 (m, 2H), 7.00 (s, 2H), 6.87 (d, $J = 8.3$ Hz, 2H), 2.96 – 2.70 (m, 4H), 2.54 (dt, $J = 17.2, 6.5$ Hz, 2H), 2.25 (dt, $J = 17.1, 5.3$ Hz, 2H), 2.06 – 1.70 (m, 8H).

^{13}C NMR (126 MHz, CDCl_3) δ 194.26, 154.88, 145.65, 141.48, 139.21, 138.44, 137.49, 136.85, 135.17, 134.68, 134.09, 132.57, 130.50 (q, $J = 33.3$ Hz), 129.33 (q, $J = 30.2$ Hz), 128.66 – 128.21 (m), 124.02 (q, $J = 273.2$ Hz), 124.06 – 123.18 (m), 120.26, 114.78, 29.92, 28.18, 23.60, 23.21.

^{19}F NMR (376 MHz, CDCl_3) δ -59.63, -63.28.

HRMS (ESI+): calc'd for $[\text{C}_{48}\text{H}_{36}\text{N}_6\text{Au}_2\text{Cl}_2\text{F}_{12}]\text{Na}$: 1411.1410, found: 1411.1427



Complex 1.10g

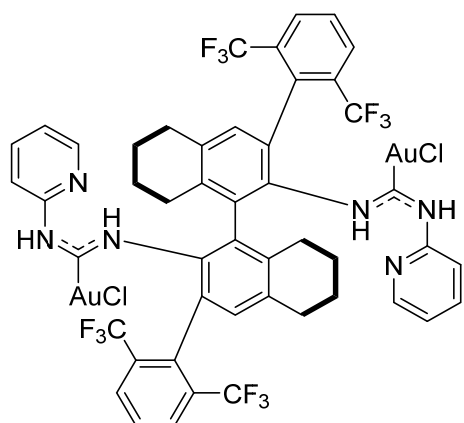
0.101 mmol scale, 65% yield (90.2 mg, 0.0649 mmol)

^1H NMR (500 MHz, CDCl_3) δ 13.50 (s, 2H), 8.69 (s, 2H), 8.31 – 8.09 (m, 4H), 7.86 – 7.45 (m, 6H), 7.08 (dd, $J = 7.4, 5.2$ Hz, 2H), 7.03 (s, 2H), 6.90 (d, $J = 8.3$ Hz, 2H), 2.81 (dh, $J = 23.0, 5.9$ Hz, 4H), 2.54 (dt, $J = 14.5, 7.0$ Hz, 2H), 2.25 (dt, $J = 17.4, 5.3$ Hz, 2H), 2.14 – 1.75 (m, 8H).

^{13}C NMR (126 MHz, CDCl_3) δ 194.64, 154.94, 145.62, 139.21, 138.68, 138.42, 137.47, 135.15, 134.71, 134.41, 133.29 (q, $J = 33.3$ Hz), 132.84 – 132.76 (m), 132.69, 131.71 (q, $J = 31.2, 30.8$ Hz), 127.10 (q, $J = 4.9$ Hz), 125.28 (q, $J = 3.8$ Hz), 124.14 (q, $J = 275.4$ Hz), 123.82 (q, $J = 274.3$ Hz), 120.22, 114.88, 29.95, 28.20, 23.64, 23.26.

^{19}F NMR (376 MHz, CDCl_3) δ -59.61, -63.25.

HRMS (ESI+): calc'd for $[\text{C}_{48}\text{H}_{36}\text{N}_6\text{Au}_2\text{Cl}_2\text{F}_{12}]\text{Na}$: 1411.1410, found: 1411.1432



Complex 1.10h

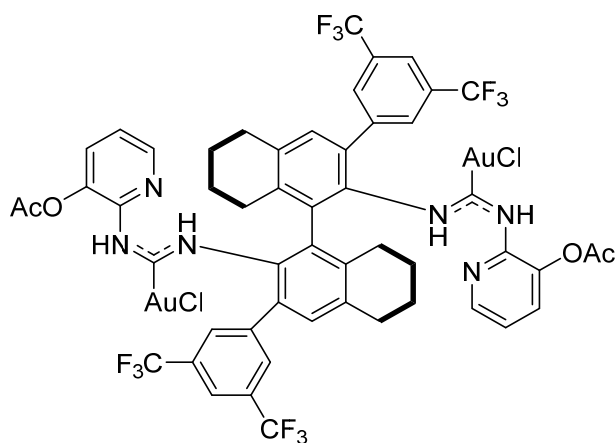
0.0977 mmol scale, 53% yield (71.7 mg, 0.0516 mmol)

^1H NMR (500 MHz, CDCl_3) δ 13.50 (s, 2H), 8.54 (s, 2H), 8.19 (d, $J = 4.3$ Hz, 2H), 8.08 (d, $J = 8.3$ Hz, 2H), 7.80 (s, 4H), 7.68 (t, $J = 8.2$ Hz, 2H), 7.09 (dd, $J = 7.6, 4.9$ Hz, 2H), 7.00 (s, 2H), 6.88 (d, $J = 8.3$ Hz, 2H), 2.79 (tdd, $J = 17.4, 14.4, 12.0, 7.8$ Hz, 4H), 2.54 (dt, $J = 14.4, 6.8$ Hz, 2H), 2.25 (dt, $J = 17.4, 5.2$ Hz, 2H), 2.06 – 1.73 (m, 8H).

^{13}C NMR (126 MHz, CDCl_3) δ 194.53, 154.82, 145.71, 141.45, 139.30, 138.52, 137.54, 136.86, 135.18, 134.72, 134.07, 132.58, 130.56 (q, $J = 33.4$ Hz), 129.38 (q, $J = 30.3$ Hz), 128.62 – 128.31 (m), 124.05 (q, $J = 274.3$ Hz), 123.79 – 123.18 (m), 120.33, 114.75, 29.94, 28.21, 23.61, 23.22.

^{19}F NMR (376 MHz, CDCl_3) δ -59.63, -63.28.

HRMS (ESI+): calc'd for $[\text{C}_{48}\text{H}_{36}\text{N}_6\text{Au}_2\text{Cl}_2\text{F}_{12}]\text{Na}$: 1411.1410, found: 1411.1429



Complex 1.10i

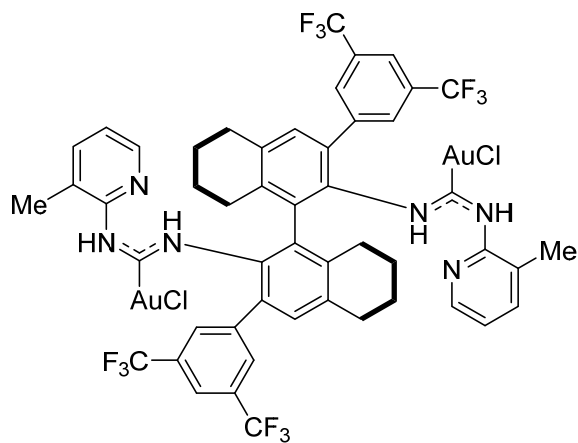
0.118 mmol scale, 35% yield (62.8 mg, 0.0417 mmol)

^1H NMR (500 MHz, CD_2Cl_2) δ 13.60 (s, 2H), 8.44 (s, 2H), 8.11 (d, $J = 4.9$ Hz, 2H), 7.81 (s, 4H), 7.73 (d, $J = 9.0$ Hz, 4H), 7.31 (s, 2H), 7.22 (dd, $J = 8.4, 4.7$ Hz, 2H), 3.02 – 2.74 (m, 4H), 2.62 (t, $J = 12.6$ Hz, 2H), 2.52 – 2.41 (m, 2H), 2.33 (s, 6H), 2.12 – 1.80 (m, 8H).

^{13}C NMR (126 MHz, CD_2Cl_2) δ 196.98, 168.10, 146.86, 142.02, 141.64, 139.79, 136.81, 133.17, 132.56, 132.34, 131.70 (q, $J = 33.5$ Hz), 131.12, 123.78 (q, $J = 273.0$ Hz), 121.23 – 120.85 (m), 120.53, 30.21, 29.11, 23.66, 23.27, 21.93.

^{19}F NMR (376 MHz, CDCl_3) δ -63.54.

HRMS (ESI+): calc'd for $[\text{C}_{52}\text{H}_{40}\text{O}_4\text{N}_6\text{Au}_2\text{Cl}_2\text{F}_{12}]\text{Na}$: 1527.1520, found: 1527.1533



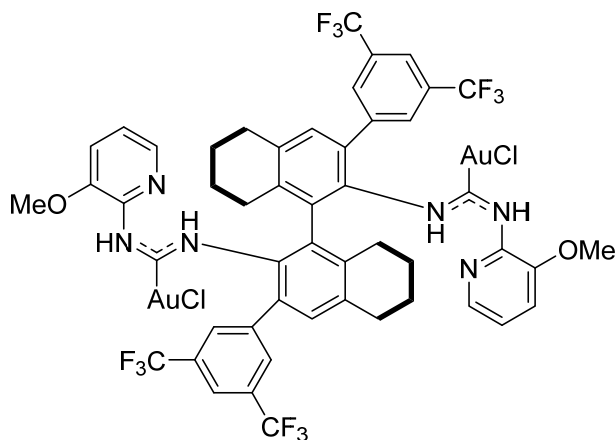
Complex 1.10j

^1H NMR (400 MHz, CD_2Cl_2) δ 14.15 (s, 2H), 8.12 (dd, $J = 5.2, 1.8$ Hz, 2H), 7.94 (s, 2H), 7.79 (d, $J = 1.6$ Hz, 4H), 7.73 (s, 2H), 7.58 (d, $J = 7.4$ Hz, 2H), 7.30 (s, 2H), 7.10 (dd, $J = 7.5, 5.0$ Hz, 2H), 2.91 (d, $J = 5.6$ Hz, 4H), 2.67 (dt, $J = 13.8, 6.5$ Hz, 2H), 2.47 (dt, $J = 17.1, 5.0$ Hz, 2H), 2.35 – 2.21 (m, 6H), 2.15 – 1.81 (m, 8H).

^{13}C NMR (126 MHz, CDCl_3) δ 196.78, 153.65, 143.15, 141.79, 140.75, 139.39, 136.87, 135.35, 135.25, 133.49, 132.33, 131.66 (q, $J = 33.2$ Hz), 131.08, 123.81 (q, $J = 272.8$ Hz), 120.98 (q, $J = 4.3$ Hz), 30.18, 29.00, 23.70, 23.30, 17.15.

^{19}F NMR (376 MHz, CDCl_3) δ -63.62.

HRMS (ESI+): calc'd for $[\text{C}_{50}\text{H}_{40}\text{N}_6\text{Au}_2\text{Cl}_2\text{F}_{12}]\text{Na}$: 1439.1723, found: 1439.1726



Complex 1.10k

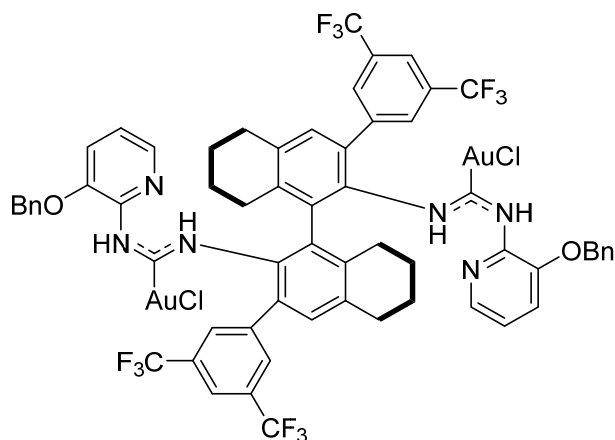
0.153 mmol scale, 51% yield (112.6 mg, 0.0777 mmol)

^1H NMR (5:1 rotamer ratio, asterisks denote minor rotamer peaks, 500 MHz, CD_2Cl_2) δ 13.93* (s, 0H), 13.72 (s, 2H), 8.58 (s, 2H), 7.83* (s, 0H), 7.82* (s, 0H), 7.78* (d, $J = 1.4$ Hz, 0H), 7.77 (t, $J = 1.3$ Hz, 4H), 7.73 (s, 2H), 7.71 – 7.68* (m, 0H), 7.29 (s, 2H), 7.26* (dd, $J = 8.3, 1.3$ Hz, 0H), 7.23* (s, 0H), 7.21 (dd, $J = 8.3, 1.4$ Hz, 2H), 7.13 (dd, $J = 8.2, 5.1$ Hz, 2H), 7.11 – 7.07* (m, 0H), 3.87* (s, 0H), 3.83 (s, 6H), 3.10* (d, $J = 17.3$ Hz, 0H), 3.00 – 2.86 (m, 4H), 2.79* (d, $J = 17.1$ Hz, 0H), 2.64 (dt, $J = 17.4, 6.4$ Hz, 2H), 2.43 (dt, $J = 17.5, 5.8$ Hz, 2H), 2.16 – 1.69* (m, 8H, indistinguishable overlap of major and minor peaks).

^{13}C NMR (asterisks denote minor rotamer peaks, 151 MHz, CD_2Cl_2) δ 196.19, 194.94*, 145.76, 145.53*, 144.84, 144.60*, 142.07, 141.88*, 140.60*, 139.29, 139.07*, 136.96, 136.30, 135.77*, 135.21 (d, $J = 4.3$ Hz), 134.76*, 133.78, 132.51, 132.39*, 131.76 (q, $J = 33.2$ Hz), 131.48 – 130.80 (m), 124.85*, 127.01 – 121.13 (m), 121.62*, 120.98 (dd, $J = 7.8, 3.9$ Hz), 120.82, 118.96, 56.75, 30.25, 29.52*, 28.94, 23.78, 23.40, 23.24*, 22.97*.

^{19}F NMR (asterisks denote minor rotamer peaks, 376 MHz, CDCl_3) δ -63.32, -63.52*.

HRMS (ESI+): calc'd for $[\text{C}_{50}\text{H}_{40}\text{O}_2\text{N}_6\text{Au}_2\text{Cl}_2\text{F}_{12}]\text{Na}$: 1471.1622, found: 1471.1649



Complex 1.101

0.093 mmol scale, 46% yield (68.6 mg, 0.0428 mmol)

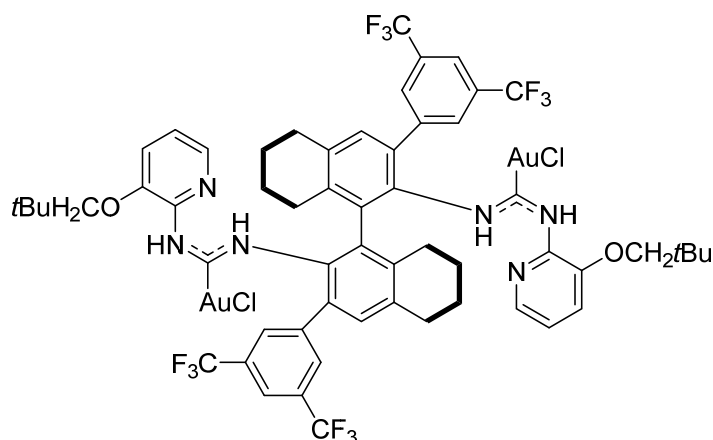
^1H NMR (7:1 rotamer ratio, asterisks denote minor rotamer peaks, 500 MHz, CDCl_3) δ 14.02* (s, 0H), 13.81 (s, 2H), 8.61 (d, $J = 6.0$ Hz, 2H), 8.56* (s, 0H), 7.83* (s, 0H), 7.79 (d, $J = 5.2$ Hz, 6H), 7.74 (s, 2H), 7.44 (d, $J = 7.1$ Hz, 4H), 7.39 – 7.34 (m, 4H), 7.33* (d, $J = 7.3$ Hz, 0H), 7.30 (d, $J = 3.3$ Hz, 2H), 7.21 (d, $J = 8.1$ Hz, 2H), 7.07 (dd, $J = 8.3, 4.7$ Hz, 2H), 5.22 – 5.06 (m, 4H), 3.08* (d, $J = 17.1$ Hz, 0H), 2.94 (t, $J = 7.7$ Hz, 4H), 2.79* (d, $J = 16.6$ Hz, 0H), 2.65 (dd, $J = 15.5, 7.1$ Hz, 2H), 2.45 (dt, $J = 17.6, 5.8$ Hz, 2H), 2.13 – 1.68* (m, 8H, indistinguishable overlap of major and minor peaks).

^{13}C NMR (asterisks denote minor rotamer peaks, 151 MHz, CD_2Cl_2) δ 196.40, 145.93, 143.83, 143.59*, 142.08, 141.89*, 139.33, 136.94, 136.51, 135.78, 135.33, 135.25, 133.81, 132.52, 131.77

(q, $J = 33.0$ Hz), 131.20, 129.28, 129.00, 128.42, 123.92 (q, $J = 272.6$ Hz), 121.50*, 121.05, 120.70, 120.26, 78.13*, 71.90, 30.26, 29.50*, 28.97, 23.79, 23.41, 23.23*, 22.97*.

^{19}F NMR (asterisks denote minor rotamer peaks, 376 MHz, CDCl_3) δ -63.35, -63.49*.

HRMS (ESI+): calc'd for $[\text{C}_{62}\text{H}_{48}\text{O}_2\text{N}_6\text{Au}_2\text{Cl}_2\text{F}_{12}]\text{Na}$: 1623.2248, found: 1623.2308



Complex 1.10m

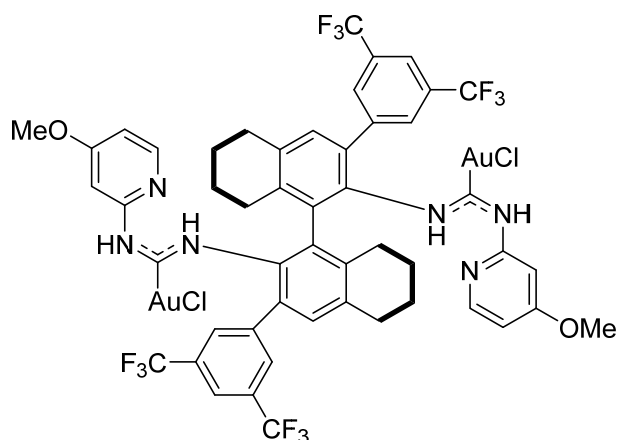
0.346 mmol scale, 43% yield (231.4 mg, 0.148 mmol)

^1H NMR (7:1 rotamer ratio, asterisks denote minor rotamer peaks, 600 MHz, CD_2Cl_2) δ 14.06* (s, 0H), 13.90 (s, 2H), 8.46 (s, 2H), 8.36* (s, 0H), 7.86* (s, 0H), 7.82* (s, 0H), 7.81 (d, $J = 5.1$ Hz, 2H), 7.79 (s, 4H), 7.73 (s, 2H), 7.69* (d, $J = 5.1$ Hz, 0H), 7.30 (s, 2H), 7.27 (s, 0H), 7.24 (d, $J = 8.0$ Hz, 2H), 7.13 (dd, $J = 8.3, 5.0$ Hz, 2H), 7.08* (dd, $J = 8.3, 5.0$ Hz, 0H), 3.73 (d, $J = 8.4$ Hz, 2H), 3.69* (d, $J = 8.9$ Hz, 0H), 3.62 (d, $J = 8.5$ Hz, 2H), 3.17 – 3.02* (m, 0H), 3.06 – 2.84 (m, 4H), 2.78* (dt, $J = 13.9, 6.1$ Hz, 0H), 2.75 – 2.61 (m, 2H), 2.46 (dt, $J = 17.3, 5.3$ Hz, 2H), 2.39* (d, $J = 17.9$ Hz, 0H), 2.10 – 1.70* (m, 8H, indistinguishable overlap of major and minor peaks), 1.02* (s, 0H), 1.01 (s, 18H).

^{13}C NMR (asterisks denote minor rotamer peaks, 151 MHz, CD_2Cl_2) δ 196.62, 195.10*, 155.55*, 145.90, 145.56*, 144.47, 144.36*, 142.00, 141.87*, 140.64*, 139.37, 139.11*, 137.72*, 136.95, 136.22*, 136.10, 135.73*, 135.40, 135.31, 134.67*, 133.61, 132.54, 132.47*, 131.75 (q, $J = 33.0$ Hz), 131.24 – 131.13* (m), 131.10 – 130.92 (m), 123.91 (q, $J = 272.9$ Hz), 121.70*, 121.16 – 120.93 (m), 120.85, 120.31*, 119.82, 80.07*, 79.84, 32.43*, 32.35, 30.31*, 30.25, 29.49*, 29.01, 27.00, 26.88*, 23.77, 23.36, 23.23*, 22.95*.

^{19}F NMR (asterisks denote minor rotamer peaks, 376 MHz, CDCl_3) δ -63.13*, -63.51.

HRMS (ESI+): calc'd for $[\text{C}_{58}\text{H}_{56}\text{O}_2\text{N}_6\text{Au}_2\text{Cl}_2\text{F}_{12}]\text{Na}$: 1583.2874, found: 1583.2883



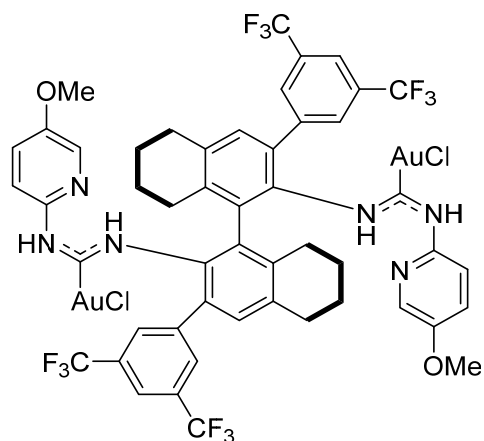
Complex 1.10n

^1H NMR (500 MHz, CDCl_3) δ 13.75 (s, 2H), 8.92 (s, 2H), 8.03 (d, $J = 6.0$ Hz, 2H), 7.76 (s, 4H), 7.73 (s, 2H), 7.23 (s, 2H), 6.67 (dd, $J = 5.9, 2.4$ Hz, 2H), 6.45 (d, $J = 2.5$ Hz, 2H), 3.79 (s, 6H), 2.88 (t, $J = 6.0$ Hz, 4H), 2.60 (dt, $J = 16.8, 6.6$ Hz, 2H), 2.39 (dt, $J = 16.7, 5.2$ Hz, 2H), 2.15 – 1.76 (m, 8H).

^{13}C NMR (126 MHz, CDCl_3) δ 195.44, 167.89, 156.98, 146.66, 141.85, 138.90, 136.66, 135.37, 133.71, 132.19, 131.57 (q, $J = 33.1$ Hz), 131.16 – 130.98 (m), 123.87 (q, $J = 272.8$ Hz), 121.25 – 120.80 (m), 108.74, 98.98, 56.13, 30.13, 28.86, 23.72, 23.35.

^{19}F NMR (376 MHz, CDCl_3) δ -63.49.

HRMS (ESI+): calc'd for $[\text{C}_{50}\text{H}_{40}\text{O}_2\text{N}_6\text{Au}_2\text{Cl}_2\text{F}_{12}]\text{Na}$: 1471.1622, found: 1471.1630



Complex 1.10o

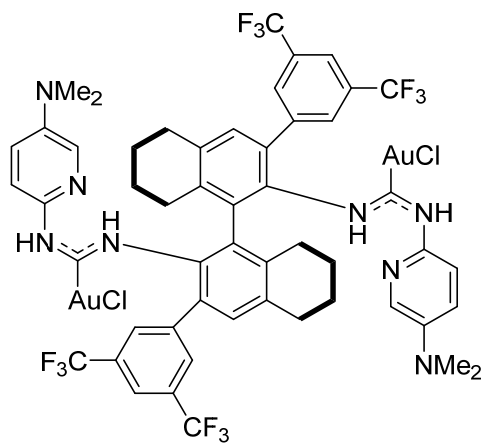
0.447 mmol scale, 73% yield (473.2 mg, 0.326 mmol)

^1H NMR (500 MHz, CD_2Cl_2) δ 13.22 (s, 2H), 9.17 – 8.40 (m, 2H), 7.89 (d, $J = 3.0$ Hz, 2H), 7.80 – 7.76 (m, 4H), 7.73 (s, 2H), 7.31 (dd, $J = 9.0, 2.9$ Hz, 2H), 7.25 (s, 2H), 6.90 (d, $J = 9.0$ Hz, 2H), 3.88 (d, $J = 1.6$ Hz, 6H), 2.90 (t, $J = 6.0$ Hz, 4H), 2.61 (dt, $J = 16.2, 6.1$ Hz, 2H), 2.43 (dt, $J = 16.8, 5.4$ Hz, 2H), 2.23 – 1.76 (m, 8H).

^{13}C NMR (126 MHz, CD_3CN) δ 194.09, 153.91, 149.39, 142.60, 139.56, 137.73, 136.10, 135.63, 134.35, 132.39, 131.82 – 131.75 (m), 131.72 (q, $J = 33.2$ Hz), 126.54, 124.37 (q, $J = 272.3$ Hz), 121.20 (dd, $J = 7.4, 4.0$ Hz), 118.31, 56.84, 30.23, 28.91, 23.89, 23.54.

^{19}F NMR (376 MHz, CDCl_3) δ -63.49.

HRMS (ESI+): calc'd for $[\text{C}_{50}\text{H}_{40}\text{O}_2\text{N}_6\text{Au}_2\text{Cl}_2\text{F}_{12}]\text{Na}$: 1471.1622, found: 1471.1639



Complex 1.10p

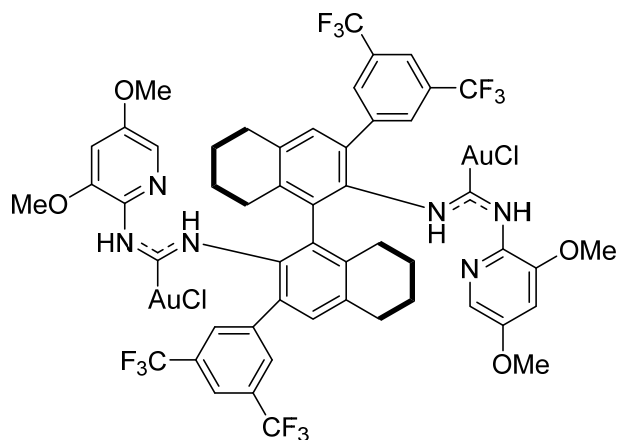
0.101 mmol scale, 31% yield (46.4 mg, 0.0314 mmol)

^1H NMR (500 MHz, CD_2Cl_2) δ 13.38 (s, 2H), 8.27 (s, 2H), 7.81 (s, 4H), 7.73 (s, 2H), 7.70 – 7.61 (m, 2H), 7.23 (s, 2H), 7.12 (dt, $J = 8.6, 2.1$ Hz, 2H), 6.76 (d, $J = 8.8$ Hz, 2H), 3.09 – 2.97 (m, 12H), 2.90 (t, $J = 6.3$ Hz, 4H), 2.74 – 2.52 (m, 2H), 2.43 (dt, $J = 17.2, 5.5$ Hz, 2H), 2.10 – 1.82 (m, 8H).

^{13}C NMR (126 MHz, CD_2Cl_2) δ 193.07, 145.56, 144.22, 142.11, 138.66, 136.70, 135.58, 135.35, 133.83, 132.17, 131.52 (q, $J = 33.2$ Hz), 131.19 – 130.98 (m), 128.63, 123.90 (q, $J = 272.8$ Hz), 123.26, 121.00 – 120.75 (m), 114.97, 40.61, 30.11, 28.90, 23.78, 23.36.

^{19}F NMR (376 MHz, CDCl_3) δ -63.37.

HRMS (ESI+): calc'd for $[\text{C}_{52}\text{H}_{46}\text{N}_8\text{Au}_2\text{Cl}_2\text{F}_{12}]\text{Na}$: 1497.2254, found: 1497.2255



Complex 1.10q

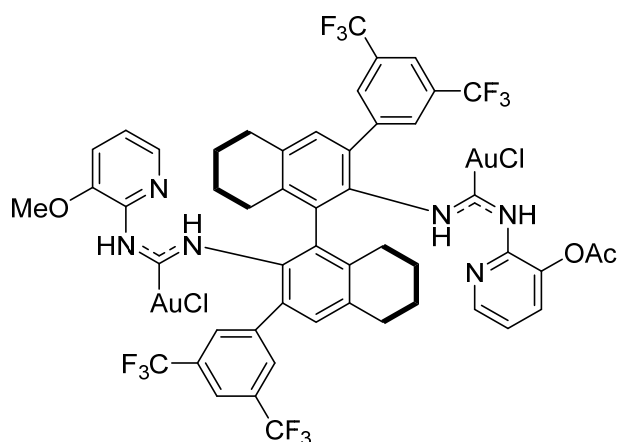
0.252 mmol scale, 46% yield (173.0 mg, 0.115 mmol)

^1H NMR (9:1 rotamer ratio, asterisks denote minor rotamer peaks, 600 MHz, CD_2Cl_2) δ 13.45* (s, 0H), 13.41 (s, 2H), 8.42 (s, 2H), 7.88* (s, 0H), 7.82* (s, 0H), 7.78 (s, 4H), 7.73 (s, 2H), 7.41 (t, $J = 1.9$ Hz, 2H), 7.29 (s, 2H), 7.27* (d, $J = 9.2$ Hz, 0H), 6.87* (s, 0H), 6.85 – 6.76 (m, 2H), 3.89 (d, $J = 1.6$ Hz, 6H), 3.86* (s, 0H), 3.82 (d, $J = 1.4$ Hz, 6H), 3.67* (s, 0H), 3.09* (d, $J = 17.4$ Hz, 0H), 2.96 (p, $J = 9.6, 8.2$ Hz, 4H), 2.76* (d, $J = 17.8$ Hz, 0H), 2.63 (dt, $J = 17.0, 6.6$ Hz, 2H), 2.43 (dt, $J = 17.2, 5.6$ Hz, 2H), 2.15 – 1.69* (m, 8H, indistinguishable overlap of major and minor peaks).

^{13}C NMR (151 MHz, CD_2Cl_2) δ 194.58, 154.42, 145.77, 142.18, 139.87, 138.99, 136.85, 135.24, 133.89, 132.49, 131.71 (q, $J = 33.3$ Hz), 123.93 (q, $J = 272.8$ Hz), 121.01 – 120.84 (m), 120.77, 107.70, 56.85, 56.79, 30.27, 28.90, 23.84, 23.45.

^{19}F NMR (376 MHz, CDCl_3) δ -63.45.

HRMS (ESI+): calc'd for $[\text{C}_{52}\text{H}_{44}\text{O}_4\text{N}_6\text{Au}_2\text{Cl}_2\text{F}_{12}]\text{Na}$: 1531.1833, found: 1531.1846



Complex 1.10r

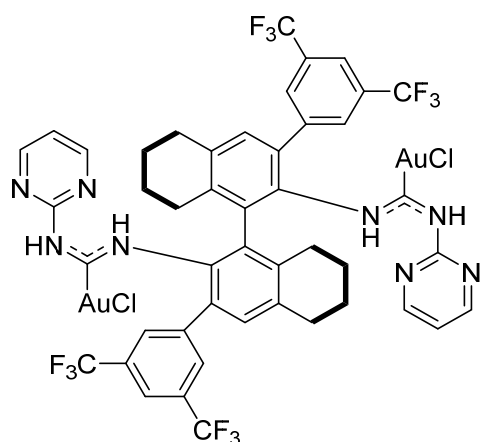
0.0412 mmol scale, 57% yield (34.7 mg, 0.0235 mmol)

^1H NMR (500 MHz, CDCl_3) δ 13.68 (s, 1H), 13.59 (s, 1H), 8.61 (s, 1H), 8.46 (s, 1H), 8.10 (d, $J = 5.0$ Hz, 1H), 7.83 (d, $J = 5.2$ Hz, 1H), 7.79 (d, $J = 7.5$ Hz, 4H), 7.75 – 7.71 (m, 4H), 7.30 (d, $J = 11.6$ Hz, 2H), 7.26 – 7.19 (m, 2H), 7.14 (dd, $J = 8.2, 5.1$ Hz, 1H), 3.83 (s, 3H), 2.92 (dq, $J = 13.5, 6.0$ Hz, 4H), 2.76 – 2.57 (m, 2H), 2.46 (dq, $J = 16.6, 5.5$ Hz, 2H), 2.33 (s, 3H), 2.14 – 1.76 (m, 8H).

^{13}C NMR (126 MHz, CDCl_3) δ 197.07, 196.08, 168.13, 146.87, 145.67, 144.67, 141.95, 141.88, 141.67, 139.63, 139.42, 136.97, 136.68, 136.38, 135.44, 135.43, 135.38, 135.16, 135.11, 133.43, 133.35, 132.65, 132.27, 132.20, 131.66 (q, $J = 33.3$ Hz), 131.22 – 130.84 (m), 123.79 (q, $J = 272.8$ Hz), 121.22 – 120.91 (m), 120.87, 120.43, 118.94, 56.74, 30.20, 30.17, 29.07, 28.98, 23.69, 23.67, 23.30, 21.96.

^{19}F NMR (376 MHz, CDCl_3) δ -63.54.

HRMS (ESI+): calc'd for $[\text{C}_{51}\text{H}_{40}\text{O}_3\text{N}_6\text{Au}_2\text{Cl}_2\text{F}_{12}]\text{Na}$: 1499.1571, found: 1499.1585



Complex 1.10s

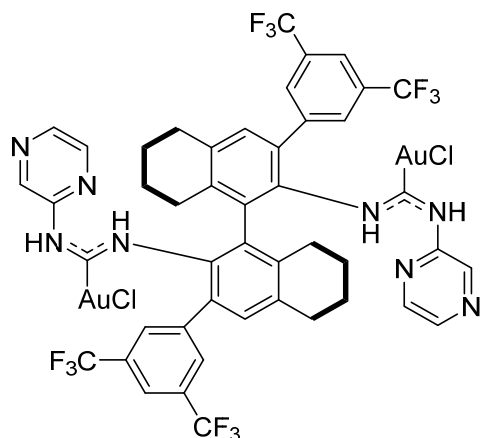
0.100 mmol scale, 39% yield (53.9 mg, 0.0387 mmol)

^1H NMR (500 MHz, CD_2Cl_2) δ 12.95 (s, 2H), 9.07 (s, 2H), 8.63 (s, 4H), 7.77 (s, 4H), 7.74 (s, 2H), 7.31 (s, 2H), 7.19 (t, $J = 5.1$ Hz, 2H), 2.92 (t, $J = 6.1$ Hz, 4H), 2.60 (dt, $J = 16.9, 6.3$ Hz, 2H), 2.44 (dt, $J = 16.9, 5.3$ Hz, 2H), 2.16 – 1.81 (m, 8H).

^{13}C NMR (126 MHz, CD_2Cl_2) δ 197.59, 159.04, 141.49, 139.73, 136.73, 135.47, 134.88, 133.34, 132.66, 131.75 (q, $J = 33.2$ Hz), 131.23 – 130.71 (m), 123.73 (q, $J = 272.8$ Hz), 121.27 – 121.03 (m), 118.13, 30.17, 29.04, 23.65, 23.34.

^{19}F NMR (376 MHz, CDCl_3) δ -63.53.

HRMS (ESI+): calc'd for $[\text{C}_{46}\text{H}_{34}\text{N}_8\text{Au}_2\text{Cl}_2\text{F}_{12}]\text{Na}$: 1413.1315, found: 1413.1350



Complex 1.10t

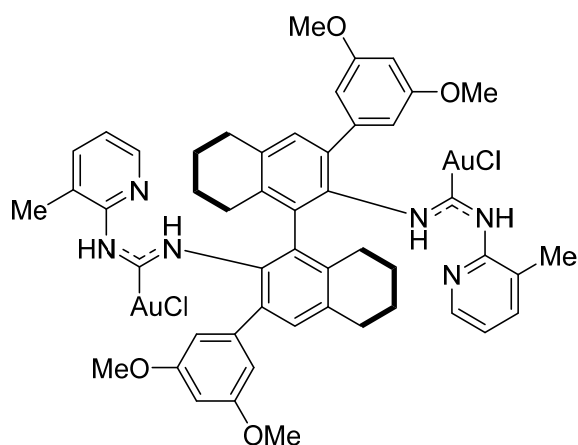
0.0953 mmol scale, 38% yield (51.0 mg, 0.0366 mmol)

^1H NMR (500 MHz, CD_2Cl_2) δ 12.74 (s, 2H), 10.19 (s, 2H), 8.44 (s, 2H), 8.36 (d, $J = 2.9$ Hz, 2H), 8.15 – 8.01 (m, 2H), 7.72 (s, 2H), 7.65 (s, 4H), 7.26 (s, 2H), 2.94 (q, $J = 6.2$ Hz, 4H), 2.61 – 2.47 (m, 2H), 2.48 – 2.28 (m, 2H), 2.07 – 1.80 (m, 8H).

^{13}C NMR (126 MHz, CD_2Cl_2) δ 195.72, 151.11, 141.43, 140.20, 139.11, 138.95, 138.74, 136.54, 135.11, 134.61, 133.55, 132.50, 131.67 (q, $J = 33.5$ Hz), 131.07, 123.79 (q, $J = 272.5$ Hz), 121.39 – 120.83 (m), 30.11, 28.78, 23.73, 23.44.

^{19}F NMR (376 MHz, CDCl_3) δ -56.55.

HRMS (ESI+): calc'd for $[\text{C}_{46}\text{H}_{34}\text{N}_8\text{Au}_2\text{Cl}_2\text{F}_{12}]\text{Na}$: 1413.1315, found: 1413.1339



Complex 1.10u

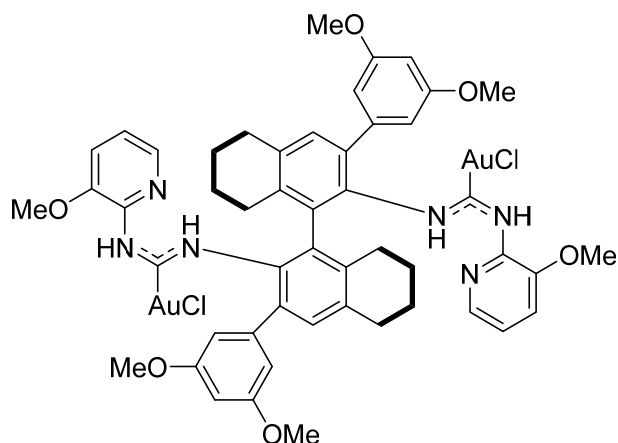
0.199 mmol scale, 13% yield (32.9 mg, 0.0260 mmol)

^1H NMR (500 MHz, CD_2Cl_2) δ 13.94 (s, 2H), 8.24 – 8.04 (m, 2H), 7.92 (s, 2H), 7.54 (d, $J = 7.5$ Hz, 2H), 7.19 (s, 2H), 7.04 (dd, $J = 7.5, 5.1$ Hz, 2H), 6.46 (d, $J = 2.3$ Hz, 4H), 6.29 (t, $J = 2.3$ Hz,

2H), 3.58 (s, 12H), 2.86 (d, $J = 6.5$ Hz, 4H), 2.62 (dt, $J = 14.3, 6.8$ Hz, 2H), 2.40 (dt, $J = 16.4, 5.6$ Hz, 2H), 2.32 (s, 6H), 2.11 – 1.78 (m, 8H).

^{13}C NMR (151 MHz, CD_2Cl_2) δ 196.04, 161.04, 153.95, 143.20, 141.80, 140.59, 138.60, 138.57, 135.32, 135.23, 133.44, 132.44, 123.07, 120.25, 108.51, 100.64, 55.84, 30.24, 28.87, 23.94, 23.49, 17.33.

HRMS (ESI+): calc'd for $[\text{C}_{50}\text{H}_{52}\text{O}_4\text{N}_6\text{Au}_2\text{Cl}_2\text{F}_{12}]\text{Na}$: 1287.2651, found: 1287.2666



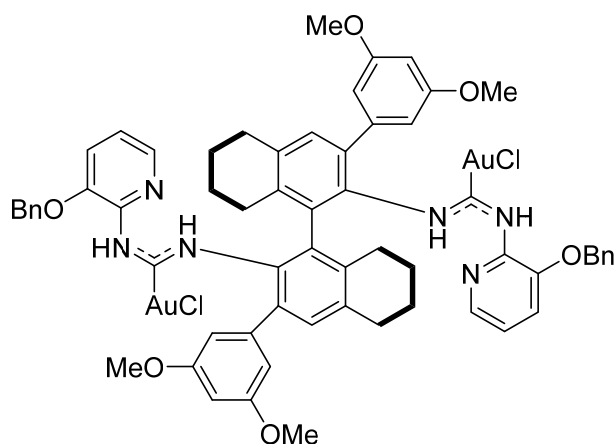
Complex 1.10v

0.179 mmol scale, 79% yield (183.5 mg, 0.141 mmol)

^1H NMR (4:1 rotamer ratio, asterisks denote minor rotamer peaks, 600 MHz, CD_2Cl_2) δ 13.66* (s, 0H), 13.56 (s, 2H), 8.54 (s, 2H), 8.51* (s, 0H), 7.73 (d, $J = 5.1$ Hz, 2H), 7.60* (d, $J = 5.4$ Hz, 0H), 7.32* (s, 0H), 7.20 (s, 2H), 7.16 (d, $J = 8.1$ Hz, 2H), 7.13* (s, 0H), 7.06 (dd, $J = 8.3, 5.1$ Hz, 2H), 7.03 – 6.96* (m, 0H), 6.47* (s, 0H), 6.45 (t, $J = 1.8$ Hz, 4H), 6.36* (d, $J = 2.2$ Hz, 0H), 6.29 (q, $J = 2.0$ Hz, 2H), 3.87* (s, 0H), 3.84 (s, 6H), 3.75* (s, 0H), 3.61 (s, 12H), 3.11 – 3.01* (m, 0H), 2.97 – 2.81 (m, 4H), 2.71* (dd, $J = 15.8, 8.0$ Hz, 0H), 2.58 (dt, $J = 17.1, 6.6$ Hz, 2H), 2.36 (dt, $J = 16.9, 6.0$ Hz, 2H), 2.16 – 1.66* (m, 8H, indistinguishable overlap of major and minor peaks).

^{13}C NMR (asterisks denote minor rotamer peaks, 126 MHz, CDCl_3) δ 195.07, 161.02*, 160.92, 145.87, 145.37*, 144.65, 144.14*, 141.87, 141.46*, 139.39*, 138.27, 138.14, 137.44*, 137.19*, 136.96*, 136.14, 135.14, 134.93, 133.57, 132.43, 132.26*, 120.81*, 120.27, 118.57*, 118.45, 108.87*, 108.54, 100.17, 99.75*, 56.54, 56.02*, 55.78, 30.19, 29.28*, 28.69, 23.89, 23.50, 23.38*, 23.10*.

HRMS (ESI+): calc'd for $[\text{C}_{50}\text{H}_{52}\text{O}_6\text{N}_6\text{Au}_2\text{Cl}_2\text{F}_{12}]\text{Na}$: 1319.2549, found: 1319.2584



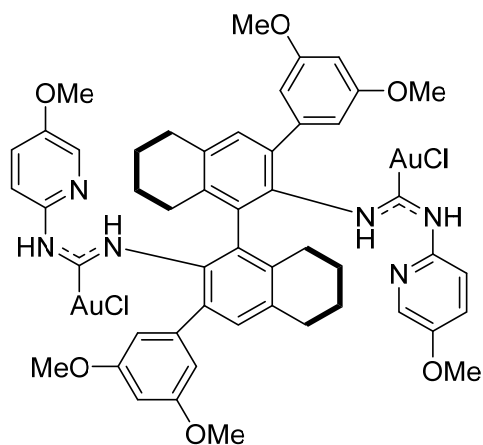
Complex 1.10w

0.176 mmol scale, 50% yield (128.5 mg, 0.0886 mmol)

^1H NMR (5:1 rotamer ratio, asterisks denote minor rotamer peaks, 500 MHz, CD_2Cl_2) δ 13.76* (s, 0H), 13.65 (s, 2H), 8.61 (s, 2H), 8.50* (s, 0H), 7.76 (dd, $J = 5.1, 1.4$ Hz, 2H), 7.62* (dd, $J = 5.2, 1.4$ Hz, 0H), 7.50 – 7.44 (m, 4H), 7.40 – 7.36 (m, 6H), 7.35 – 7.32 (m, 2H), 7.32 – 7.30* (m, 0H), 7.25* (dd, $J = 8.5, 1.4$ Hz, 0H), 7.22 (s, 2H), 7.18 (dd, $J = 8.2, 1.4$ Hz, 2H), 7.14* (s, 0H), 6.47 (d, $J = 2.2$ Hz, 4H), 6.37* (t, $J = 2.3$ Hz, 0H), 6.31 (t, $J = 2.3$ Hz, 2H), 5.12 (q, $J = 12.0$ Hz, 4H), 3.74 (s, 2H), 3.60 (s, 12H), 3.06* (dt, $J = 17.2, 5.7$ Hz, 0H), 2.91 (q, $J = 7.0, 6.5$ Hz, 4H), 2.76 – 2.67* (m, 0H), 2.61 (dt, $J = 17.6, 6.5$ Hz, 2H), 2.39 (dt, $J = 17.1, 5.6$ Hz, 2H), 2.10 – 1.68* (m, 8H, indistinguishable overlap of major and minor peaks).

^{13}C NMR (asterisks denote minor rotamer peaks, 126 MHz, CDCl_3) δ 195.31, 193.83*, 161.03*, 160.92, 146.05, 145.52*, 143.66, 143.15*, 141.89, 141.48*, 139.38*, 138.31, 137.42*, 137.17*, 137.14*, 136.39, 135.79, 135.28*, 135.12, 135.03, 133.56, 132.52*, 132.43, 132.31*, 129.40*, 129.38*, 129.20, 128.89, 128.44*, 128.40, 120.74*, 120.16, 120.07*, 119.86, 108.88*, 108.48, 100.30, 99.75*, 71.75, 56.00*, 55.78, 30.19, 29.26*, 28.73, 23.89, 23.49, 23.36*, 23.10*.

HRMS (ESI+): calc'd for $[\text{C}_{62}\text{H}_{60}\text{O}_6\text{N}_6\text{Au}_2\text{Cl}_2\text{F}_{12}]\text{Na}$: 1471.3175, found: 1471.3206



Complex 1.10x

0.187 mmol scale, 66% yield (161.2 mg, 0.124 mmol)

^1H NMR (400 MHz, CD_2Cl_2) δ 13.04 (s, 2H), 8.19 (s, 2H), 7.89 (d, $J = 3.0$ Hz, 2H), 7.30 (dd, $J = 9.0, 3.0$ Hz, 2H), 7.15 (s, 2H), 6.86 (d, $J = 9.0$ Hz, 2H), 6.47 (d, $J = 2.3$ Hz, 4H), 6.31 (t, $J = 2.3$ Hz, 2H), 3.86 (s, 6H), 3.63 (s, 12H), 2.83 (d, $J = 6.4$ Hz, 4H), 2.69 – 2.49 (m, 2H), 2.44 – 2.27 (m, 2H), 2.12 – 1.75 (m, 8H).

^{13}C NMR (151 MHz, CD_2Cl_2) δ 193.87, 161.02, 153.30, 149.11, 141.84, 138.70, 138.29, 135.44, 135.13, 133.50, 132.30, 131.53, 125.71, 115.79, 108.67, 100.31, 56.63, 55.92, 30.18, 28.81, 23.96, 23.54.

HRMS (ESI+): calc'd for $[\text{C}_{50}\text{H}_{52}\text{O}_6\text{N}_6\text{Au}_2\text{Cl}_2\text{F}_{12}]\text{Na}$: 1319.2549, found: 1319.2568

References

- (1) *Homogeneous Gold Catalysis*; Slaughter, L. M., Ed.; Topics in Current Chemistry; Springer International Publishing: Cham, 2015; Vol. 357.
- (2) Ito, Y.; Sawamura, M.; Hayashi, T. *J. Am. Chem. Soc.* **1986**, *108* (20), 6405.
- (3) Ito, Y.; Sawamura, M.; Shirakawa, E.; Hayashizaki, K.; Hayashi, T. *Tetrahedron* **1988**, *44* (17), 5253.
- (4) Ito, Y.; Sawamura, M.; Hamashima, H.; Emura, T.; Hayashi, T. *Tetrahedron Lett.* **1989**, *30* (35), 4681.
- (5) Togni, A.; Pastor, S. D. *Tetrahedron Lett.* **1989**, *30* (9), 1071.
- (6) Togni, A.; Pastor, S. D. *Helv. Chim. Acta* **1989**, *72* (5), 1038.
- (7) Zhou, X.-T.; Lin, Y.-R.; Dai, L.-X.; Sun, J.; Xia, L.-J.; Tang, M.-H. *J. Org. Chem.* **1999**, *64* (4), 1331.
- (8) Bachi, M. D.; Melman, A. *J. Org. Chem.* **1997**, *62* (6), 1896.
- (9) Hayashi, T.; Kumada, M. *Acc. Chem. Res.* **1982**, *15* (12), 395.
- (10) Knowles, W. S. *Acc. Chem. Res.* **1983**, *16* (3), 106.
- (11) Li, W.; Zhang, X. In *Phosphorus(III) Ligands in Homogeneous Catalysis: Design and Synthesis*; Kamer, P. C. J., Leeuwen, P. W. N. M. van, Eds.; John Wiley & Sons, Ltd, 2012; pp 27–80.
- (12) Miyashita, A.; Yasuda, A.; Takaya, H.; Toriumi, K.; Ito, T.; Souchi, T.; Noyori, R. *J. Am. Chem. Soc.* **1980**, *102* (27), 7932.
- (13) Schmid, R.; Foricher, J.; Cereghetti, M.; Schönholzer, P. *Helv. Chim. Acta* **1991**, *74* (2), 370.
- (14) Saito, T.; Yokozawa, T.; Ishizaki, T.; Moroi, T.; Sayo, N.; Miura, T.; Kumobayashi, H. *Adv. Synth. Catal.* **2001**, *343* (3), 264.
- (15) Muñoz, M. P.; Adrio, J.; Carretero, J. C.; Echavarren, A. M. *Organometallics* **2005**, *24* (6), 1293.
- (16) Johansson, M. J.; Gorin, D. J.; Staben, S. T.; Toste, F. D. *J. Am. Chem. Soc.* **2005**, *127* (51), 18002.
- (17) Zhang, Z.; Widenhoefer, R. A. *Angew. Chem. Int. Ed.* **2007**, *46* (1-2), 283.
- (18) LaLonde, R. L.; Sherry, B. D.; Kang, E. J.; Toste, F. D. *J. Am. Chem. Soc.* **2007**, *129* (9), 2452.
- (19) Luzung, M. R.; Mauleón, P.; Toste, F. D. *J. Am. Chem. Soc.* **2007**, *129* (41), 12402.
- (20) Chao, C.-M.; Vitale, M. R.; Toullec, P. Y.; Genêt, J.-P.; Michelet, V. *Chem. – Eur. J.* **2009**, *15* (6), 1319.
- (21) Kleinbeck, F.; Toste, F. D. *J. Am. Chem. Soc.* **2009**, *131* (26), 9178.
- (22) Martínez, A.; García-García, P.; Fernández-Rodríguez, M. A.; Rodríguez, F.; Sanz, R. *Angew. Chem. Int. Ed.* **2010**, *49* (27), 4633.
- (23) Sethofer, S. G.; Mayer, T.; Toste, F. D. *J. Am. Chem. Soc.* **2010**, *132* (24), 8276.
- (24) Gawade, S. A.; Bhunia, S.; Liu, R.-S. *Angew. Chem. Int. Ed.* **2012**, *51* (31), 7835.
- (25) Briones, J. F.; Davies, H. M. L. *J. Am. Chem. Soc.* **2012**, *134* (29), 11916.
- (26) Zi, W.; Toste, F. D. *J. Am. Chem. Soc.* **2013**, *135* (34), 12600.
- (27) Briones, J. F.; Davies, H. M. L. *J. Am. Chem. Soc.* **2013**, *135* (36), 13314.
- (28) Uria, U.; Vila, C.; Lin, M.-Y.; Rueping, M. *Chem. – Eur. J.* **2014**, *20* (43), 13913.
- (29) Zi, W.; Wu, H.; Toste, F. D. *J. Am. Chem. Soc.* **2015**, *137* (9), 3225.
- (30) Jia, M.; Monari, M.; Yang, Q.-Q.; Bandini, M. *Chem. Commun.* **2015**, *51* (12), 2320.
- (31) Burk, M. J. *J. Am. Chem. Soc.* **1991**, *113* (22), 8518.

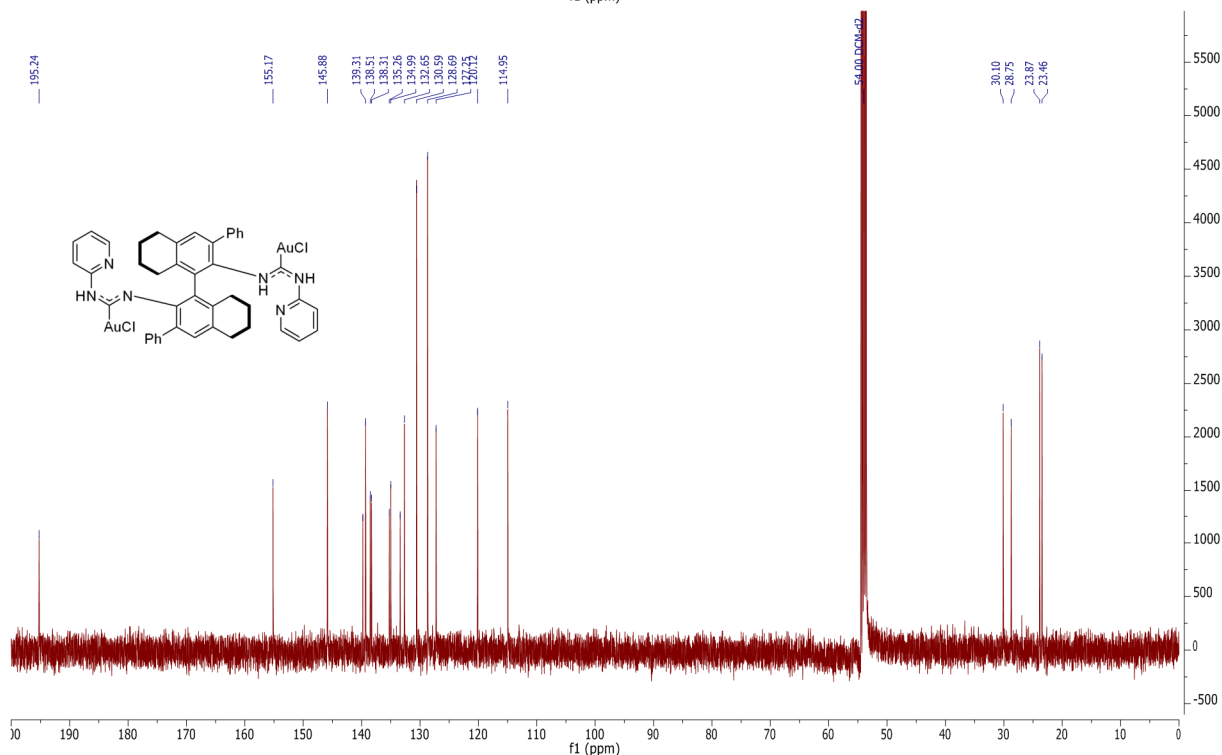
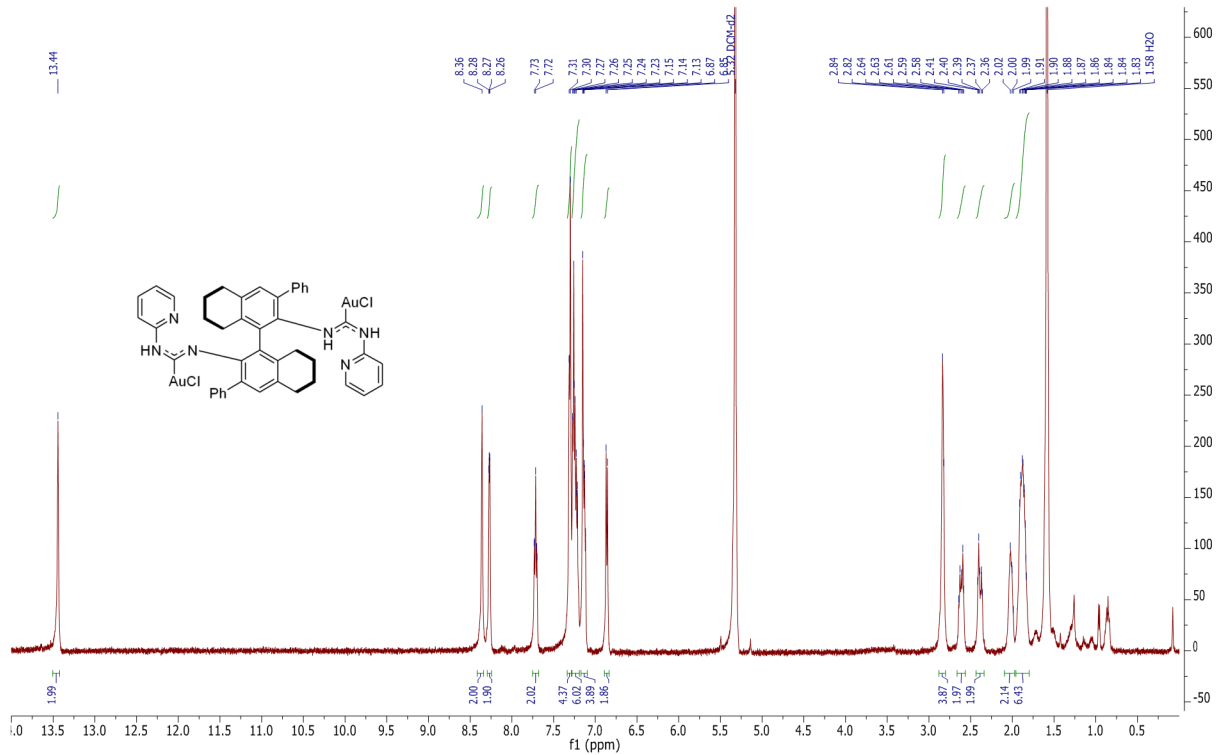
- (32) González-Arellano, C.; Corma, A.; Iglesias, M.; Sánchez, F. *Chem. Commun.* **2005**, No. 27, 3451.
- (33) Pye, P. J.; Rossen, K.; Reamer, R. A.; Tsou, N. N.; Volante, R. P.; Reider, P. J. *J. Am. Chem. Soc.* **1997**, *119* (26), 6207.
- (34) Felix, R. J.; Weber, D.; Gutierrez, O.; Tantillo, D. J.; Gagné, M. R. *Nat. Chem.* **2012**, *4* (5), 405.
- (35) Hulst, R.; de Vries, N. K.; Feringa, B. L. *Tetrahedron Asymmetry* **1994**, *5* (4), 699.
- (36) de Vries, A. H. M.; Meetsma, A.; Feringa, B. L. *Angew. Chem. Int. Ed. Engl.* **1996**, *35* (20), 2374.
- (37) Alonso, I.; Trillo, B.; López, F.; Montserrat, S.; Ujaque, G.; Castedo, L.; Lledós, A.; Mascareñas, J. L. *J. Am. Chem. Soc.* **2009**, *131* (36), 13020.
- (38) González, A. Z.; Benitez, D.; Tkatchouk, E.; Goddard, W. A.; Toste, F. D. *J. Am. Chem. Soc.* **2011**, *133* (14), 5500.
- (39) Suárez-Pantiga, S.; Hernández-Díaz, C.; Rubio, E.; González, J. M. *Angew. Chem. Int. Ed.* **2012**, *51* (46), 11552.
- (40) Li, G.-H.; Zhou, W.; Li, X.-X.; Bi, Q.-W.; Wang, Z.; Zhao, Z.-G.; Hu, W.-X.; Chen, Z. *Chem. Commun.* **2013**, *49* (42), 4770.
- (41) Liu, B.; Li, K.-N.; Luo, S.-W.; Huang, J.-Z.; Pang, H.; Gong, L.-Z. *J. Am. Chem. Soc.* **2013**, *135* (9), 3323.
- (42) Wang, Y.; Zhang, P.; Liu, Y.; Xia, F.; Zhang, J. *Chem. Sci.* **2015**, *6* (10), 5564.
- (43) Lam, H. *Synthesis* **2011**, *2011* (13), 2011.
- (44) Teller, H.; Flügge, S.; Goddard, R.; Fürstner, A. *Angew. Chem. Int. Ed.* **2010**, *49* (11), 1949.
- (45) Teller, H.; Corbet, M.; Mantilli, L.; Gopakumar, G.; Goddard, R.; Thiel, W.; Fürstner, A. *J. Am. Chem. Soc.* **2012**, *134* (37), 15331.
- (46) Yavari, K.; Aillard, P.; Zhang, Y.; Nuter, F.; Retailleau, P.; Voituriez, A.; Marinetti, A. *Angew. Chem. Int. Ed.* **2014**, *53* (3), 861.
- (47) Aillard, P.; Voituriez, A.; Dova, D.; Cauteruccio, S.; Licandro, E.; Marinetti, A. *Chem. – Eur. J.* **2014**, *20* (39), 12373.
- (48) Wu, Z.; Retailleau, P.; Gandon, V.; Voituriez, A.; Marinetti, A. *Eur. J. Org. Chem.* **2016**, *2016* (1), 70.
- (49) Pedersen, H. L.; Johannsen, M. *Chem. Commun.* **1999**, No. 24, 2517.
- (50) Wurm, T.; Mohamed Asiri, A.; Hashmi, A. S. K. In *N-Heterocyclic Carbenes*; Nolan, S. P., Ed.; Wiley-VCH Verlag GmbH & Co. KGaA, 2014; pp 243–270.
- (51) Han, X.; Widenhofer, R. A. *Angew. Chem. Int. Ed.* **2006**, *45* (11), 1747.
- (52) Bender, C. F.; Widenhofer, R. A. *Org. Lett.* **2006**, *8* (23), 5303.
- (53) Marion, N.; Díez-González, S.; de Frémont, P.; Noble, A. R.; Nolan, S. P. *Angew. Chem. Int. Ed.* **2006**, *45* (22), 3647.
- (54) Wang, F.; Liu, L.; Wang, W.; Li, S.; Shi, M. *Coord. Chem. Rev.* **2012**, *256* (9–10), 804.
- (55) Arduengo, A. J.; Harlow, R. L.; Kline, M. *J. Am. Chem. Soc.* **1991**, *113* (1), 361.
- (56) Seiders, T. J.; Ward, D. W.; Grubbs, R. H. *Org. Lett.* **2001**, *3* (20), 3225.
- (57) Matsumoto, Y.; Selim, K. B.; Nakanishi, H.; Yamada, K.; Yamamoto, Y.; Tomioka, K. *Tetrahedron Lett.* **2010**, *51* (2), 404.
- (58) Yamada, K.; Matsumoto, Y.; Selim, K. B.; Yamamoto, Y.; Tomioka, K. *Tetrahedron* **2012**, *68* (22), 4159.
- (59) Gung, B. W.; Bailey, L. N.; Craft, D. T.; Barnes, C. L.; Kirschbaum, K. *Organometallics* **2010**, *29* (15), 3450.

- (60) Holmes, M. R.; Manganaro, J. F.; Barnes, C. L.; Gung, B. W. *J. Organomet. Chem.* **2015**, 795, 18.
- (61) Banerjee, D.; Buzas, A. K.; Besnard, C.; Kündig, E. P. *Organometallics* **2012**, 31 (23), 8348.
- (62) Wilckens, K.; Uhlemann, M.; Czekelius, C. *Chem. – Eur. J.* **2009**, 15 (48), 13323.
- (63) Wilckens, K.; Lentz, D.; Czekelius, C. *Organometallics* **2011**, 30 (6), 1287.
- (64) Liu, L.; Wang, F.; Wang, W.; Zhao, M.; Shi, M. *Beilstein J. Org. Chem.* **2011**, 7 (1), 555.
- (65) Wang, W.; Yang, J.; Wang, F.; Shi, M. *Organometallics* **2011**, 30 (14), 3859.
- (66) Yang, J.; Zhang, R.; Wang, W.; Zhang, Z.; Shi, M. *Tetrahedron Asymmetry* **2011**, 22 (23), 2029.
- (67) Wang, F.; Li, S.; Qu, M.; Zhao, M.-X.; Liu, L.-J.; Shi, M. *Beilstein J. Org. Chem.* **2012**, 8, 726.
- (68) Sun, Y.; Xu, Q.; Shi, M. *Beilstein J. Org. Chem.* **2013**, 9 (1), 2224.
- (69) Usui, K.; Yoshida, T.; Nakada, M. *Tetrahedron Asymmetry* **2016**, 27 (2–3), 107.
- (70) Francos, J.; Grande-Carmona, F.; Faustino, H.; Iglesias-Sigüenza, J.; Díez, E.; Alonso, I.; Fernández, R.; Lassaletta, J. M.; López, F.; Mascareñas, J. L. *J. Am. Chem. Soc.* **2012**, 134 (35), 14322.
- (71) Slaughter, L. M. *ACS Catal.* **2012**, 2 (8), 1802.
- (72) Bonati, F.; Minghetti, G. *Synth. React. Inorg. Met.-Org. Chem.* **1971**, 1 (4), 299.
- (73) Bartolomé, C.; Ramiro, Z.; Pérez-Galán, P.; Bour, C.; Raducan, M.; Echavarren, A. M.; Espinet, P. *Inorg. Chem.* **2008**, 47 (23), 11391.
- (74) Bartolomé, C.; García-Cuadrado, D.; Ramiro, Z.; Espinet, P. *Inorg. Chem.* **2010**, 49 (21), 9758.
- (75) Wang, Y.-M.; Kuzniewski, C. N.; Rauniyar, V.; Hoong, C.; Toste, F. D. *J. Am. Chem. Soc.* **2011**, 133 (33), 12972.
- (76) Handa, S.; Slaughter, L. M. *Angew. Chem. Int. Ed.* **2012**, 51 (12), 2912.
- (77) Akana, J. A.; Bhattacharyya, K. X.; Müller, P.; Sadighi, J. P. *J. Am. Chem. Soc.* **2007**, 129 (25), 7736.
- (78) Kano, T.; Tanaka, Y.; Osawa, K.; Yurino, T.; Maruoka, K. *J. Org. Chem.* **2008**, 73 (18), 7387.
- (79) Lacerda, R. B.; de Lima, C. K. F.; da Silva, L. L.; Romeiro, N. C.; Miranda, A. L. P.; Barreiro, E. J.; Fraga, C. A. M. *Bioorg. Med. Chem.* **2009**, 17 (1), 74.
- (80) Pirrung, M. C.; Ghorai, S. *J. Am. Chem. Soc.* **2006**, 128 (36), 11772.
- (81) Bartolomé, C.; Carrasco-Rando, M.; Coco, S.; Cordovilla, C.; Martín-Alvarez, J. M.; Espinet, P. *Inorg. Chem.* **2008**, 47 (5), 1616.

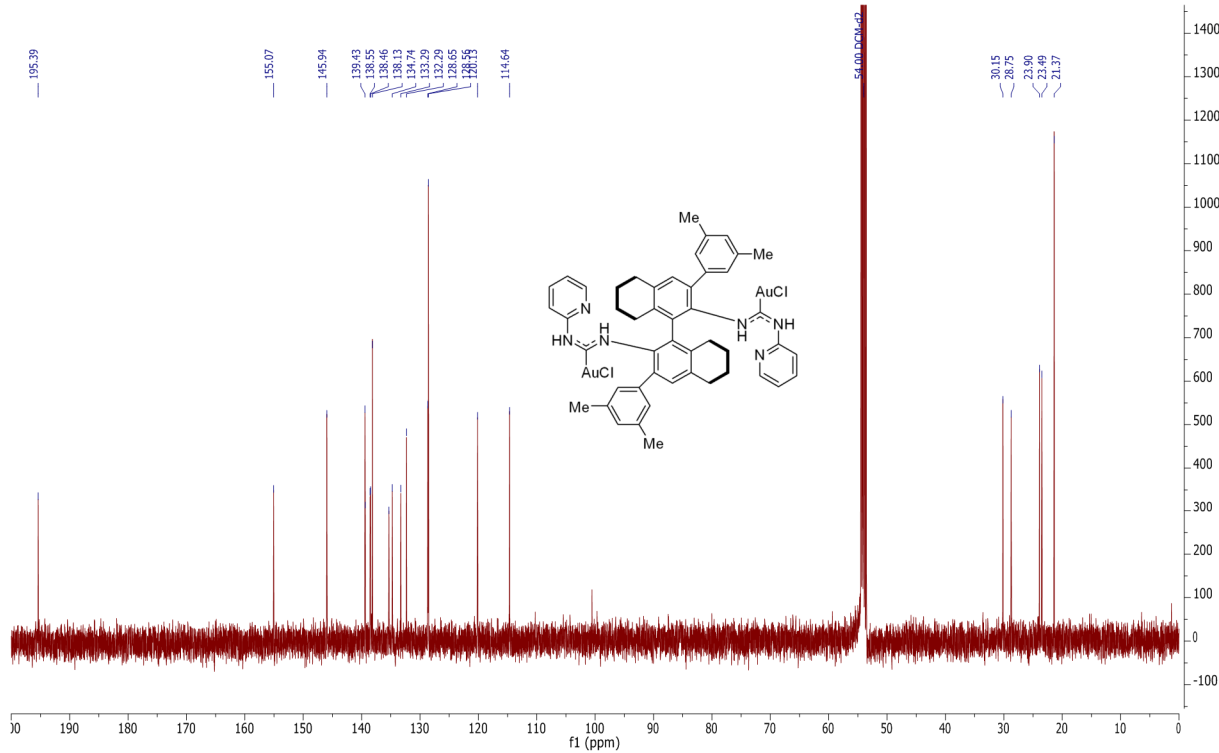
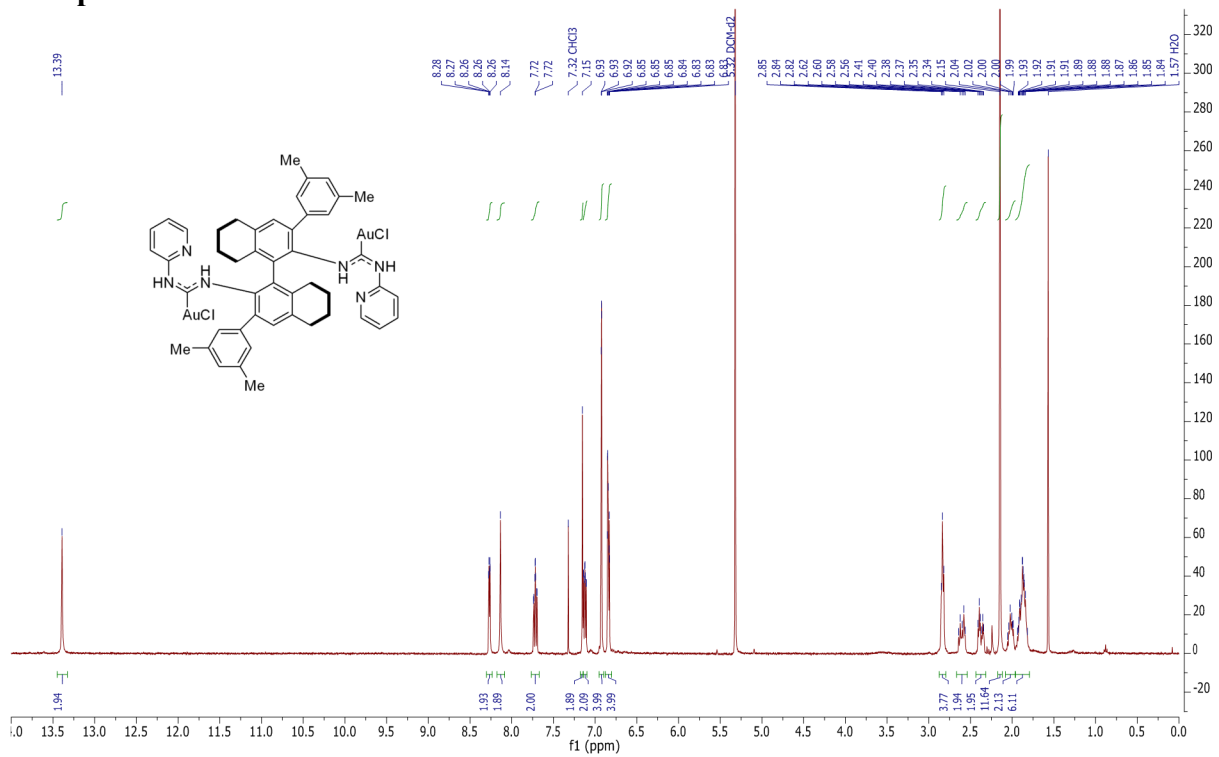
Appendix 1 - NMR Spectra

In some cases, unintegrated resonances in the 0-2 ppm region may appear. These correspond to trace quantities of residual solvents, including water, grease, and other aliphatic hydrocarbons.

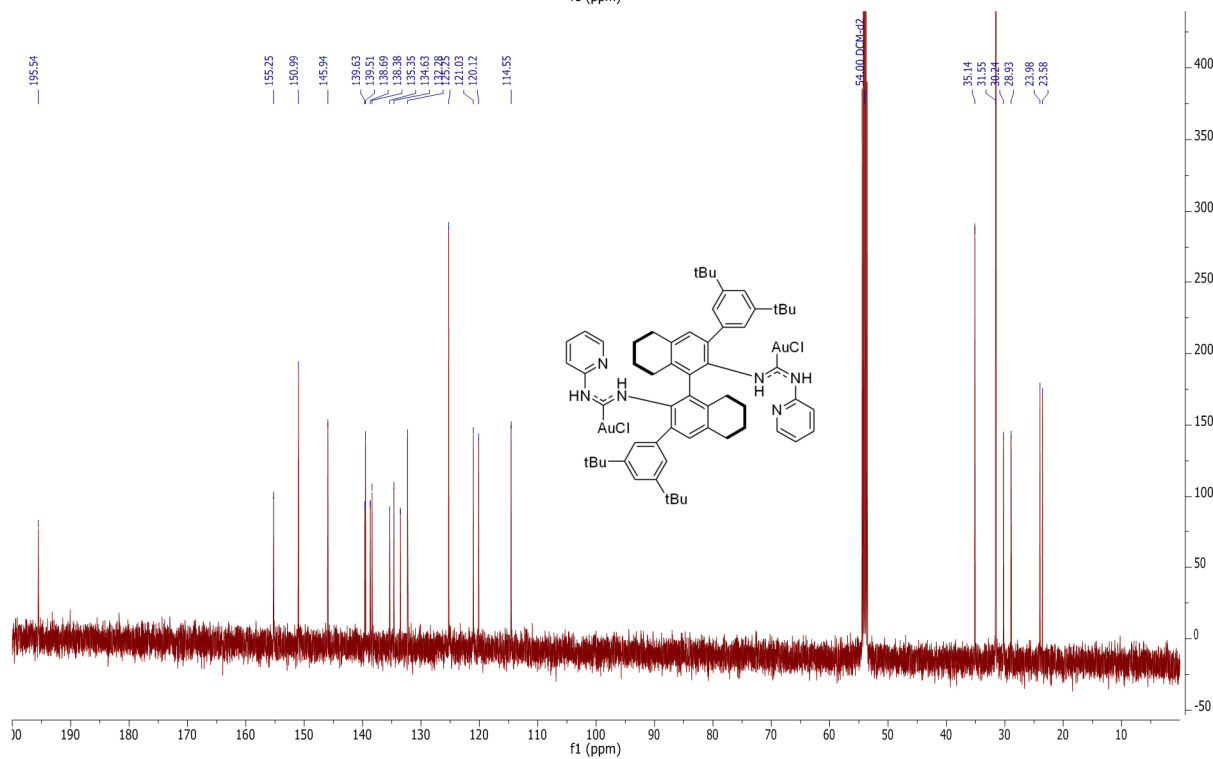
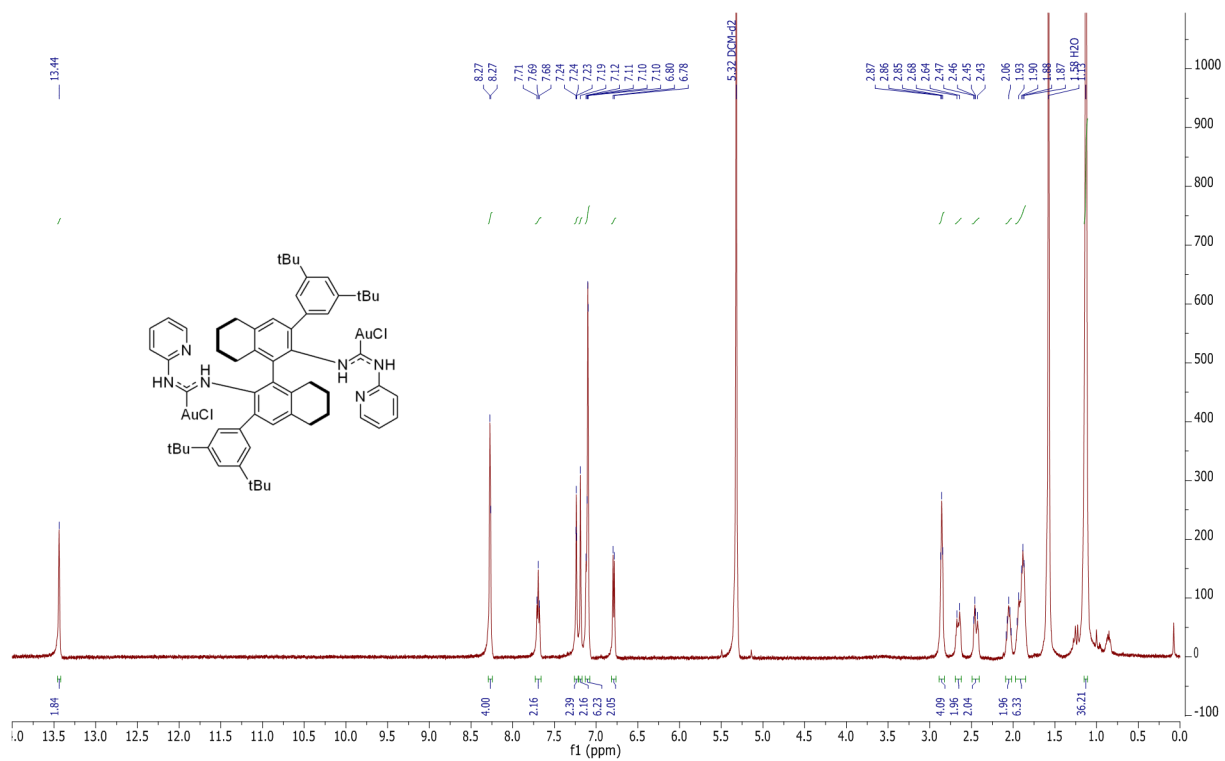
Complex 1.10a



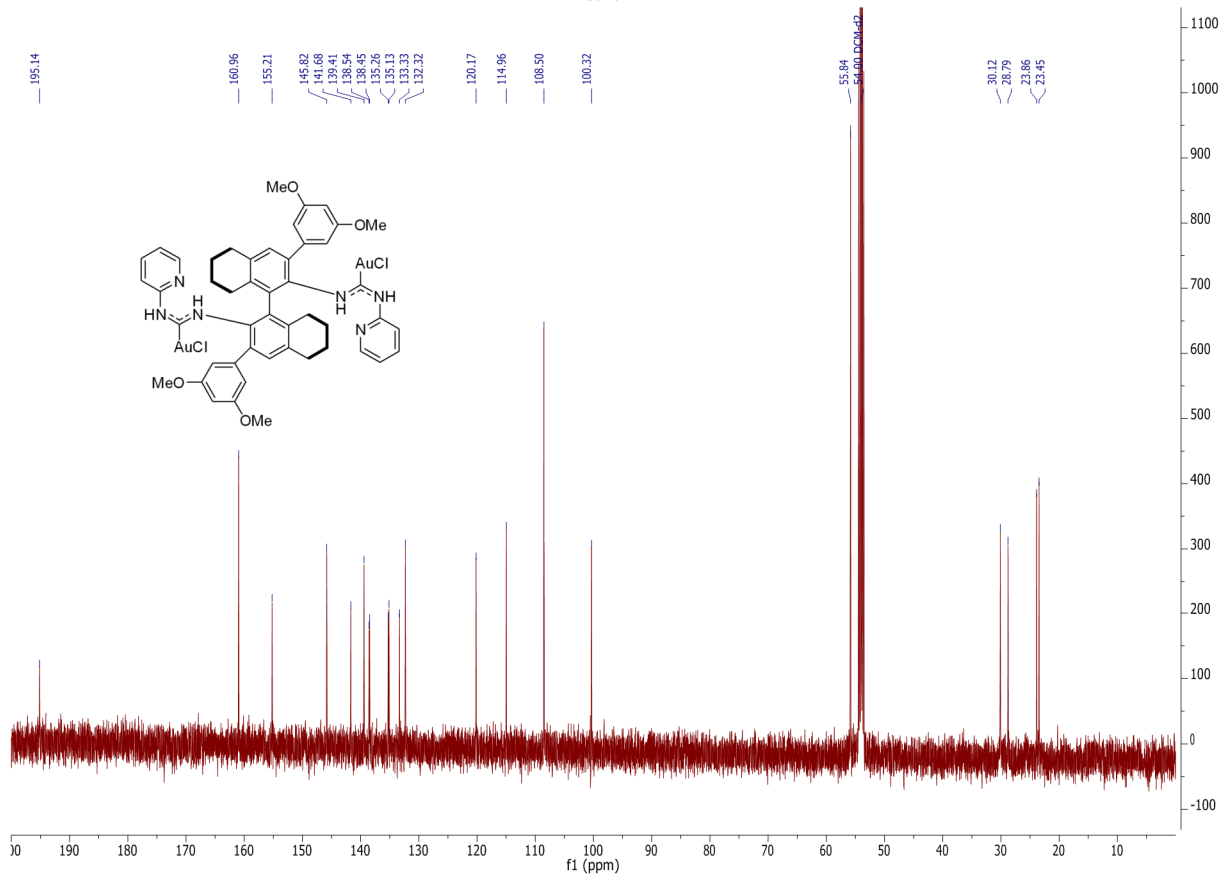
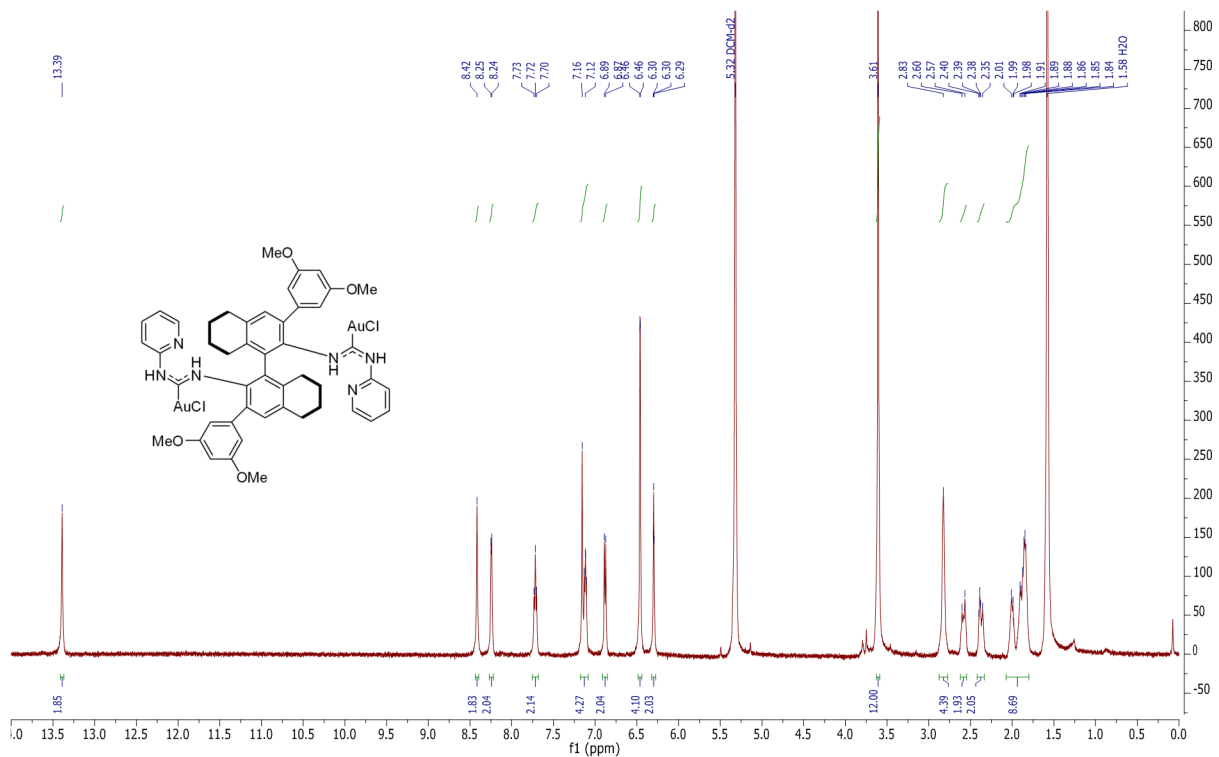
Complex 1.10b



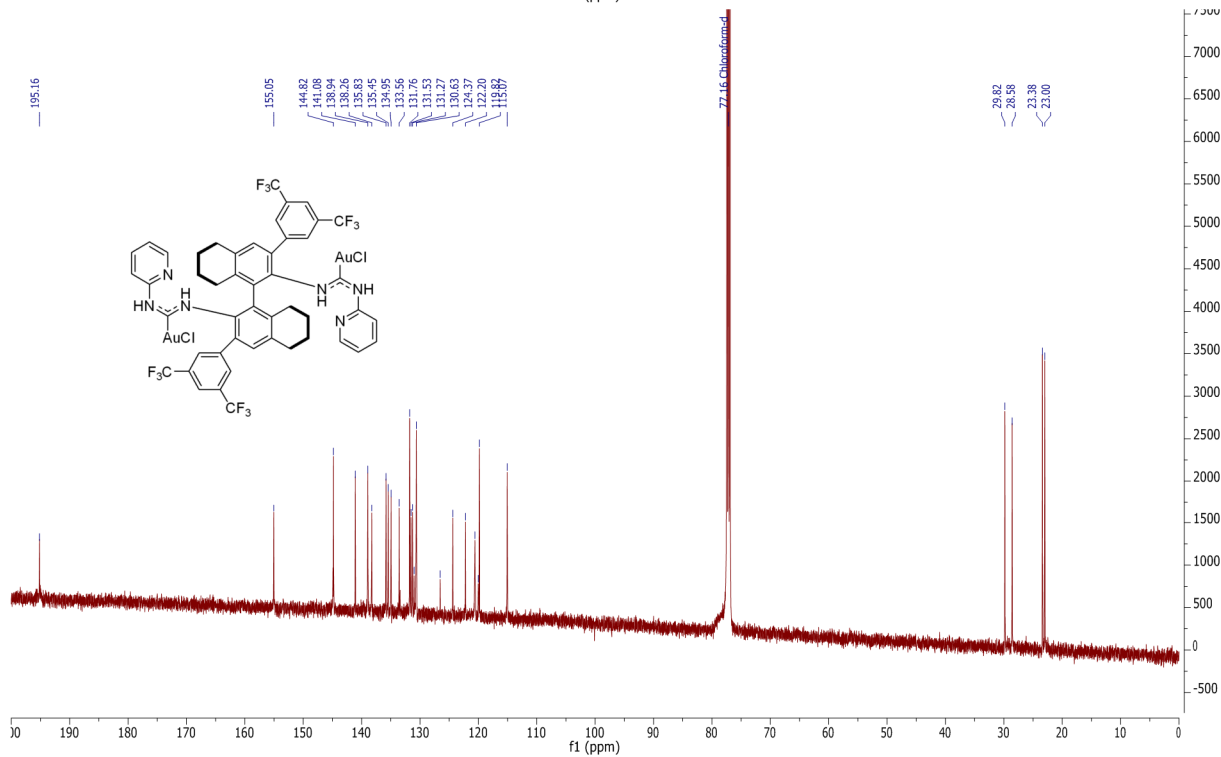
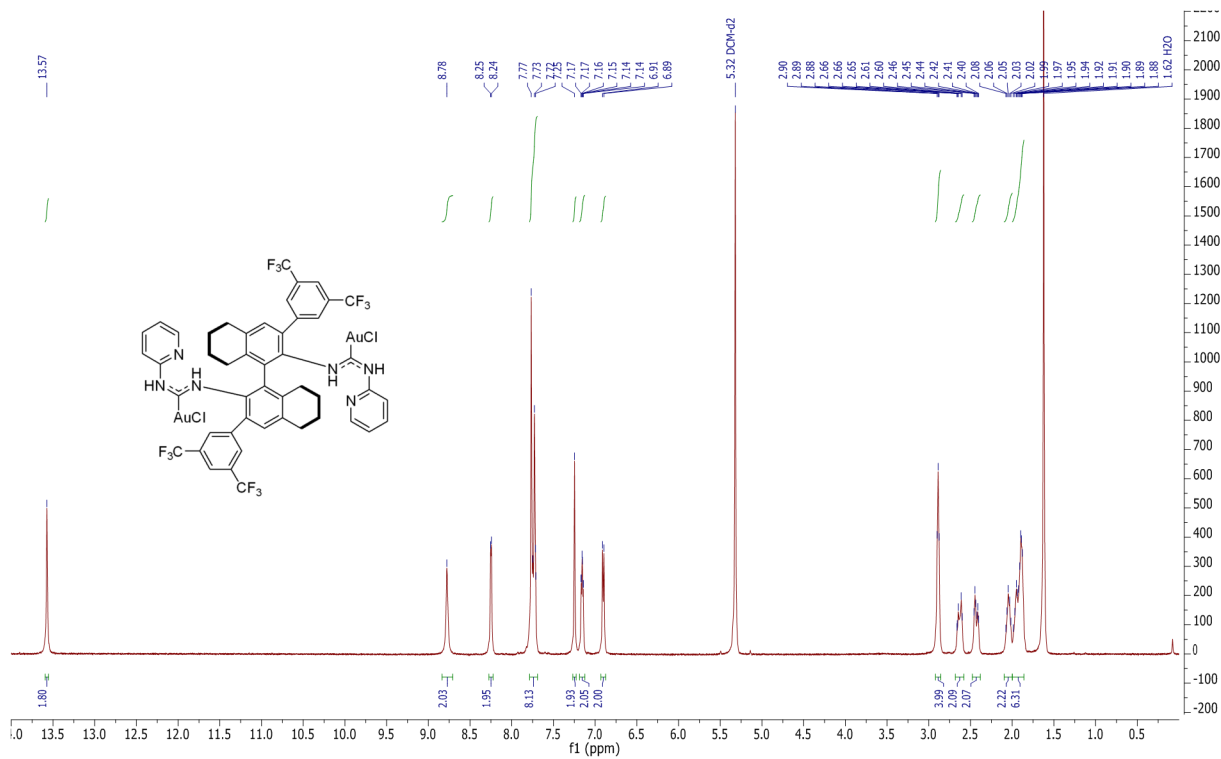
Complex 1.10c



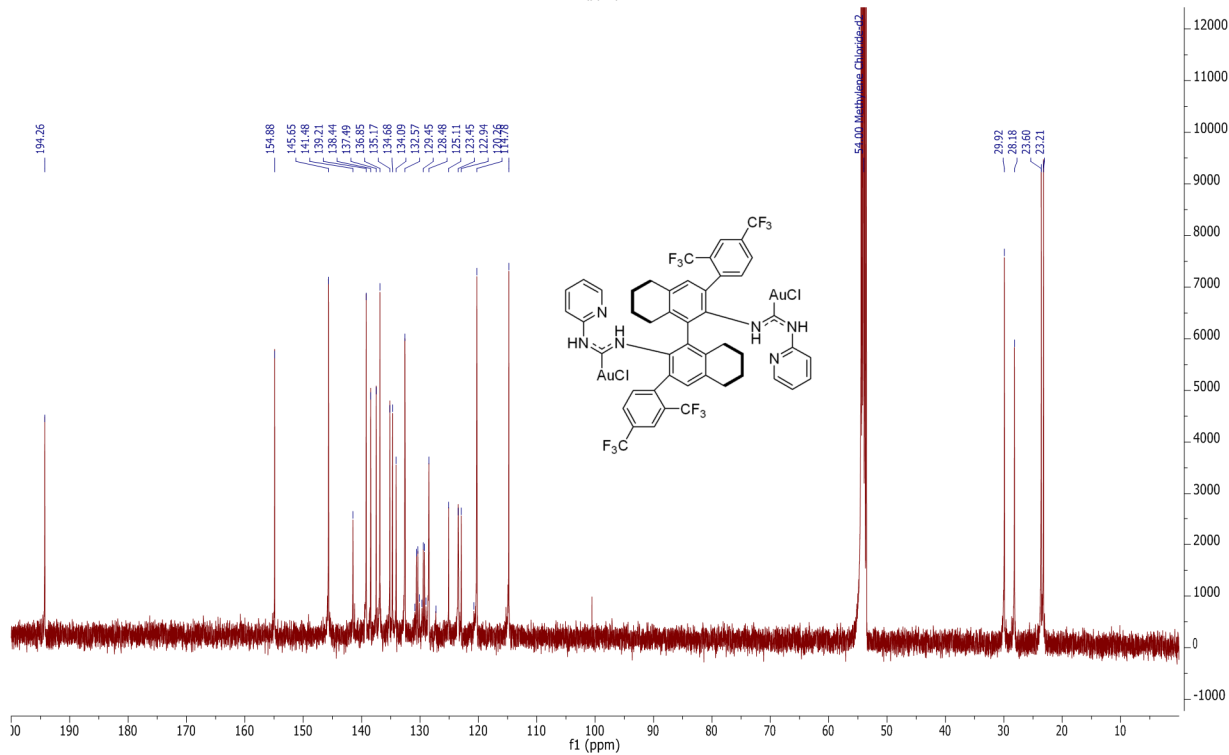
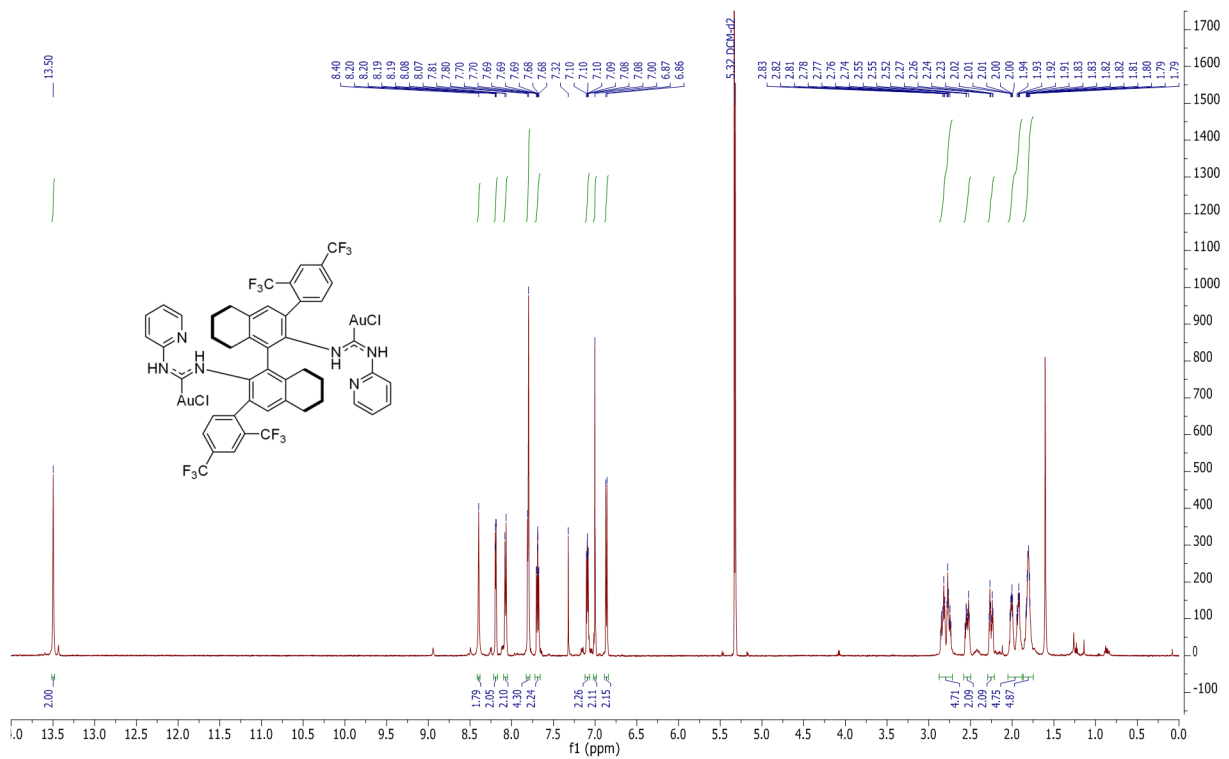
Complex 1.10d



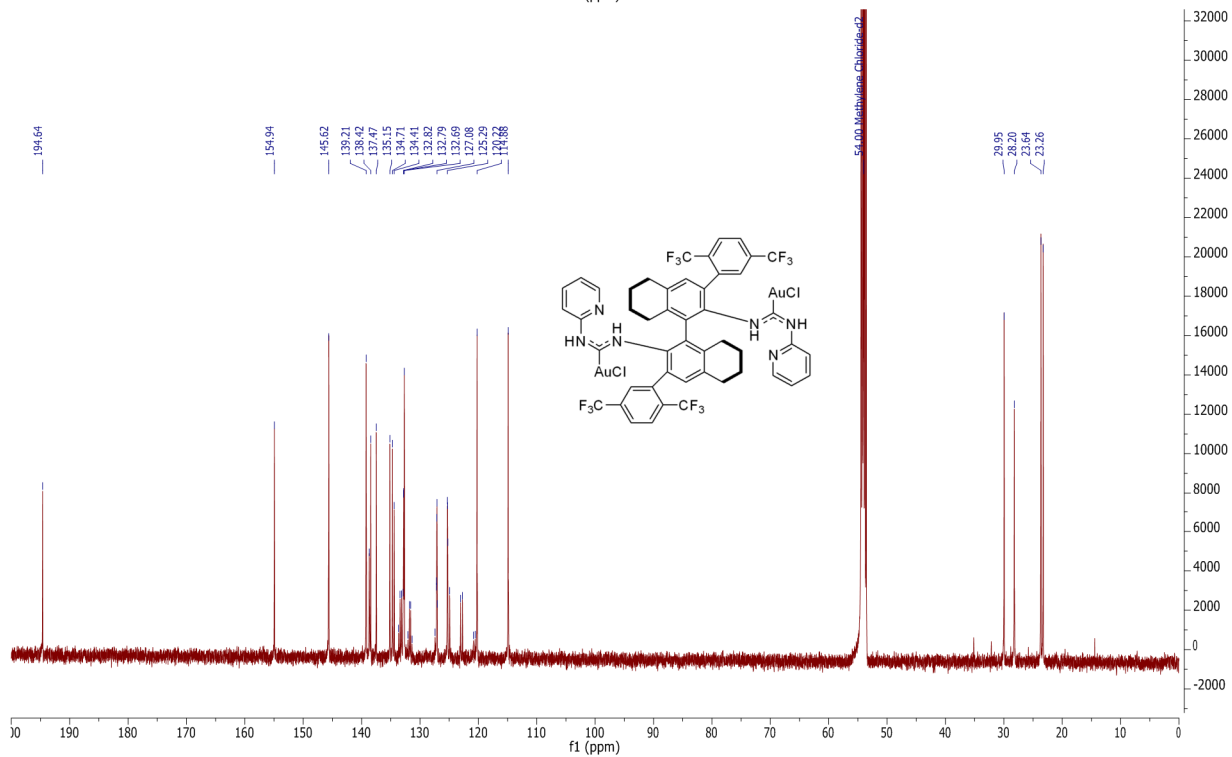
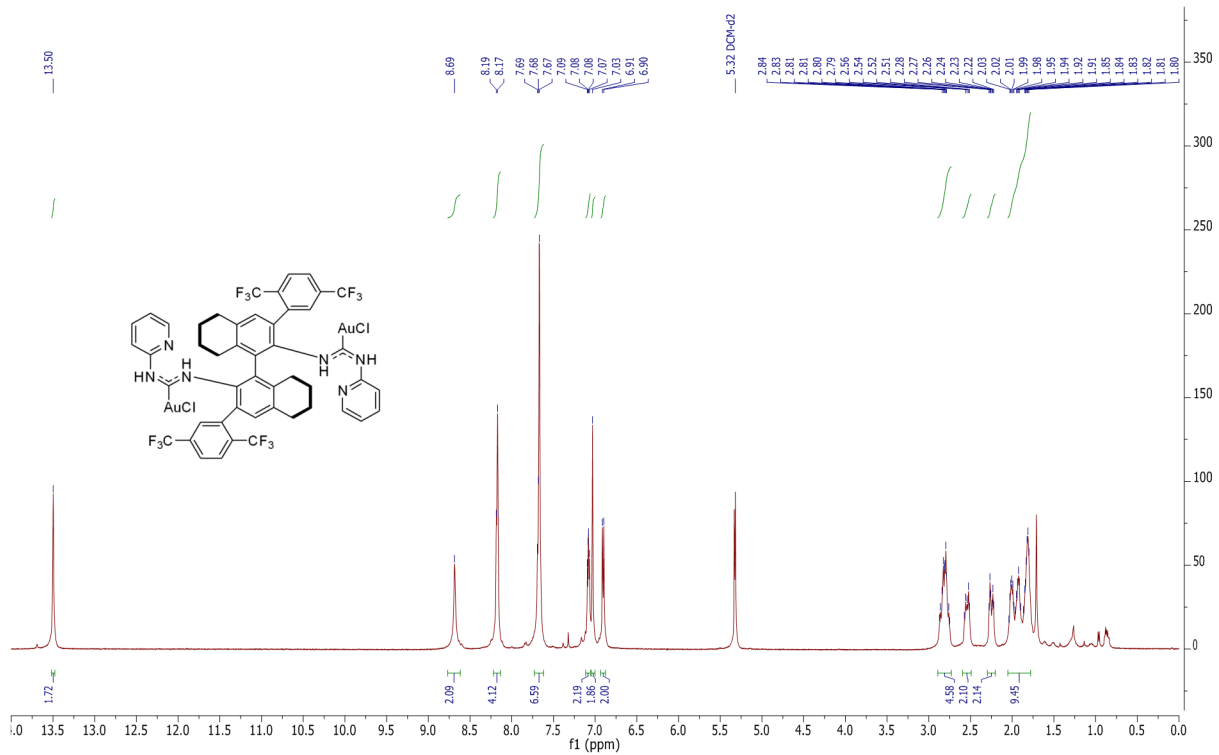
Complex 1.10e



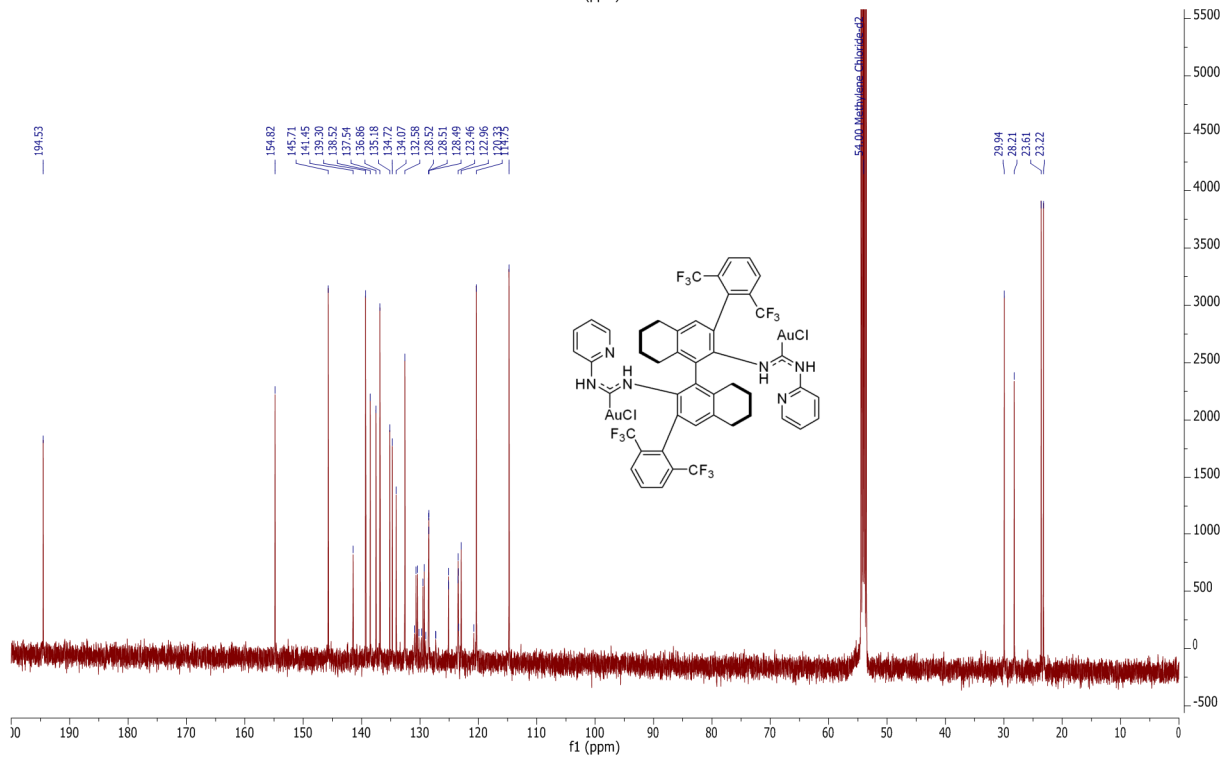
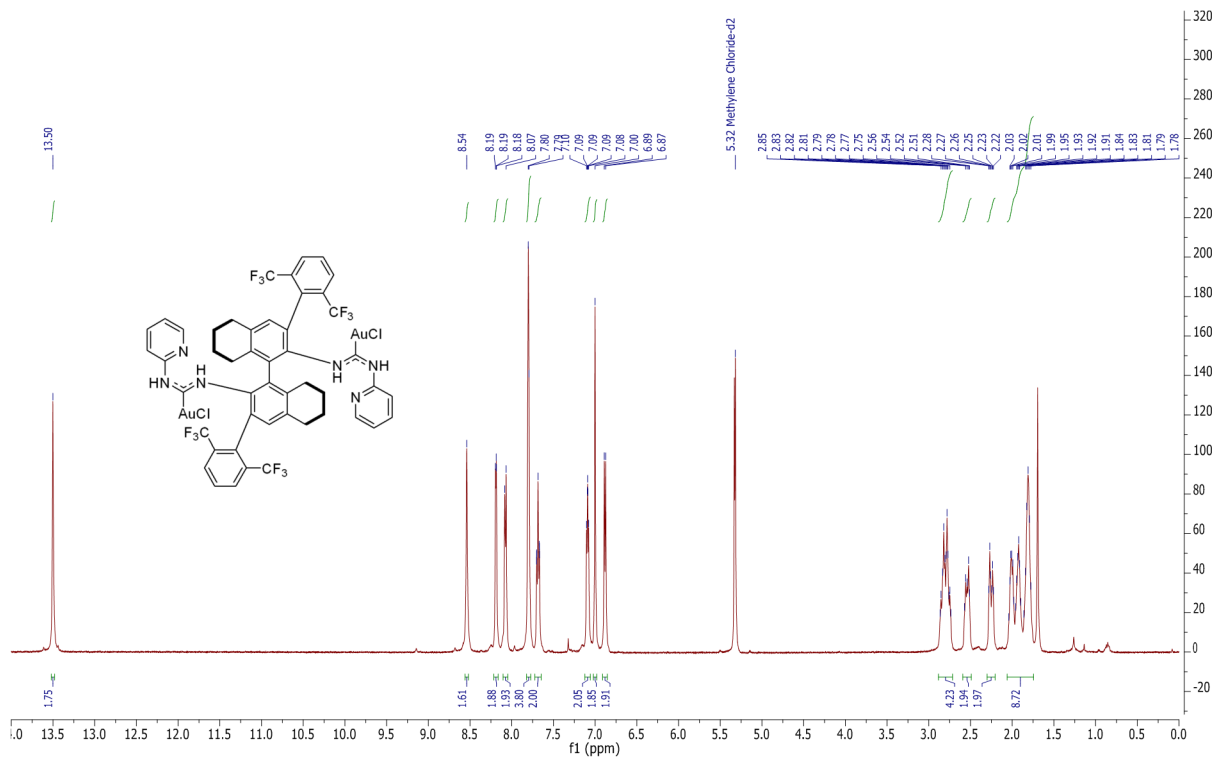
Complex 1.10f



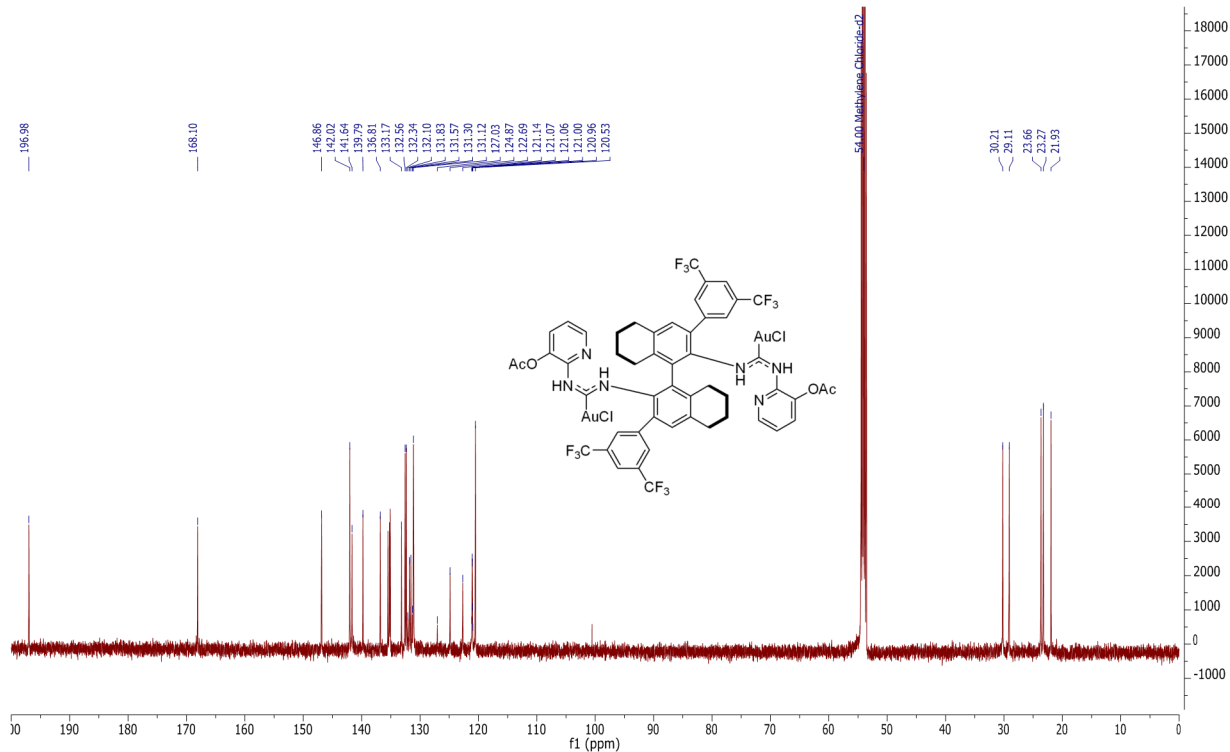
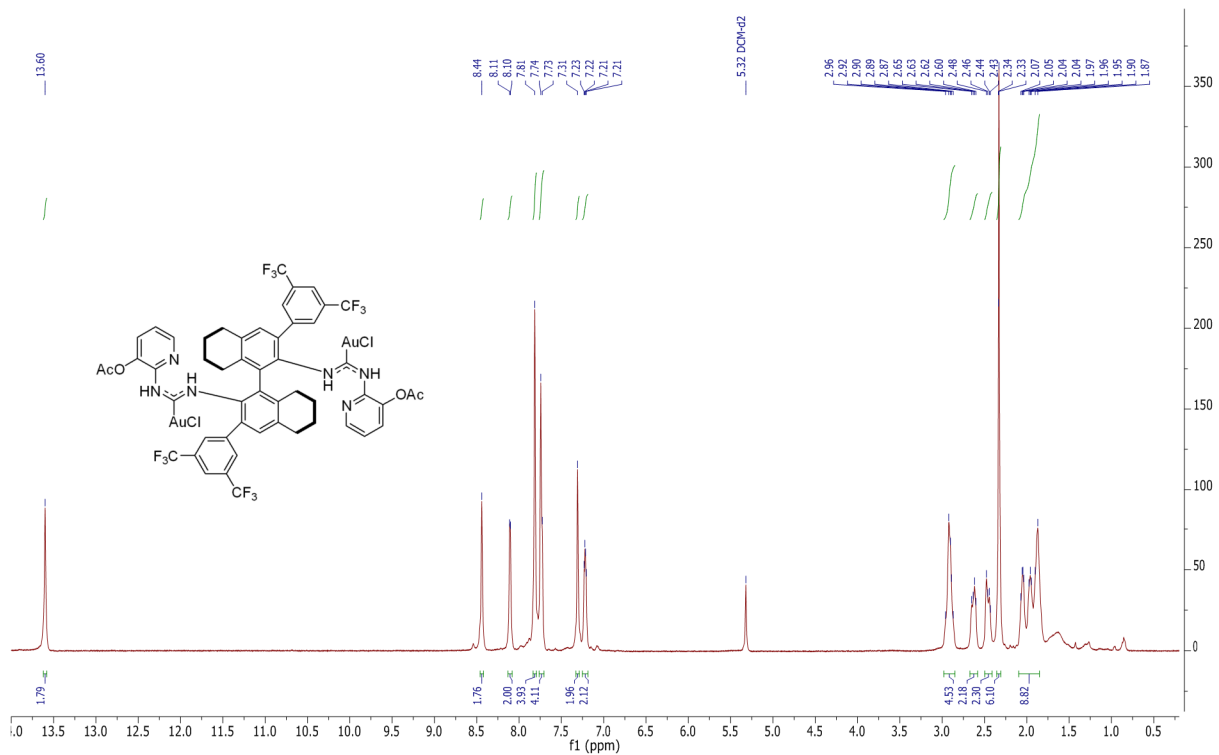
Complex 1.10g



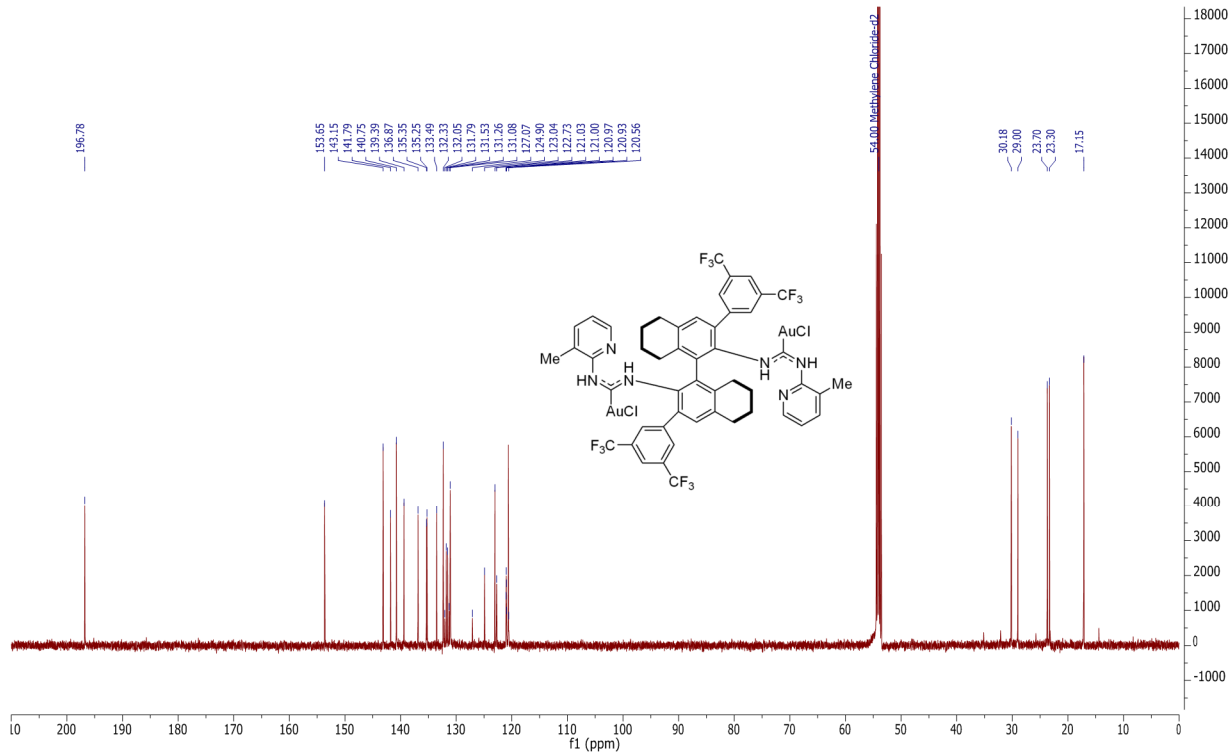
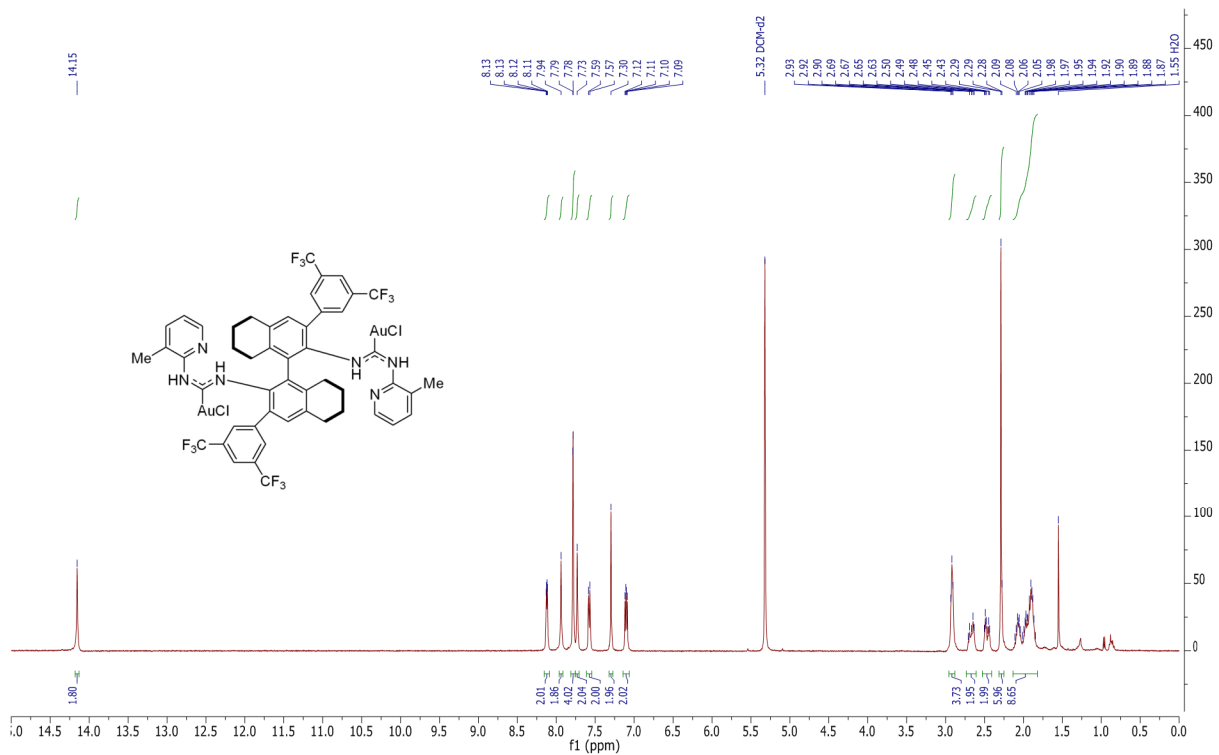
Complex 1.10h



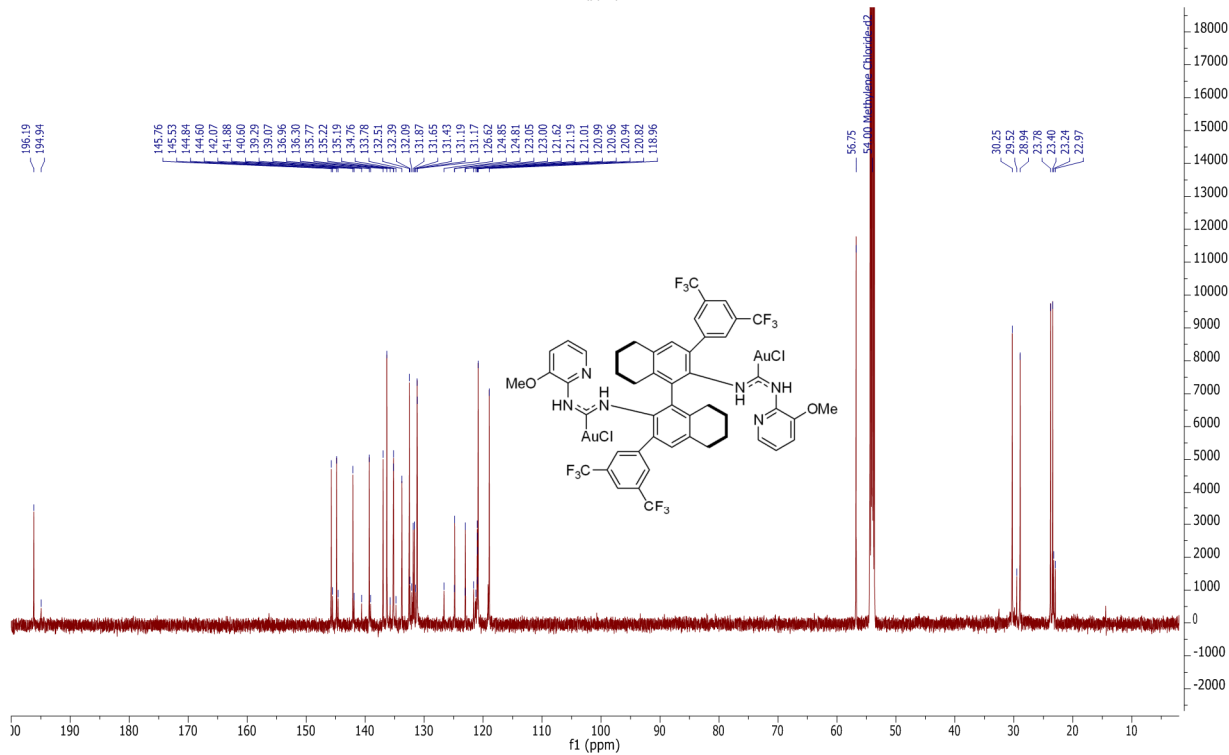
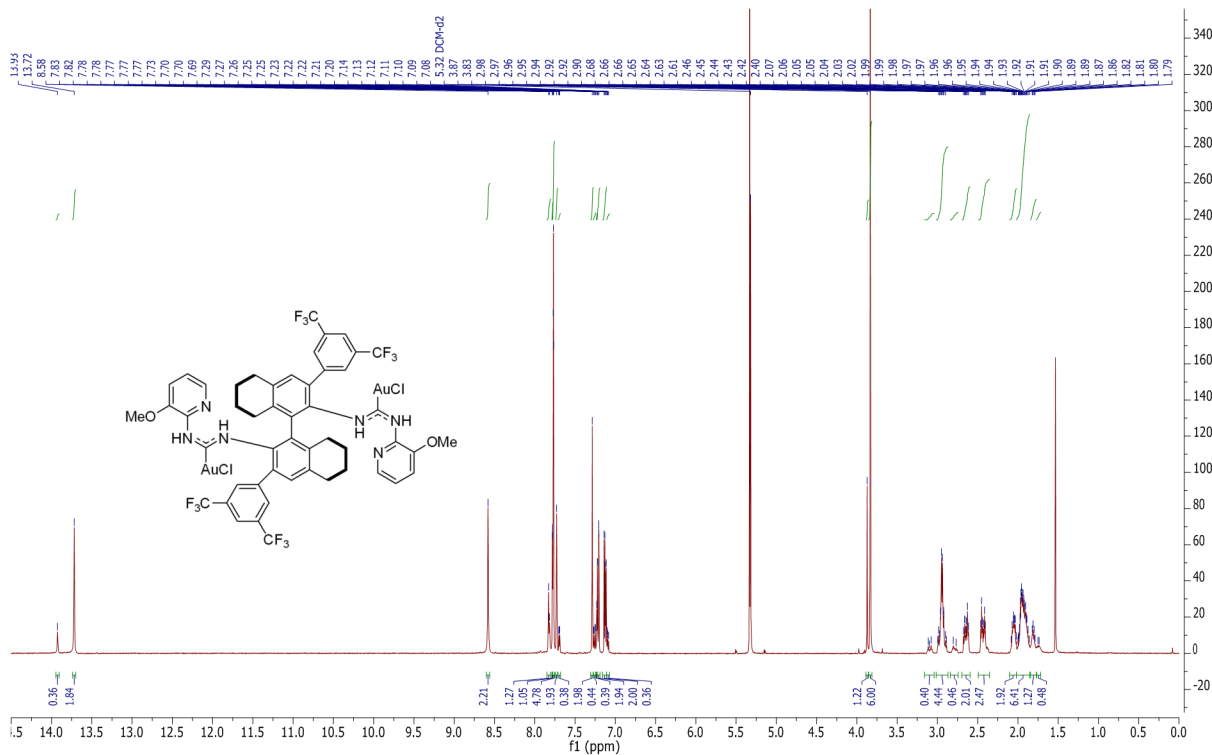
Complex 1.10i



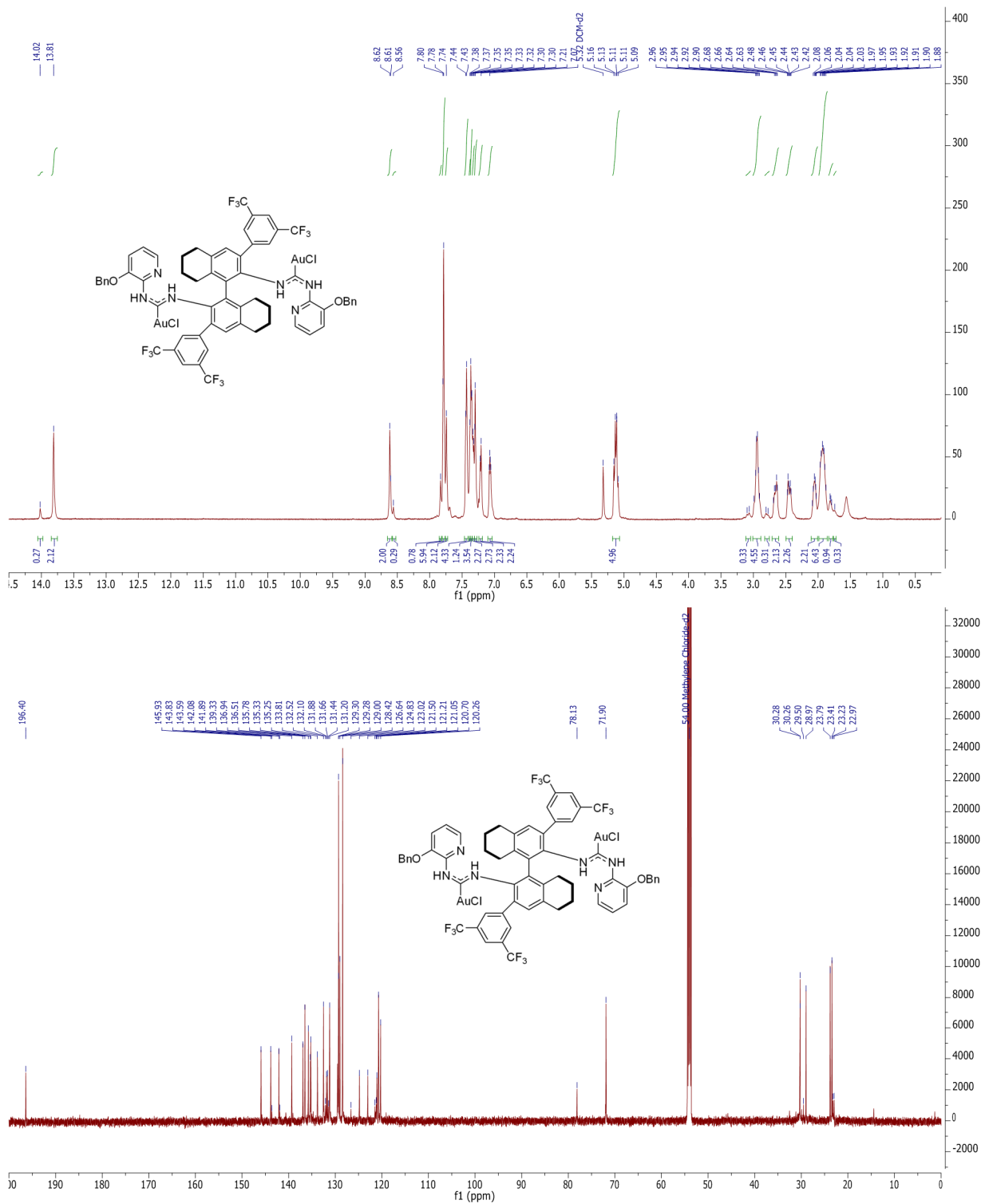
Complex 1.10j



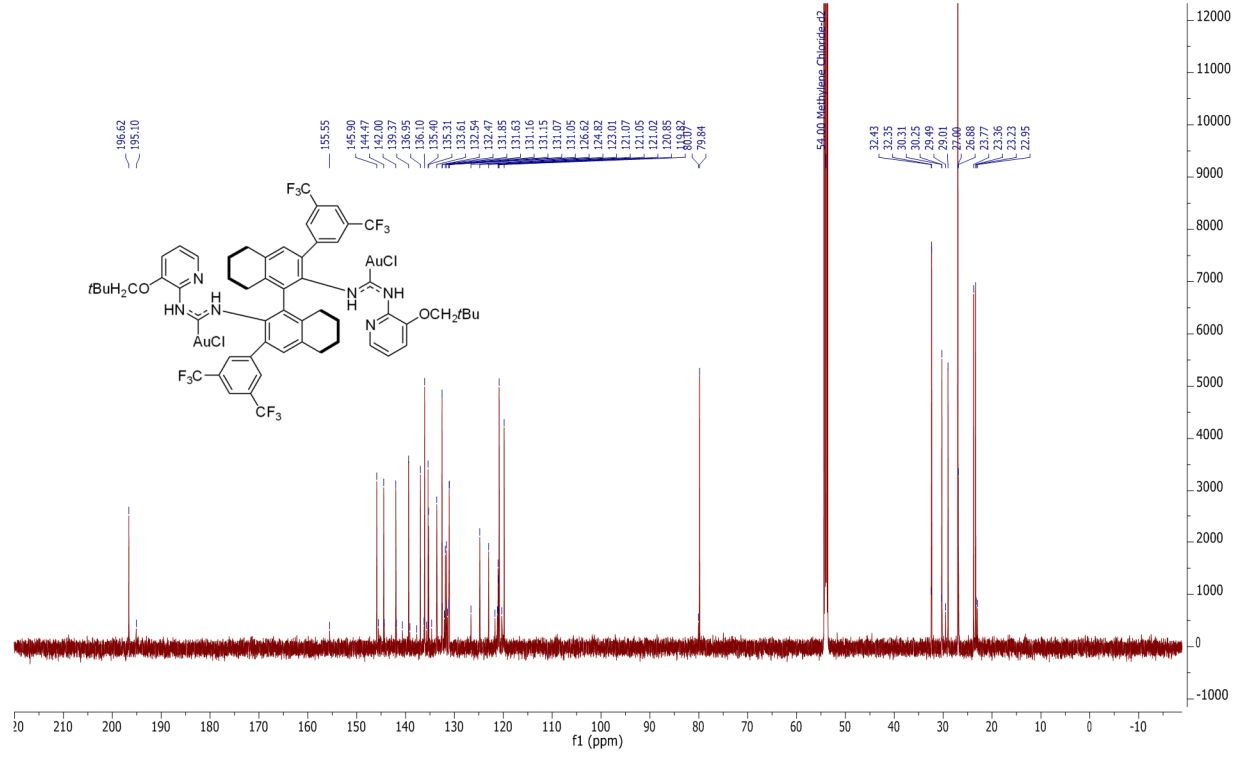
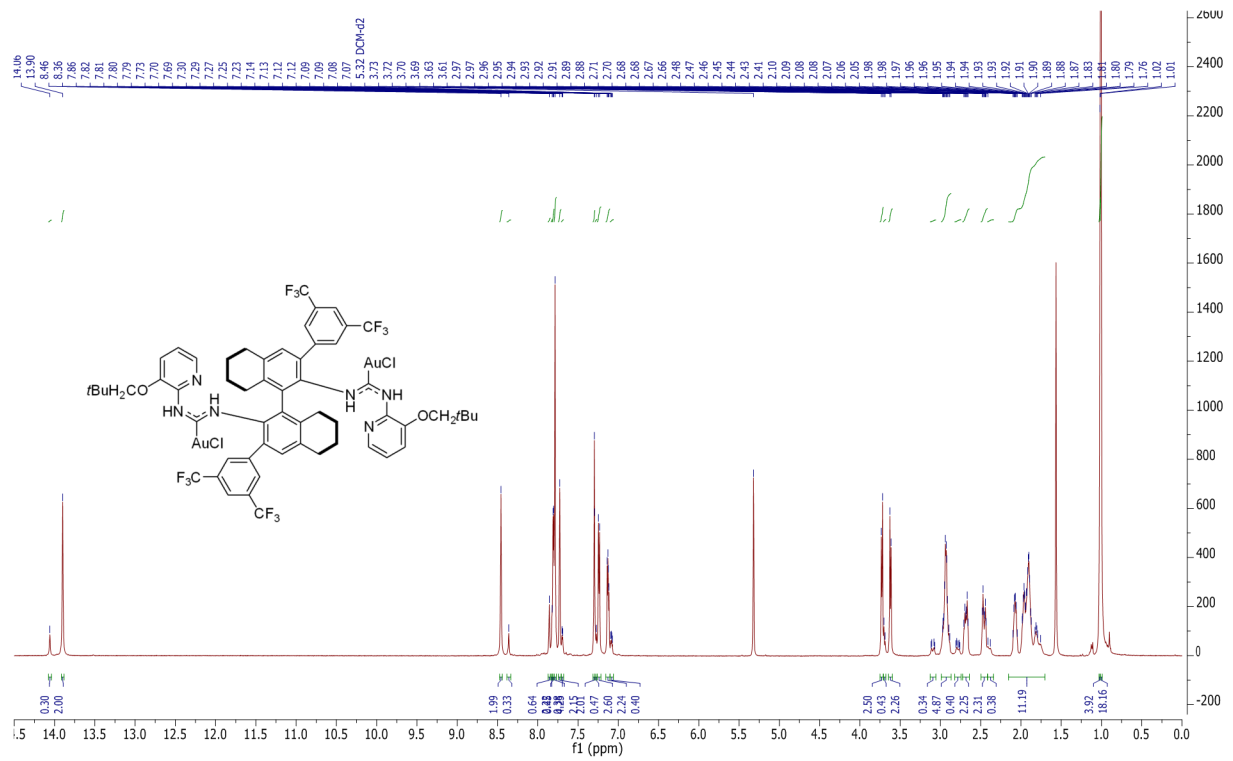
Complex 1.10k



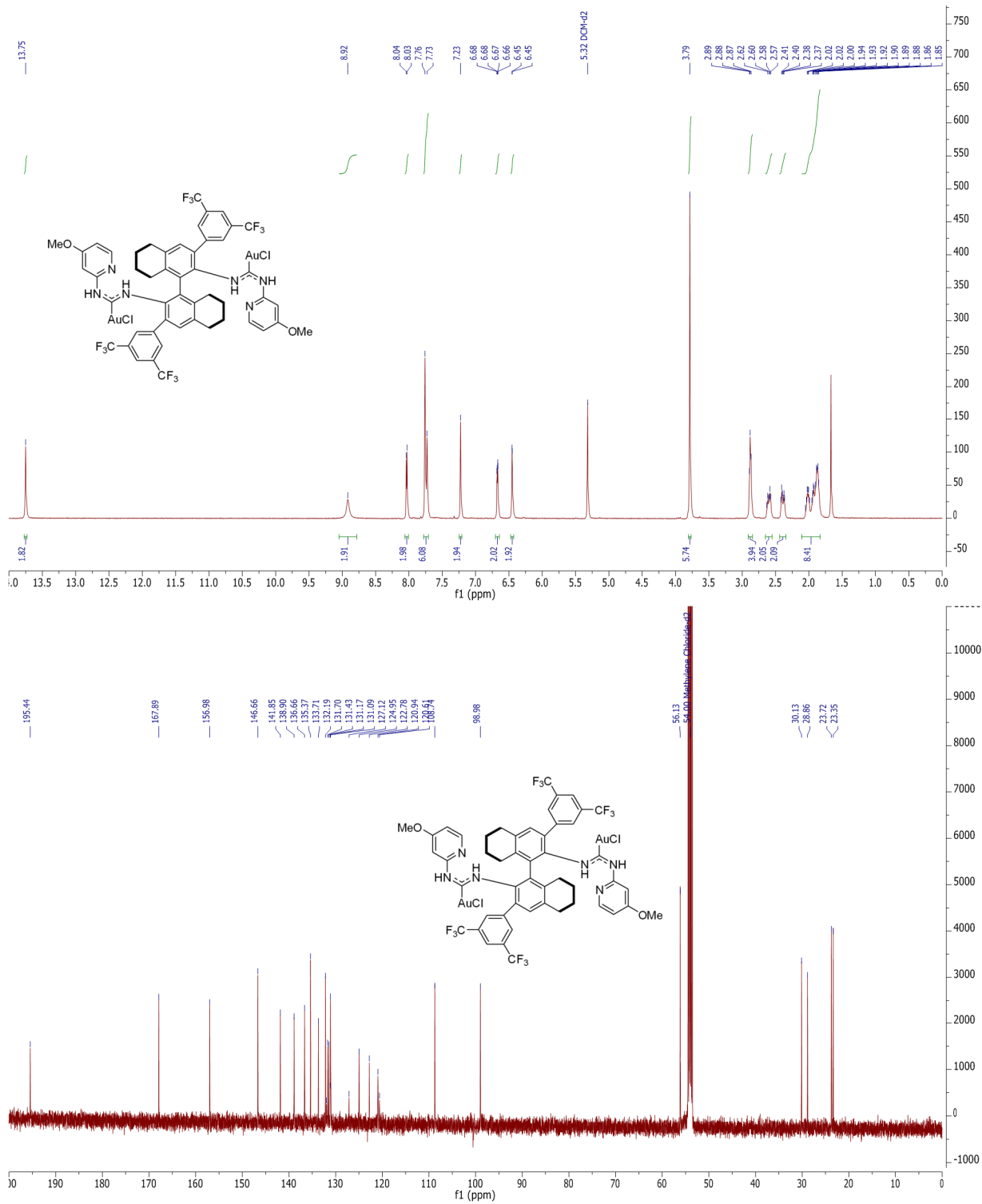
Complex 1.101



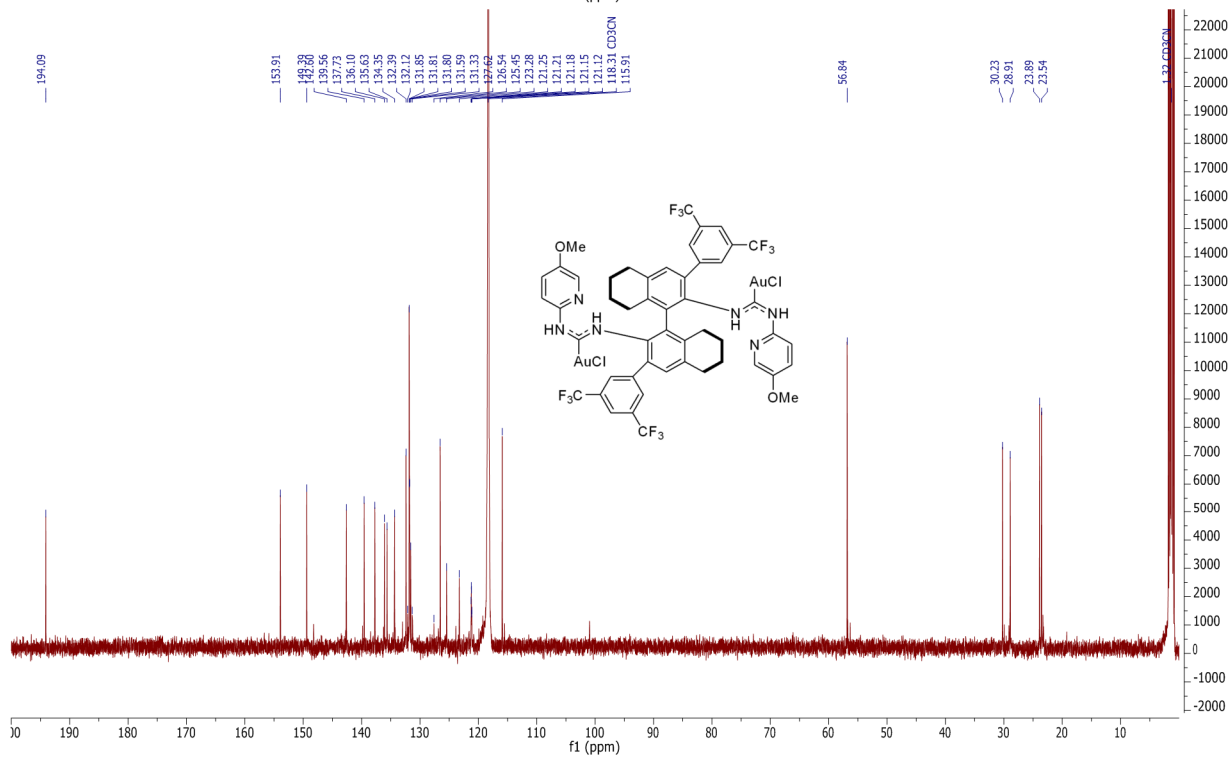
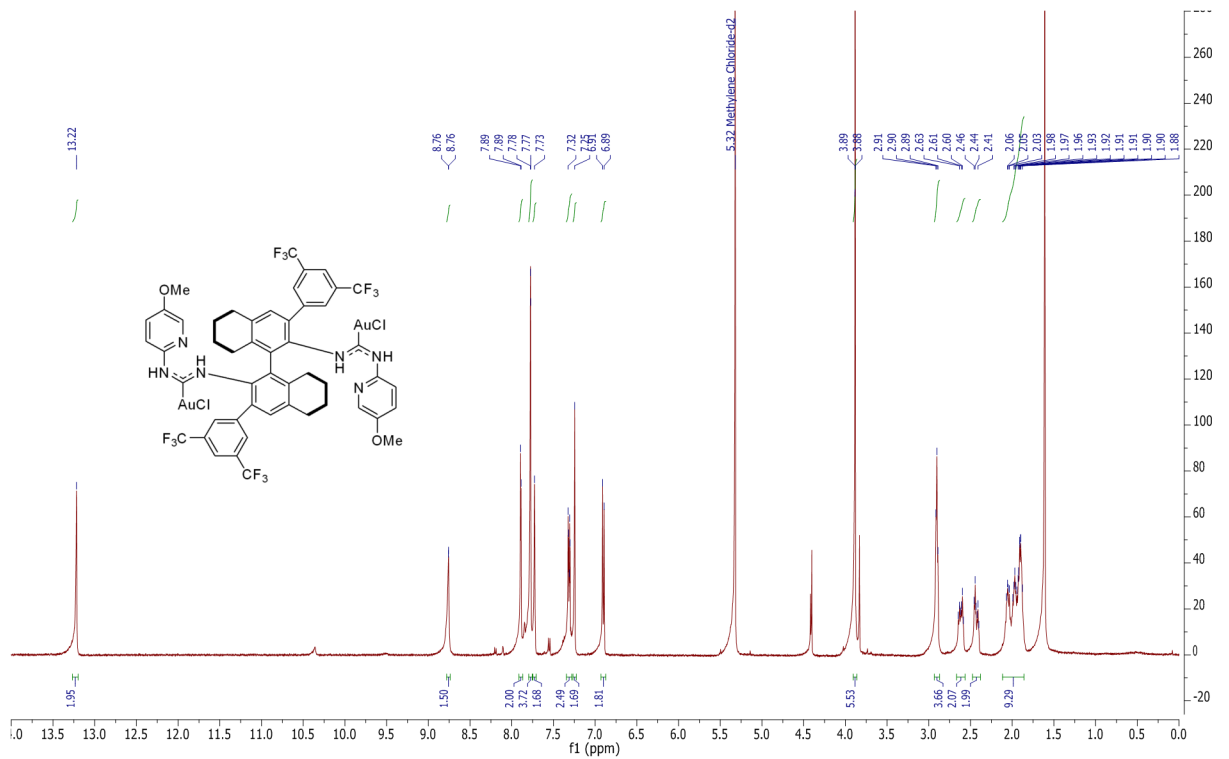
Complex 1.10m



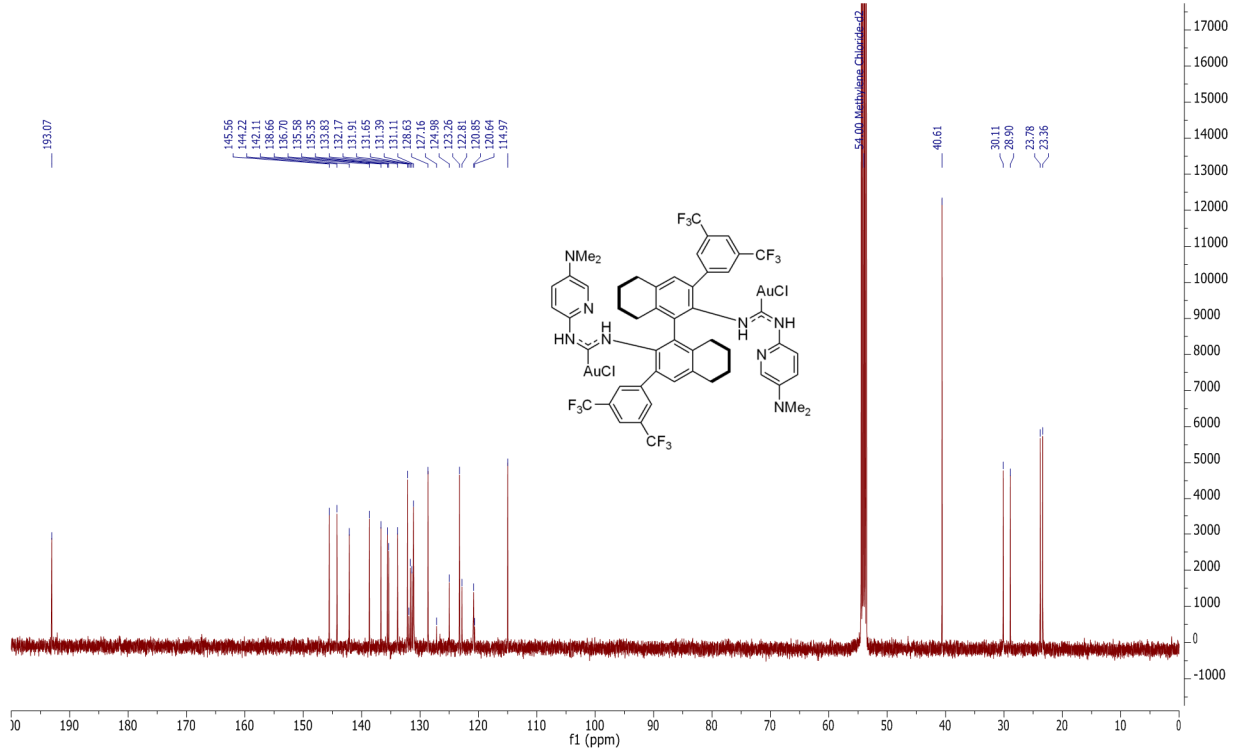
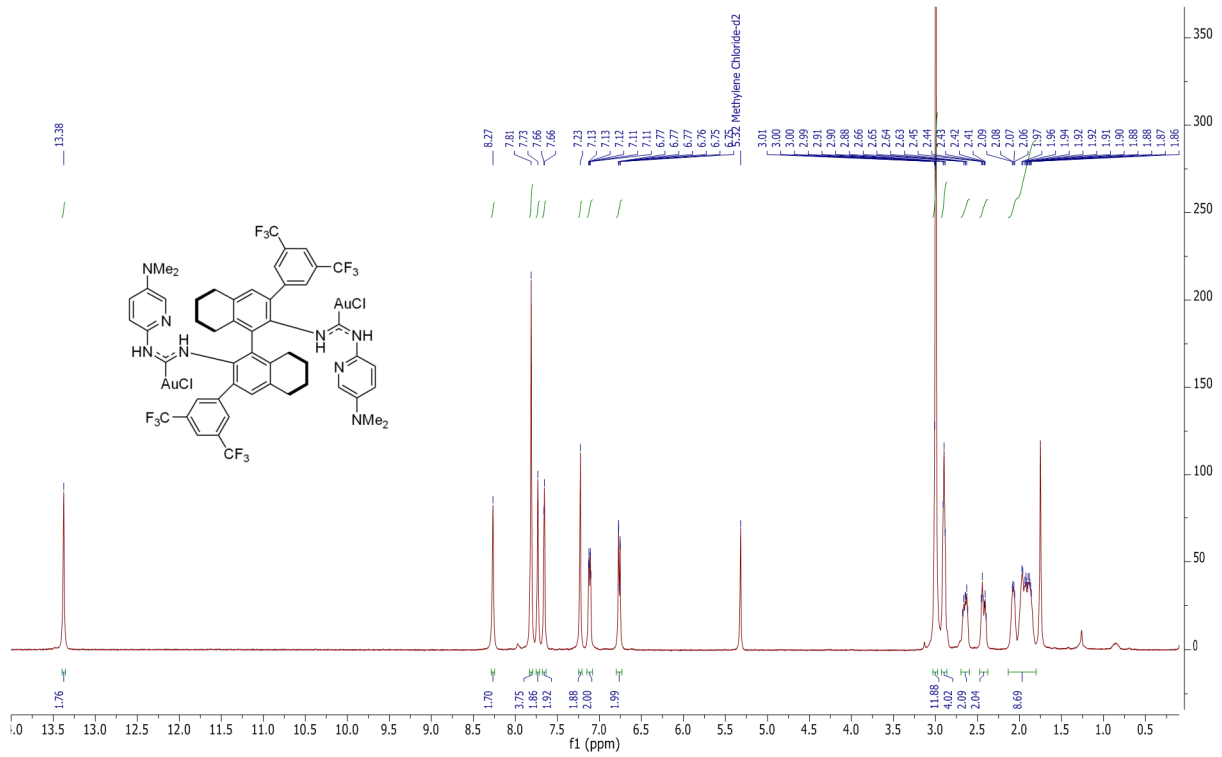
Complex 1.10n



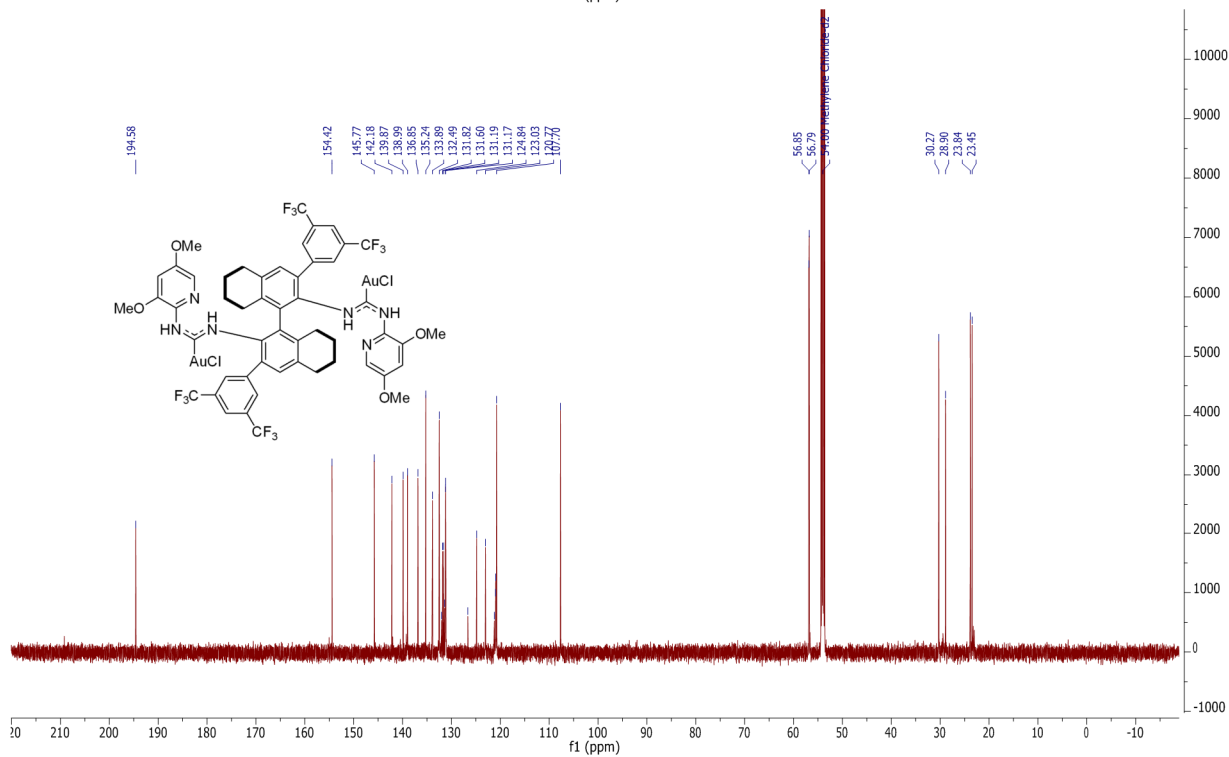
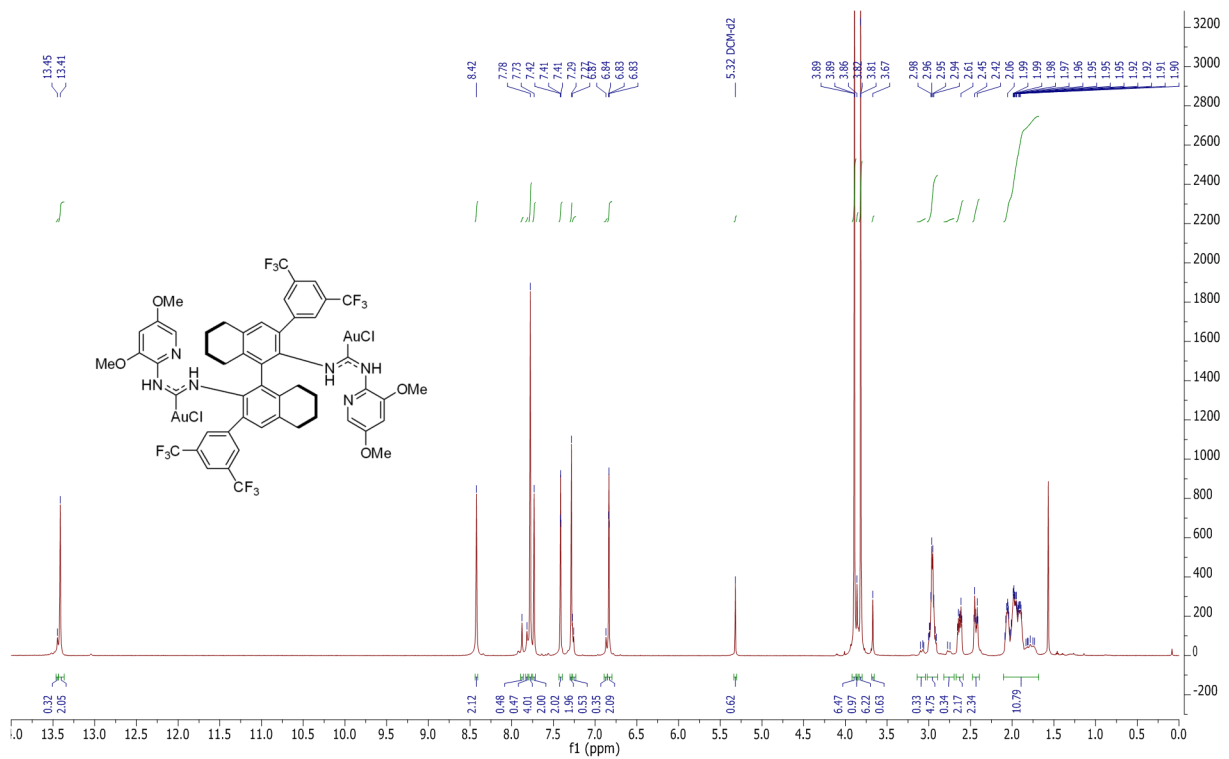
Complex 1.10o



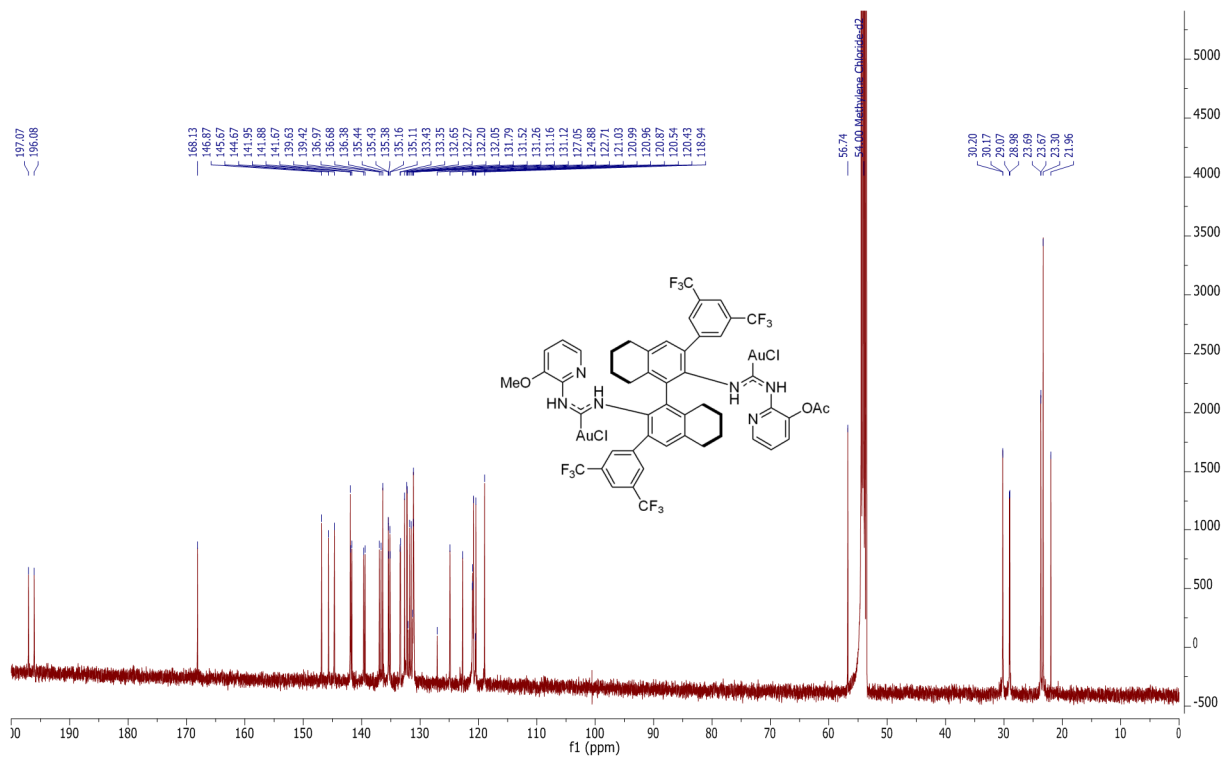
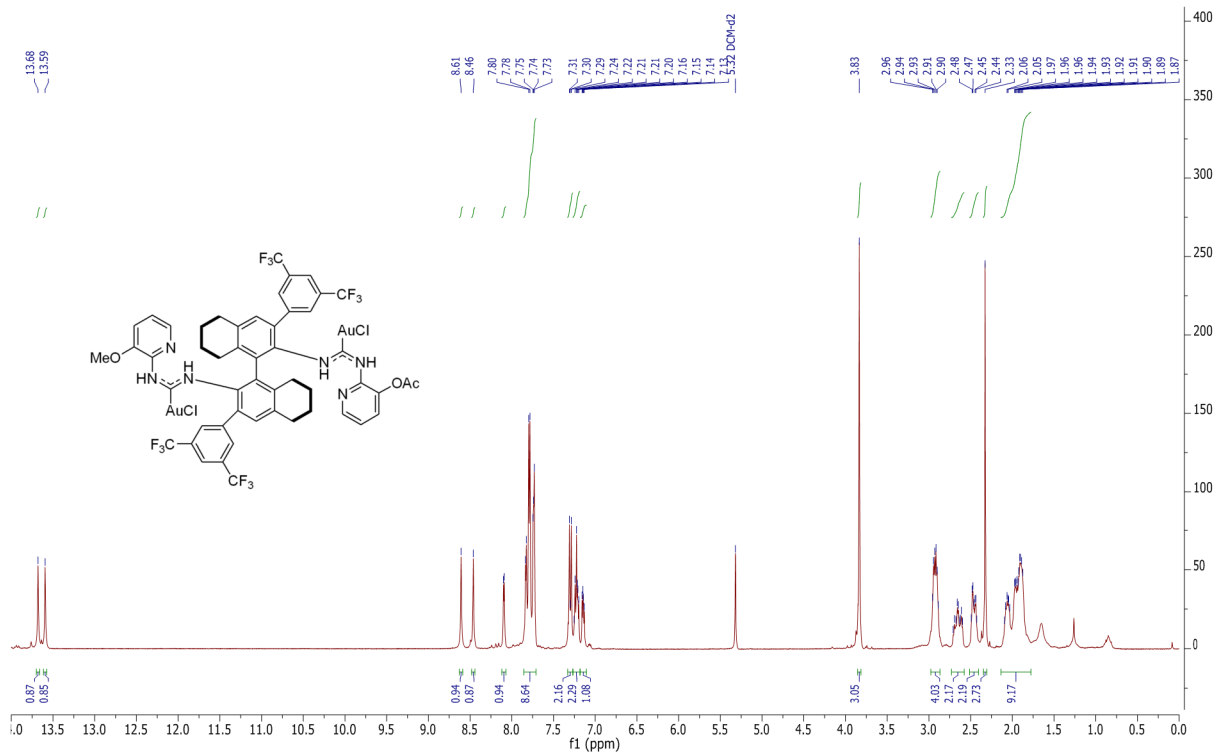
Complex 1.10p



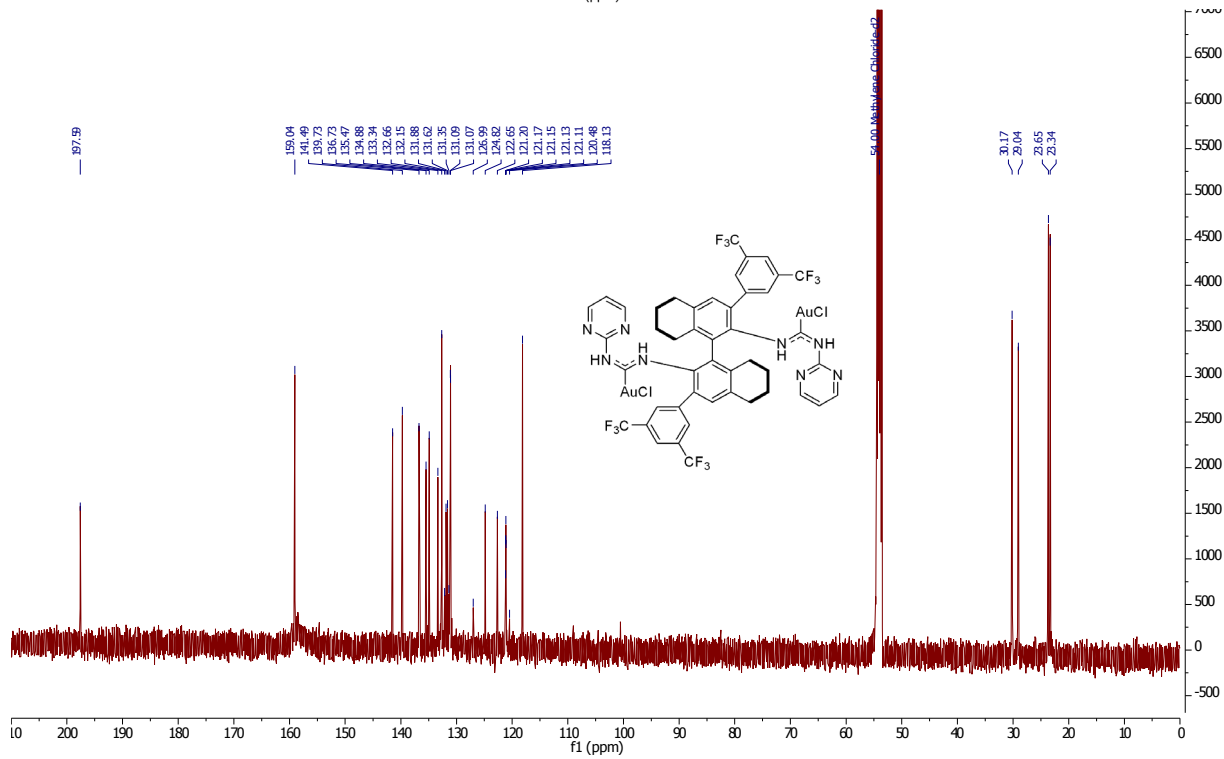
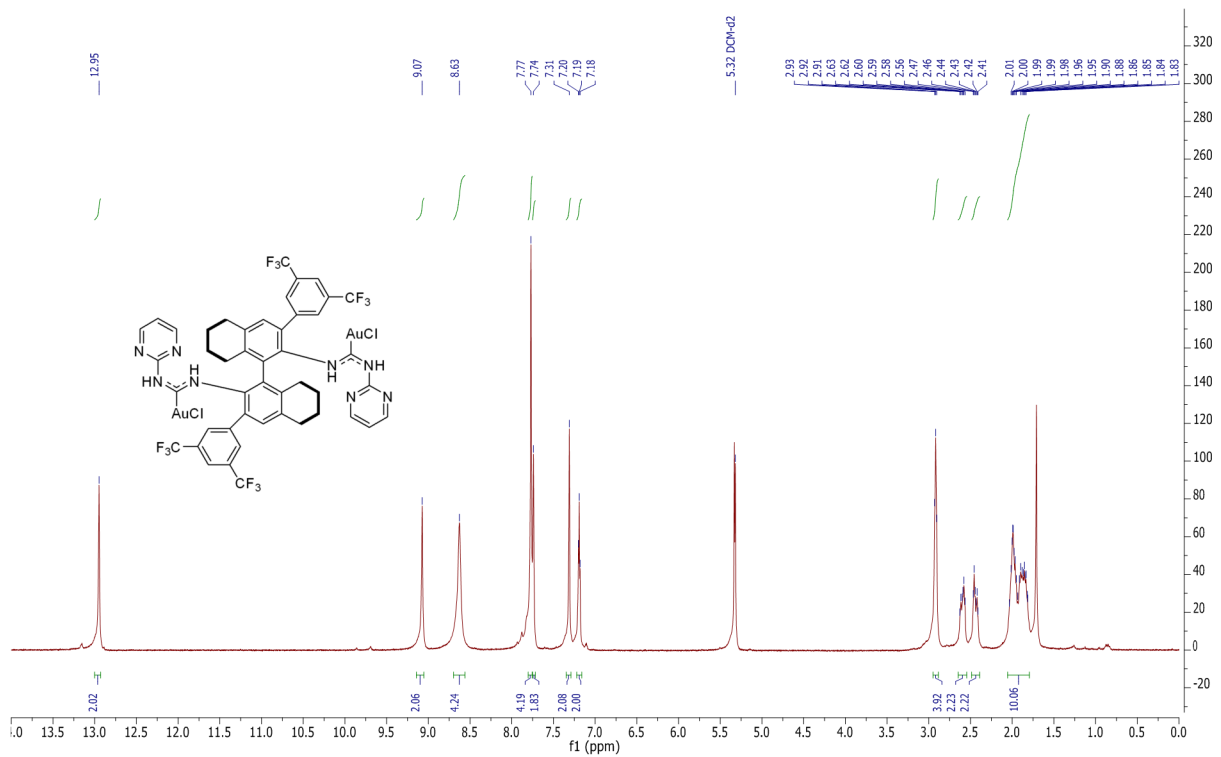
Complex 1.10q



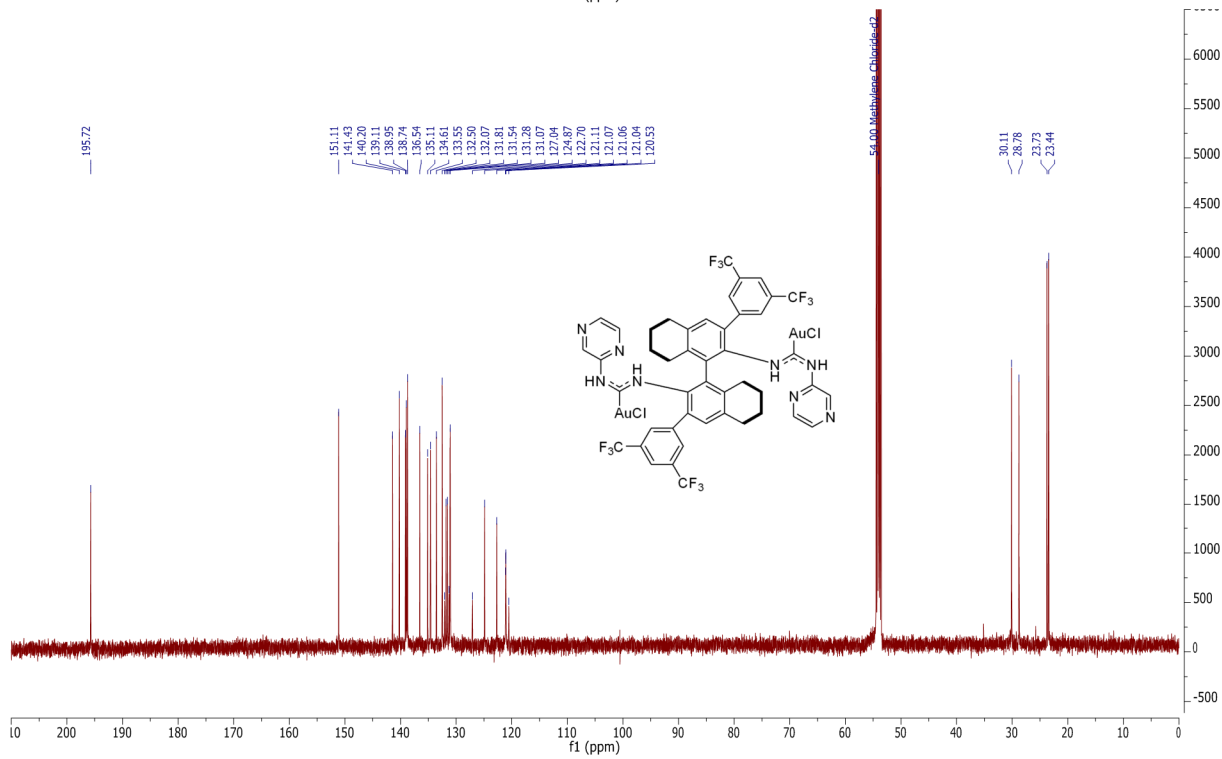
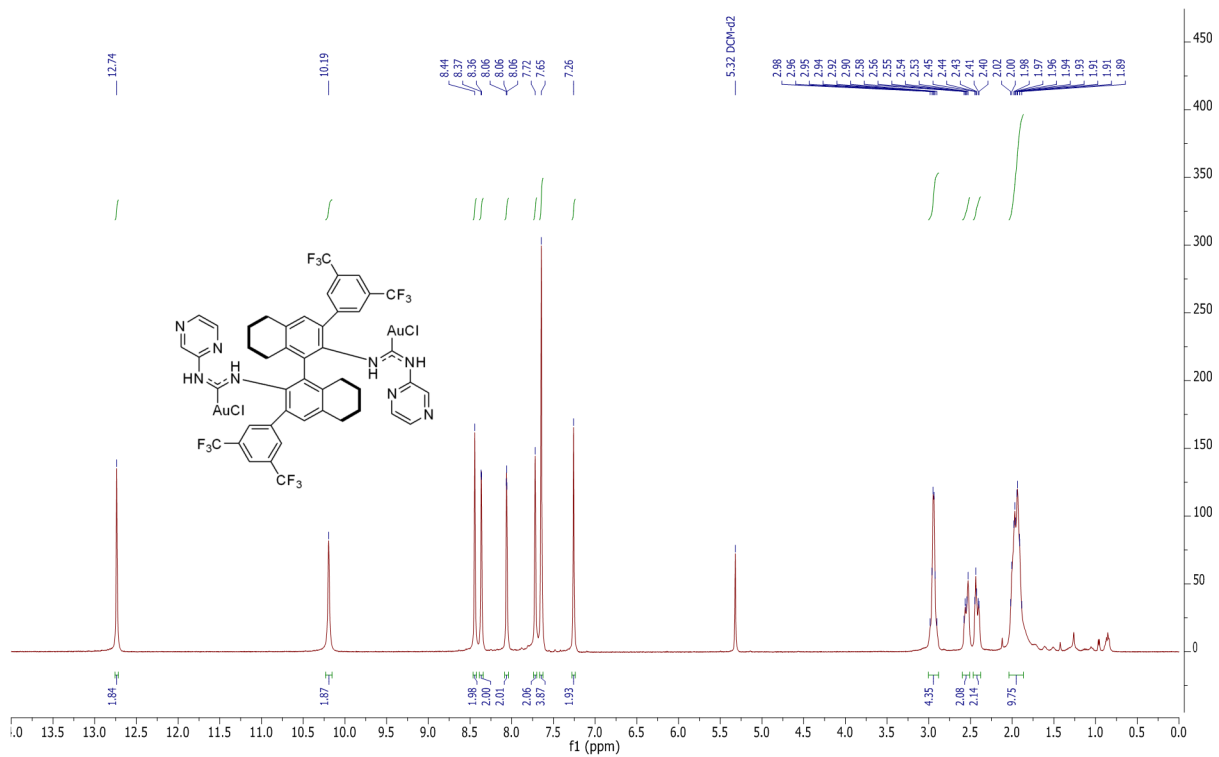
Complex 1.10r



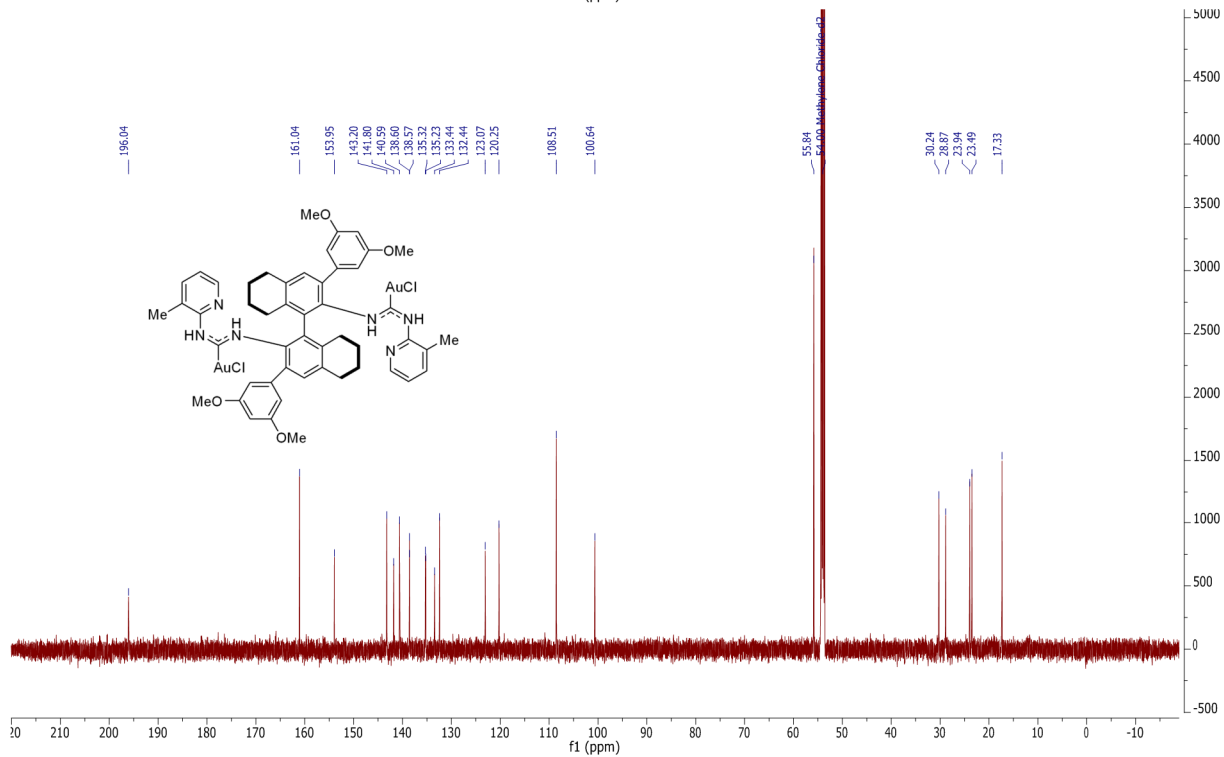
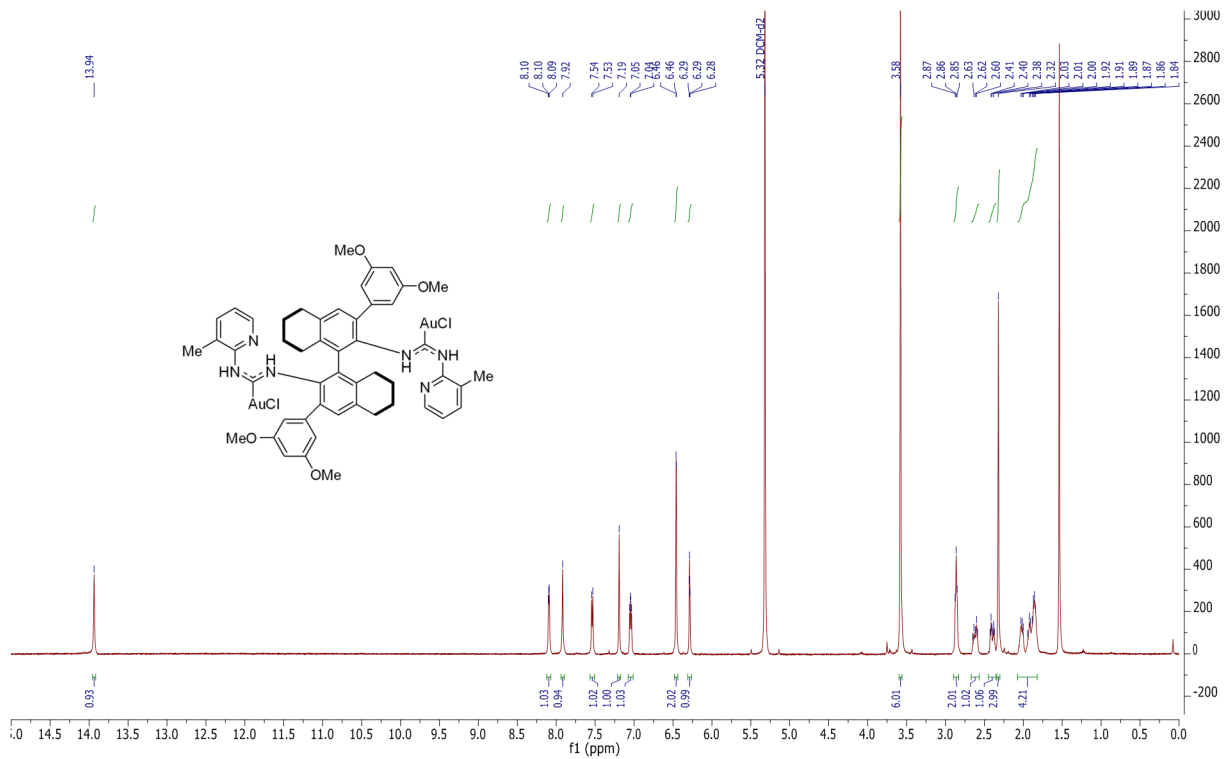
Complex 1.10s



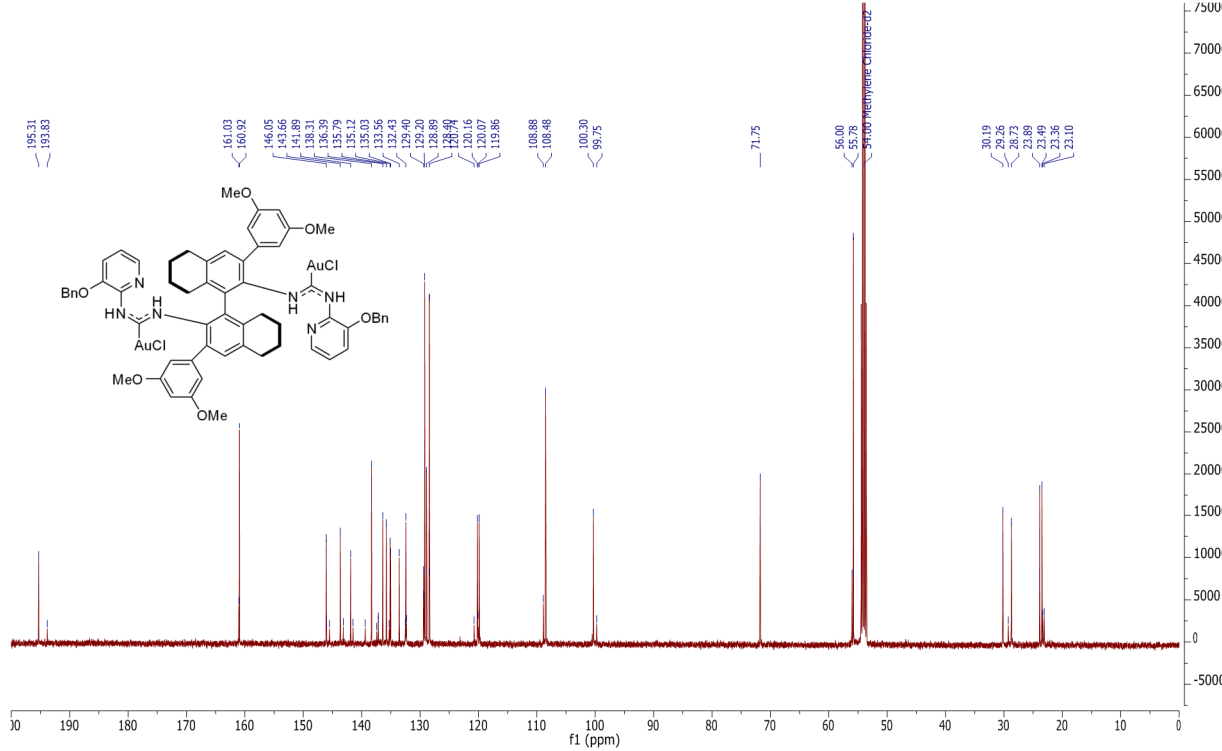
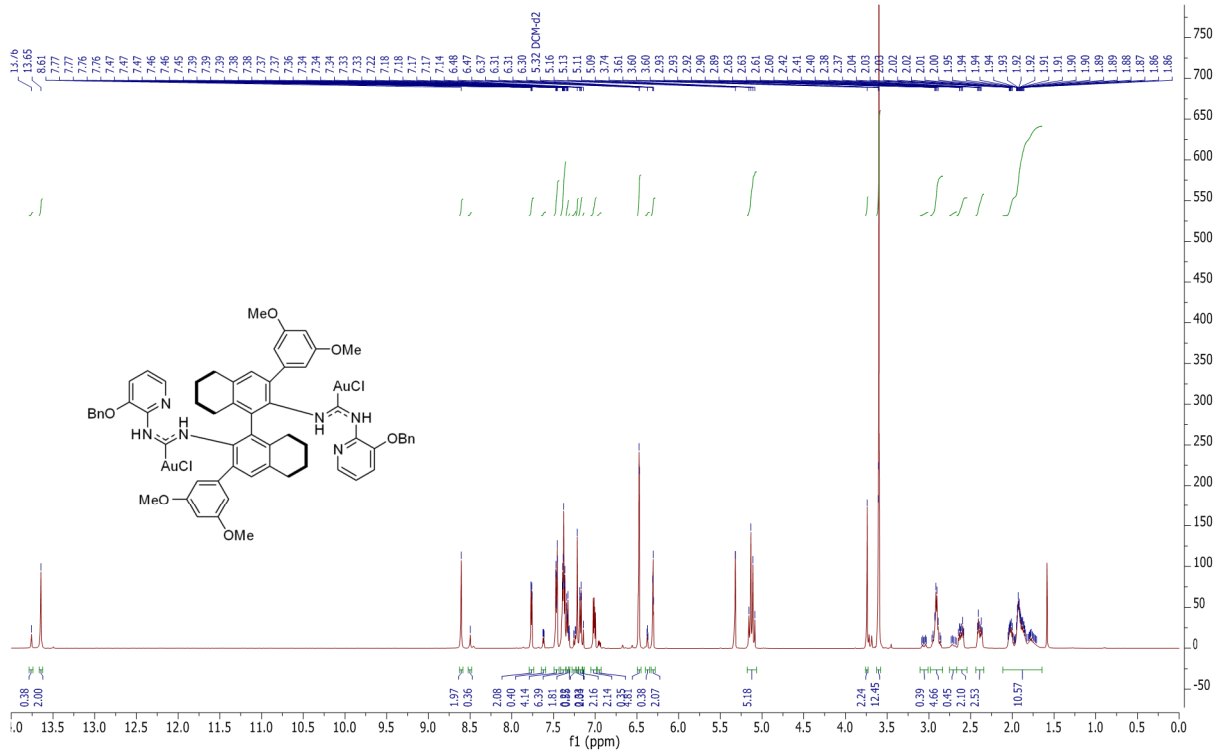
Complex 1.10t



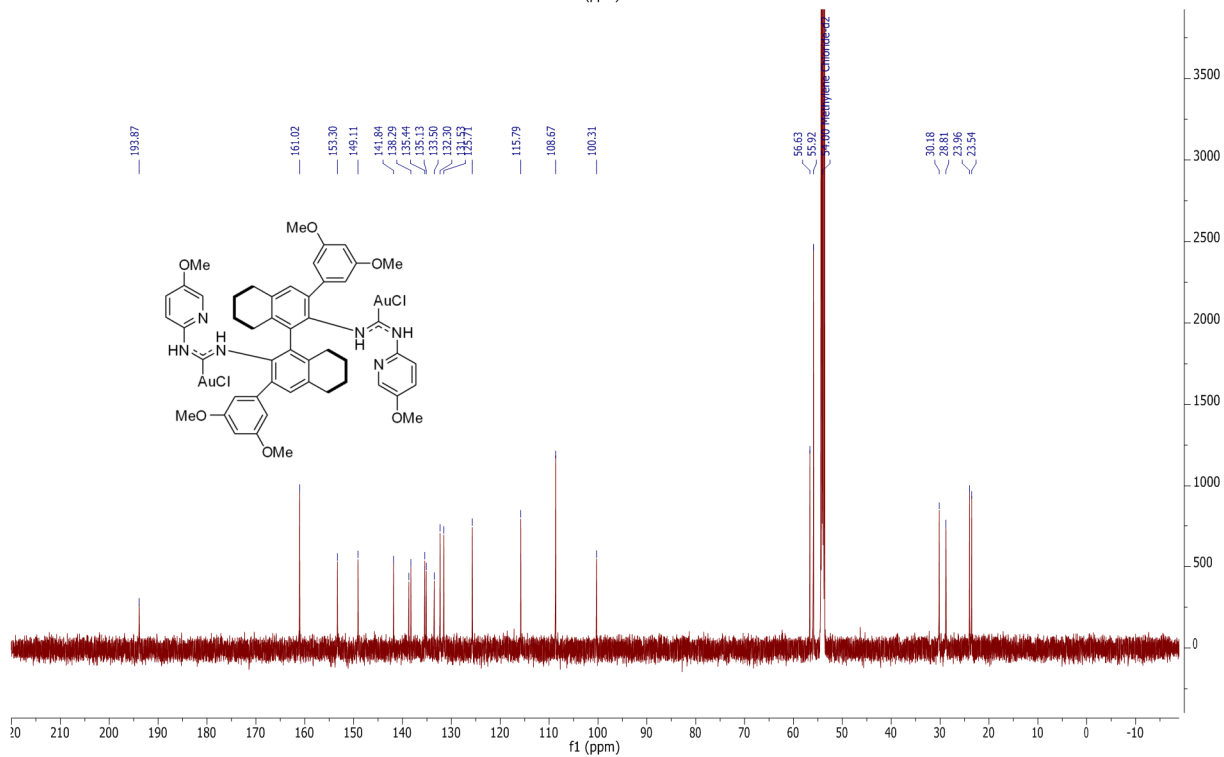
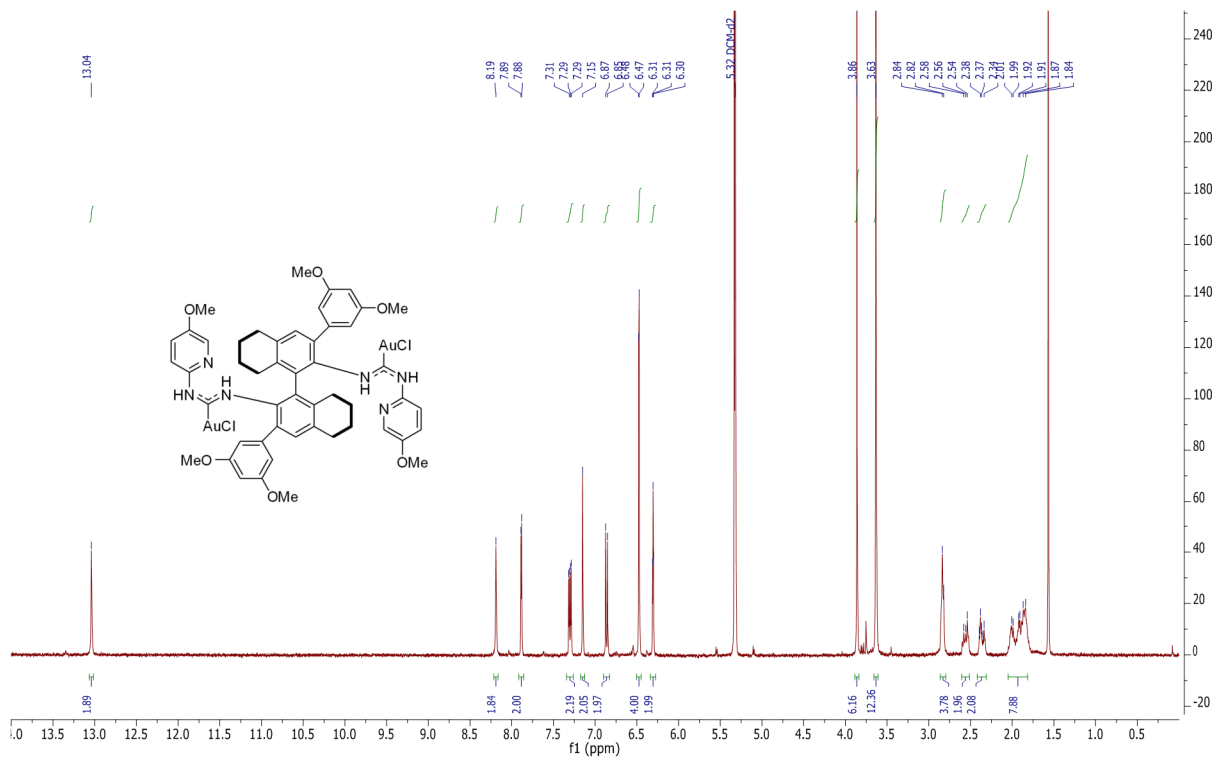
Complex 1.10u



Complex 1.10w

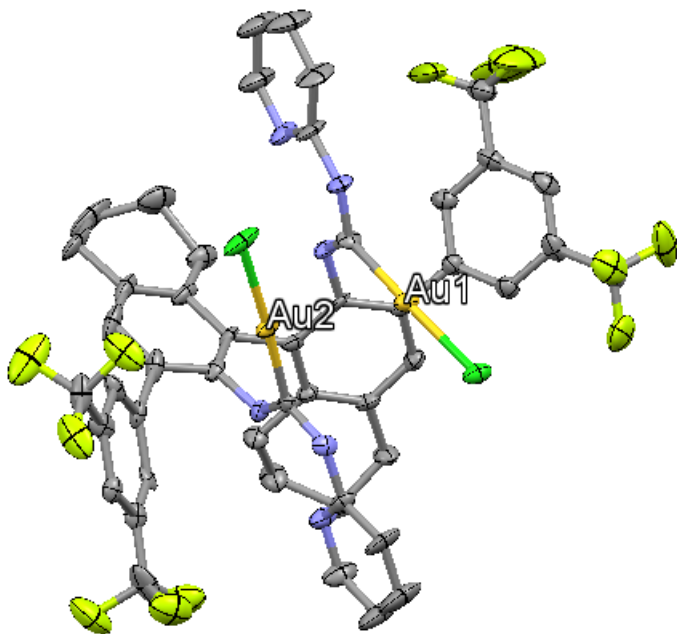


Complex 1.10x



Appendix 2 - Crystallographic Data

Thermal ellipsoid plot of **Complex 1.10e** (50% probability, hydrogen atoms omitted for clarity).



Crystallographic tables for **Complex 1.10e**

Table 1. Crystal data and structure refinement for dak002.

| | | |
|------------------------|---|----------|
| Identification code | shelx | |
| Empirical formula | C _{3.92} H _{2.78} Au _{0.16} Cl _{0.16} F _{0.98} N _{0.49} | |
| Formula weight | 113.28 | |
| Temperature | 100(2) K | |
| Wavelength | 0.71073 Å | |
| Crystal system | Orthorhombic | |
| Space group | P 21 21 2 | |
| Unit cell dimensions | a = 20.5902(11) Å | α = 90°. |
| | b = 22.9784(11) Å | β = 90°. |
| | c = 11.4576(6) Å | γ = 90°. |
| Volume | 5420.9(5) Å ³ | |
| Z | 49 | |
| Density (calculated) | 1.700 Mg/m ³ | |
| Absorption coefficient | 5.583 mm ⁻¹ | |
| F(000) | 2656 | |
| Crystal size | 0.050 x 0.050 x 0.050 mm ³ | |

| | |
|-----------------------------------|---|
| Theta range for data collection | 1.772 to 35.247°. |
| Index ranges | -32<=h<=33, -33<=k<=37, -18<=l<=18 |
| Reflections collected | 200842 |
| Independent reflections | 24200 [R(int) = 0.0494] |
| Completeness to theta = 25.000° | 100.0 % |
| Absorption correction | Semi-empirical from equivalents |
| Max. and min. transmission | 0.7452 and 0.5521 |
| Refinement method | Full-matrix least-squares on F ² |
| Data / restraints / parameters | 24200 / 30 / 746 |
| Goodness-of-fit on F ² | 1.080 |
| Final R indices [I>2sigma(I)] | R1 = 0.0446, wR2 = 0.1261 |
| R indices (all data) | R1 = 0.0612, wR2 = 0.1310 |
| Absolute structure parameter | 0.033(2) |
| Extinction coefficient | n/a |
| Largest diff. peak and hole | 2.374 and -2.734 e.Å ⁻³ |

Table 2. Atomic coordinates ($\times 10^4$) and equivalent isotropic displacement parameters ($\text{\AA}^2 \times 10^3$) for dak002. $U(\text{eq})$ is defined as one third of the trace of the orthogonalized U^{ij} tensor.

| | x | y | z | $U(\text{eq})$ |
|-------|----------|---------|----------|----------------|
| C(1) | 9503(4) | 3635(3) | 6708(6) | 23(1) |
| C(2) | 10950(3) | 3781(3) | 4540(5) | 19(1) |
| C(3) | 9366(5) | 3645(4) | 8849(6) | 35(2) |
| C(4) | 9196(6) | 4017(4) | 9777(7) | 51(3) |
| C(5) | 9111(8) | 3765(5) | 10861(8) | 65(4) |
| C(6) | 9199(8) | 3165(5) | 10998(8) | 69(4) |
| C(7) | 9360(7) | 2842(5) | 10049(7) | 53(3) |
| C(8) | 10878(4) | 3804(3) | 2404(6) | 26(1) |
| C(9) | 10822(5) | 4198(4) | 1464(6) | 43(2) |
| C(10) | 10837(8) | 3979(5) | 360(8) | 64(4) |
| C(11) | 10929(8) | 3395(4) | 192(8) | 55(3) |
| C(12) | 10975(6) | 3039(4) | 1146(7) | 41(2) |
| C(13) | 10722(3) | 2469(3) | 5982(5) | 21(1) |
| C(14) | 11167(4) | 2879(3) | 5585(6) | 24(1) |
| C(15) | 11766(4) | 2955(3) | 6164(8) | 32(2) |
| C(16) | 11862(5) | 2636(4) | 7207(9) | 42(2) |
| C(17) | 11420(5) | 2237(4) | 7623(7) | 36(2) |
| C(18) | 11577(6) | 1906(5) | 8743(7) | 52(3) |
| C(19) | 11138(9) | 1429(5) | 8992(9) | 73(5) |
| C(20) | 10463(7) | 1601(6) | 8756(9) | 58(3) |
| C(21) | 10340(5) | 1723(4) | 7427(8) | 40(2) |
| C(22) | 10841(5) | 2148(3) | 7008(6) | 32(2) |
| C(23) | 10100(3) | 2397(3) | 5314(5) | 20(1) |
| C(24) | 9546(3) | 2719(3) | 5640(5) | 17(1) |
| C(25) | 8979(4) | 2687(3) | 5015(5) | 20(1) |
| C(26) | 8967(3) | 2336(3) | 4008(6) | 25(1) |
| C(27) | 9510(4) | 2016(3) | 3658(6) | 24(1) |
| C(28) | 9456(4) | 1660(4) | 2574(6) | 31(2) |
| C(29) | 10083(4) | 1465(4) | 2084(7) | 33(2) |
| C(30) | 10498(5) | 1211(4) | 3097(9) | 38(2) |
| C(31) | 10652(4) | 1682(3) | 3968(7) | 30(1) |

| | | | | |
|--------|-----------|----------|----------|--------|
| C(32) | 10067(3) | 2035(3) | 4314(6) | 21(1) |
| C(33) | 8382(3) | 3011(3) | 5340(7) | 25(1) |
| C(34) | 8088(4) | 3371(3) | 4542(7) | 27(2) |
| C(35) | 7560(4) | 3713(4) | 4847(9) | 32(2) |
| C(36) | 7334(4) | 3705(4) | 5987(9) | 33(2) |
| C(37) | 7625(4) | 3343(4) | 6800(8) | 30(2) |
| C(38) | 8145(4) | 2994(4) | 6482(7) | 28(1) |
| C(39) | 7260(4) | 4146(4) | 4013(11) | 45(2) |
| C(40) | 7381(5) | 3326(5) | 8035(8) | 39(2) |
| N(1) | 10874(3) | 4038(2) | 3536(5) | 23(1) |
| N(2) | 11036(3) | 3194(3) | 4565(5) | 21(1) |
| N(3) | 9579(3) | 3059(3) | 6685(5) | 23(1) |
| N(4) | 9426(3) | 3892(3) | 7743(5) | 26(1) |
| N(5) | 10947(4) | 3237(3) | 2254(6) | 31(1) |
| N(6) | 9441(4) | 3070(3) | 8963(6) | 36(2) |
| F(1) | 6615(3) | 4141(4) | 4026(8) | 79(3) |
| F(2) | 7420(4) | 4002(3) | 2893(6) | 60(2) |
| F(3) | 7456(4) | 4665(3) | 4173(7) | 56(2) |
| F(4) | 7047(7) | 3783(6) | 8319(9) | 134(6) |
| F(5) | 7796(5) | 3236(8) | 8776(6) | 146(7) |
| F(6) | 6936(6) | 2928(6) | 8151(7) | 120(5) |
| Cl(1) | 9228(1) | 4568(1) | 3503(2) | 29(1) |
| Cl(2) | 10985(2) | 4763(1) | 7722(2) | 47(1) |
| Au(1) | 9411(1) | 4104(1) | 5242(1) | 23(1) |
| Au(2) | 10946(1) | 4248(1) | 6014(1) | 25(1) |
| C(48) | 13253(10) | 4694(8) | 6540(20) | 40(5) |
| F(10) | 12749(8) | 5023(7) | 6906(18) | 56(5) |
| F(11) | 13640(6) | 5045(6) | 5909(19) | 62(5) |
| F(12) | 13527(15) | 4496(7) | 7527(19) | 85(8) |
| C(41) | 12312(6) | 3364(5) | 5557(13) | 24(4) |
| C(42) | 12572(7) | 3804(6) | 6247(10) | 28(4) |
| C(43) | 13017(6) | 4193(5) | 5775(12) | 30(5) |
| C(44) | 13203(5) | 4142(4) | 4613(12) | 24(3) |
| C(45) | 12944(6) | 3702(5) | 3924(10) | 25(3) |
| C(46) | 12499(6) | 3313(5) | 4396(12) | 21(3) |
| C(47A) | 13160(11) | 3665(14) | 2720(40) | 53(9) |

| | | | | |
|--------|-----------|----------|----------|---------|
| F(7) | 13730(12) | 3349(10) | 2600(30) | 77(7) |
| F(8) | 13202(9) | 4138(8) | 2134(17) | 67(5) |
| F(9) | 12751(10) | 3352(9) | 2080(17) | 65(5) |
| C(44A) | 13165(12) | 4191(10) | 5410(30) | 46(7) |
| C(43A) | 12908(8) | 4188(8) | 6510(20) | 44(5) |
| C(42A) | 12428(9) | 3782(7) | 6790(30) | 41(5) |
| C(45A) | 12965(10) | 3810(11) | 4560(20) | 48(5) |
| C(46A) | 12489(10) | 3394(9) | 4877(17) | 31(4) |
| C(41A) | 12235(11) | 3388(10) | 5985(18) | 32(4) |
| F(12A) | 13199(9) | 4375(7) | 8487(19) | 82(6) |
| F(11A) | 13700(10) | 4845(10) | 7070(30) | 127(11) |
| F(10A) | 12661(15) | 5032(10) | 7670(30) | 146(14) |
| C(48A) | 13069(12) | 4632(11) | 7510(40) | 68(9) |
| F(8A) | 13294(12) | 4322(7) | 3000(20) | 103(9) |
| C(47) | 13257(15) | 3840(13) | 3490(30) | 64(7) |
| F(7A) | 13792(17) | 3556(18) | 3270(30) | 160(19) |
| F(9A) | 12930(20) | 3532(16) | 2700(30) | 150(17) |

Table 3. Bond lengths [Å] and angles [°] for dak002.

| | |
|--------------|-----------|
| C(1)-N(3) | 1.335(9) |
| C(1)-N(4) | 1.335(8) |
| C(1)-Au(1) | 2.003(7) |
| C(2)-N(1) | 1.303(8) |
| C(2)-N(2) | 1.359(9) |
| C(2)-Au(2) | 2.000(6) |
| C(3)-N(6) | 1.337(11) |
| C(3)-N(4) | 1.393(9) |
| C(3)-C(4) | 1.409(10) |
| C(4)-C(5) | 1.382(14) |
| C(5)-C(6) | 1.398(17) |
| C(6)-C(7) | 1.358(13) |
| C(7)-N(6) | 1.360(11) |
| C(8)-N(5) | 1.322(10) |
| C(8)-N(1) | 1.404(9) |
| C(8)-C(9) | 1.412(10) |
| C(9)-C(10) | 1.363(12) |
| C(10)-C(11) | 1.369(15) |
| C(11)-C(12) | 1.368(13) |
| C(12)-N(5) | 1.350(10) |
| C(13)-C(14) | 1.391(11) |
| C(13)-C(22) | 1.410(9) |
| C(13)-C(23) | 1.502(9) |
| C(14)-N(2) | 1.401(9) |
| C(14)-C(15) | 1.412(10) |
| C(15)-C(41A) | 1.40(2) |
| C(15)-C(16) | 1.417(12) |
| C(15)-C(41) | 1.622(13) |
| C(16)-C(17) | 1.377(15) |
| C(17)-C(22) | 1.399(12) |
| C(17)-C(18) | 1.527(11) |
| C(18)-C(19) | 1.45(2) |
| C(19)-C(20) | 1.47(2) |
| C(20)-C(21) | 1.570(14) |

| | |
|-------------|------------|
| C(21)-C(22) | 1.499(14) |
| C(23)-C(24) | 1.409(9) |
| C(23)-C(32) | 1.418(9) |
| C(24)-C(25) | 1.370(9) |
| C(24)-N(3) | 1.431(8) |
| C(25)-C(26) | 1.407(9) |
| C(25)-C(33) | 1.486(10) |
| C(26)-C(27) | 1.398(10) |
| C(27)-C(32) | 1.372(10) |
| C(27)-C(28) | 1.492(10) |
| C(28)-C(29) | 1.478(12) |
| C(29)-C(30) | 1.554(13) |
| C(30)-C(31) | 1.506(11) |
| C(31)-C(32) | 1.506(10) |
| C(33)-C(34) | 1.373(11) |
| C(33)-C(38) | 1.397(11) |
| C(34)-C(35) | 1.387(11) |
| C(35)-C(36) | 1.388(13) |
| C(35)-C(39) | 1.511(13) |
| C(36)-C(37) | 1.384(13) |
| C(37)-C(38) | 1.388(11) |
| C(37)-C(40) | 1.502(12) |
| C(39)-F(3) | 1.272(13) |
| C(39)-F(1) | 1.328(11) |
| C(39)-F(2) | 1.366(14) |
| C(40)-F(5) | 1.222(13) |
| C(40)-F(4) | 1.297(14) |
| C(40)-F(6) | 1.302(14) |
| Cl(1)-Au(1) | 2.2917(18) |
| Cl(2)-Au(2) | 2.2886(19) |
| Au(1)-Au(2) | 3.2988(4) |
| C(48)-F(11) | 1.34(3) |
| C(48)-F(10) | 1.35(3) |
| C(48)-F(12) | 1.35(3) |
| C(48)-C(43) | 1.52(2) |
| C(41)-C(42) | 1.3900 |

| | |
|-----------------|-----------|
| C(41)-C(46) | 1.3900 |
| C(42)-C(43) | 1.3900 |
| C(43)-C(44) | 1.3900 |
| C(44)-C(45) | 1.3900 |
| C(45)-C(46) | 1.3900 |
| C(45)-C(47A) | 1.45(5) |
| C(47A)-F(9) | 1.33(5) |
| C(47A)-F(8) | 1.28(3) |
| C(47A)-F(7) | 1.39(4) |
| C(44A)-C(43A) | 1.36(4) |
| C(44A)-C(45A) | 1.37(4) |
| C(43A)-C(42A) | 1.40(3) |
| C(43A)-C(48A) | 1.57(4) |
| C(42A)-C(41A) | 1.35(3) |
| C(45A)-C(47) | 1.38(3) |
| C(45A)-C(46A) | 1.41(3) |
| C(46A)-C(41A) | 1.37(2) |
| F(12A)-C(48A) | 1.30(4) |
| F(11A)-C(48A) | 1.48(4) |
| F(10A)-C(48A) | 1.26(3) |
| F(8A)-C(47) | 1.24(3) |
| C(47)-F(7A) | 1.30(4) |
| C(47)-F(9A) | 1.33(5) |
| | |
| N(3)-C(1)-N(4) | 118.0(7) |
| N(3)-C(1)-Au(1) | 121.8(5) |
| N(4)-C(1)-Au(1) | 119.8(5) |
| N(1)-C(2)-N(2) | 118.9(6) |
| N(1)-C(2)-Au(2) | 120.1(5) |
| N(2)-C(2)-Au(2) | 121.0(4) |
| N(6)-C(3)-N(4) | 118.8(7) |
| N(6)-C(3)-C(4) | 123.7(7) |
| N(4)-C(3)-C(4) | 117.4(8) |
| C(5)-C(4)-C(3) | 117.1(9) |
| C(4)-C(5)-C(6) | 119.9(9) |
| C(7)-C(6)-C(5) | 118.7(10) |

| | |
|--------------------|-----------|
| C(6)-C(7)-N(6) | 123.6(10) |
| N(5)-C(8)-N(1) | 119.9(6) |
| N(5)-C(8)-C(9) | 122.8(7) |
| N(1)-C(8)-C(9) | 117.3(7) |
| C(10)-C(9)-C(8) | 118.0(9) |
| C(9)-C(10)-C(11) | 119.7(9) |
| C(10)-C(11)-C(12) | 118.9(9) |
| N(5)-C(12)-C(11) | 123.1(8) |
| C(14)-C(13)-C(22) | 120.9(7) |
| C(14)-C(13)-C(23) | 118.0(6) |
| C(22)-C(13)-C(23) | 121.0(7) |
| C(13)-C(14)-N(2) | 119.7(6) |
| C(13)-C(14)-C(15) | 120.3(7) |
| N(2)-C(14)-C(15) | 119.8(7) |
| C(14)-C(15)-C(41A) | 128.4(11) |
| C(14)-C(15)-C(16) | 117.1(8) |
| C(41A)-C(15)-C(16) | 113.2(11) |
| C(14)-C(15)-C(41) | 118.4(8) |
| C(16)-C(15)-C(41) | 124.4(8) |
| C(17)-C(16)-C(15) | 122.9(8) |
| C(16)-C(17)-C(22) | 119.2(7) |
| C(16)-C(17)-C(18) | 118.8(9) |
| C(22)-C(17)-C(18) | 122.0(10) |
| C(19)-C(18)-C(17) | 114.2(9) |
| C(18)-C(19)-C(20) | 110.5(9) |
| C(19)-C(20)-C(21) | 112.2(10) |
| C(22)-C(21)-C(20) | 108.5(9) |
| C(17)-C(22)-C(13) | 119.4(8) |
| C(17)-C(22)-C(21) | 121.4(7) |
| C(13)-C(22)-C(21) | 119.2(8) |
| C(24)-C(23)-C(32) | 118.9(6) |
| C(24)-C(23)-C(13) | 119.9(6) |
| C(32)-C(23)-C(13) | 121.1(6) |
| C(25)-C(24)-C(23) | 121.5(6) |
| C(25)-C(24)-N(3) | 120.5(6) |
| C(23)-C(24)-N(3) | 117.9(6) |

| | |
|-------------------|-----------|
| C(24)-C(25)-C(26) | 118.4(6) |
| C(24)-C(25)-C(33) | 123.1(6) |
| C(26)-C(25)-C(33) | 118.5(6) |
| C(25)-C(26)-C(27) | 121.4(6) |
| C(32)-C(27)-C(26) | 119.6(6) |
| C(32)-C(27)-C(28) | 122.5(7) |
| C(26)-C(27)-C(28) | 117.9(7) |
| C(29)-C(28)-C(27) | 114.6(7) |
| C(28)-C(29)-C(30) | 108.1(7) |
| C(31)-C(30)-C(29) | 110.0(8) |
| C(32)-C(31)-C(30) | 113.1(7) |
| C(27)-C(32)-C(23) | 120.1(6) |
| C(27)-C(32)-C(31) | 120.5(6) |
| C(23)-C(32)-C(31) | 119.4(6) |
| C(34)-C(33)-C(38) | 119.2(7) |
| C(34)-C(33)-C(25) | 120.0(6) |
| C(38)-C(33)-C(25) | 120.6(7) |
| C(33)-C(34)-C(35) | 121.3(7) |
| C(34)-C(35)-C(36) | 119.5(8) |
| C(34)-C(35)-C(39) | 122.3(8) |
| C(36)-C(35)-C(39) | 117.9(8) |
| C(37)-C(36)-C(35) | 119.8(7) |
| C(36)-C(37)-C(38) | 120.4(8) |
| C(36)-C(37)-C(40) | 120.3(8) |
| C(38)-C(37)-C(40) | 119.3(8) |
| C(37)-C(38)-C(33) | 119.9(8) |
| F(3)-C(39)-F(1) | 108.9(9) |
| F(3)-C(39)-F(2) | 106.6(8) |
| F(1)-C(39)-F(2) | 104.4(10) |
| F(3)-C(39)-C(35) | 113.3(10) |
| F(1)-C(39)-C(35) | 113.4(8) |
| F(2)-C(39)-C(35) | 109.6(8) |
| F(5)-C(40)-F(4) | 109.4(12) |
| F(5)-C(40)-F(6) | 107.6(12) |
| F(4)-C(40)-F(6) | 99.8(11) |
| F(5)-C(40)-C(37) | 115.2(8) |

| | |
|--------------------|-----------|
| F(4)-C(40)-C(37) | 113.1(10) |
| F(6)-C(40)-C(37) | 110.5(9) |
| C(2)-N(1)-C(8) | 129.9(6) |
| C(2)-N(2)-C(14) | 123.7(6) |
| C(1)-N(3)-C(24) | 123.6(6) |
| C(1)-N(4)-C(3) | 129.7(7) |
| C(8)-N(5)-C(12) | 117.3(7) |
| C(3)-N(6)-C(7) | 117.1(7) |
| C(1)-Au(1)-Cl(1) | 174.0(2) |
| C(1)-Au(1)-Au(2) | 74.8(2) |
| Cl(1)-Au(1)-Au(2) | 110.13(5) |
| C(2)-Au(2)-Cl(2) | 177.4(2) |
| C(2)-Au(2)-Au(1) | 73.98(19) |
| Cl(2)-Au(2)-Au(1) | 108.37(8) |
| F(11)-C(48)-F(10) | 106.7(16) |
| F(11)-C(48)-F(12) | 114(2) |
| F(10)-C(48)-F(12) | 104(2) |
| F(11)-C(48)-C(43) | 110(2) |
| F(10)-C(48)-C(43) | 110.9(15) |
| F(12)-C(48)-C(43) | 111.2(15) |
| C(42)-C(41)-C(46) | 120.0 |
| C(42)-C(41)-C(15) | 116.4(9) |
| C(46)-C(41)-C(15) | 123.5(9) |
| C(43)-C(42)-C(41) | 120.0 |
| C(42)-C(43)-C(44) | 120.0 |
| C(42)-C(43)-C(48) | 118.3(13) |
| C(44)-C(43)-C(48) | 121.6(13) |
| C(45)-C(44)-C(43) | 120.0 |
| C(46)-C(45)-C(44) | 120.0 |
| C(46)-C(45)-C(47A) | 122.3(15) |
| C(44)-C(45)-C(47A) | 117.7(15) |
| C(45)-C(46)-C(41) | 120.0 |
| F(9)-C(47A)-F(8) | 102(3) |
| F(9)-C(47A)-F(7) | 101(3) |
| F(8)-C(47A)-F(7) | 110(2) |
| F(9)-C(47A)-C(45) | 111.3(18) |

| | |
|----------------------|-----------|
| F(8)-C(47A)-C(45) | 118(3) |
| F(7)-C(47A)-C(45) | 112(3) |
| C(43A)-C(44A)-C(45A) | 122(2) |
| C(44A)-C(43A)-C(42A) | 119(2) |
| C(44A)-C(43A)-C(48A) | 126(2) |
| C(42A)-C(43A)-C(48A) | 114(2) |
| C(41A)-C(42A)-C(43A) | 120(2) |
| C(47)-C(45A)-C(44A) | 118(3) |
| C(47)-C(45A)-C(46A) | 124(3) |
| C(44A)-C(45A)-C(46A) | 117(2) |
| C(41A)-C(46A)-C(45A) | 120(2) |
| C(42A)-C(41A)-C(46A) | 121(2) |
| C(42A)-C(41A)-C(15) | 125.4(18) |
| C(46A)-C(41A)-C(15) | 113.8(19) |
| F(10A)-C(48A)-F(12A) | 110(4) |
| F(10A)-C(48A)-F(11A) | 113(3) |
| F(12A)-C(48A)-F(11A) | 105(2) |
| F(10A)-C(48A)-C(43A) | 116(2) |
| F(12A)-C(48A)-C(43A) | 112(2) |
| F(11A)-C(48A)-C(43A) | 99(3) |
| F(8A)-C(47)-F(7A) | 108(3) |
| F(8A)-C(47)-F(9A) | 101(3) |
| F(7A)-C(47)-F(9A) | 92(4) |
| F(8A)-C(47)-C(45A) | 118(3) |
| F(7A)-C(47)-C(45A) | 121(3) |
| F(9A)-C(47)-C(45A) | 111(2) |

Symmetry transformations used to generate equivalent atoms:

Table 4. Anisotropic displacement parameters ($\text{\AA}^2 \times 10^3$) for dak002. The anisotropic displacement factor exponent takes the form: $-2\pi^2 [h^2 a^{*2} U^{11} + \dots + 2 h k a^* b^* U^{12}]$

| | U ¹¹ | U ²² | U ³³ | U ²³ | U ¹³ | U ¹² |
|-------|-----------------|-----------------|-----------------|-----------------|-----------------|-----------------|
| C(1) | 33(4) | 15(3) | 22(3) | -7(2) | 4(3) | 6(2) |
| C(2) | 14(2) | 24(3) | 17(2) | 0(2) | -2(2) | -2(2) |
| C(3) | 66(5) | 31(4) | 8(2) | -2(2) | -4(3) | 6(4) |
| C(4) | 98(9) | 37(5) | 19(3) | -17(3) | -2(4) | 15(5) |
| C(5) | 128(12) | 49(6) | 19(4) | -7(4) | 14(5) | 9(7) |
| C(6) | 133(13) | 57(7) | 15(3) | -1(4) | 3(5) | 24(7) |
| C(7) | 99(9) | 44(5) | 18(3) | 0(3) | 3(4) | 21(6) |
| C(8) | 35(4) | 25(3) | 18(3) | 7(2) | 0(3) | -4(3) |
| C(9) | 82(7) | 33(4) | 13(3) | 6(3) | -9(3) | -4(4) |
| C(10) | 123(12) | 50(6) | 18(3) | 7(4) | -13(5) | 4(7) |
| C(11) | 110(10) | 40(5) | 17(3) | 0(3) | -12(5) | 6(6) |
| C(12) | 72(6) | 24(4) | 26(4) | -3(3) | 2(4) | 6(4) |
| C(13) | 35(3) | 20(3) | 9(2) | 0(2) | -7(2) | 5(2) |
| C(14) | 33(3) | 19(3) | 19(3) | -5(2) | -9(2) | 6(3) |
| C(15) | 32(4) | 19(3) | 44(5) | -2(3) | -20(3) | 4(3) |
| C(16) | 56(5) | 24(4) | 45(5) | -1(3) | -34(4) | 10(4) |
| C(17) | 55(5) | 30(4) | 22(3) | -4(3) | -17(3) | 21(4) |
| C(18) | 90(8) | 45(6) | 21(4) | 1(3) | -24(4) | 31(5) |
| C(19) | 152(14) | 40(6) | 29(4) | 8(4) | -31(7) | 28(7) |
| C(20) | 90(9) | 49(6) | 36(5) | 18(5) | 12(5) | 11(6) |
| C(21) | 62(6) | 28(4) | 29(4) | 8(3) | 6(4) | 14(4) |
| C(22) | 55(5) | 24(3) | 15(3) | 3(2) | -5(3) | 15(3) |
| C(23) | 29(3) | 18(3) | 12(2) | 2(2) | 2(2) | 3(2) |
| C(24) | 29(3) | 16(3) | 6(2) | 2(2) | -4(2) | 6(2) |
| C(25) | 29(3) | 19(3) | 12(2) | 1(2) | 3(2) | 2(2) |
| C(26) | 25(3) | 28(3) | 21(3) | -3(3) | -5(3) | 0(2) |
| C(27) | 32(4) | 26(3) | 13(2) | -2(2) | 1(2) | -4(3) |
| C(28) | 32(4) | 39(4) | 22(3) | -13(3) | 1(3) | 1(3) |
| C(29) | 33(4) | 42(5) | 24(3) | -11(3) | 0(3) | -3(3) |
| C(30) | 37(4) | 35(5) | 43(5) | -19(4) | -6(4) | 2(3) |
| C(31) | 35(4) | 26(3) | 29(3) | -8(3) | -1(3) | 5(3) |

| | | | | | | |
|--------|---------|---------|---------|--------|---------|--------|
| C(32) | 26(3) | 21(3) | 16(2) | -3(2) | -1(2) | 2(2) |
| C(33) | 25(3) | 24(3) | 26(3) | 4(3) | 2(3) | 1(2) |
| C(34) | 25(3) | 28(4) | 28(3) | 4(3) | 5(3) | 0(3) |
| C(35) | 24(3) | 25(4) | 47(5) | 14(3) | 9(3) | 1(3) |
| C(36) | 32(4) | 25(4) | 43(4) | 0(4) | 10(3) | 7(3) |
| C(37) | 27(3) | 28(4) | 35(4) | -5(3) | 11(3) | -2(3) |
| C(38) | 29(3) | 26(4) | 27(3) | -1(3) | 5(3) | -4(3) |
| C(39) | 34(4) | 35(5) | 64(6) | 20(5) | 7(4) | 8(3) |
| C(40) | 36(4) | 49(6) | 34(4) | -6(4) | 11(3) | -1(4) |
| N(1) | 36(3) | 10(2) | 24(2) | 2(2) | 6(2) | 5(2) |
| N(2) | 23(3) | 21(3) | 20(2) | 1(2) | -5(2) | 2(2) |
| N(3) | 35(3) | 22(3) | 13(2) | -4(2) | -2(2) | 4(2) |
| N(4) | 38(3) | 28(3) | 12(2) | -6(2) | 0(2) | -1(3) |
| N(5) | 50(4) | 27(3) | 18(2) | -1(2) | 0(3) | 7(3) |
| N(6) | 58(4) | 36(4) | 15(2) | -4(3) | -9(3) | 11(3) |
| F(1) | 35(3) | 91(6) | 110(6) | 69(5) | 0(4) | 11(3) |
| F(2) | 66(4) | 64(5) | 51(4) | 24(3) | -13(3) | 16(3) |
| F(3) | 66(4) | 30(3) | 70(4) | 15(3) | 14(4) | 10(3) |
| F(4) | 191(13) | 148(11) | 64(6) | -2(6) | 61(7) | 99(10) |
| F(5) | 63(5) | 350(20) | 21(3) | -12(6) | 10(3) | 30(8) |
| F(6) | 126(8) | 188(13) | 46(4) | 1(6) | 38(5) | -85(9) |
| Cl(1) | 46(1) | 21(1) | 19(1) | 1(1) | 2(1) | 0(1) |
| Cl(2) | 98(2) | 27(1) | 16(1) | -1(1) | -13(1) | 10(1) |
| Au(1) | 32(1) | 19(1) | 18(1) | 0(1) | 4(1) | 0(1) |
| Au(2) | 38(1) | 20(1) | 17(1) | 2(1) | -5(1) | 5(1) |
| C(48) | 34(9) | 18(8) | 67(14) | 3(8) | -21(10) | -3(7) |
| F(10) | 47(8) | 27(7) | 95(13) | -17(8) | 19(9) | -17(6) |
| F(11) | 37(6) | 38(7) | 111(14) | -29(9) | -3(8) | -16(5) |
| F(12) | 150(20) | 25(7) | 74(13) | -4(8) | -53(14) | 1(11) |
| C(41) | 23(9) | 19(8) | 30(12) | 3(8) | -13(9) | 0(6) |
| C(42) | 19(8) | 21(8) | 44(11) | 11(7) | 5(7) | 4(6) |
| C(43) | 37(13) | 15(9) | 39(11) | 9(8) | 9(9) | 6(8) |
| C(44) | 28(7) | 16(7) | 29(8) | 3(6) | -6(6) | 1(6) |
| C(45) | 29(8) | 12(6) | 32(9) | 1(6) | -3(8) | 1(5) |
| C(46) | 14(6) | 15(7) | 34(9) | -1(7) | 3(7) | 7(5) |
| C(47A) | 23(9) | 45(14) | 90(30) | 20(16) | 16(12) | -7(9) |

| | | | | | | |
|--------|---------|---------|---------|---------|---------|---------|
| F(7) | 56(10) | 60(12) | 110(20) | 6(12) | 40(12) | 16(8) |
| F(8) | 88(11) | 46(9) | 67(11) | 17(8) | 28(9) | 7(8) |
| F(9) | 83(12) | 65(11) | 48(9) | 2(8) | 12(9) | -25(9) |
| C(44A) | 31(9) | 17(8) | 90(20) | 16(11) | -4(13) | -8(7) |
| C(43A) | 28(7) | 24(8) | 81(15) | 3(10) | -12(9) | 5(6) |
| C(42A) | 23(8) | 12(6) | 88(16) | -6(9) | -4(9) | -12(5) |
| C(45A) | 39(10) | 45(12) | 60(14) | 14(11) | 11(10) | 7(9) |
| C(46A) | 35(8) | 36(10) | 23(8) | 12(7) | 8(8) | 10(7) |
| C(41A) | 33(8) | 35(9) | 28(10) | 9(8) | -2(8) | 6(6) |
| F(12A) | 101(12) | 43(8) | 101(14) | -5(8) | -38(11) | -22(8) |
| F(11A) | 72(12) | 85(16) | 220(30) | 1(19) | -21(16) | -54(11) |
| F(10A) | 160(20) | 69(14) | 210(30) | -78(19) | -90(20) | 72(15) |
| C(48A) | 43(12) | 33(11) | 130(30) | 7(14) | -27(15) | -1(9) |
| F(8A) | 153(19) | 40(9) | 117(17) | 28(10) | 80(15) | 26(10) |
| C(47) | 69(17) | 60(16) | 64(16) | 12(14) | 35(14) | 4(13) |
| F(7A) | 130(20) | 190(40) | 170(30) | 90(30) | 90(30) | 100(20) |
| F(9A) | 210(40) | 160(30) | 77(17) | -52(18) | 80(20) | -70(30) |

Table 5. Hydrogen coordinates ($\times 10^4$) and isotropic displacement parameters ($\text{\AA}^2 \times 10^3$) for dak002.

| | x | y | z | U(eq) |
|--------|-------|------|-------|-------|
| H(4) | 9143 | 4424 | 9663 | 62 |
| H(5) | 8992 | 3998 | 11512 | 78 |
| H(6) | 9148 | 2988 | 11741 | 82 |
| H(7) | 9420 | 2435 | 10149 | 64 |
| H(9) | 10776 | 4604 | 1598 | 51 |
| H(10) | 10783 | 4230 | -292 | 76 |
| H(11) | 10961 | 3239 | -574 | 67 |
| H(12) | 11029 | 2633 | 1022 | 49 |
| H(16) | 12250 | 2699 | 7639 | 50 |
| H(18A) | 12024 | 1751 | 8685 | 62 |
| H(18B) | 11567 | 2182 | 9405 | 62 |
| H(19A) | 11182 | 1313 | 9821 | 88 |
| H(19B) | 11253 | 1089 | 8502 | 88 |
| H(20A) | 10359 | 1955 | 9211 | 70 |
| H(20B) | 10168 | 1287 | 9020 | 70 |
| H(21A) | 10372 | 1356 | 6977 | 48 |
| H(21B) | 9900 | 1887 | 7313 | 48 |
| H(26) | 8580 | 2317 | 3557 | 29 |
| H(28A) | 9188 | 1312 | 2746 | 37 |
| H(28B) | 9224 | 1890 | 1975 | 37 |
| H(29A) | 10312 | 1797 | 1719 | 40 |
| H(29B) | 10010 | 1164 | 1480 | 40 |
| H(30A) | 10256 | 894 | 3487 | 46 |
| H(30B) | 10906 | 1047 | 2781 | 46 |
| H(31A) | 10841 | 1501 | 4676 | 36 |
| H(31B) | 10984 | 1945 | 3631 | 36 |
| H(34) | 8249 | 3385 | 3766 | 33 |
| H(36) | 6980 | 3946 | 6210 | 40 |
| H(38) | 8340 | 2743 | 7041 | 33 |
| H(1) | 10810 | 4416 | 3573 | 28 |

| | | | | |
|--------|-------|------|------|----|
| H(2) | 11007 | 3002 | 3904 | 25 |
| H(3) | 9654 | 2877 | 7348 | 28 |
| H(4A) | 9410 | 4275 | 7726 | 31 |
| H(42) | 12444 | 3839 | 7041 | 34 |
| H(44) | 13507 | 4408 | 4291 | 29 |
| H(46) | 12322 | 3012 | 3924 | 25 |
| H(44A) | 13493 | 4466 | 5224 | 55 |
| H(42A) | 12237 | 3784 | 7542 | 49 |
| H(46A) | 12345 | 3117 | 4318 | 38 |

Chapter 2. Enantioselective Hydroazidation of Allenes

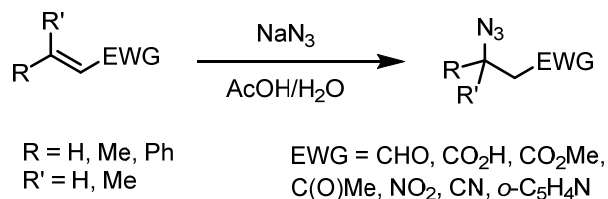
This work has been published in D. A. Khrakovsky, C. Tao, M. W. Johnson, R. T. Thornbury, S. L. Shevick, F. D. Toste, *Angew. Chem. Int. Ed.* **2016**, *55*, 6079–6083.¹

¹ Sophia L. Shevick performed the initial reactions. Richard T. Thornbury synthesized enantiopure product for the first racemization studies. Dr. Miles W. Johnson carried out early optimization studies. Dr. Chuanzhou Tao performed additional optimization experiments and contributed to substrate scope.

Introduction

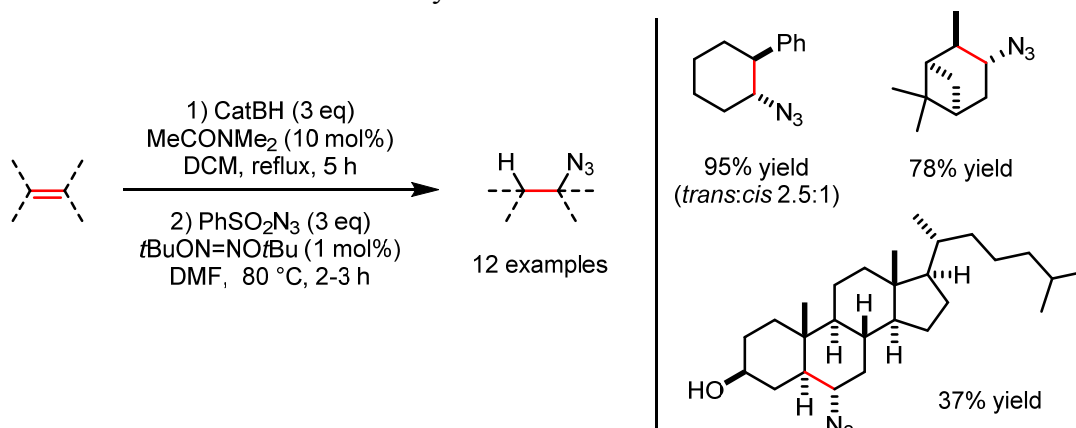
Organic azides hold a special place in organic chemistry due to their utility in a diversity of synthetic transformations.¹ Hydroazidation of olefins is an atom-economical approach for generating organic azides first reported by Boyer in the early 1950s.² In this report, hydrazoic acid, generated *in situ* from sodium azide and acetic acid, was added to substrates containing electron-deficient double bonds (Figure 2.1). Many of the advancements within this reaction manifold, including catalytic applications to unactivated olefins, have been covered elsewhere,³ but some of the most recent developments deserve mention.

Figure 2.1 Boyer's hydroazidation of electron-deficient olefins



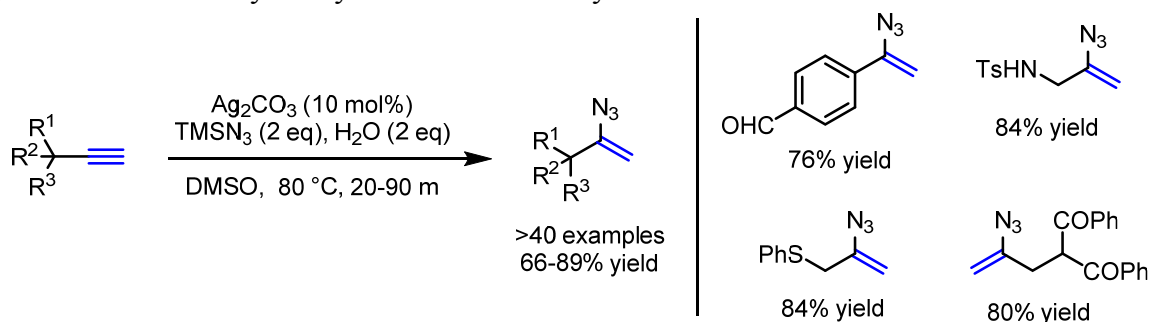
Renaud and coworkers demonstrated that a sequential hydroboration-azidation protocol may be used to achieve anti-Markovnikov selectivity of the overall hydroazidation process (Figure 2.2).⁴ The radical character of the second step was supported by the use of substrates that underwent rearrangement.

Figure 2.2 Anti-Markovnikov radical hydroazidation of alkenes



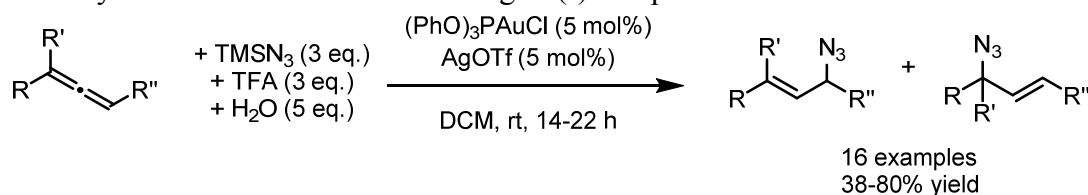
Researchers in the lab of Bi have disclosed a silver-catalyzed hydroazidation of carbon-carbon triple bonds for rapid access to vinyl azides. Their original report was limited to propargyl alcohols,⁵ but has been expanded more generally to terminal alkynes (Figure 2.3).⁶ The methodology is notable for its broad substrate scope and use of commercially available starting materials.

Figure 2.3 Silver-catalyzed hydroazidation of alkynes



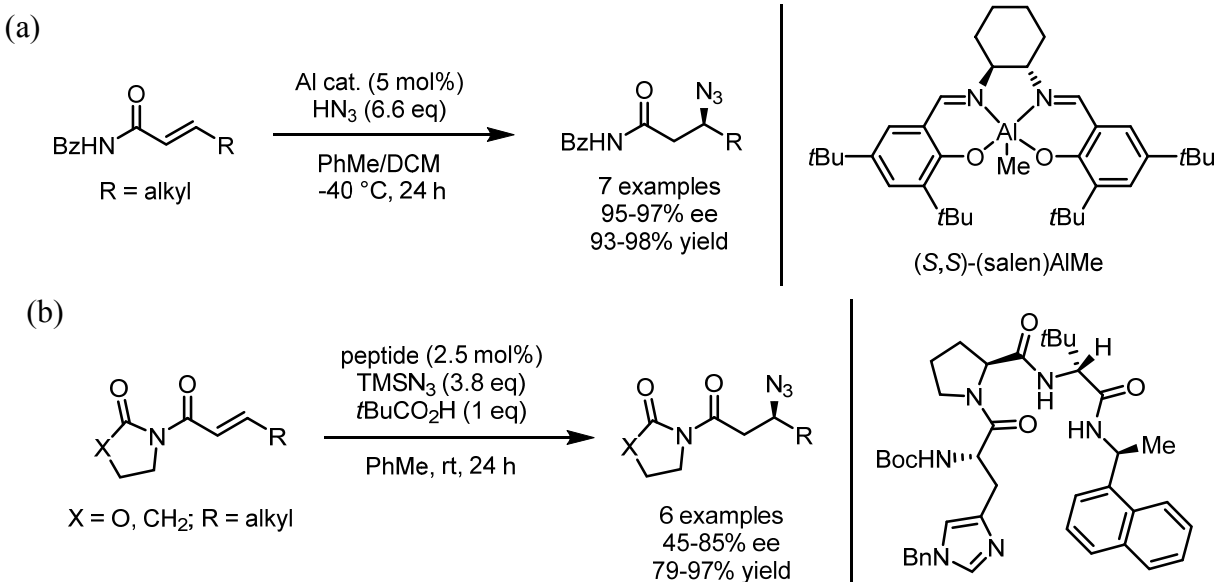
Muñoz and coworkers published the gold(I)-catalyzed hydroazidation of allenes in 2014,⁷ reporting a broad substrate scope and moderate to good yields (Figure 2.4). Mechanistic studies could not discriminate between inner-sphere and outer-sphere attack, as both gold-allene and gold-azide coordination complexes were observed by ¹H and ³¹P NMR analysis.

Figure 2.4 Hydroazidation of allenes with a gold(I) complex



The potential to render this last transformation enantioselective, and thereby access chiral allylic azides – precursors for biologically important allylic amines^{8,9} – piqued our interest in this area of reactivity. We were additionally encouraged by the relative dearth of enantioselective hydroazidation reactions, which have only been reported in a formal sense *via* conjugate addition to activated double bonds.

Figure 2.5 Two catalytic strategies for asymmetric conjugate azidation of imides



Jacobsen and coworkers employed a chiral aluminum-salen complex to catalyze the hydroazidation reaction with α,β -unsaturated imides¹⁰ (Figure 2.5a) and later extended the

substrate scope to α,β -unsaturated ketones.¹¹ Miller and colleagues demonstrated a similar reaction using artificial peptide catalysts and pyrrolidinone- and oxazolidinone-derived α,β -unsaturated imide substrates (Figure 2.5b).^{12,13} Recently, researchers in the lab of Della Sala disclosed the enantioselective hydroazidation of nitro-olefins with a chiral thiourea catalyst (Figure 2.6).¹⁴ In all three of these cases, the catalyst interaction with the substrates' C-O or N-O bonds was implicated as the origin of facial selectivity, limiting the applicability of such methodologies to unconjugated substrates.

Figure 2.6 Enantioselective hydroazidation of nitroalkenes with a chiral thiourea catalyst

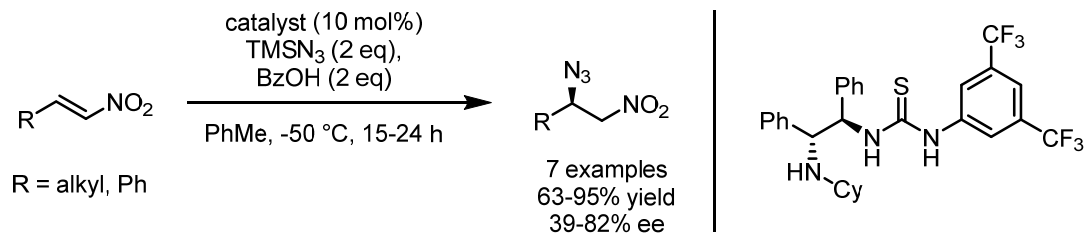
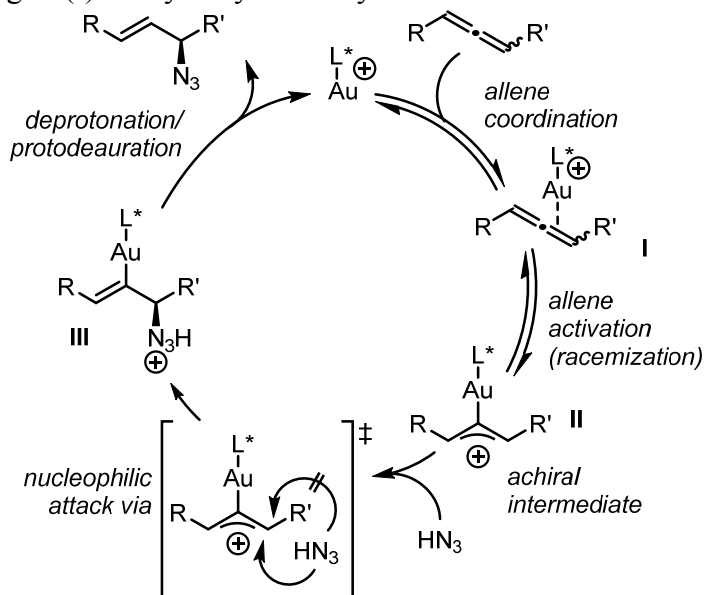


Figure 2.7 Proposed gold(I) catalytic cycle for hydroazidation of allenes



Inspired by examples of rhodium-catalyzed asymmetric additions of nitrogen nucleophiles to allenes,^{15,16} we sought to develop a gold(I)-catalyzed enantioselective hydroazidation of allenes as an entry to allylic azides. We first considered the mechanistic implications of two closely related transformations: the racemization of chiral aryl allenes, reported by Widenhoefer and coworkers,¹⁷ and the nucleophilic intermolecular addition of hydrazides to allenes, reported by Toste and coworkers.¹⁸ Both these reports identify a cationic allylic gold(I) complex as a likely low-energy intermediate on their respective reaction coordinates. Envisioning a plausible catalytic cycle for hydroazidation (Figure 2.7), we hypothesized that if we could introduce a chiral environment around the gold center in this planar, achiral intermediate (II), then facial selectivity of subsequent nucleophilic addition could be achieved. This would enable the use of easily accessible racemic allene substrates in an asymmetric transformation.

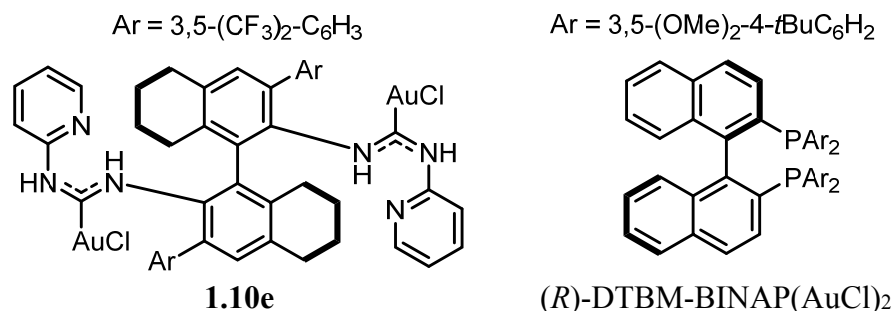
Results and Discussion

The first task was to interrogate whether the key achiral intermediate could be accessed using carbene gold(I) catalysts, as both previous Widenhoefer and Toste reports used phosphine gold(I) catalysts. If chiral, non-racemic allene starting material is used, this intermediate is implicated in the racemization pathway. We found that ADC gold(I) complex **1.10e** was extremely active in racemizing allenes relative to a chiral diphosphine gold(I) complex (Table 2.1).

Table 2.1 Racemization of chiral allenes with gold(I) catalysts

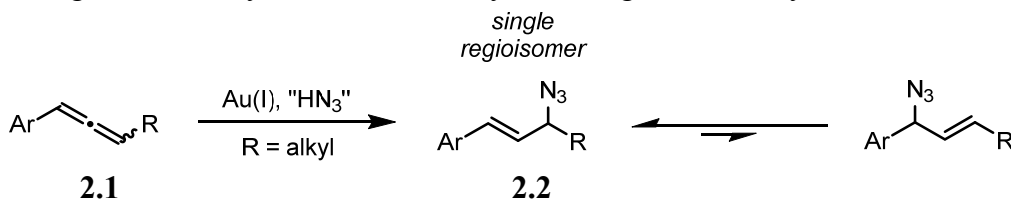
| Entry ^a | Time (min) | 1.10e^b | (<i>R</i>)-DTBM-BINAP(AuCl) ₂ ^b |
|--------------------|------------|--------------------------|---|
| 1 | 5 | racemic | 79 |
| 2 | 30 | racemic | 54 |
| 3 | 120 | racemic | 21 |

[a] Conditions: 0.05 mmol **2.1a**, 0.0025 mmol precatalyst, 0.0075 mmol AgOTf, 1.0 mL of THF (0.05 M). [b] Column entries are ee's

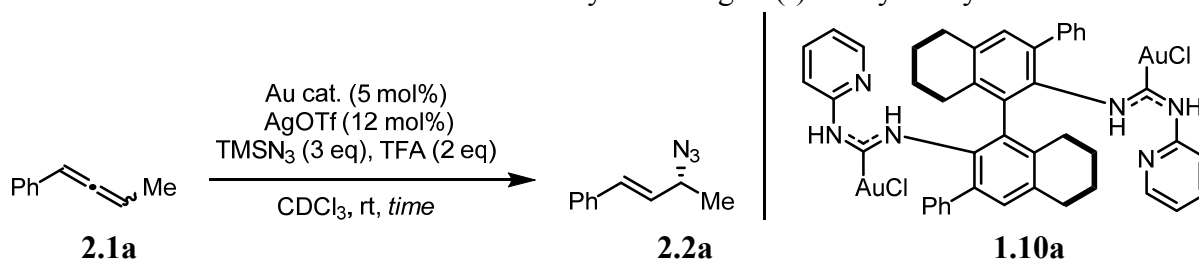


The other challenge in the development of gold(I)-catalyzed asymmetric hydroazidation related to the known rearrangement of allylic azides, first reported by Winstein and coworkers.¹⁹ Hoping to circumvent this issue entirely, we targeted aryl allene substrates **2.1** affording cinnamyl azide products **2.2** which have been isolated as single regioisomers,^{7,20} and presumably do not undergo rearrangement to a significant extent (Figure 2.8).

Figure 2.8 Regioselective hydroazidation of aryl allenes gives cinnamyl azides



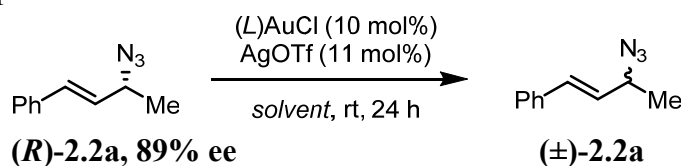
Unfortunately, our initial attempts at asymmetric hydroazidation with BINAM-derived ADC gold(I) complexes were stymied by irreproducible results, as the observed ee values degraded over the course of the reaction (Table 2.2). We suspected that a gold(I)-catalyzed racemization pathway through the aforementioned rearrangement might be responsible.

Table 2.2 Erosion of enantiomeric excess in asymmetric gold(I)-catalyzed hydrazidation

| Entry ^a | Time (min) | Yield (%) ^b | ee (%) ^c |
|--------------------|------------|------------------------|---------------------|
| 1 | 5 | 14 | 50 |
| 2 | 30 | 22 | 37 |
| 3 | 120 | 30 | 27 |
| 4 | 720 | 49 | 18 |

[a] Conditions: 0.1 mmol **2.1a**, 0.0025 mmol precatalyst, 0.06 mmol AgOTf, 0.3 mmol TMSN₃, 0.2 mmol acid, 1.0 mL of CDCl₃ (0.1 M). [b] Determined by ¹H NMR with 4-chloroanisole as an internal standard. [c] Determined by chiral HPLC.

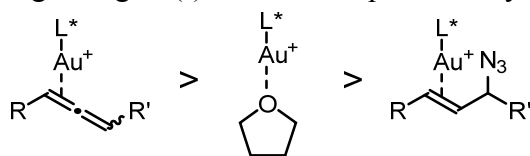
In order to investigate this possibility, chiral, non-racemic cinnamyl azide **2.2a** was synthesized²¹ and treated with achiral cationic gold(I) complexes in different solvents (Table 2.3). After 24 hours, HPLC analysis revealed that the enantiomeric excess of **2.2a** eroded in chloroform and toluene (entries 1 and 2), but not to an appreciable extent in tetrahydrofuran (entry 3). Moreover, using tetrahydrofuran as a co-solvent greatly slowed the rate of racemization (entries 4 and 5). A potential explanation for this phenomenon is the coordination of the oxygen lone pairs of the ethereal solvent to the cationic gold center. This may outcompete binding of the alkene product, preventing racemization, but still allow for allene starting material to coordinate, allowing the reaction to proceed (Figure 2.9).

Table 2.3 Solvent-dependent erosion of enantiomeric excess

| Entry ^{a,b} | Solvent | L = PPh ₃ | L = IPr |
|----------------------|------------------------------------|----------------------|---------|
| 1 | CHCl ₃ | 23 | 46 |
| 2 | PhMe | 62 | 73 |
| 3 | THF | 87 | 88 |
| 4 | THF/CHCl ₃ ^c | 72 | 84 |
| 5 | THF/PhMe ^c | 86 | 87 |

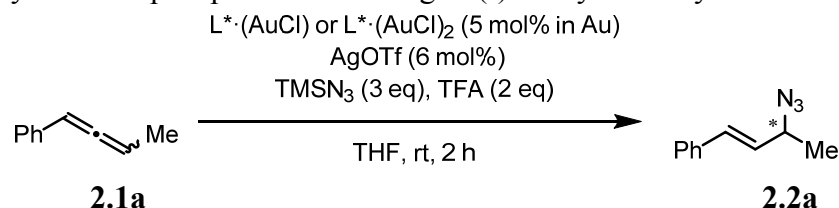
[a] Conditions: 0.5 mmol **2.2a**, 0.05 mmol Au precatalyst, 0.11 mmol AgOTf, 1.0 mL solvent (0.05 M). [b] All table entries are reported as % ee. [c] 1:1 volumetric ratio.

Figure 2.9 Coordination strength of gold(I) to reaction species in hydroazidation manifold



With the choice of solvent established, the enantioselectivities of other ligand classes were evaluated (Table 2.4). The application of conventional axially chiral phosphine and phosphoramidite ligands gave low ee values (entries 1-3). Moreover, chiral Arduengo-based NHCs also gave nearly racemic products under the same conditions (entries 4-6). The catalyst loadings were normalized to 5 mole percent in gold content for both mononuclear and dinuclear complexes.

Table 2.4 Survey of chiral phosphine and NHC gold(I) catalysts in asymmetric hydroazidation

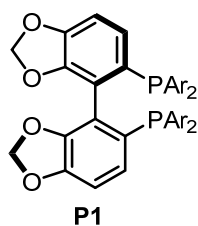


| Entry ^a | Ligand | Yield (%) ^b | ee (%) ^c |
|--------------------|-----------------------|------------------------|---------------------|
| 1 | P1^d | 50 | 20 |
| 2 | P2^d | 49 | 10 |
| 3 | P3^e | 35 | 2 |
| 4 | N1^e | 21 | 5 |
| 5 | N2^e | 51 | 3 |
| 6 | N3^e | 12 | 2 |

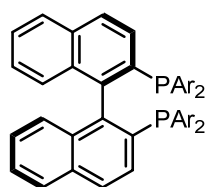
a) Conditions: 0.1 mmol **2.1a**, 0.005 mmol precatalyst (0.0025 mmol for dinuclear gold precatalysts), 0.06 mmol AgOTf, 0.3 mmol TMSN₃, 0.2 mmol TFA, 1.0 mL THF (0.1 M), 2 h at room temperature. b) Determined by ¹H NMR with 1,3,5-trimethoxybenzene as an internal standard. c) Determined by chiral HPLC. d) Dinuclear ligand. e) Mononuclear ligand

Ar = 3,5-Me₂C₆H₄

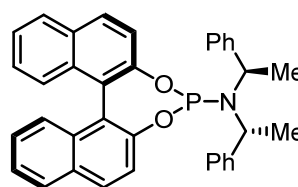
Ar = 3,5-(OMe)₂-4-*t*BuC₆H₂



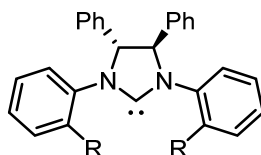
P1



P2

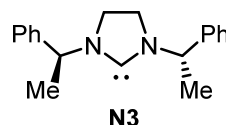


P3



N1: R = Me

N2: R = *i*Pr

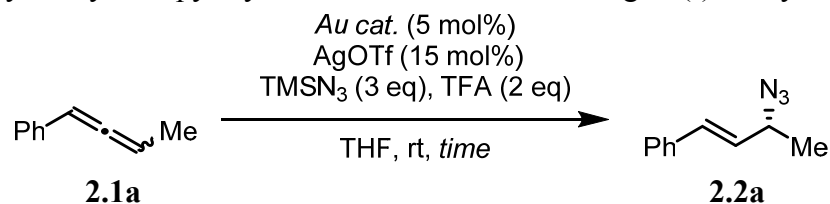


N3

Encouraged by the absence of selectivity observed with these well-established chiral gold(I) complexes, we continued testing BINAM-derived ADC gold(I) complexes in the reaction (Table 2.5). Changes to the aromatic substituents revealed several trends. Interrogation of steric and electronic effects in 3,5-disubstituted arenes (entries 1-5) showed that similarly sized electron-donating methyl groups (entry 2) and electron-withdrawing trifluoromethyl groups (entry 5) provided comparable enantioselectivity, while the latter gave slightly greater yield. In order to probe this apparent steric effect, the two trifluoromethyl substituents were introduced at various positions on the ring (entries 6-8). None of these new configurations provided the same level of enantioselectivity observed with the original 3,5-disubstitution.

Keeping this optimal aromatic fragment, we moved on to testing the effect of changes to the pyridyl residues (entries 9-13). A number of *ortho*-substituents, including acetoxy (entry 9), methyl (entry 10), and benzyloxy (entry 11), did not improve the observed enantioselectivities. Other heterocycles fared no better: a pyrimidine residue (entry 12) also led to a decreased ee value, while a pyrazine derivative (entry 13) shut down reactivity completely. A control experiment was performed to demonstrate that the silver source used for generating cationic gold(I) was not itself a competent catalyst for the reaction (entry 14).

Table 2.5 Survey of aryl and pyridyl substitution in chiral ADC gold(I) catalysts



| Entry ^a | Precatalyst | Time (h) | Yield (%) ^b | ee (%) ^c |
|--------------------|--------------|----------|------------------------|---------------------|
| 1 | 1.10a | 16 | 24 | 50 |
| 2 | 1.10b | 16 | 36 | 72 |
| 3 | 1.10c | 16 | 15 | 46 |
| 4 | 1.10d | 16 | 41 | 50 |
| 5 | 1.10e | 16 | 45 | 73 |
| 6 | 1.10f | 4 | 9 | 55 |
| 7 | 1.10g | 4 | 7 | 42 |
| 8 | 1.10h | 4 | 15 | 67 |
| 9 | 1.10i | 16 | 18 | 46 |
| 10 | 1.10j | 16 | 26 | 44 |
| 11 | 1.10l | 16 | 11 | 53 |
| 12 | 1.10s | 4 | 10 | 60 |
| 13 | 1.10t | 4 | 0 | n/d |
| 14 | none | 16 | 0 | n/d |

[a] Conditions: 0.1 mmol **2.1a**, 0.005 mmol precatalyst, 0.015 mmol AgOTf, 0.3 mmol TMSN₃, 0.2 mmol TFA, 2.0 mL of THF (0.05 M), 16 h at room temperature. [b] Determined by ¹H NMR with 4-chloroanisole as an internal standard. [c] Determined by chiral HPLC.

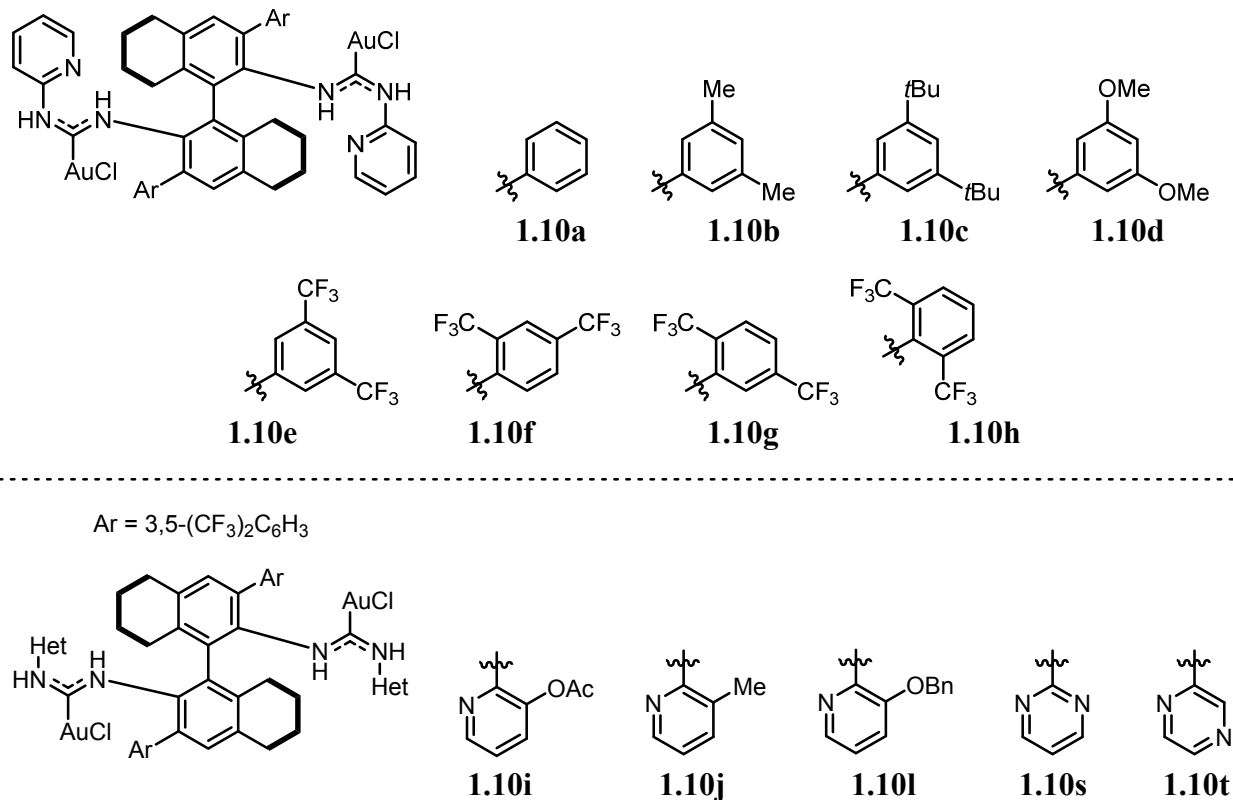
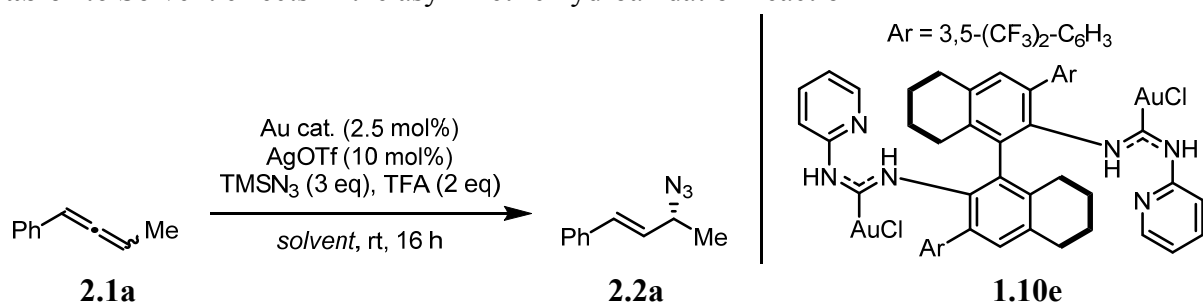


Table 2.6 Solvent effects in the asymmetric hydroazidation reaction



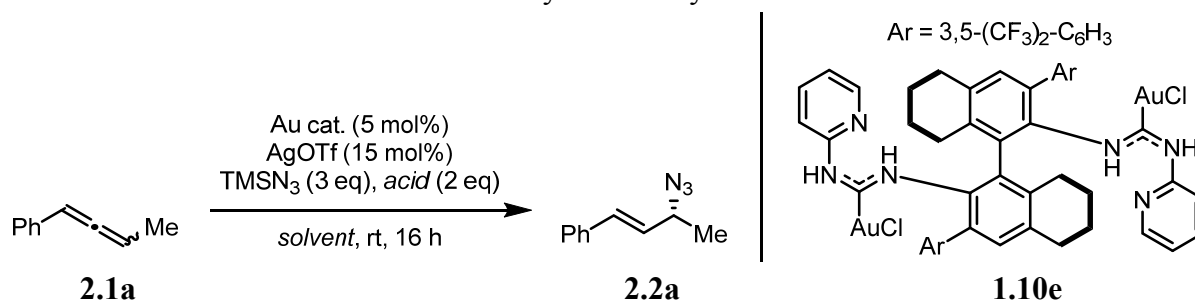
| Entry ^a | Solvent | Yield (%) ^b | ee (%) ^c |
|--------------------|--------------------------|------------------------|---------------------|
| 1 | THF | 18 | 73 |
| 2 | 2-Me-THF | 13 | 58 |
| 3 | 2,5-Me ₂ -THF | 6 | 37 |
| 4 | 3-Me-THF | 9 | 38 |
| 5 | Et ₂ O | 46 | 50 |
| 6 | 1,4-dioxane | 51 | 57 |
| 7 | DME | 34 | 62 |
| 8 | MTBE | 60 | 48 |
| 9 | CPME | 14 | 52 |

[a] Conditions: 0.1 mmol **2.1a**, 0.0025 mmol precatalyst, 0.010 mmol AgOTf, 0.3 mmol TMSN₃, 0.2 mmol acid, 2.0 mL of appropriate solvent (0.05 M), 16 h at room temperature. [b] Determined by ¹H NMR with 4-chloroanisole as an internal standard. [c] Determined by chiral HPLC.

Next, optimization of the reaction conditions was attempted by exhaustive screening of ethereal solvents (Table 2.6). While the product yields varied widely, no enantioselectivity values exceeding the benchmark value obtained with tetrahydrofuran were found.

At this point, we focused our attention on improving yield (Table 2.7). We hypothesized that the relatively low yields obtained with tetrahydrofuran could be the result of catalyst decomposition, as a strong acid (TFA) could disrupt the catalyst's stabilizing intramolecular hydrogen-bonding. This was supported by the observation that the reaction mixture turned dark purple over time, indicative of the formation of gold nanoparticles. We tried acetic acid and benzoic acid, which are roughly as acidic as hydrazoic acid,²² and found the results mostly unchanged (entries 2 and 3). On the other hand, when water was employed, a substantial increase in the yield was noted (entry 4). Luckily, the formation of the allylic alcohol from hydration of the allene²³ was not observed, presumably due to the greater nucleophilicity of azide. Many other proton donors were suitable in the reaction manifold, including numerous carboxylic and boronic acids and even silica gel, but water gave the best combination of yield and ee. Finally, the yields were raised to the desired levels by addition of toluene or chloroform as co-solvents (entries 6 and 7), and the enantioselectivities were elevated by decreasing the temperature and extending the reaction times to compensate for the slower rate of conversion (entry 8).

Table 2.7 Acid and solvent effects in the asymmetric hydroazidation reaction



| Entry ^a | Acid | Solvent | Yield (%) ^b | ee (%) ^c |
|--------------------|------------------|--|------------------------|---------------------|
| 1 | TFA | THF | 45 | 73 |
| 2 | AcOH | THF | 40 | 71 |
| 3 | PhCOOH | THF | 33 | 75 |
| 4 | H ₂ O | THF | 77 | 75 |
| 5 | H ₂ O | THF/CH ₃ NO ₂ ^d | 60 | 71 |
| 6 | H ₂ O | THF/PhMe ^d | 91 | 73 |
| 7 | H ₂ O | THF/CHCl ₃ ^d | 91 | 73 |
| 8 ^e | H ₂ O | THF/CHCl ₃ ^d | 92 ^f | 90 |

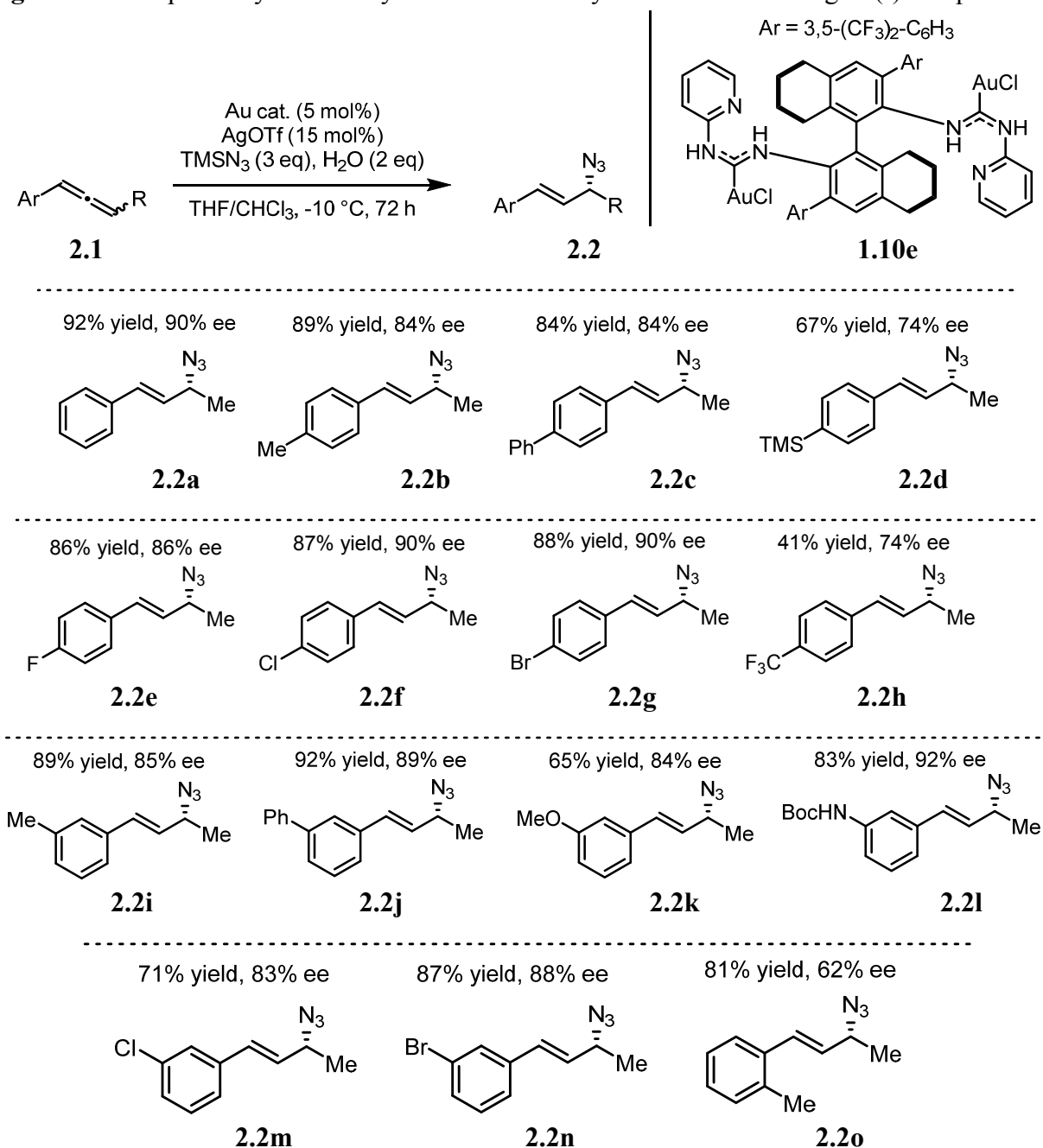
[a] Conditions: 0.1 mmol **2.1a**, 0.005 mmol precatalyst, 0.015 mmol AgOTf, 0.3 mmol TMSN₃, 0.2 mmol acid, 2.0 mL of THF (0.05 M), 16 h at room temperature.

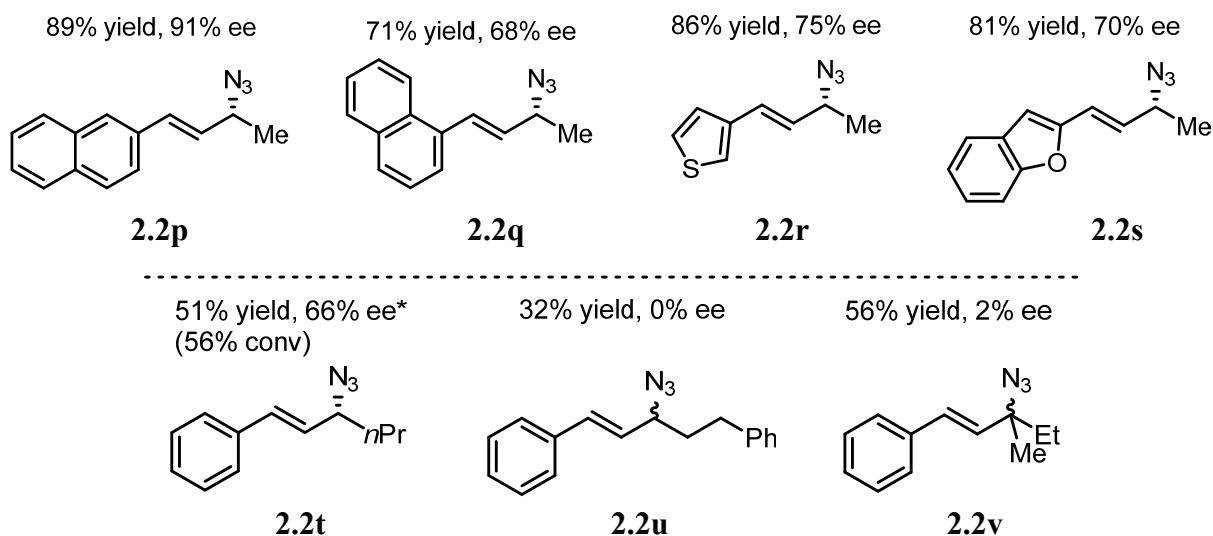
[b] Determined by ¹H NMR with 4-chloroanisole as an internal standard. [c] Determined by chiral HPLC. [d] 3:1 volumetric ratio. [e] Reaction run at -10 °C for 72 hours. [f] Isolated yield.

With these optimized conditions in hand, the substrate scope was investigated (Figure 2.10). Introduction of aromatic substituents revealed that both electron-donating and withdrawing groups were generally well-tolerated at various positions on the ring (**2.2a-o**). Polycyclic and

heterocyclic substrates also gave good yields and moderate to high enantioselectivities (**2.2p-s**). Introduction of alkyl substitutions other than methyl proved problematic. An *n*-propyl derivative required some solvent system reoptimization in order to achieve only moderate selectivity (**2.2t**), and a product displaying even larger alkyl chain was nearly racemic (**2.2u**), as was a product derived from a trisubstituted allene (**2.2v**).

Figure 2.10 Scope of asymmetric hydroazidation of aryl allenes with ADC gold(I) complex

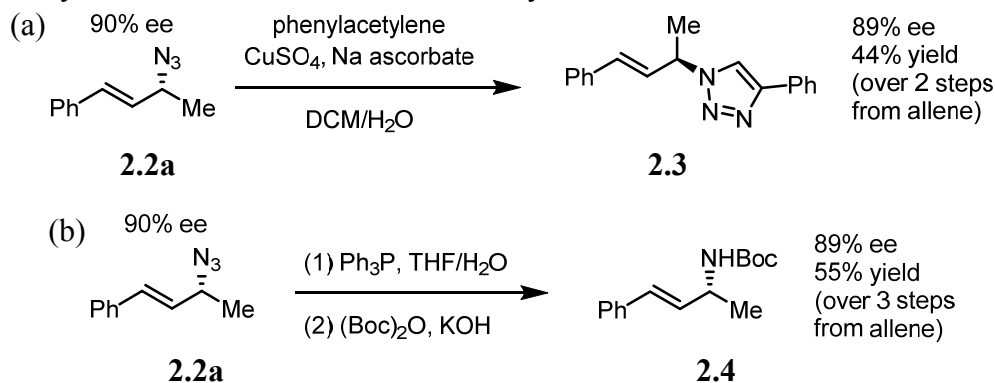




*Reaction run at -20 °C in DCM:MTBE (3:1)

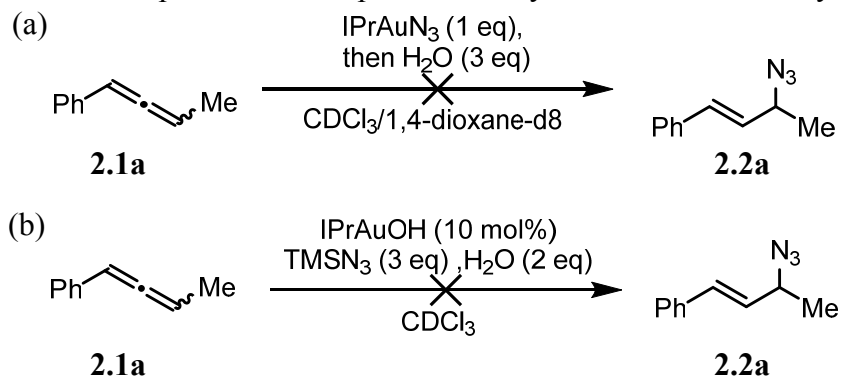
Next, we sought to demonstrate the synthetic utility of these chiral allylic azide products. First, azide **2.2a** was subjected to CuAAC²⁴ with phenylacetylene, affording the corresponding triazole product **2.3** (Figure 2.11a). Then, using Staudinger conditions,²⁵ azide **2.2a** was unmasked to the corresponding allylic amine, and a simple Boc protection was carried out in the same pot to facilitate analysis of the product, furnishing **2.4** (Figure 2.11b). Gratifyingly, no racemization of the chiral center was observed in either case.

Figure 2.11 Synthetic transformations of chiral allylic azides



Finally, some experiments to gain insight on the reaction mechanism were performed. To test the intermediacy of a gold(I) azide species, IPrAuN₃ was prepared. It was treated with a stoichiometric quantity of allene **2.1a**, and after a period of time, water was added. Both with and without water, no conversion to product **2.2a** was observed (Figure 2.12a). To test the intermediacy of a gold(I) hydroxide species, IPrAuOH was prepared, but it was not a competent catalyst for the reaction (Figure 2.12b). Thus, no conclusive evidence supporting or disproving either inner-sphere or outer-sphere azide attack was obtained.

Figure 2.12 Mechanistic experiments with putative catalytic intermediates of hydroazidation



In summary, we have demonstrated the first asymmetric hydroazidation of unconjugated carbon-carbon π -bonds. The use of ADC gold(I) catalysts derived from BINAM, 1,3-disubstituted allenes, and hydrazoic acid generated *in situ* allows for the enantioselective preparation of chiral allylic azide products. Although the substrate scope of the reaction is somewhat limited, we hope that this contribution will spur greater interest in asymmetric hydroazidation reactions in the synthetic community.

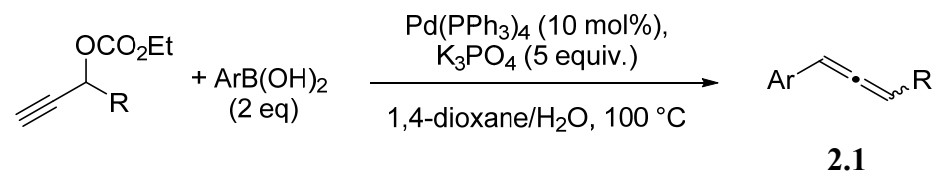
Experimental

General information

Unless otherwise noted, reagents were obtained from commercial sources and used without further purification. Trimethylsilyl azide was stored over 4 Å molecular sieves at -20 °C. Dry tetrahydrofuran, dichloromethane, and toluene were obtained by passage through activated alumina columns under argon. All other solvents used were HPLC grade. TLC analysis of reaction mixtures was performed on Merck silica gel 60 F₂₅₄ TLC plates and visualized by ultraviolet light, iodine or potassium permanganate stain. Flash chromatography was carried out with ICN SiliTech 32-63 D 60 Å silica gel. ¹H and ¹³C NMR spectra were recorded with Bruker AV-500, DRX-500, or AV-600 spectrometers and were referenced to residual ¹H and ¹³C signals of the deuterated solvents, respectively (δH 7.26, δC 77.16 for chloroform-d and δH 5.32, δC 54.00 for dichloromethane-d₂). Enantioselectivity was determined by chiral HPLC using Daicel Chiralpak AD-H, AS-H, IB, OD-H, or Regis (R,R) WHELK-O1 columns (all 0.46 cm x 25 cm). Optical rotation was recorded on a Perkin Elmer Polarimeter 241 at the D line (1.0 dm path length, c = mg/mL). Generally, racemic samples were prepared in procedures modified from those reported by Muñoz and coworkers using IPrAuCl and AgOTf.⁷ Mass spectral data were obtained via the Micro-Mass/Analytical Facility operated by the College of Chemistry, University of California, Berkeley using a Thermo LTQ-FT (ESI) instrument.

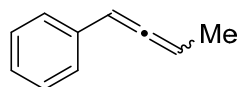
General procedure for preparation of allene substrates

The synthesis of racemic 1,3-disubstituted allenes by Pd-catalyzed cross-coupling was adapted from the procedure of Yoshida and coworkers.²⁶ A representative synthesis of **2.1a** is given.



To a round bottom flask equipped with a Teflon-coated stir bar and condenser tube were added but-3-yn-2-yl ethyl carbonate (1.25 g, 8.82 mmol, 1 equiv), phenylboronic acid (2.20 g, 18.1 mmol, 2.1 equiv), potassium phosphate tribasic (9.61 g, 45.3 mmol, 5.1 equiv), palladium(0) tetrakis(triphenylphosphine) (261 mg, 0.226 mmol, 0.025 equiv), 1,4-dioxane (30 mL) and water (15 mL) at room temperature, and the biphasic solution was heated to 100 °C with vigorous stirring for 15 min. The reaction mixture was cooled to room temperature, then the aqueous phase was separated and extracted with DCM (10 mL). The combined organic layers were diluted with cyclohexane (75 mL), filtered through a pad of silica gel and Celite, then washed with brine and dried over MgSO₄. The solvent was removed *in vacuo*, and the crude residue was chromatographed on silica gel with hexane as eluent (with Et₂O as co-eluent for allenes bearing polar functionalities) to afford the allene.

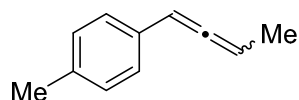
Allenes were stored in pentane at -20 °C to prevent decomposition, then passed through short silica gel plugs (washing with pentane) and the solvent removed *in vacuo* prior to use in reactions.



2.1a, buta-1,2-dien-1-ylbenzene²⁷

¹H NMR (600 MHz, CDCl₃) δ 7.29 (d, *J* = 4.4 Hz, 4H), 7.17 (dq, *J* = 8.6, 4.2 Hz, 1H), 6.09 (dq, *J* = 6.3, 3.2 Hz, 1H), 5.53 (p, *J* = 7.0 Hz, 1H), 1.78 (dd, *J* = 7.1, 3.3 Hz, 3H).

¹³C NMR (151 MHz, CDCl₃) δ 206.12, 135.17, 128.65, 126.77, 94.13, 89.68, 14.20.

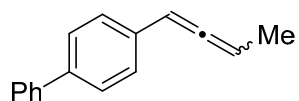


2.1b, 1-(buta-1,2-dien-1-yl)-4-methylbenzene²⁷

¹H NMR (600 MHz, CDCl₃) δ 7.22 (d, *J* = 8.0 Hz, 2H), 7.14 (d, *J* = 7.8 Hz, 1H), 6.11 (dq, *J* = 6.6, 3.3 Hz, 1H), 5.55 (p, *J* = 6.9 Hz, 1H), 2.37 (s, 4H), 1.82 (dd, *J* = 7.1, 3.3 Hz, 3H).

¹³C NMR (151 MHz, CDCl₃) δ 205.82, 136.49, 132.16, 129.38, 126.67, 93.90, 89.57, 21.29, 14.32.

HRMS (EI⁺): calcd. for [C₁₁H₁₂]⁺: 144.0939, found: 144.0943.

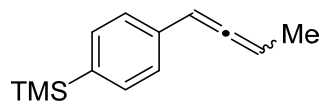


2.1c, 4-(buta-1,2-dien-1-yl)-1,1'-biphenyl

¹H NMR (600 MHz, CDCl₃) δ 7.63 (dd, *J* = 8.1, 1.2 Hz, 2H), 7.58 (d, *J* = 8.2 Hz, 2H), 7.47 (t, *J* = 7.7 Hz, 2H), 7.40 (d, *J* = 8.3 Hz, 2H), 7.37 (t, *J* = 7.4 Hz, 1H), 6.18 (dq, *J* = 6.4, 3.2 Hz, 1H), 5.61 (p, *J* = 7.0 Hz, 1H), 1.85 (dd, *J* = 7.1, 3.2 Hz, 3H).

¹³C NMR (151 MHz, CDCl₃) δ 206.35, 141.00, 139.62, 134.26, 128.88, 127.40, 127.29, 127.18, 127.04, 93.80, 89.83, 14.26.

HRMS (EI⁺): calcd. for [C₁₆H₁₄]⁺: 206.1096, found: 206.1093.

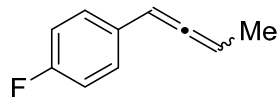


2.1d, (4-(buta-1,2-dien-1-yl)phenyl)trimethylsilane

¹H NMR (600 MHz, CDCl₃) δ 7.48 (d, *J* = 8.0 Hz, 2H), 7.30 (d, *J* = 7.8 Hz, 2H), 6.11 (dq, *J* = 6.4, 3.1 Hz, 1H), 5.56 (p, *J* = 6.9 Hz, 1H), 1.80 (dd, *J* = 7.1, 3.2 Hz, 3H), 0.28 (s, 9H).

¹³C NMR (151 MHz, CDCl₃) δ 206.38, 138.84, 135.71, 133.72, 126.13, 94.12, 89.68, 14.22, -0.95.

HRMS (EI⁺): calcd. for [C₁₃H₁₈Si]⁺: 202.1178, found: 202.1180.

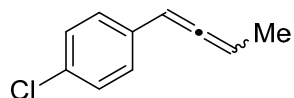


2.1e, 1-(buta-1,2-dien-1-yl)-4-fluorobenzene

$^1\text{H NMR}$ (600 MHz, CDCl_3) δ 7.25 – 7.21 (m, 2H), 7.03 – 6.91 (m, 2H), 6.06 (dq, $J = 6.4, 3.2$ Hz, 1H), 5.53 (p, $J = 6.9$ Hz, 1H), 1.78 (dd, $J = 7.1, 3.2$ Hz, 3H).

$^{13}\text{C NMR}$ (151 MHz, CDCl_3) δ 205.70 (d, $J = 2.4$ Hz), 161.71 (d, $J = 245.6$ Hz), 130.92 (d, $J = 3.3$ Hz), 127.95 (d, $J = 8.0$ Hz), 115.38 (d, $J = 21.7$ Hz), 92.97, 89.80, 14.05.

HRMS (EI $^+$): calcd. for $[\text{C}_{10}\text{H}_9\text{F}]^+$: 148.0688, found: 148.0686.

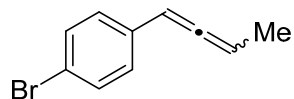


2.1f, 1-(buta-1,2-dien-1-yl)-4-chlorobenzene

$^1\text{H NMR}$ (600 MHz, CDCl_3) δ 7.28 (d, $J = 8.4$ Hz, 2H), 7.23 (d, $J = 8.6$ Hz, 2H), 6.08 (dq, $J = 6.4, 3.2$ Hz, 1H), 5.57 (p, $J = 7.0$ Hz, 1H), 1.81 (dd, $J = 7.1, 3.2$ Hz, 3H).

$^{13}\text{C NMR}$ (151 MHz, CDCl_3) δ 206.19, 133.74, 132.29, 128.78, 127.94, 93.27, 90.16, 14.12.

HRMS (EI $^+$): calcd. for $[\text{C}_{10}\text{H}_9\text{Cl}]^+$: 164.0395, found: 164.0394.

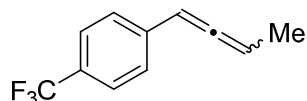


2.1g, 1-bromo-4-(buta-1,2-dien-1-yl)benzene²⁷

$^1\text{H NMR}$ (500 MHz, CDCl_3) δ 7.44 (d, $J = 8.1$ Hz, 2H), 7.18 (d, $J = 8.2$ Hz, 2H), 6.07 (dq, $J = 6.2, 3.2$ Hz, 1H), 5.57 (p, $J = 6.9, 6.3$ Hz, 1H), 1.82 (dd, $J = 7.2, 3.3$ Hz, 3H).

$^{13}\text{C NMR}$ (126 MHz, CDCl_3) δ 206.12, 134.14, 131.65, 128.24, 120.30, 93.32, 90.20, 14.08.

HRMS (EI $^+$): calcd. for $[\text{C}_{10}\text{H}_9\text{Br}]^+$: 207.9888, found: 207.9886.

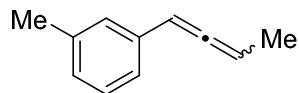


2.1h, 1-(buta-1,2-dien-1-yl)-4-(trifluoromethyl)benzene²⁷

$^1\text{H NMR}$ (500 MHz, CDCl_3) δ 7.56 (d, $J = 8.0$ Hz, 2H), 7.40 (d, $J = 8.0$ Hz, 2H), 6.14 (dt, $J = 6.6, 3.5$ Hz, 1H), 5.63 (p, $J = 7.0$ Hz, 1H), 1.84 (dd, $J = 7.1, 3.3$ Hz, 3H).

$^{13}\text{C NMR}$ (126 MHz, CDCl_3) δ 207.03, 139.21, 128.66 (q, $J = 32.3$ Hz), 126.86, 125.58 (q, $J = 3.8$ Hz), 123.40, 93.36, 90.38, 13.90.

HRMS (EI $^+$): calcd. for $[\text{C}_{11}\text{H}_9\text{F}_3]^+$: 198.0656, found: 198.0655.

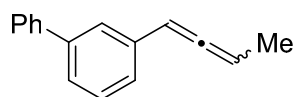


2.1i, 1-(buta-1,2-dien-1-yl)-3-methylbenzene

^1H NMR (600 MHz, CDCl_3) δ 7.27 (t, $J = 7.6$ Hz, 1H), 7.22 – 7.14 (m, 2H), 7.08 (d, $J = 7.6$ Hz, 1H), 6.15 (dq, $J = 6.5, 3.2$ Hz, 1H), 5.60 (p, $J = 7.0$ Hz, 1H), 2.41 (s, 3H), 1.87 (dd, $J = 7.1, 3.2$ Hz, 3H).

^{13}C NMR (151 MHz, CDCl_3) δ 206.08, 138.20, 135.03, 128.55, 127.61, 127.41, 123.96, 94.12, 89.54, 21.47, 14.25.

HRMS (EI+): calcd. for $[\text{C}_{11}\text{H}_{12}]^+$: 144.0939, found: 144.0937.

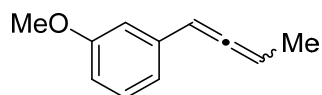


2.1j, 3-(buta-1,2-dien-1-yl)-1,1'-biphenyl

^1H NMR (600 MHz, CDCl_3) δ 7.65 (d, $J = 7.6$ Hz, 2H), 7.56 (s, 1H), 7.51 – 7.44 (m, 3H), 7.41 (dt, $J = 12.4, 7.5$ Hz, 2H), 7.34 (d, $J = 7.6$ Hz, 1H), 6.22 (dq, $J = 6.6, 3.2$ Hz, 1H), 5.62 (p, $J = 6.8$ Hz, 1H), 1.86 (dd, $J = 6.9, 3.0$ Hz, 3H).

^{13}C NMR (151 MHz, CDCl_3) δ 206.25, 141.70, 141.31, 135.66, 129.07, 128.84, 127.42, 127.31, 125.74, 125.73, 125.60, 94.11, 89.89, 14.25.

HRMS (EI+): calcd. for $[\text{C}_{16}\text{H}_{14}]^+$: 206.1096, found: 206.1092.

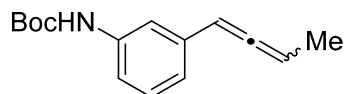


2.1k, 1-(buta-1,2-dien-1-yl)-3-methoxybenzene

^1H NMR (600 MHz, CDCl_3) δ 7.24 (t, $J = 7.9$ Hz, 1H), 6.91 (d, $J = 7.9$ Hz, 1H), 6.87 (t, $J = 2.1$ Hz, 1H), 6.77 (dd, $J = 8.2, 2.6$ Hz, 1H), 6.09 (dq, $J = 6.3, 3.1$ Hz, 1H), 5.56 (p, $J = 7.0$ Hz, 1H), 3.82 (s, 3H), 1.81 (dd, $J = 7.1, 3.2$ Hz, 3H).

^{13}C NMR (151 MHz, CDCl_3) δ 206.17, 159.96, 136.67, 129.59, 119.46, 112.46, 112.03, 94.07, 89.78, 55.28, 14.19.

HRMS (EI+): calcd. for $[\text{C}_{11}\text{H}_{12}\text{O}]^+$: 160.0888, found: 160.0888.

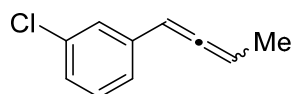


2.1l, tert-butyl (3-(buta-1,2-dien-1-yl)phenyl)carbamate

^1H NMR (500 MHz, CDCl_3) δ 7.29 – 7.17 (m, 3H), 6.98 (d, $J = 7.3$ Hz, 1H), 6.66 (s, 1H), 6.06 (dq, $J = 6.1, 3.3$ Hz, 1H), 5.53 (p, $J = 6.9, 6.2$ Hz, 1H), 1.78 (dd, $J = 6.9, 3.3$ Hz, 3H), 1.53 (s, 9H).

^{13}C NMR (126 MHz, CDCl_3) δ 206.07, 152.86, 138.74, 135.99, 129.15, 121.48, 116.97, 116.61, 93.97, 89.76, 80.51, 28.41, 14.17.

HRMS (EI $^+$): calcd. for $[\text{C}_{15}\text{H}_{19}\text{NO}_2]^+$: 245.1416, found: 245.1416.

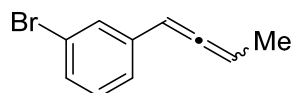


2.1m, 1-(3-chlorophenyl)-3-methylbut-1,2-diene

^1H NMR (500 MHz, CDCl_3) δ 7.32 (s, 1H), 7.24 (t, $J = 7.7$ Hz, 1H), 7.18 (t, $J = 6.6$ Hz, 2H), 6.07 (dq, $J = 6.4, 3.0$ Hz, 1H), 5.60 (p, $J = 6.9$ Hz, 1H), 1.83 (dd, $J = 7.2, 3.2$ Hz, 3H).

^{13}C NMR (126 MHz, CDCl_3) δ 206.38, 137.28, 134.60, 129.84, 126.77, 126.60, 124.96, 93.24, 90.36, 14.13.

HRMS (EI $^+$): calcd. for $[\text{C}_{10}\text{H}_9\text{Cl}]^+$: 164.0393, found: 164.0394.

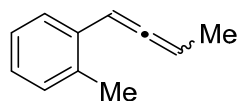


2.1n, 1-bromo-3-(3-methylbut-1,2-dienyl)benzene

^1H NMR (600 MHz, CDCl_3) δ 7.45 (t, $J = 1.7$ Hz, 1H), 7.31 (dt, $J = 7.8, 1.7$ Hz, 1H), 7.20 (d, $J = 7.7$ Hz, 1H), 7.16 (t, $J = 7.7$ Hz, 1H), 6.04 (dq, $J = 6.5, 3.2$ Hz, 1H), 5.59 (p, $J = 7.0$ Hz, 1H), 1.81 (dd, $J = 7.2, 3.2$ Hz, 3H).

^{13}C NMR (151 MHz, CDCl_3) δ 206.38, 137.56, 130.10, 129.65, 129.52, 125.39, 122.87, 93.15, 90.34, 14.11.

HRMS (EI $^+$): calcd. for $[\text{C}_{10}\text{H}_9\text{Br}]^+$: 207.9888, found: 207.9885.

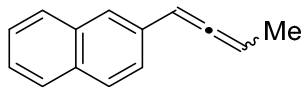


2.1o, 1-(2-methylphenyl)-3-methylbut-1,2-diene²⁷

^1H NMR (500 MHz, CDCl_3) δ 7.40 (d, $J = 7.7$ Hz, 1H), 7.23 – 7.06 (m, 3H), 6.37 – 6.26 (m, 1H), 5.53 (p, $J = 7.1$ Hz, 1H), 2.40 (s, 2H), 1.82 (dt, $J = 6.5, 2.9$ Hz, 3H).

^{13}C NMR (126 MHz, CDCl_3) δ 206.86, 135.00, 133.27, 130.57, 127.31, 126.70, 126.17, 91.42, 88.76, 20.01, 14.34.

HRMS (EI $^+$): calcd. for $[\text{C}_{11}\text{H}_{12}]^+$: 144.0939, found: 144.0941.

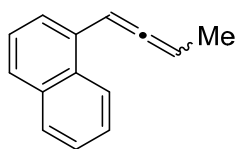


2.1p, 2-(buta-1,2-dien-1-yl)naphthalene²⁸

¹H NMR (600 MHz, CDCl₃) δ 7.88 – 7.80 (m, 3H), 7.71 (s, 1H), 7.57 (dd, *J* = 8.5, 1.8 Hz, 1H), 7.49 (dddd, *J* = 18.9, 8.1, 6.8, 1.4 Hz, 2H), 6.35 (dq, *J* = 6.4, 3.2 Hz, 1H), 5.68 (p, *J* = 7.0 Hz, 1H), 1.90 (dd, *J* = 7.2, 3.3 Hz, 3H).

¹³C NMR (151 MHz, CDCl₃) δ 206.67, 133.85, 132.70, 132.66, 128.25, 127.82, 127.76, 126.26, 125.59, 125.41, 124.85, 94.51, 89.98, 14.31.

HRMS (EI+): calcd. for [C₁₄H₁₂]⁺: 180.0939, found: 180.0940.

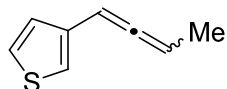


2.1q, 1-(buta-1,2-dien-1-yl)naphthalene²⁸

¹H NMR (600 MHz, CDCl₃) δ 8.27 (d, *J* = 8.3 Hz, 1H), 7.96 – 7.84 (m, 1H), 7.76 (d, *J* = 8.1 Hz, 1H), 7.62 – 7.58 (m, 1H), 7.53 (dddd, *J* = 19.2, 8.1, 6.8, 1.4 Hz, 2H), 7.48 (t, *J* = 7.7 Hz, 1H), 6.83 (dq, *J* = 6.5, 3.2 Hz, 1H), 5.62 (p, *J* = 7.0 Hz, 1H), 1.89 (dd, *J* = 7.2, 3.3 Hz, 3H).

¹³C NMR (151 MHz, CDCl₃) δ 207.48, 133.93, 131.22, 130.85, 128.63, 127.24, 125.92, 125.62, 125.60, 125.26, 123.60, 90.58, 88.51, 14.18.

HRMS (EI+): calcd. for [C₁₄H₁₂]⁺: 180.0939, found: 180.0938.

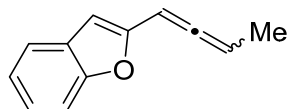


2.1r, 3-(buta-1,2-dien-1-yl)thiophene²⁹

¹H NMR (600 MHz, CDCl₃) δ 7.29 (dt, *J* = 5.0, 2.2 Hz, 1H), 7.14 – 7.12 (m, 1H), 7.09 (s, 1H), 6.22 (dp, *J* = 5.4, 2.8 Hz, 1H), 5.52 (p, *J* = 7.0 Hz, 1H), 1.82 (dt, *J* = 5.4, 2.5 Hz, 3H).

¹³C NMR (151 MHz, CDCl₃) δ 206.28, 136.52, 126.43, 125.80, 120.35, 88.87, 88.70, 14.35.

HRMS (EI+): calcd. for [C₈H₈S]⁺: 136.0347, found: 136.0347.

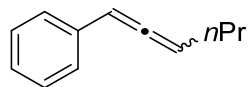


2.1s, 2-(buta-1,2-dien-1-yl)benzofuran

¹H NMR (600 MHz, CDCl₃) δ 7.51 (dd, *J* = 18.6, 7.8 Hz, 2H), 7.25 (dt, *J* = 25.1, 7.5 Hz, 2H), 6.59 (s, 1H), 6.23 (dq, *J* = 6.4, 3.2 Hz, 1H), 5.73 (p, *J* = 7.0 Hz, 1H), 1.89 (dd, *J* = 7.2, 3.2 Hz, 3H).

^{13}C NMR (151 MHz, CDCl_3) δ 206.70, 155.01, 151.60, 129.28, 123.98, 122.81, 120.45, 111.02, 103.53, 90.70, 85.18, 14.24.

HRMS (EI+): calcd. for $[\text{C}_{12}\text{H}_{10}\text{O}]^+$: 170.0732, found: 170.0730.



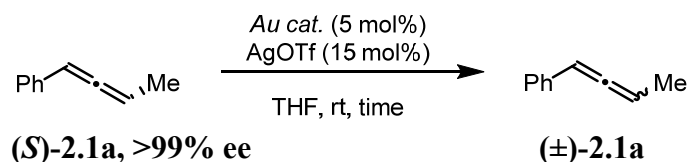
2.1t, hexa-1,2-dien-1-ylbenzene³⁰

^1H NMR (500 MHz, CDCl_3) δ 7.30 (dd, $J = 4.4, 1.4$ Hz, 4H), 7.19 (dtt, $J = 8.7, 5.3, 2.5$ Hz, 1H), 6.13 (dtd, $J = 6.1, 3.0, 1.4$ Hz, 1H), 5.57 (qd, $J = 6.7, 1.3$ Hz, 1H), 2.26 – 2.08 (m, 2H), 1.52 (qd, $J = 7.4, 1.3$ Hz, 2H), 0.98 (td, $J = 7.3, 1.4$ Hz, 3H).

^{13}C NMR (126 MHz, CDCl_3) δ 205.31, 135.25, 128.67, 126.73, 126.68, 95.05, 94.62, 30.98, 22.55, 13.92.

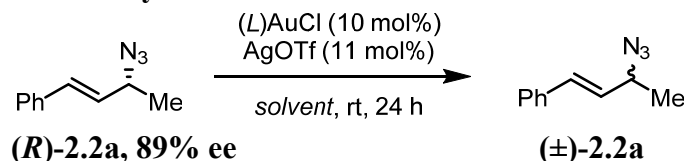
HRMS (EI+): calcd. for $[\text{C}_{12}\text{H}_{14}]^+$: 158.1096, found: 158.1098.

Chiral allene racemization studies



Complex 1.10e (3.5 mg, 0.0025 mmol, 0.05 equiv) or (*R*)-DTBM-BINAP(AuCl)₂ (4.0 mg, 0.0025 mmol, 0.05 equiv) and silver triflate (1.9 mg, 0.0075 mmol, 0.15 equiv) were weighed in a dram vial and a THF was added (1.0 mL). The heterogeneous mixture was sonicated for 5 min using a commercial ultrasonic cleaner, and then filtered through glass fiber into a second dram vial containing **(S)-2.1a**³¹ (6.5 mg, 0.05 mmol, 1.0 equiv). Aliquots of 0.15 mL were taken at 5, 30, and 120 minutes. Aliquots were diluted with hexane (2 mL) and then passed through a short plug of silica gel, washing with hexanes. The solvent was then removed *in vacuo* and the crude residue was analyzed by HPLC (OD-H column, 100% hexanes, 0.25 mL/min).

Chiral allylic azide racemization studies



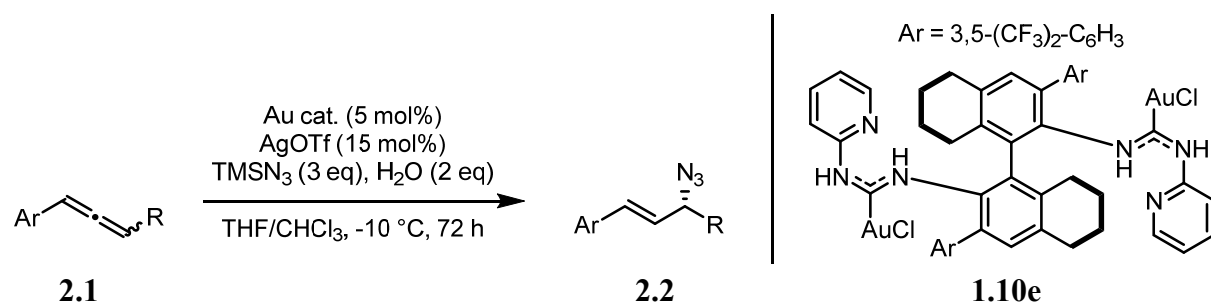
$\text{PPh}_3(\text{AuCl})$ (4.9 mg, 0.010 mmol, 0.10 equiv) or IPrAuCl (6.2 mg, 0.010 mmol, 0.10 equiv) and silver triflate (2.8 mg, 0.011 mmol, 0.11 equiv) were weighed in a dram vial and the appropriate solvent was added (1.0 mL). The heterogeneous mixture was sonicated for 5 min using a commercial ultrasonic cleaner, and then filtered through glass fiber into a second dram vial, which

had been pre-weighed with the allylic azide **2.2a** (17.3 mg, 0.10 mmol, 1.0 equiv). The reaction vial was kept at room temperature for 24 h and then the reaction was quenched by addition of Et₃N (ca. 200 μL, 1.4 mmol). The solvent was then removed *in vacuo* and the crude reaction mixture was passed through a short silica gel plug, washing with Et₂O/hexanes. A sample of the product was then submitted for chiral HPLC analysis (WHELK column, 100% Hexanes, 0.50 mL/min, t_R = major: 13.1 min, minor: 12.4 min.) The results are summarized in Table 2.3.

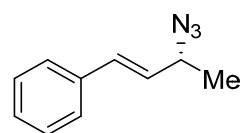
The synthesis of **2.2a** for racemization studies was initially carried out according to the procedure of Murahashi and coworkers.²¹ The maximum enantioselectivity achieved by utilizing this methodology was 80% ee. Subsequent racemization experiments (including those in Table 2.3) used **2.2a** obtained from the optimized gold(I)-catalyzed methodology described below.

Optimized procedure for gold(I)-catalyzed enantioselective hydrazidation

Caution! This protocol generates hydrazoic acid (HN₃), which is acutely toxic and extremely shock sensitive. Handle with care, and do not scale up significantly.



Complex 1.10e (7.0 mg, 0.005 mmol, 0.05 equiv) and silver triflate (3.8 mg, 0.015 mmol, 0.15 equiv) were weighed in a dram vial and a 3:1 volumetric mixture of THF:CHCl₃ was added (1.0 mL). The heterogeneous mixture was sonicated for 5 min using a commercial ultrasonic cleaner, and then filtered through glass fiber into a second dram vial. Substrate **2.1** (0.10 mmol, 1.0 equiv) was weighed in a third dram vial and a 3:1 volumetric mixture of THF:CHCl₃ was added (1.0 mL). TMSN₃ (39 μL, 0.30 mmol, 3 equiv) and water (3.6 μL, 0.20 mmol, 2 equiv) were added *via* microscale syringe. Both vials were cooled to -10 °C, and then the catalyst mixture was added to the reactant mixture *via* pipette. The temperature was maintained for 72 h and then the reaction was quenched by addition of Et₃N (ca. 200 μL, 1.4 mmol). The reaction mixture was diluted with hexane (4 mL) and then passed through a short plug of silica gel, washing with hexane/Et₂O. The solvent was then removed *in vacuo* and the crude reaction mixture was purified by flash column chromatography (hexane/Et₂O, 4 mL Pasteur pipette column) to afford the pure product **2.2**.



2.2a, (*R,E*)-(3-azidobut-1-en-1-yl)benzene³²

0.10 mmol scale, 92% yield (15.9 mg, 0.0918 mmol)

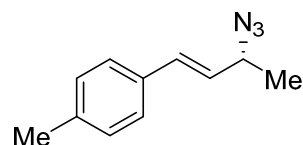
^1H NMR (600 MHz, CDCl_3) δ 7.41 (d, $J = 7.5$ Hz, 2H), 7.34 (t, $J = 7.6$ Hz, 2H), 7.28 (t, $J = 7.4$ Hz, 1H), 6.61 (d, $J = 15.8$ Hz, 1H), 6.15 (dd, $J = 15.8, 7.4$ Hz, 1H), 4.18 (p, $J = 6.8$ Hz, 1H), 1.38 (d, $J = 6.7$ Hz, 3H).

^{13}C NMR (151 MHz, CDCl_3) δ 136.17, 132.31, 128.78, 128.46, 128.21, 126.77, 59.81, 20.37.

HRMS (EI+): calcd. for $[\text{C}_{10}\text{H}_{11}\text{N}_3]^+$: 173.0953, found: 173.0953.

HPLC: WHELK column, 100% Hexanes, 0.50 mL/min, t_{R} = major: 13.1 min, minor: 12.4 min. 90% ee.

$[\alpha]_{\text{D}}^{20} +65.3^\circ$ (c 2.45, CHCl_3)



2.2b, (*R,E*)-1-(3-azidobut-1-en-1-yl)-4-methylbenzene³²

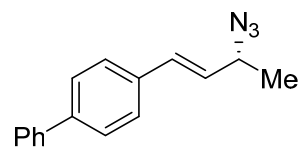
0.10 mmol scale, 89% yield (16.6 mg, 0.0887 mmol)

^1H NMR (600 MHz, CDCl_3) δ 7.30 (d, $J = 7.8$ Hz, 2H), 7.14 (d, $J = 7.8$ Hz, 2H), 6.57 (d, $J = 15.8$ Hz, 1H), 6.10 (dd, $J = 15.8, 7.5$ Hz, 1H), 4.16 (p, $J = 6.8$ Hz, 1H), 2.35 (s, 3H), 1.37 (d, $J = 6.7$ Hz, 3H).

^{13}C NMR (151 MHz, CDCl_3) δ 138.14, 133.38, 132.26, 129.48, 127.41, 126.68, 59.95, 21.36, 20.42.

HRMS (EI+): calcd. for $[\text{C}_{11}\text{H}_{13}\text{N}_3]^+$: 187.1109, found: 187.1112.

HPLC: AD-H column, 100% hexanes, 0.25 mL/min, t_{R} = major: 16.3 min, minor: 17.3 min. 84% ee.



2.2c, (*R,E*)-4-(3-azidobut-1-en-1-yl)-1,1'-biphenyl

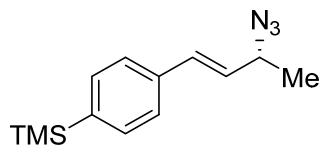
0.10 mmol scale, 84% yield (15.9 mg, 0.0842 mmol)

^1H NMR (600 MHz, CDCl_3) δ 7.62 – 7.58 (m, 4H), 7.51 – 7.42 (m, 4H), 7.36 (t, $J = 7.4$ Hz, 1H), 6.65 (d, $J = 15.8$ Hz, 1H), 6.20 (dd, $J = 15.8, 7.4$ Hz, 1H), 4.21 (p, $J = 6.8$ Hz, 1H), 1.40 (d, $J = 6.7$ Hz, 3H).

^{13}C NMR (151 MHz, CDCl_3) δ 141.03, 140.71, 135.19, 131.86, 128.95, 128.54, 127.56, 127.47, 127.21, 127.10, 59.86, 20.39.

HRMS (EI+): calcd. for $[\text{C}_{16}\text{H}_{15}\text{N}_3]^+$: 249.1269, found: 249.1266.

HPLC: AD-H column, 100% hexanes, 1.00 mL/min, t_R = major: 29.0 min, minor: 33.8 min. 84% ee.



2.2d, (*R,E*)-4-(3-azidobut-1-en-1-yl)phenyltrimethylsilane

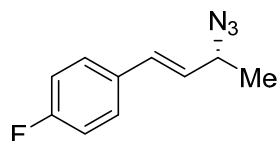
0.10 mmol scale, 67% yield (16.4 mg, 0.0668 mmol)

^1H NMR (600 MHz, CDCl_3) δ 7.50 (d, $J = 7.9$ Hz, 2H), 7.39 (d, $J = 7.8$ Hz, 2H), 6.60 (d, $J = 15.8$ Hz, 1H), 6.18 (dd, $J = 15.8, 7.4$ Hz, 1H), 4.18 (p, $J = 6.8$ Hz, 1H), 1.38 (d, $J = 6.7$ Hz, 3H), 0.27 (s, 9H).

^{13}C NMR (151 MHz, CDCl_3) δ 140.76, 136.54, 133.80, 132.32, 128.70, 126.05, 59.84, 20.38, -1.02.

HRMS (EI⁺): calcd. for $[\text{C}_{13}\text{H}_{19}\text{N}_3\text{Si}]^+$: 245.1348, found: 245.1348.

HPLC: AD-H column, 100% hexanes, 0.50 mL/min, t_R = major: 13.8 min, minor: 16.1 min. 74% ee.



2.2e, (*R,E*)-1-(3-azidobut-1-en-1-yl)-4-fluorobenzene

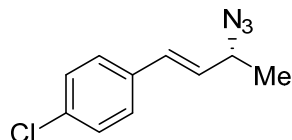
0.10 mmol scale, 86% yield (16.4 mg, 0.0858 mmol)

^1H NMR (600 MHz, CDCl_3) δ 7.37 (dd, $J = 8.5, 5.5$ Hz, 2H), 7.02 (t, $J = 8.6$ Hz, 2H), 6.57 (d, $J = 15.8$ Hz, 1H), 6.06 (dd, $J = 15.8, 7.4$ Hz, 1H), 4.16 (p, $J = 6.8$ Hz, 1H), 1.37 (d, $J = 6.7$ Hz, 3H).

^{13}C NMR (151 MHz, CDCl_3) δ 162.72 (d, $J = 247.6$ Hz), 132.33 (d, $J = 3.2$ Hz), 131.11, 128.33 (d, $J = 8.1$ Hz), 128.25 (d, $J = 1.7$ Hz), 115.72 (d, $J = 21.7$ Hz), 59.73, 20.35.

HRMS (EI⁺): calcd. for $[\text{C}_{10}\text{H}_{10}\text{N}_3\text{F}]^+$: 191.0859, found: 191.0857.

HPLC: AS-H column, 100% hexanes, 0.25 mL/min, t_R = major: 41.4 min, minor: 34.3 min. 86% ee.



2.2f, (*R,E*)-1-(3-azidobut-1-en-1-yl)-4-chlorobenzene

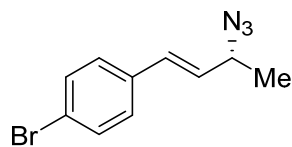
0.10 mmol scale, 87% yield (18.1 mg, 0.0872 mmol)

^1H NMR (600 MHz, CDCl_3) δ 7.34 – 7.28 (m, 4H), 6.55 (d, $J = 15.8$ Hz, 1H), 6.12 (dd, $J = 15.8$, 7.3 Hz, 1H), 4.20 – 4.13 (m, 1H), 1.38 (d, $J = 6.7$ Hz, 3H).

^{13}C NMR (151 MHz, CDCl_3) δ 134.70, 133.91, 131.00, 129.20, 128.97, 127.98, 59.63, 20.29.

HRMS (EI^+): calcd. for $[\text{C}_{10}\text{H}_{10}\text{N}_3\text{Cl}]^+$: 207.0563, found: 207.0561.

HPLC: AD-H column, 100% hexanes, 0.25 mL/min, t_{R} = major: 41.3 min, minor: 42.9 min. 89% ee.



2.2g, (*R,E*)-1-(3-azidobut-1-en-1-yl)-4-bromobenzene³²

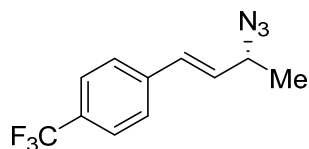
0.10 mmol scale, 88% yield (22.1 mg, 0.0877 mmol)

^1H NMR (600 MHz, CDCl_3) δ 7.48 (d, $J = 8.3$ Hz, 2H), 7.35 – 7.22 (m, 2H), 6.57 (d, $J = 15.8$ Hz, 1H), 6.16 (dd, $J = 15.8$, 7.3 Hz, 1H), 4.19 (p, $J = 6.8$ Hz, 1H), 1.41 (d, $J = 6.7$ Hz, 2H).

^{13}C NMR (151 MHz, CDCl_3) δ 135.15, 131.92, 131.05, 129.34, 128.28, 122.06, 59.61, 20.27.

HRMS (EI^+): calcd. for $[\text{C}_{10}\text{H}_{10}\text{N}_3\text{Br}]^+$: 251.0058, found: 251.0058.

HPLC: AD-H column, 100% hexanes, 0.50 mL/min, t_{R} = major: 23.5 min, minor: 25.2 min. 90% ee.



2.2h, (*R,E*)-1-(3-azidobut-1-en-1-yl)-4-(trifluoromethyl)benzene

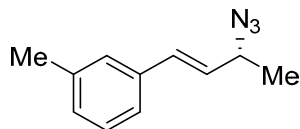
0.10 mmol scale, 41% yield (9.9 mg, 0.0410 mmol)

^1H NMR (600 MHz, CDCl_3) δ 7.59 (d, $J = 8.1$ Hz, 2H), 7.49 (d, $J = 8.0$ Hz, 2H), 6.64 (d, $J = 15.8$ Hz, 1H), 6.24 (dd, $J = 15.8$, 7.1 Hz, 1H), 4.20 (p, $J = 6.8$ Hz, 1H), 1.40 (d, $J = 6.7$ Hz, 3H).

^{13}C NMR (151 MHz, CDCl_3) δ 139.71, 131.24, 130.75, 130.05 (q, $J = 32.5$ Hz), 126.94, 125.76 (q, $J = 3.9$ Hz), 59.42, 20.19.

HRMS (EI^+): calcd. for $[\text{C}_{11}\text{H}_{10}\text{N}_3\text{F}_3]^+$: 241.0827, found: 241.0827.

HPLC: AS-H column, 100% hexanes, 0.50 mL/min, t_{R} = major: 14.8 min, minor: 13.3 min. 74% ee.



2.2i, (*R,E*)-1-(3-azidobut-1-en-1-yl)-3-methylbenzene

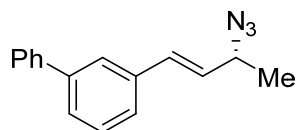
0.10 mmol scale, 89% yield (16.7 mg, 0.0892 mmol)

^1H NMR (600 MHz, CDCl_3) δ 7.25 – 7.18 (m, 3H), 7.09 (d, $J = 7.0$ Hz, 1H), 6.57 (d, $J = 15.8$ Hz, 1H), 6.13 (dd, $J = 15.8, 7.4$ Hz, 1H), 4.17 (p, $J = 6.8$ Hz, 1H), 2.35 (s, 3H), 1.37 (d, $J = 6.6$ Hz, 3H).

^{13}C NMR (151 MHz, CDCl_3) δ 138.38, 136.13, 132.45, 129.02, 128.69, 128.25, 127.47, 123.96, 59.88, 21.52, 20.41.

HRMS (EI+): calcd. for $[\text{C}_{11}\text{H}_{13}\text{N}_3]^+$: 187.1109, found: 187.1110.

HPLC: AD-H column, 100% hexanes, 0.25 mL/min, t_{R} = major: 30.2 min, minor: 32.4 min. 85% ee.



2.2j, (*R,E*)-3-(3-azidobut-1-en-1-yl)-1,1'-biphenyl

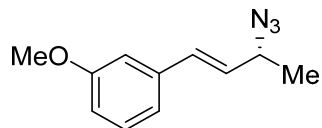
0.10 mmol scale, 92% yield (23.0 mg, 0.0923 mmol)

^1H NMR (600 MHz, CDCl_3) δ 7.62 (m, 3H), 7.52 (d, $J = 7.2$ Hz, 1H), 7.47 (t, $J = 7.6$ Hz, 2H), 7.40 (m, 3H), 6.69 (d, $J = 15.8$ Hz, 1H), 6.23 (dd, $J = 15.8, 7.4$ Hz, 1H), 4.21 (p, $J = 6.8$ Hz, 1H), 1.41 (d, $J = 6.7$ Hz, 3H).

^{13}C NMR (151 MHz, CDCl_3) δ 141.84, 141.04, 136.63, 132.20, 129.20, 128.92, 128.85, 127.58, 127.30, 127.09, 125.68, 125.62, 59.81, 20.38.

HRMS (EI+): calcd. for $[\text{C}_{16}\text{H}_{15}\text{N}_3]^+$: 249.1266, found: 249.1266.

HPLC: WHELK column, 100% hexanes 0.75 mL/min, t_{R} = major: 22.0 min, minor: 20.2 min. 89% ee.



2.2k, (*R,E*)-1-(3-azidobut-1-en-1-yl)-3-methoxybenzene

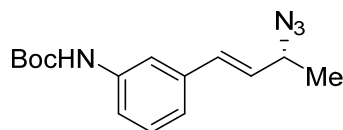
0.10 mmol scale, 65% yield (13.2 mg, 0.0649 mmol)

^1H NMR (600 MHz, CDCl_3) δ 7.29 – 7.24 (m, 1H), 7.02 (d, $J = 7.7$ Hz, 1H), 6.95 (s, 1H), 6.85 (dd, $J = 8.2, 2.0$ Hz, 1H), 6.60 (d, $J = 15.8$ Hz, 1H), 6.16 (dd, $J = 15.8, 7.4$ Hz, 1H), 4.20 (p, $J = 6.8$ Hz, 1H), 3.85 (s, 3H), 1.40 (d, $J = 6.7$ Hz, 3H).

^{13}C NMR (151 MHz, CDCl_3) δ 160.01, 137.64, 132.19, 129.78, 128.81, 119.44, 113.92, 112.09, 59.76, 55.41, 20.36.

HRMS (EI+): calcd. for $[\text{C}_{11}\text{H}_{13}\text{N}_3\text{O}]^+$: 203.1059, found: 203.1058.

HPLC: AD-H column, 100% hexanes, 1.00 mL/min, t_{R} = major: 23.0 min, minor: 25.5 min. 84% ee.



2.2l, *tert*-butyl (*R,E*)-(3-(3-azidobut-1-en-1-yl)phenyl)carbamate

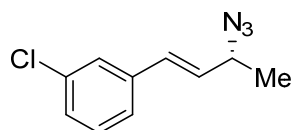
0.10 mmol scale, 83% yield (23.8 mg, 0.0825 mmol)

^1H NMR (500 MHz, CDCl_3) δ 7.53 (s, 1H), 7.28 – 7.20 (m, 1H), 7.21 – 7.14 (m, 1H), 7.07 (dt, J = 7.5, 1.3 Hz, 1H), 6.56 (d, J = 15.7 Hz, 1H), 6.49 (s, 1H), 6.15 (dd, J = 15.8, 7.4 Hz, 1H), 4.16 (p, J = 6.8 Hz, 1H), 1.52 (s, 9H), 1.36 (d, J = 6.7 Hz, 3H).

^{13}C NMR (151 MHz, CDCl_3) δ 152.83, 138.88, 137.12, 132.04, 129.30, 128.91, 121.59, 118.27, 116.61, 80.77, 59.73, 28.48, 20.30.

HRMS (EI+): calcd. for $[\text{C}_{15}\text{H}_{20}\text{N}_4\text{O}_2]^+$: 288.1586, found: 288.1582.

HPLC: AS-H column, 99:1 hexanes:isopropanol, 1.00 mL/min, t_{R} = major: 15.1 min, minor: 13.5 min. 92% ee.



2.2m, (*R,E*)-1-(3-azidobut-1-en-1-yl)-3-chlorobenzene

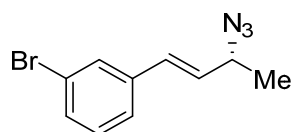
0.10 mmol scale, 71% yield (14.6 mg, 0.0703 mmol)

^1H NMR (600 MHz, CDCl_3) δ 7.42 (s, 1H), 7.28 (m, 3H), 6.57 (d, J = 15.8 Hz, 1H), 6.18 (dd, J = 15.8, 7.3 Hz, 1H), 4.20 (p, J = 6.8 Hz, 1H), 1.41 (d, J = 6.7 Hz, 3H).

^{13}C NMR (151 MHz, CDCl_3) δ 138.09, 134.80, 130.86, 130.08, 130.01, 128.17, 126.69, 125.02, 59.51, 20.27.

HRMS (EI+): calcd. for $[\text{C}_{10}\text{H}_{10}\text{N}_3\text{Cl}]^+$: 207.0563, found: 207.0561.

HPLC: WHELK column, 100% hexanes, 0.30 mL/min, t_{R} = major: 24.9 min, minor: 22.7 min. 87% ee.



2.2n, (*R,E*)-1-(3-azidobut-1-en-1-yl)-3-bromobenzene

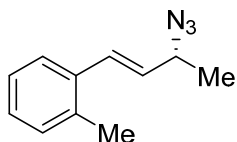
0.10 mmol scale, 87% yield (21.9 mg, 0.0869 mmol)

^1H NMR (600 MHz, CDCl_3) δ 7.55 (s, 1H), 7.39 (d, $J = 7.8$ Hz, 1H), 7.30 (d, $J = 7.7$ Hz, 1H), 7.20 (t, $J = 7.8$ Hz, 1H), 6.53 (d, $J = 15.7$ Hz, 1H), 6.15 (dd, $J = 15.8, 7.2$ Hz, 1H), 4.17 (p, $J = 6.8$ Hz, 1H), 1.38 (d, $J = 6.7$ Hz, 3H).

^{13}C NMR (151 MHz, CDCl_3) δ 138.35, 131.08, 130.74, 130.29, 130.11, 129.61, 125.47, 122.98, 59.51, 20.28.

HRMS (EI+): calcd. for $[\text{C}_{10}\text{H}_{10}\text{N}_3\text{Br}]^+$: 251.0058, found: 251.0062.

HPLC: WHELK column, 100% hexanes, 0.25 mL/min, t_{R} = major: 40.0 min, minor: 37.7 min. 88% ee.



2.2o, (*R,E*)-1-(3-azidobut-1-en-1-yl)-2-methylbenzene

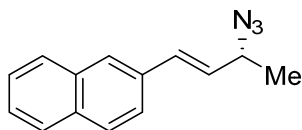
0.10 mmol scale, 81% yield (15.2 mg, 0.0812 mmol)

^1H NMR (600 MHz, CDCl_3) δ 7.47 – 7.42 (m, 1H), 7.22 – 7.15 (m, 3H), 6.82 (d, $J = 15.6$ Hz, 1H), 6.02 (dd, $J = 15.6, 7.5$ Hz, 1H), 4.20 (p, $J = 6.8$ Hz, 1H), 2.37 (s, 3H), 1.39 (d, $J = 6.7$ Hz, 3H).

^{13}C NMR (151 MHz, CDCl_3) δ 135.79, 135.41, 130.47, 130.38, 129.78, 128.10, 126.29, 126.00, 60.04, 20.46, 19.95.

HRMS (EI+): calcd. for $[\text{C}_{11}\text{H}_{13}\text{N}_3]^+$: 187.1109, found: 187.1110.

HPLC: AD-H column, 100% hexanes, 0.50 mL/min, t_{R} = major: 12.4 min, minor: 13.3 min. 62% ee.



2.2p, (*R,E*)-2-(3-azidobut-1-en-1-yl)naphthalene

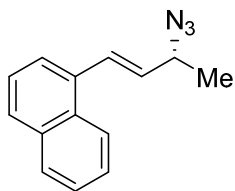
0.10 mmol scale, 89% yield (19.9 mg, 0.0891 mmol)

^1H NMR (600 MHz, CDCl_3) δ 7.81 (m, 3H), 7.77 (s, 1H), 7.61 (d, $J = 8.5$ Hz, 1H), 7.47 (m, 2H), 6.77 (d, $J = 15.8$ Hz, 1H), 6.28 (dd, $J = 15.8, 7.4$ Hz, 1H), 4.24 (p, $J = 6.8$ Hz, 1H), 1.43 (d, $J = 6.7$ Hz, 3H).

^{13}C NMR (151 MHz, CDCl_3) δ 133.65, 133.62, 133.33, 132.39, 128.81, 128.46, 128.17, 127.82, 126.99, 126.52, 126.26, 123.63, 59.90, 20.41.

HRMS (EI+): calcd. for $[\text{C}_{14}\text{H}_{13}\text{N}_3]^+$: 223.1109, found: 223.1109.

HPLC: WHELK column, 100% hexanes, 0.75 mL/min, t_R = major: 26.5 min, minor: 24.2 min. 91% ee.



2.2q, (*R,E*)-1-(3-azidobut-1-en-1-yl)naphthalene³²

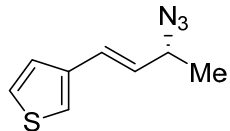
0.10 mmol scale, 71% yield (15.8 mg, 0.0708 mmol)

¹H NMR (600 MHz, CDCl₃) δ 8.10 (d, J = 8.3 Hz, 1H), 7.87 (d, J = 8.0 Hz, 1H), 7.82 (d, J = 8.2 Hz, 1H), 7.61 (d, J = 7.1 Hz, 1H), 7.53 (dt, J = 14.7, 7.1 Hz, 2H), 7.46 (t, J = 7.6 Hz, 1H), 7.36 (d, J = 15.5 Hz, 1H), 6.18 (dd, J = 15.5, 7.3 Hz, 1H), 4.31 (p, J = 6.8 Hz, 1H), 1.46 (d, J = 6.7 Hz, 3H).

¹³C NMR (151 MHz, CDCl₃) δ 134.02, 133.72, 131.72, 131.26, 129.72, 128.72, 128.56, 126.38, 126.03, 125.70, 124.33, 123.82, 59.91, 20.44.

HRMS (EI⁺): calcd. for [C₁₄H₁₃N₃]⁺: 223.1109, found: 223.1108.

HPLC: WHELK column, 100% hexanes, 0.50 mL/min, t_R = major: 26.4 min, minor: 23.1 min. 68% ee.



2.2r, (*R,E*)-3-(3-azidobut-1-en-1-yl)thiophene

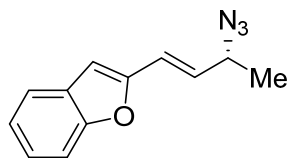
0.10 mmol scale, 86% yield (15.5 mg, 0.0865 mmol)

¹H NMR (600 MHz, CDCl₃) δ 7.29 (dd, J = 5.1, 2.9 Hz, 1H), 7.24 – 7.12 (m, 2H), 6.61 (d, J = 15.7 Hz, 1H), 6.00 (dd, J = 15.8, 7.4 Hz, 1H), 4.14 (p, J = 6.9 Hz, 1H), 1.36 (d, J = 6.7 Hz, 3H).

¹³C NMR (151 MHz, CDCl₃) δ 138.79, 128.31, 126.42, 126.40, 125.10, 123.17, 59.81, 20.36.

HRMS (EI⁺): calcd. for [C₈H₉N₃S]⁺: 179.0517, found: 179.0517.

HPLC: WHELK column, 100% hexanes, 0.30 mL/min, t_R = major: 27.7 min, minor: 25.9 min. 75% ee.



2.2s, (*R,E*)-2-(3-azidobut-1-en-1-yl)benzofuran

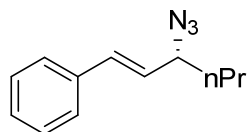
0.10 mmol scale, 81% yield (17.7 mg, 0.0830 mmol)

^1H NMR (500 MHz, CDCl_3) δ 8.16 (d, $J = 7.5$ Hz, 1H), 8.08 (dd, $J = 8.3, 2.3$ Hz, 1H), 7.97 – 7.86 (m, 2H), 7.84 (td, $J = 7.5, 2.4$ Hz, 1H), 7.18 (dd, $J = 15.7, 2.4$ Hz, 1H), 7.03 (ddd, $J = 15.7, 7.1, 2.4$ Hz, 1H), 4.84 (h, $J = 6.9, 6.2$ Hz, 1H), 2.05 (dd, $J = 6.8, 2.4$ Hz, 3H).

^{13}C NMR (126 MHz, CDCl_3) δ 154.94, 153.49, 130.33, 128.84, 125.00, 123.05, 121.16, 120.27, 111.10, 105.79, 59.17, 20.18.

HRMS (EI+): calcd. for $[\text{C}_{12}\text{H}_{11}\text{N}_3\text{O}]^+$: 213.0902, found: 213.0902.

HPLC: AD-H column, 100% hexanes, 0.50 mL/min, t_{R} = major: 23.7 min, minor: 28.7 min. 70% ee.



2.2t, (*R,E*)-(3-azidohex-1-en-1-yl)benzene³³

0.10 mmol scale, 51% yield (10.3 mg, 0.0512 mmol)

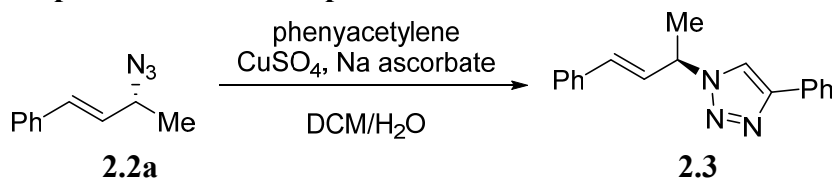
^1H NMR (600 MHz, CDCl_3) δ 7.41 (d, $J = 7.5$ Hz, 2H), 7.34 (t, $J = 7.6$ Hz, 2H), 7.30 – 7.26 (m, 1H), 6.61 (d, $J = 15.8$ Hz, 1H), 6.11 (dd, $J = 15.8, 8.1$ Hz, 1H), 4.01 (q, $J = 7.3$ Hz, 1H), 1.69 – 1.61 (m, 1H), 1.61 – 1.55 (m, 1H), 1.50 – 1.36 (m, 2H), 0.95 (t, $J = 7.4$ Hz, 3H).

^{13}C NMR (151 MHz, CDCl_3) δ 136.08, 133.12, 128.65, 128.09, 127.29, 126.64, 64.66, 36.85, 19.17, 13.76.

HRMS (EI+): calcd. for $[\text{C}_{12}\text{H}_{15}\text{N}_3]^+$: 201.1266, found: 201.1264.

HPLC: WHELK column, 100% hexanes, 0.50 mL/min, t_{R} = major: 11.7 min, minor: 11.0 min. 66% ee.

Preparation of triazole product



2.3, (*R,E*)-4-phenyl-1-(4-phenylbut-3-en-2-yl)-1H-1,2,3-triazole

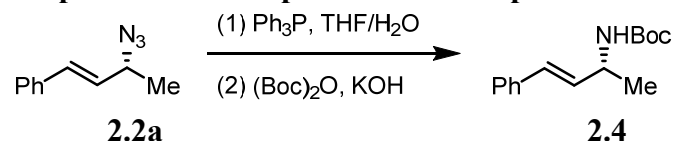
The title compound was prepared in a procedure modified from Creary and coworkers.³⁴ Crude azide **2.2a** (from 0.1 mmol of allene **2.1a**) and phenylacetylene (22 μL , 0.20 mmol, 2 equiv) were dissolved in a mixture of DCM (1.0 mL) and H_2O (0.5 mL) and treated with CuSO_4 (1.6 mg, 0.010 mmol, 0.10 equiv) and Na ascorbate (4.0 mg, 0.020 mmol, 0.20 equiv). The reaction mixture was stirred for 24 hours at room temperature, then the phases were separated, the aqueous layer was extracted with DCM, and the combined organic layers were dried over MgSO_4 . The solvent was

removed *in vacuo*, and the crude residue was chromatographed on silica gel with hexane/Et₂O as eluent to afford the pure product as a white powder (12.2 mg, 0.044 mmol, 44% yield).

The spectral data are in agreement with those previously reported.³³

HPLC: AD-H column, 95:5 hexanes:isopropanol, 1.00 mL/min, *t_R* = major: 28.8 min, minor: 27.6 min. 89% ee.

Preparation of Boc-protected amine product



2.4, tert-butyl (*R,E*)-(4-phenylbut-3-en-2-yl)carbamate

The title compound was prepared in a procedure modified from Rueping³⁵ and Atlan.³⁶ Crude azide **2.2a** (from 0.1 mmol of allene **2.1a**) was dissolved in a mixture of THF (1.5 mL) and H₂O (0.3 mL) and treated with PPh₃ (57.7 mg, 0.22 mmol, 2.2 equiv). The reaction mixture was stirred at room temperature until TLC analysis showed full consumption of starting material. The reaction mixture was then made basic with KOH (2M) and di-*tert*-butyldicarbonate was added (92 μL, 0.4 mmol, 4.0 equiv.). The reaction mixture was stirred at room temperature for 24 hours and then THF was removed *in vacuo*. The aqueous material was acidified with aqueous NH₄Cl (saturated solution) and extracted with DCM. The combined organic layers were dried over MgSO₄. The solvent was removed *in vacuo*, and the crude residue was chromatographed on silica gel with hexane/EtOAc as eluent to afford the pure product as a white powder (13.6 mg, 0.055 mmol, 55% yield).

The spectral data are in agreement with those previously reported.³⁷

HPLC: AD-H column, 95:5 hexanes:isopropanol, 1.00 mL/min, *t_R* = major: 6.5 min, minor: 8.1 min. 89% ee.

References

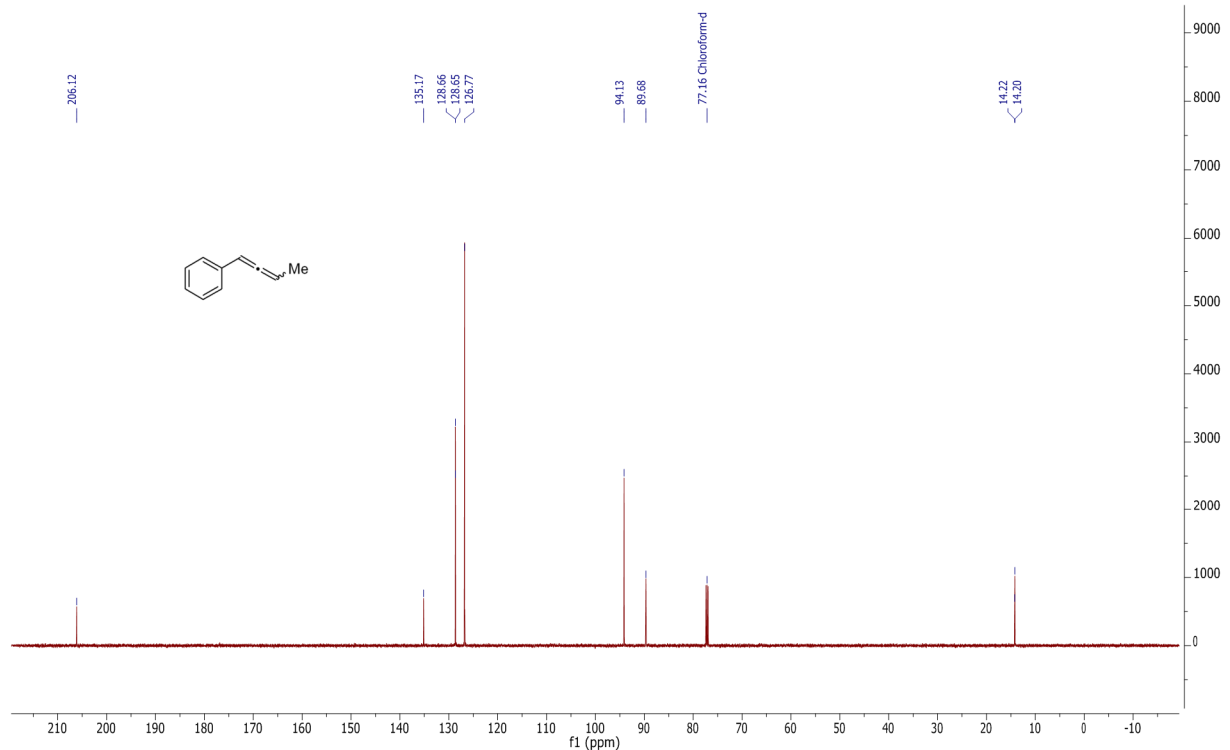
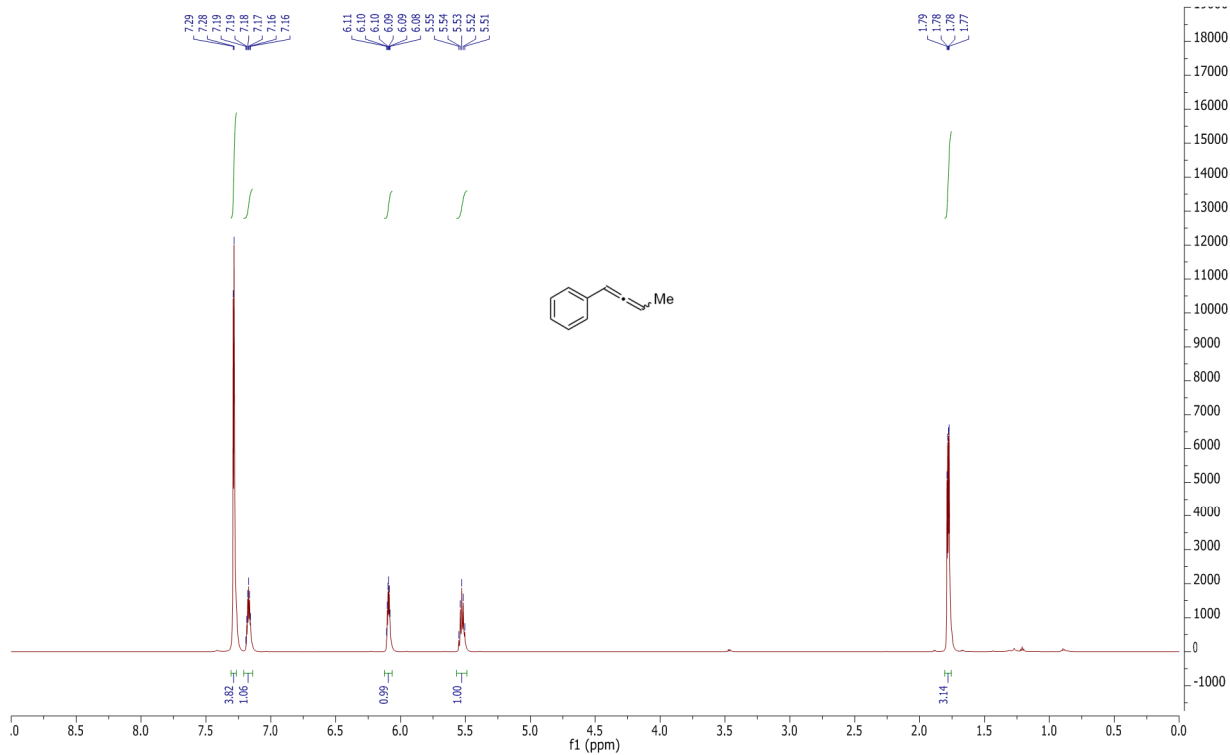
- (1) Bräse, S.; Gil, C.; Knepper, K.; Zimmermann, V. *Angew. Chem. Int. Ed.* **2005**, *44* (33), 5188.
- (2) Boyer, J. H. *J. Am. Chem. Soc.* **1951**, *73* (11), 5248.
- (3) Waser, J.; Carreira, E. M. In *Organic Azides*; Bräse, S., Banert, K., Eds.; John Wiley & Sons, Ltd, 2009; pp 95–111.
- (4) Kapat, A.; König, A.; Montermini, F.; Renaud, P. *J. Am. Chem. Soc.* **2011**, *133* (35), 13890.
- (5) Liu, Z.; Liu, J.; Zhang, L.; Liao, P.; Song, J.; Bi, X. *Angew. Chem. Int. Ed.* **2014**, *53* (21), 5305.
- (6) Liu, Z.; Liao, P.; Bi, X. *Org. Lett.* **2014**, *16* (14), 3668.
- (7) Hurtado-Rodrigo, C.; Hoehne, S.; Muñoz, M. P. *Chem. Commun.* **2014**, *50* (12), 1494.
- (8) Trost, B. M.; Pulley, S. R. *Tetrahedron Lett.* **1995**, *36* (48), 8737.
- (9) Gagnon, D.; Lauzon, S.; Godbout, C.; Spino, C. *Org. Lett.* **2005**, *7* (21), 4769.
- (10) Myers, J. K.; Jacobsen, E. N. *J. Am. Chem. Soc.* **1999**, *121* (38), 8959.
- (11) Taylor, M. S.; Zalatan, D. N.; Lerchner, A. M.; Jacobsen, E. N. *J. Am. Chem. Soc.* **2005**, *127* (4), 1313.
- (12) Horstmann, T. E.; Guerin, D. J.; Miller, S. J. *Angew. Chem. Int. Ed.* **2000**, *39* (20), 3635.
- (13) Guerin, D. J.; Miller, S. J. *J. Am. Chem. Soc.* **2002**, *124* (10), 2134.
- (14) Bellavista, T.; Meninno, S.; Lattanzi, A.; Della Sala, G. *Adv. Synth. Catal.* **2015**, *357* (14-15), 3365.
- (15) Haydl, A. M.; Xu, K.; Breit, B. *Angew. Chem.* **2015**, *127* (24), 7255.
- (16) Xu, K.; Gilles, T.; Breit, B. *Nat. Commun.* **2015**, *6*, 7616.
- (17) Harris, R. J.; Nakafuku, K.; Widenhoefer, R. A. *Chem. – Eur. J.* **2014**, *20* (38), 12245.
- (18) Wang, Z. J.; Benitez, D.; Tkatchouk, E.; Goddard III, W. A.; Toste, F. D. *J. Am. Chem. Soc.* **2010**, *132* (37), 13064.
- (19) Gagneux, A.; Winstein, S.; Young, W. G. *J. Am. Chem. Soc.* **1960**, *82* (22), 5956.
- (20) Wang, T.-T.; Wang, F.-X.; Yang, F.-L.; Tian, S.-K. *Chem. Commun.* **2014**, *50* (29), 3802.
- (21) Murahashi, S.; Taniguchi, Y.; Imada, Y.; Tanigawa, Y. *J. Org. Chem.* **1989**, *54* (14), 3292.
- (22) Bordwell, F. G. *Acc. Chem. Res.* **1988**, *21* (12), 456.
- (23) Zhang, Z.; Du Lee, S.; Fisher, A. S.; Widenhoefer, R. A. *Tetrahedron* **2009**, *65* (9), 1794.
- (24) Rostovtsev, V. V.; Green, L. G.; Fokin, V. V.; Sharpless, K. B. *Angew. Chem. Int. Ed.* **2002**, *41* (14), 2596.
- (25) Staudinger, H.; Meyer, J. *Helv. Chim. Acta* **1919**, *2* (1), 635.
- (26) Yoshida, M.; Okada, T.; Shishido, K. *Tetrahedron* **2007**, *63* (30), 6996.
- (27) Butler, K. L.; Tragni, M.; Widenhoefer, R. A. *Angew. Chem. Int. Ed.* **2012**, *51* (21), 5175.
- (28) Caporusso, A. M.; Zampieri, A.; Aronica, L. A.; Banti, D. *J. Org. Chem.* **2006**, *71* (5), 1902.
- (29) Tran, D. N.; Cramer, N. *Angew. Chem. Int. Ed.* **2013**, *52* (40), 10630.
- (30) Zhang, H.; Fu, X.; Chen, J.; Wang, E.; Liu, Y.; Li, Y. *J. Org. Chem.* **2009**, *74* (24), 9351.
- (31) Myers, A. G.; Zheng, B. *J. Am. Chem. Soc.* **1996**, *118* (18), 4492.
- (32) Surendra Reddy, P.; Ravi, V.; Sreedhar, B. *Tetrahedron Lett.* **2010**, *51* (31), 4037.
- (33) Hou, J.; Feng, C.; Li, Z.; Fang, Q.; Wang, H.; Gu, G.; Shi, Y.; Liu, P.; Xu, F.; Yin, Z.; Shen, J.; Wang, P. *Eur. J. Med. Chem.* **2011**, *46* (8), 3190.
- (34) Creary, X.; Anderson, A.; Brophy, C.; Crowell, F.; Funk, Z. *J. Org. Chem.* **2012**, *77* (19), 8756.
- (35) Rueping, M.; Vila, C.; Uria, U. *Org. Lett.* **2012**, *14* (3), 768.

- (36) Atlan, V.; Racouchot, S.; Rubin, M.; Bremer, C.; Ollivier, J.; de Meijere, A.; Salaün, J. *Tetrahedron Asymmetry* **1998**, *9* (7), 1131.
- (37) Reginato, G.; Mordini, A.; Messina, F.; Degl'Innocenti, A.; Poli, G. *Tetrahedron* **1996**, *52* (33), 10985.

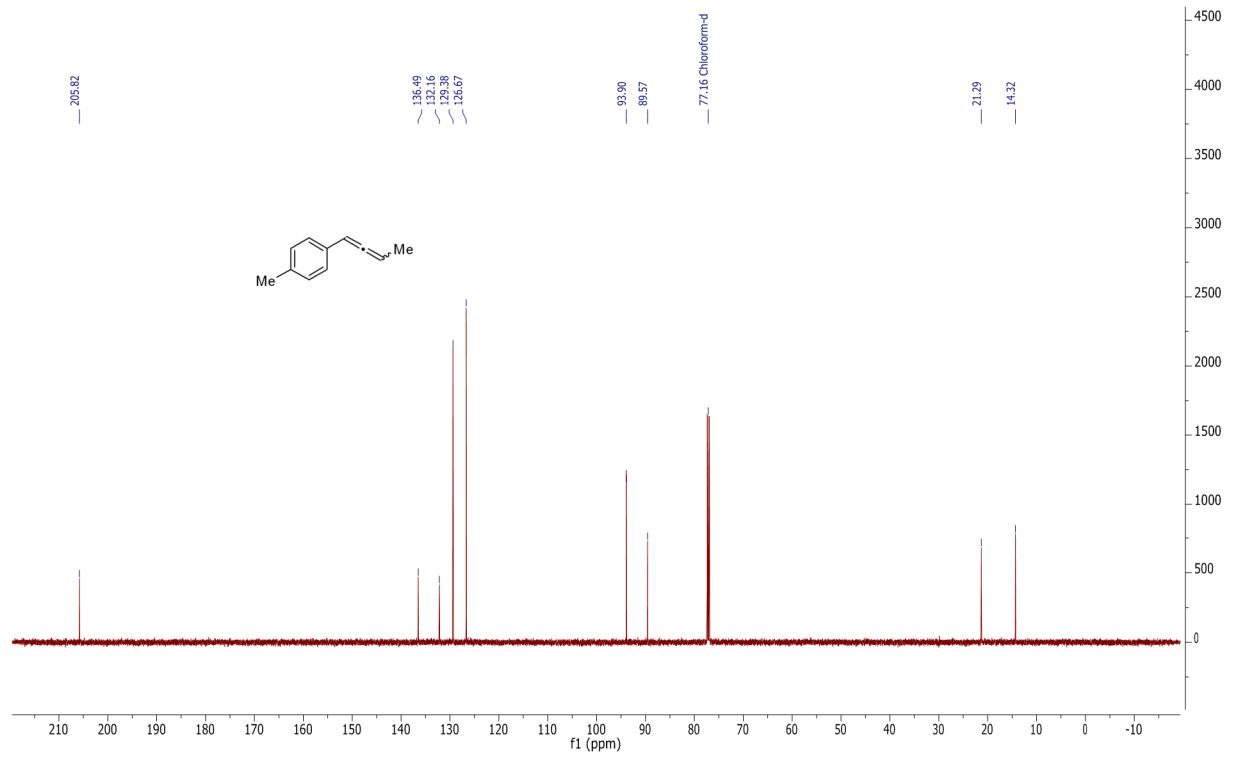
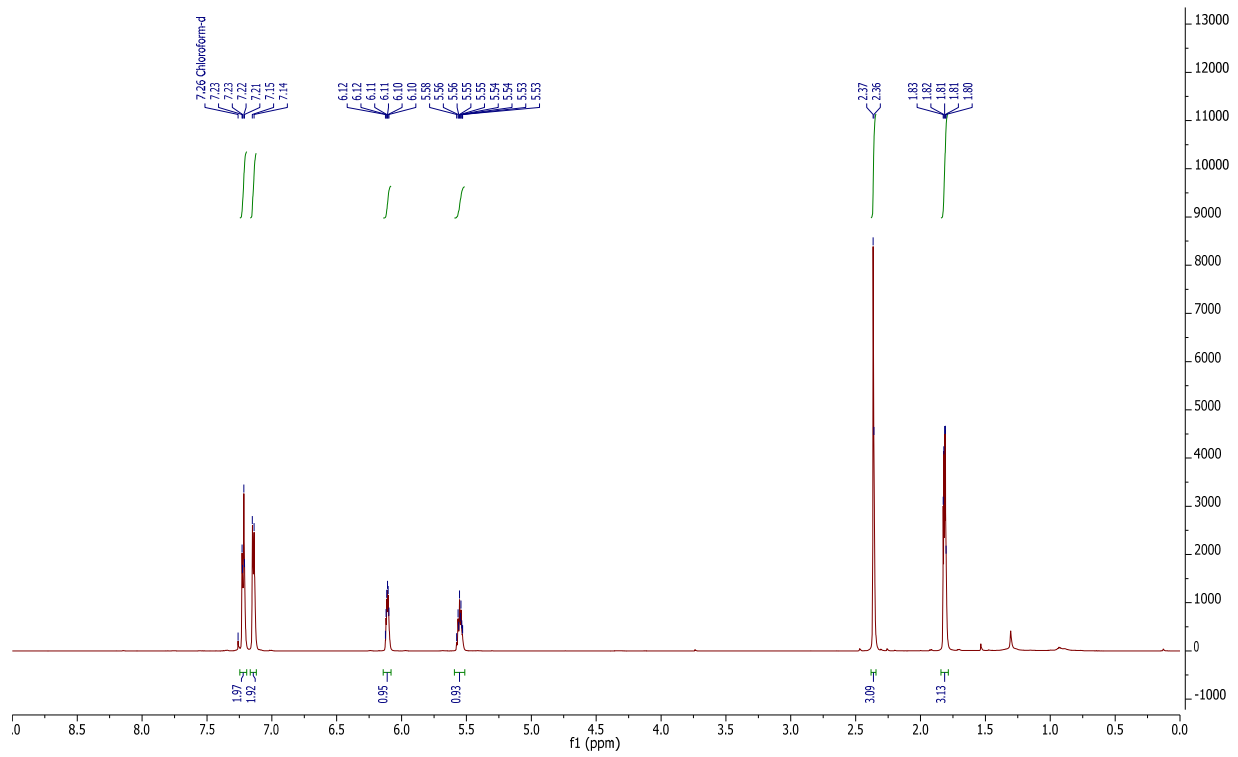
Appendix 1 - NMR Spectra

In some cases, unintegrated resonances in the 0-2 ppm region may appear. These correspond to trace quantities of residual solvents, including water, grease, and other aliphatic hydrocarbons.

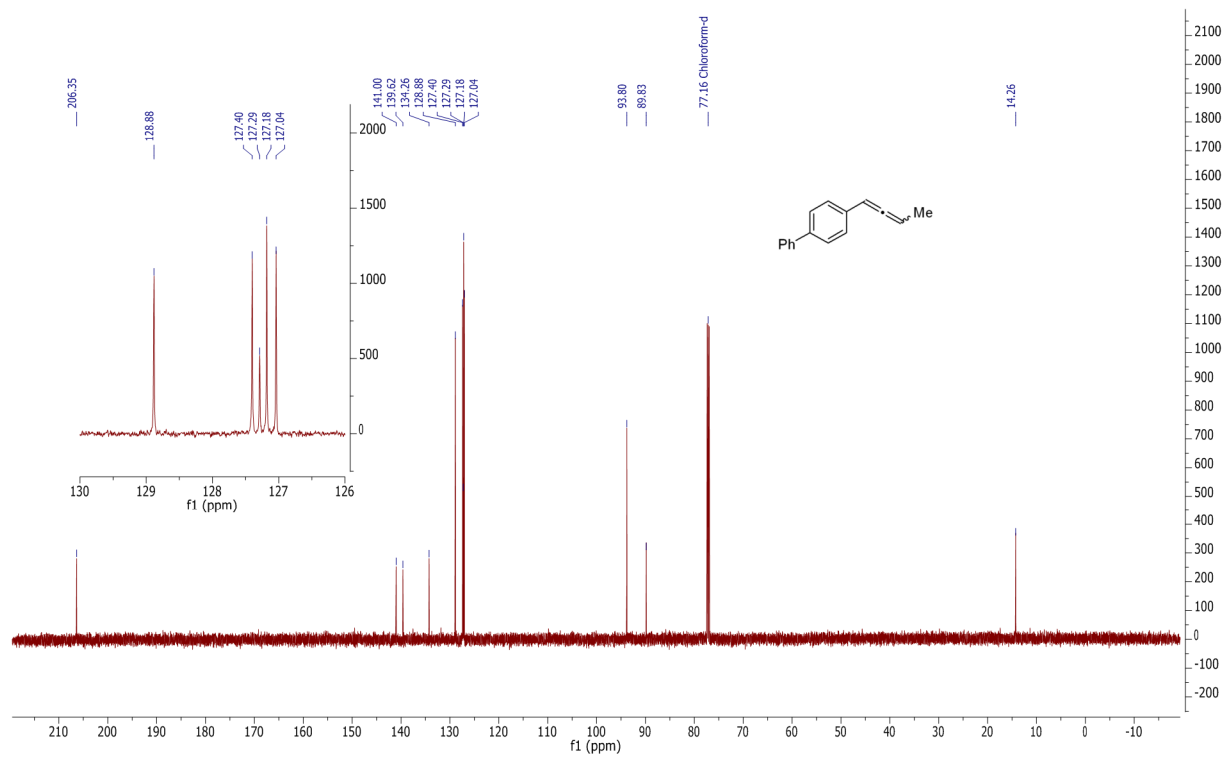
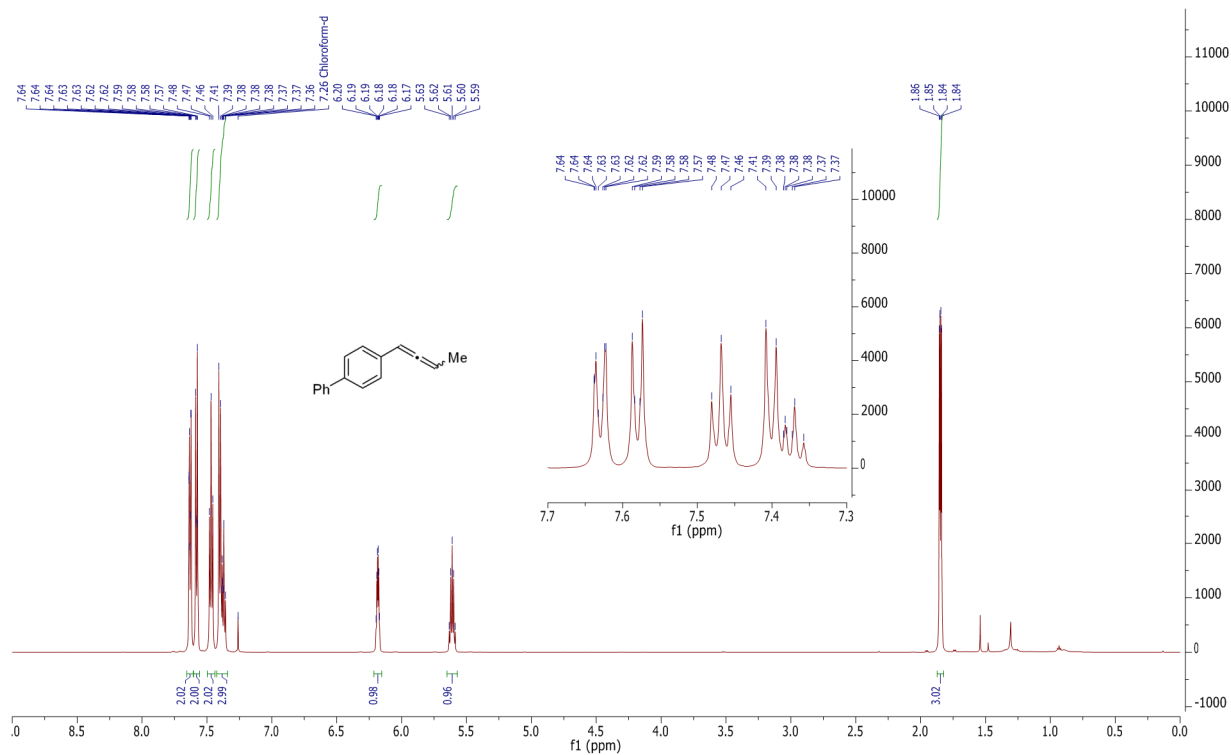
2.1a



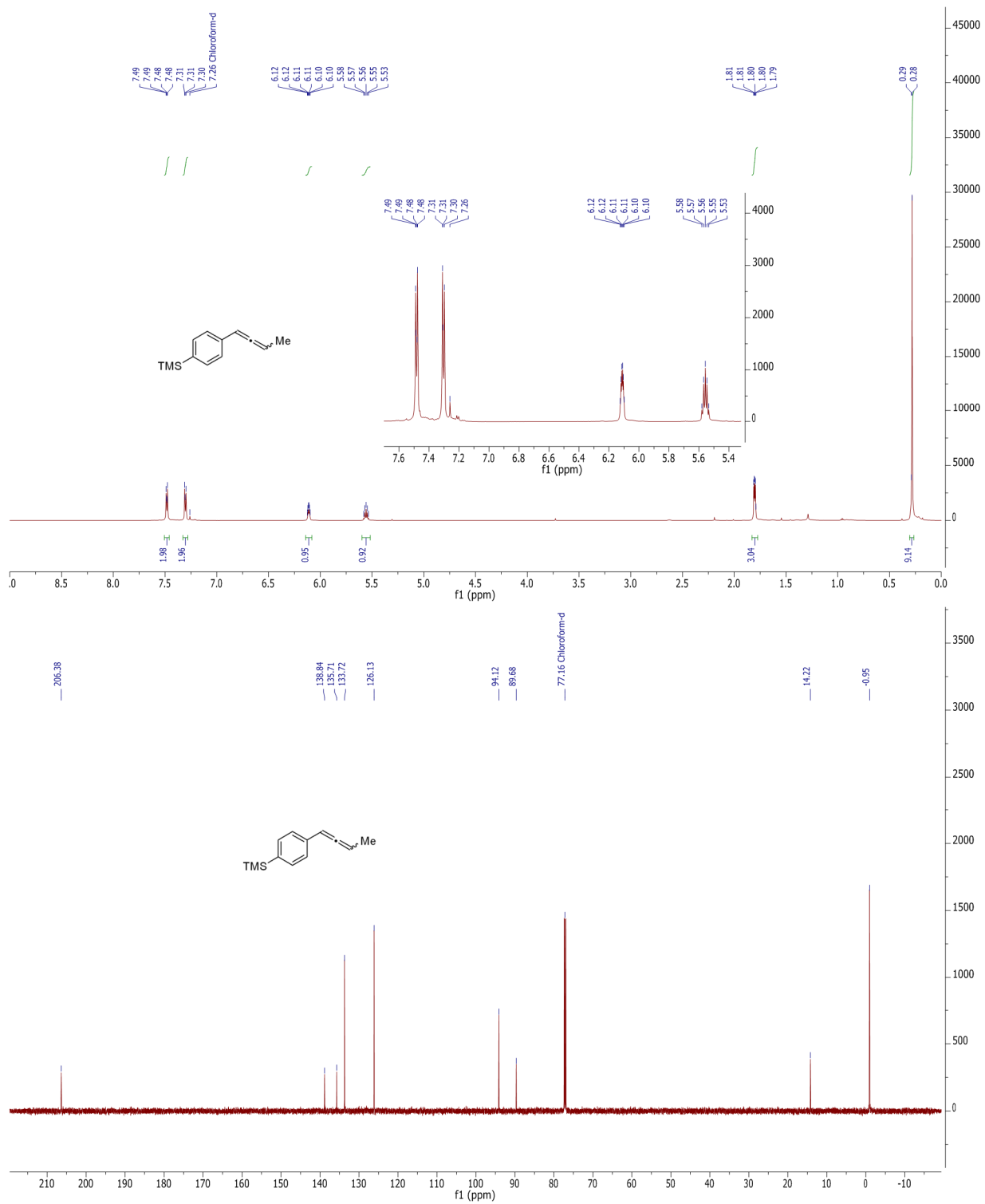
2.1b



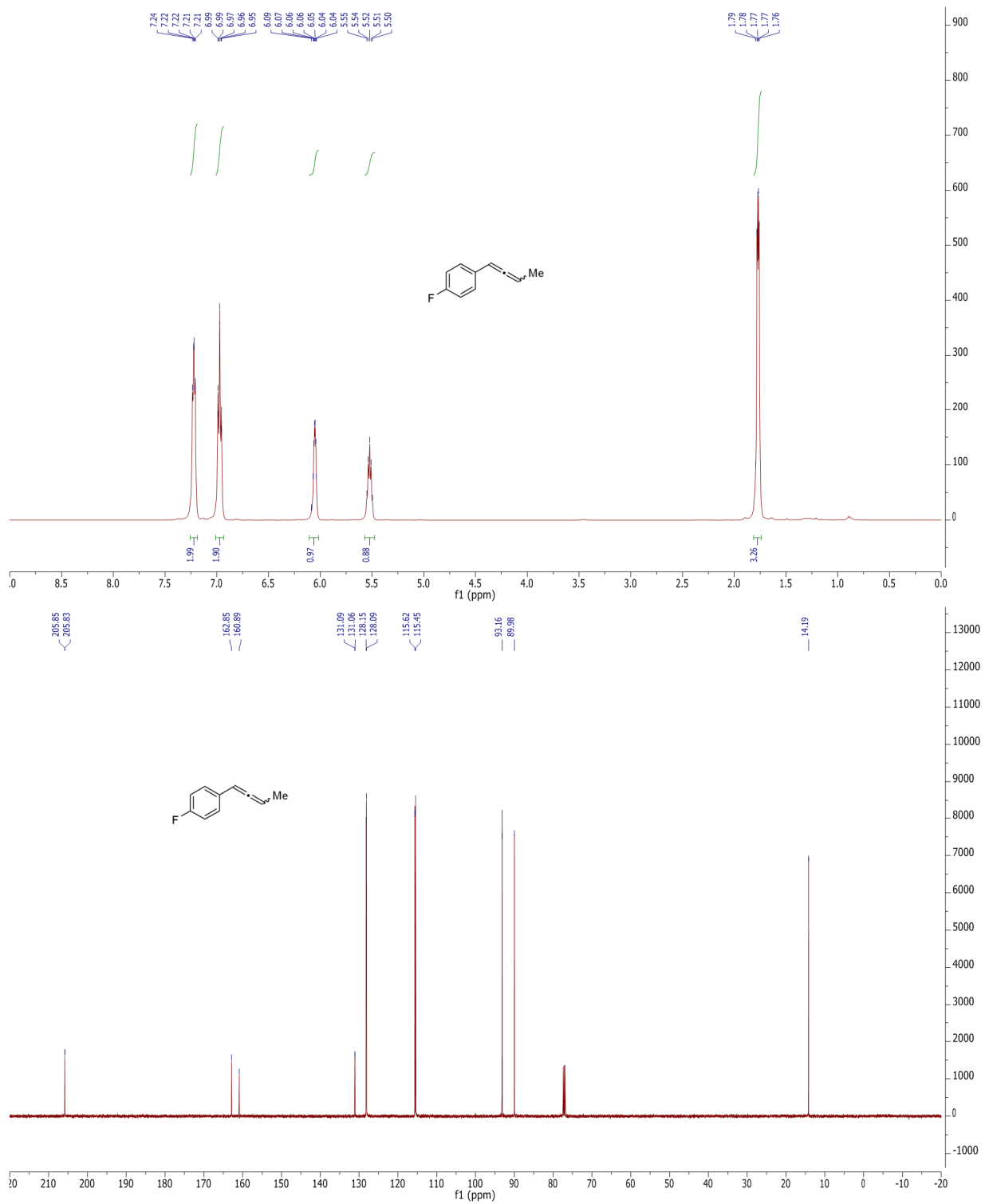
2.1c



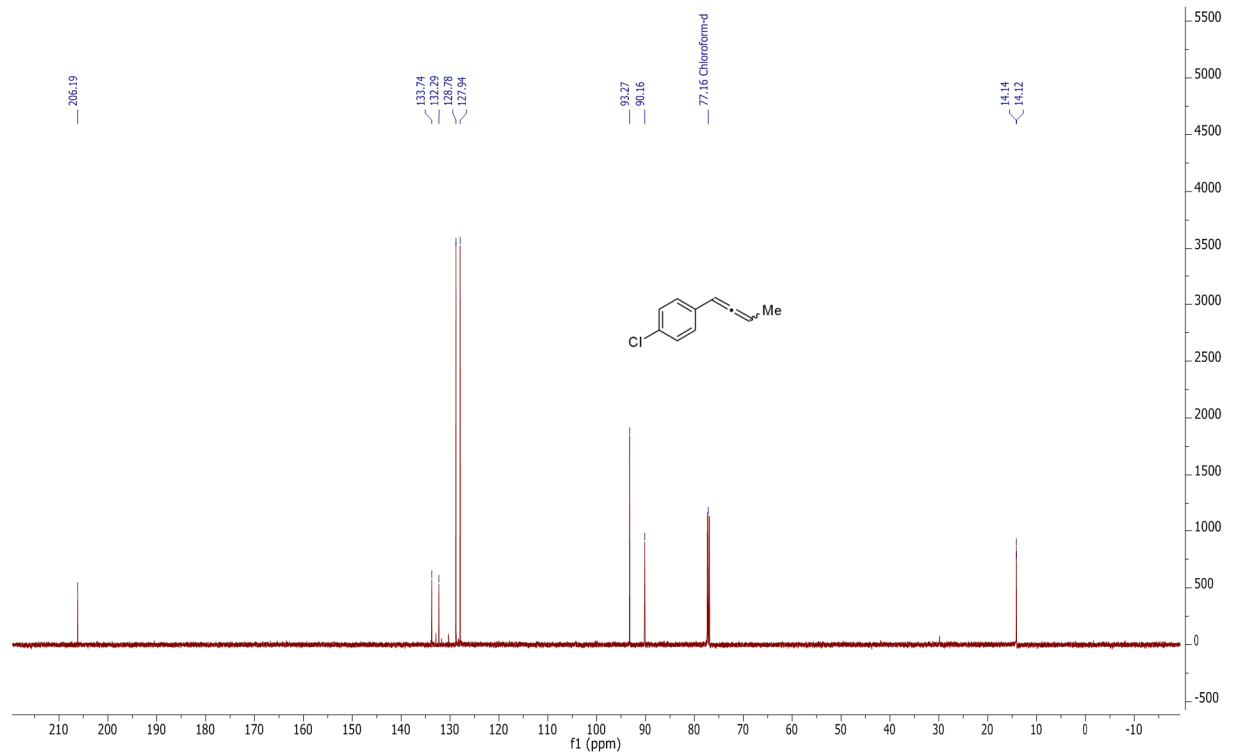
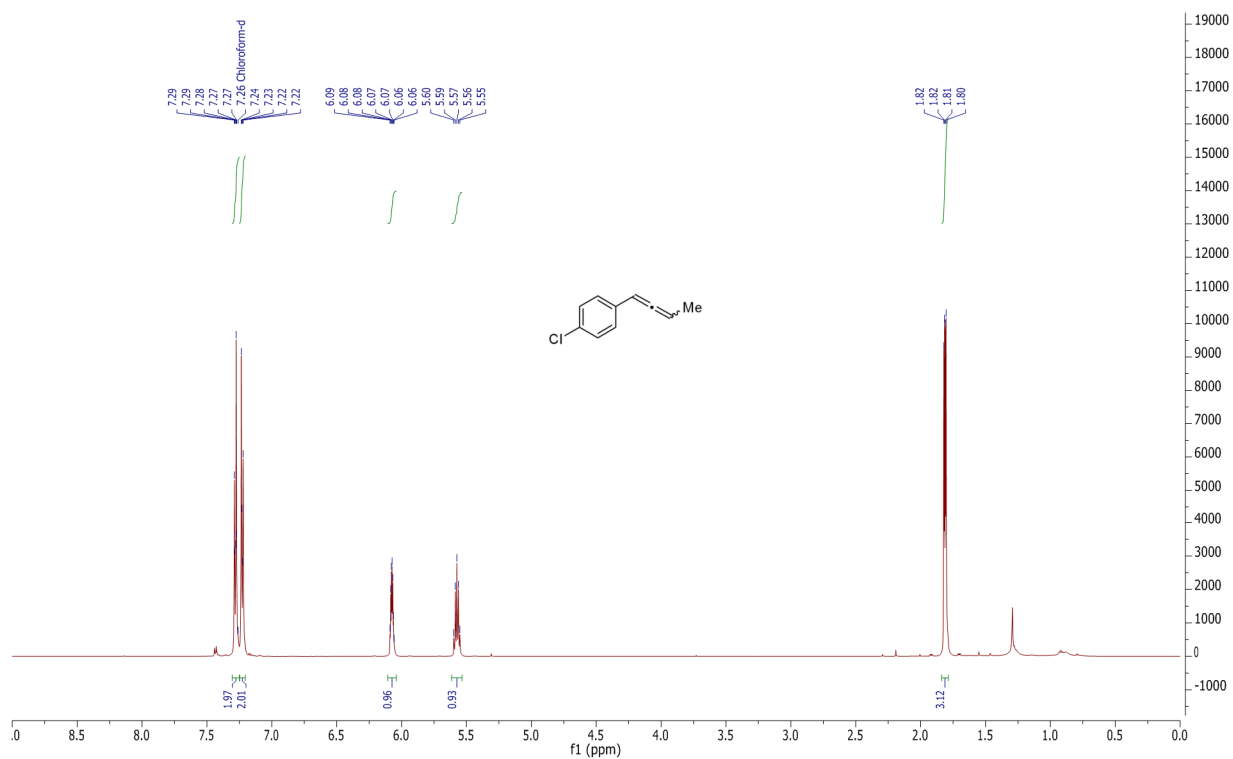
2.1d



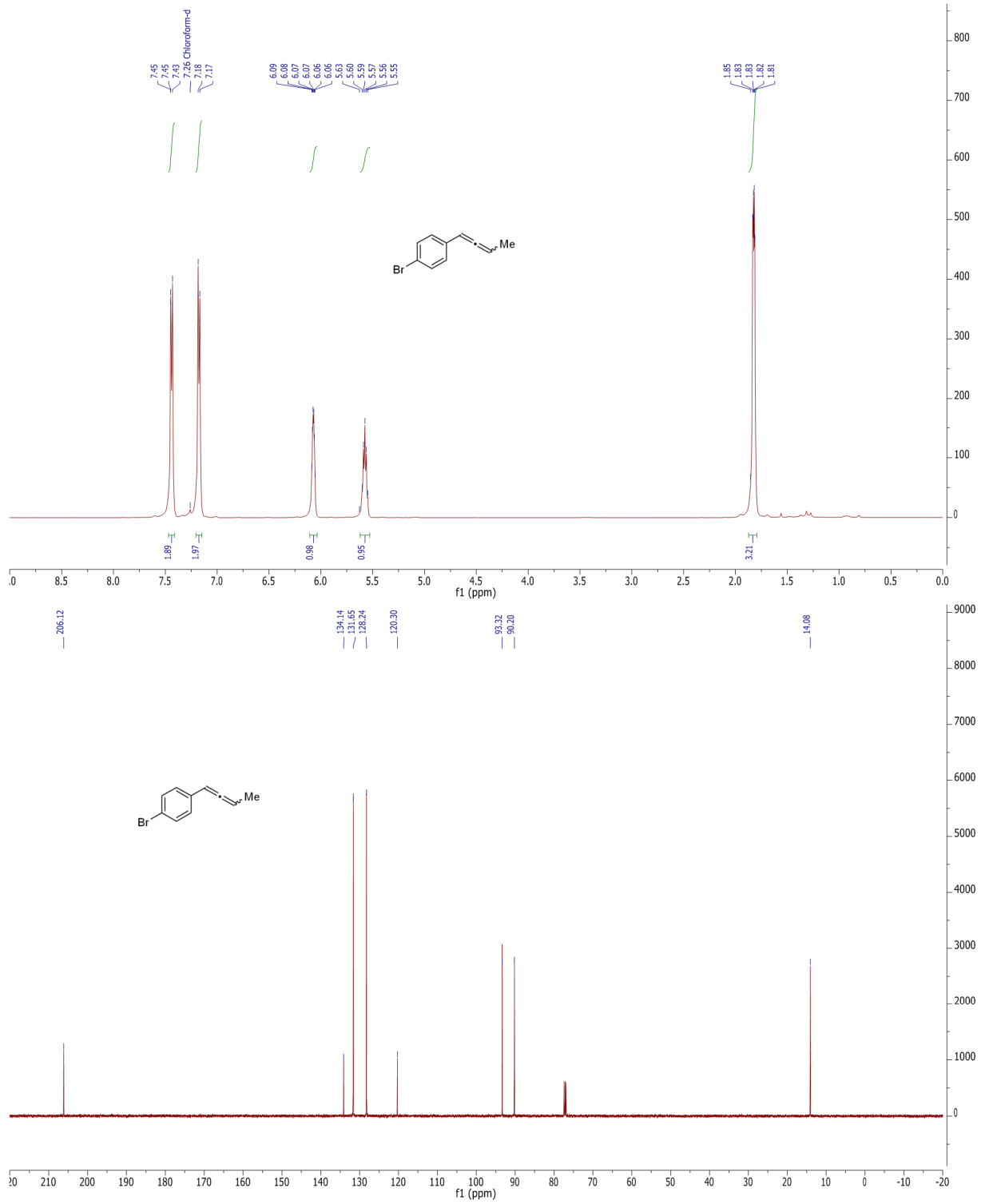
2.1e



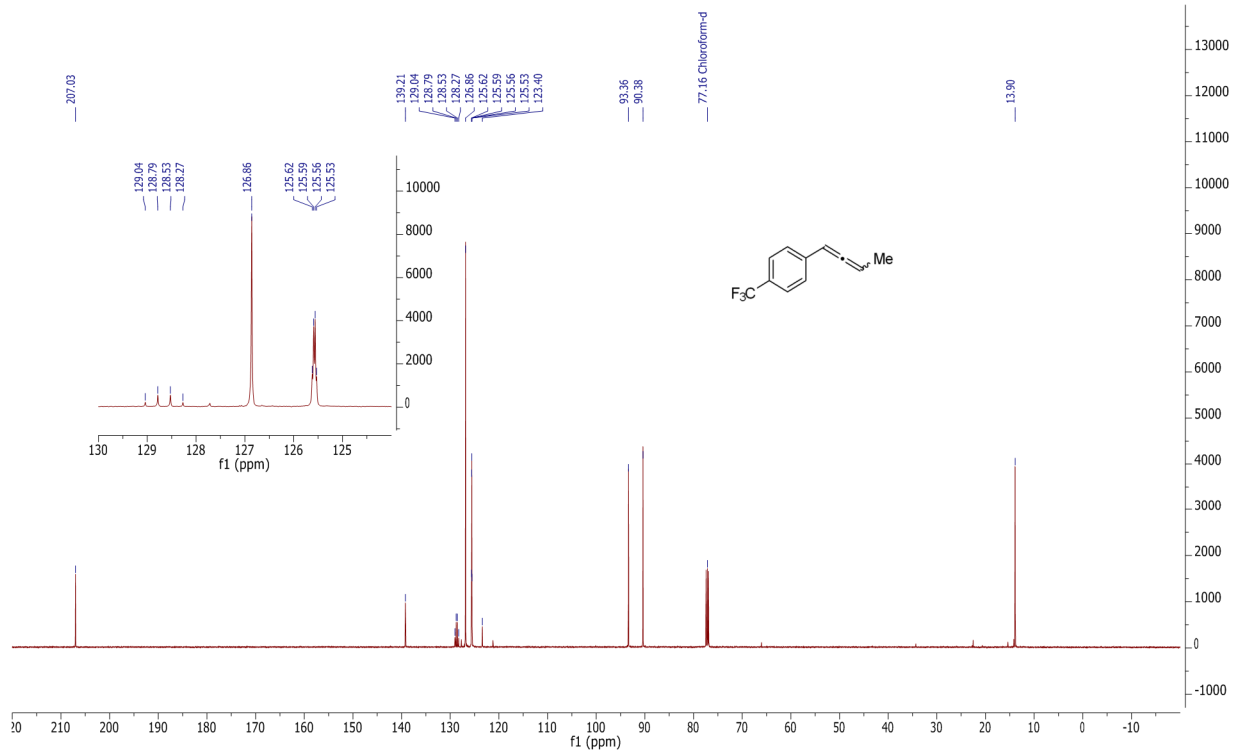
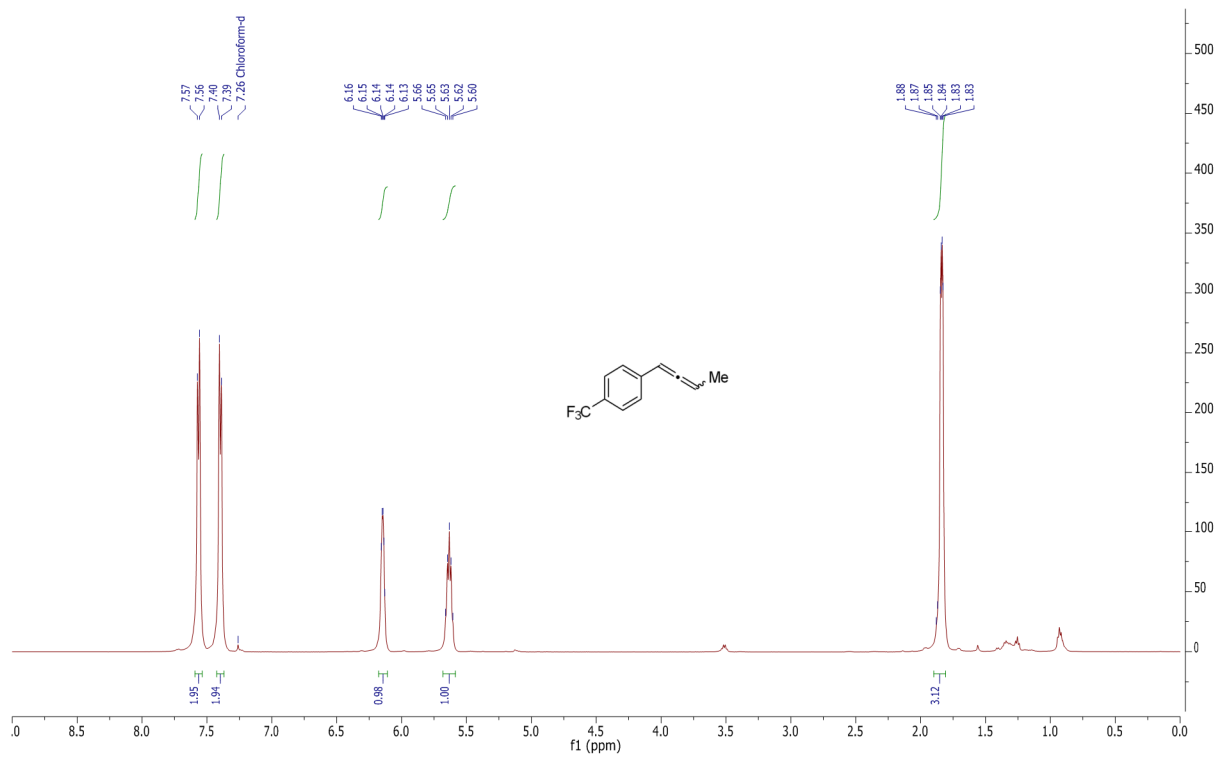
2.1f



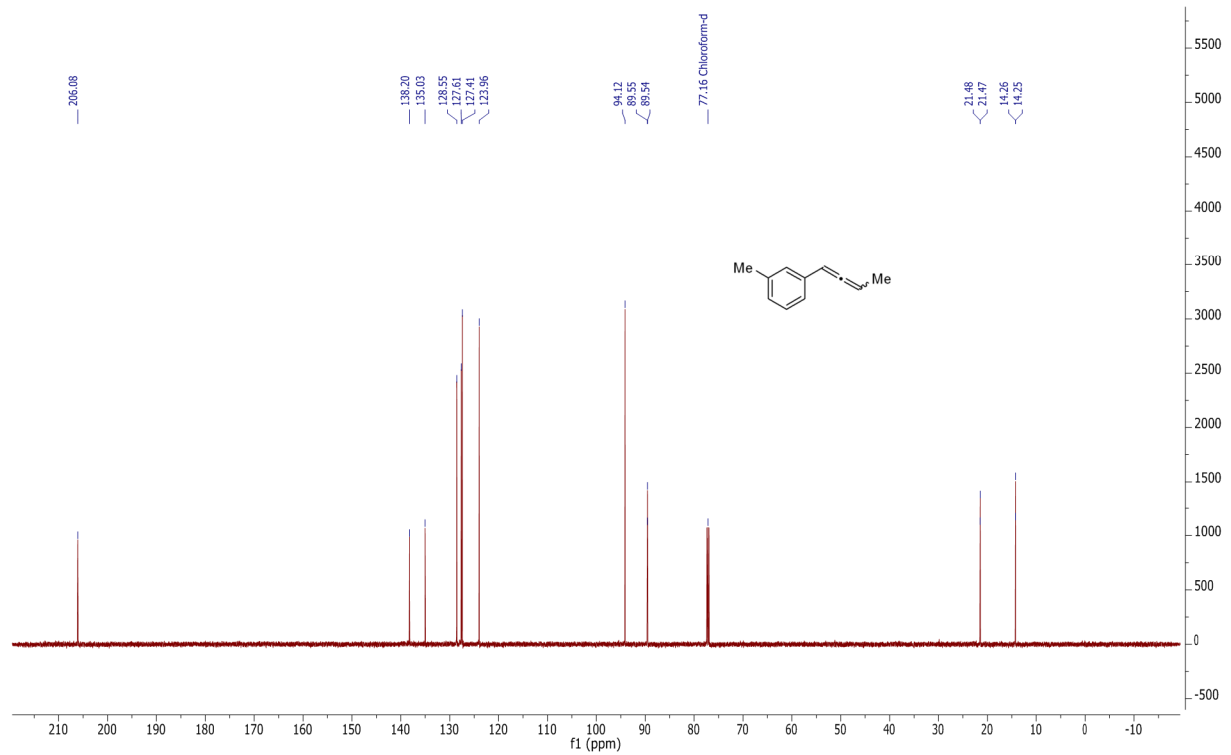
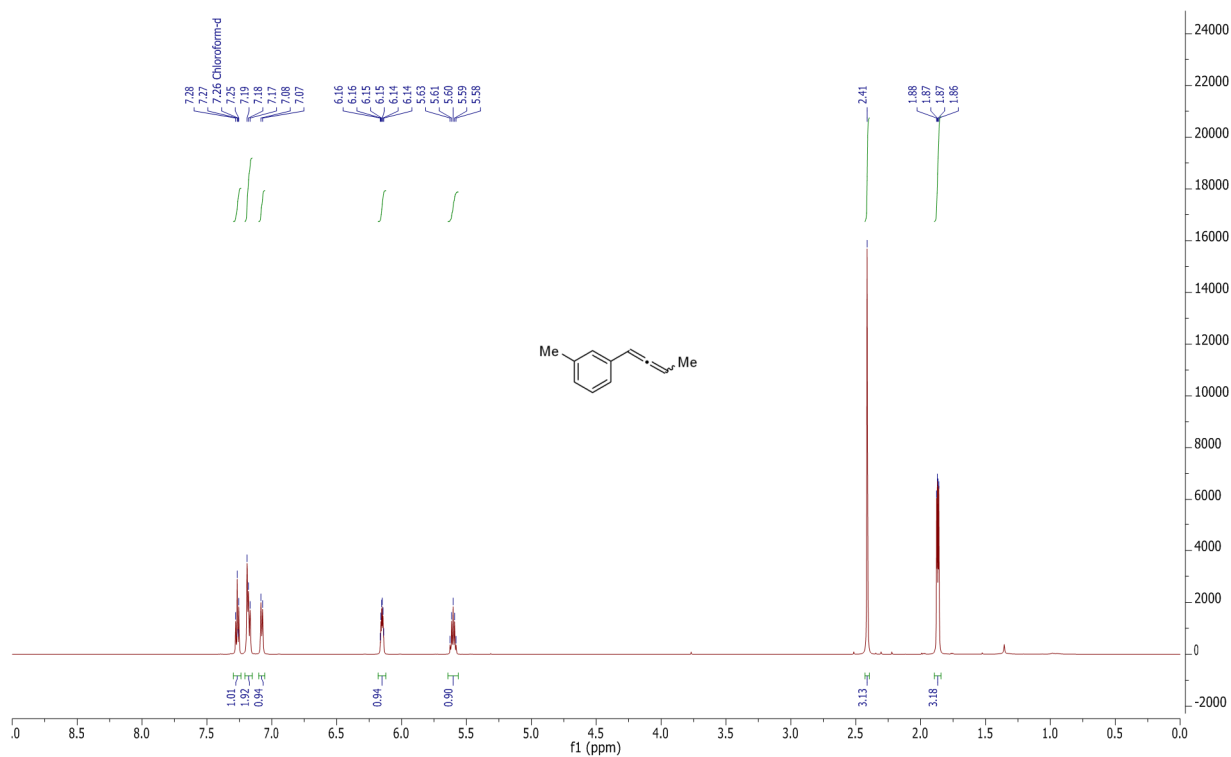
2.1g



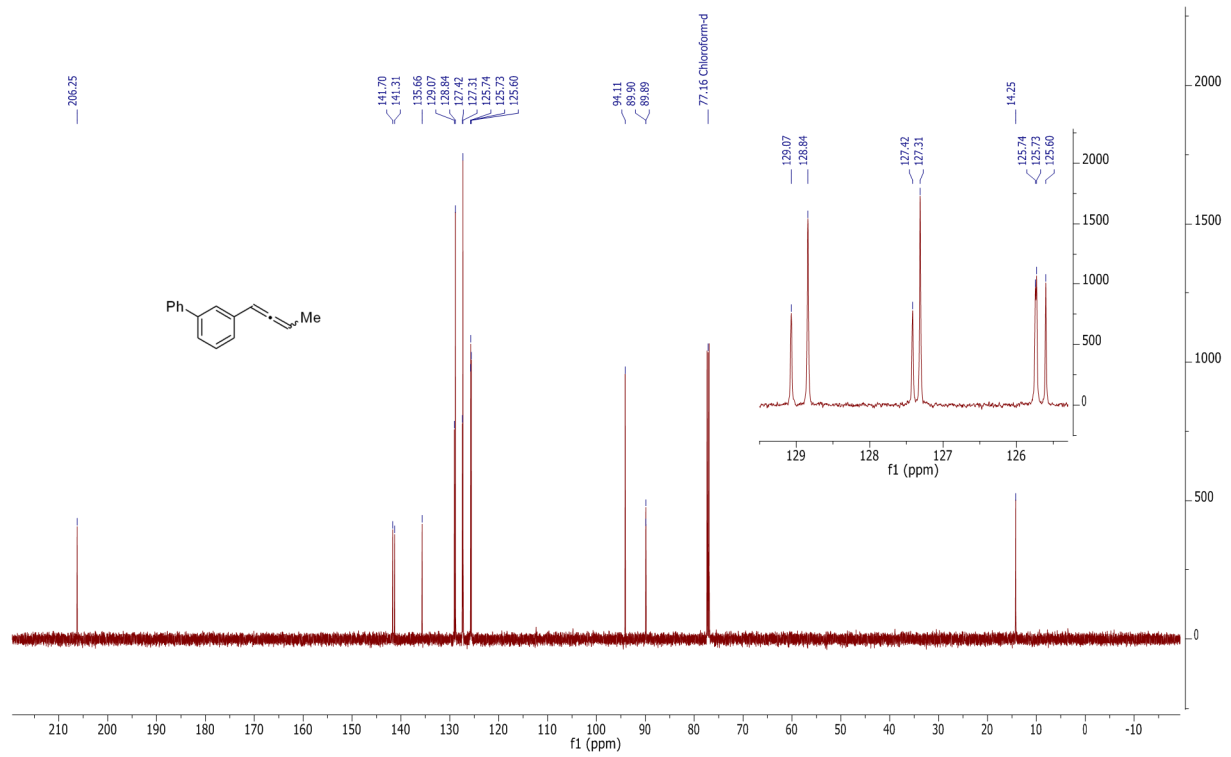
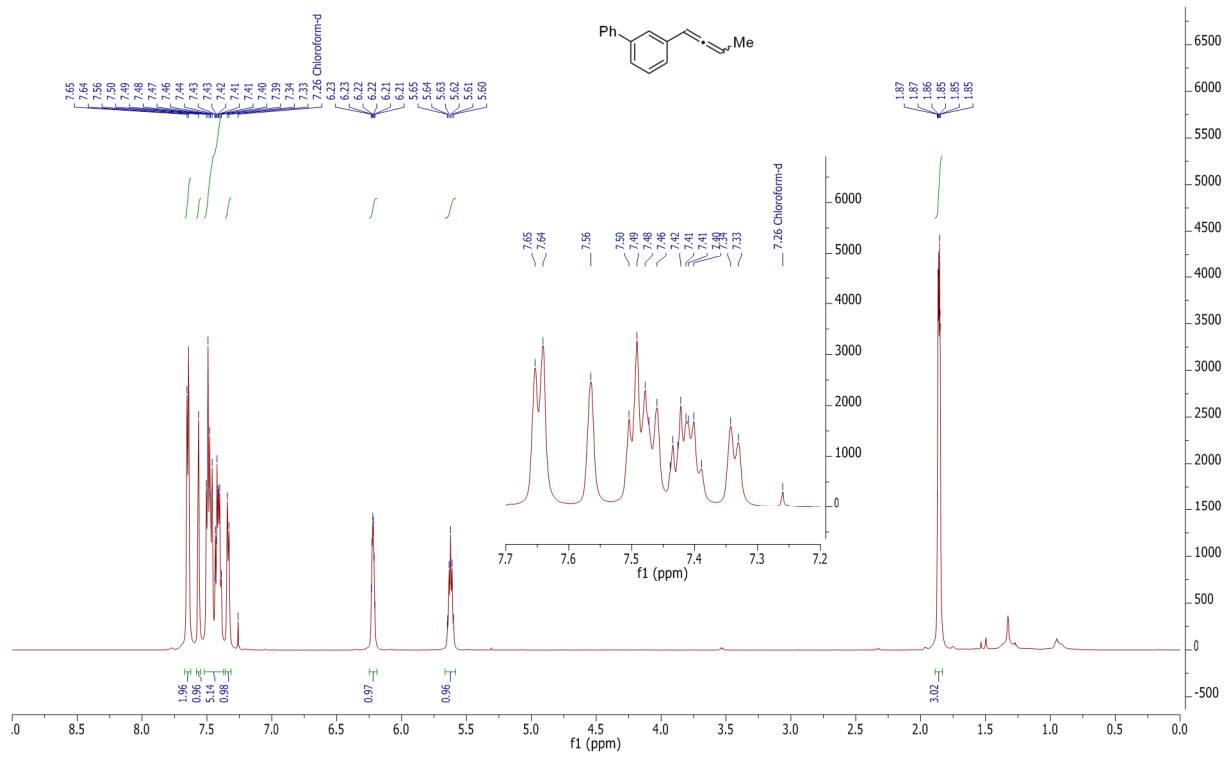
2.1h



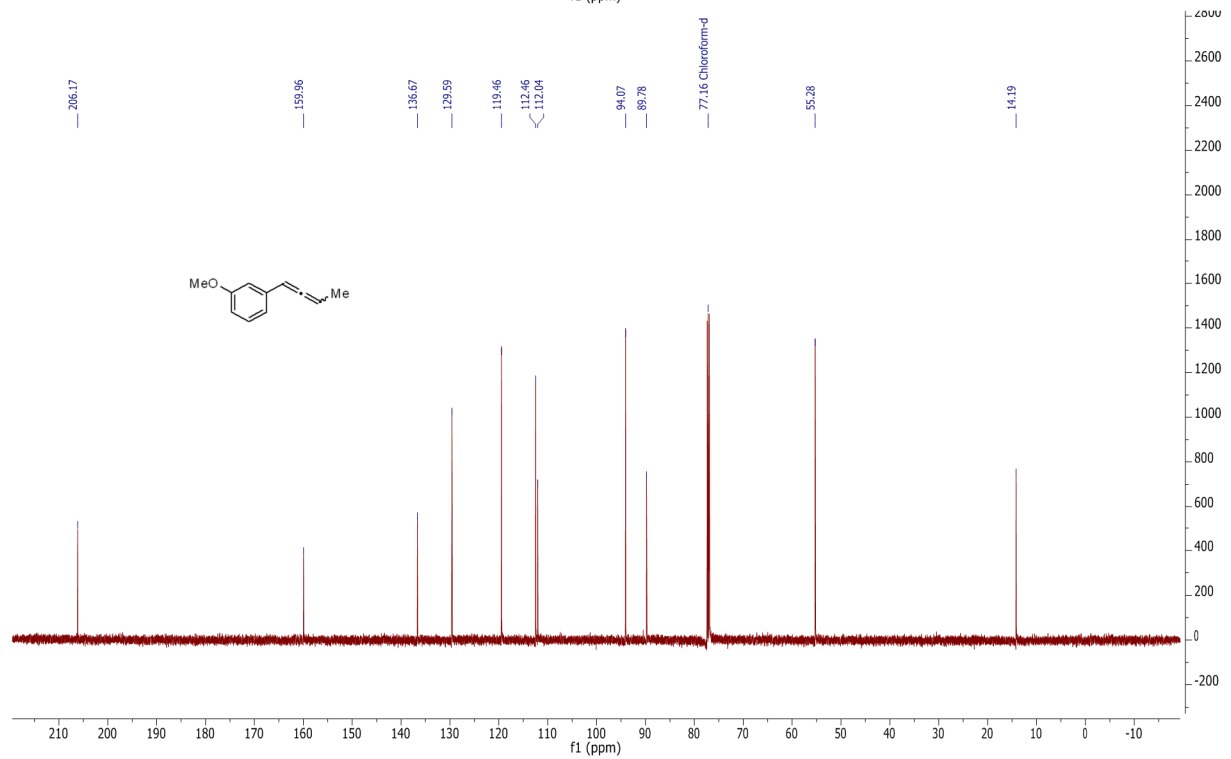
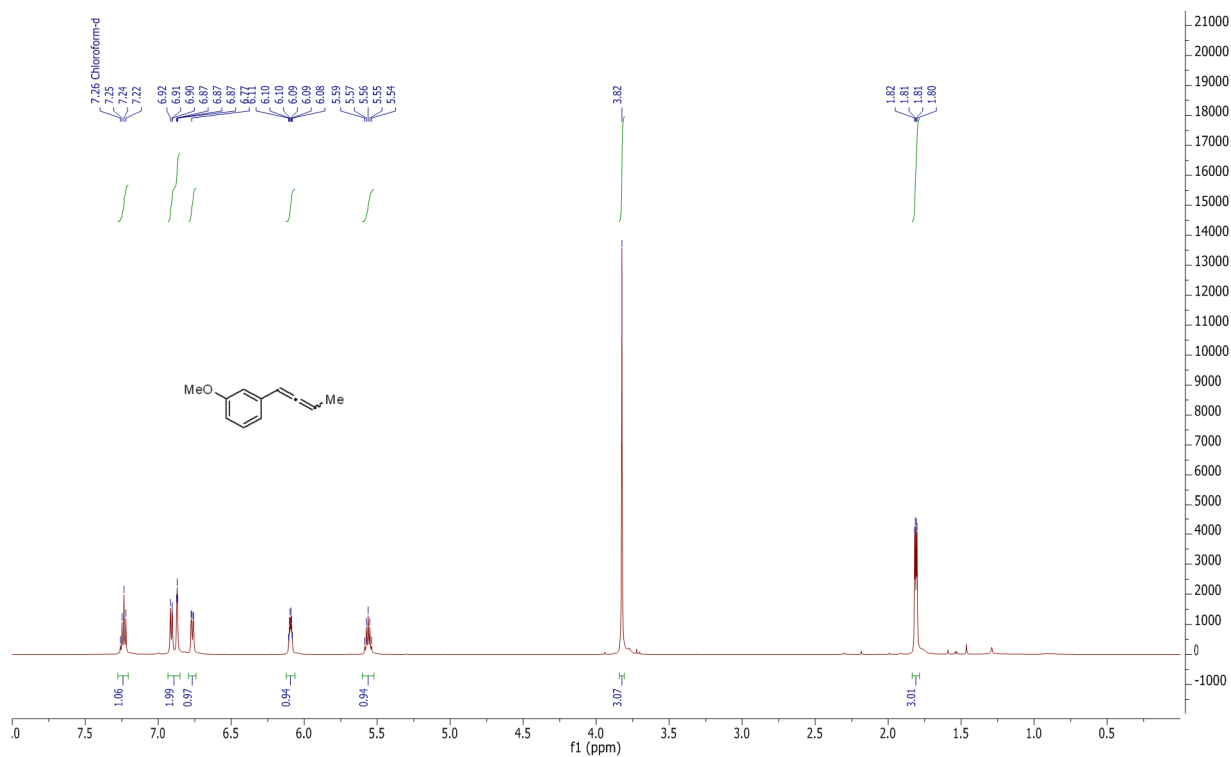
2.1i



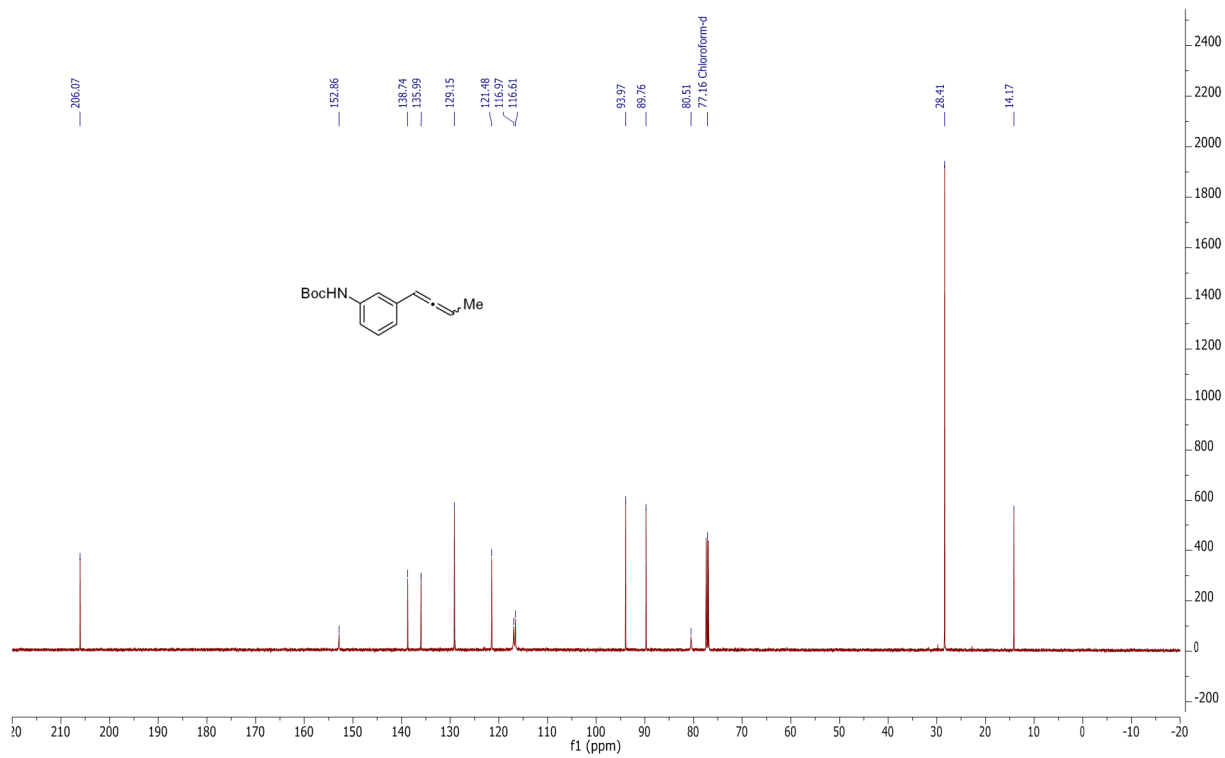
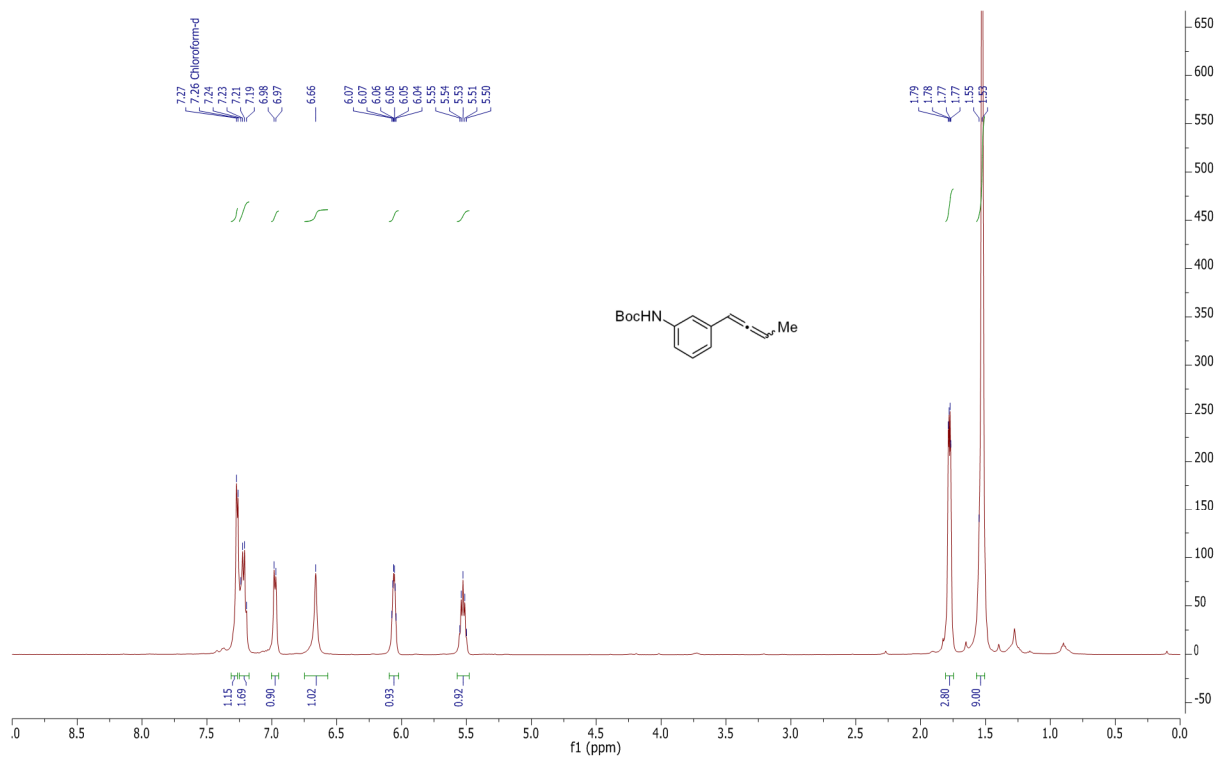
2.1j



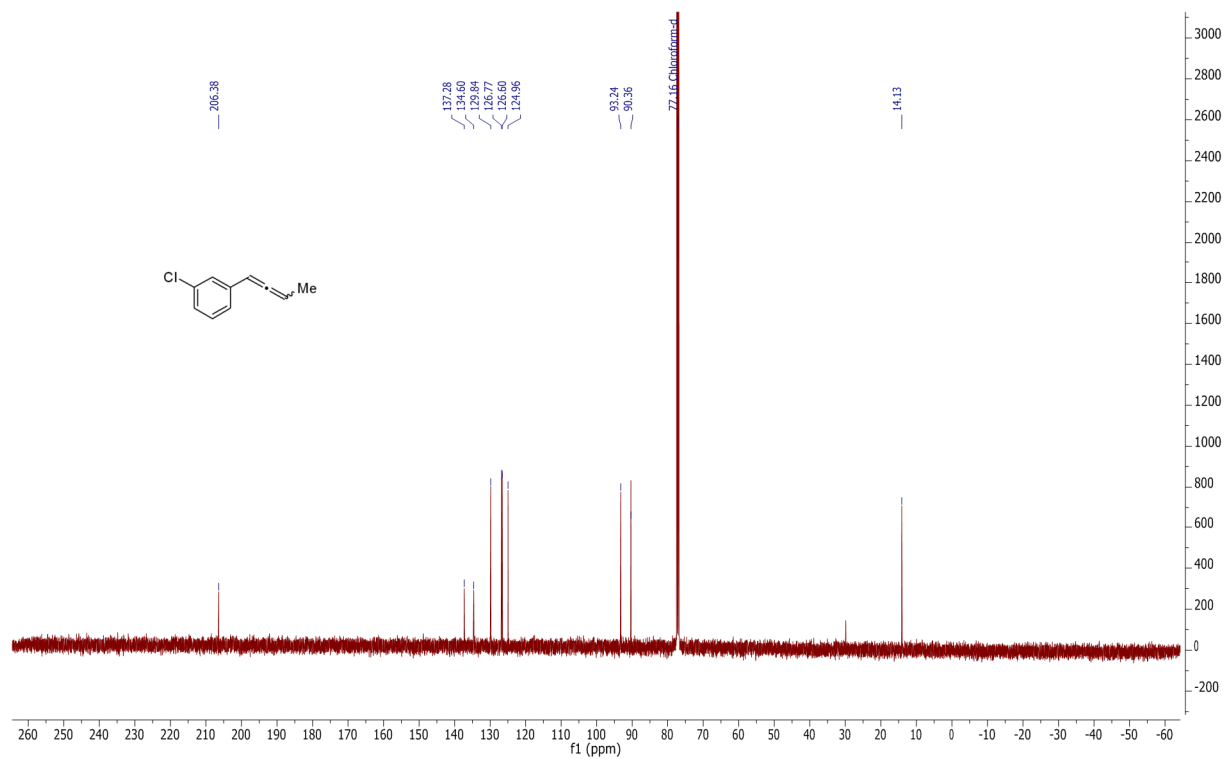
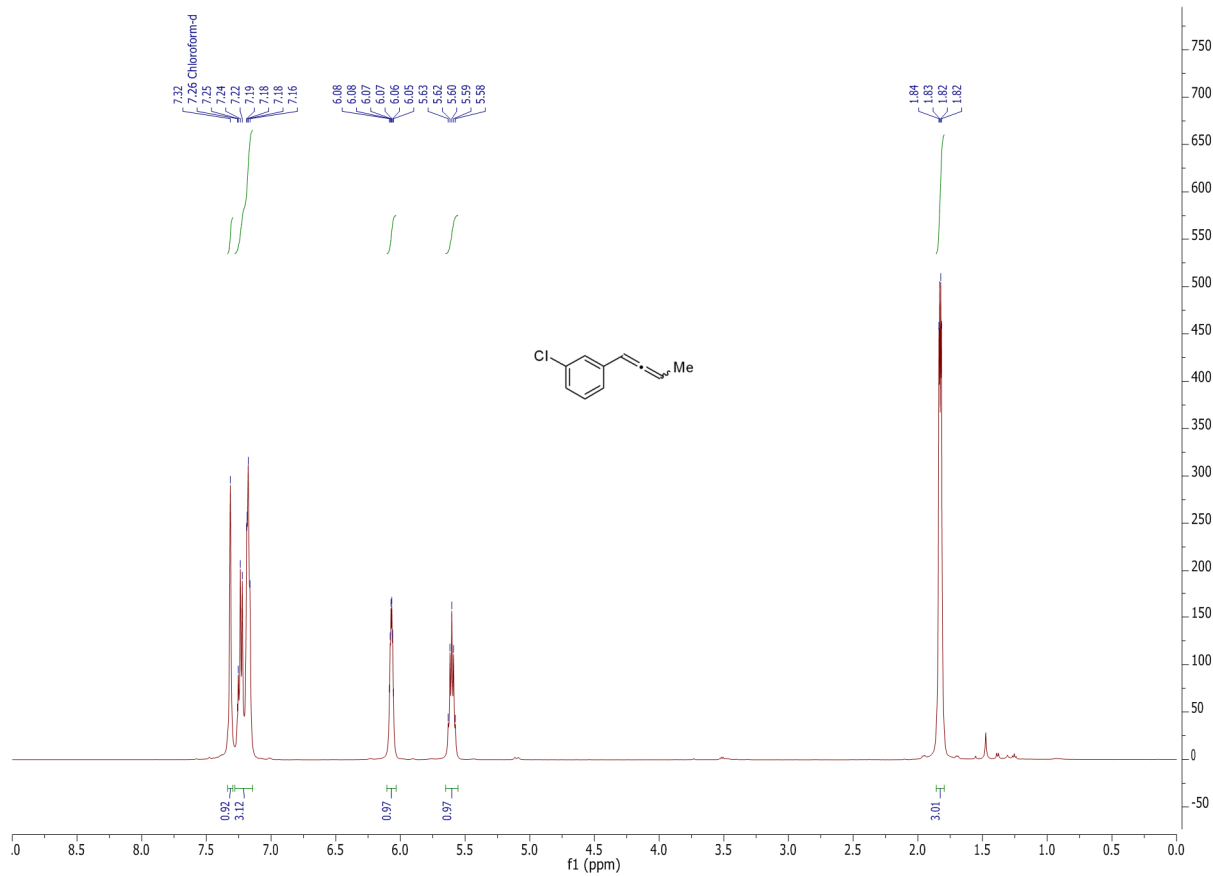
2.1k



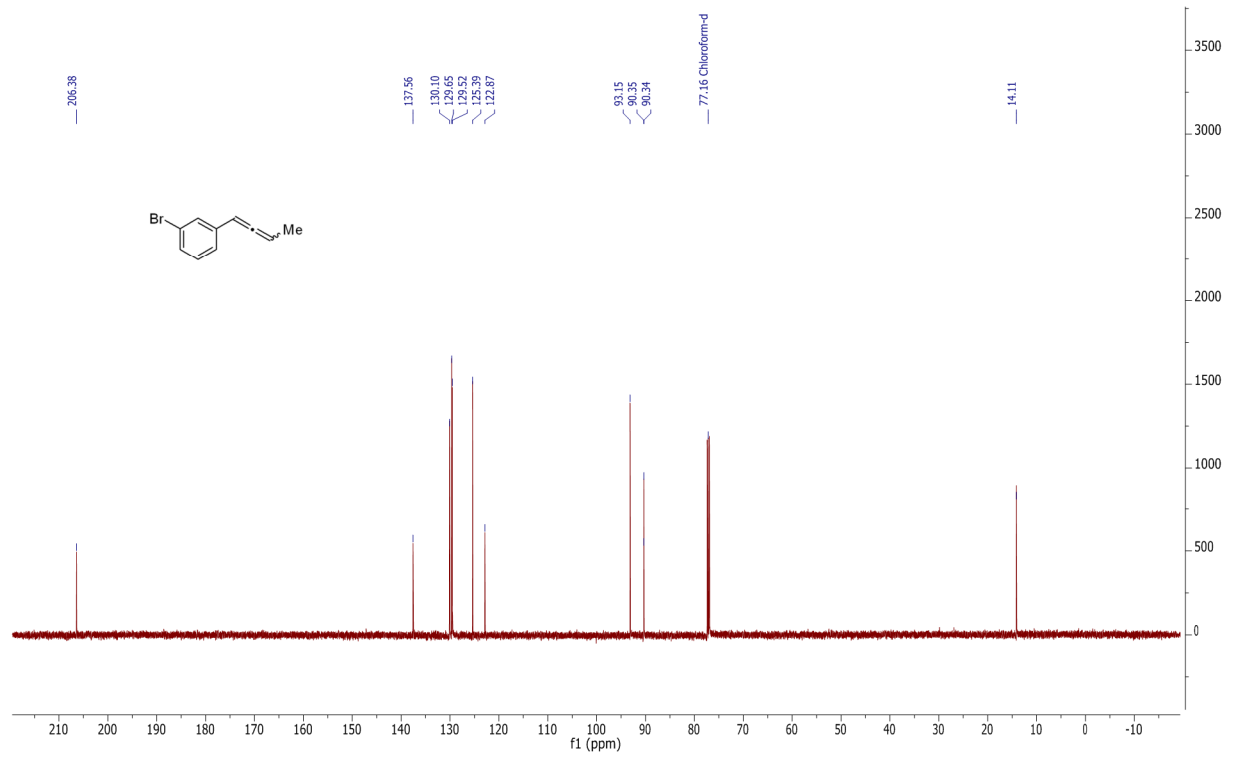
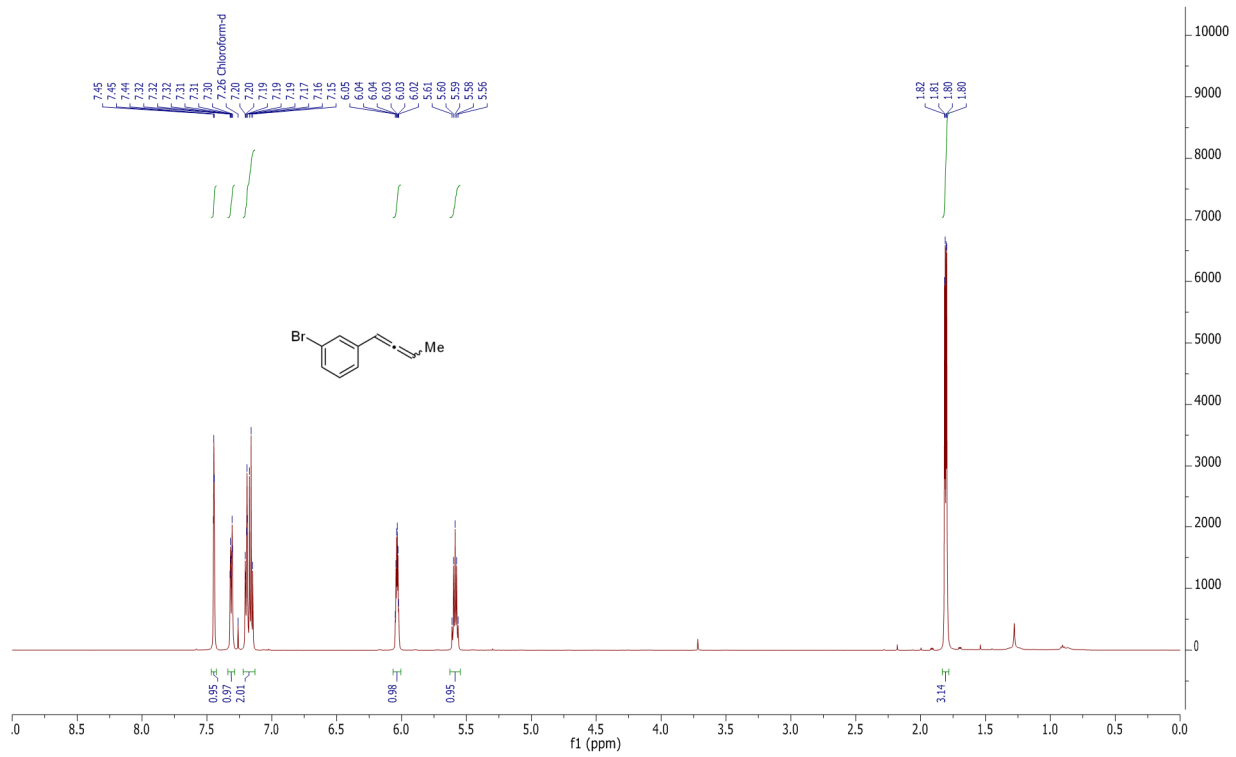
2.11



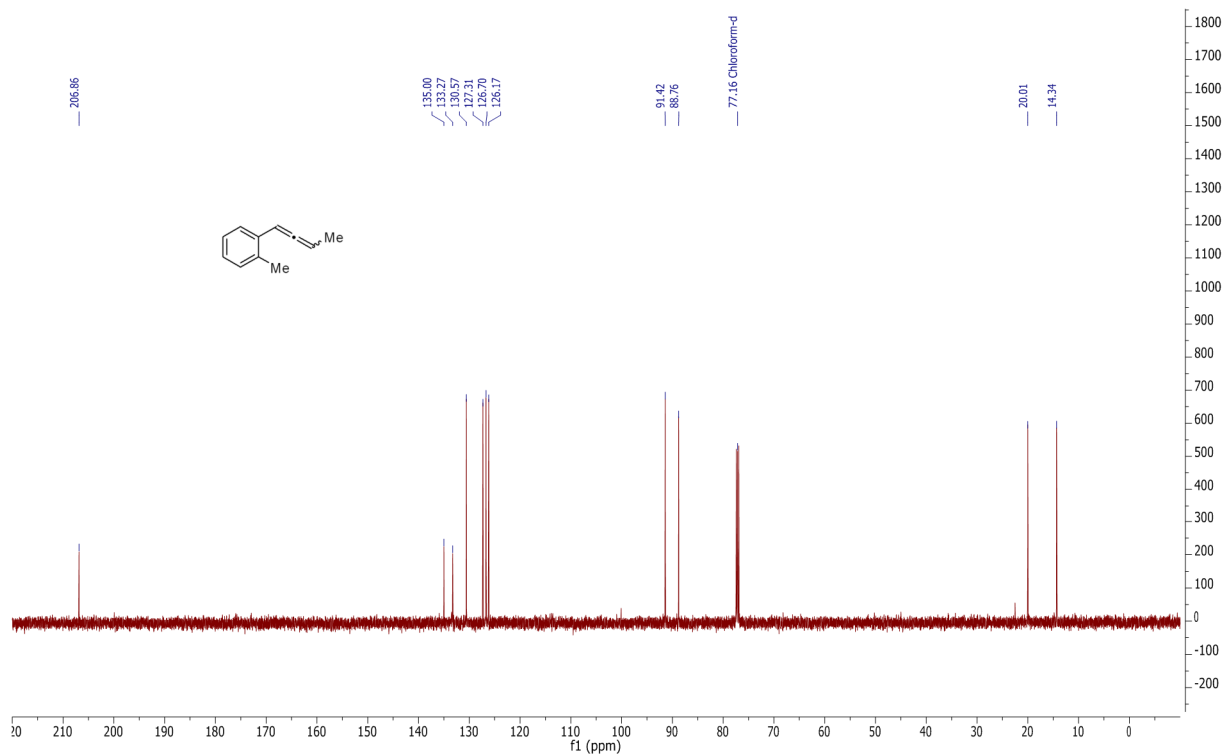
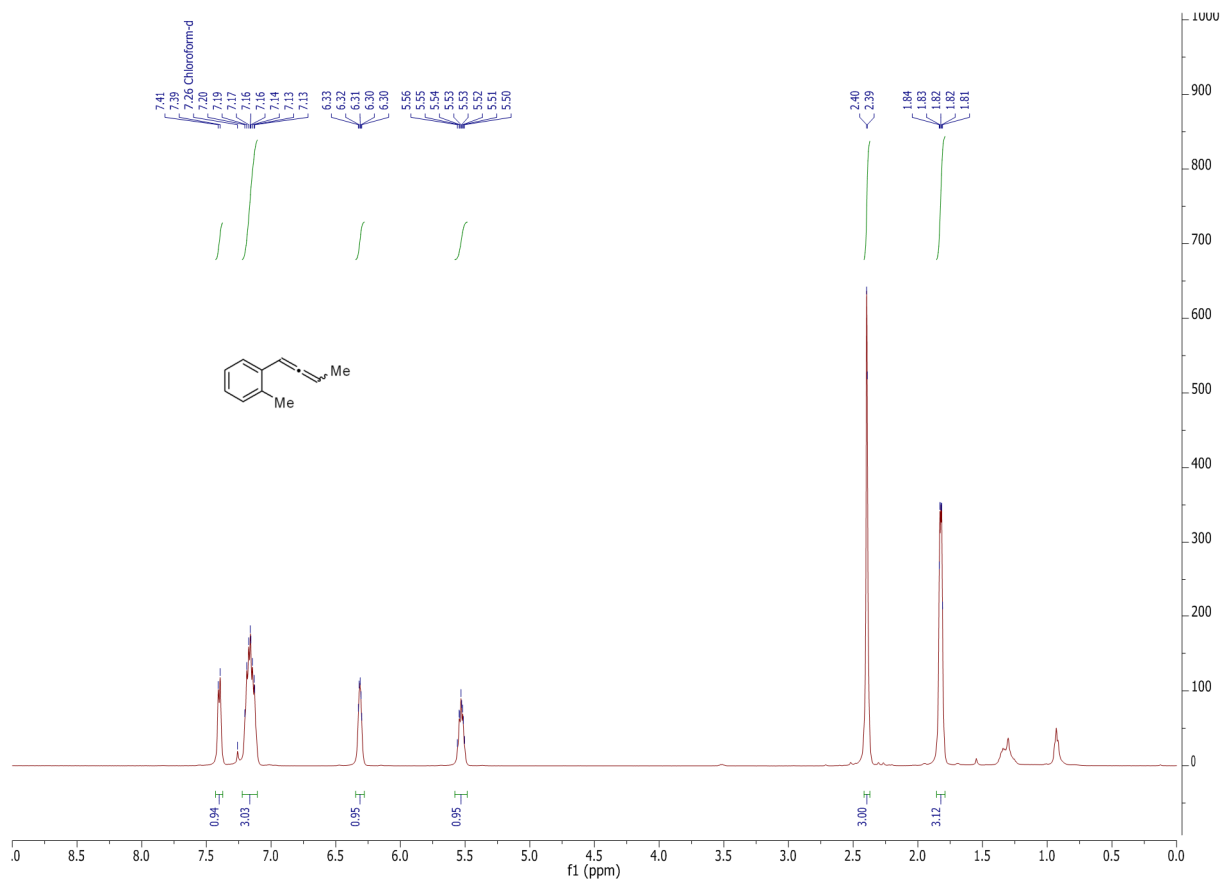
2.1m



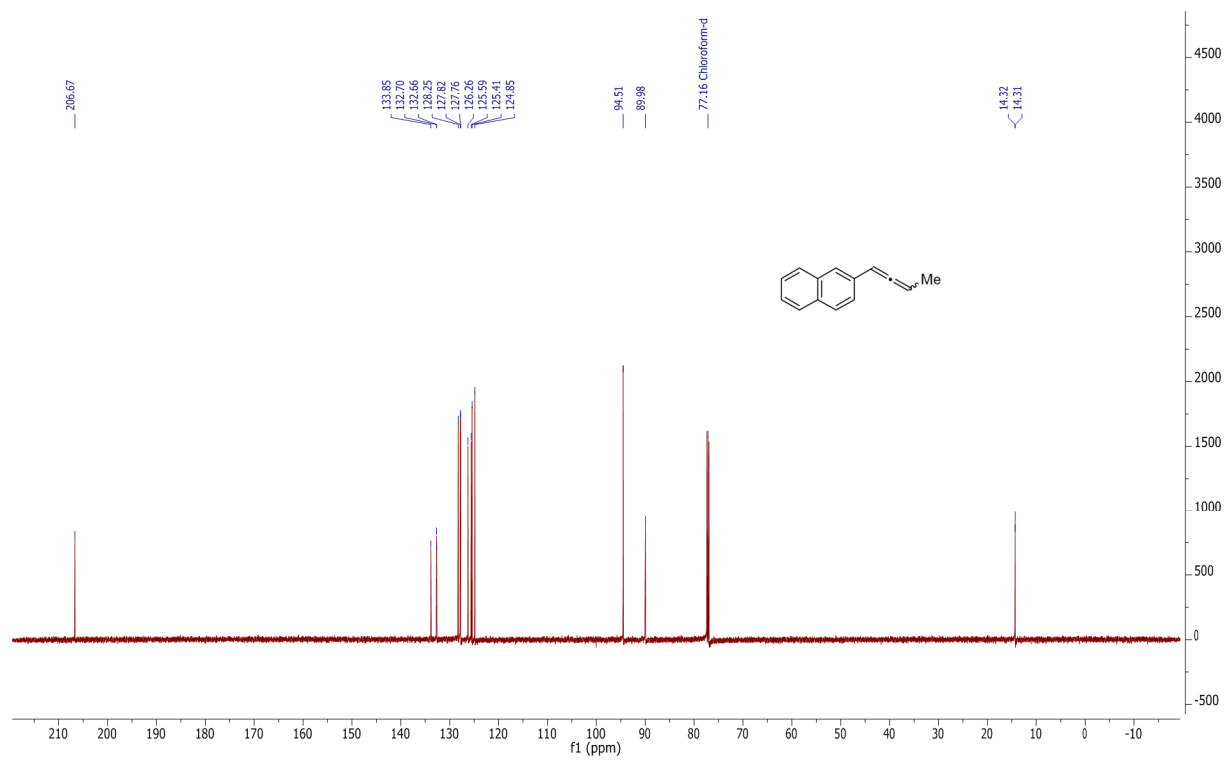
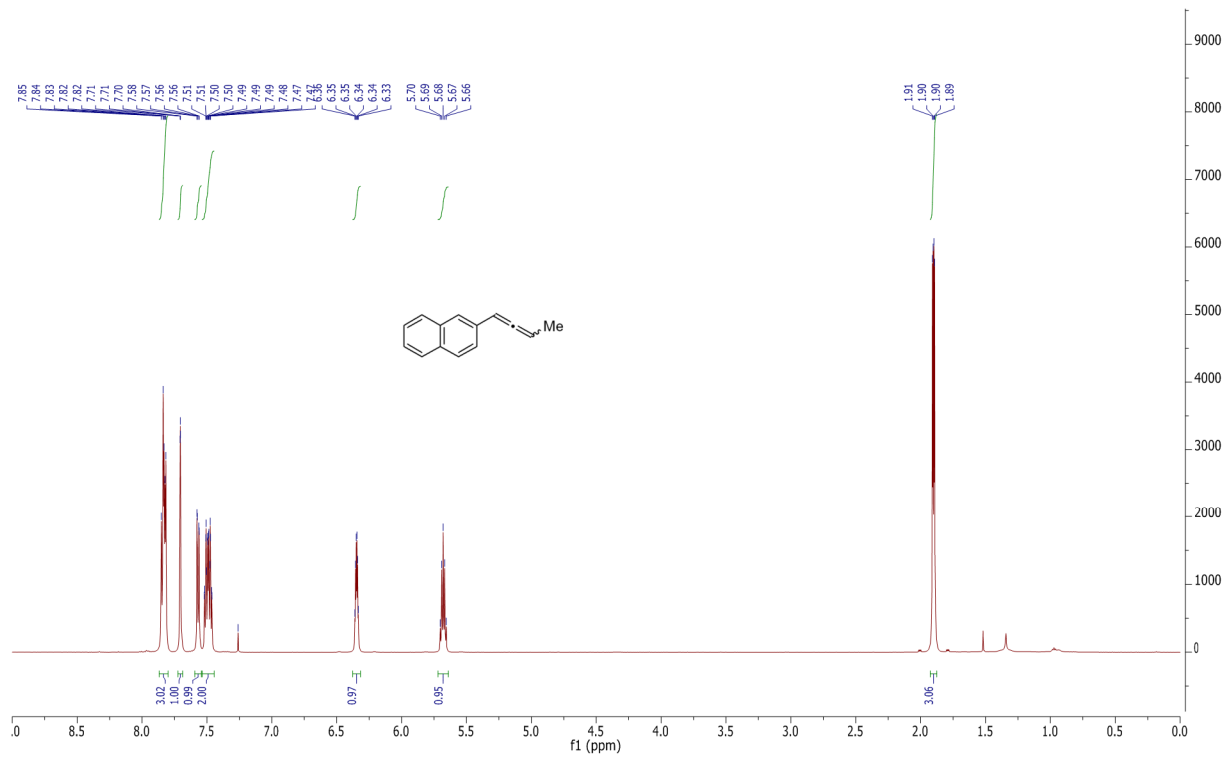
2.1n



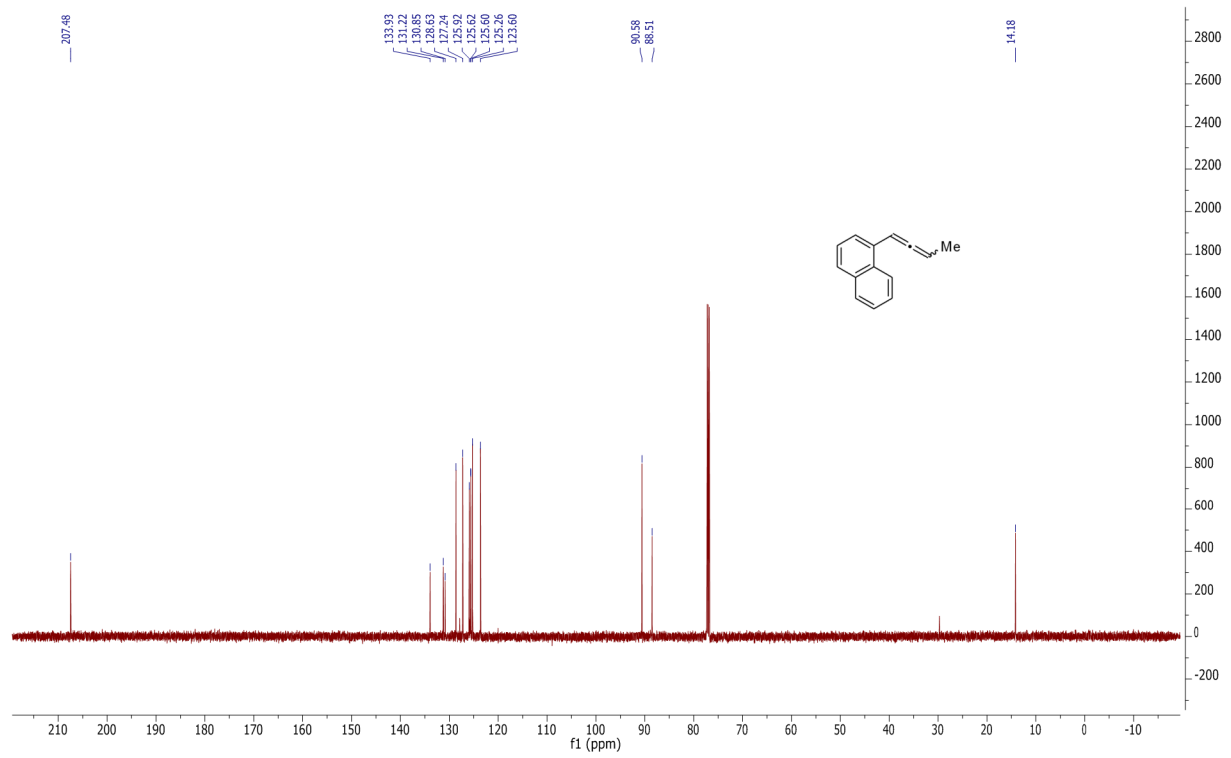
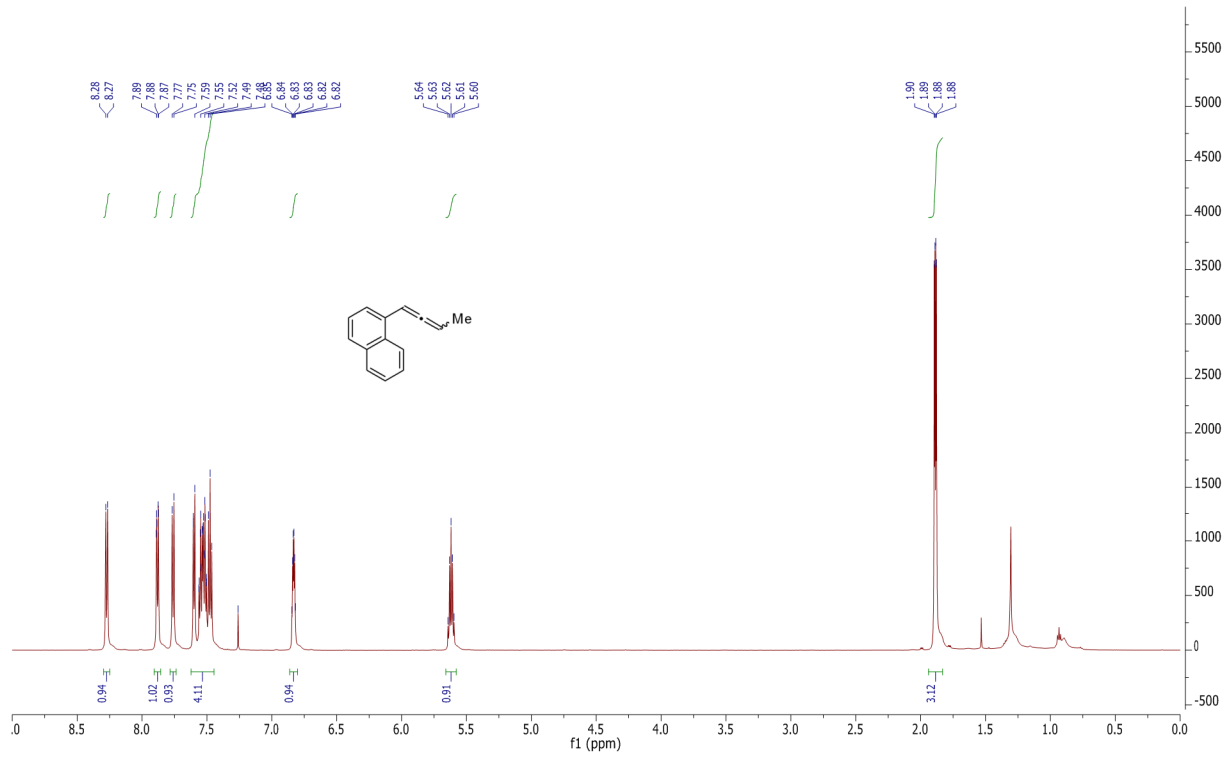
2.10



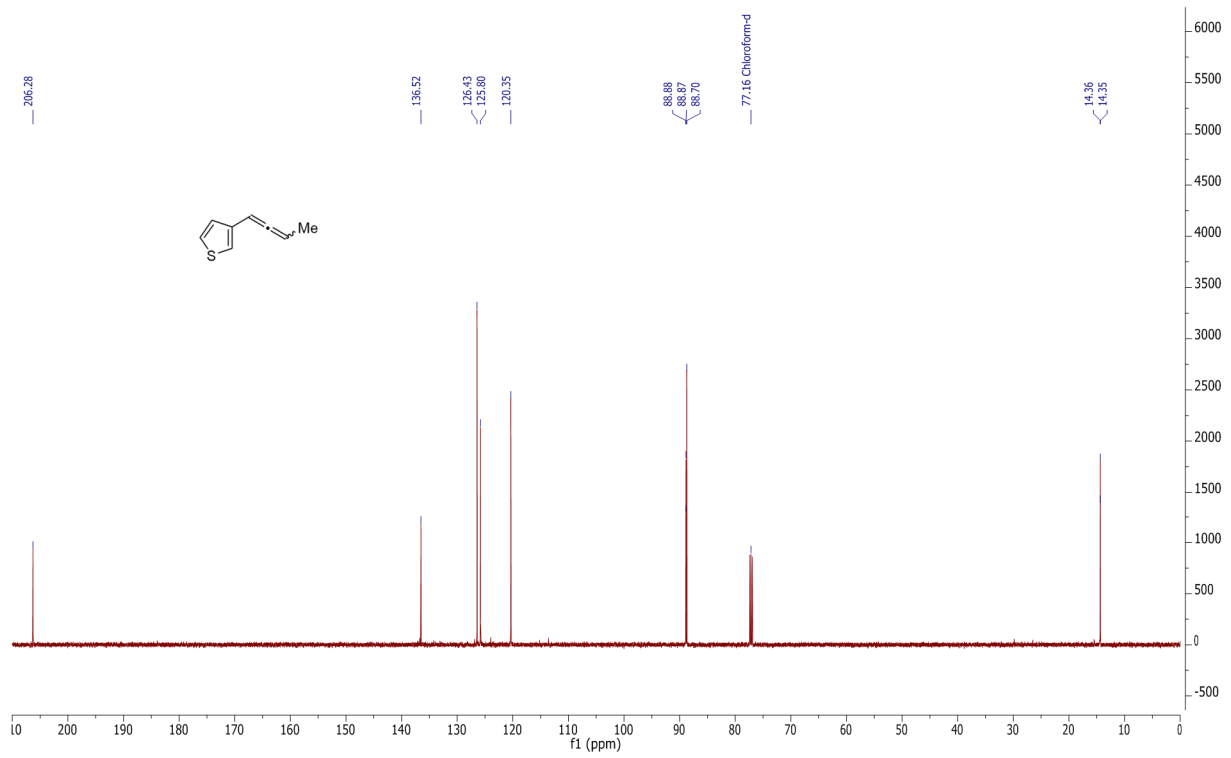
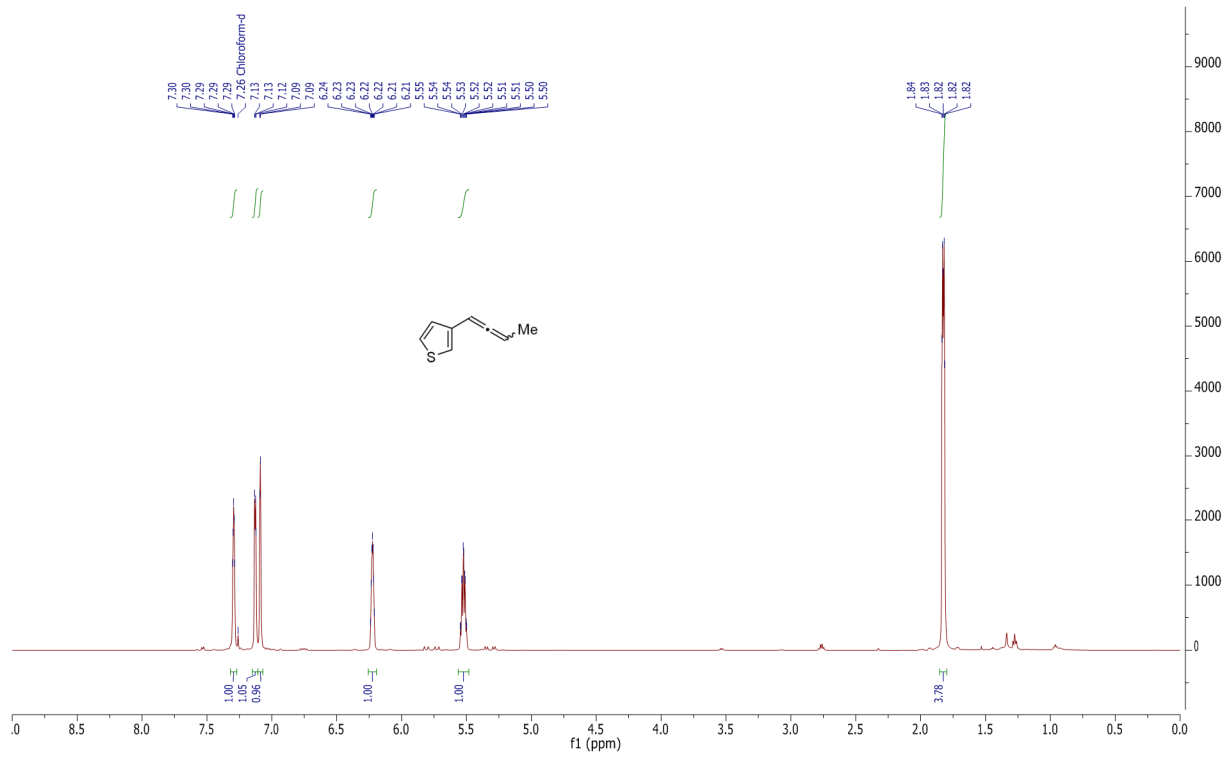
2.1p



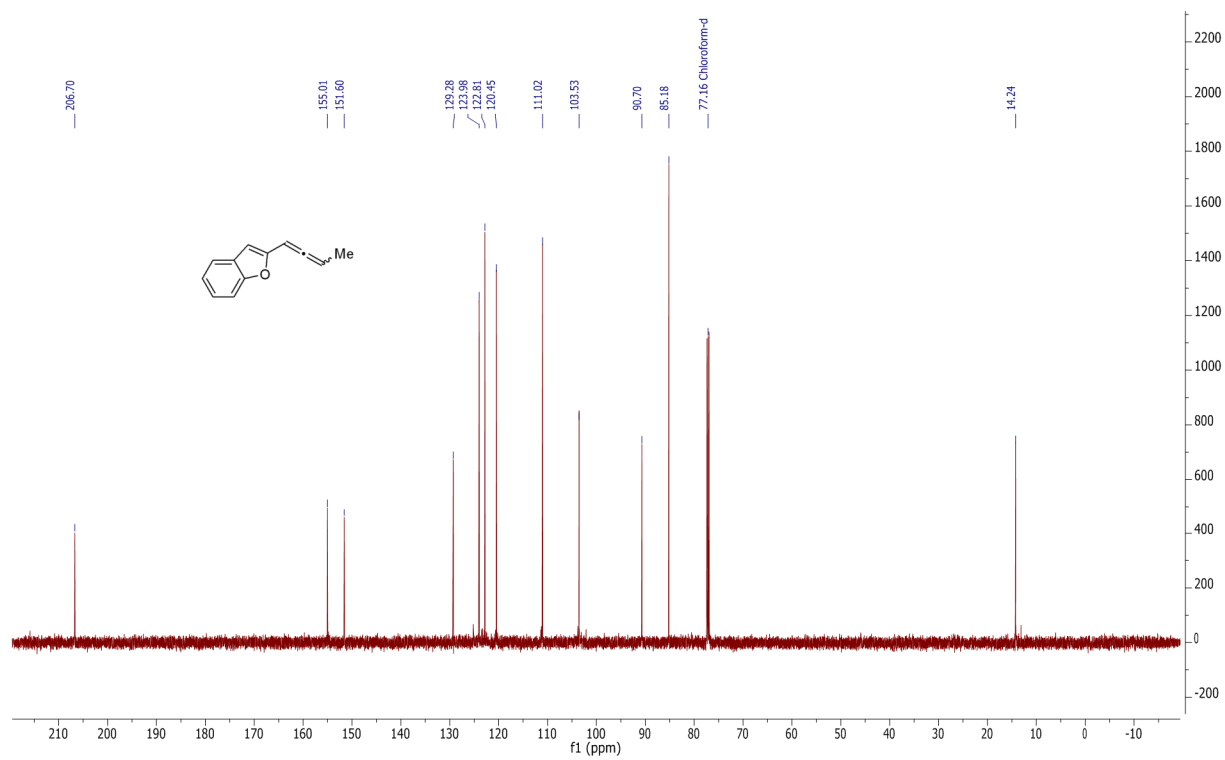
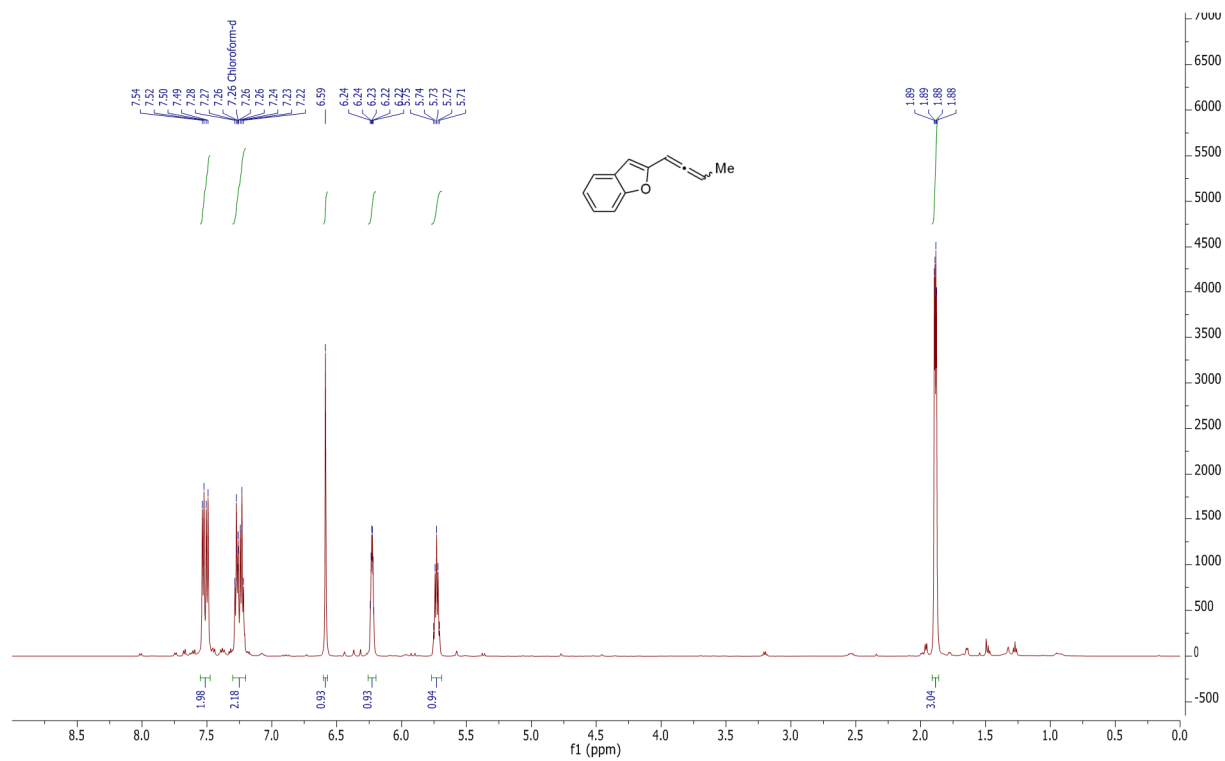
2.1q



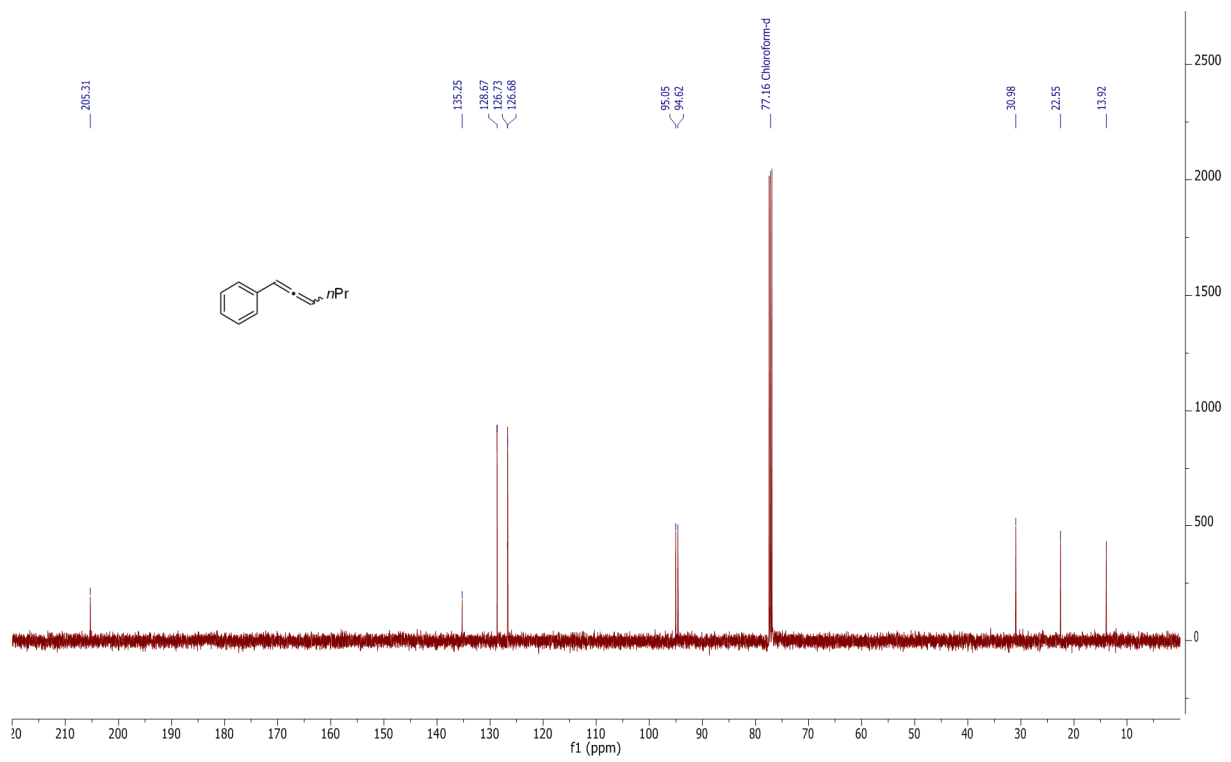
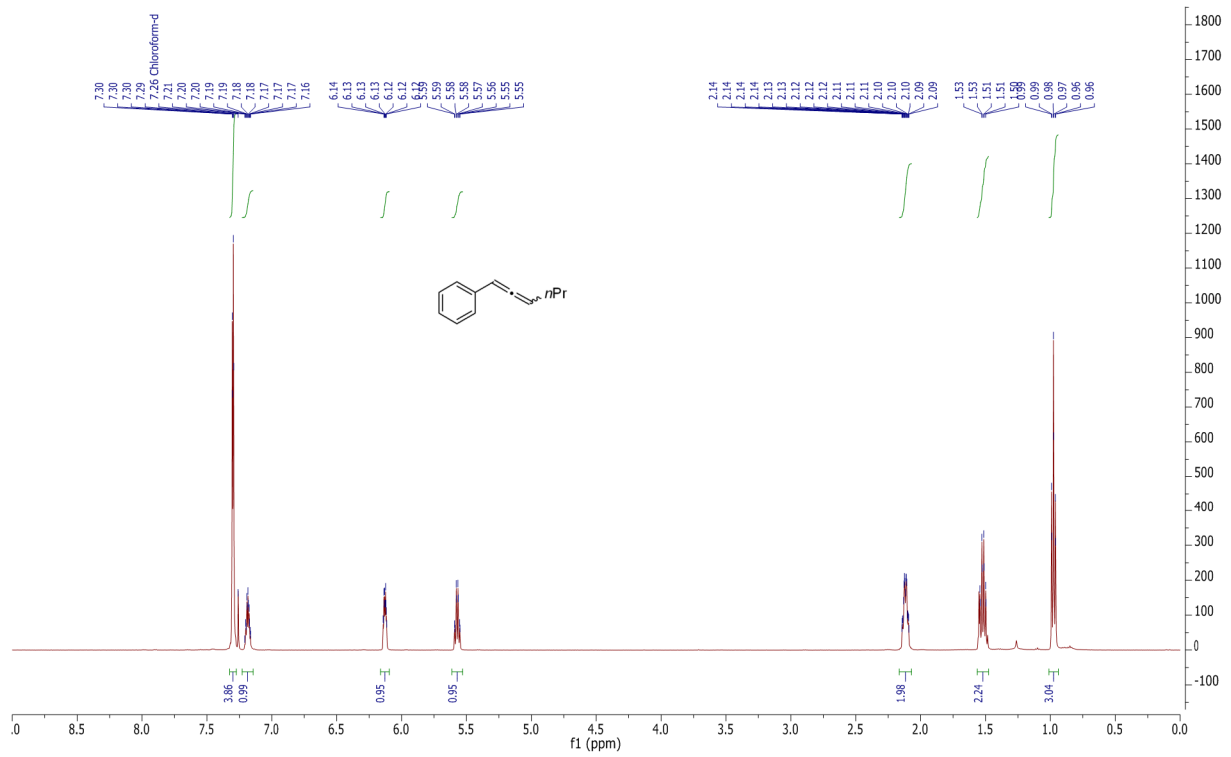
2.1r



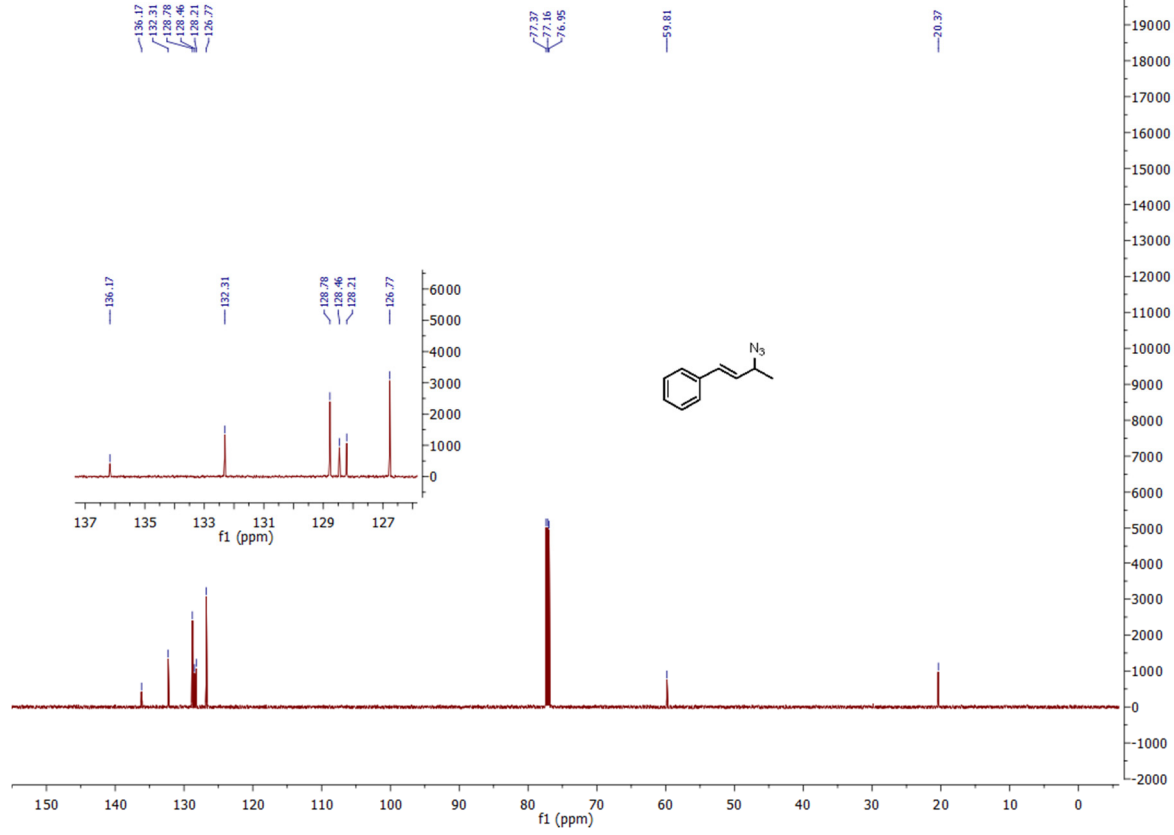
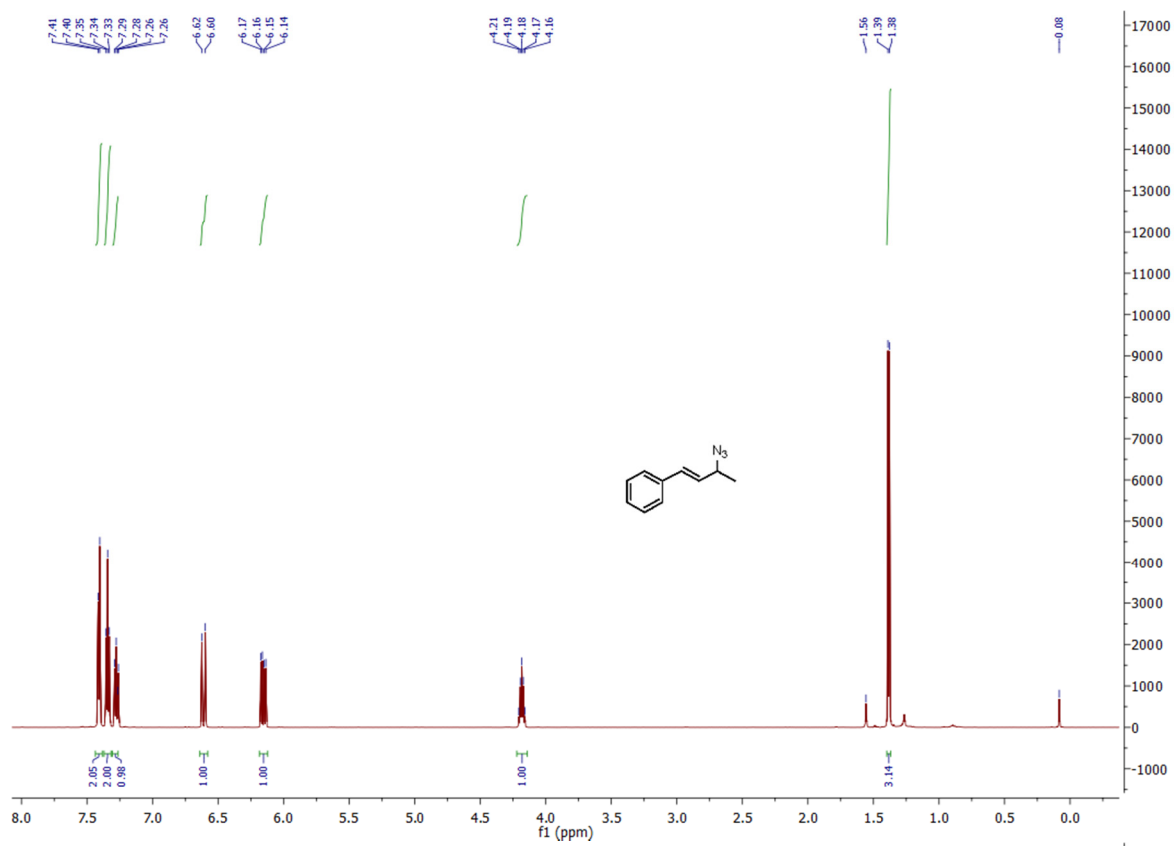
2.1s



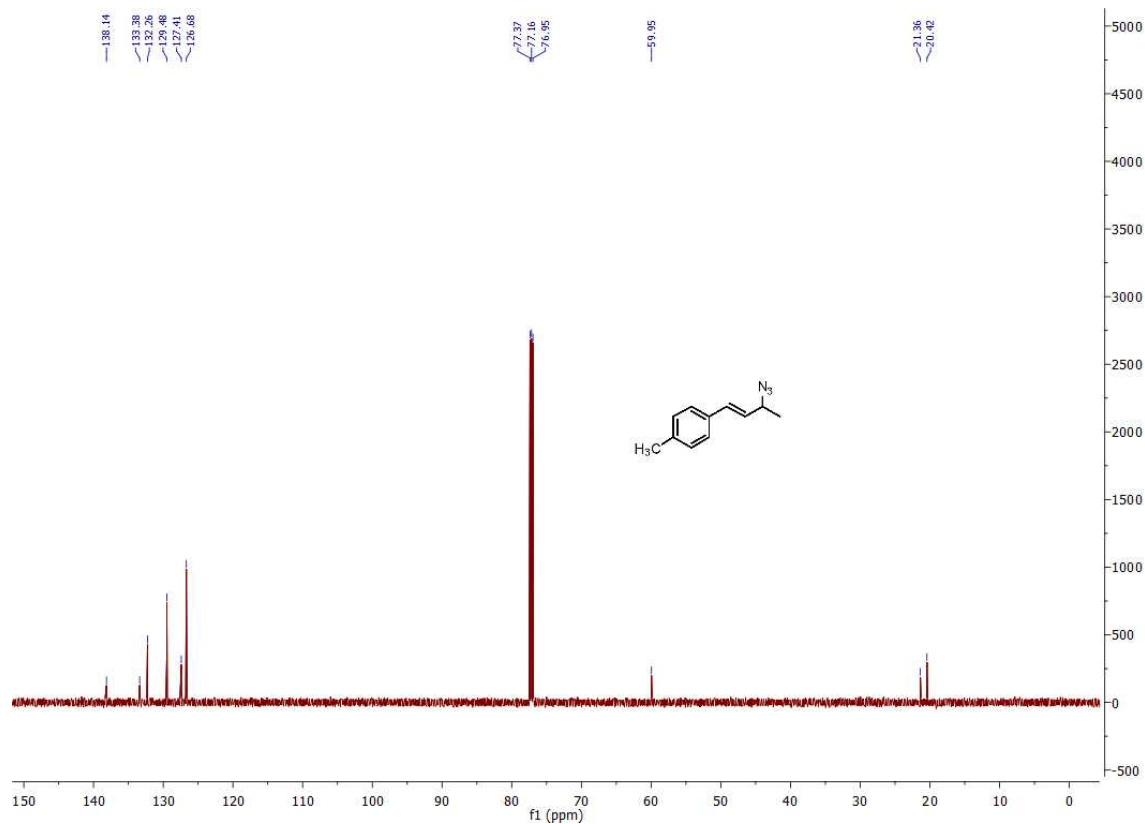
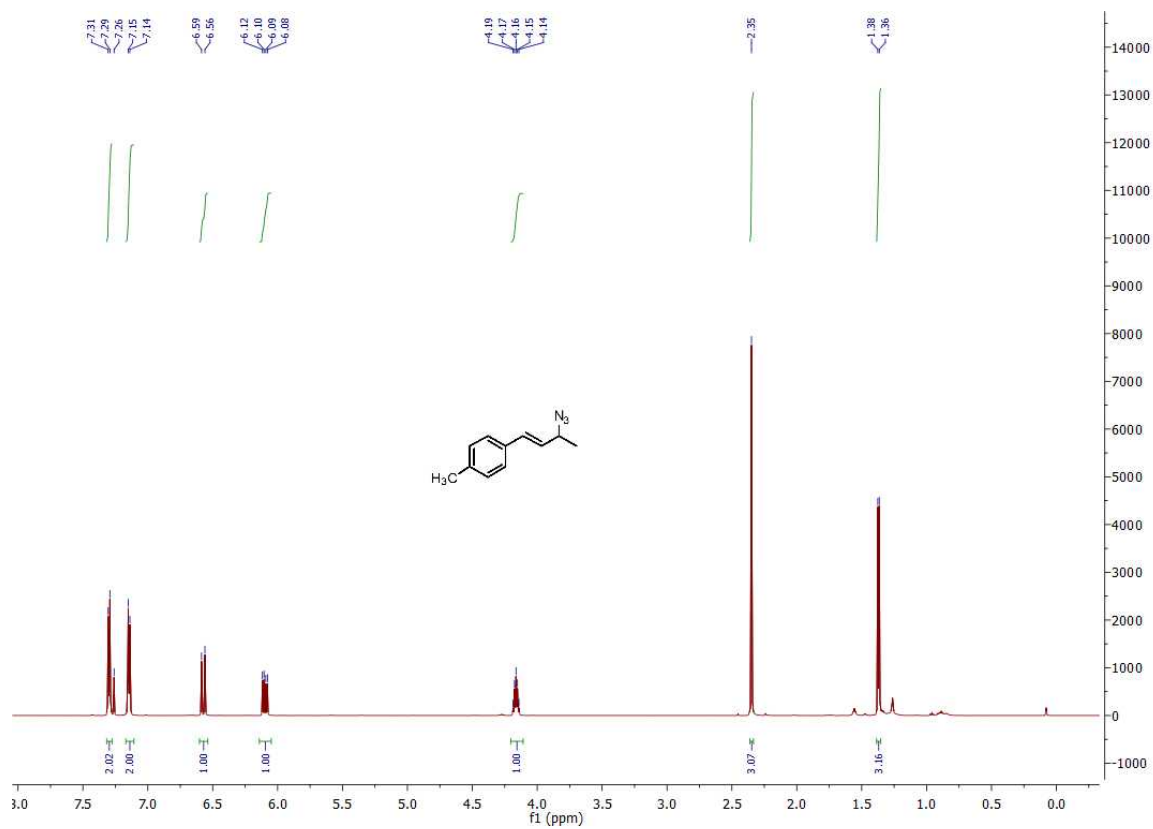
2.1t



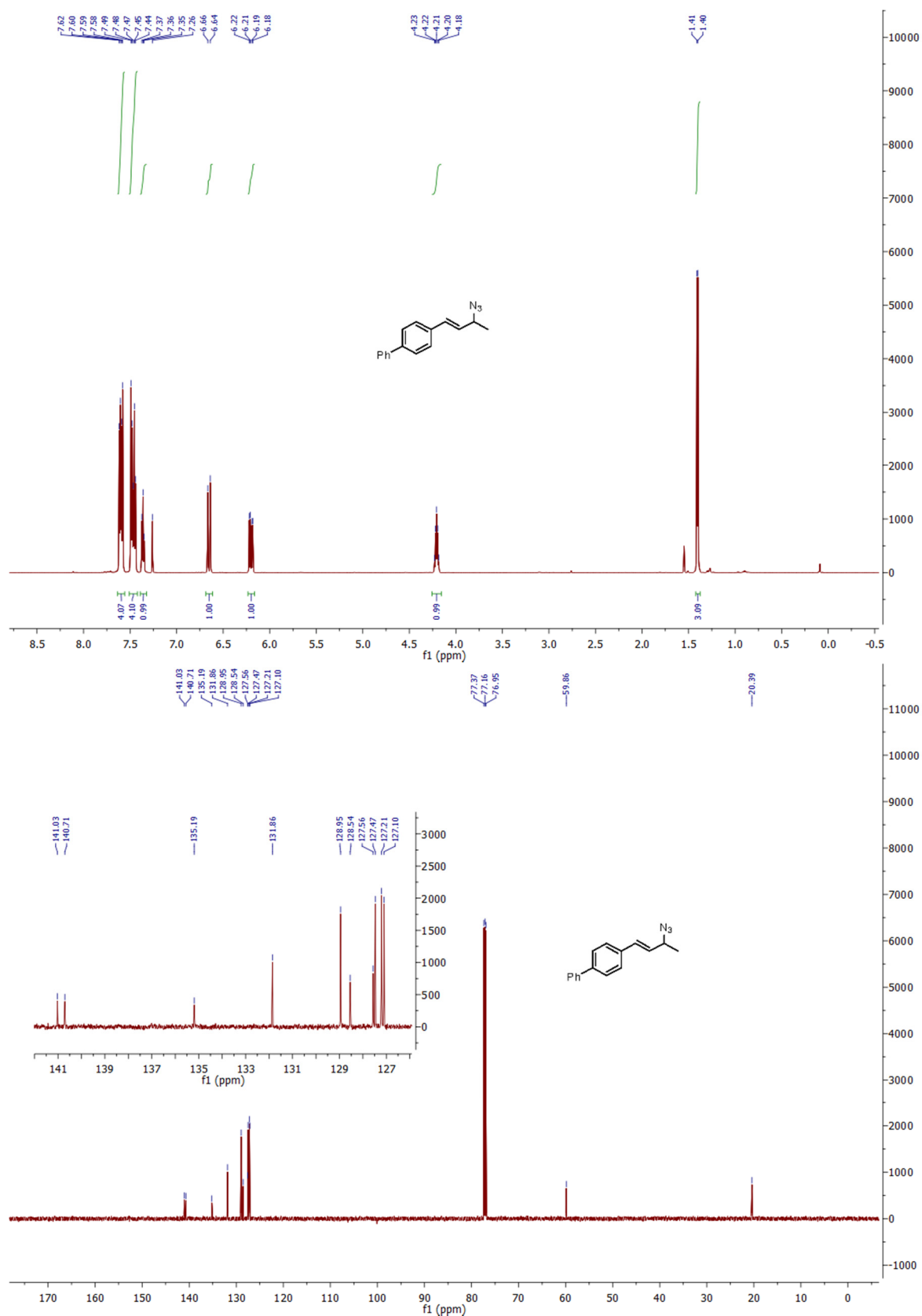
2.2a



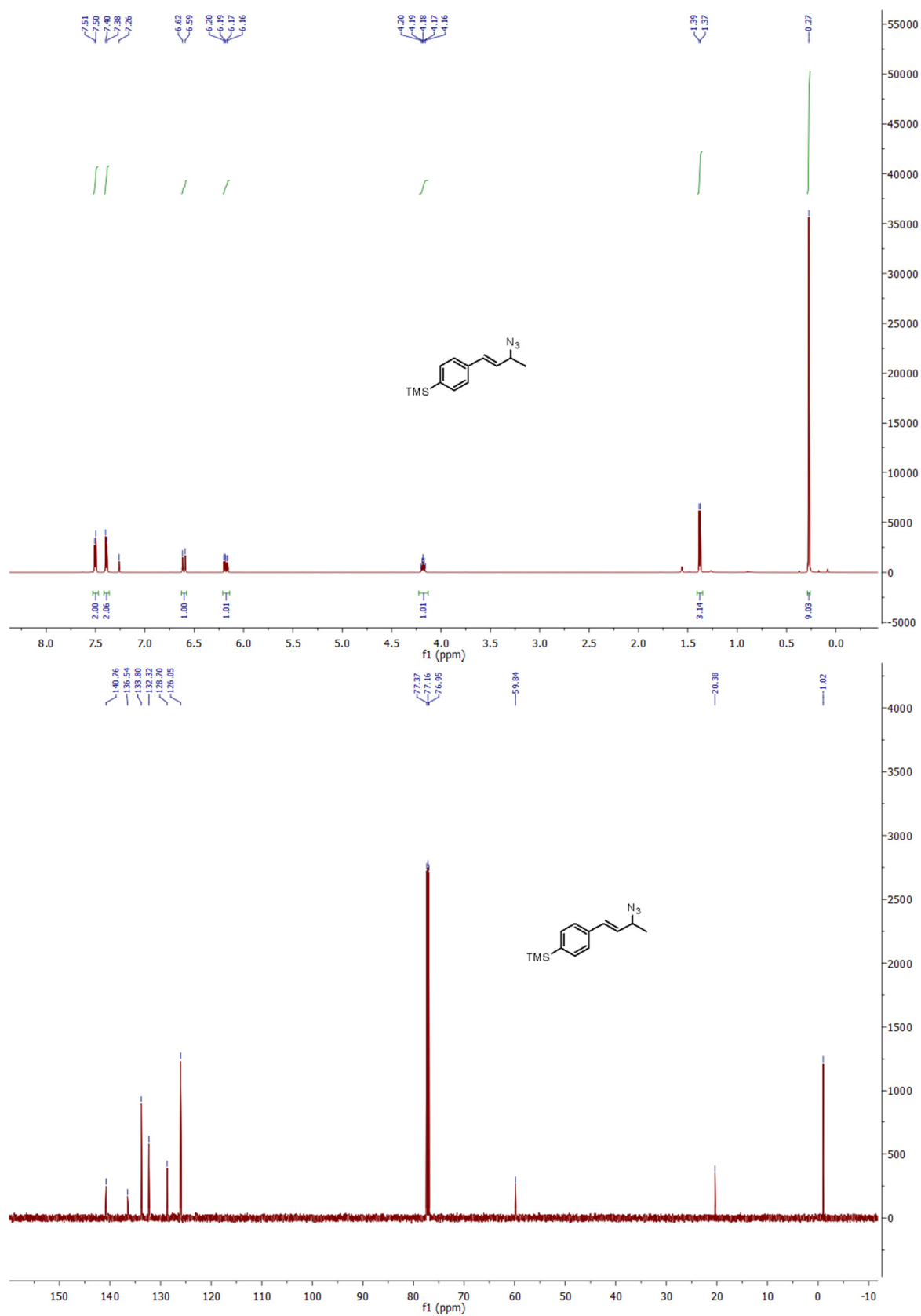
2.2b



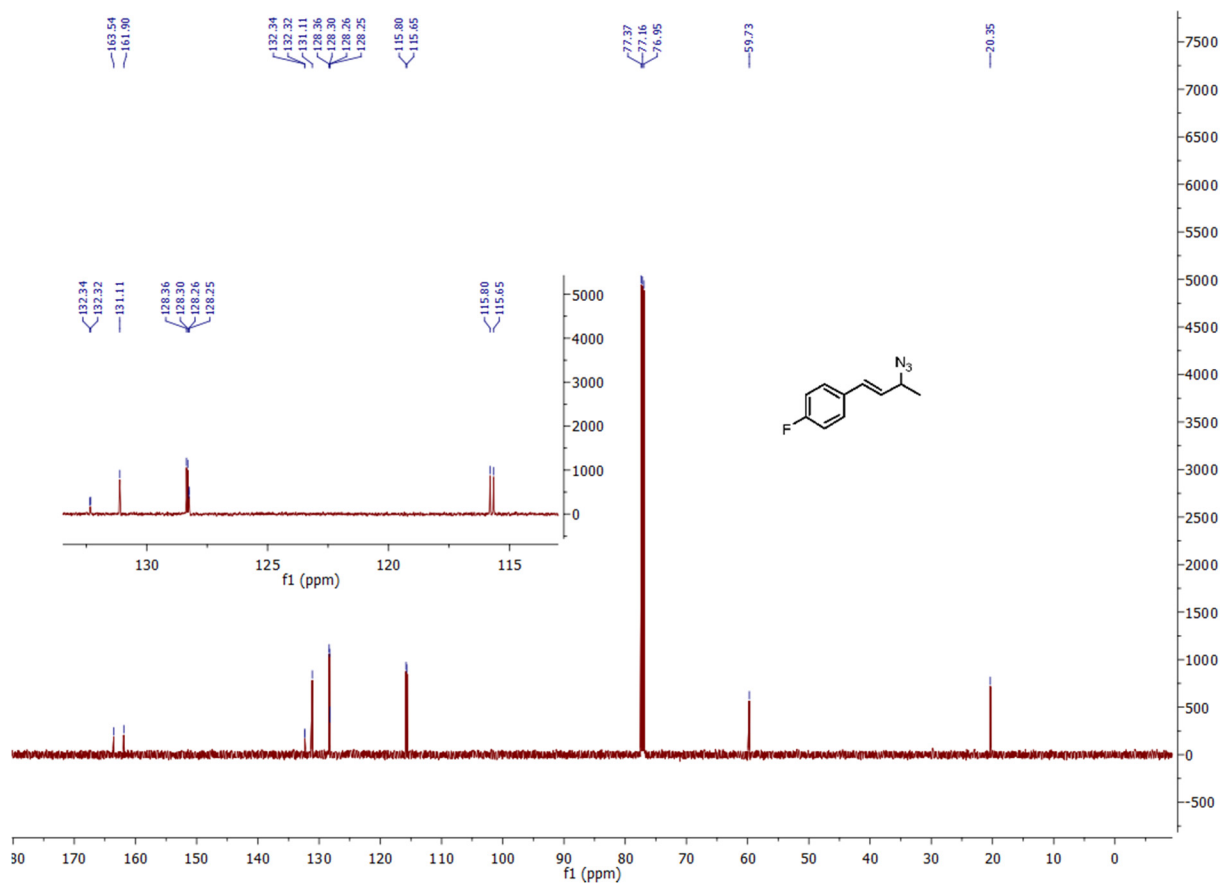
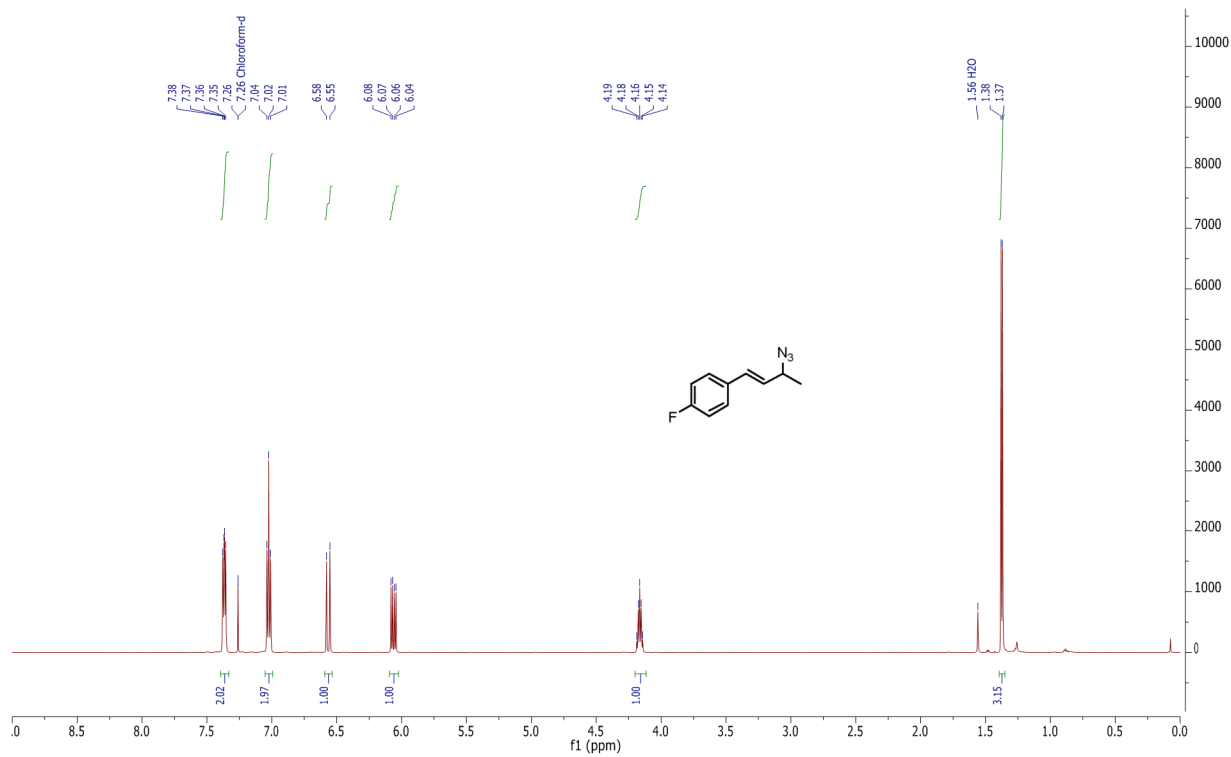
2.2c



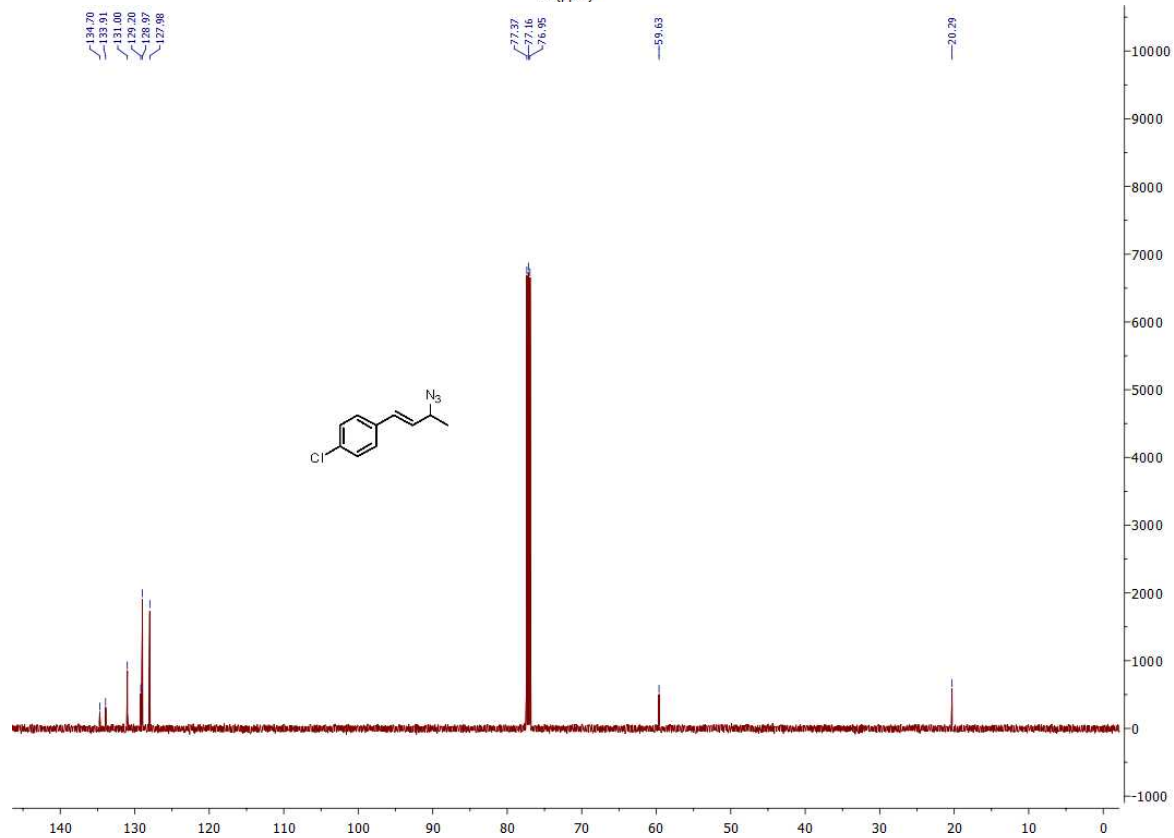
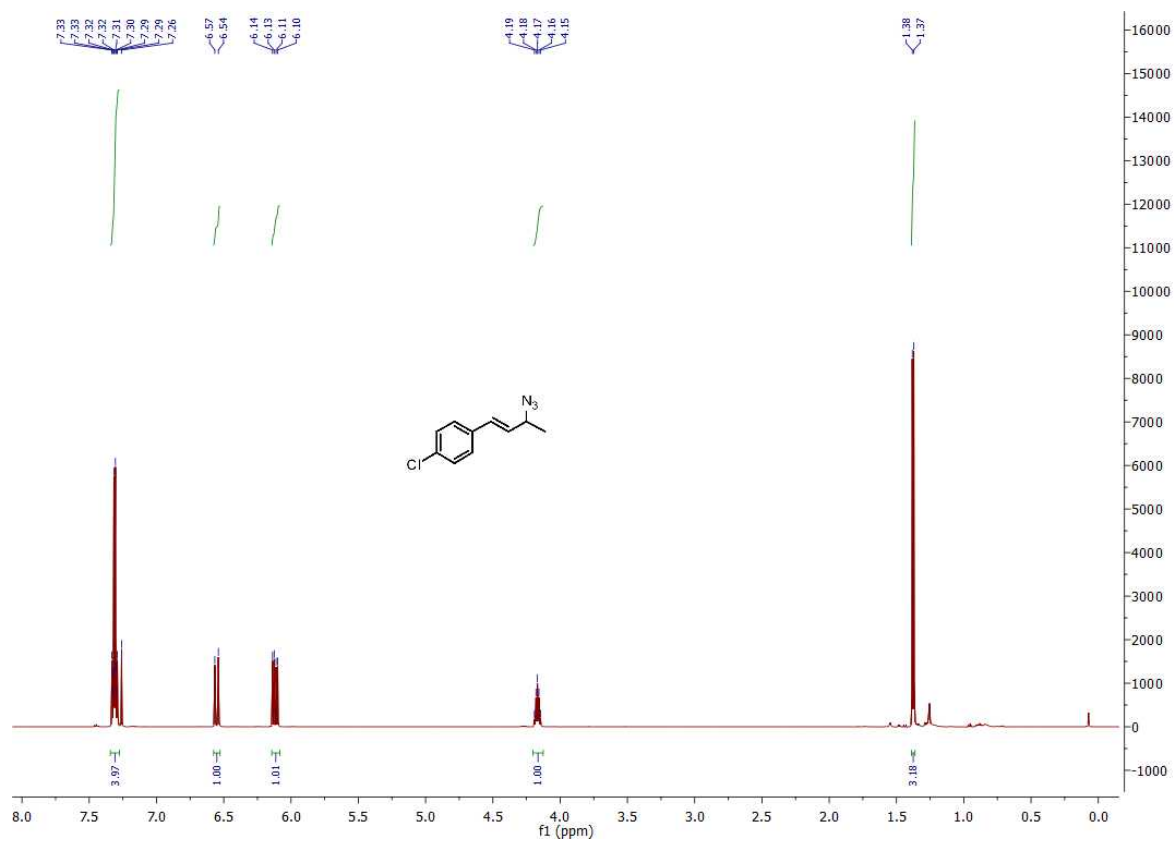
2.2d



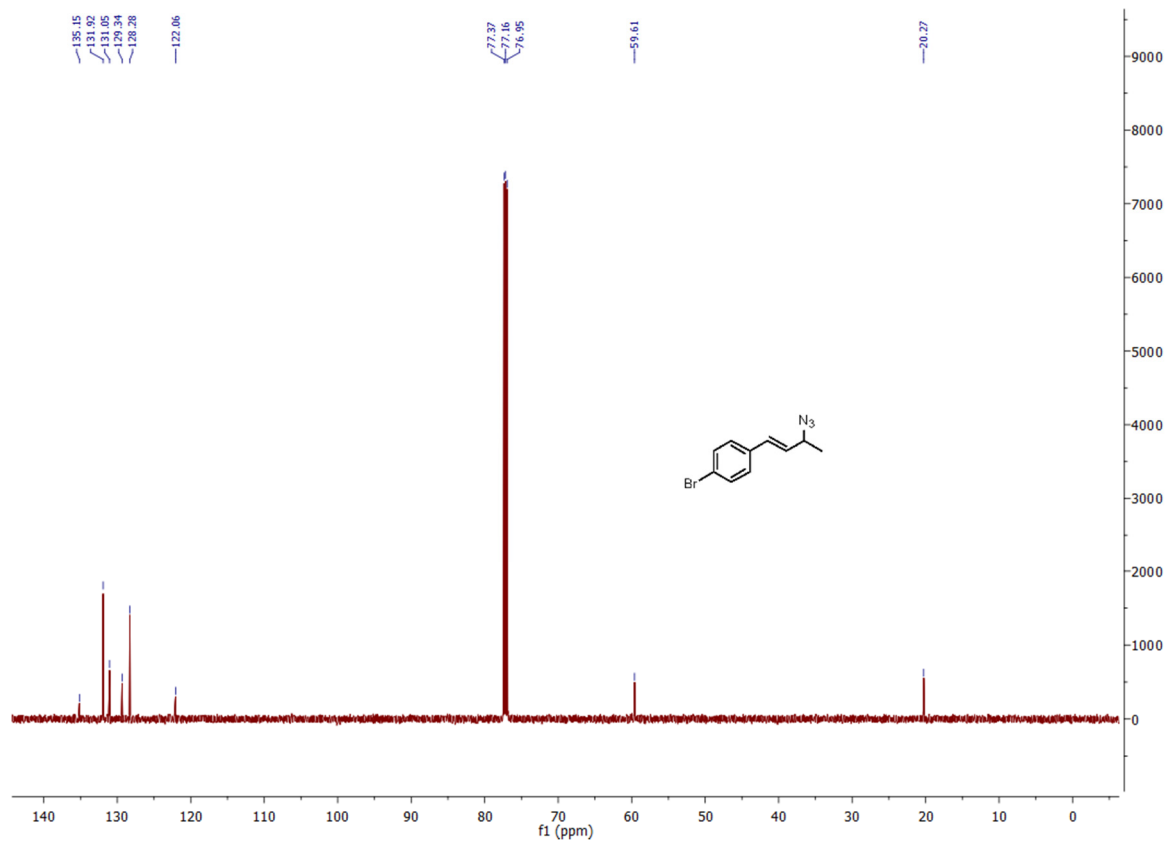
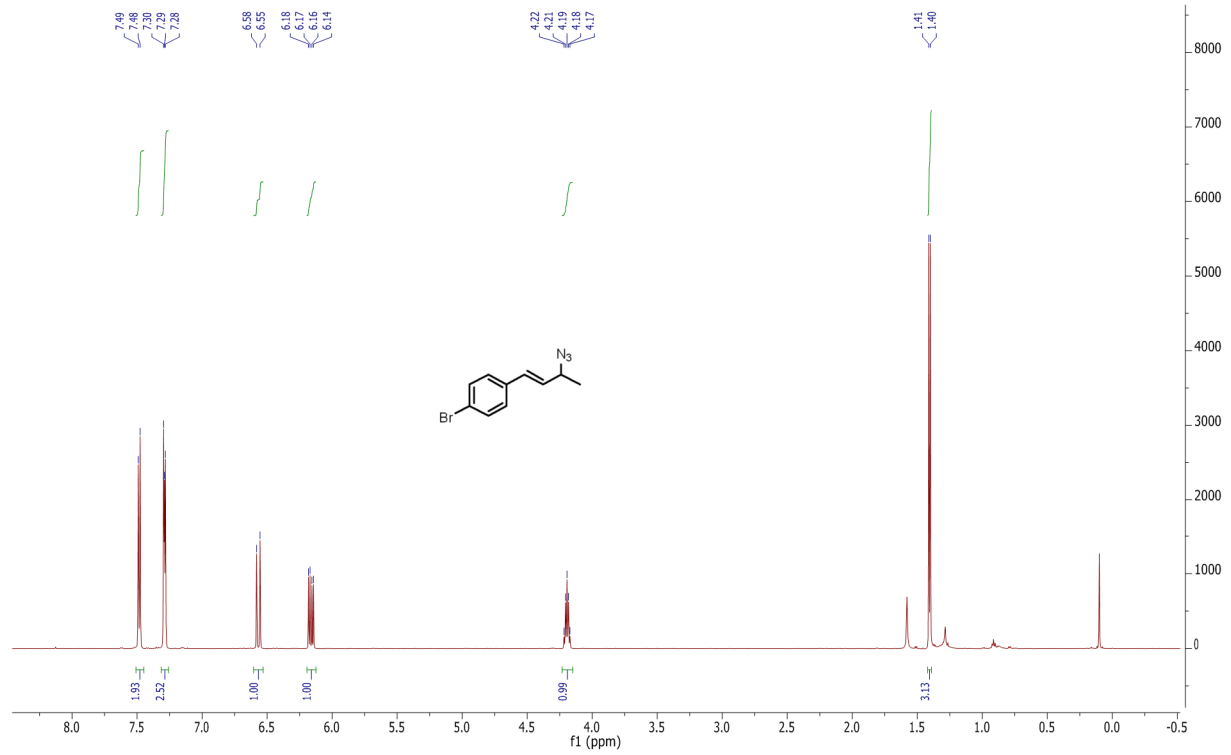
2.2e



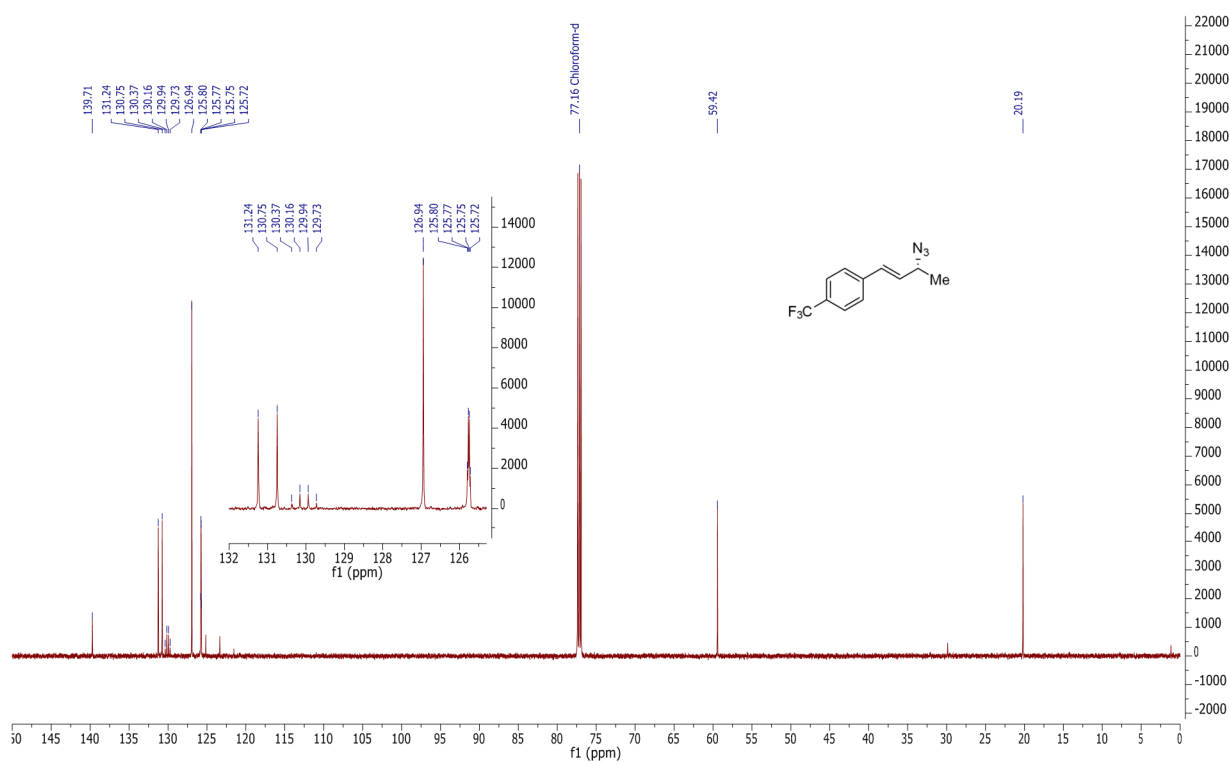
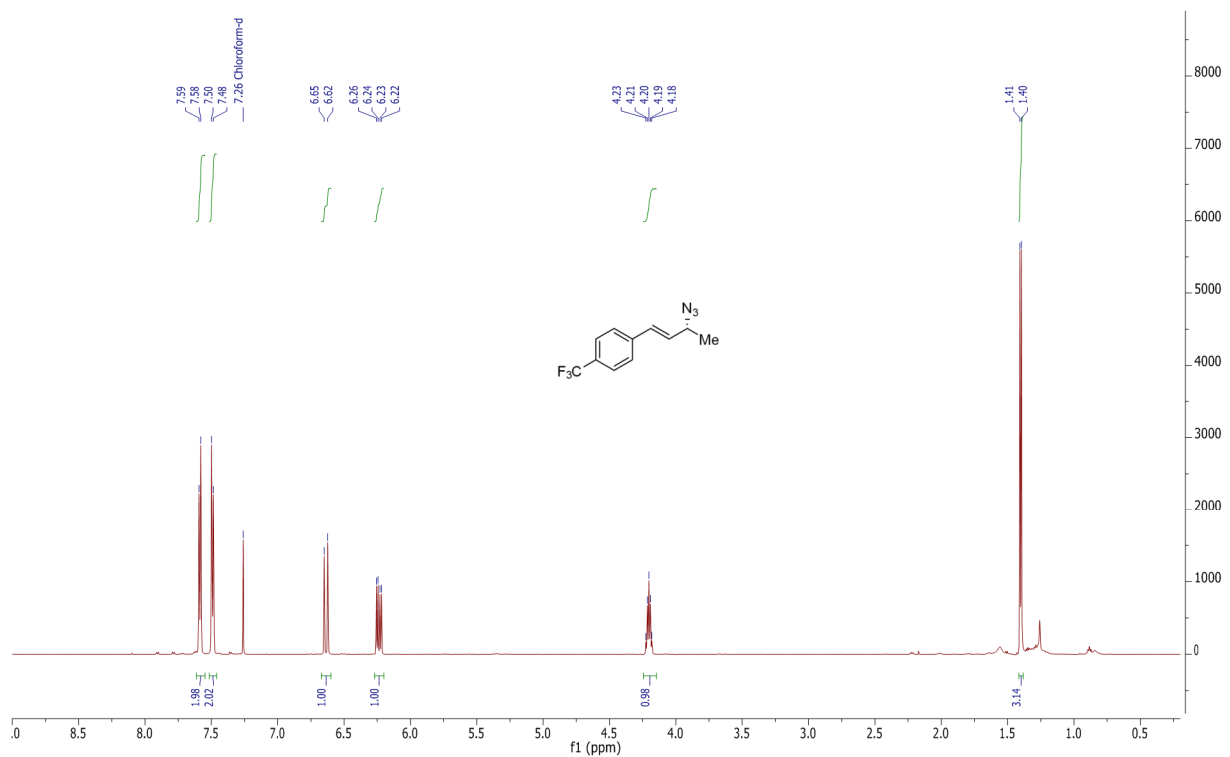
2.2f



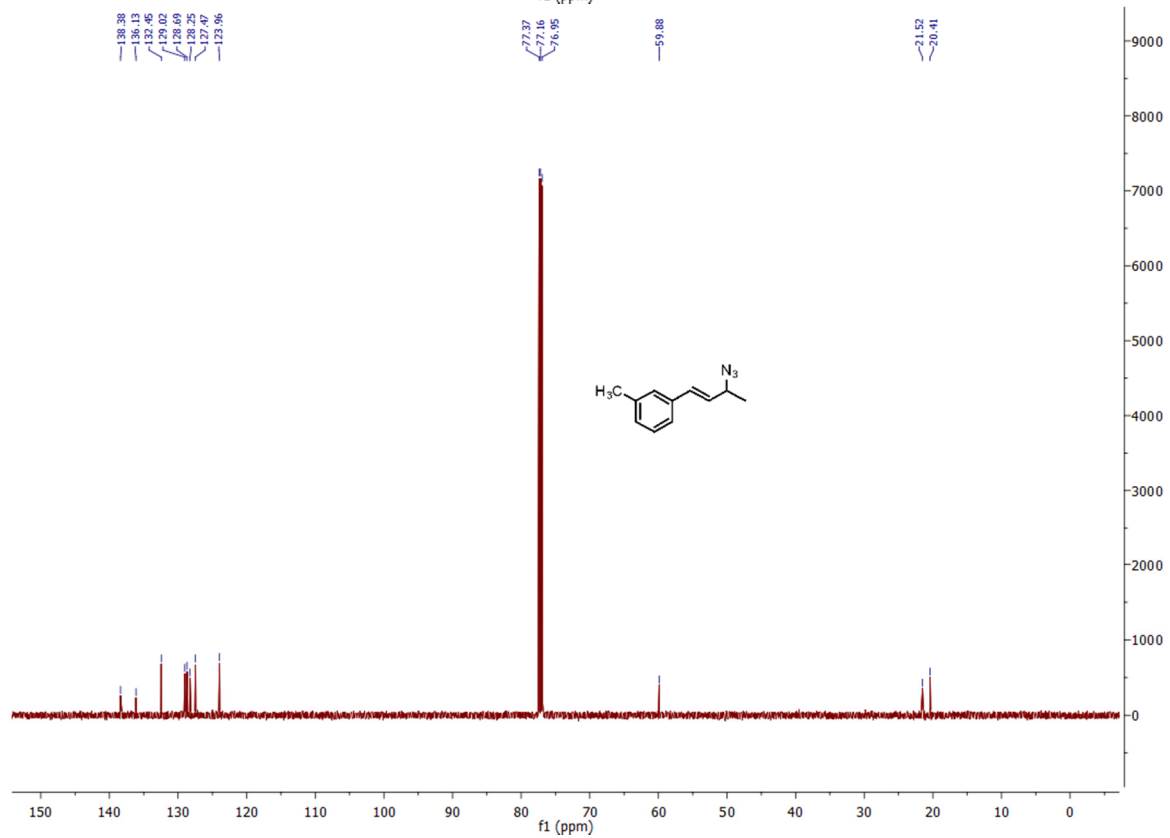
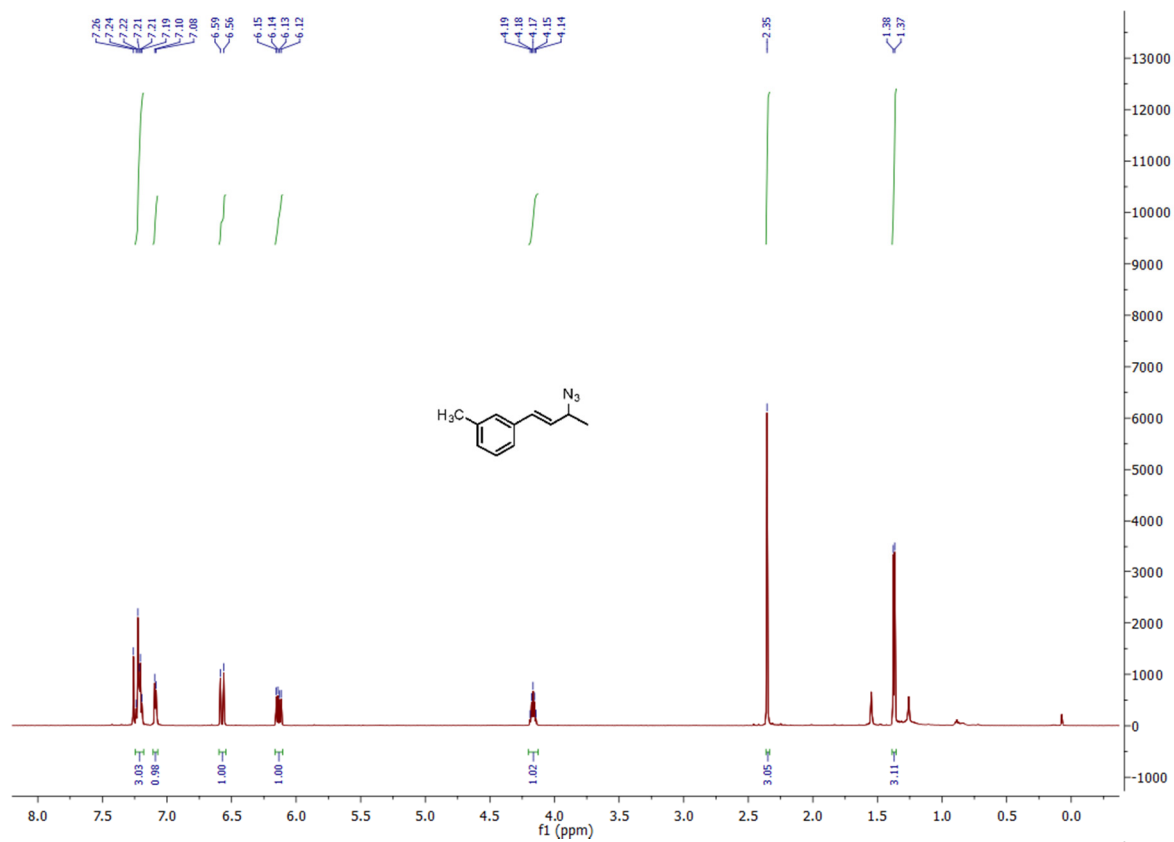
2.2g



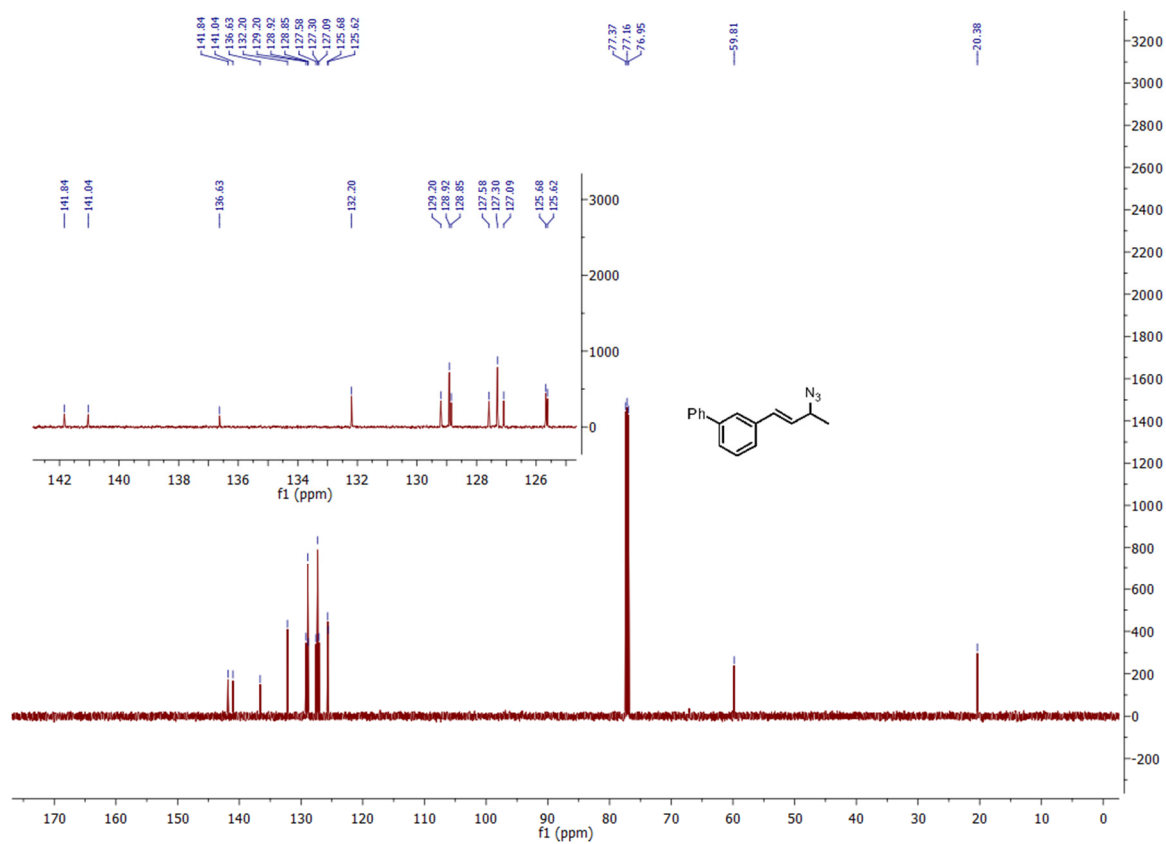
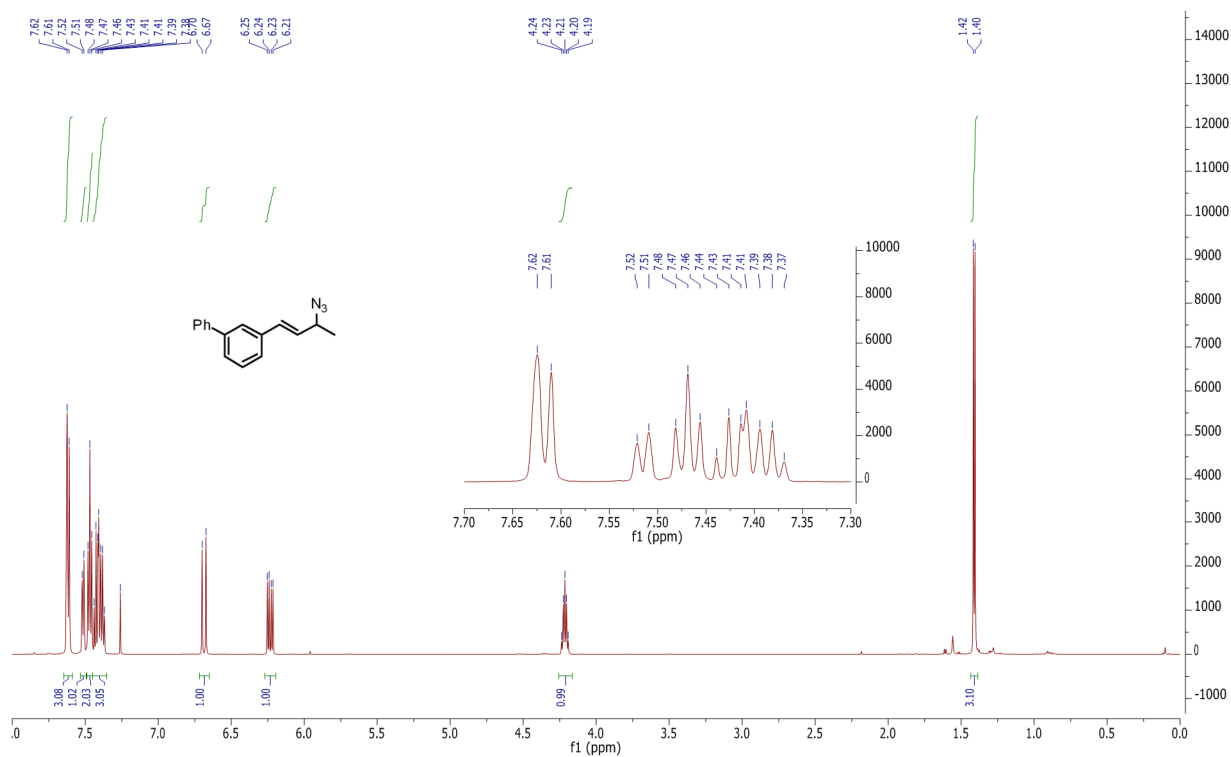
2.2h



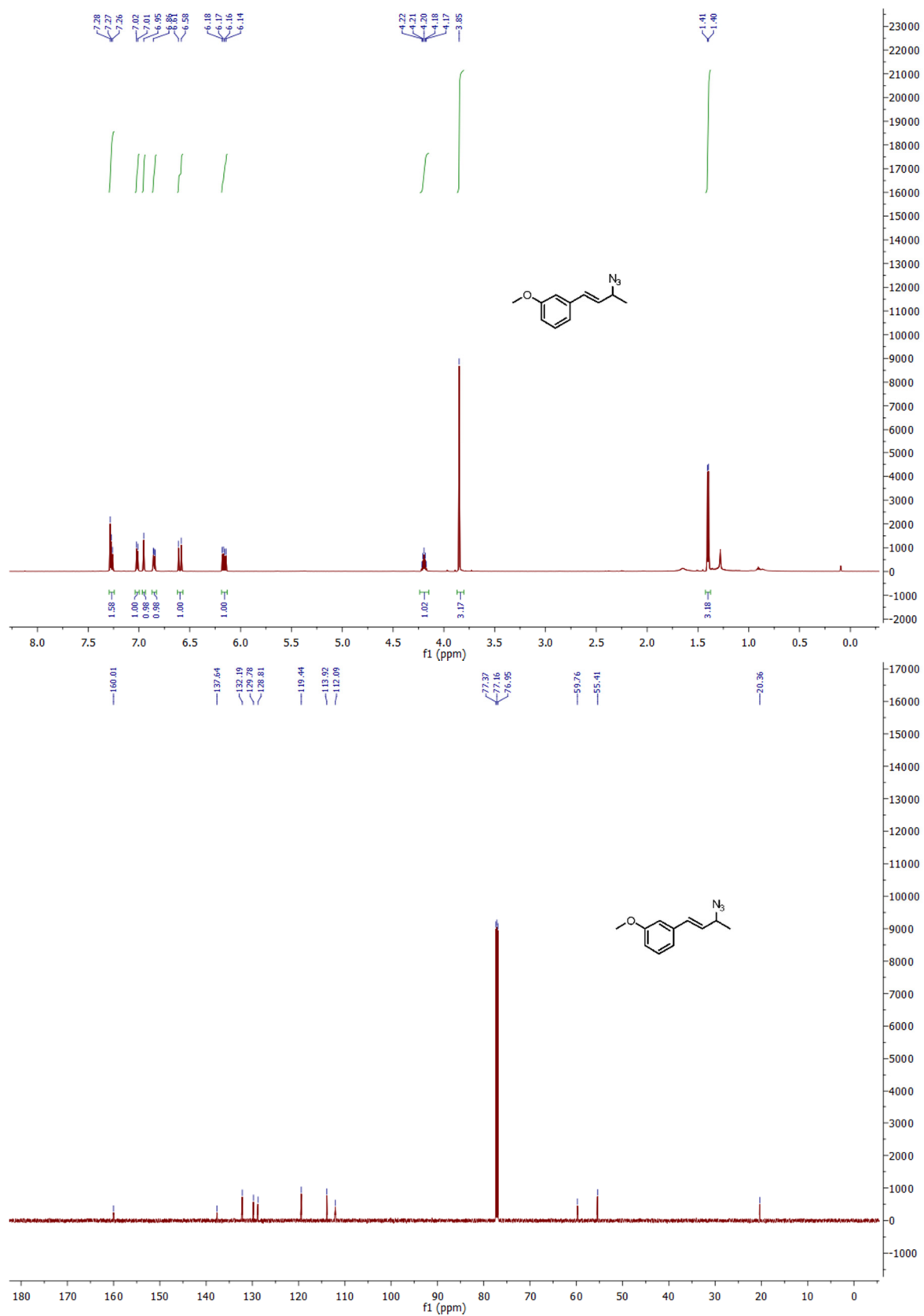
2.2i



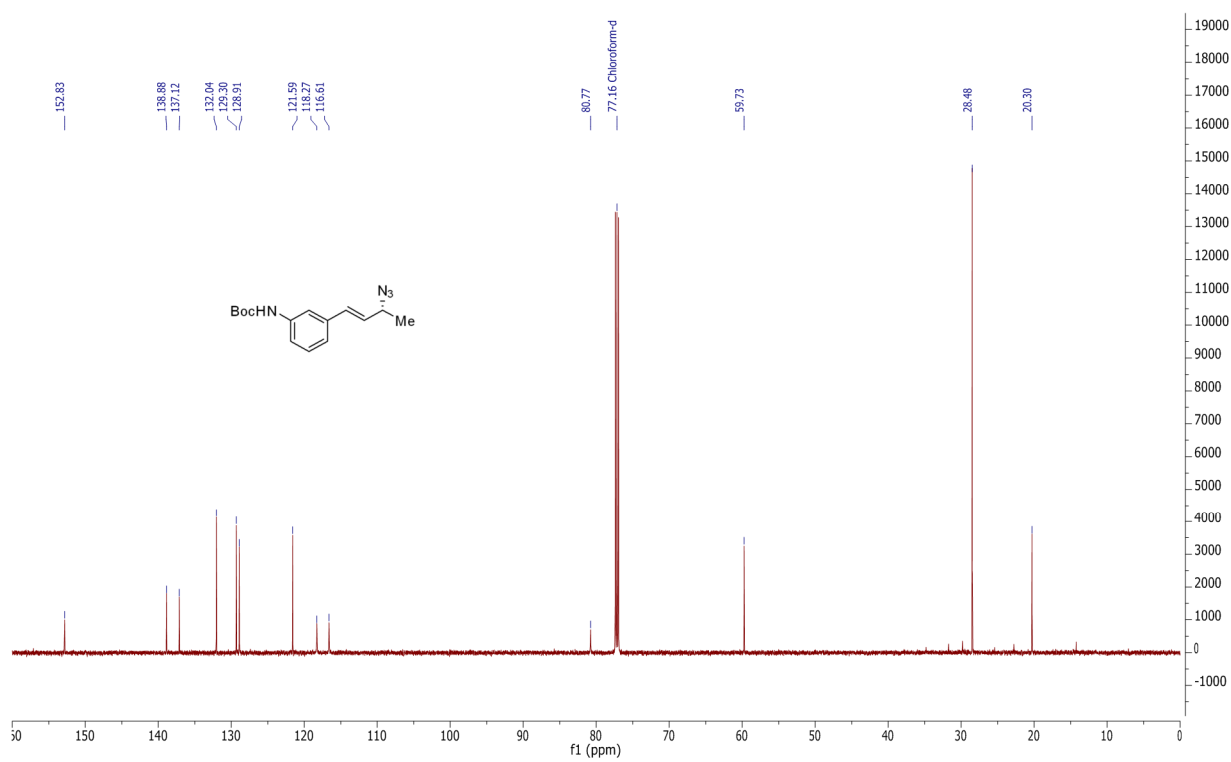
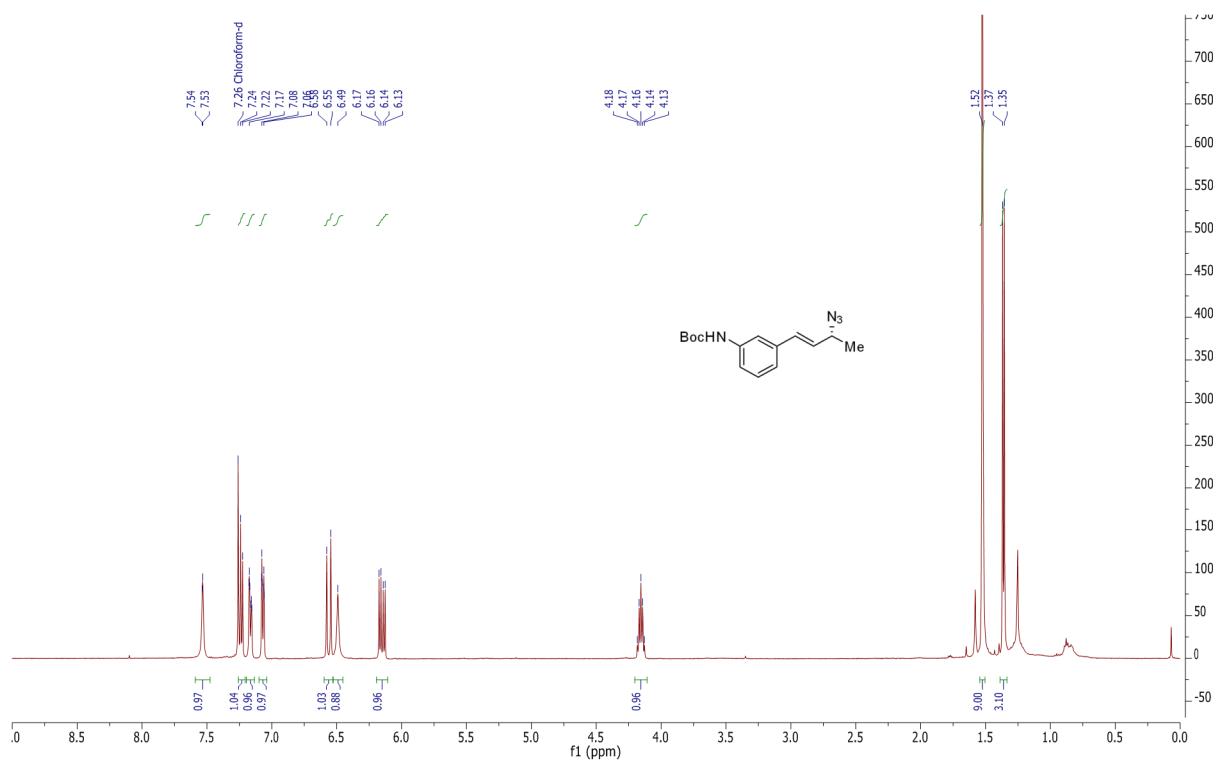
2.2j



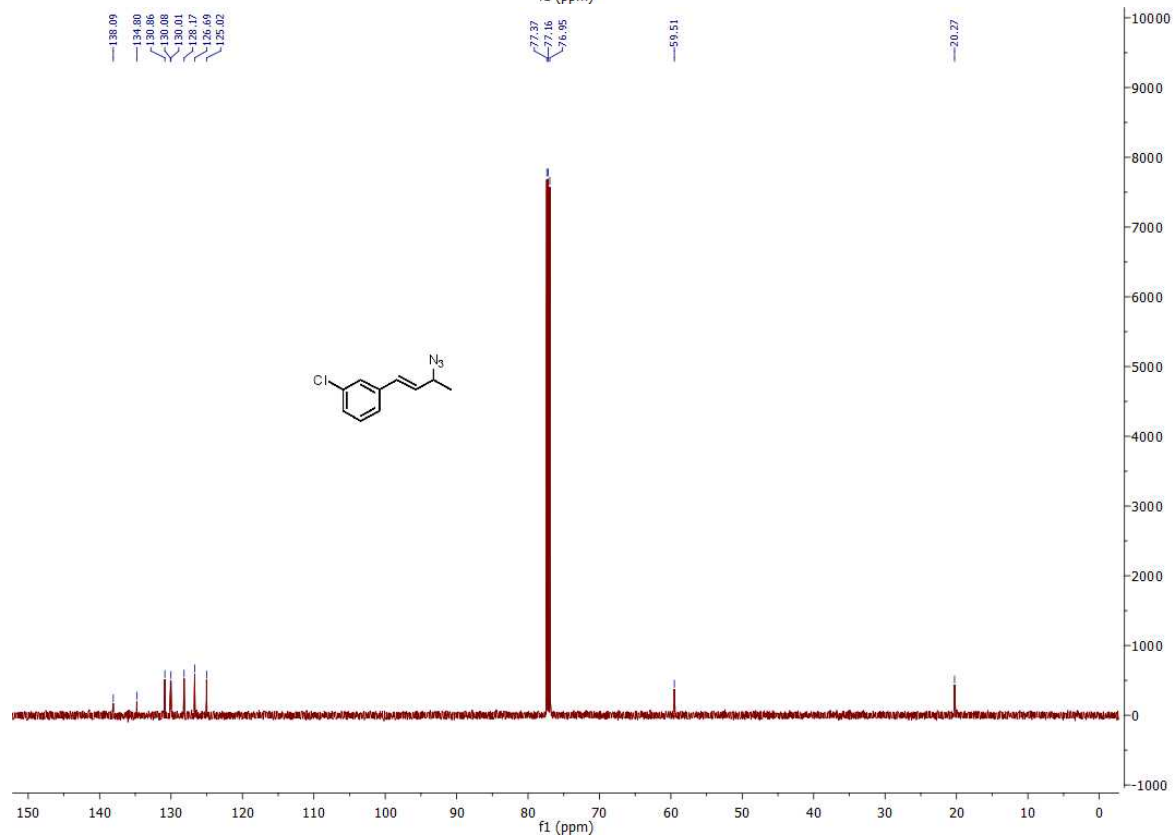
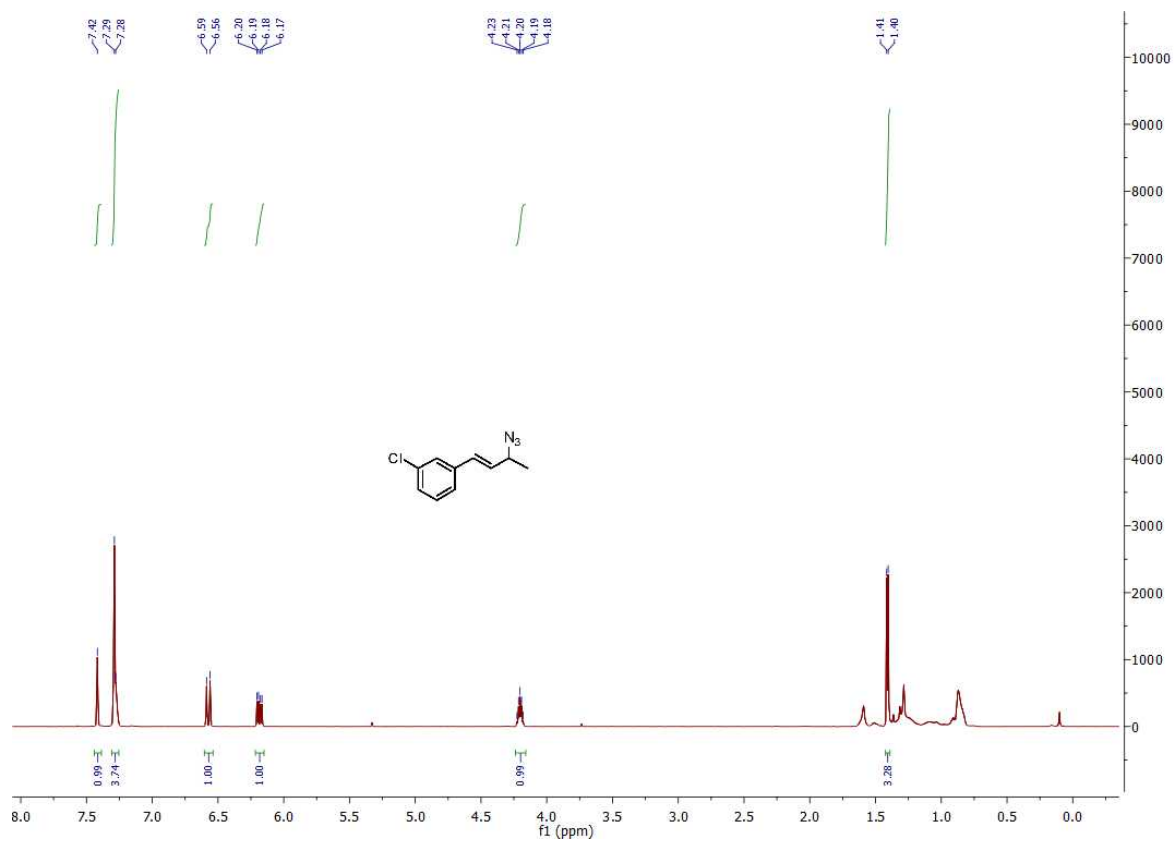
2.2k



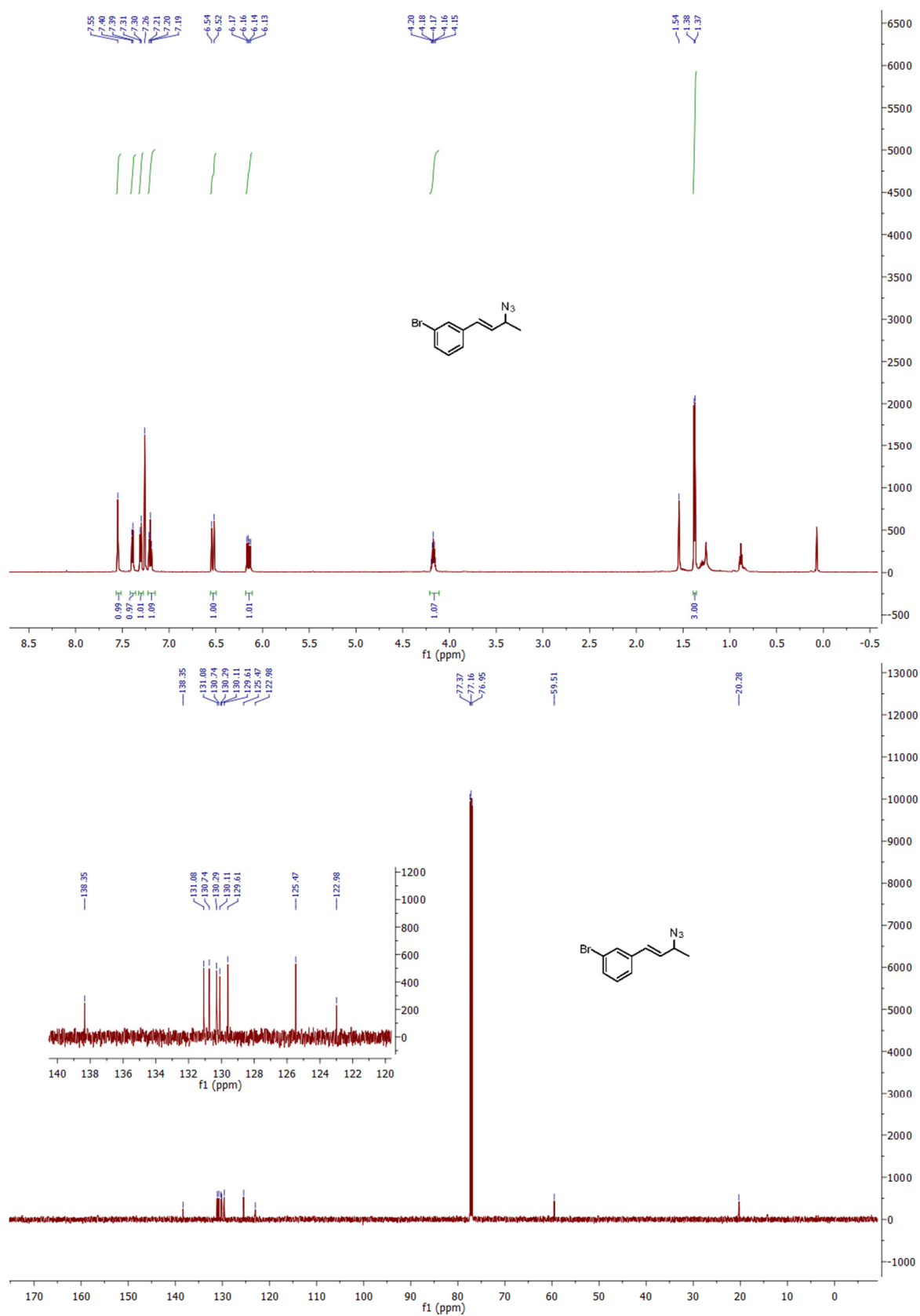
2.21



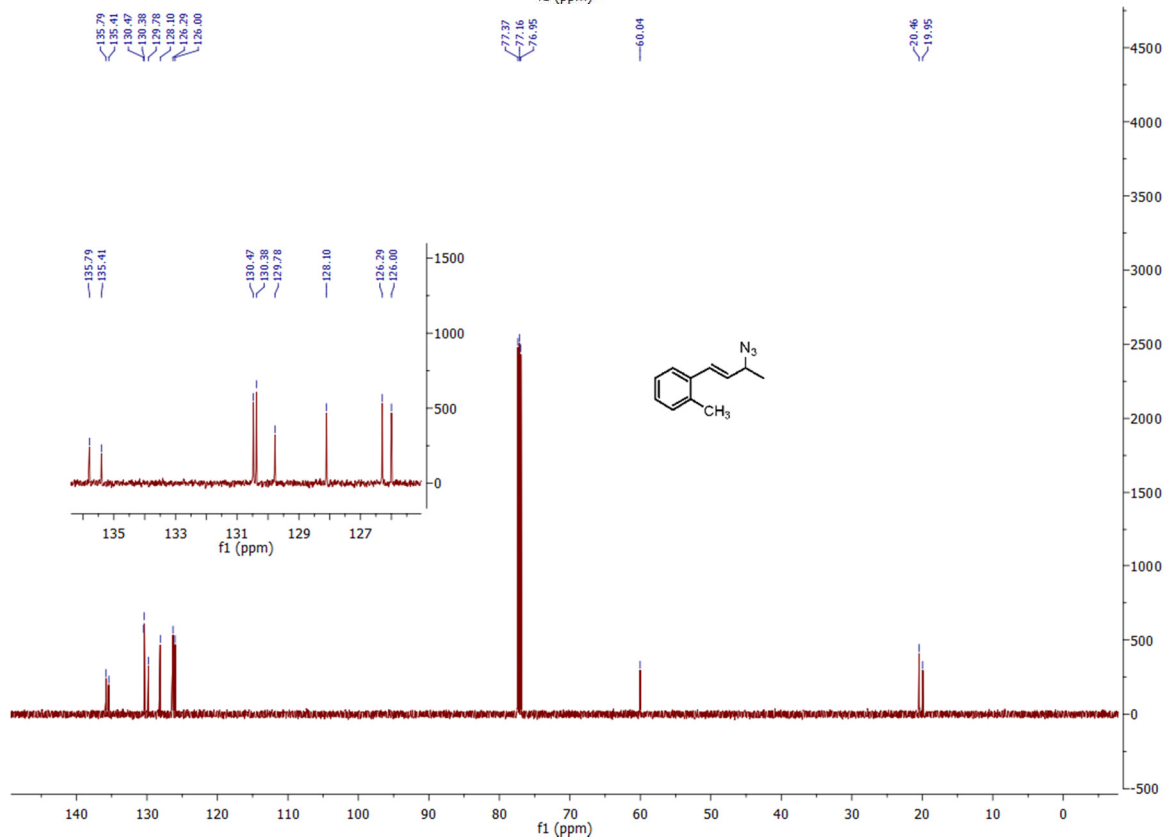
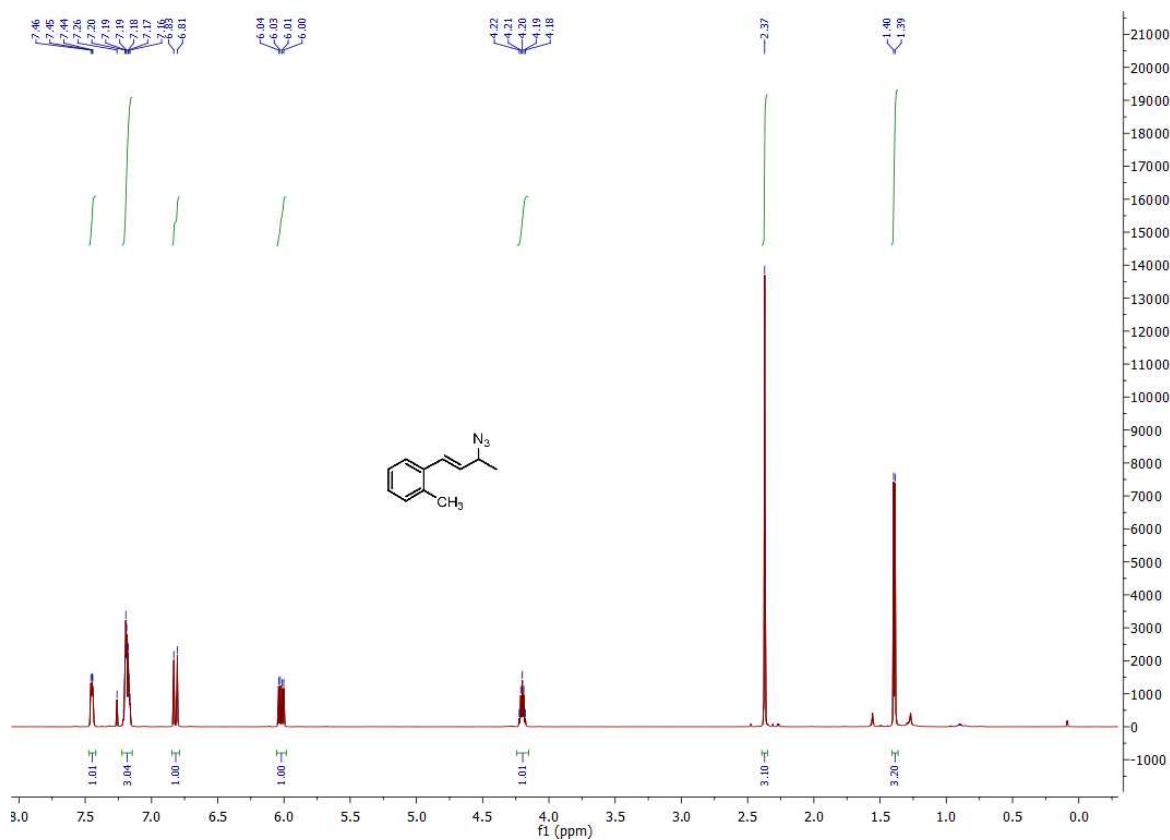
2.2m



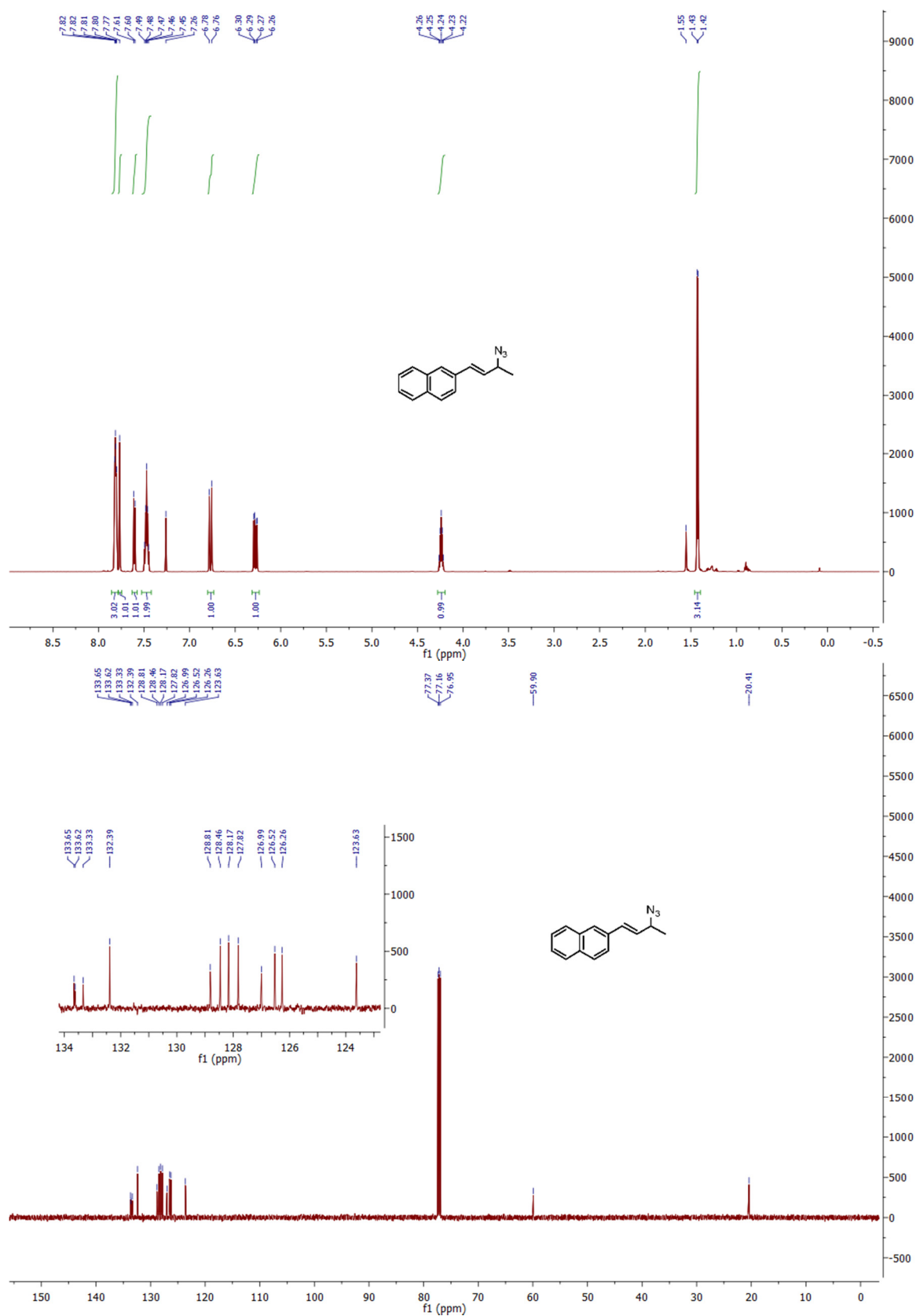
2.2n



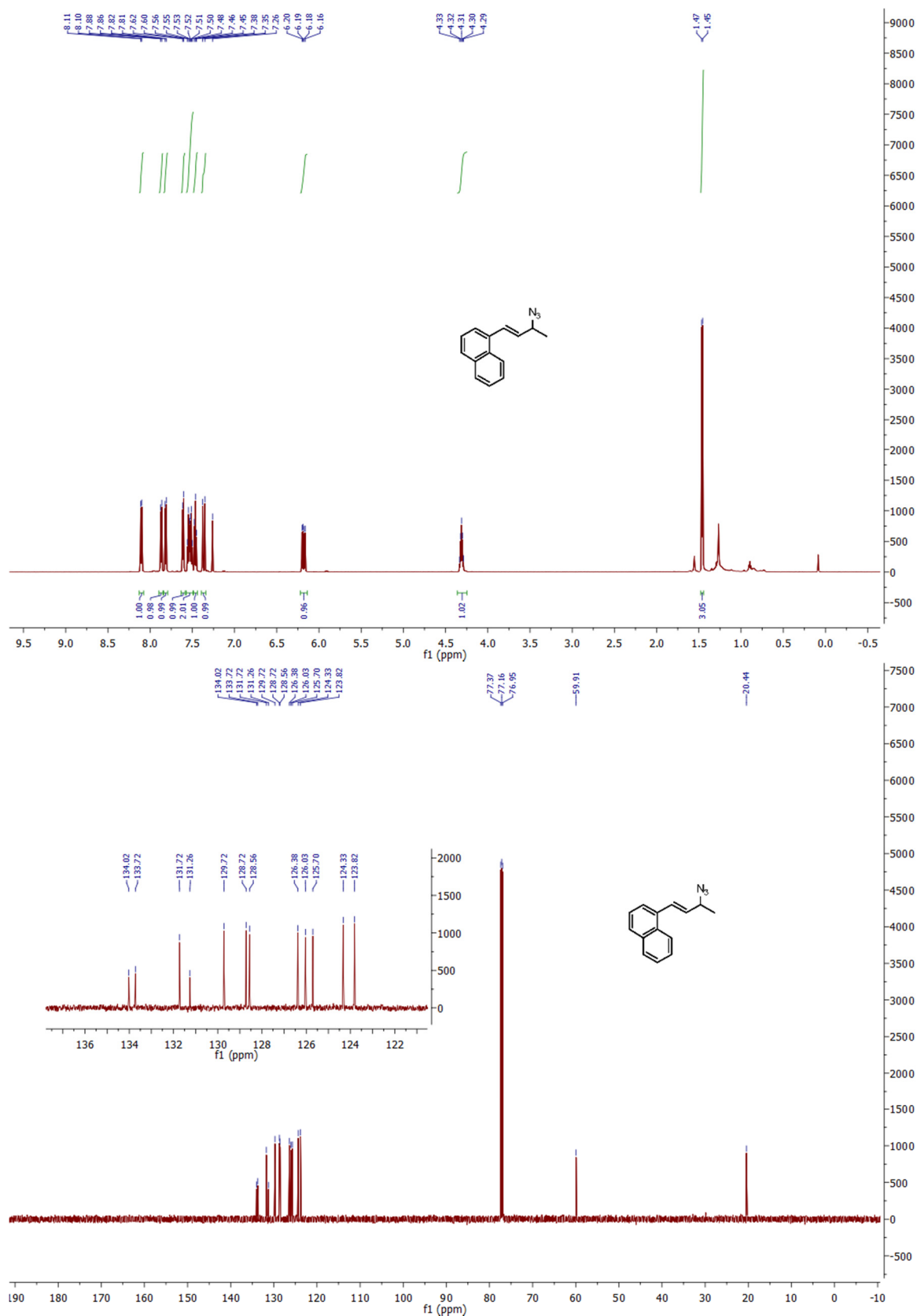
2.20



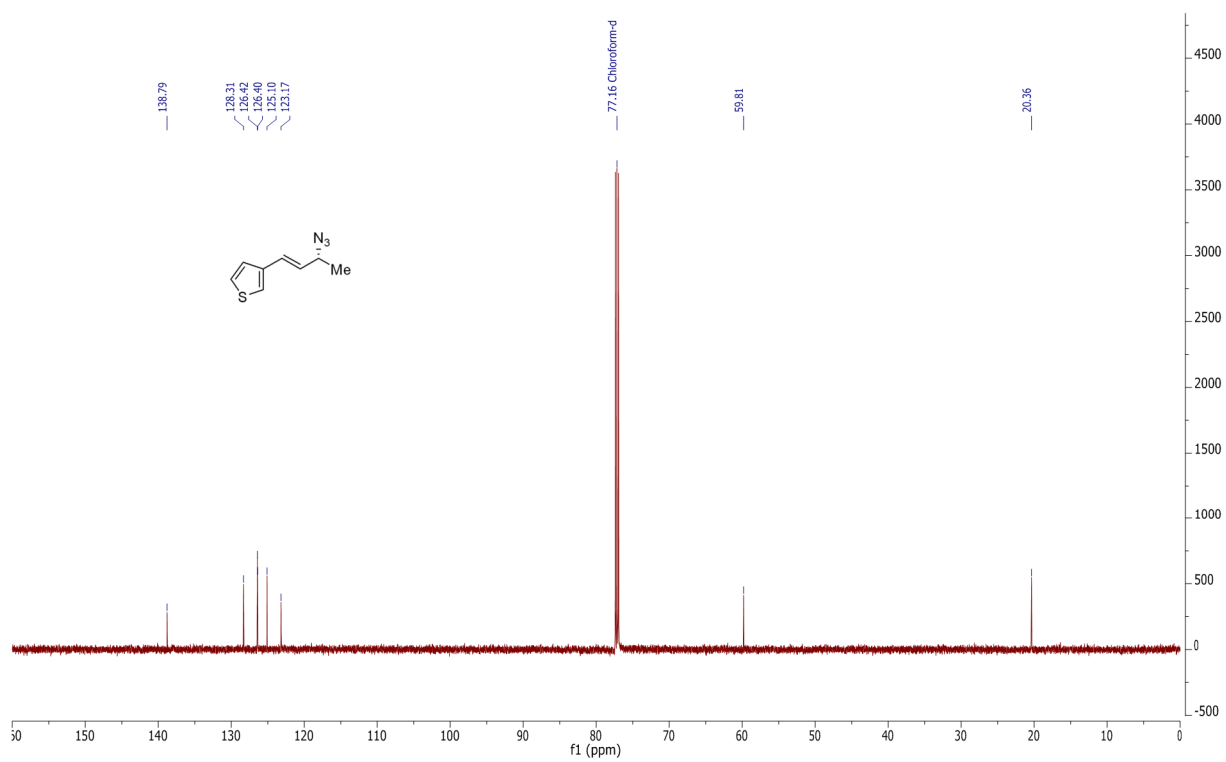
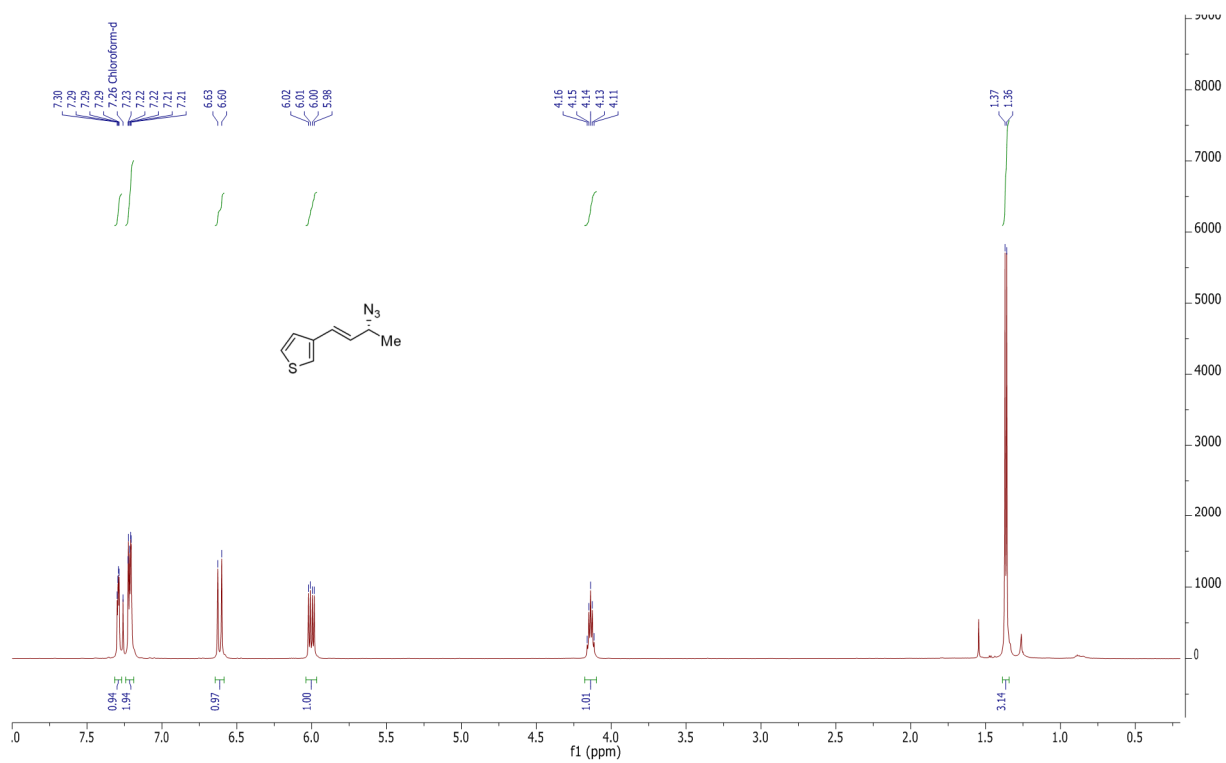
2.2p



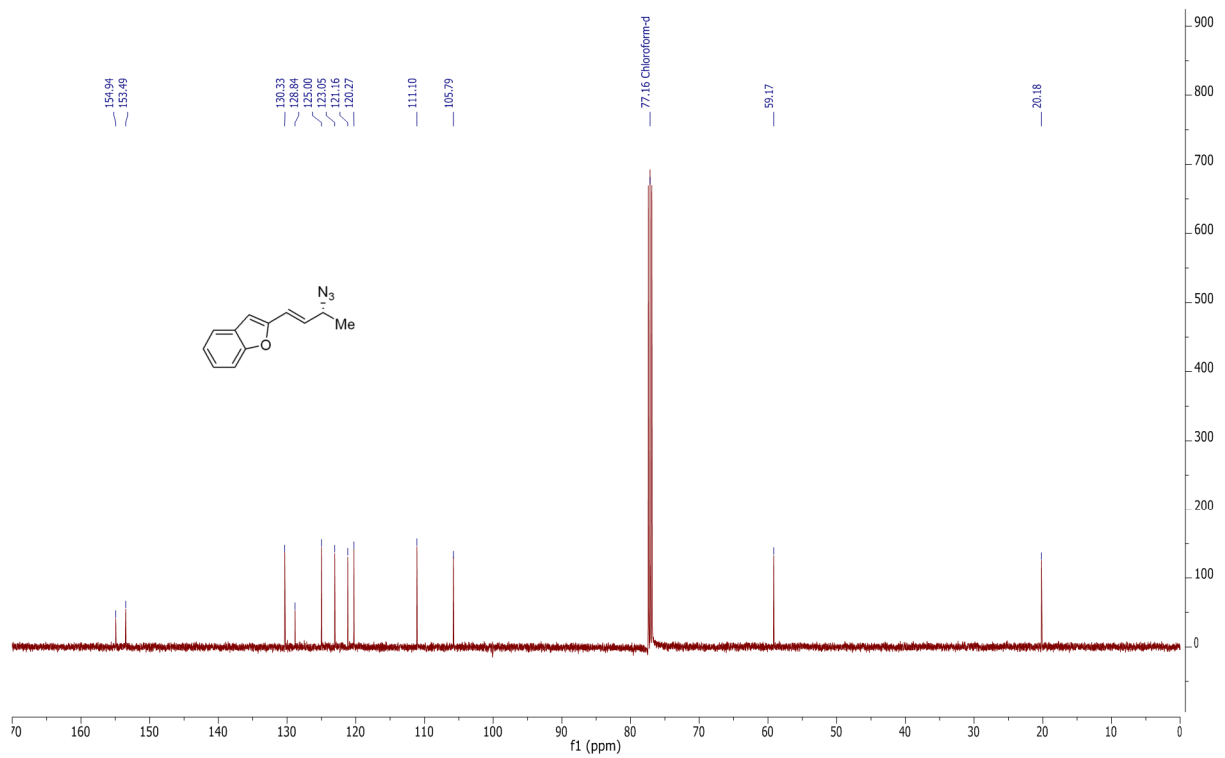
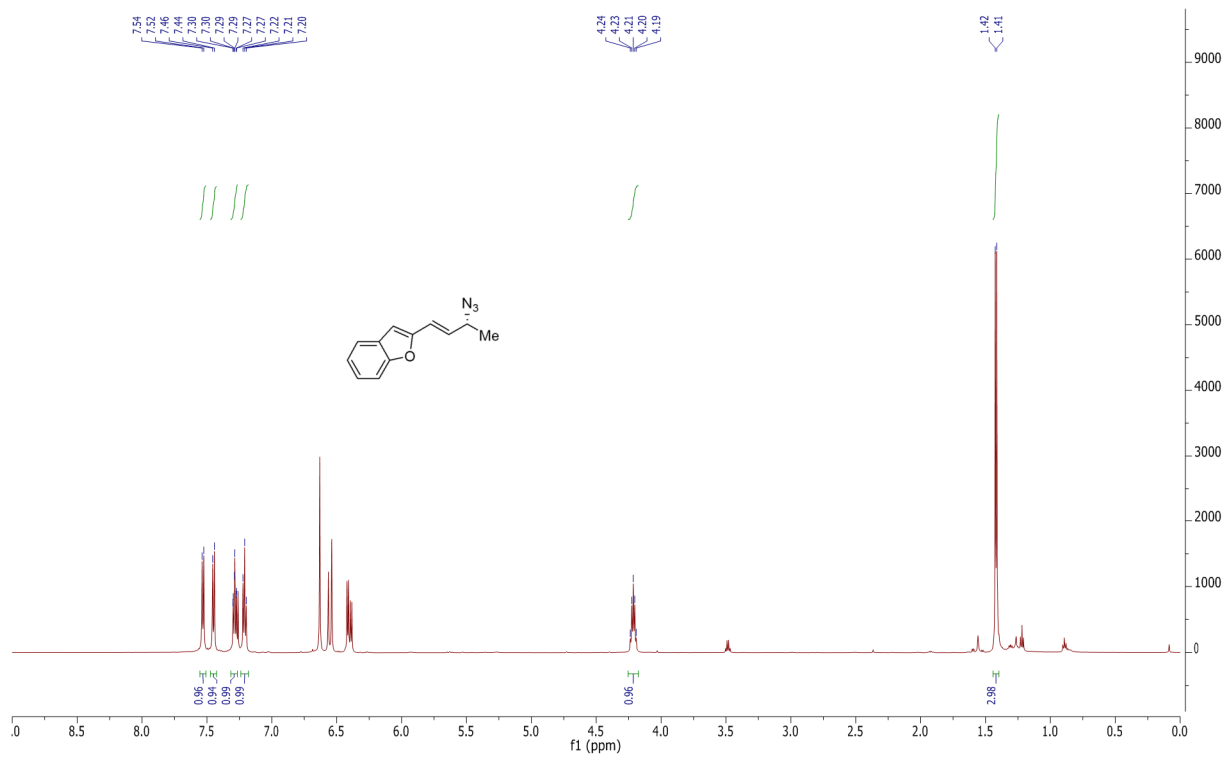
2.2q



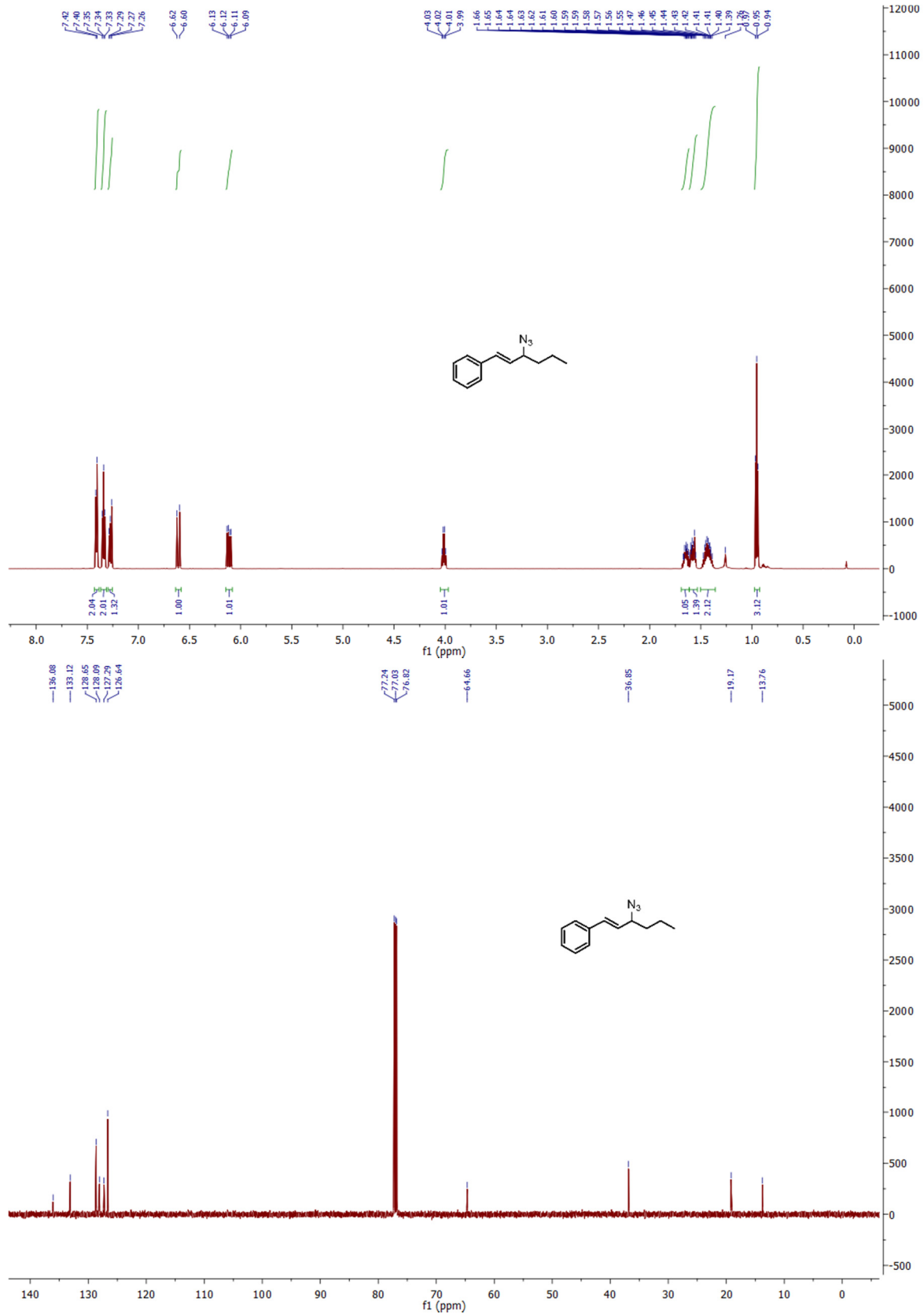
2.2r



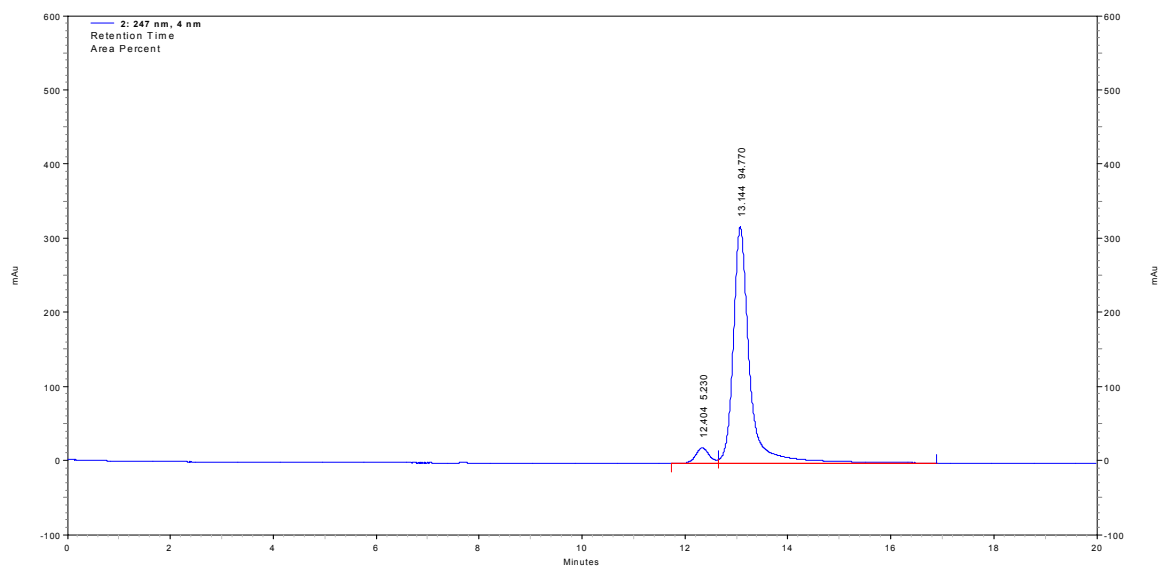
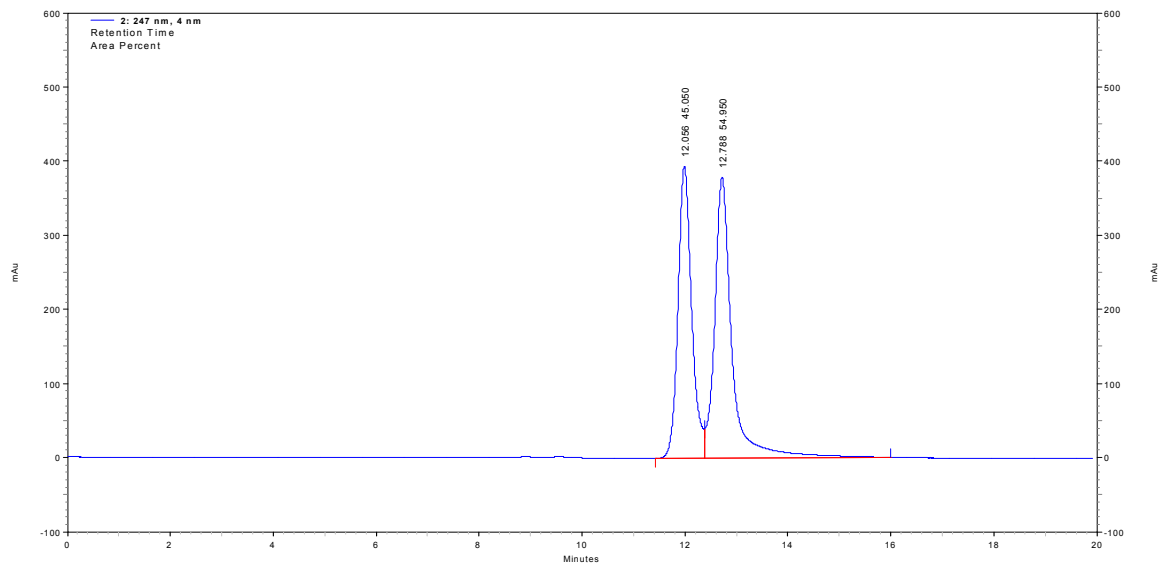
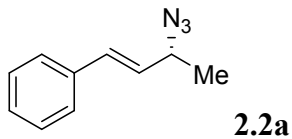
2.2s



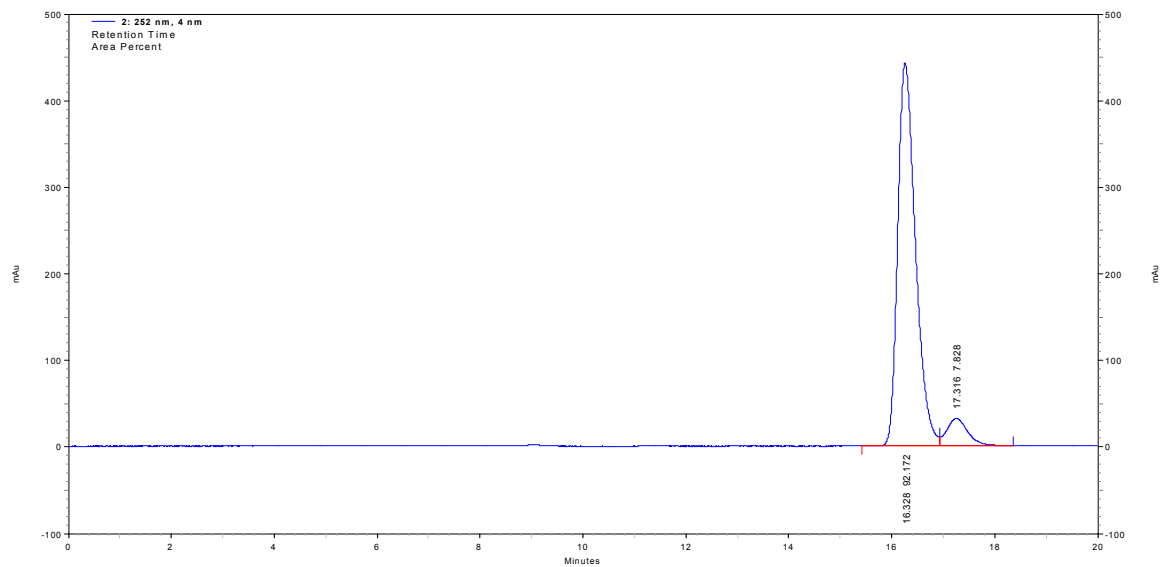
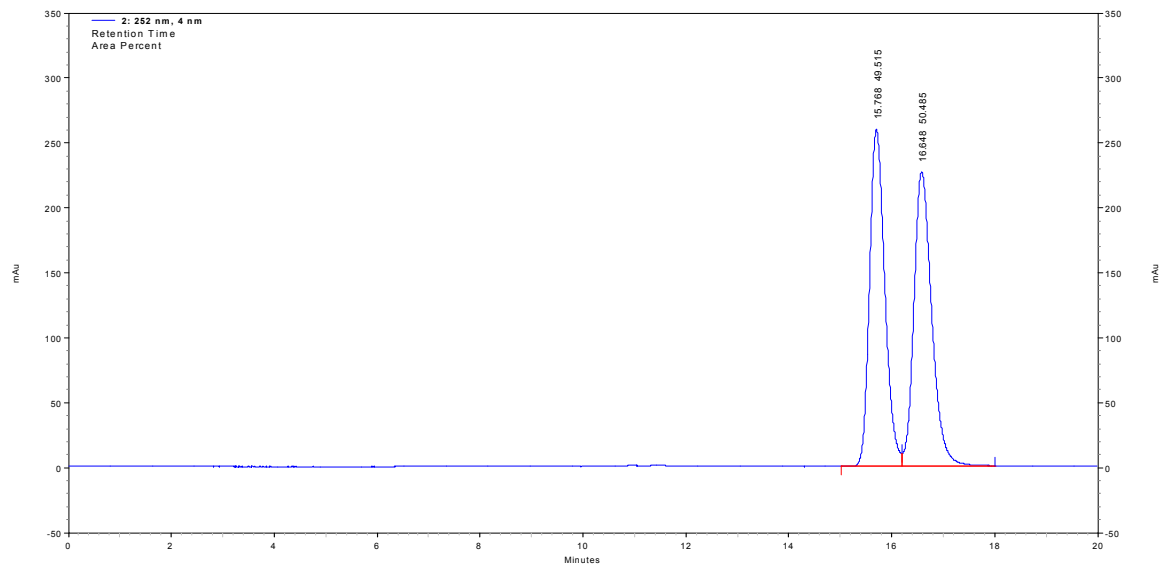
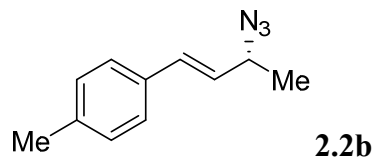
2.2t



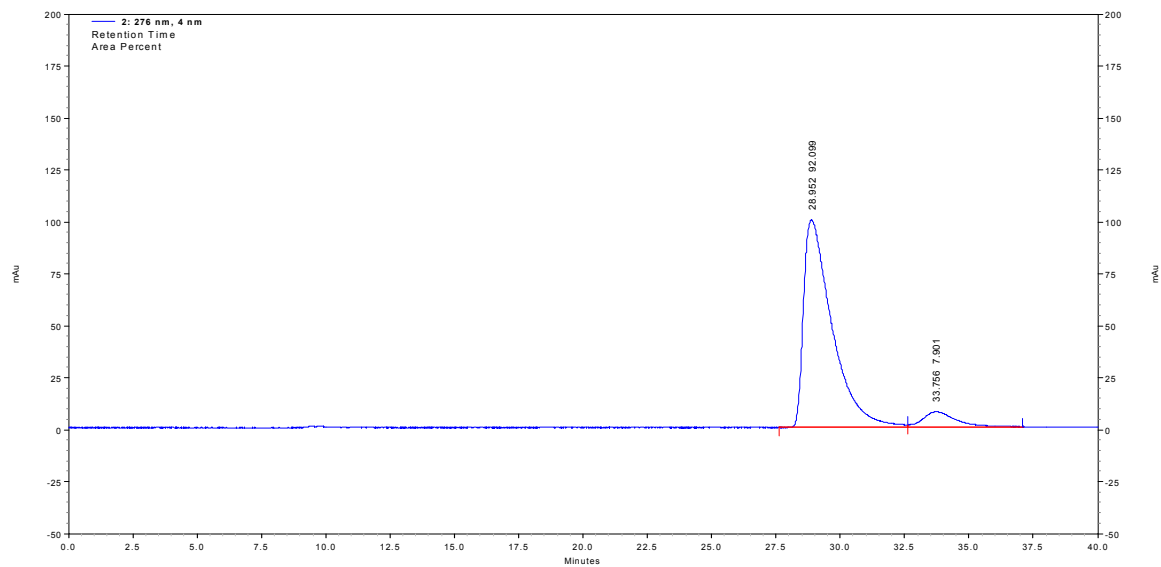
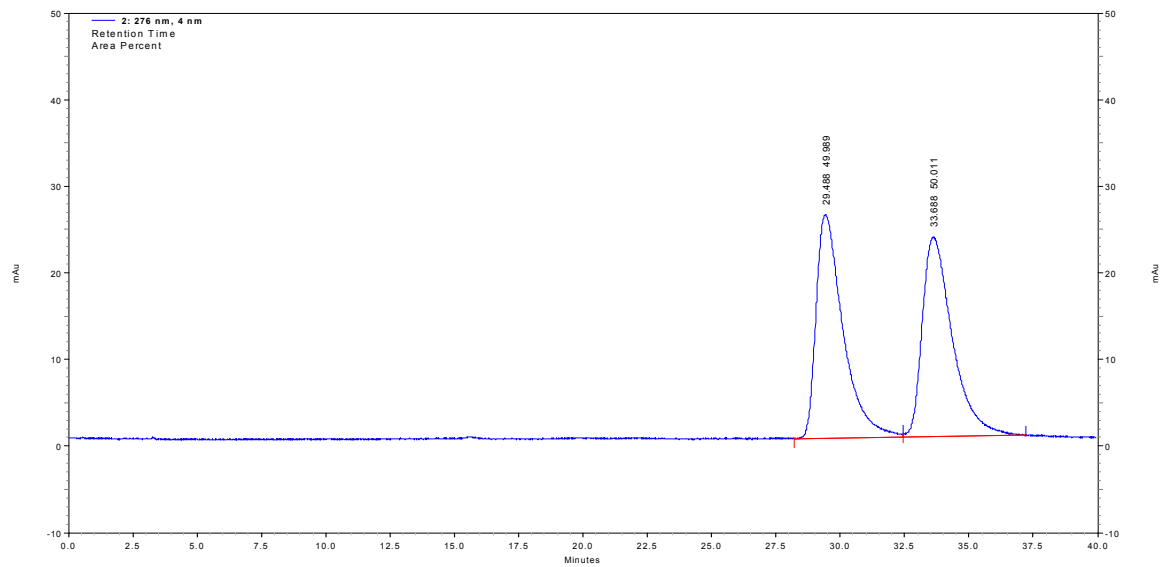
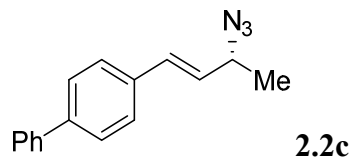
Appendix 2 - HPLC Traces



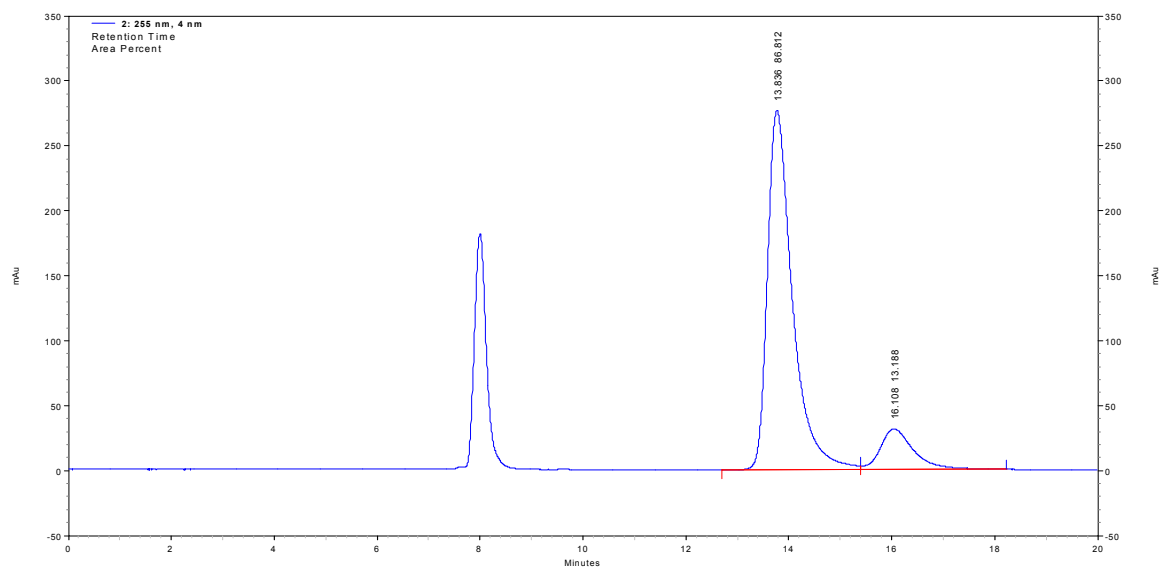
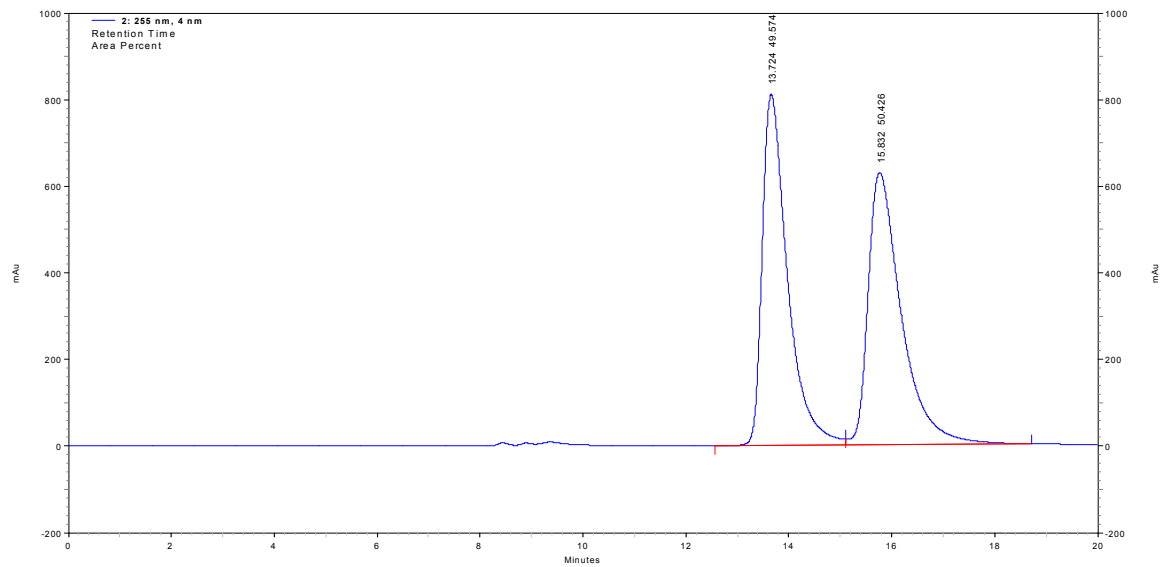
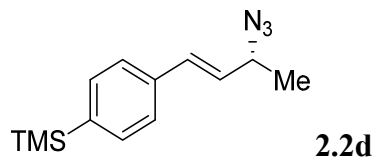
| Retention Time | Area Percent |
|----------------|--------------|
| 12.404 | 5.230 |
| 13.144 | 94.770 |



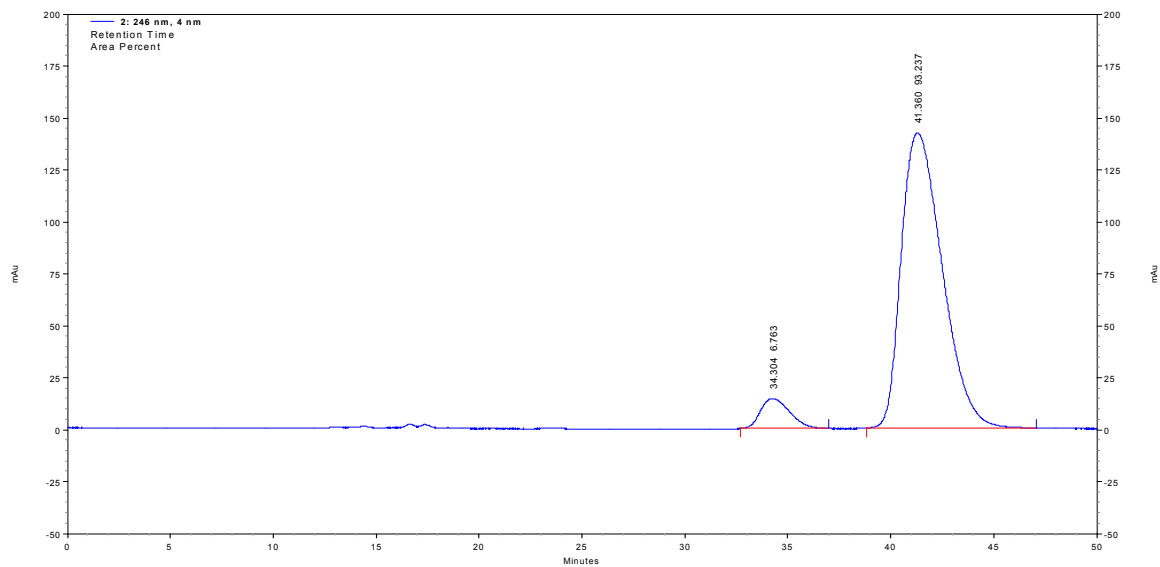
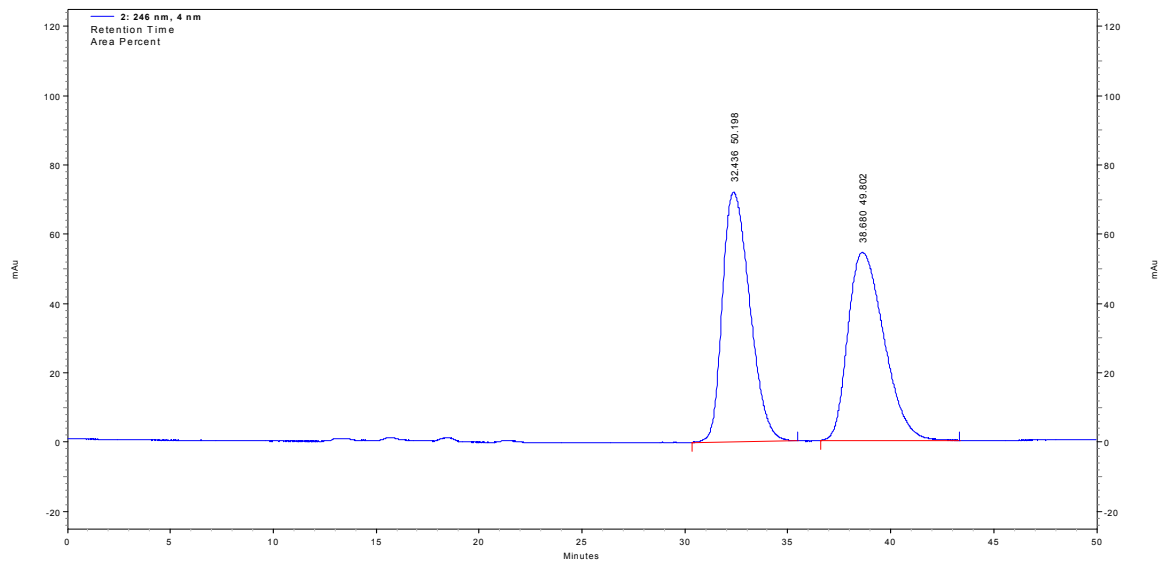
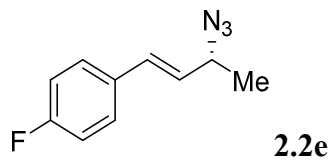
| 252 nm | |
|----------------|--------------|
| Retention Time | Area Percent |
| 16.328 | 92.172 |
| 17.316 | 7.828 |



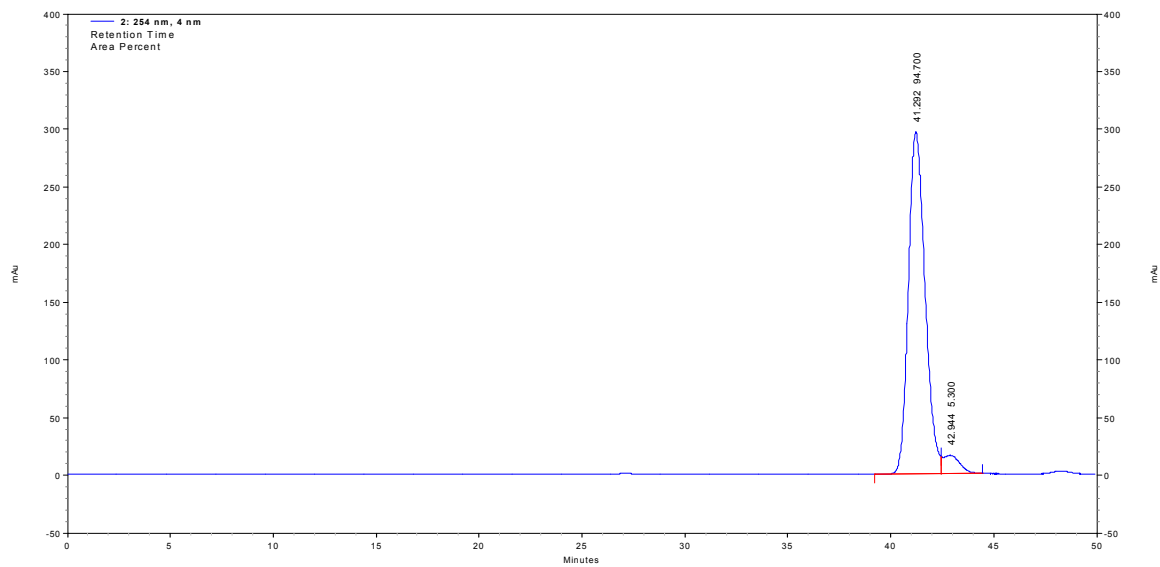
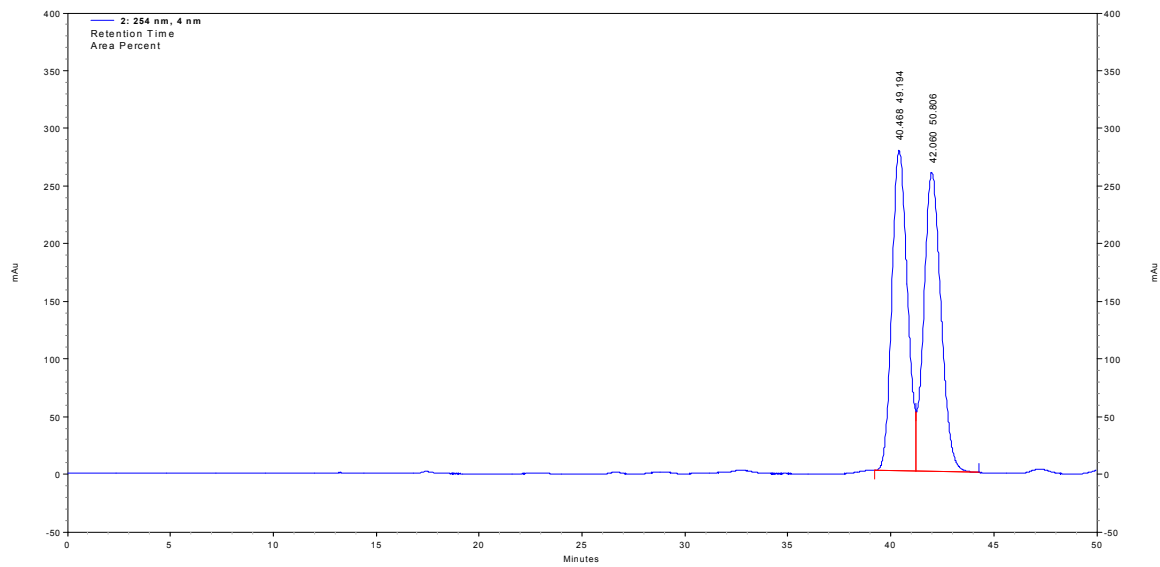
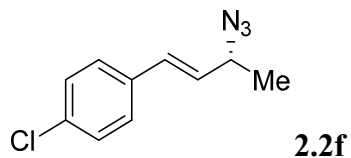
| Retention Time | Area Percent |
|----------------|--------------|
| 28.952 | 92.099 |
| 33.756 | 7.901 |



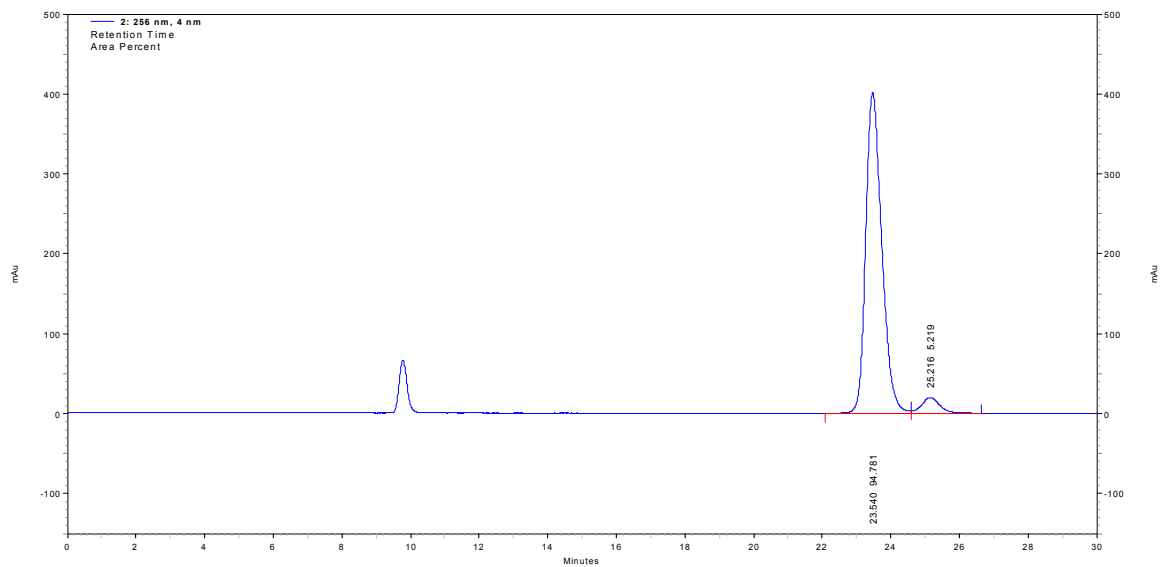
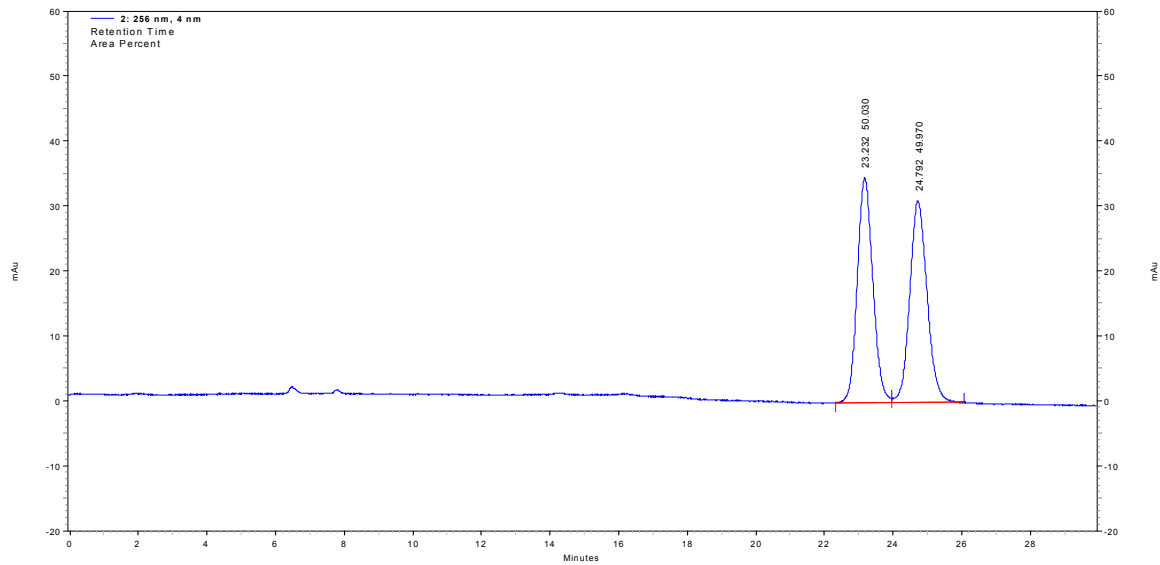
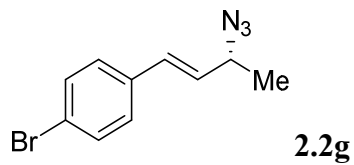
| 255 nm | |
|----------------|--------------|
| Retention Time | Area Percent |
| 13.836 | 86.812 |
| 16.108 | 13.188 |



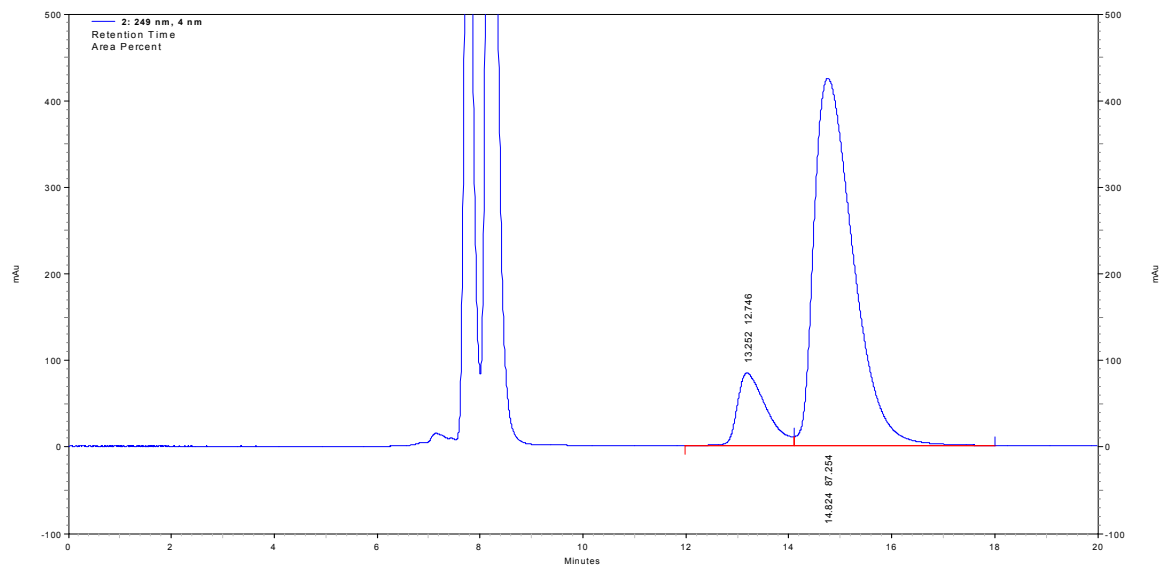
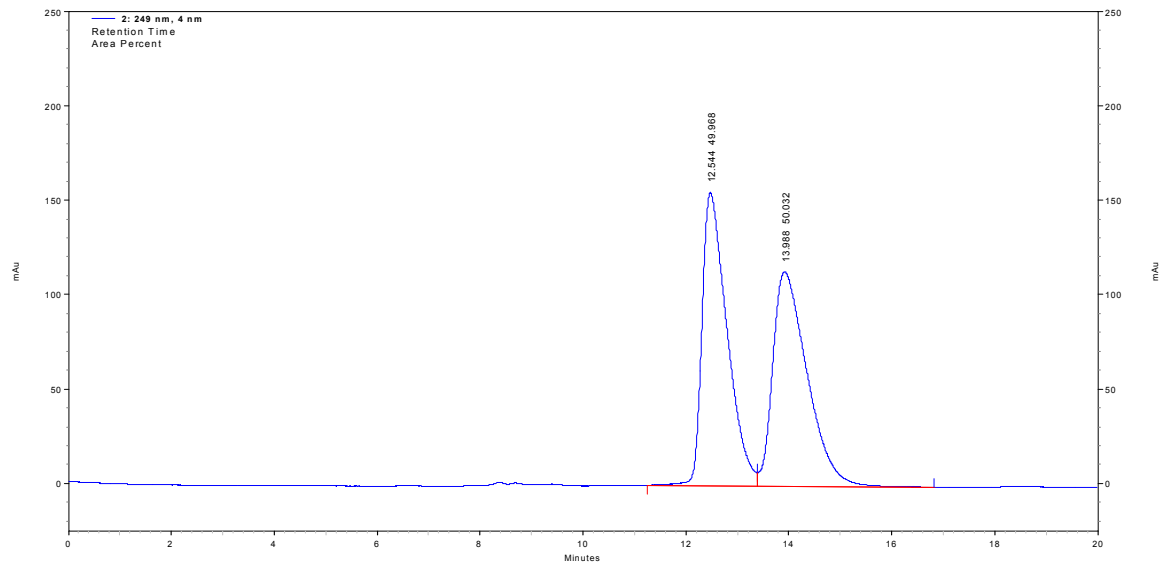
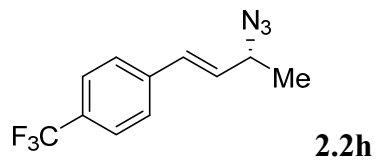
| 246 nm | |
|----------------|--------------|
| Retention Time | Area Percent |
| 34.304 | 6.763 |
| 41.360 | 93.237 |



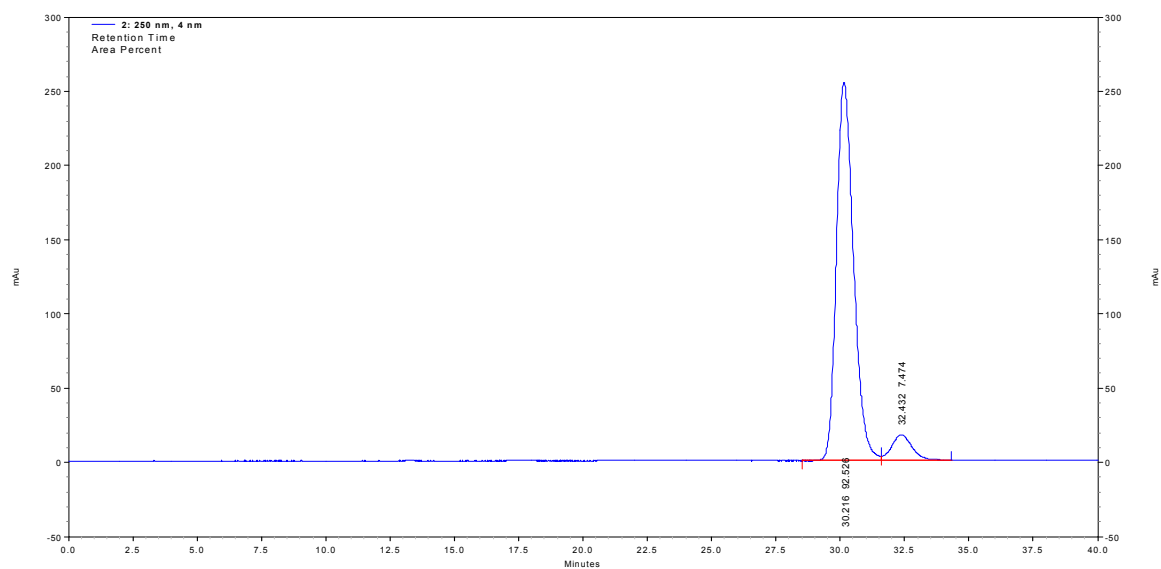
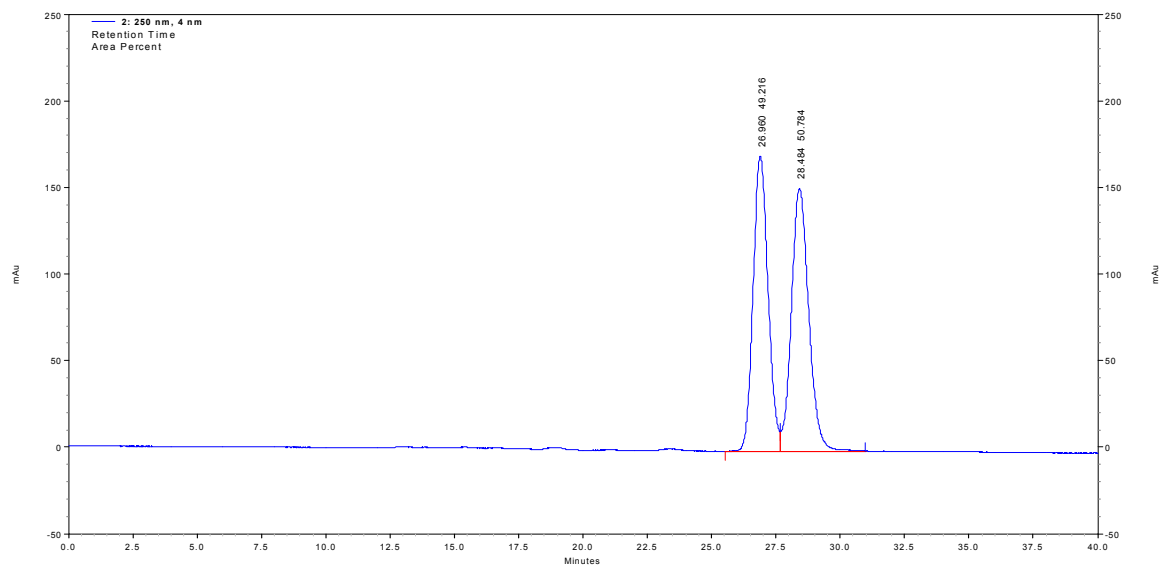
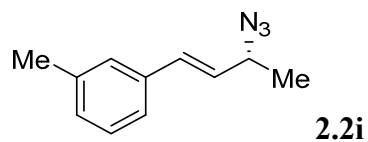
| 254 nm | |
|----------------|--------------|
| Retention Time | Area Percent |
| 41.292 | 94.700 |
| 42.944 | 5.300 |



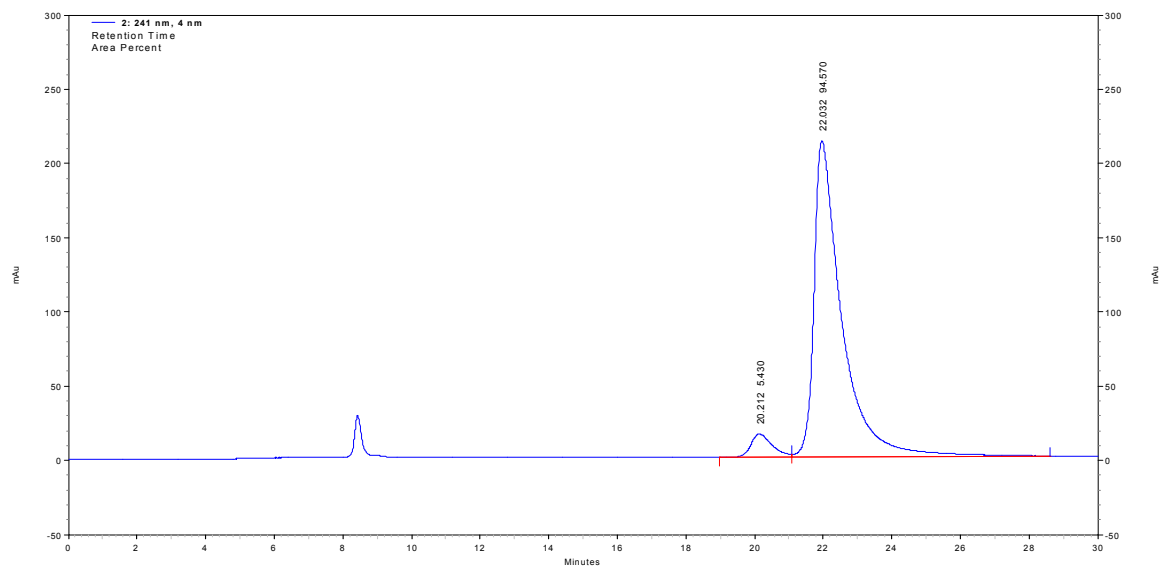
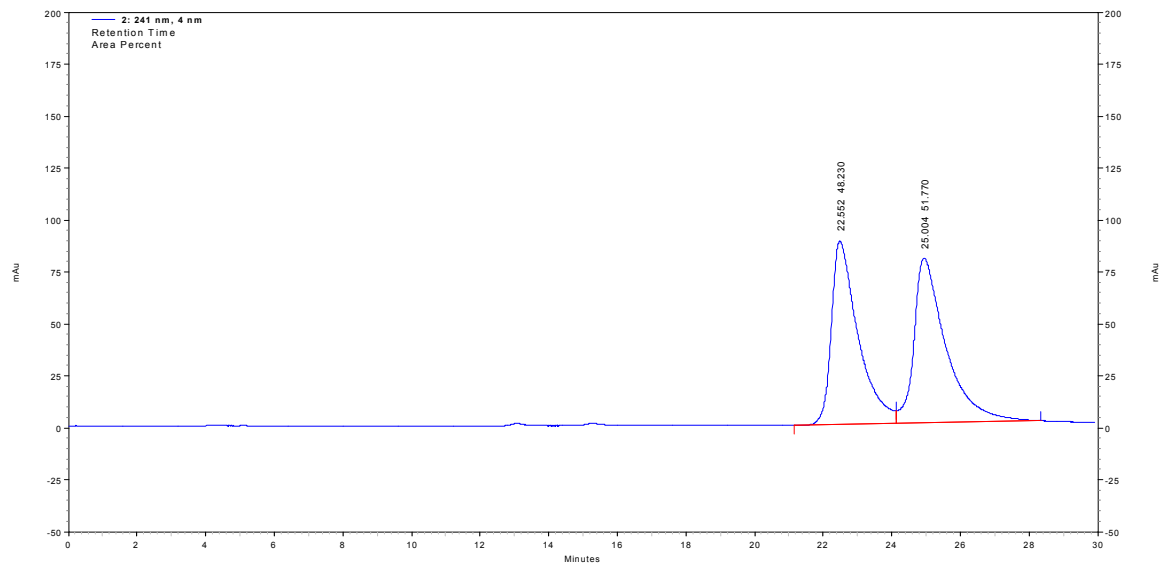
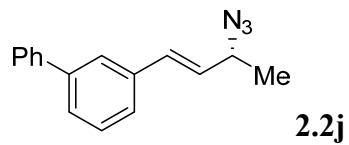
| 256 nm | Retention Time | Area Percent |
|--------|----------------|--------------|
| | 23.540 | 94.781 |
| | 25.216 | 5.219 |



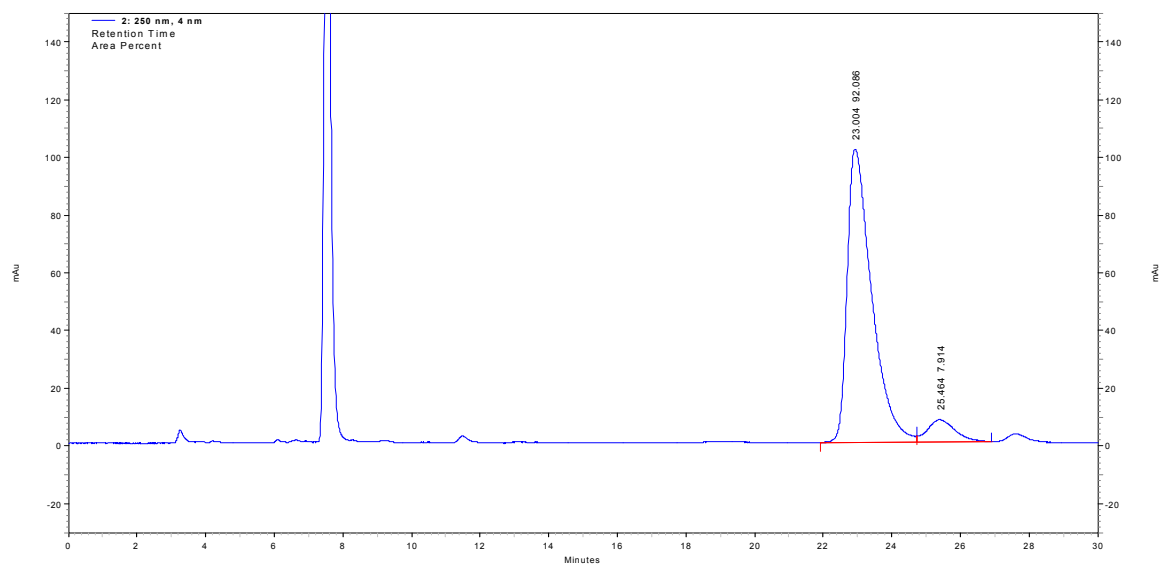
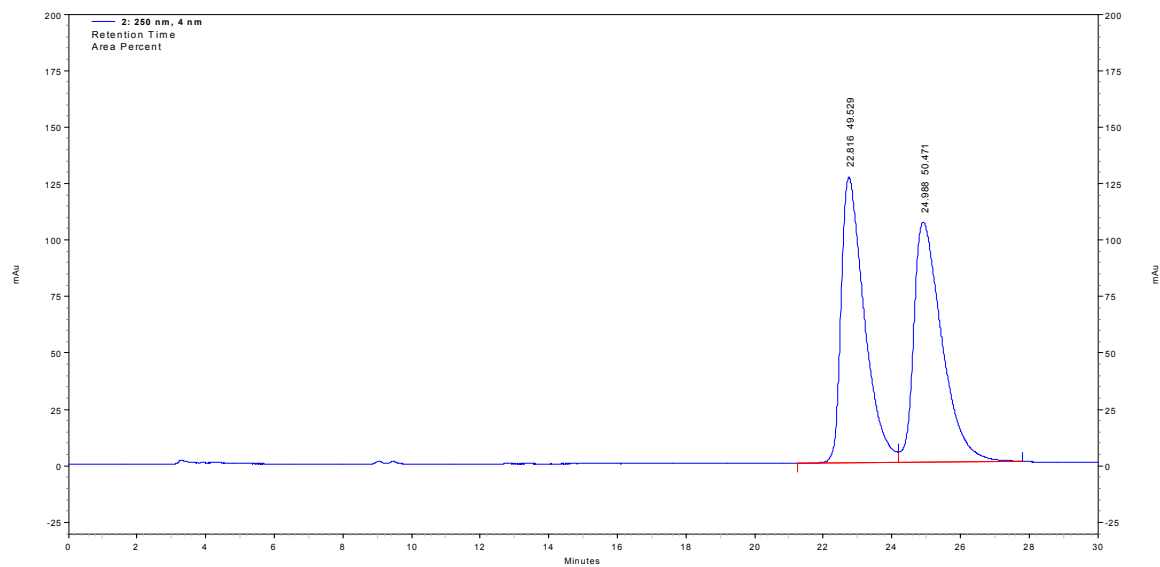
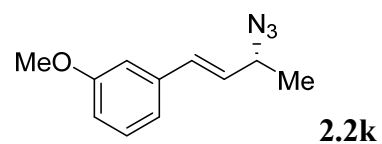
| 249 nm | |
|----------------|--------------|
| Retention Time | Area Percent |
| 13.252 | 12.746 |
| 14.824 | 87.254 |



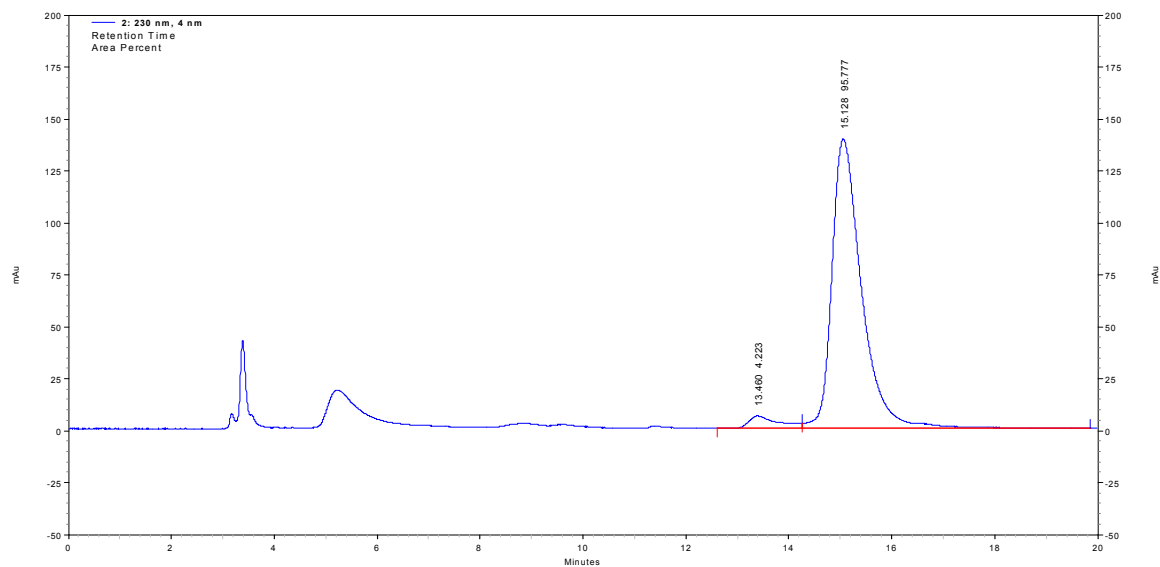
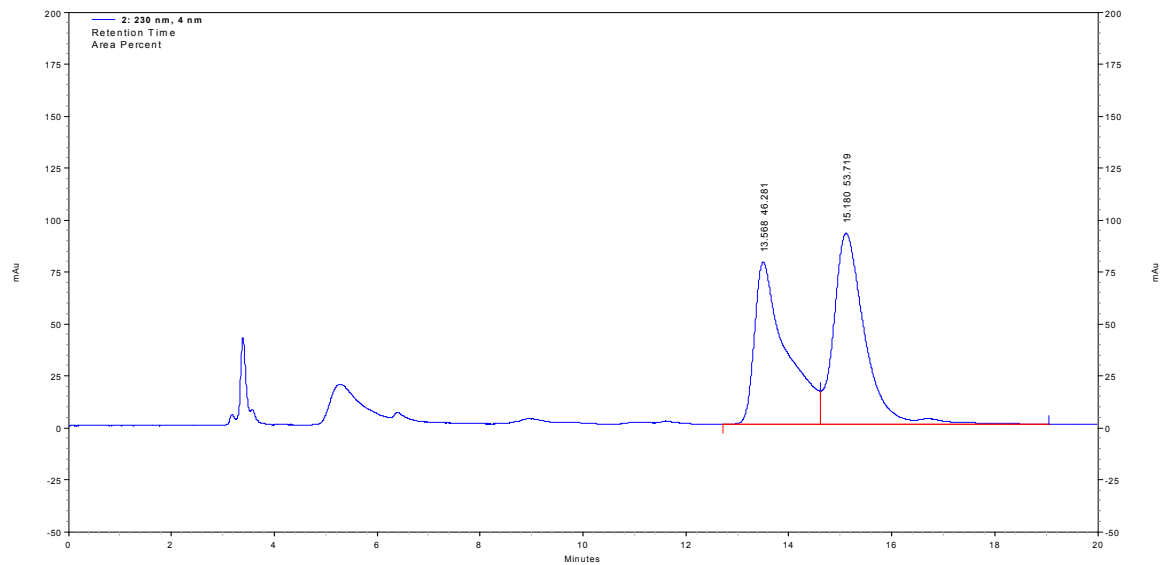
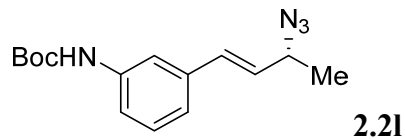
| Retention Time | Area Percent |
|----------------|--------------|
| 30.216 | 92.526 |
| 32.432 | 7.474 |



| Retention Time | Area Percent |
|----------------|--------------|
| 20.212 | 5.430 |
| 22.032 | 94.570 |



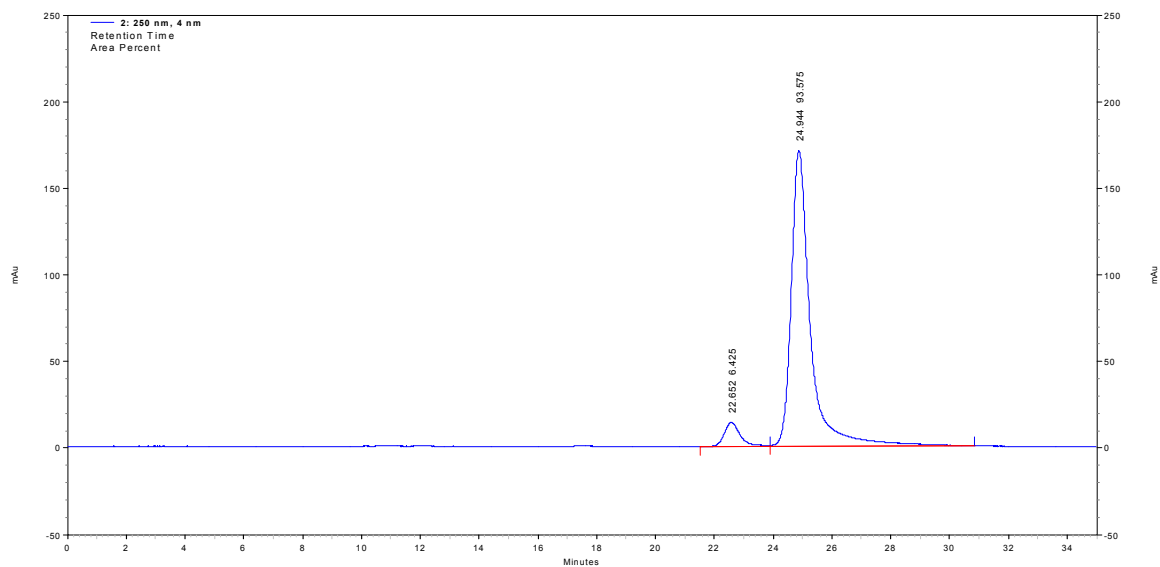
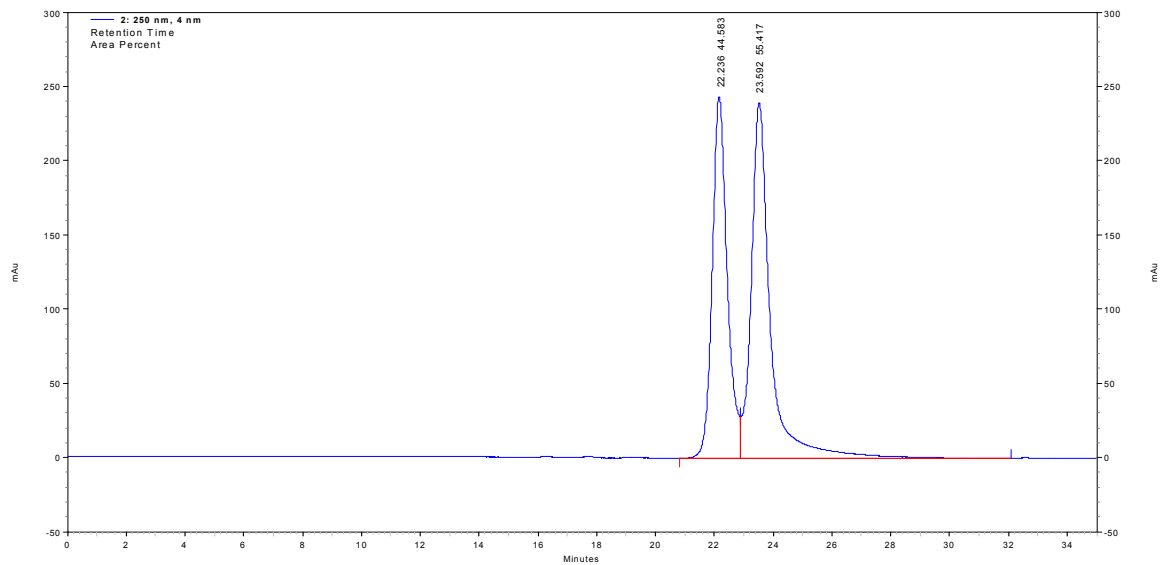
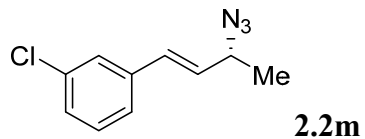
| Retention Time | Area Percent |
|----------------|--------------|
| 23.004 | 92.086 |
| 25.464 | 7.914 |



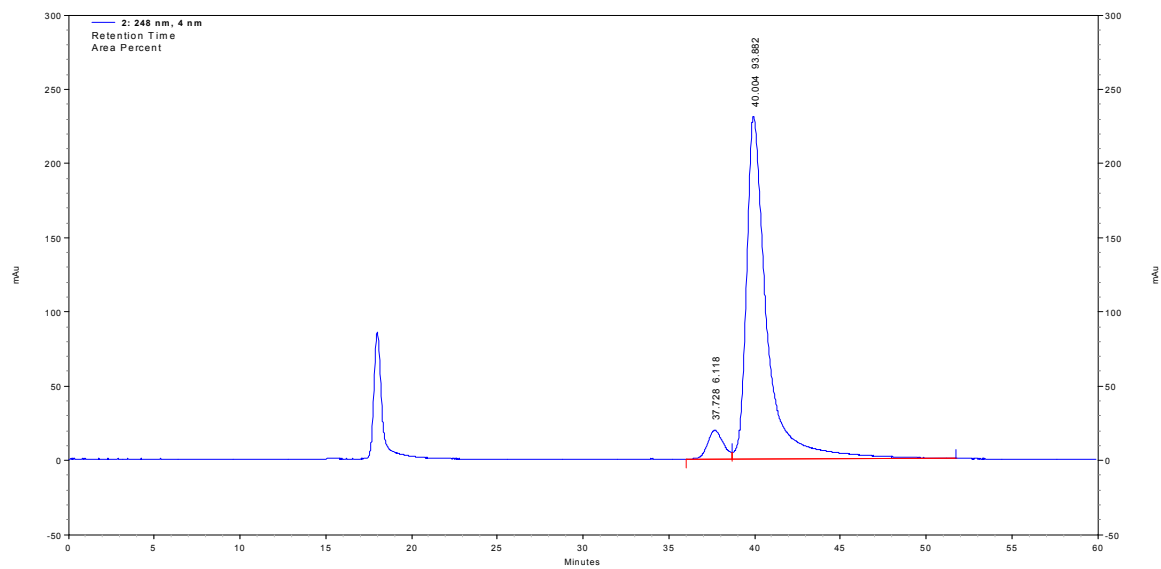
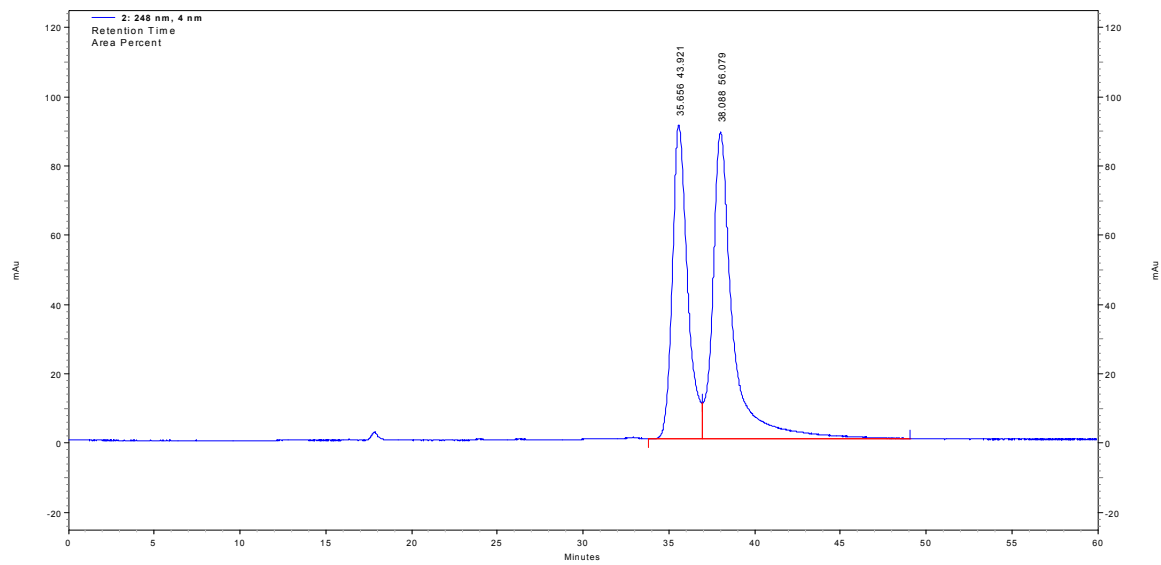
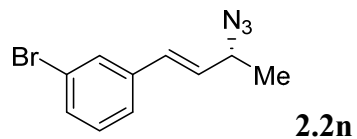
230 nm

Retention Time Area Percent

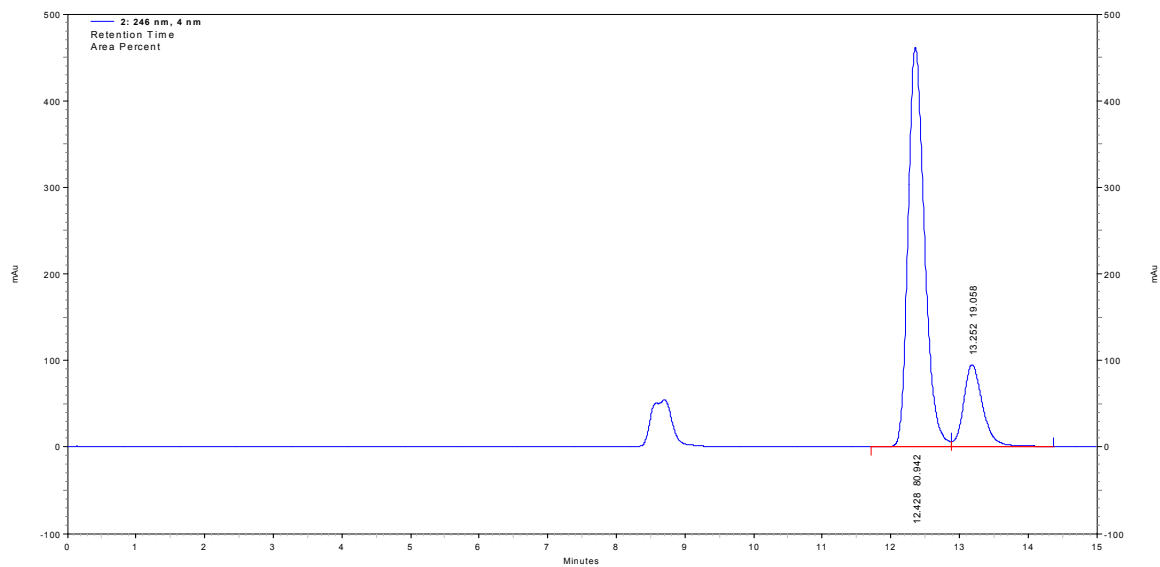
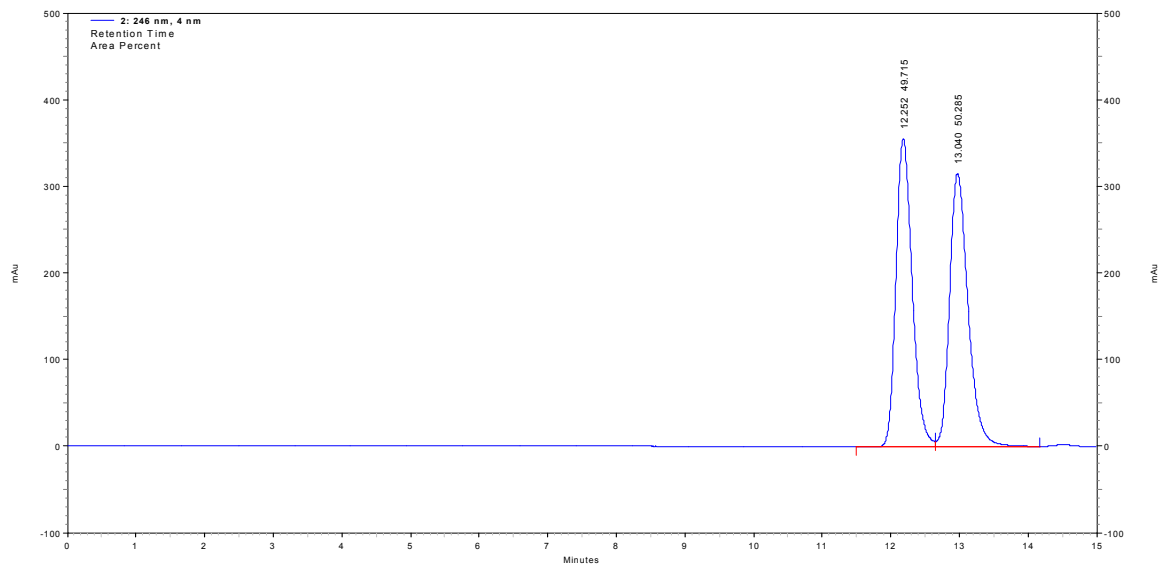
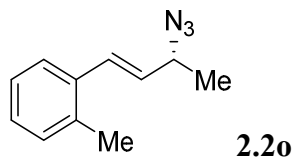
| | |
|--------|--------|
| 13.460 | 4.223 |
| 15.128 | 95.777 |



| Retention Time | Area Percent |
|----------------|--------------|
| 22.652 | 6.425 |
| 24.944 | 93.575 |



| Retention Time | Area Percent |
|----------------|--------------|
| 37.728 | 6.118 |
| 40.004 | 93.882 |



246 nm

Retention Time

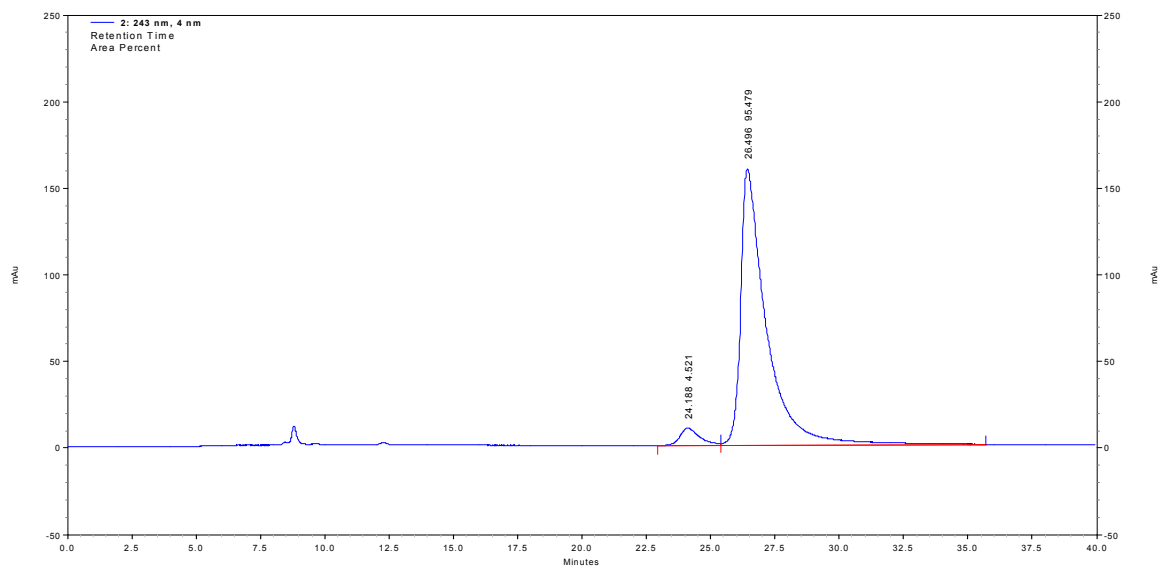
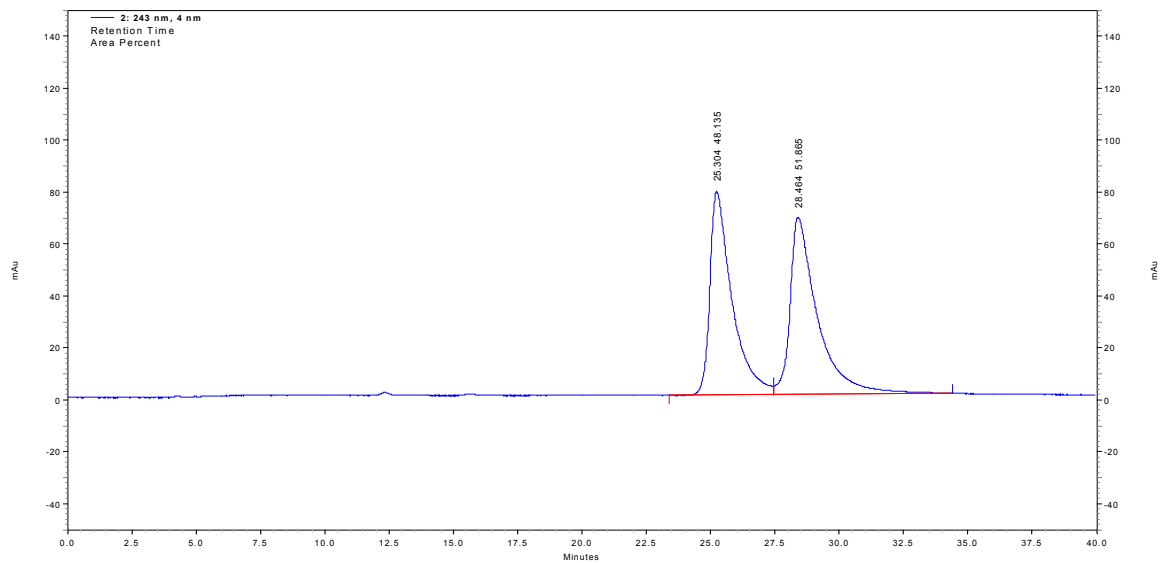
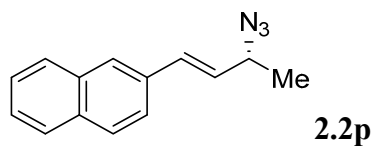
Area Percent

12.428

80.942

13.252

19.058



243 nm

Retention Time

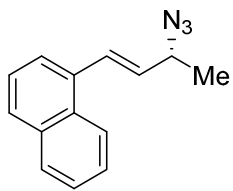
Area Percent

24.188

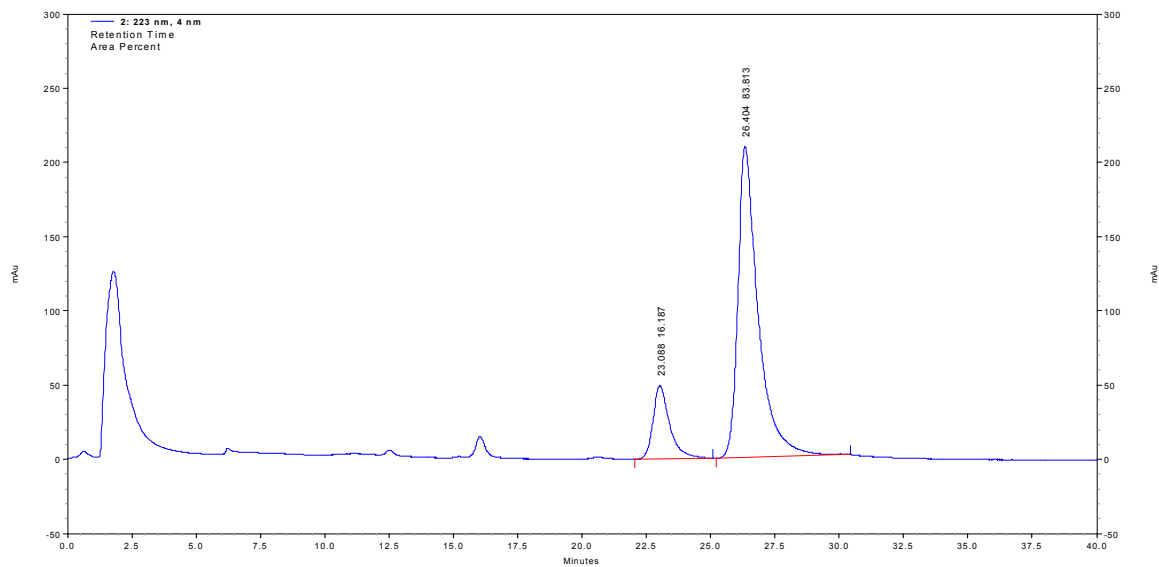
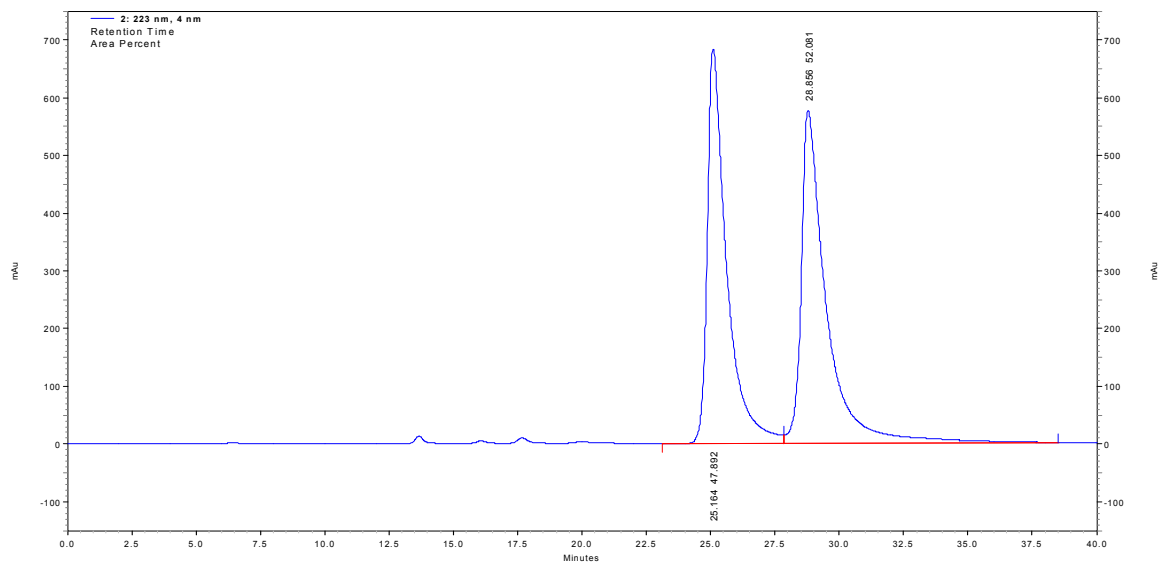
4.521

26.496

95.479



2.2q



223 nm

Retention Time

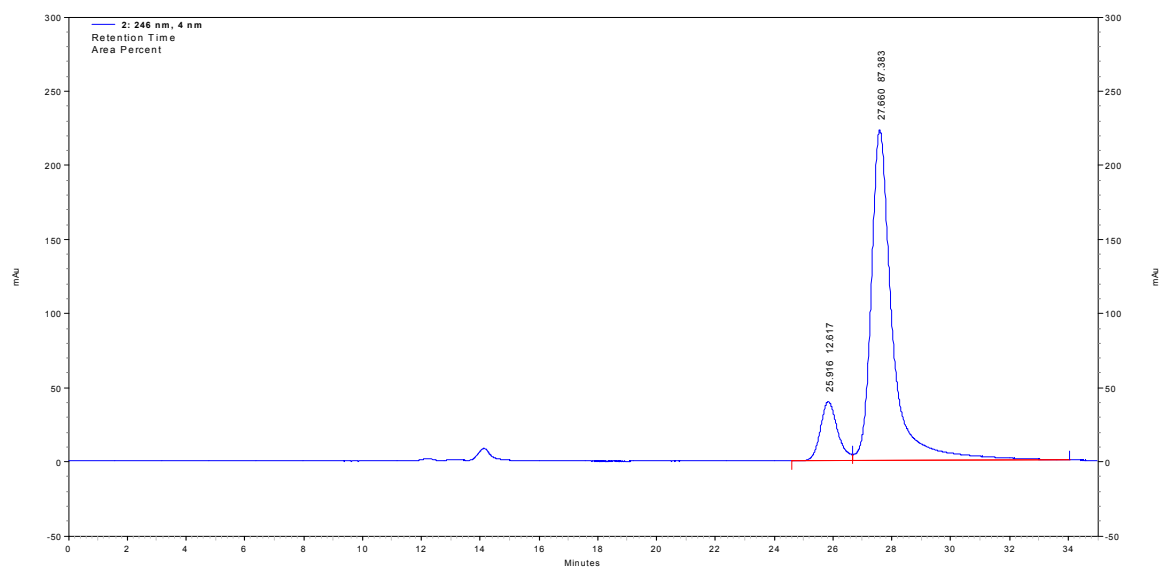
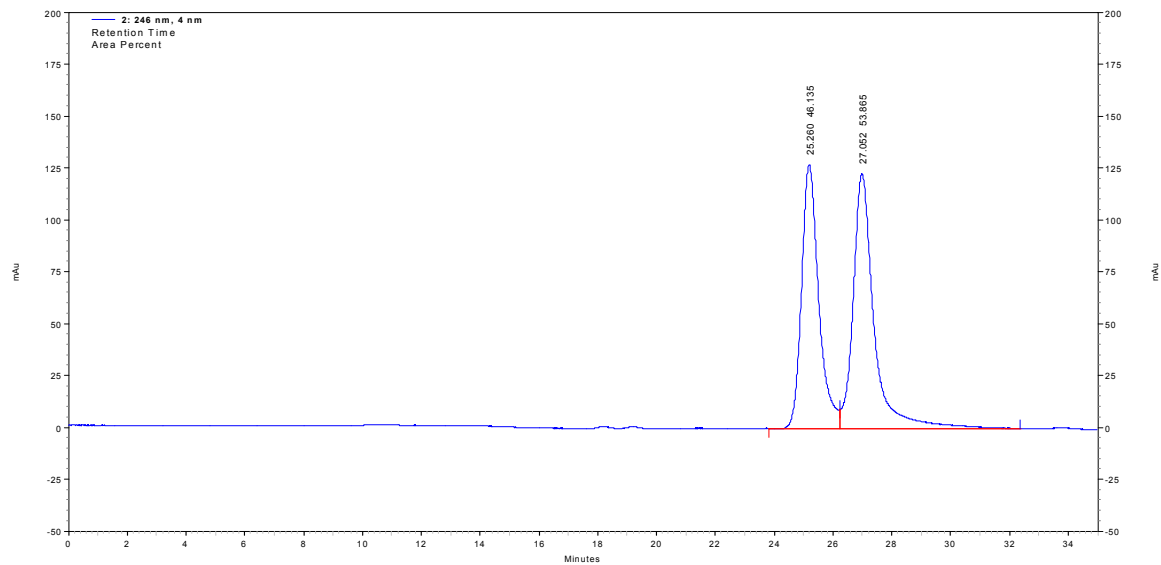
Area Percent

23.088

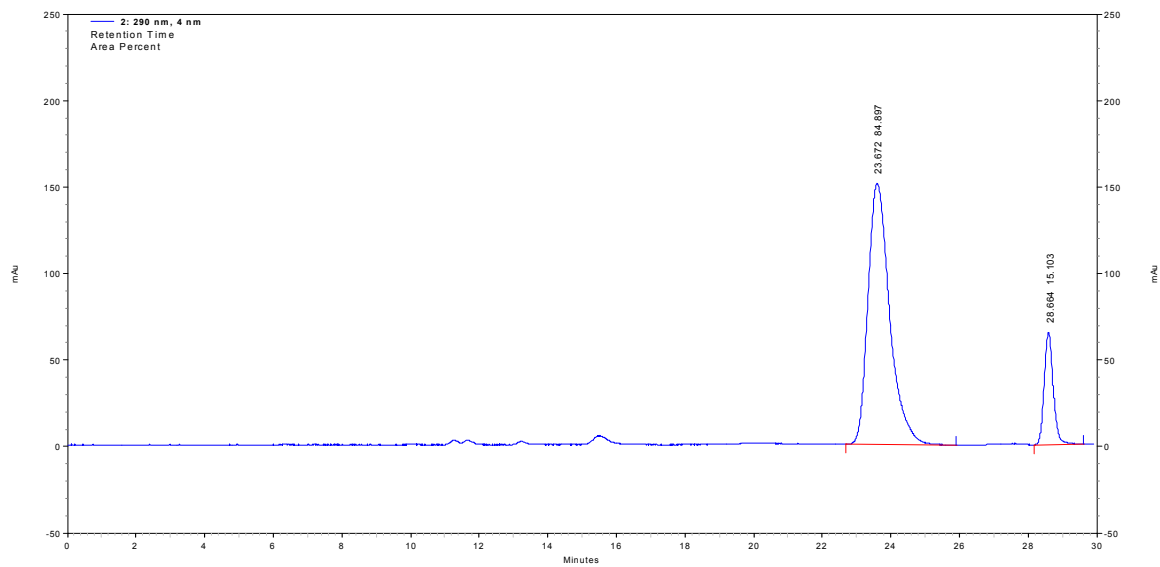
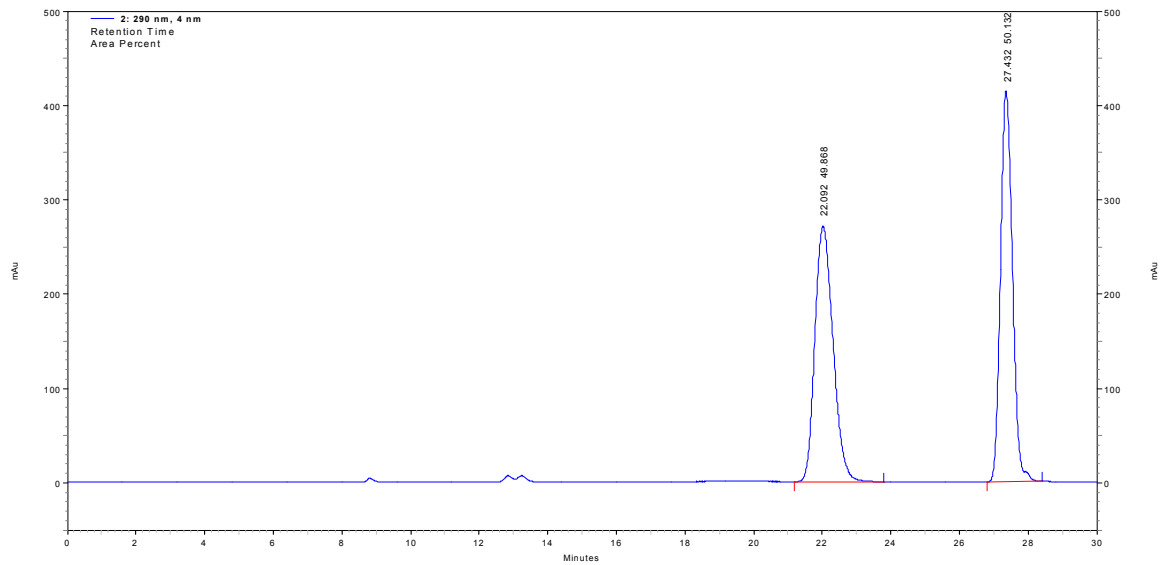
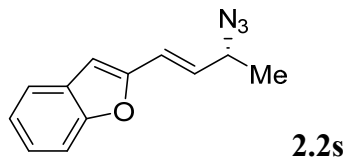
16.187

26.404

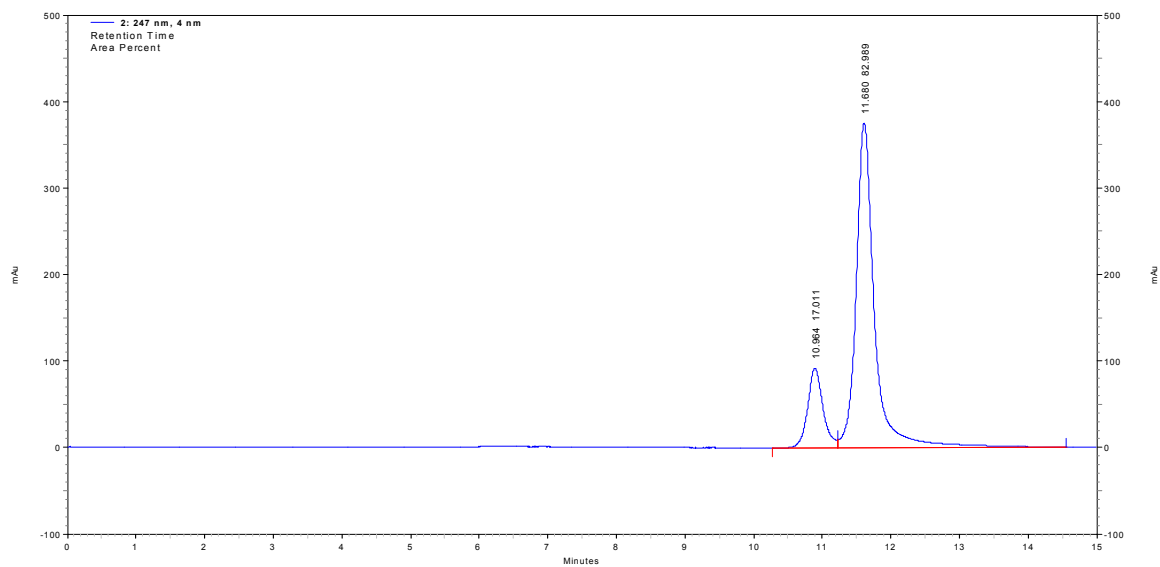
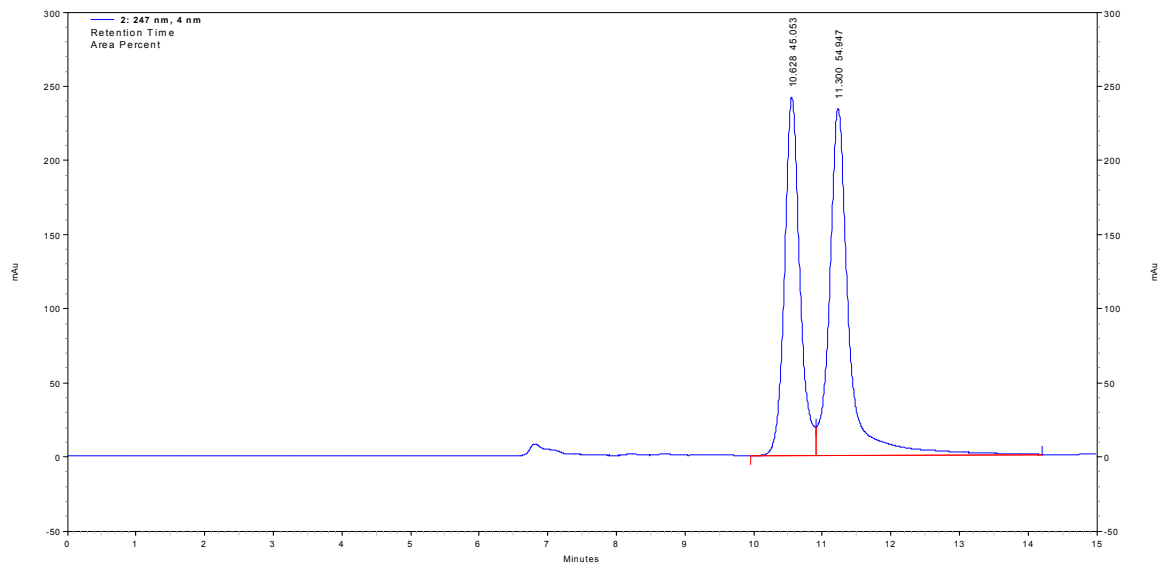
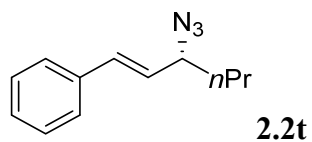
83.813



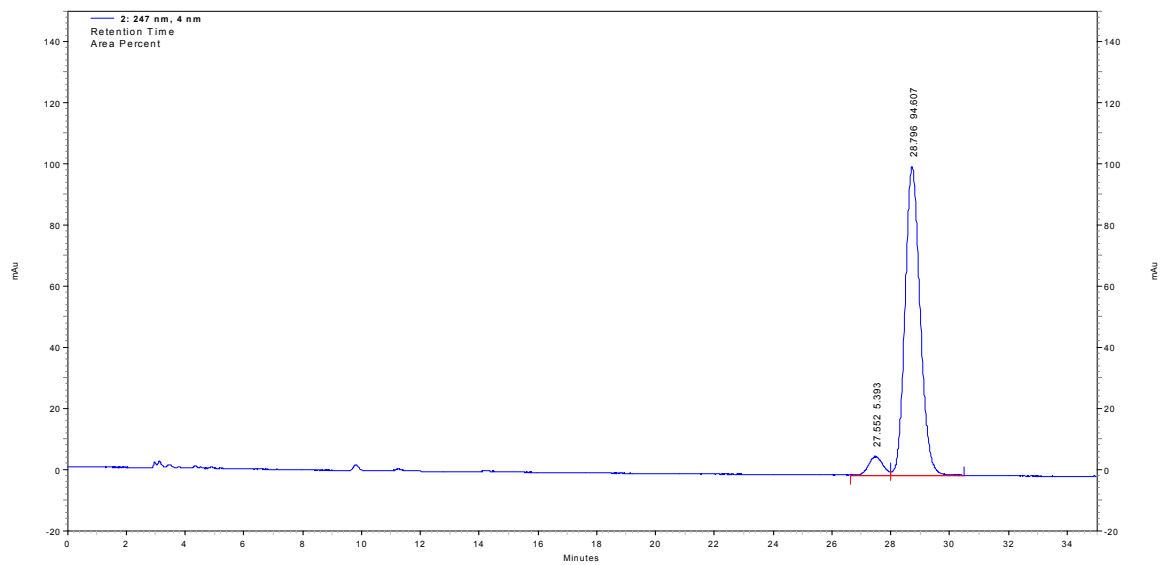
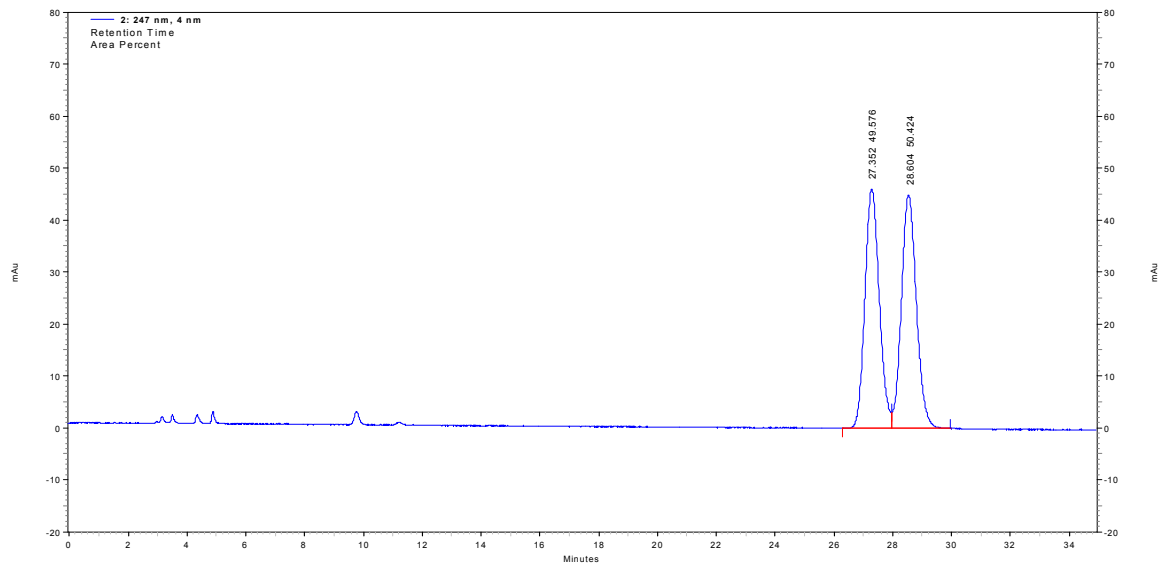
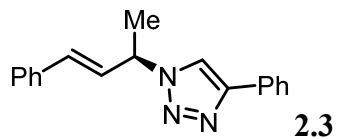
| Retention Time | Area Percent |
|----------------|--------------|
| 25.916 | 12.617 |
| 27.660 | 87.383 |



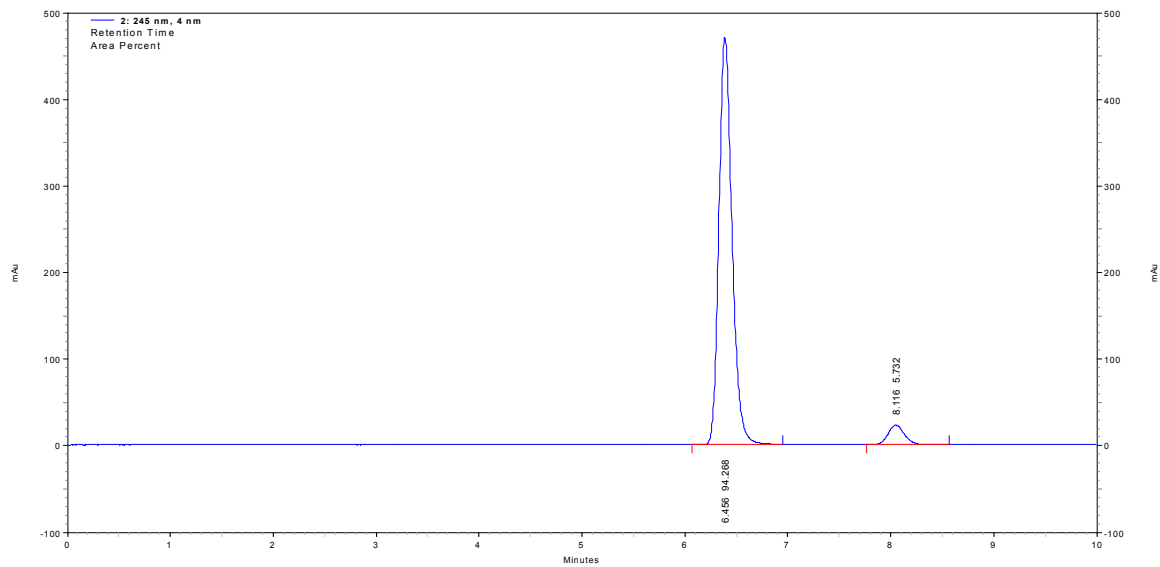
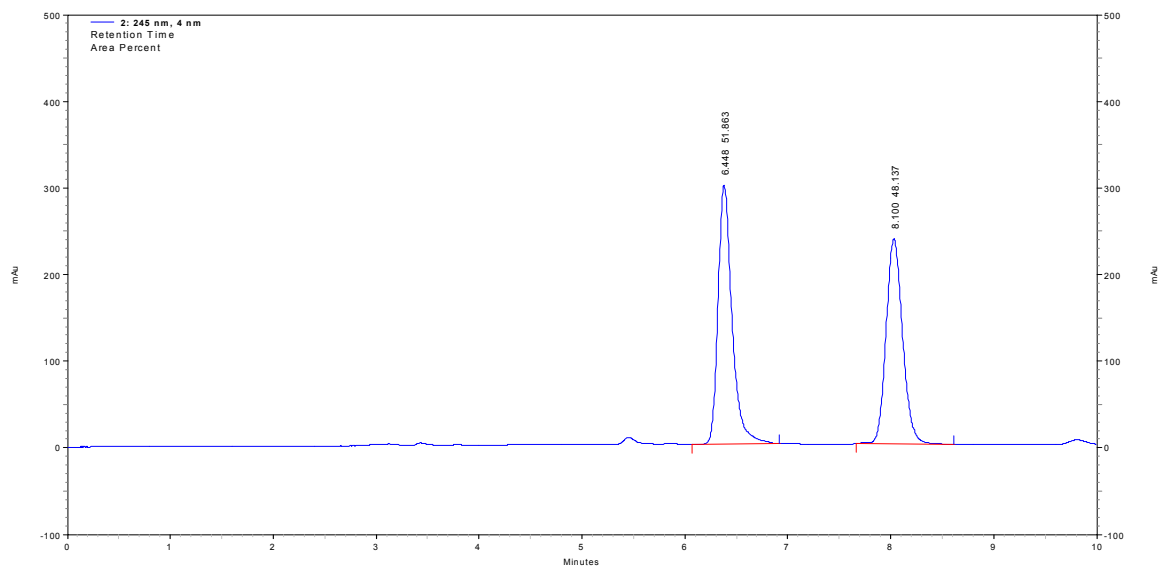
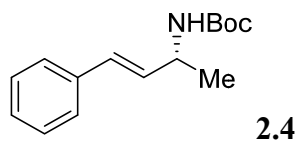
| 290 nm Retention Time | Area Percent |
|--------------------------|--------------|
| 23.672 | 84.897 |
| 28.664 | 15.103 |



| Retention Time | Area Percent |
|----------------|--------------|
| 10.964 | 17.011 |
| 11.680 | 82.989 |



| Retention Time | Area Percent |
|----------------|--------------|
| 27.552 | 5.393 |
| 28.796 | 94.607 |



| Retention Time | Area Percent |
|----------------|--------------|
| 6.456 | 94.268 |
| 8.116 | 5.732 |

Chapter 3. Enantioselective Hydroamination of Allenes

This work has been published in D. A. Khrakovsky, C. Tao, M. W. Johnson, R. T. Thornbury, S. L. Shevick, F. D. Toste, *Angew. Chem. Int. Ed.* **2016**, *55*, 6079–6083.¹

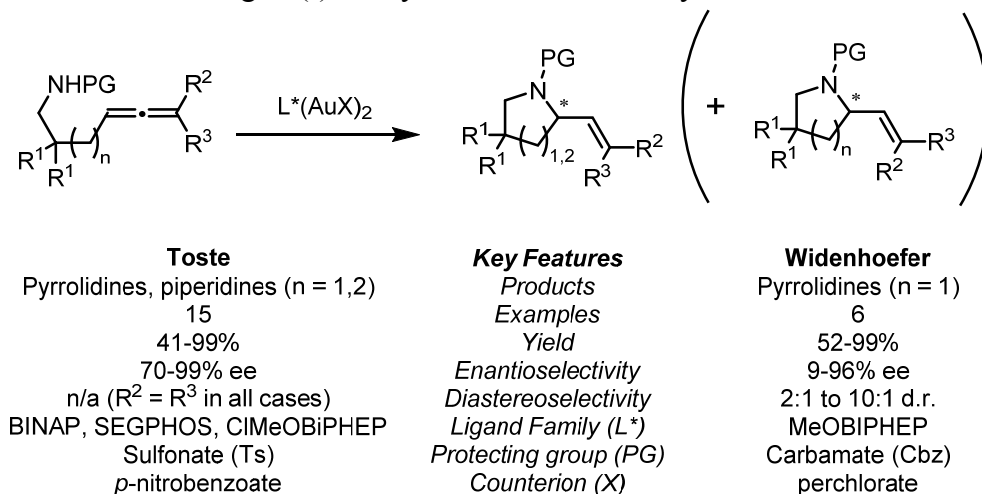
¹ Dr. Christian N. Kuzniewski performed the initial reactions.

Introduction

Enantioselective hydroamination is a powerful, atom-economical reaction for generating chiral amines using ubiquitous carbon-carbon unsaturated bonds. Gold catalysis is uniquely suited for enabling this reactivity *via* activation of the π -system towards nucleophilic attack by the amine moiety. This introduction will focus on the applications of enantioselective gold(I) catalysis to this reaction manifold. Related cascade reactions in which an achiral gold catalyst is paired with a chiral organocatalyst (typically a chiral phosphoric acid,¹⁻⁷ urea,^{8,9} or cinchona alkaloid¹⁰), represent a potent alternative strategy, but will not be discussed. Additionally, a more general perspective¹¹ on asymmetric hydroamination and a review of applications to total synthesis¹² are both recommended to the reader.

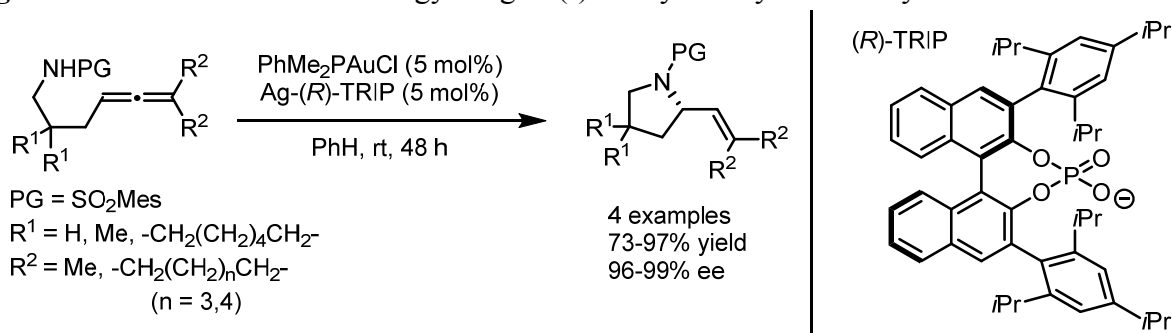
In 2007, Toste and coworkers reported the first enantioselective gold(I)-catalyzed hydroamination reaction.¹³ The substrate scope was limited to trisubstituted symmetrical allenes with tethered nucleophiles, but high yields and excellent enantioselectivities (up to 99% ee) were observed in the formation of chiral pyrrolidines and piperidines (Figure 3.1, bottom left). Later that year, Widenhofer and colleagues extended this intramolecular reaction to trisubstituted unsymmetrical allenes,¹⁴ thereby achieving a dynamic kinetic enantioselective transformation. The authors reported good yields and enantioselectivities (up to 96% ee), albeit with low to moderate diastereoselectivities (Figure 3.1, bottom right). In both cases, axially chiral diphosphine ligands enabled the high levels of enantioselectivity.

Figure 3.1 Enantioselective gold(I)-catalyzed intramolecular hydroaminations of allenes



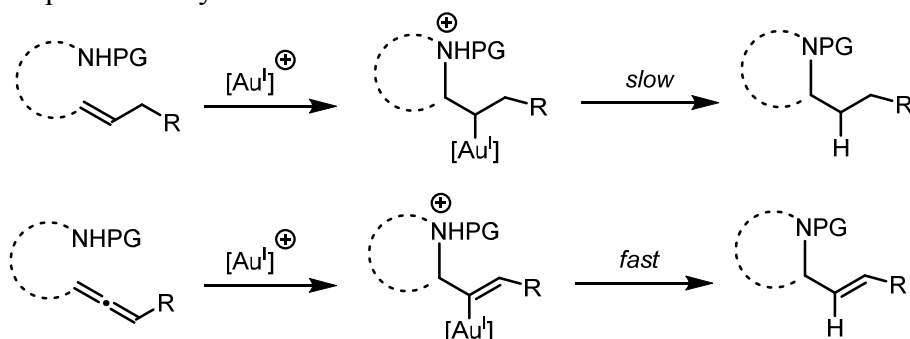
Around the same time, a very different approach to asymmetric hydroamination was also disclosed by researchers in the Toste group.¹⁵ The authors demonstrated the use of an achiral gold(I) complex in combination with a silver salt bearing a chiral phosphate counterion derived from BINOL to achieve enantioselectivity (Figure 3.2). The use of a non-polar solvent (benzene) was critical for optimization of the reaction, as the formation of a tight ion pair between the source of chirality (TRIP anion) and the site of reactivity (cationic gold center) proved imperative for efficient stereoinduction. This chiral counterion strategy was also applied to related hydroalkoxylation and hydrocarboxylation reactions.

Figure 3.2 Chiral counterion strategy for gold(I)-catalyzed asymmetric hydroamination



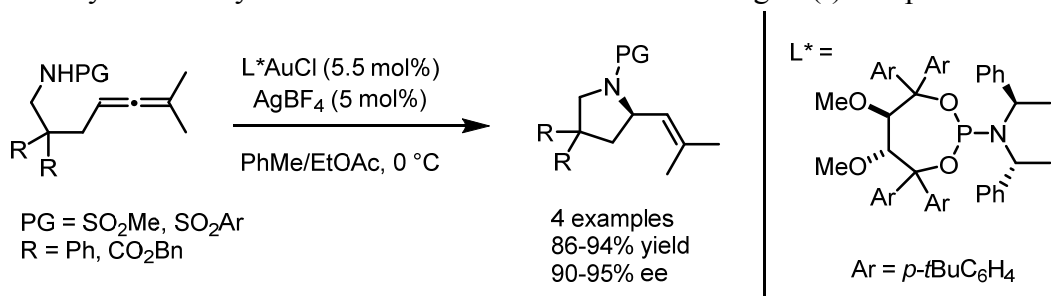
These seminal reports established enantioselective hydroamination of allenes as a benchmark reaction in asymmetric gold(I) catalysis. The related hydroamination of alkenes has also been explored,^{16–21} although these reactions typically exhibit lower enantioselectivities due to the requirement of higher reaction temperatures. This is a consequence of the lower kinetic basicity of alkyl-gold (sp³) intermediates compared to vinyl-gold (sp²) species,²² which manifests in a slower rate of protodeauration for the former relative to the latter (Figure 3.3).

Figure 3.3 Comparison of hydroamination of alkenes and allenes



Besides axially chiral diphosphines, several other ligand classes have been shown to induce enantioselectivity in gold(I)-catalyzed hydroaminations of allenes.²³ Researchers in the Fürstner group applied their acyclic TADDOL-related ligands to the transformation (Figure 3.4).²⁴ Related asymmetric hydrofunctionalization reactions, including hydroarylation and hydroalkoxylation, were also demonstrated with this class of gold(I) complexes.

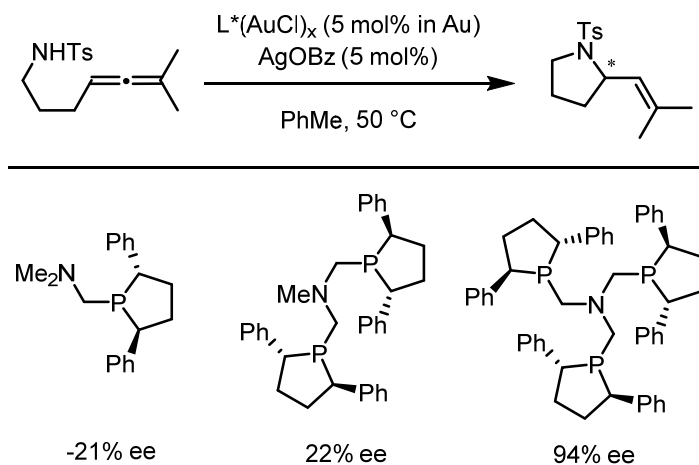
Figure 3.4 Asymmetric hydroamination with a TADDOL-related gold(I) complex



Gade and coworkers investigated chiral mono-, bi-, and tridentate phospholane ligands—originally applied to rhodium-catalyzed hydrogenations²⁵—in the gold-catalyzed hydroamination

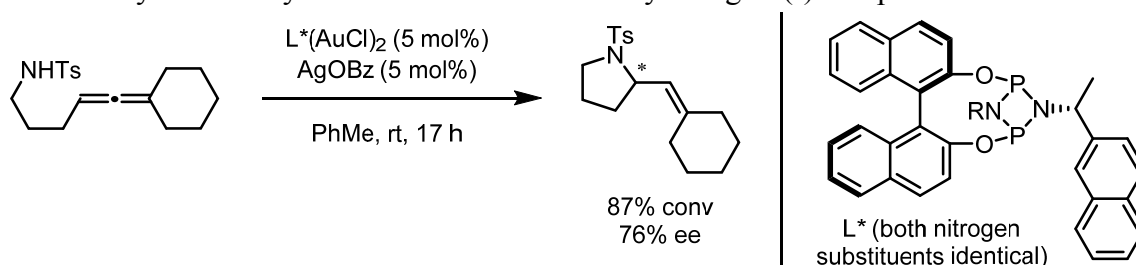
manifold.²⁶ Interestingly, these ligands displayed increasing enantioselectivity corresponding to their increased nuclearity (Figure 3.5).

Figure 3.5 Asymmetric hydroamination with mono-, bi-, and tridentate phospholane gold(I) complexes



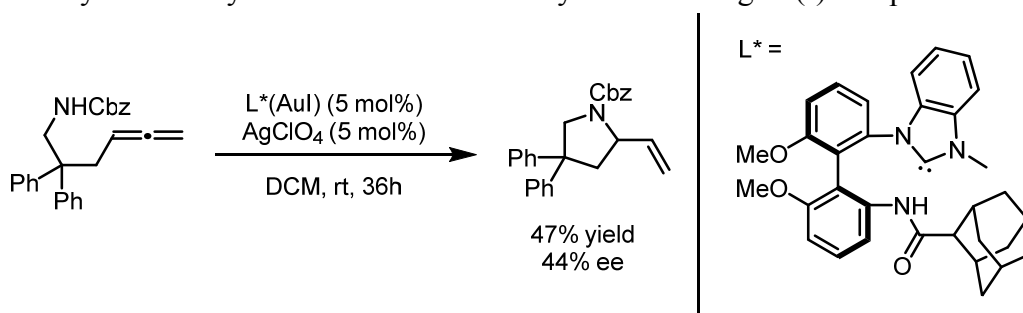
The Gade group has also synthesized a series of novel cyclophosphazane (CycloP) ligands derived from axially chiral diols.²⁷ A survey of these ligands in gold(I)-catalyzed hydroamination revealed that one variant afforded promising levels of enantioselectivity (Figure 3.6).

Figure 3.6 Asymmetric hydroamination with chiral CycloP gold(I) complex



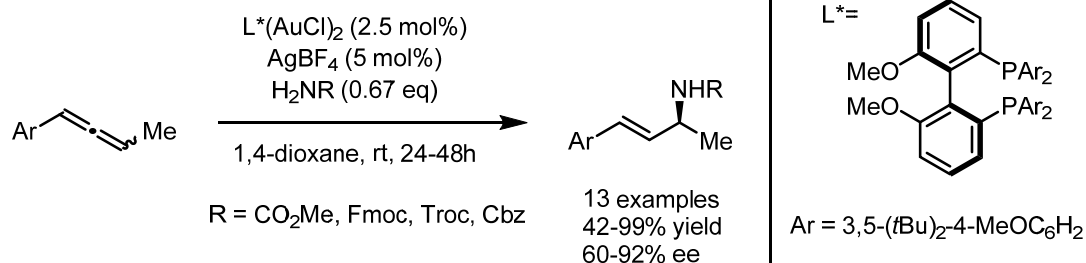
Mirroring the general trend in asymmetric gold(I) catalysis, there is a striking lack of chiral carbene ligands demonstrated to be effective in asymmetric hydroamination. Shi and coworkers reported such complexes derived from axially chiral 2,2'-dimethoxy-1,1'-biphenyl scaffolds,²⁸ but even with a bulky adamantyl substituent, the best reported ee value was still far from synthetically useful (Figure 3.7).

Figure 3.7 Asymmetric hydroamination with axially chiral NHC gold(I) complex



All the examples so far are intramolecular hydroaminations, which rely on allene substrates with tethered nitrogen residues to facilitate a large effective concentration of nucleophile. Only one report in the literature from Widenhoefer and coworkers has tackled the more difficult intermolecular variant (Figure 3.8).²⁹

Figure 3.8 Asymmetric intermolecular hydroamination with MeOBIPHEP gold(I) complex

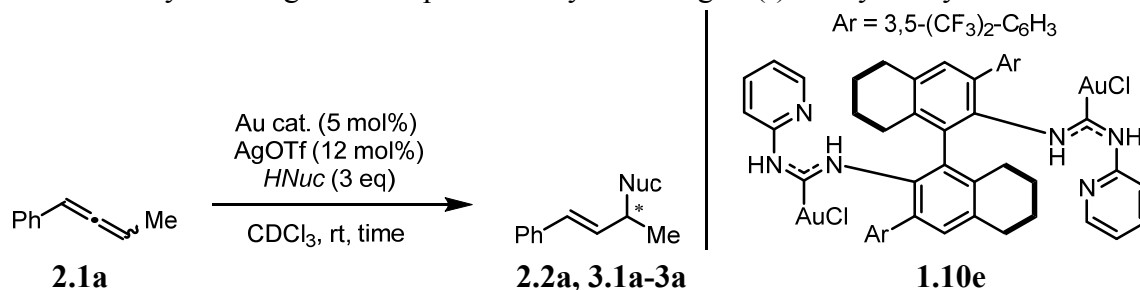


Given the scarcity of both chiral carbenes in asymmetric gold(I)-catalyzed hydroaminations, and intermolecular versions of this reaction, we sought to address both these deficits through the application of our BINAM-derived ADC ligand library.

Results and Discussion

Our investigations began with a survey of nitrogen nucleophiles using the optimal precatalyst **1.10e** from the hydroazidation work in the previous chapter (Table 3.1). Interestingly, under the same reaction conditions, the allylic amine products (**3.1a-3.3a**) obtained from these nucleophiles—*tert*-butyl carbamate, *tert*-butyl carbazate, and aniline—were the opposite enantiomers relative to the hydroazidation product **2.2a**, hinting at a switch from an inner-sphere^{30,31} to an outer-sphere^{32,33} mechanism.

Table 3.1 Survey of nitrogen nucleophiles in asymmetric gold(I)-catalyzed hydroamination



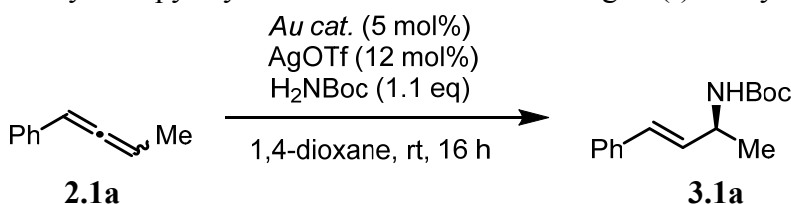
| Entry ^a | Nucleophile | Product | Time | Major enantiomer ^b | ee (%) ^c |
|--------------------|------------------------------|-------------|------|-------------------------------|---------------------|
| 1 | HN ₃ ^d | 2.2a | 60 m | <i>R</i> | 35 |
| 2 | H ₂ NBoc | 3.1a | 24 h | <i>S</i> | 27 |
| 3 | H ₂ NNHBoc | 3.2a | 14 d | <i>S</i> | 65 |
| 4 | H ₂ NPh | 3.3a | 14 d | <i>S</i> | 30 |

[a] Conditions: 0.05 mmol **2.1a**, 0.0025 mmol precatalyst **1.10e**, 0.006 mmol AgOTf, 0.15 mmol nucleophile, 1.0 mL CDCl₃ (0.05 M). [b] Determined by optical rotation and comparison to literature precedents (see Experimental section for details) [c] Determined by chiral HPLC. [d] Generated *in situ* from TMSN₃ (0.15 mmol) and TFA (0.10 mmol).

Enantiodivergence in synthetic protocols has been widely reported,³⁴⁻³⁷ and is usually brought about by modification of various reaction parameters, including catalyst identity (e.g. changes to metal or ligand), temperature, solvent, and additives, among others. However, the dependence of product stereochemistry on the identity of nucleophile is relatively rare.³⁸

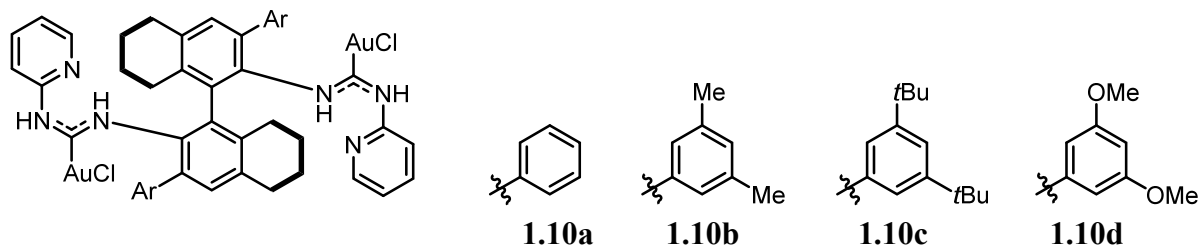
From these data, we decided to pursue optimization of the intermolecular hydroamination of allenes with *tert*-butyl carbamate. Even though it gave a lower ee value than the other two nucleophiles, the reaction was much faster, and the Boc-protected products (**3.1**) are easily unmasked to the corresponding free allylic amines. Switching to 1,4-dioxane solvent, as suggested by the Widenhoefer precedent,²⁹ and applying the library of BINAM-derived ADC gold(I) precatalysts immediately furnished high levels of enantioselectivity (Table 3.2).

Table 3.2 Survey of aryl and pyridyl substitution in chiral ADC gold(I) catalyts

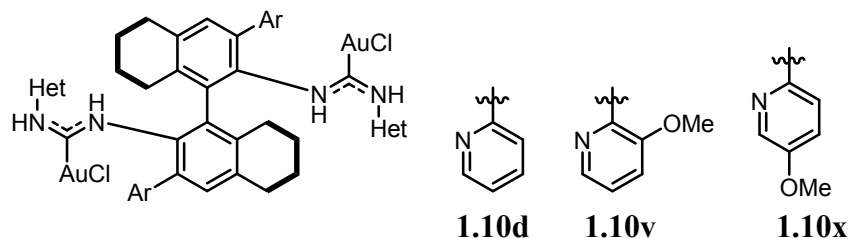


| Entry ^a | Precatalyst | Yield (%) ^b | ee (%) ^c |
|--------------------|--------------|------------------------|---------------------|
| 1 | 1.10a | 33 | 77 |
| 2 | 1.10b | 32 | 79 |
| 3 | 1.10c | 28 | 85 |
| 4 | 1.10d | 53 | 89 |
| 5 | 1.10e | 46 | 81 |
| 6 | 1.10v | 26 | 59 |
| 7 | 1.10x | 48 | 83 |
| 8 | 1.10k | 15 | 61 |
| 9 | 1.10m | 20 | 82 |
| 10 | 1.10o | 0 | n/d |

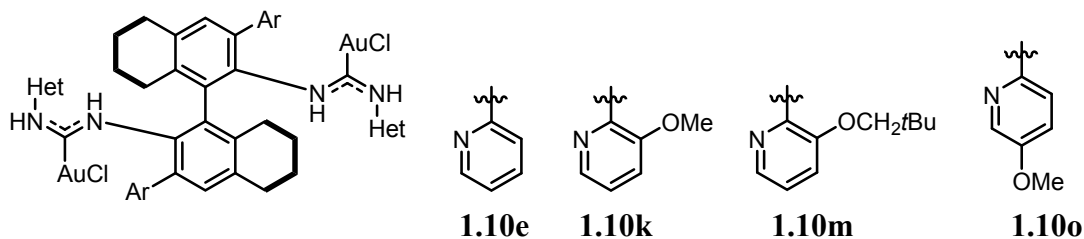
[a] Conditions: 0.05 mmol 2.1a, 0.0025 mmol precatalyst 1.10, 0.006 mmol AgOTf, 0.055 mmol H₂NBoc, 1.0 mL of 1,4-dioxane (0.05 M), 16 h at room temperature. [b] Determined by ¹H NMR with 1,3,5-trimethoxybenzene as an internal standard. The mass balance is unconsumed starting material and traces of the hydration product. [c] Determined by chiral HPLC.



Ar = 3,5-(OMe)₂C₆H₃



Ar = 3,5-(CF₃)₂C₆H₃

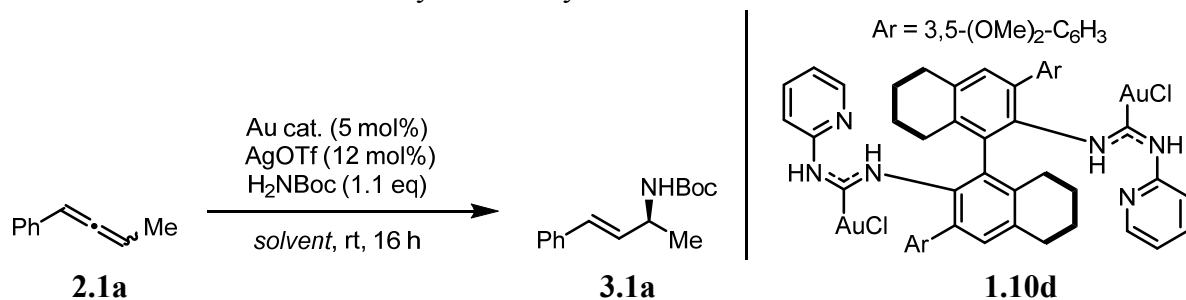


Small selectivity changes were observed among aryl substituents on the precatalysts (entries 1-5), and 3,5-dimethoxyphenyl groups (entry 4, **1.10d**) proved optimal. Keeping that aryl group, the effect of pyridyl substituents was briefly investigated, and the introduction of methoxy

substituents at two positions on the ring both gave diminished selectivity (compare entries 4, 6, and 7). The same substitutions were also explored with catalysts bearing 3,5-bis(trifluoromethyl)phenyl groups, and similar negative outcomes resulted (compare entries 5, 8, and 10). Introduction of a bulky neopentoxy substituent gave selectivities similar to those of the parent compound (compare entries 5 and 9). However, both precatalysts' ee values were less than those obtained with **1.10d**, which was taken on to further optimization of reaction parameters.

The effect of different solvents on reaction outcomes was examined next (Table 3.3). Of the solvents surveyed, 1,4-dioxane still gave the best enantioselectivity (entries 1-8). However, a marked increase in yield was observed with aromatic solvents (entries 3 and 4). In light of this, mixed solvents systems, specifically mixtures of 1,4-dioxane and a given aromatic solvent, were investigated (entries 9-12). Unfortunately, in all cases the desired increases in yield were not attained, and moreover, the ee values decreased from two to eleven percentage points.

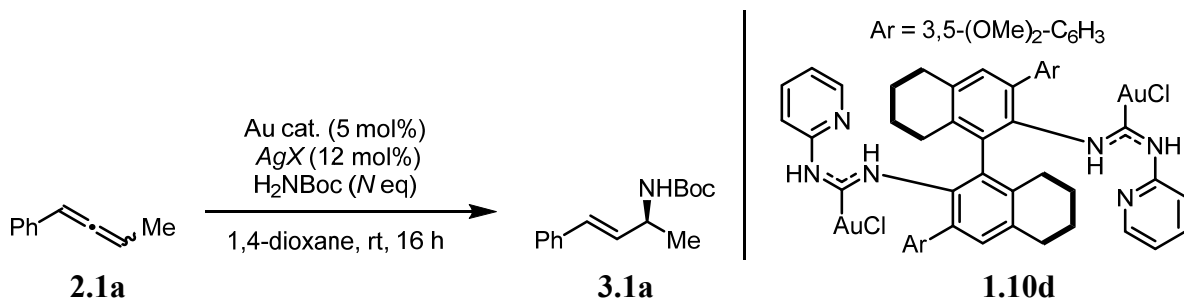
Table 3.3 Solvent effects in the asymmetric hydroamination reaction



| Entry ^a | Solvent | Yield (%) ^b | ee (%) ^c |
|--------------------|--|------------------------|---------------------|
| 1 | 1,4-dioxane | 53 | 89 |
| 2 | DCM | 54 | 30 |
| 3 | PhMe | 73 | 75 |
| 4 | PhCF ₃ | 88 | 65 |
| 5 | THF | 30 | 82 |
| 6 | Et ₂ O | 12 | 77 |
| 7 | DMM | 48 | 84 |
| 8 | CPME | 22 | 75 |
| 9 | 1,4-dioxane/PhH ^d | 53 | 86 |
| 10 | 1,4-dioxane/PhMe ^d | 45 | 87 |
| 11 | 1,4-dioxane/PhF ^d | 52 | 84 |
| 12 | 1,4-dioxane/PhCF ₃ ^d | 20 | 78 |

[a] Conditions: 0.05 mmol **2.1a**, 0.0025 mmol precatalyst **1.10d**, 0.006 mmol AgOTf, 0.055 mmol H₂NBoc, 1.0 mL of appropriate solvent (0.05 M), 16 h at room temperature. [b] Determined by ¹H NMR with 1,3,5-trimethoxy-benzene as an internal standard. The mass balance is unconsumed starting material and traces of the hydration product. [c] Determined by chiral HPLC. [d] 1:1 volumetric ratio

Table 3.4 Silver salt and nucleophile equivalency effects in the asymmetric hydroamination reaction



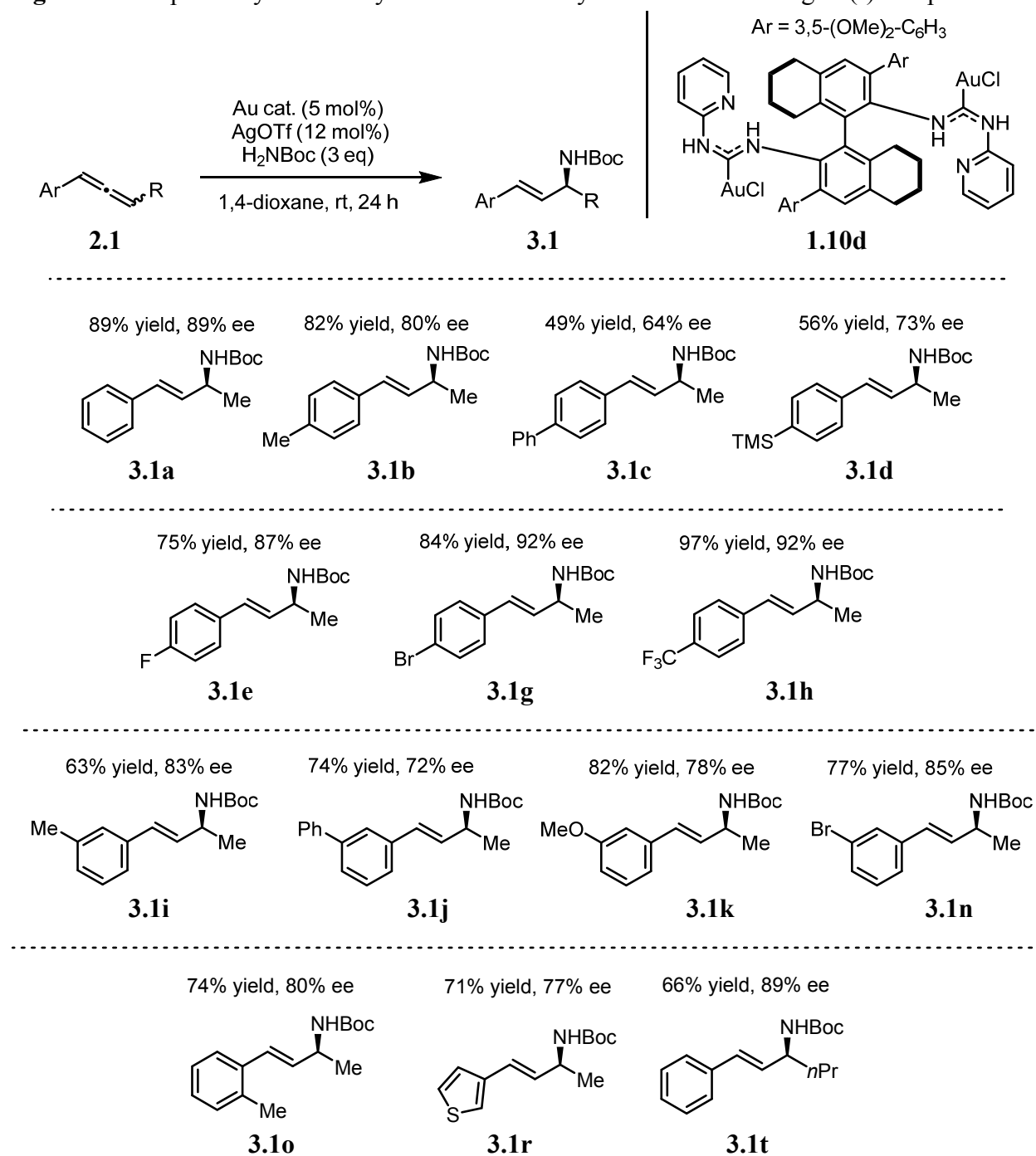
| Entry ^a | Ag salt | Nucleophile equivalents | Yield (%) ^b | ee (%) ^c |
|--------------------|--------------------|-------------------------|------------------------|---------------------|
| 1 | AgOTf | 1.1 | 53 | 89 |
| 2 | AgBF ₄ | 1.1 | 25 | 69 |
| 3 | AgClO ₄ | 1.1 | 31 | 73 |
| 4 | AgSbF ₆ | 1.1 | trace | 32 |
| 5 | AgNTf ₂ | 1.1 | 25 | 58 |
| 6 | AgOTf | 2.0 | 62 | 89 |
| 7 | AgOTf | 3.0 | 64 | 89 |
| 8 ^d | AgOTf | 3.0 | 89 ^e | 89 |

[a] Conditions: 0.05 mmol 2.1a, 0.0025 mmol precatalyst 1.10d, 0.006 mmol appropriate silver salt, 0.055 to 0.15 mmol H₂NBoc, 1.0 mL of appropriate solvent (0.05 M), 16 h at room temperature. [b] Determined by ¹H NMR with 1,3,5-trimethoxybenzene as an internal standard. The mass balance is unconsumed starting material and traces of the hydration product. [c] Determined by chiral HPLC. [d] Reaction run for 24 hours. [e] Isolated yield.

The counterion effect was explored next (Table 3.4, entries 1-5). No improvement in enantioselectivity or yield was achieved from this study. Ultimately, the yield of the reaction was improved by the addition of super-stoichiometric quantities of carbamate nucleophile (entries 6 and 7) and extension of the reaction time (entry 8). This established the optimized reaction conditions for asymmetric intermolecular hydroamination.

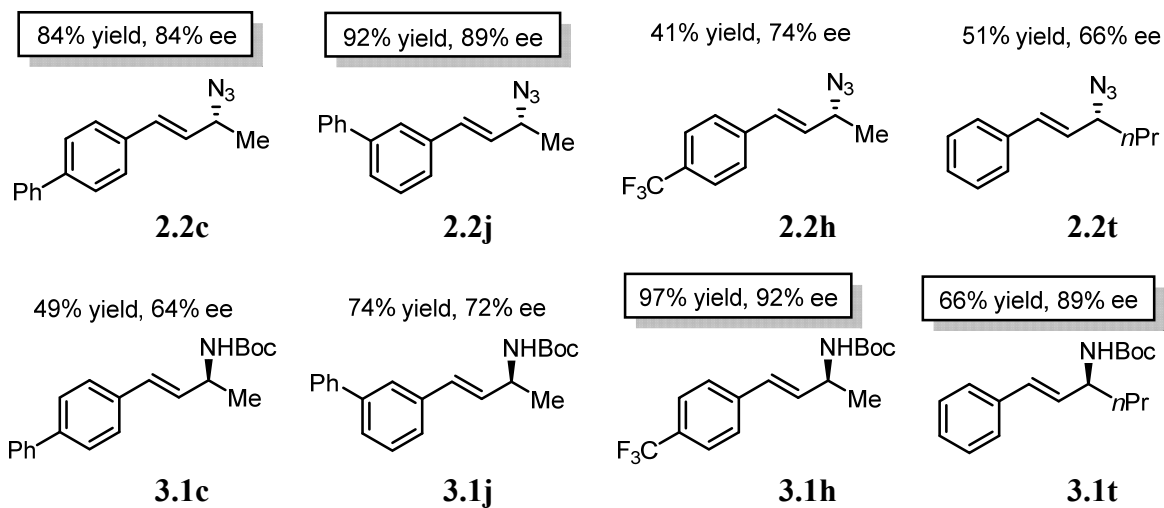
With these optimal conditions, the substrate scope tolerated in the reaction was investigated. Electron-donating and withdrawing groups were generally well tolerated in the *para*- and *meta*- positions of the aryl ring (Figure 3.9, **3.1a-3.1n**). One example each of an *ortho*-substituent (**3.1o**), a heteroaromatic ring (**3.1r**), and a non-methyl R substituent (**3.1t**) were also demonstrated.

Figure 3.9 Scope of asymmetric hydroazidation of aryl allenes with ADC gold(I) complex



Perhaps the most significant consequence of this methodology is its complementarity to the hydroamination reaction outlined in Chapter 2. Taken together, the two transformations allow access to a range of enantioenriched allylic amine products using the same catalyst family. Notably, a single enantiomer of the catalysts can generate allylic amines with opposite chirality. Moreover, in cases where the hydroamination fails to provide allylic amines with useful enantioselectivities, the hydroazidation reaction can be used to address these deficiencies and *vice versa* (Figure 3.10).

Figure 3.10 Complementarity of hydroazidation and hydroamination reaction products from identical substrates



Experimental

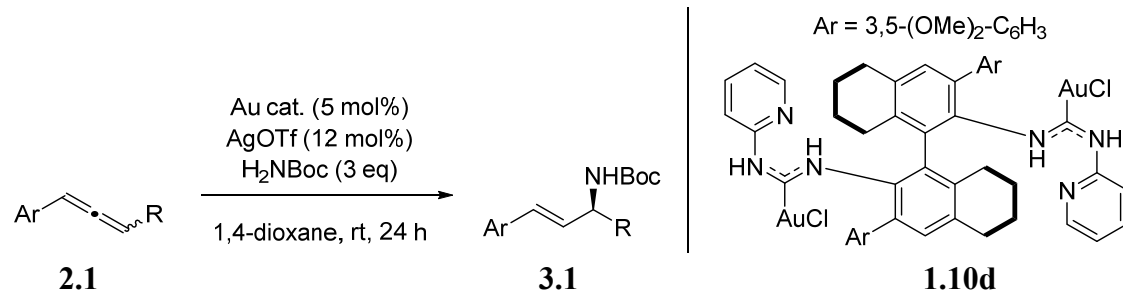
General information

Unless otherwise noted, reagents were obtained from commercial sources and used without further purification. Anhydrous 1,4-dioxane was purchased from Sigma-Aldrich. All other solvents used are HPLC grade. TLC analysis of reaction mixtures was performed on Merck silica gel 60 F₂₅₄ TLC plates and visualized by ultraviolet light, iodine or potassium permanganate stain. Flash chromatography was carried out with ICN SiliTech 32-63 D 60 Å silica gel. ¹H and ¹³C NMR spectra were recorded with Bruker AV-500, DRX-500, or AV-600 spectrometers and were referenced to residual ¹H and ¹³C signals of the deuterated solvent (δ H 7.26, δ C 77.16 for chloroform-d). Enantioselectivity was determined by chiral HPLC using Daicel Chiralpak AD-H, AS-H, IB, OD-H, or Regis (R,R) WHELK-O1 columns (all 0.46 cm x 25 cm). Optical rotation was recorded on a Perkin Elmer Polarimeter 241 at the D line (1.0 dm path length, *c* = mg/mL). Generally, racemic samples were prepared in procedures modified from those reported by Widenhoefer and coworkers using IPrAuCl and AgOTf.³⁹ Mass spectral data were obtained via the Micro-Mass/Analytical Facility operated by the College of Chemistry, University of California, Berkeley using a Thermo LTQ-FT (ESI) instrument.

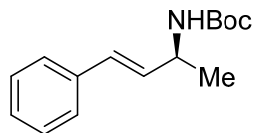
General procedure for preparation of allene substrates

The procedure and characterization data were outlined in the Experimental section of Chapter 2.

Optimized procedure for gold(I)-catalyzed enantioselective hydroamination



Precatalyst **1.10d** (3.1 mg, 0.0025 mmol, 0.05 equiv) and silver triflate (1.6 mg, 0.006 mmol, 0.12 equiv) were weighed in a dram vial and a 1,4-dioxane (anhydrous) was added (1.0 mL). The heterogeneous mixture was sonicated for 5 min using a commercial ultrasonic cleaner, and then filtered through glass fiber into a second dram vial, which had been pre-weighed with the appropriate substrate **2.1** (0.05 mmol, 1.0 equiv) and *tert*-butyl carbamate (17.6 mg, 0.15 mmol, 3 equiv). The reaction vial was kept at room temperature for 24 h and then the reaction was quenched by addition of Et₃N (ca. 200 μ L, 1.4 mmol). The reaction solvent was then removed *in vacuo* and the crude reaction mixture was purified by flash column chromatography (hexane/Et₂O, silica gel, 4 mL Pasteur pipette column) to afford the product **3.1**.



3.1a, *tert*-butyl (*S,E*)-(4-phenylbut-3-en-2-yl)carbamate⁴⁰

0.0507 mmol scale, 89% yield (11.2 mg, 0.0453 mmol)

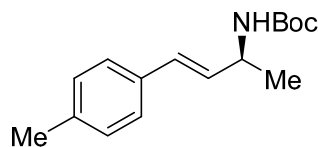
¹H NMR (600 MHz, CDCl₃) δ 7.36 (d, *J* = 8.3 Hz, 2H), 7.30 (t, *J* = 7.7 Hz, 2H), 7.23 (t, *J* = 6.8 Hz, 1H), 6.50 (d, *J* = 16.1 Hz, 1H), 6.16 (dd, *J* = 15.8, 5.9 Hz, 1H), 4.56 (brs, 1H), 4.41 (brs, 1H), 1.46 (s, 9H), 1.31 (d, *J* = 6.7 Hz, 3H).

¹³C NMR (151 MHz, CDCl₃) δ 155.26, 137.00, 131.88, 129.33, 128.67, 127.61, 126.51, 79.53, 48.01, 28.58, 21.29.

HRMS (EI⁺): calcd. for [C₁₅H₂₁NO₂]⁺: 247.1572, found: 247.1569.

HPLC: AD-H column, 95:5 hexanes:isopropanol, 1.00 mL/min, *t*_R = major: 8.3 min, minor: 6.6 min. 89% ee.

[α]_D²⁰ -60.1° (*c* 1.0, CHCl₃); Lit.: [α]_D²⁰ -60.9° (*c* 1.08, CHCl₃, *S*-enantiomer, 98% ee)



3.1b, *tert*-butyl (*S,E*)-(4-(*p*-tolyl)but-3-en-2-yl)carbamate

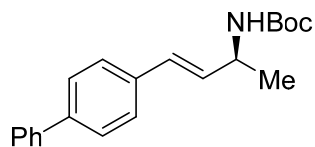
0.0492 mmol scale, 82% yield (10.5 mg, 0.0402 mmol)

¹H NMR (600 MHz, CDCl₃) δ 7.25 (d, *J* = 8.7 Hz, 2H), 7.11 (d, *J* = 7.7 Hz, 2H), 6.46 (d, *J* = 15.9 Hz, 1H), 6.10 (dd, *J* = 16.0, 5.8 Hz, 1H), 4.54 (brs, 1H), 4.39 (brs, 1H), 2.33 (s, 3H), 1.46 (d, *J* = 2.0 Hz, 9H), 1.30 (d, *J* = 6.7 Hz, 3H).

¹³C NMR (151 MHz, CDCl₃) δ 155.27, 137.42, 134.19, 130.81, 129.37, 129.21, 126.41, 79.50, 48.00, 28.59, 21.31.

HRMS (EI⁺): calcd. for [C₁₆H₂₃NO₂]⁺: 261.1729, found: 261.1728.

HPLC: AD-H column, 95:5 hexanes:isopropanol, 1.00 mL/min, *t*_R = major: 9.8 min, minor: 6.3 min. 80% ee.



3.1c, *tert*-butyl (*S,E*)-(4-([1,1'-biphenyl]-4-yl)but-3-en-2-yl)carbamate

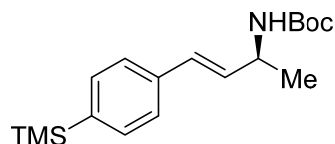
0.0499 mmol scale, 49% yield (7.9 mg, 0.0244 mmol)

^1H NMR (500 MHz, CDCl_3) δ 7.64 – 7.52 (m, 4H), 7.44 (dt, $J = 7.5, 3.5$ Hz, 4H), 7.38 – 7.31 (m, 1H), 6.53 (d, $J = 15.9$ Hz, 1H), 6.20 (dd, $J = 15.6, 5.8$ Hz, 1H), 4.57 (brs, 1H), 4.43 (brs, 1H), 1.47 (s, 9H), 1.33 (d, $J = 6.8$ Hz, 3H).

^{13}C NMR (126 MHz, CDCl_3) δ 155.24, 140.81, 140.36, 136.00, 131.97, 128.91, 128.83, 127.42, 127.36, 127.05, 126.93, 79.57, 48.01, 28.58, 21.30.

HRMS (EI+): calcd. for $[\text{C}_{21}\text{H}_{25}\text{NO}_2]^+$: 323.1885, found: 323.1885.

HPLC: AD-H column, 95:5 hexanes:isopropanol, 1.00 mL/min, t_{R} = major: 14.1 min, minor: 9.7 min. 64% ee.



3.1d, *tert*-butyl (*S,E*)-(4-(4-(trimethylsilyl)phenyl)but-3-en-2-yl)carbamate

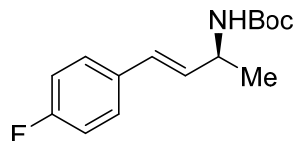
0.0469 mmol scale, 56% yield (8.4 mg, 0.0263 mmol)

^1H NMR (600 MHz, CDCl_3) δ 7.46 (d, $J = 7.8$ Hz, 2H), 7.34 (d, $J = 7.6$ Hz, 2H), 6.49 (d, $J = 15.9$ Hz, 1H), 6.18 (dd, $J = 15.8, 5.9$ Hz, 1H), 4.55 (brs, 1H), 4.41 (brs, 1H), 1.46 (s, 9H), 1.31 (d, $J = 6.8$ Hz, 3H), 0.26 (s, 9H).

^{13}C NMR (151 MHz, CDCl_3) δ 155.26, 139.91, 137.42, 133.72, 132.18, 129.33, 125.83, 79.55, 48.04, 28.59, 21.28, -0.99.

HRMS (EI+): calcd. for $[\text{C}_{18}\text{H}_{29}\text{NO}_2\text{Si}]^+$: 319.1968, found: 319.1959.

HPLC: AD-H column, 95:5 hexanes:isopropanol, 1.00 mL/min, t_{R} = major: 5.9 min, minor: 5.0 min. 73% ee.



3.1e, *tert*-butyl (*S,E*)-(4-(4-fluorophenyl)but-3-en-2-yl)carbamate

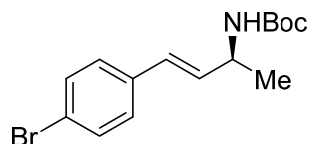
0.0513 mmol scale, 75% yield (10.2 mg, 0.0384 mmol)

^1H NMR (600 MHz, CDCl_3) δ 7.40 – 7.28 (m, 2H), 7.11 – 6.92 (m, 2H), 6.45 (d, $J = 15.9$ Hz, 1H), 6.06 (dd, $J = 15.8, 5.7$ Hz, 1H), 4.54 (brs, 1H), 4.38 (brs, 1H), 1.46 (s, 9H), 1.30 (d, $J = 6.8$ Hz, 3H).

^{13}C NMR (151 MHz, CDCl_3) δ 162.39 (d, $J = 246.6$ Hz), 155.24, 133.14 (d, $J = 3.3$ Hz), 131.67, 128.17, 127.99 (d, $J = 8.0$ Hz), 115.55 (d, $J = 21.5$ Hz), 79.58, 47.96, 28.58, 21.27.

HRMS (EI+): calcd. for $[\text{C}_{15}\text{H}_{20}\text{FNO}_2]^+$: 265.1478, found: 265.1482.

HPLC: AD-H column, 95:5 hexanes:isopropanol, 1.00 mL/min, t_{R} = major: 8.6 min, minor: 7.1 min. 87% ee.



3.1g, *tert*-butyl (*S,E*)-(4-(4-bromophenyl)but-3-en-2-yl)carbamate⁴¹

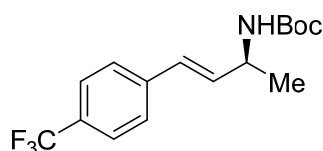
0.0493 mmol scale, 84% yield (13.5 mg, 0.0414 mmol)

¹H NMR (600 MHz, CDCl₃) δ 7.42 (d, *J* = 8.5 Hz, 2H), 7.21 (d, *J* = 8.5 Hz, 2H), 6.42 (d, *J* = 15.9 Hz, 1H), 6.14 (dd, *J* = 15.9, 5.8 Hz, 1H), 4.54 (brs, 1H), 4.38 (brs, 1H), 1.45 (s, 9H), 1.30 (d, *J* = 6.8 Hz, 3H).

¹³C NMR (151 MHz, CDCl₃) δ 155.22, 135.96, 132.76, 131.76, 128.17, 128.05, 121.34, 79.64, 47.96, 28.57, 21.19.

HRMS (EI⁺): calcd. for [C₁₅H₂₀BrNO₂]⁺: 325.0677, found: 325.0677.

HPLC: AD-H column, 95:5 hexanes:isopropanol, 1.00 mL/min, *t_R* = major: 11.0 min, minor: 8.0 min. 92% ee.



3.1h, *tert*-butyl (*S,E*)-(4-(4-(trifluoromethyl)phenyl)but-3-en-2-yl)carbamate

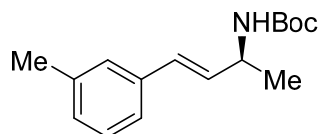
0.0500 mmol scale, 97% yield (15.3 mg, 0.0485 mmol)

¹H NMR (600 MHz, CDCl₃) δ 7.55 (d, *J* = 8.2 Hz, 2H), 7.44 (d, *J* = 8.2 Hz, 2H), 6.52 (d, *J* = 15.9 Hz, 1H), 6.25 (dd, *J* = 15.8, 5.7 Hz, 1H), 4.56 (brs, 1H), 4.42 (brs, 1H), 1.46 (s, 9H), 1.32 (d, *J* = 6.9 Hz, 3H).

¹³C NMR (151 MHz, CDCl₃) δ 155.21, 140.51, 134.69, 129.43 (q, *J* = 32.6 Hz), 128.01, 126.67, 125.62 (q, *J* = 3.8 Hz), 124.33 (q, *J* = 271.8 Hz), 79.72, 47.96, 28.56, 21.13.

HRMS (EI⁺): calcd. for [C₁₆H₂₀F₃NO₂]⁺: 315.1446, found: 315.1440.

HPLC: AD-H column, 95:5 hexanes:isopropanol, 1.00 mL/min, *t_R* = major: 9.6 min, minor: 7.5 min. 92% ee.



3.1i, *tert*-butyl (*S,E*)-(4-(*m*-tolyl)but-3-en-2-yl)carbamate

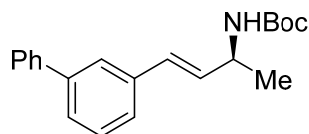
0.0520 mmol scale, 63% yield (8.6 mg, 0.0329 mmol)

^1H NMR (600 MHz, CDCl_3) δ 7.22 – 7.13 (m, 3H), 7.05 (d, $J = 7.4$ Hz, 1H), 6.46 (d, $J = 15.9$ Hz, 1H), 6.14 (dd, $J = 16.2, 5.4$ Hz, 1H), 4.55 (brs, 1H), 4.41 (brs, 1H), 2.34 (s, 3H), 1.46 (s, 9H), 1.31 (d, $J = 6.8$ Hz, 3H).

^{13}C NMR (151 MHz, CDCl_3) δ 155.08, 138.01, 136.75, 131.48, 129.23, 128.37, 128.22, 127.03, 123.49, 79.32, 47.82, 28.40, 21.32, 21.11.

HRMS (EI+): calcd. for $[\text{C}_{16}\text{H}_{23}\text{NO}_2]^+$: 261.1729, found: 261.1723.

HPLC: AD-H column, 95:5 hexanes:isopropanol, 1.00 mL/min, t_{R} = major: 7.0 min, minor: 5.9 min. 83% ee.



3.1j, *tert*-butyl (*S,E*)-(4-([1,1'-biphenyl]-3-yl)but-3-en-2-yl)carbamate

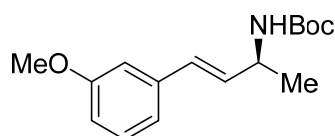
0.0494 mmol scale, 74% yield (11.9 mg, 0.0368 mmol)

^1H NMR (600 MHz, CDCl_3) δ 7.64 – 7.55 (m, 3H), 7.48 – 7.42 (m, 3H), 7.41 – 7.31 (m, 3H), 6.57 (d, $J = 15.8$ Hz, 1H), 6.23 (dd, $J = 15.8, 6.8$ Hz, 1H), 4.57 (brs, 1H), 4.44 (brs, 1H), 1.47 (s, 9H), 1.33 (d, $J = 6.8$ Hz, 3H).

^{13}C NMR (151 MHz, CDCl_3) δ 155.26, 141.73, 141.25, 137.48, 132.32, 129.27, 129.09, 128.89, 127.49, 127.31, 126.52, 125.46, 125.41, 79.59, 48.05, 28.60, 21.32.

HRMS (EI+): calcd. for $[\text{C}_{21}\text{H}_{25}\text{NO}_2]^+$: 323.1885, found: 323.1880.

HPLC: AD-H column, 95:5 hexanes:isopropanol, 1.00 mL/min, t_{R} = major: 13.6 min, minor: 9.1 min. 72% ee.



3.1k, *tert*-butyl (*S,E*)-(4-(3-methoxyphenyl)but-3-en-2-yl)carbamate⁴¹

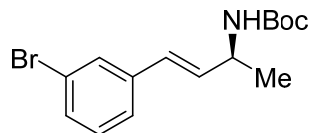
0.0524 mmol scale, 82% yield (11.9 mg, 0.0429 mmol)

^1H NMR (600 MHz, CDCl_3) δ 7.22 (t, $J = 7.9$ Hz, 1H), 6.95 (dt, $J = 7.5, 1.1$ Hz, 1H), 6.92 – 6.86 (m, 1H), 6.78 (ddd, $J = 8.1, 2.6, 0.9$ Hz, 1H), 6.46 (d, $J = 15.9$ Hz, 1H), 6.15 (dd, $J = 15.6, 5.7$ Hz, 1H), 4.56 (brs, 1H), 4.41 (brs, 1H), 3.81 (s, 3H), 1.46 (s, 9H), 1.31 (d, $J = 6.6$ Hz, 3H).

^{13}C NMR (151 MHz, CDCl_3) δ 159.77, 155.07, 138.29, 132.03, 129.44, 129.06, 119.00, 113.14, 111.66, 79.37, 55.17, 47.82, 28.39, 21.07.

HRMS (EI+): calcd. for $[\text{C}_{16}\text{H}_{23}\text{NO}_2]^+$: 277.1678, found: 277.1677.

HPLC: AD-H column, 95:5 hexanes:isopropanol, 1.00 mL/min, t_R = major: 12.3 min, minor: 9.0 min. 78% ee.



3.1n, *tert*-butyl (*S,E*)-(4-(3-bromophenyl)but-3-en-2-yl)carbamate

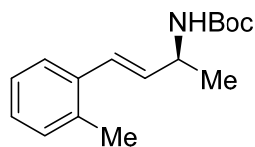
0.0516 mmol scale, 77% yield (13.0 mg, 0.0398 mmol)

^1H NMR (600 MHz, CDCl_3) δ 7.51 (t, J = 1.8 Hz, 1H), 7.34 (d, J = 8.0 Hz, 1H), 7.25 (d, J = 6.4 Hz, 1H), 7.16 (t, J = 7.8 Hz, 1H), 6.42 (d, J = 15.9 Hz, 1H), 6.16 (dd, J = 15.8, 5.7 Hz, 1H), 4.55 (brs, 1H), 4.40 (brs, 1H), 1.46 (s, 9H), 1.30 (d, J = 6.8 Hz, 3H).

^{13}C NMR (151 MHz, CDCl_3) δ 155.20, 139.19, 133.56, 130.45, 130.16, 129.34, 127.91, 125.24, 122.86, 79.65, 47.90, 28.57, 21.20.

HRMS (EI+): calcd. for $[\text{C}_{15}\text{H}_{20}\text{BrNO}_2]^+$: 325.0677, found: 325.0672.

HPLC: AD-H column, 95:5 hexanes:isopropanol, 1.00 mL/min, t_R = major: 8.3 min, minor: 6.7 min. 85% ee.



3.1o, *tert*-butyl (*S,E*)-(4-(*o*-tolyl)but-3-en-2-yl)carbamate⁴¹

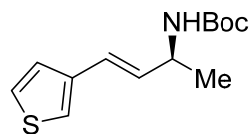
0.0506 mmol scale, 60% yield (8.0 mg, 0.0306 mmol)

^1H NMR (600 MHz, CDCl_3) δ 7.44 – 7.34 (m, 1H), 7.18 – 7.08 (m, 3H), 6.70 (d, J = 15.7 Hz, 1H), 6.02 (dd, J = 15.7, 5.7 Hz, 1H), 4.55 (brs, 1H), 4.41 (brs, 1H), 2.33 (s, 3H), 1.46 (s, 9H), 1.32 (d, J = 6.8 Hz, 3H).

^{13}C NMR (151 MHz, CDCl_3) δ 155.27, 136.19, 135.57, 133.28, 130.36, 127.53, 127.27, 126.19, 125.82, 79.52, 48.26, 28.60, 21.39, 19.92.

HRMS (EI+): calcd. for $[\text{C}_{16}\text{H}_{23}\text{NO}_2]^+$: 261.1729, found: 261.1726.

HPLC: AD-H column, 95:5 hexanes:isopropanol, 1.00 mL/min, t_R = major: 6.9 min, minor: 6.2 min. 80% ee.



3.1r, *tert*-butyl (*S,E*)-(4-(thiophen-3-yl)but-3-en-2-yl)carbamate

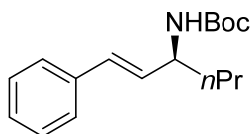
0.0543 mmol scale, 71% yield (9.7 mg, 0.0383 mmol)

^1H NMR (600 MHz, CDCl_3) δ 7.26 – 7.24 (m, 1H), 7.18 (d, $J = 4.4$ Hz, 1H), 7.13 (d, $J = 2.9$ Hz, 1H), 6.51 (d, $J = 15.9$ Hz, 1H), 6.01 (dd, $J = 15.8, 5.7$ Hz, 1H), 4.52 (brs, 1H), 4.37 (brs, 1H), 1.46 (s, 9H), 1.29 (d, $J = 6.8$ Hz, 3H).

^{13}C NMR (151 MHz, CDCl_3) δ 155.24, 139.57, 131.77, 126.12, 125.11, 123.62, 122.05, 79.54, 47.91, 28.59, 21.25.

HRMS (EI+): calcd. for $[\text{C}_{13}\text{H}_{19}\text{NO}_2\text{S}]^+$: 253.1137, found: 253.1131.

HPLC: AD-H column, 95:5 hexanes:isopropanol, 1.00 mL/min, t_{R} = major: 10.1 min, minor: 7.9 min. 77% ee.



3.1t, *tert*-butyl (*S,E*)-(1-phenylhex-1-en-3-yl)carbamate

0.0499 mmol scale, 66% yield (9.1 mg, 0.033 mmol)

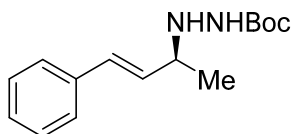
^1H NMR (600 MHz, CDCl_3) δ 7.36 (d, $J = 8.5$ Hz, 2H), 7.30 (t, $J = 7.8$ Hz, 2H), 7.22 (t, $J = 7.3$ Hz, 1H), 6.50 (d, $J = 15.8$ Hz, 1H), 6.08 (dd, $J = 16.5, 6.8$ Hz, 1H), 4.54 (brs, 1H), 4.27 (brs, 1H), 1.59 – 1.53 (m, 2H), 1.46 (s, 9H), 1.44 – 1.36 (m, 2H), 0.94 (t, $J = 7.4$ Hz, 3H).

^{13}C NMR (151 MHz, CDCl_3) δ 155.47, 137.11, 130.97, 130.02, 128.66, 127.56, 126.51, 79.48, 52.46, 37.95, 28.59, 19.22, 14.04.

HRMS (EI+): calcd. for $[\text{C}_{17}\text{H}_{25}\text{NO}_2]^+$: 275.1885, found: 275.1880.

HPLC: AD-H column, 95:5 hexanes:isopropanol, 1.00 mL/min, t_{R} = major: 8.6 min, minor: 6.3 min. 89% ee.

Products obtained from other nucleophiles



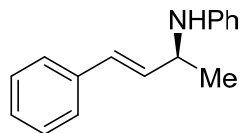
3.2a, *tert*-butyl (*S,E*)-2-(4-phenylbut-3-en-2-yl)hydrazine-1-carboxylate

0.0515 mmol scale, 50% yield (6.8 mg, 0.0259 mmol)

The spectral data are consistent with those previously reported.⁴²

HPLC: AD-H column, 95:5 hexanes:isopropanol, 1.00 mL/min, t_{R} = major: 10.2 min, minor: 12.1 min. 65% ee.

$[\alpha]_{\text{D}}^{20} -68.5^\circ$ (c 0.68, CHCl_3); Lit.: $[\alpha]_{\text{D}}^{20} -143^\circ$ (c 0.99, CHCl_3 , S-enantiomer, 94% ee)



3.3a, (*S,E*)-*N*-(4-phenylbut-3-en-2-yl)aniline

0.0515 mmol scale, 31% yield (3.6 mg, 0.0161 mmol)

The spectral data are consistent with those previously reported.^{43,44}

HPLC: IB column, 99:1 hexanes:isopropanol, 1.00 mL/min, t_R = major: 11.0 min, minor: 13.1 min. 30% ee.

$[\alpha]_D^{20}$ -9.9° (c 0.9, CHCl_3); Lit.: $[\alpha]_D^{20}$ -17.4° (c 1.0, CHCl_3 , *S*-enantiomer, 74% ee)

References

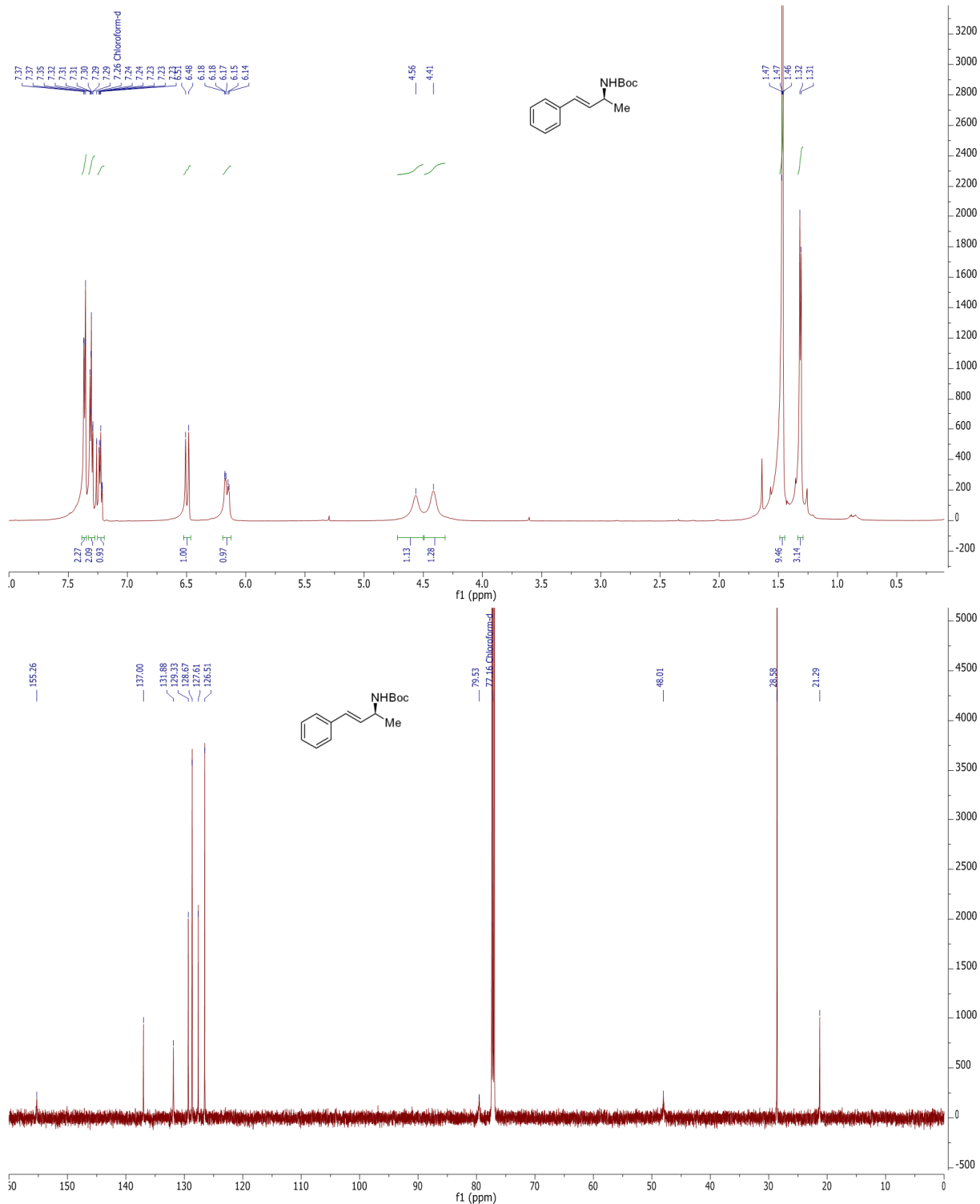
- (1) Han, Z.-Y.; Xiao, H.; Chen, X.-H.; Gong, L.-Z. *J. Am. Chem. Soc.* **2009**, *131* (26), 9182.
- (2) Liu, X.-Y.; Che, C.-M. *Org. Lett.* **2009**, *11* (18), 4204.
- (3) Wang, C.; Han, Z.-Y.; Luo, H.-W.; Gong, L.-Z. *Org. Lett.* **2010**, *12* (10), 2266.
- (4) Gregory, A. W.; Jakubec, P.; Turner, P.; Dixon, D. J. *Org. Lett.* **2013**, *15* (17), 4330.
- (5) He, Y.-P.; Wu, H.; Chen, D.-F.; Yu, J.; Gong, L.-Z. *Chem. – Eur. J.* **2013**, *19* (17), 5232.
- (6) Du, Y.-L.; Hu, Y.; Zhu, Y.-F.; Tu, X.-F.; Han, Z.-Y.; Gong, L.-Z. *J. Org. Chem.* **2015**, *80* (9), 4754.
- (7) Zhao, F.; Li, N.; Zhu, Y.-F.; Han, Z.-Y. *Org. Lett.* **2016**, *18* (7), 1506.
- (8) Barber, D. M.; Sanganee, H. J.; Dixon, D. J. *Org. Lett.* **2012**, *14* (20), 5290.
- (9) Barber, D. M.; Đuriš, A.; Thompson, A. L.; Sanganee, H. J.; Dixon, D. J. *ACS Catal.* **2014**, *4* (2), 634.
- (10) Chen, X.; Chen, H.; Ji, X.; Jiang, H.; Yao, Z.-J.; Liu, H. *Org. Lett.* **2013**, *15* (8), 1846.
- (11) Reznichenko, A. L.; Nawara-Hultsch, A. J.; Hultsch, K. C. In *Stereoselective Formation of Amines*; Li, W., Zhang, X., Eds.; Topics in Current Chemistry; Springer Berlin Heidelberg, 2013; pp 191–260.
- (12) Ghorai, M. K.; Tiwari, D. P.; Bhattacharyya, A. In *Stereoselective Synthesis of Drugs and Natural Products*; John Wiley & Sons, Inc., 2013; Vol. 1, pp 1173–1184.
- (13) LaLonde, R. L.; Sherry, B. D.; Kang, E. J.; Toste, F. D. *J. Am. Chem. Soc.* **2007**, *129* (9), 2452.
- (14) Zhang, Z.; Bender, C. F.; Widenhofer, R. A. *J. Am. Chem. Soc.* **2007**, *129* (46), 14148.
- (15) Hamilton, G. L.; Kang, E. J.; Mba, M.; Toste, F. D. *Science* **2007**, *317* (5837), 496.
- (16) Zhang, Z.; Lee, S. D.; Widenhofer, R. A. *J. Am. Chem. Soc.* **2009**, *131* (15), 5372.
- (17) Kanno, O.; Kuriyama, W.; Wang, Z. J.; Toste, F. D. *Angew. Chem. Int. Ed.* **2011**, *50* (42), 9919.
- (18) Sun, Y.; Xu, Q.; Shi, M. *Beilstein J. Org. Chem.* **2013**, *9* (1), 2224.
- (19) Abadie, M.-A.; Trivelli, X.; Medina, F.; Capet, F.; Roussel, P.; Agbossou-Niedercorn, F.; Michon, C. *ChemCatChem* **2014**, *6* (8), 2235.
- (20) Lee, S. D.; Timmerman, J. C.; Widenhofer, R. A. *Adv. Synth. Catal.* **2014**, *356* (14-15), 3187.
- (21) Michon, C.; Abadie, M.-A.; Medina, F.; Agbossou-Niedercorn, F. *Catal. Today* **2014**, *235*, 2.
- (22) Roth, K. E.; Blum, S. A. *Organometallics* **2010**, *29* (7), 1712.
- (23) Michon, C.; Medina, F.; Abadie, M.-A.; Agbossou-Niedercorn, F. *Organometallics* **2013**, *32* (19), 5589.
- (24) Teller, H.; Corbet, M.; Mantilli, L.; Gopakumar, G.; Goddard, R.; Thiel, W.; Fürstner, A. *J. Am. Chem. Soc.* **2012**, *134* (37), 15331.
- (25) Lloret Fillol, J.; Kruckenberg, A.; Scherl, P.; Wadepohl, H.; Gade, L. H. *Chem. – Eur. J.* **2011**, *17* (50), 14047.
- (26) Rodríguez, L.-I.; Roth, T.; Lloret Fillol, J.; Wadepohl, H.; Gade, L. H. *Chem. – Eur. J.* **2012**, *18* (12), 3721.
- (27) Roth, T.; Wadepohl, H.; Wright, D. S.; Gade, L. H. *Chem. – Eur. J.* **2013**, *19* (41), 13823.
- (28) Liu, L.; Wang, F.; Wang, W.; Zhao, M.; Shi, M. *Beilstein J. Org. Chem.* **2011**, *7* (1), 555.
- (29) Butler, K. L.; Tragni, M.; Widenhofer, R. A. *Angew. Chem. Int. Ed.* **2012**, *51* (21), 5175.
- (30) Nishina, N.; Yamamoto, Y. *Angew. Chem. Int. Ed.* **2006**, *45* (20), 3314.
- (31) Hesp, K. D.; Stradiotto, M. *J. Am. Chem. Soc.* **2010**, *132* (51), 18026.

- (32) Wang, Z. J.; Benitez, D.; Tkatchouk, E.; Goddard III, W. A.; Toste, F. D. *J. Am. Chem. Soc.* **2010**, *132* (37), 13064.
- (33) Zhdanko, A.; Maier, M. E. *Angew. Chem. Int. Ed.* **2014**, *53* (30), 7760.
- (34) Zaroni, G.; Castronovo, F.; Franzini, M.; Vidari, G.; Giannini, E. *Chem. Soc. Rev.* **2003**, *32* (3), 115.
- (35) Tanaka, T.; Hayashi, M. *Synthesis* **2008**, *2008* (21), 3361.
- (36) Bartók, M. *Chem. Rev.* **2010**, *110* (3), 1663.
- (37) Escorihuela, J.; Burguete, M. I.; Luis, S. V. *Chem. Soc. Rev.* **2013**, *42* (12), 5595.
- (38) Henrich, M.; Delgado, A.; Molins, E.; Roig, A.; Llebaria, A. *Tetrahedron Lett.* **1999**, *40* (22), 4259.
- (39) Kinder, R. E.; Zhang, Z.; Widenhoefer, R. A. *Org. Lett.* **2008**, *10* (14), 3157.
- (40) Reginato, G.; Mordini, A.; Messina, F.; Degl'Innocenti, A.; Poli, G. *Tetrahedron* **1996**, *52* (33), 10985.
- (41) Dellaria Jr., J. F.; Sallin, K. J. *Tetrahedron Lett.* **1990**, *31* (19), 2661.
- (42) Wang, Y.; Xu, J.-K.; Gu, Y.; Tian, S.-K. *Org. Chem.* **2014**, *1* (7), 812.
- (43) Ozawa, F.; Okamoto, H.; Kawagishi, S.; Yamamoto, S.; Minami, T.; Yoshifuji, M. *J. Am. Chem. Soc.* **2002**, *124* (37), 10968.
- (44) Malkov, A. V.; Stončius, S.; MacDougall, K. N.; Mariani, A.; McGeoch, G. D.; Kočovský, P. *Organocatalysis Org. Synth.* **2006**, *62* (2–3), 264.

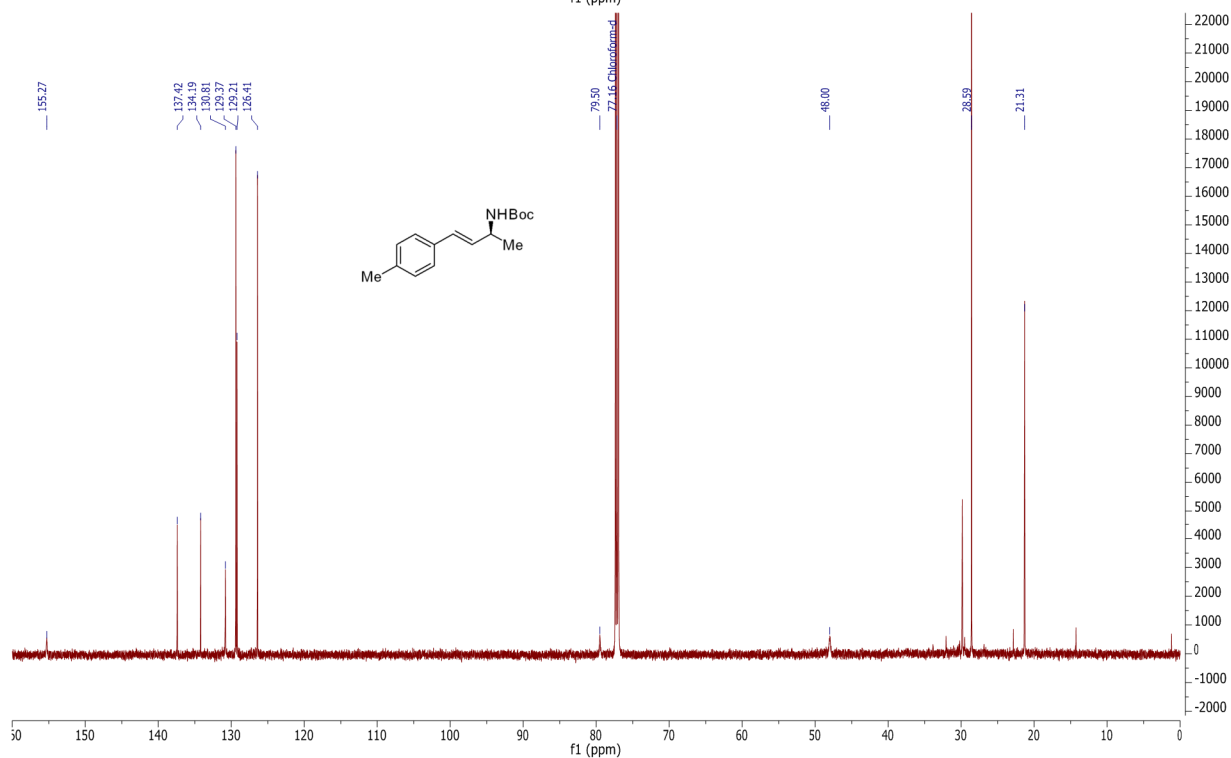
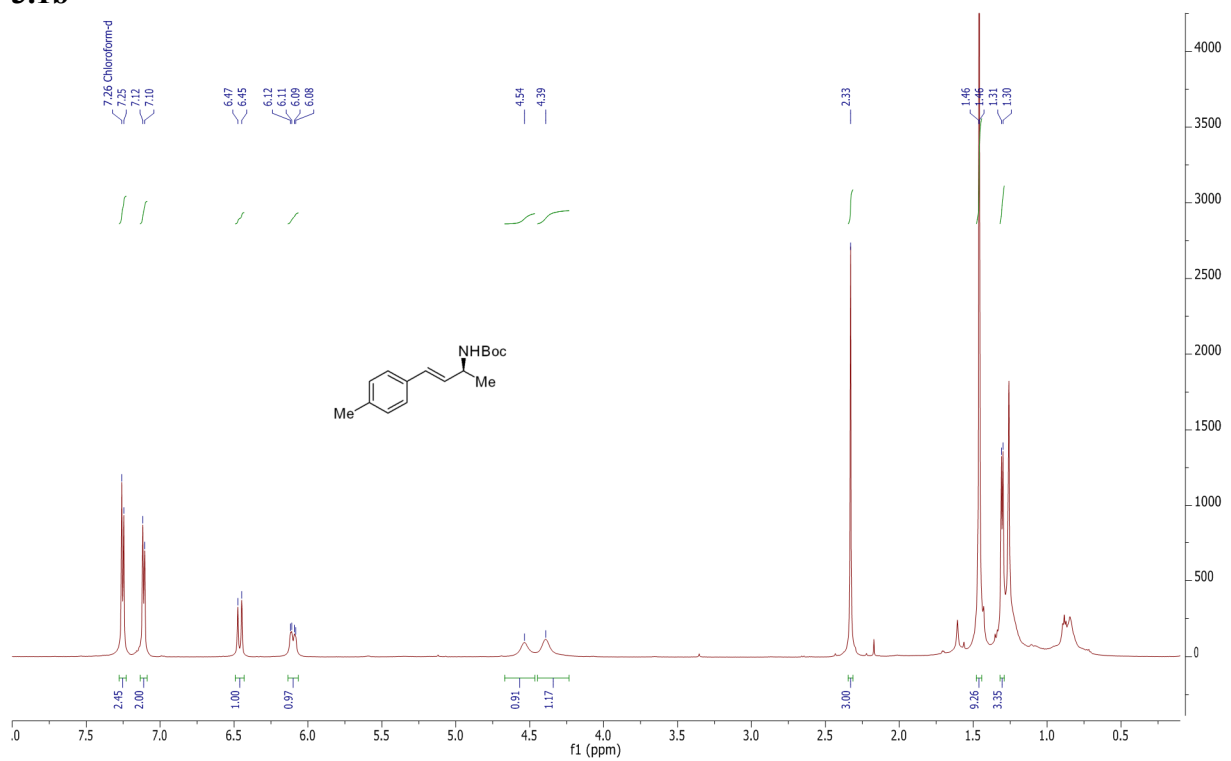
Appendix 1 - NMR Spectra

In some cases, unintegrated resonances in the 0-2 ppm region may appear. These correspond to trace quantities of residual solvents, including water, grease, and other aliphatic hydrocarbons.

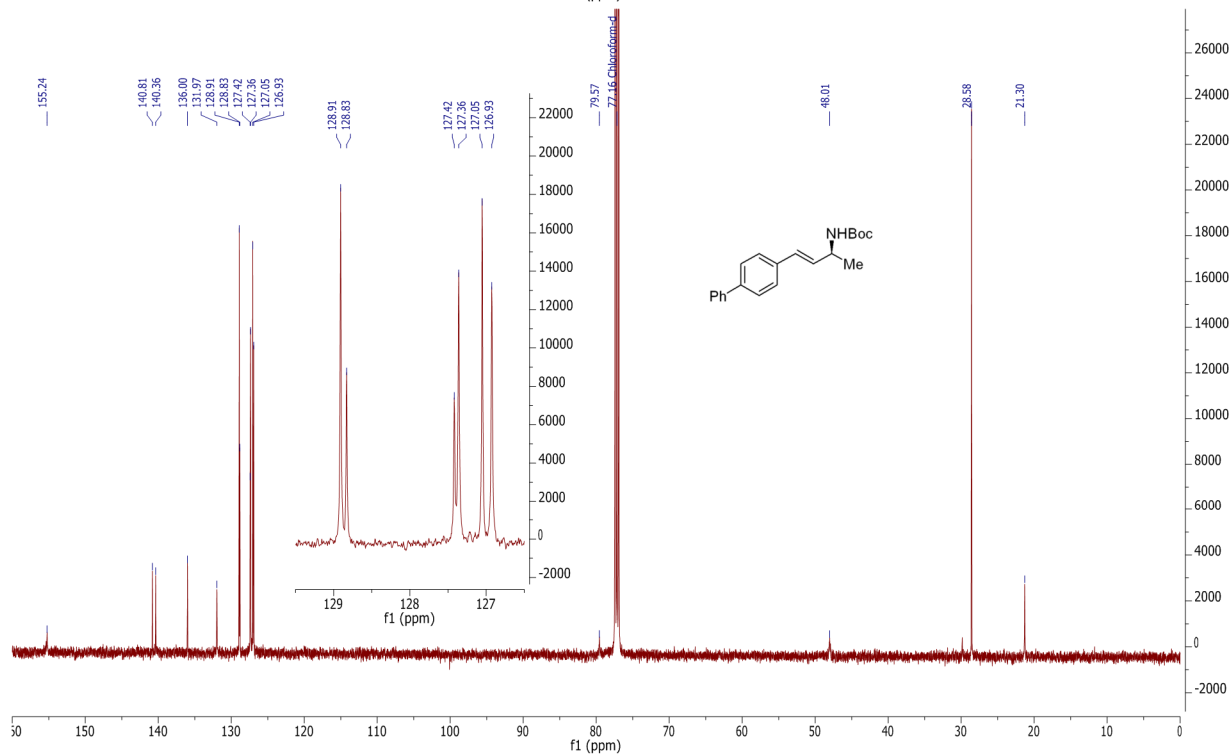
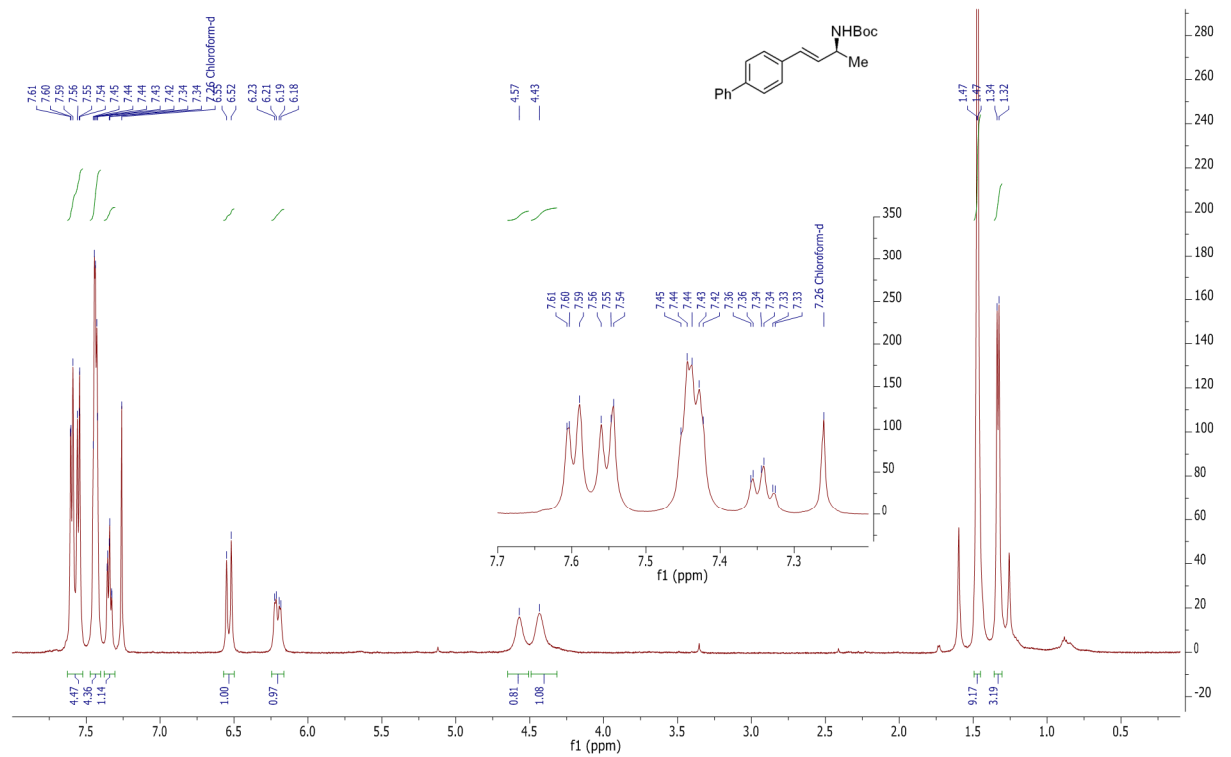
3.1a



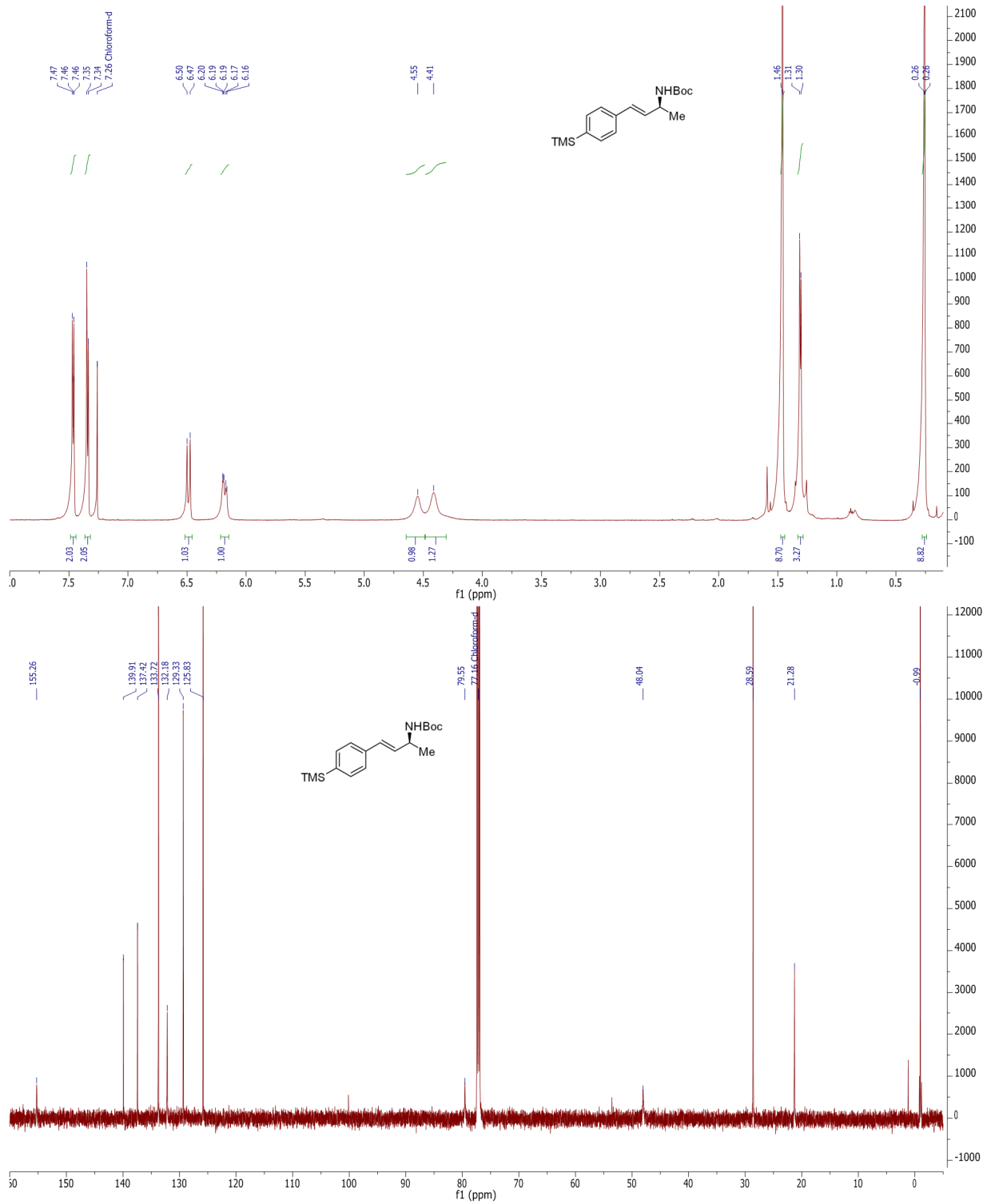
3.1b



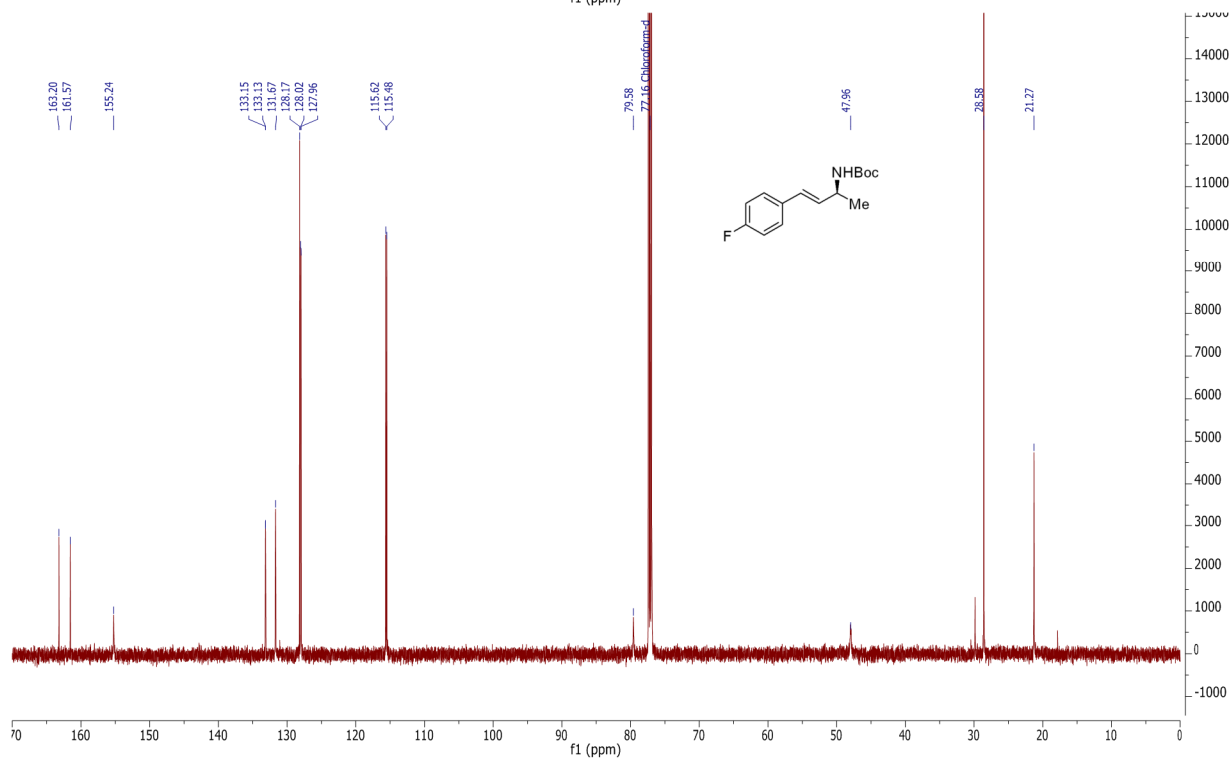
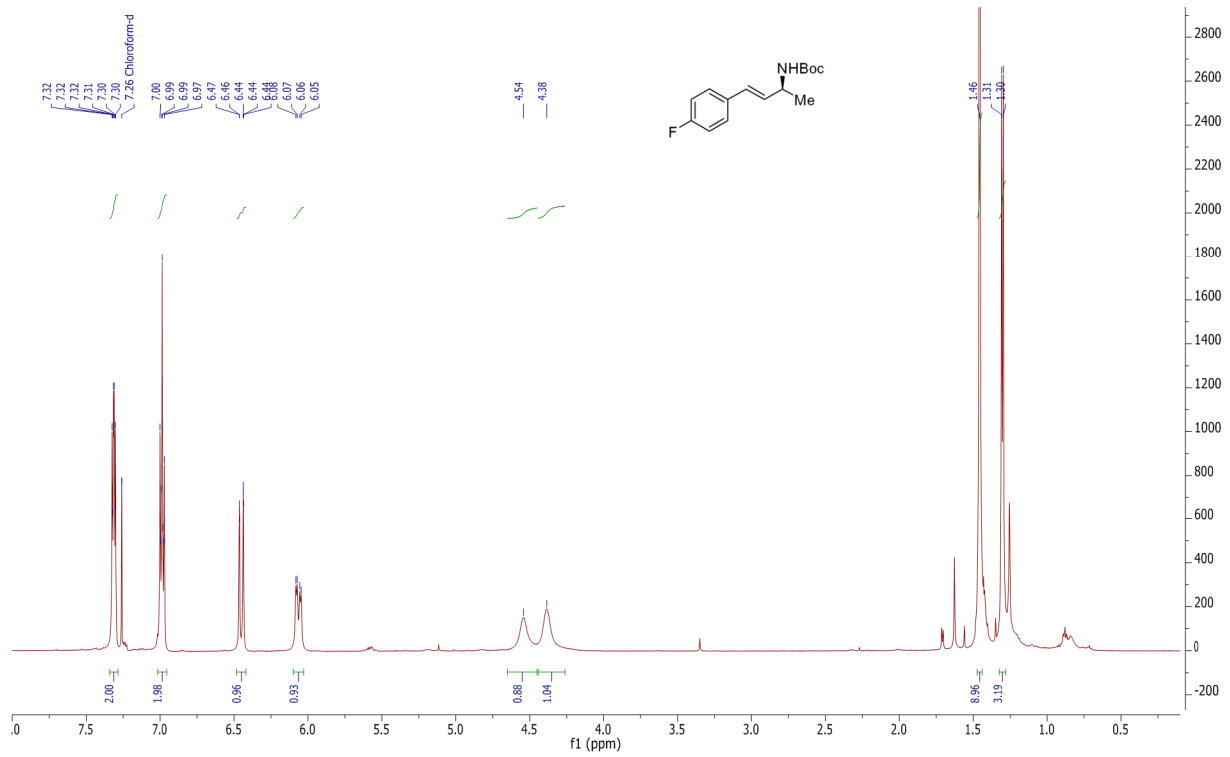
3.1c



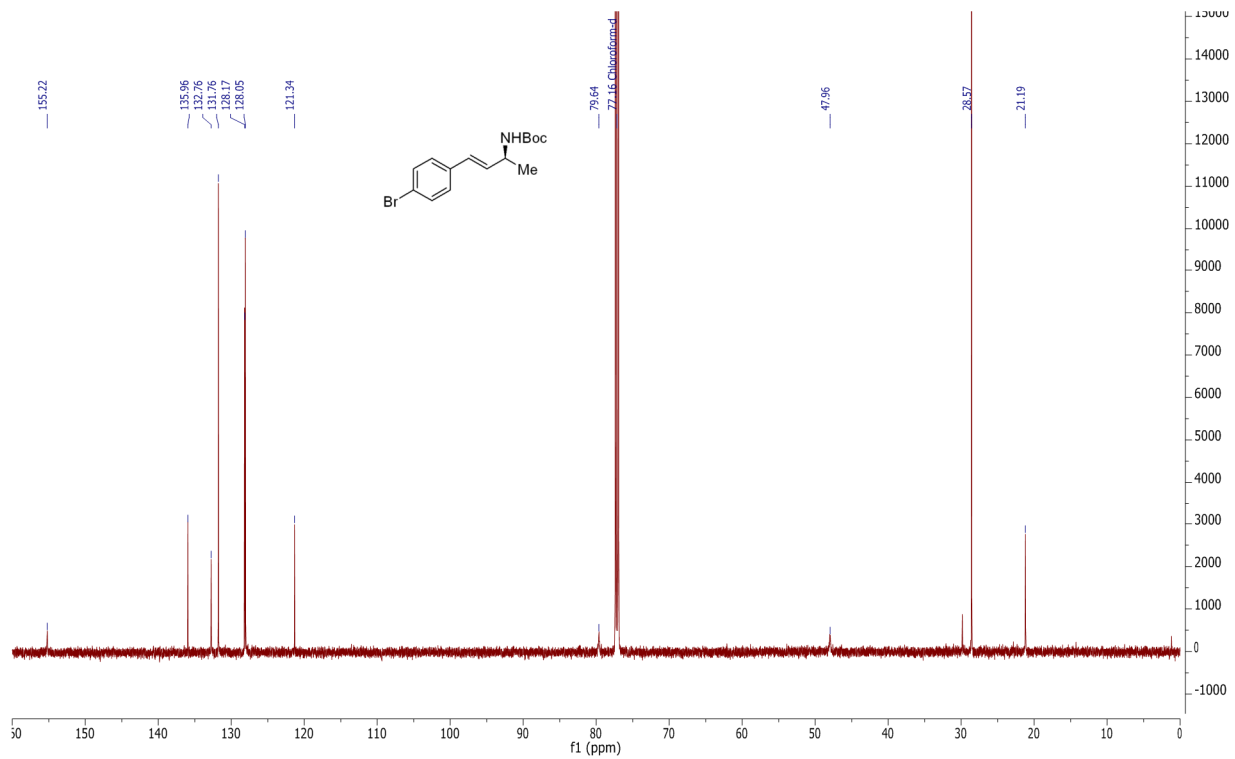
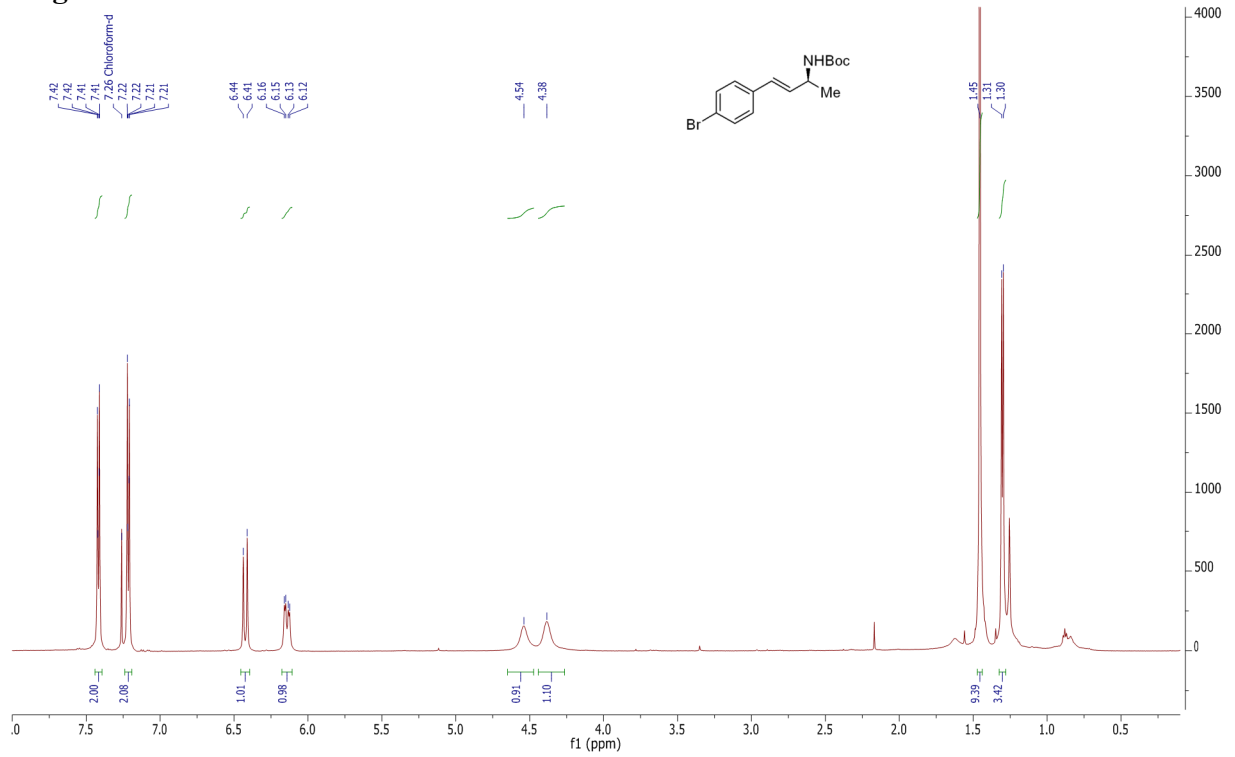
3.1d



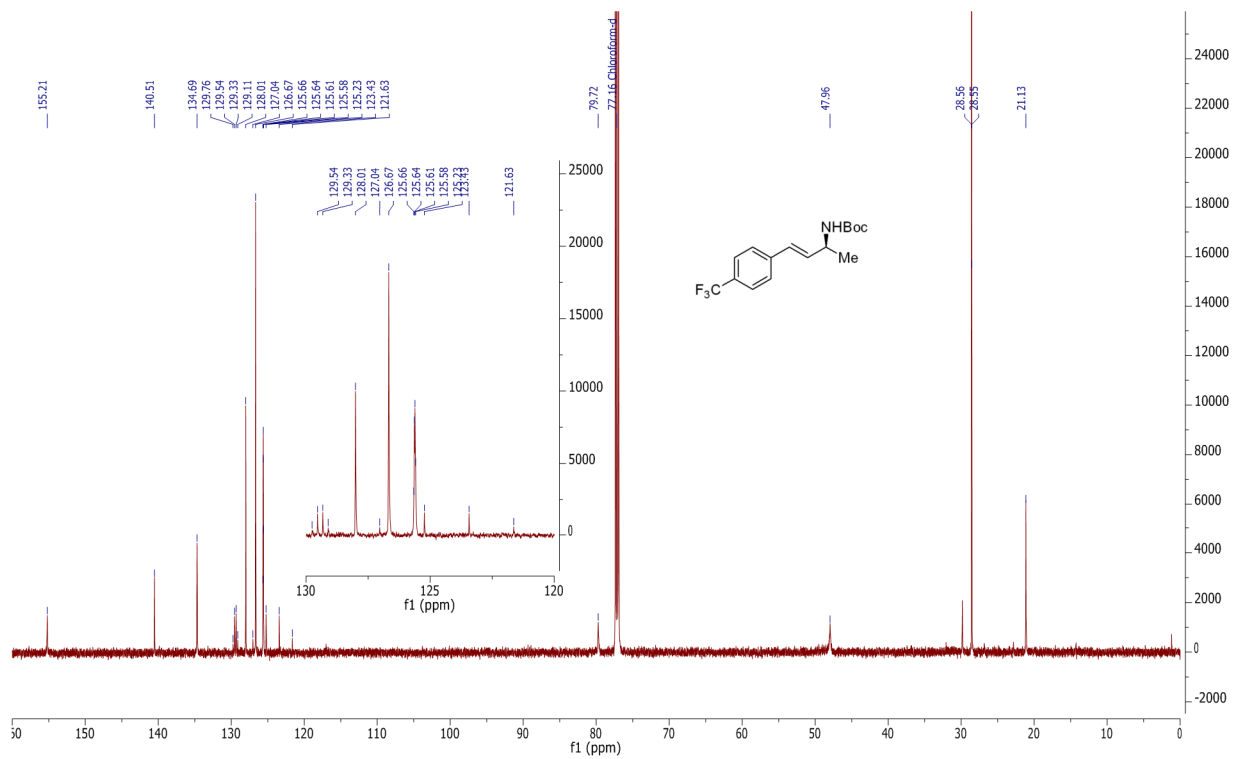
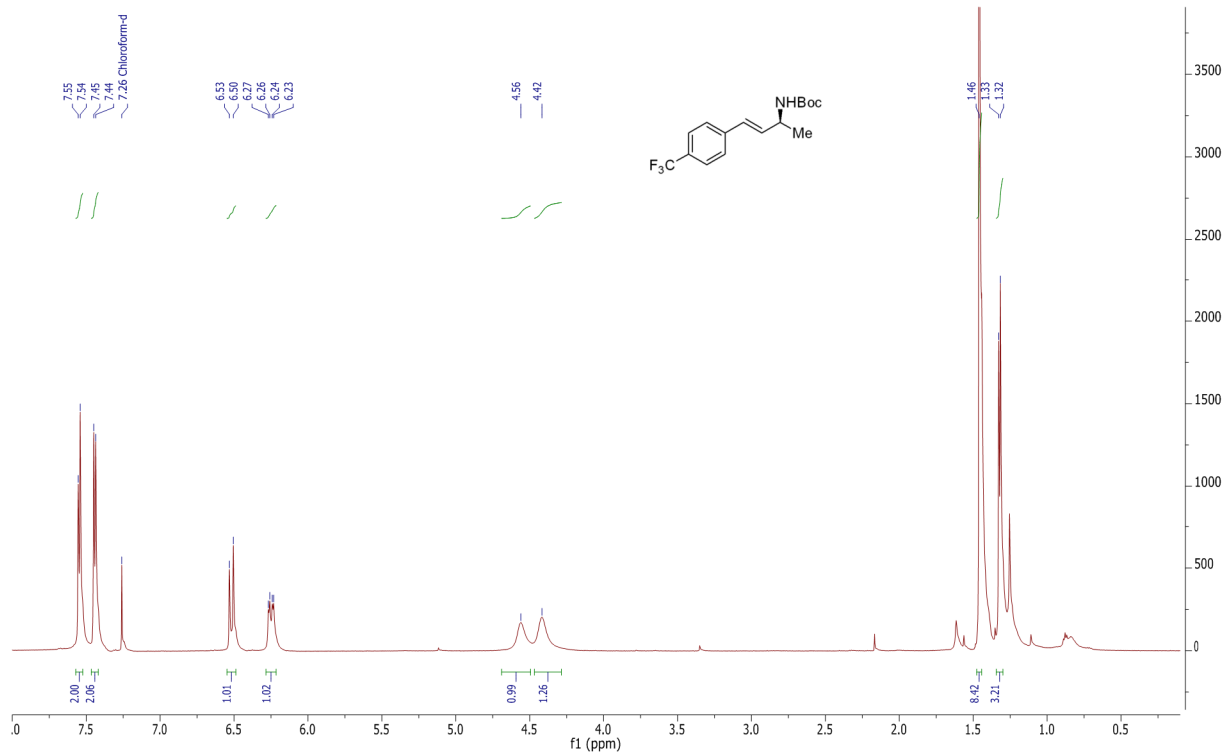
3.1e



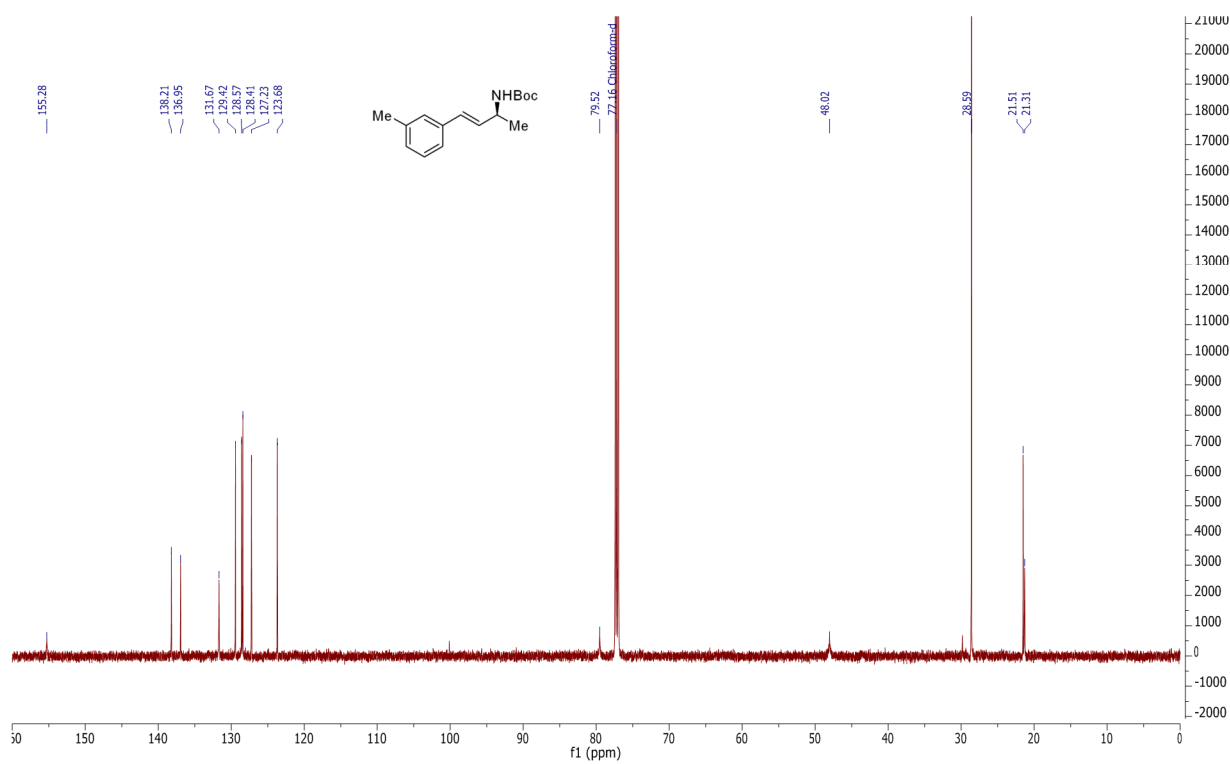
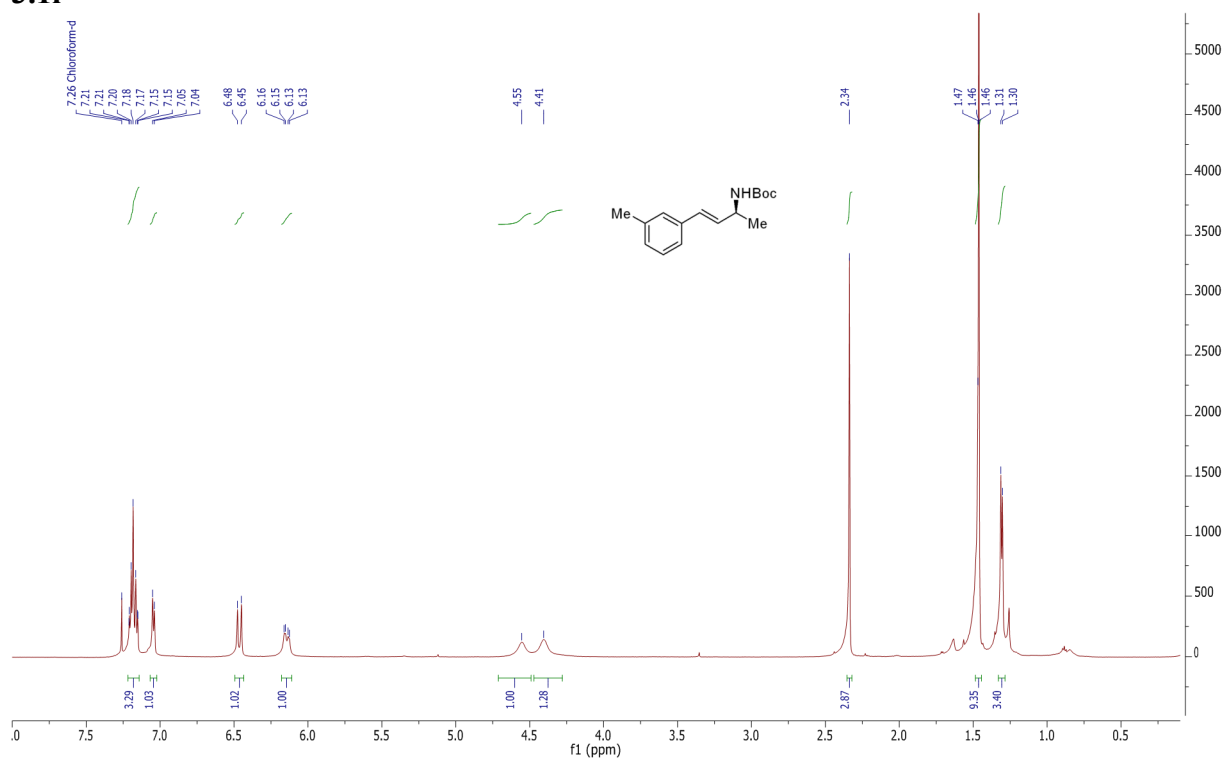
3.1g



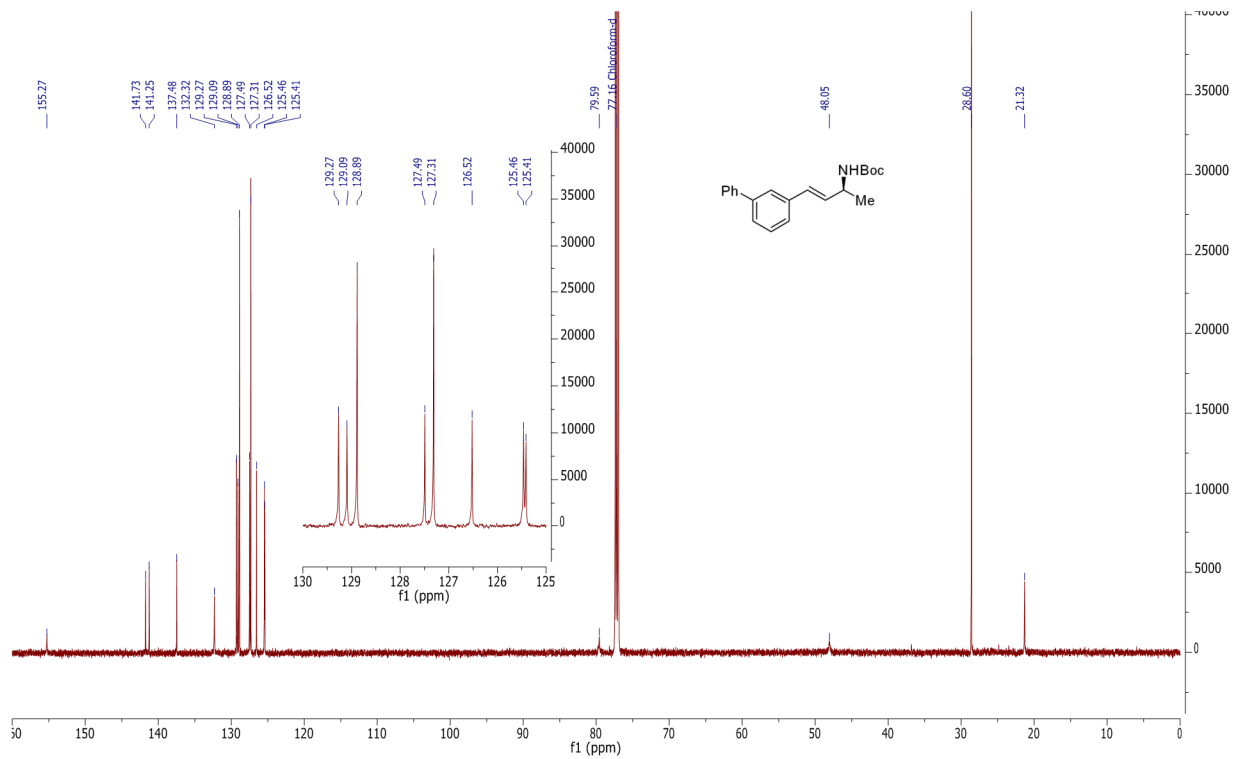
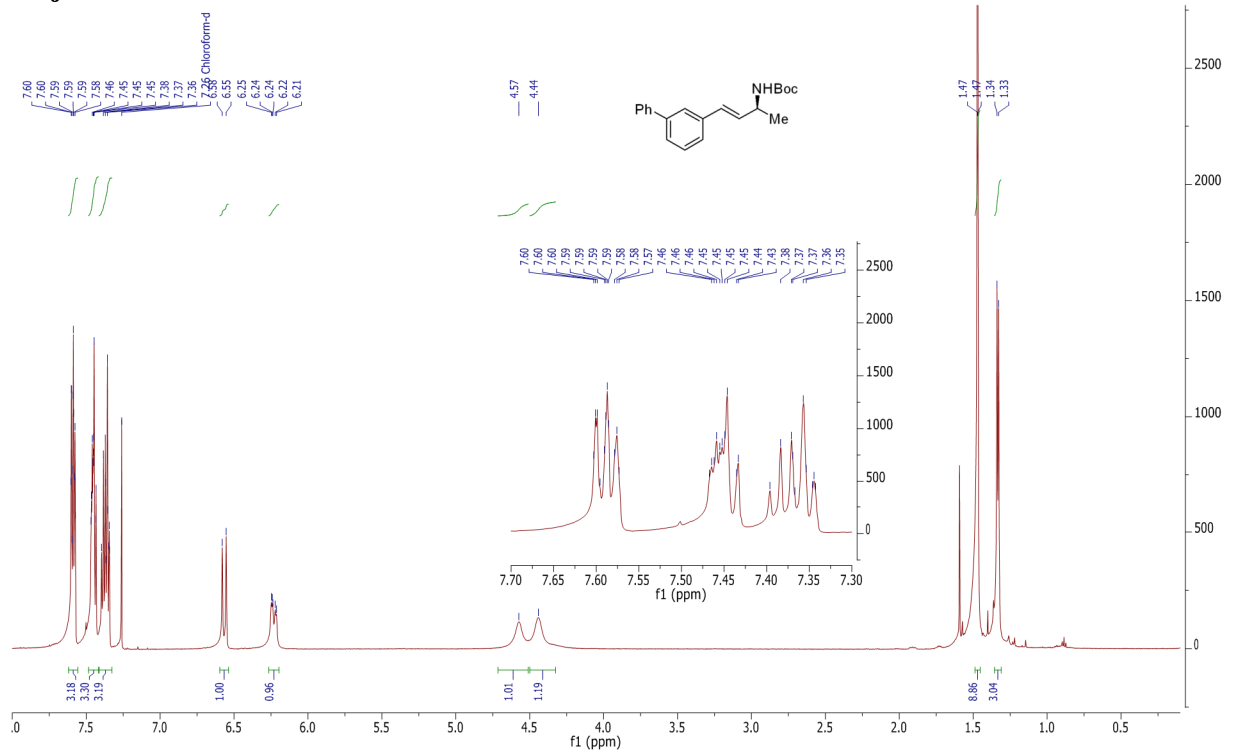
3.1h



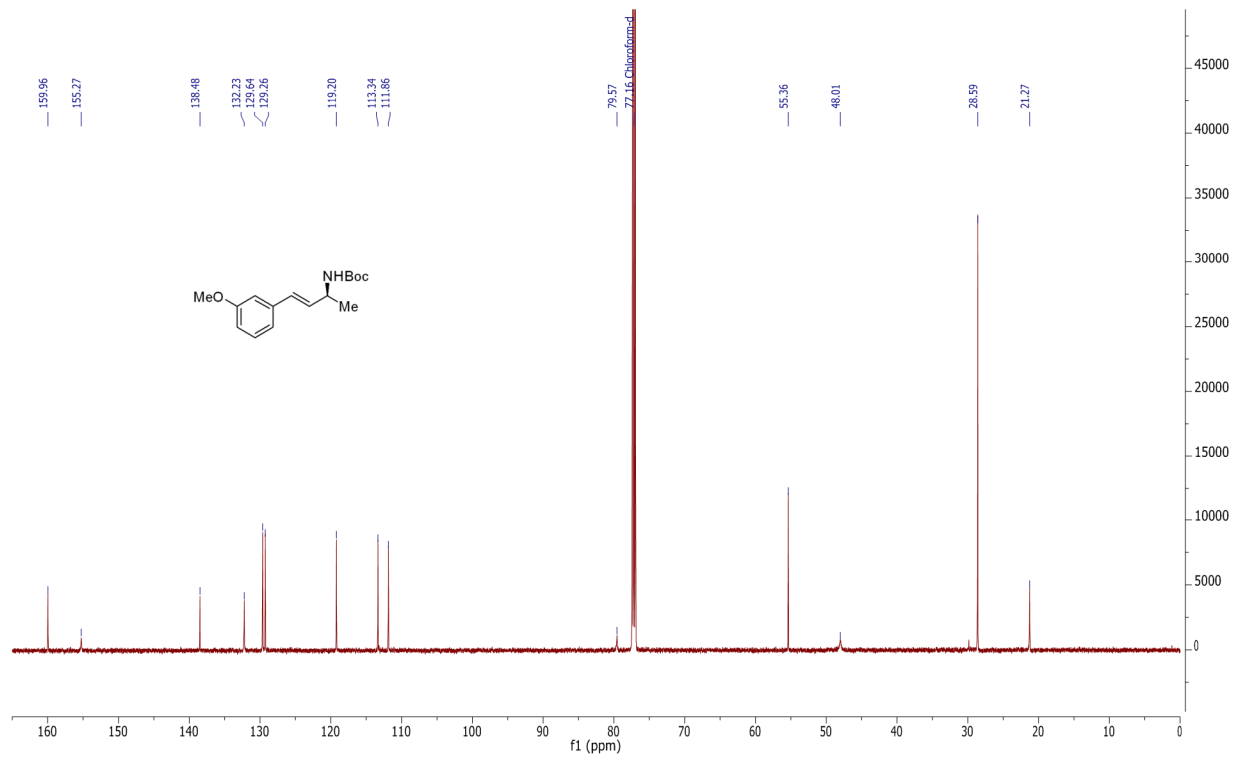
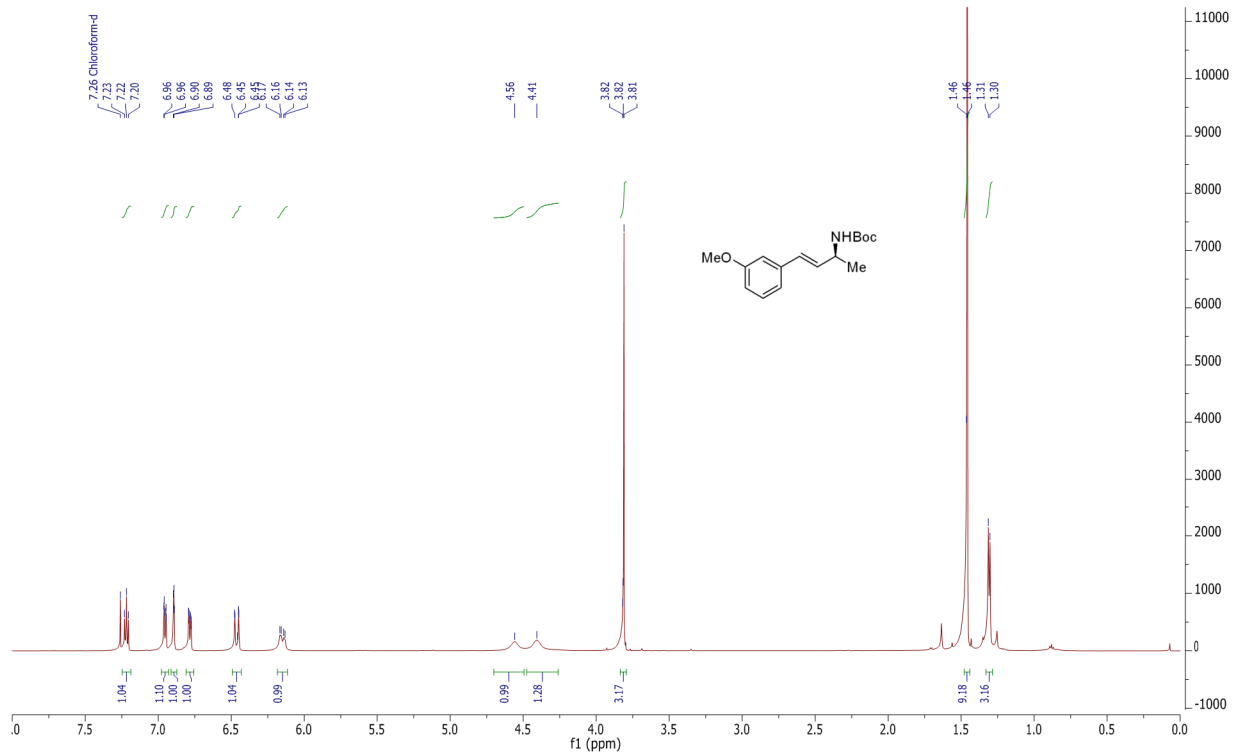
3.1i



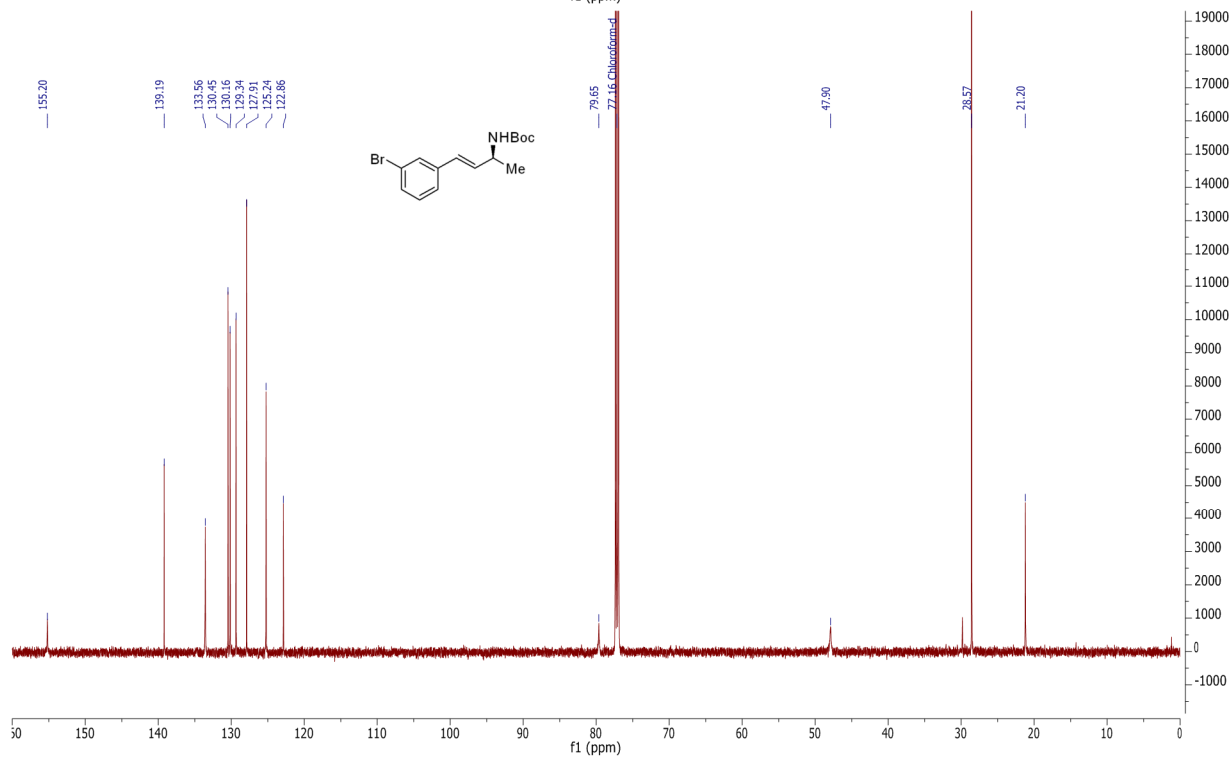
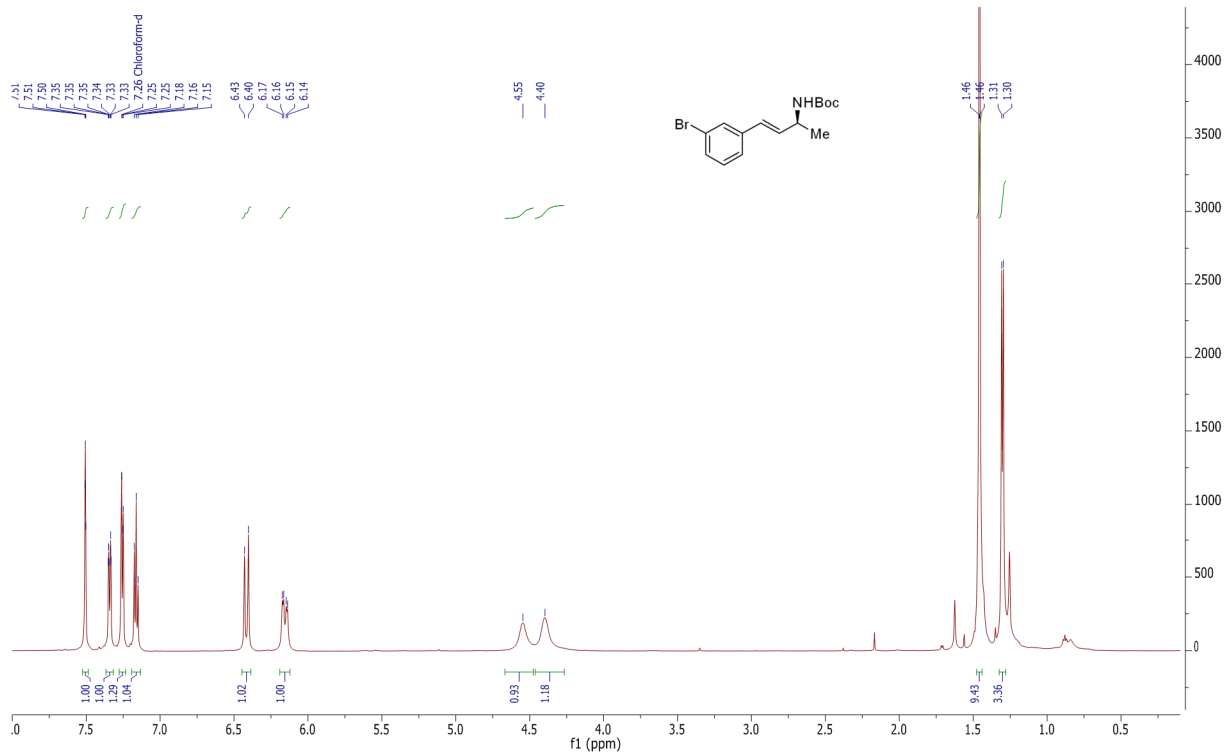
3.1j



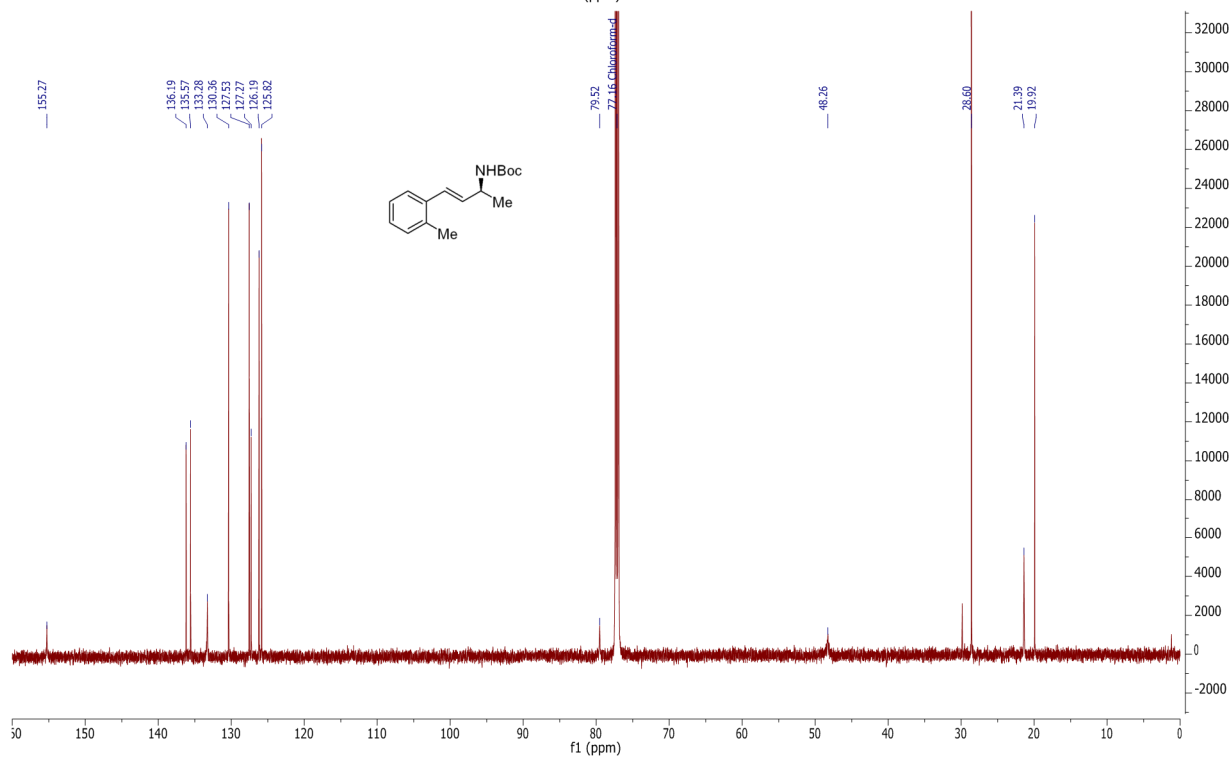
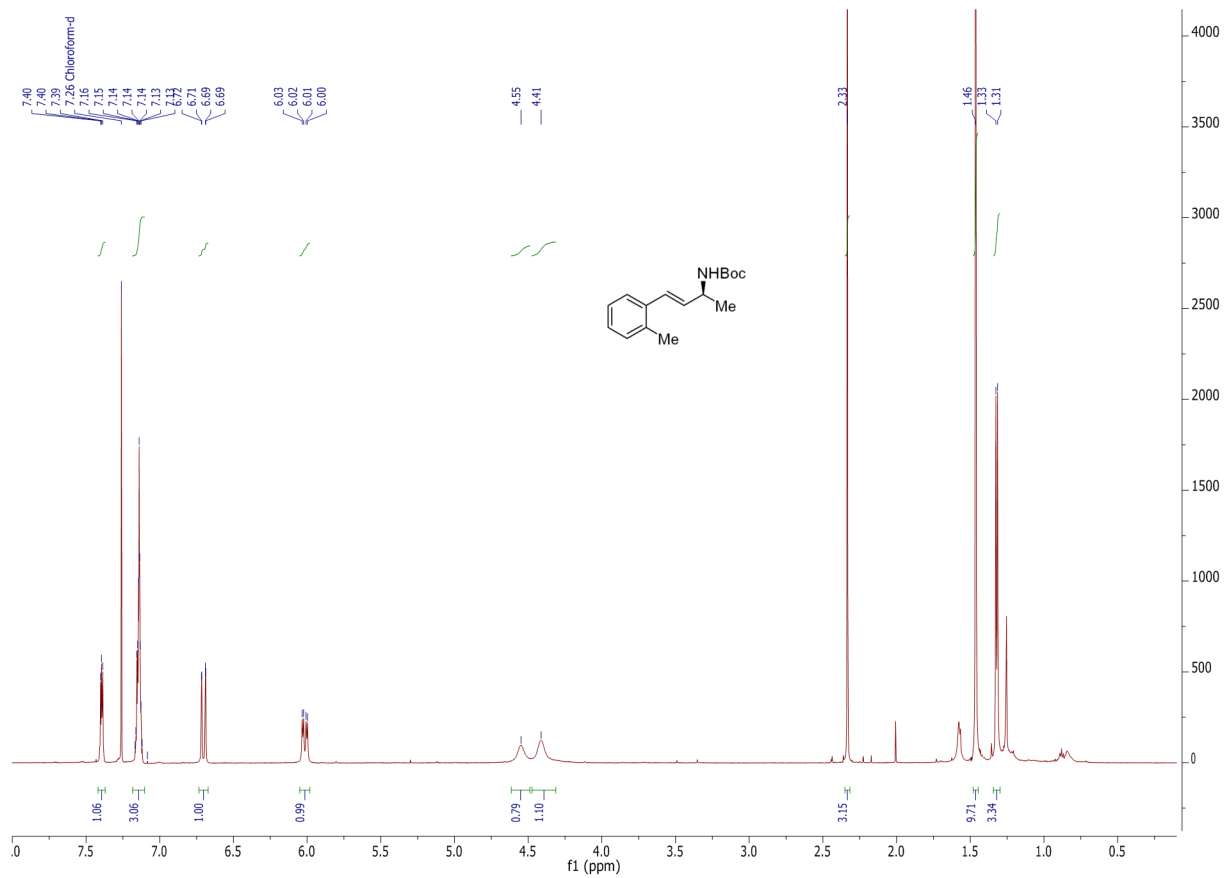
3.1k



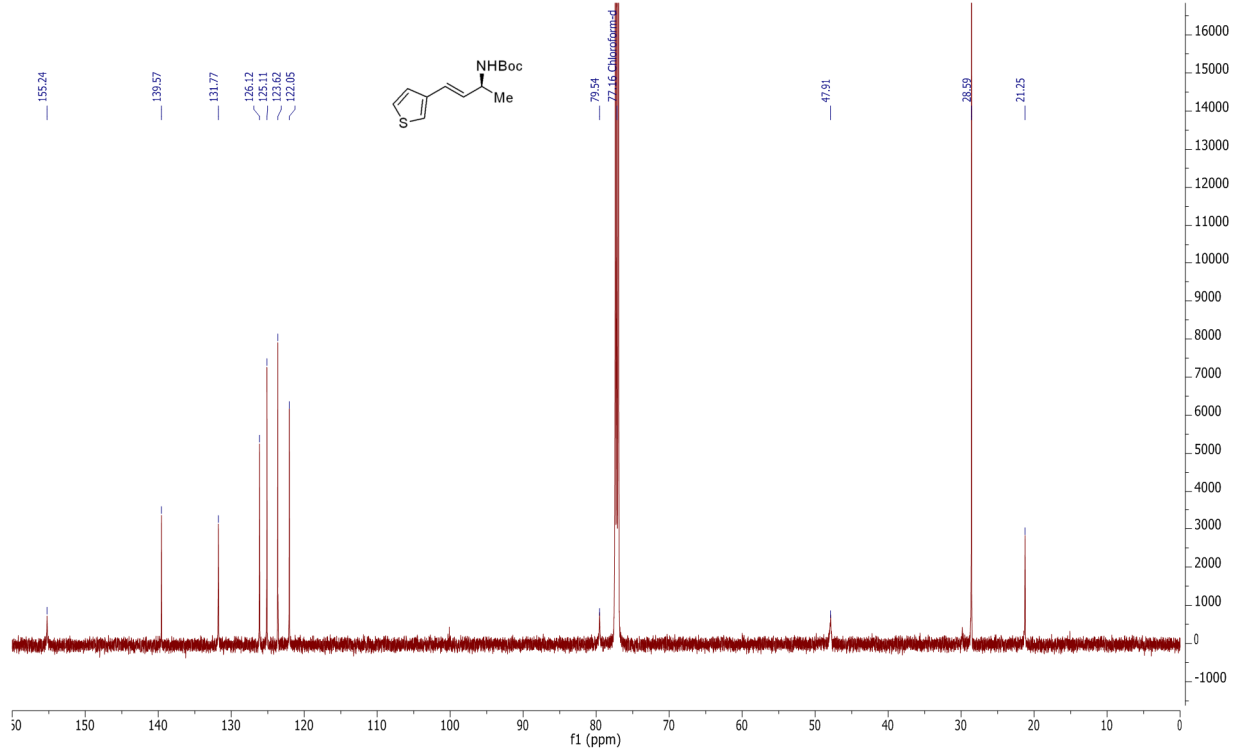
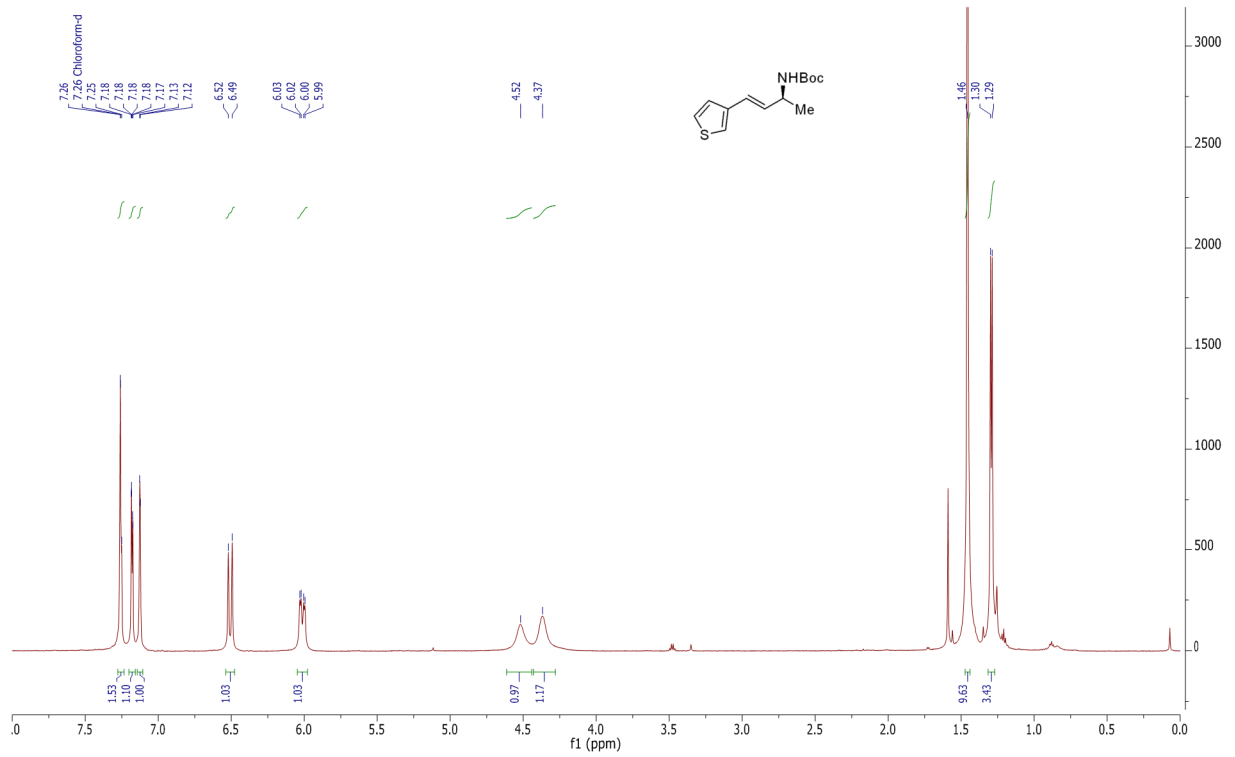
3.1n



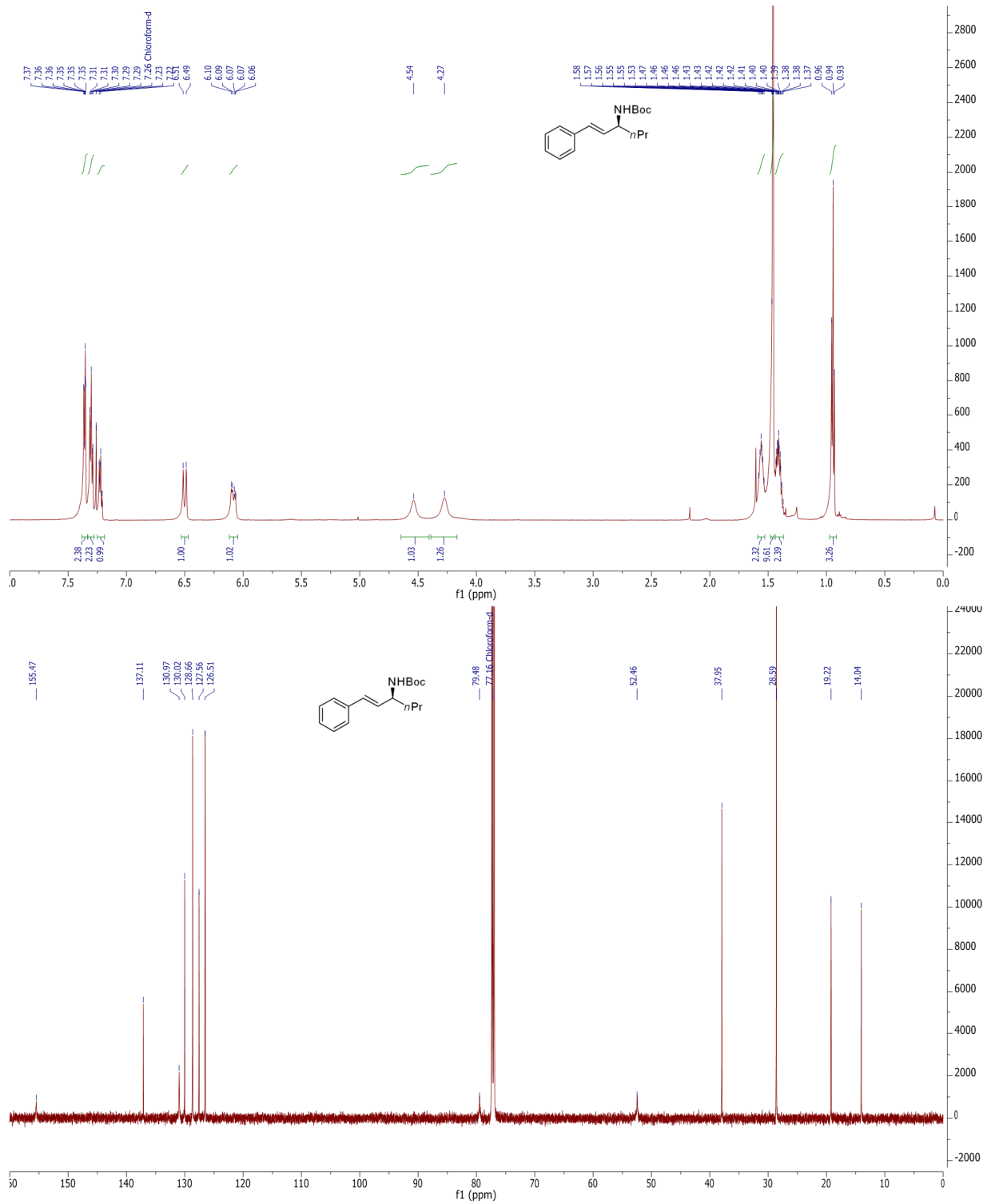
3.1o



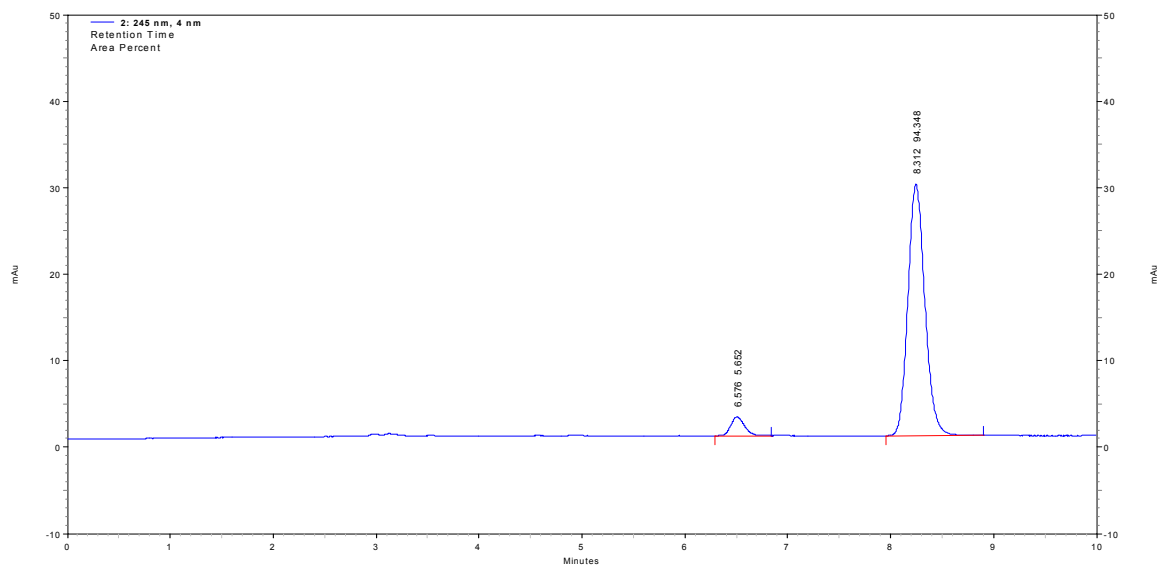
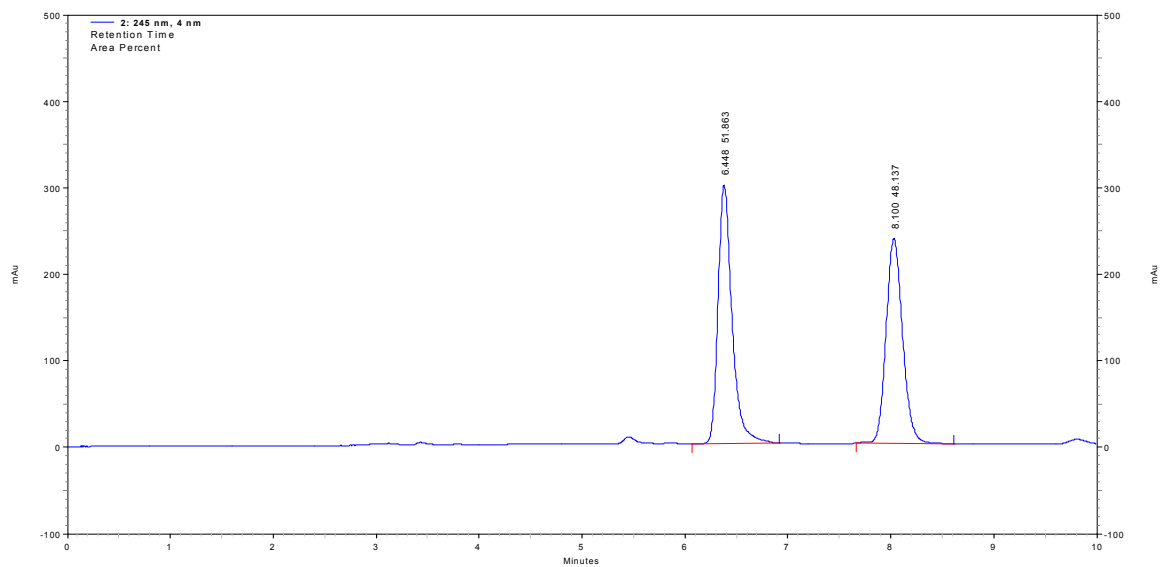
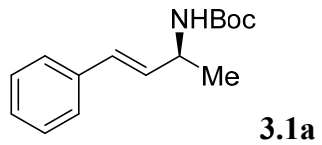
3.1r



3.1t



Appendix 2 - HPLC Traces



245 nm

Retention Time

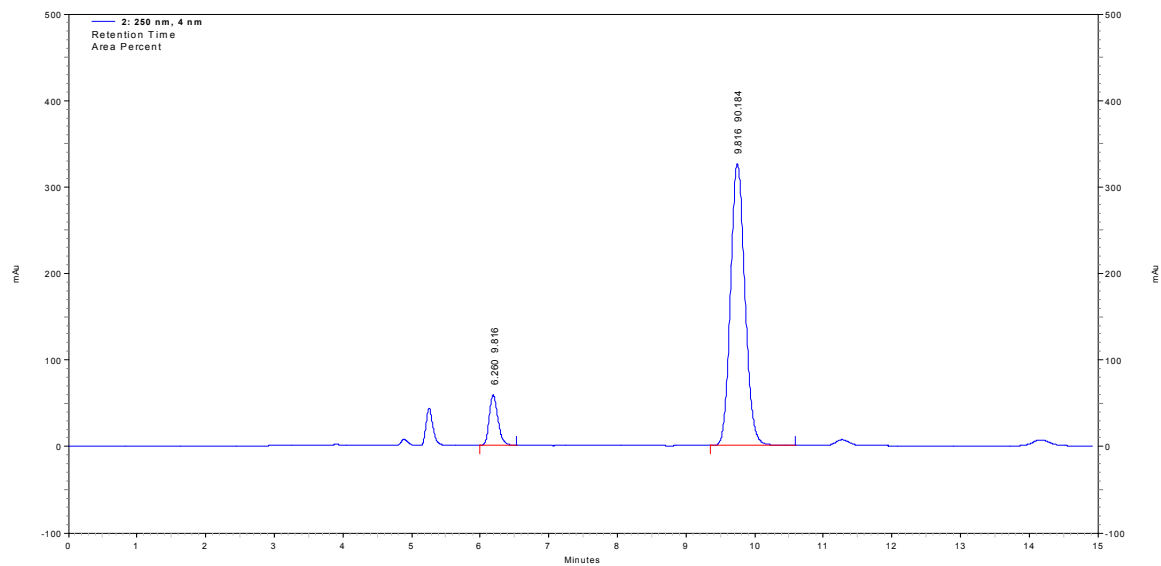
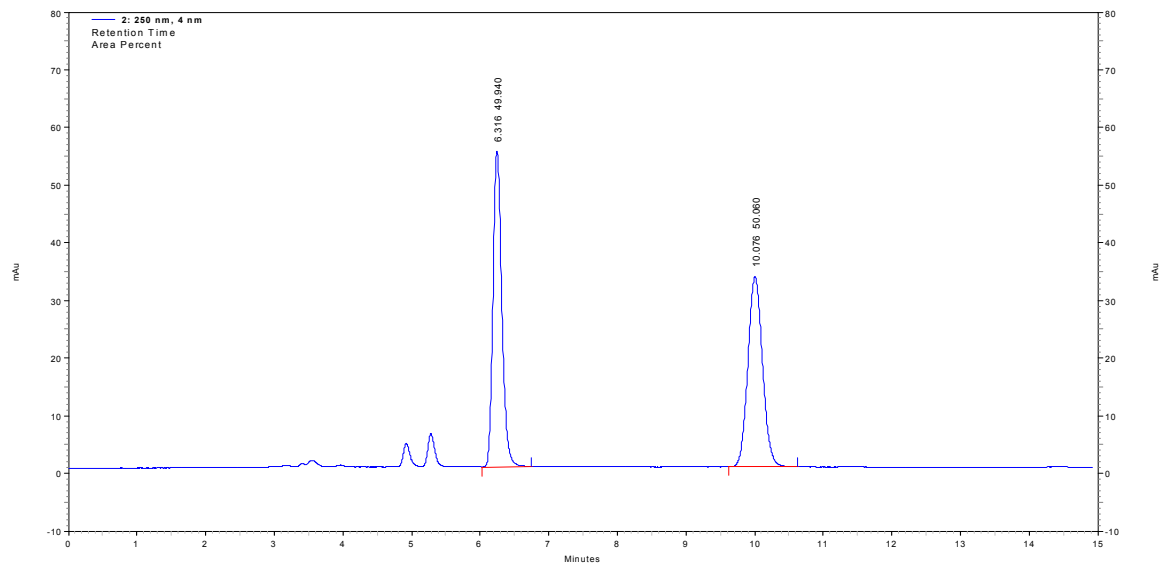
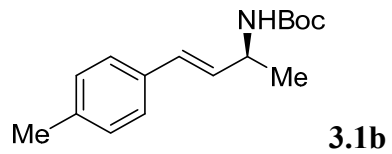
Area Percent

6.576

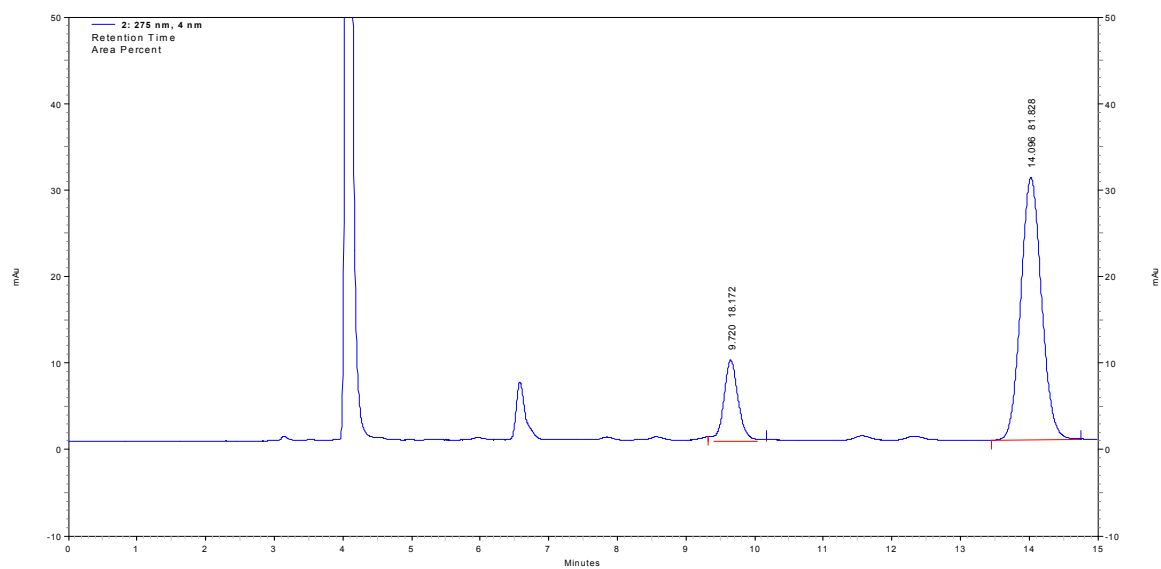
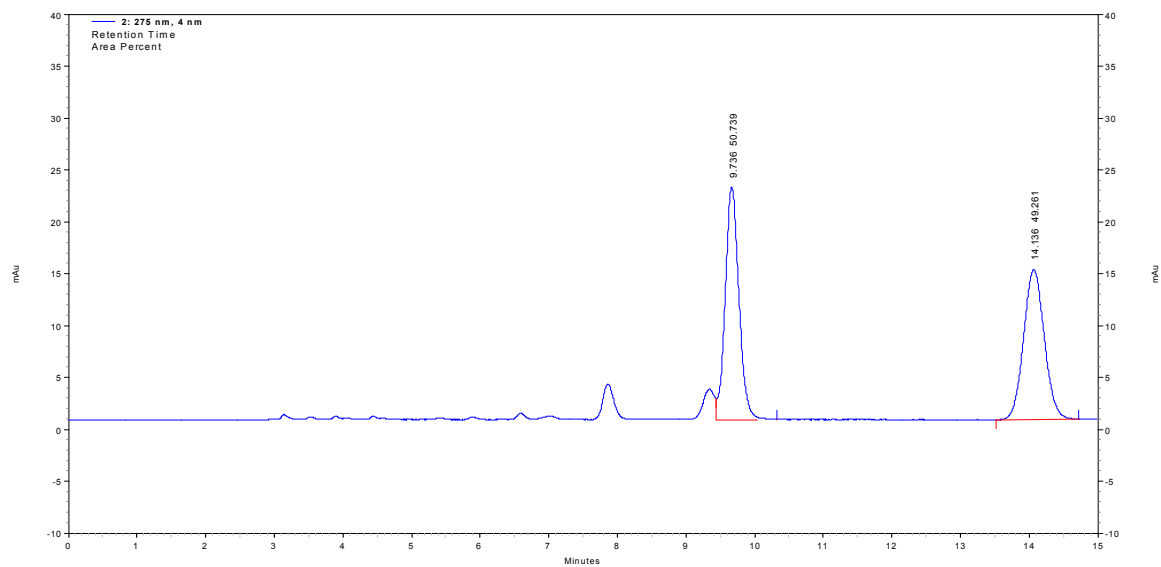
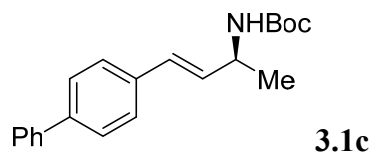
5.652

8.312

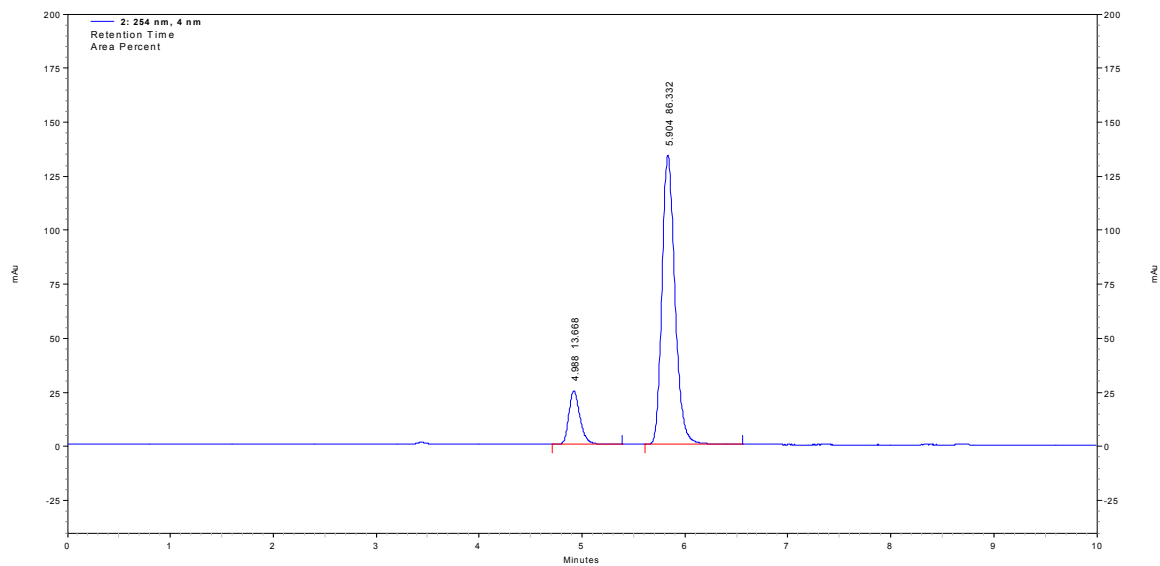
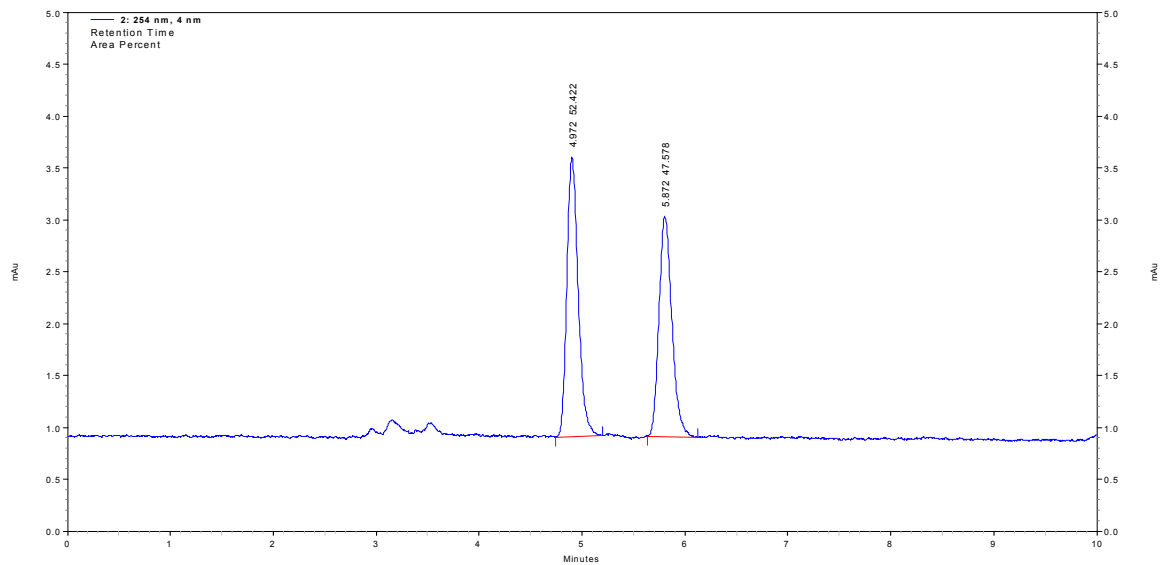
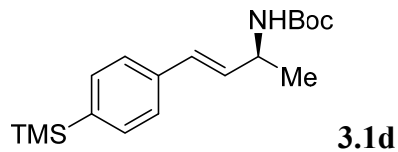
94.348



| 250 nm | Retention Time | Area Percent |
|--------|----------------|--------------|
| | 6.260 | 9.816 |
| | 9.816 | 90.184 |



| 275 nm Retention Time | Area Percent |
|--------------------------|--------------|
| 9.720 | 18.172 |
| 14.096 | 81.828 |



254 nm

Retention Time

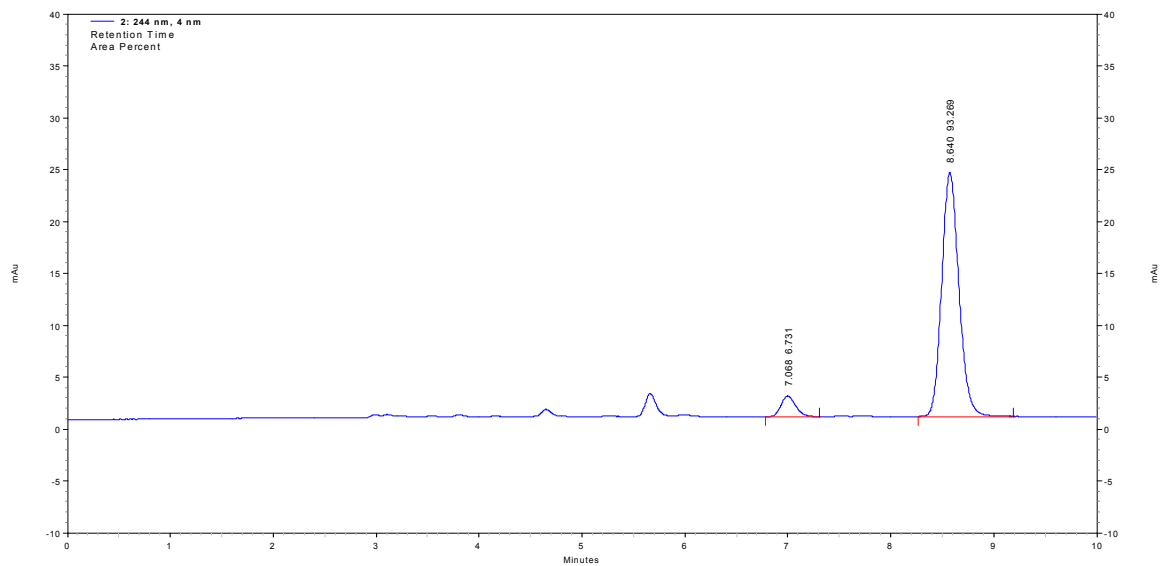
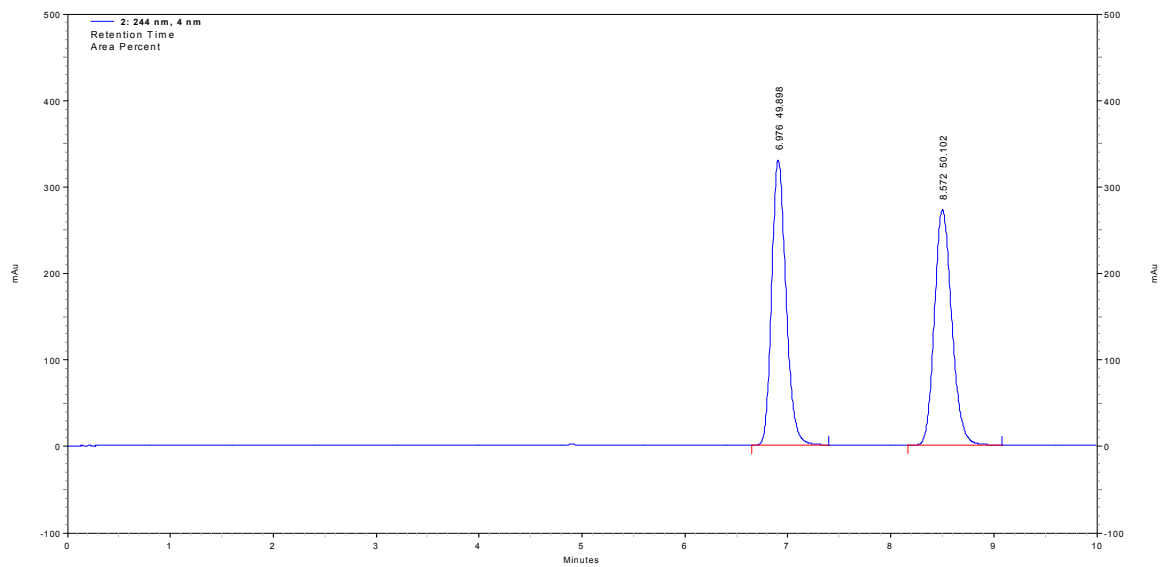
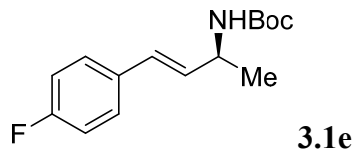
Area Percent

4.988

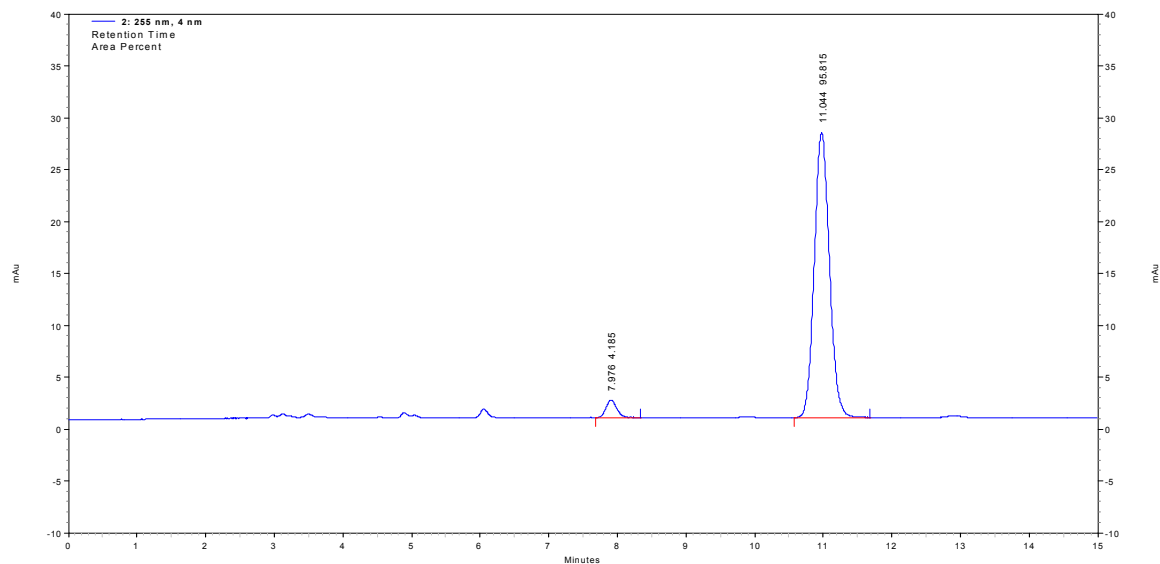
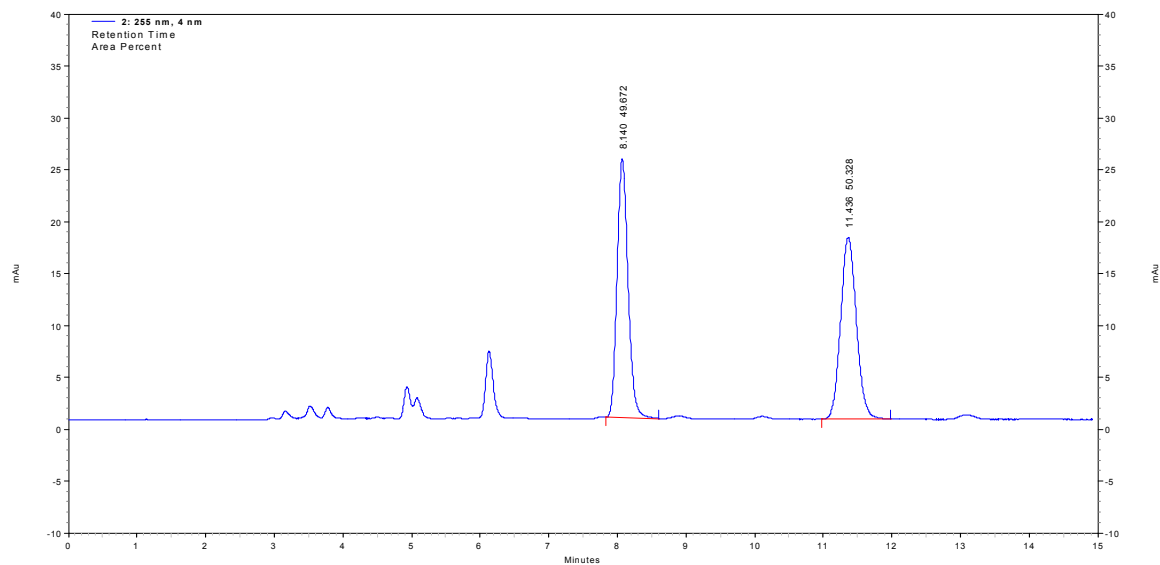
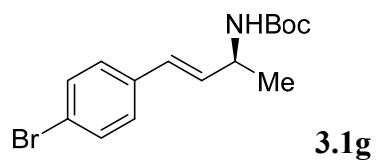
13.668

5.904

86.332



| 244 nm | |
|----------------|--------------|
| Retention Time | Area Percent |
| 7.068 | 6.731 |
| 8.640 | 93.269 |



255 nm

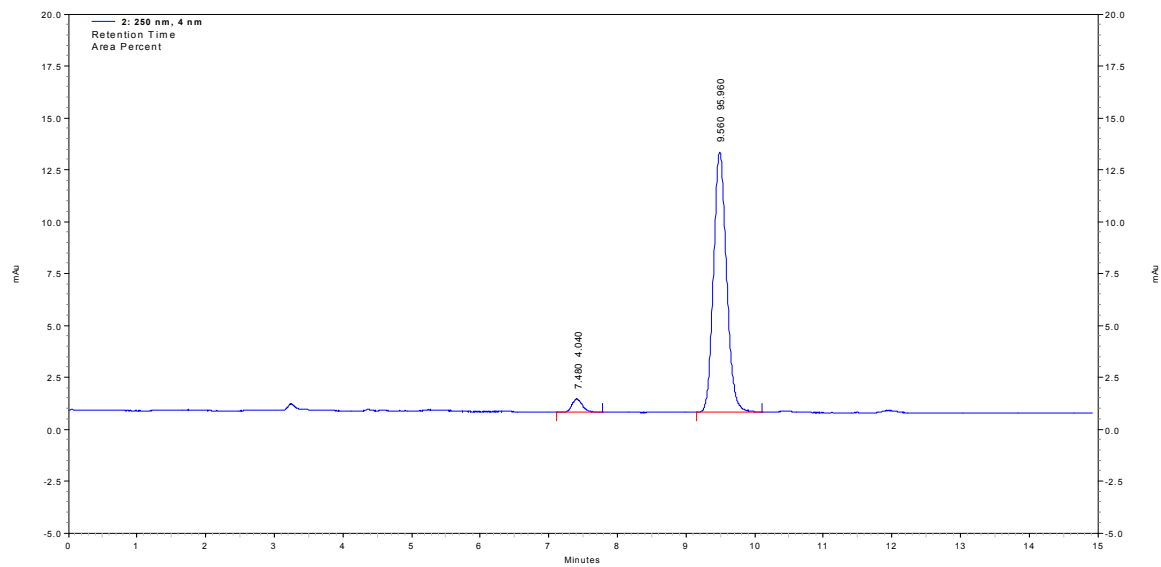
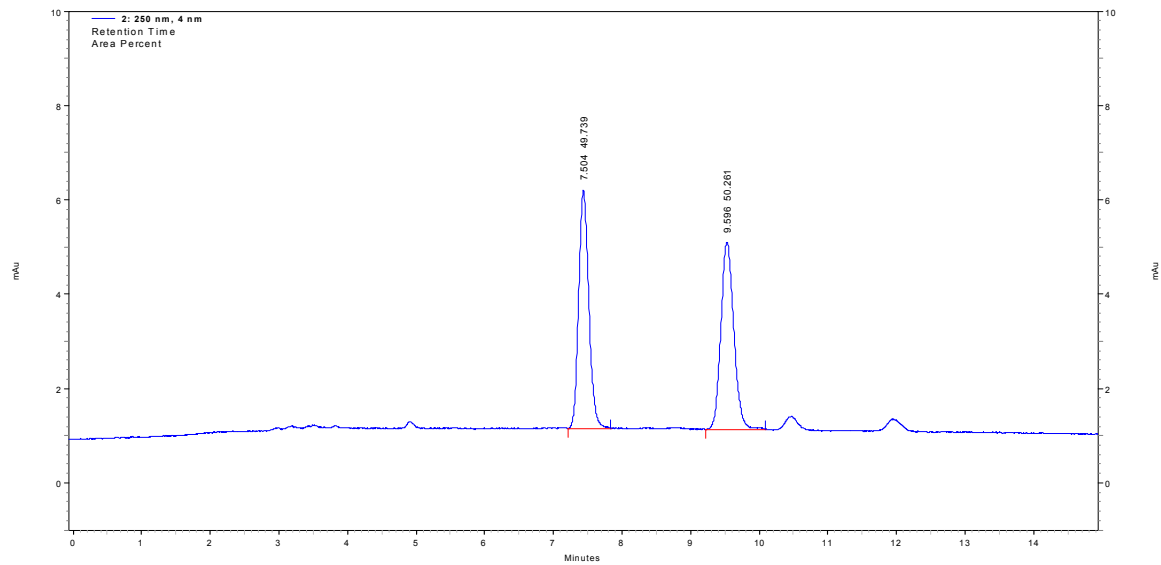
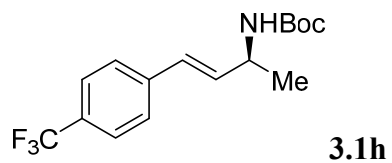
Retention Time Area Percent

7.976

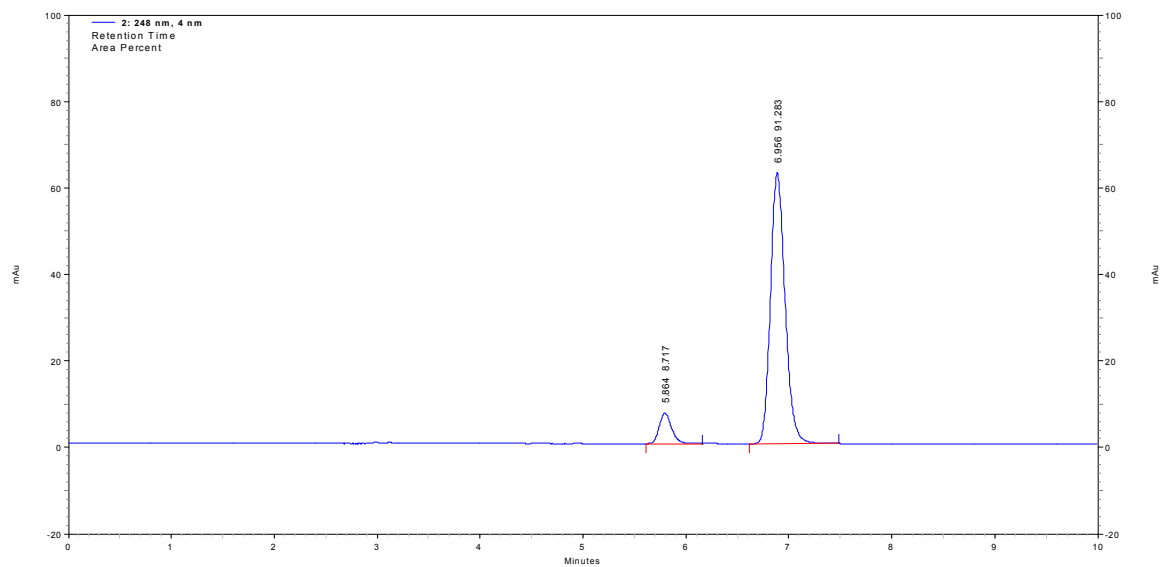
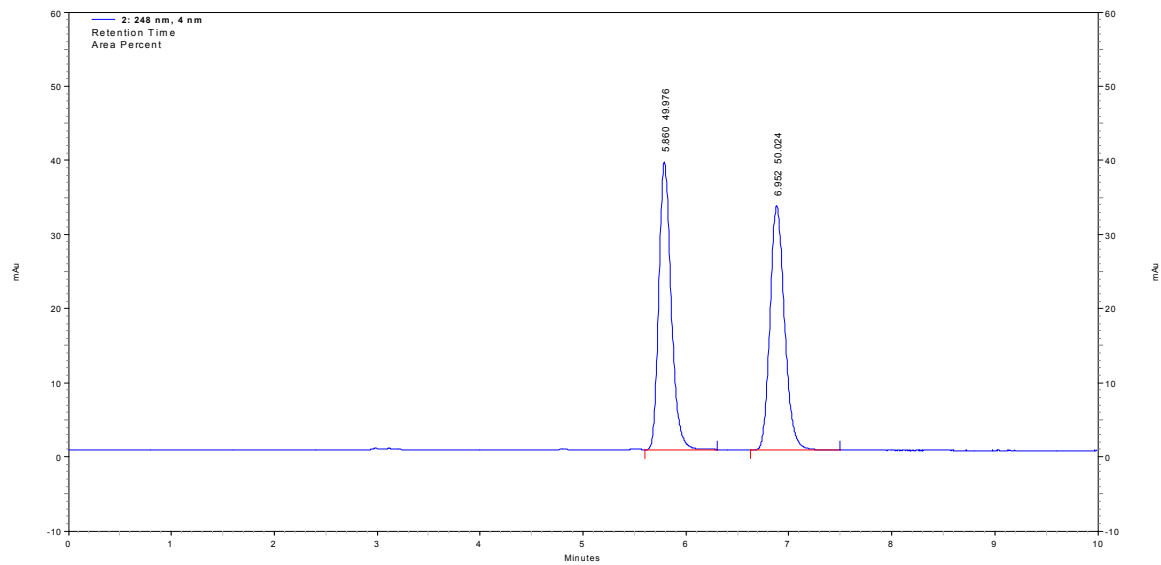
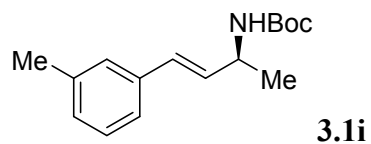
4.185

11.044

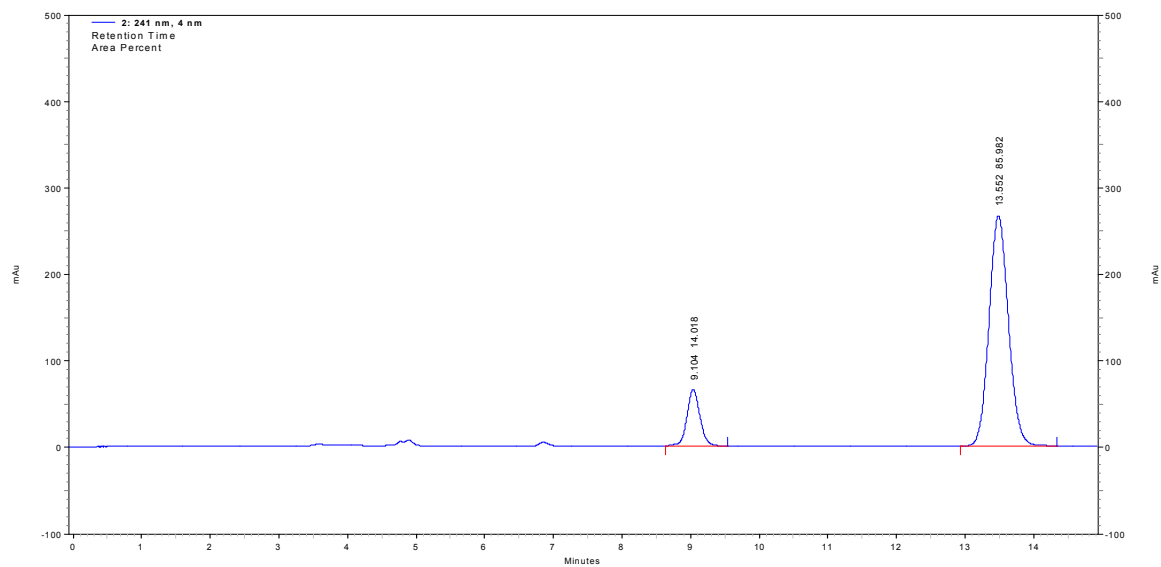
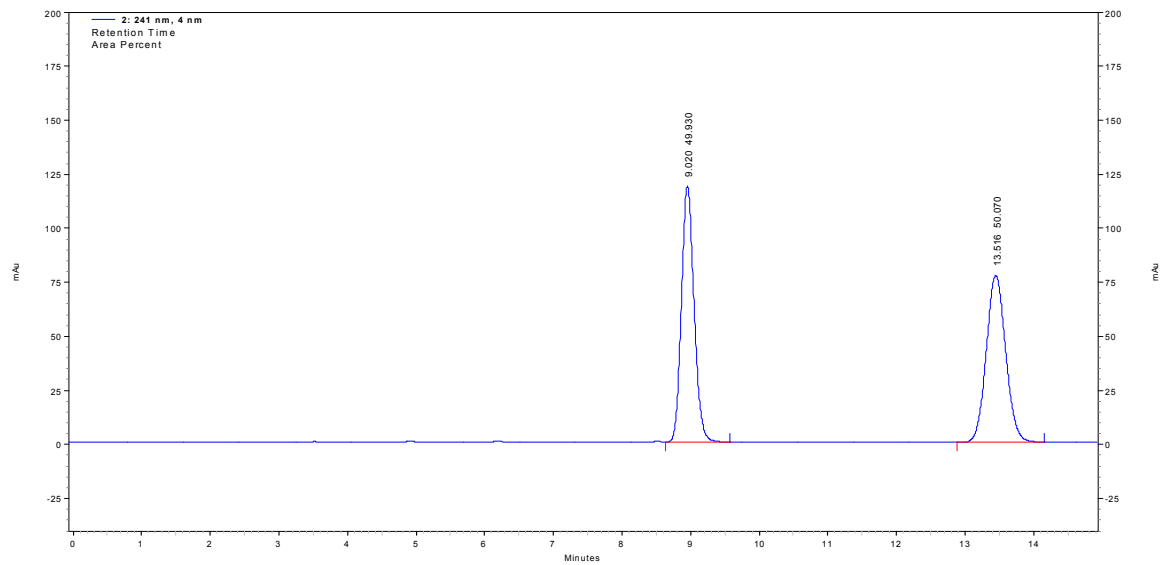
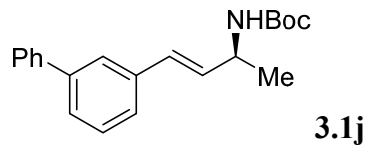
95.815



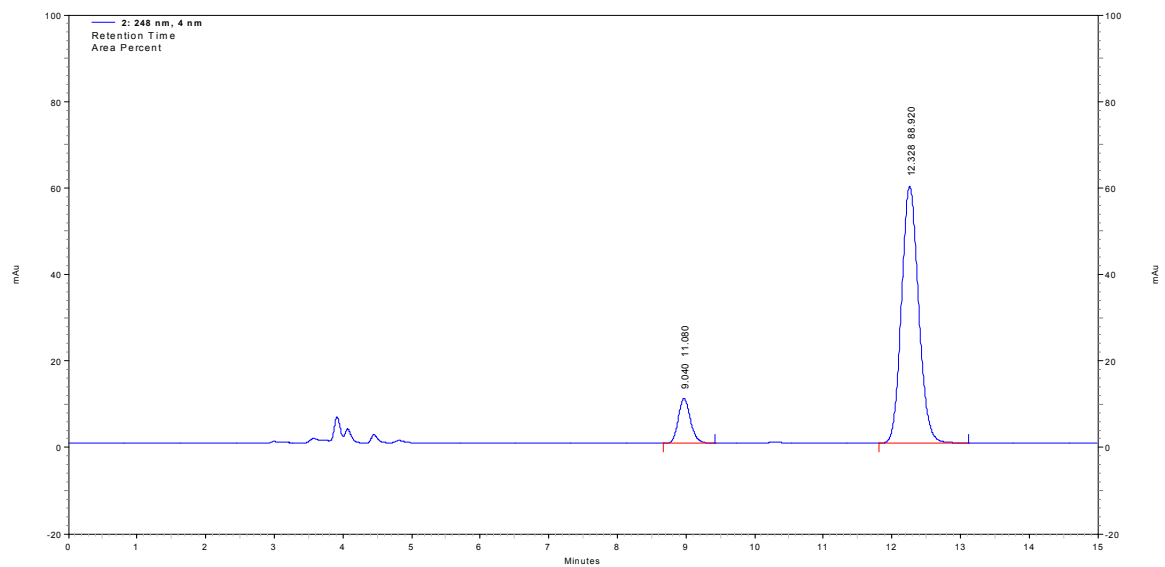
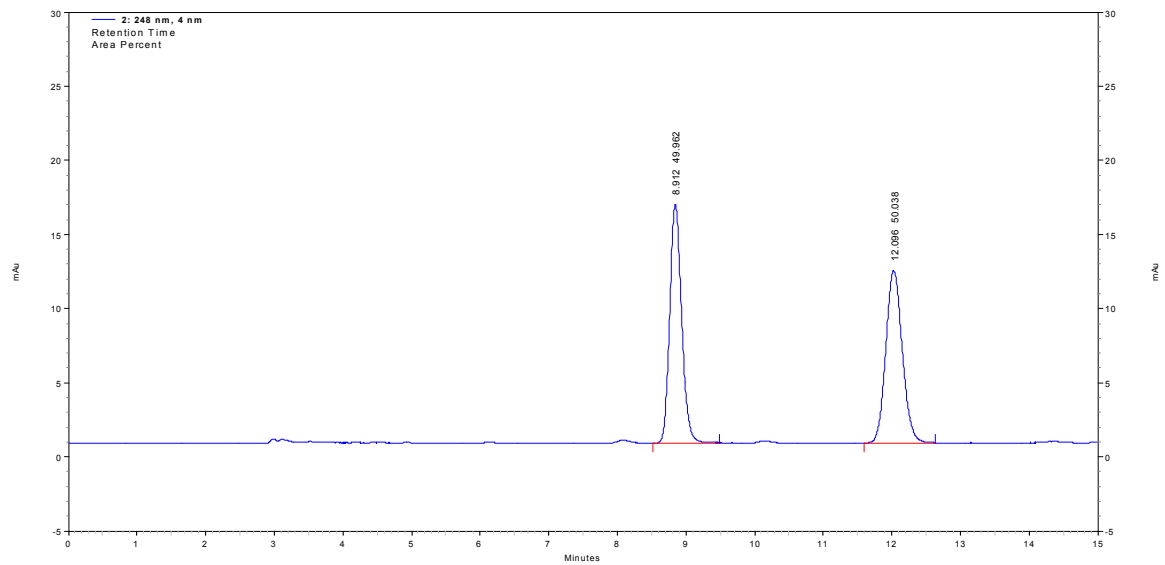
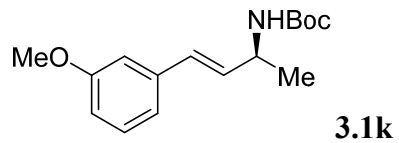
| Retention Time | Area Percent |
|----------------|--------------|
| 7.480 | 4.040 |
| 9.560 | 95.960 |



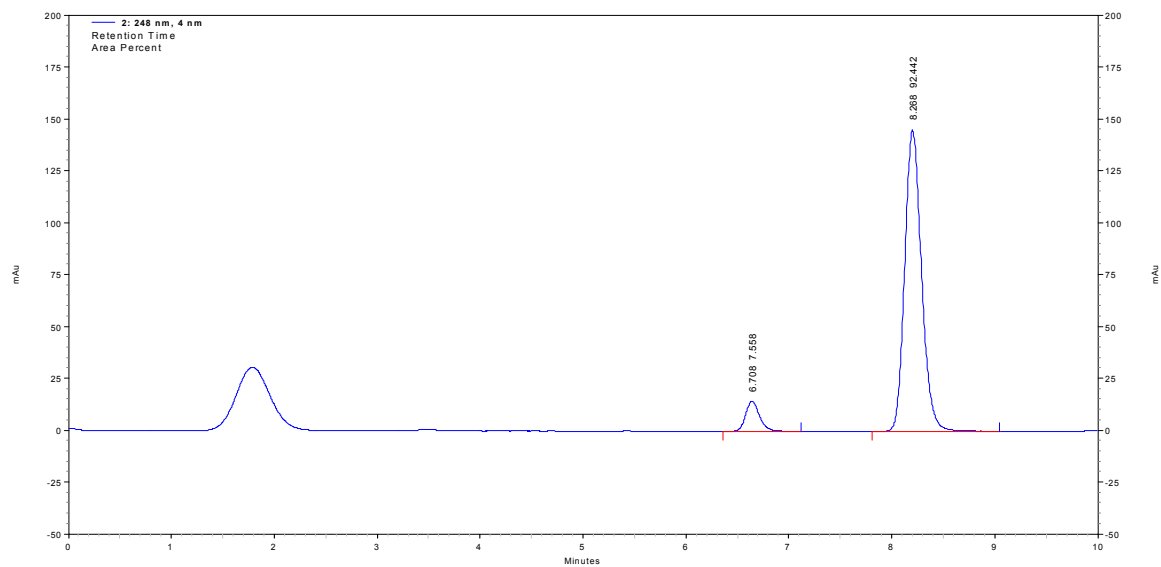
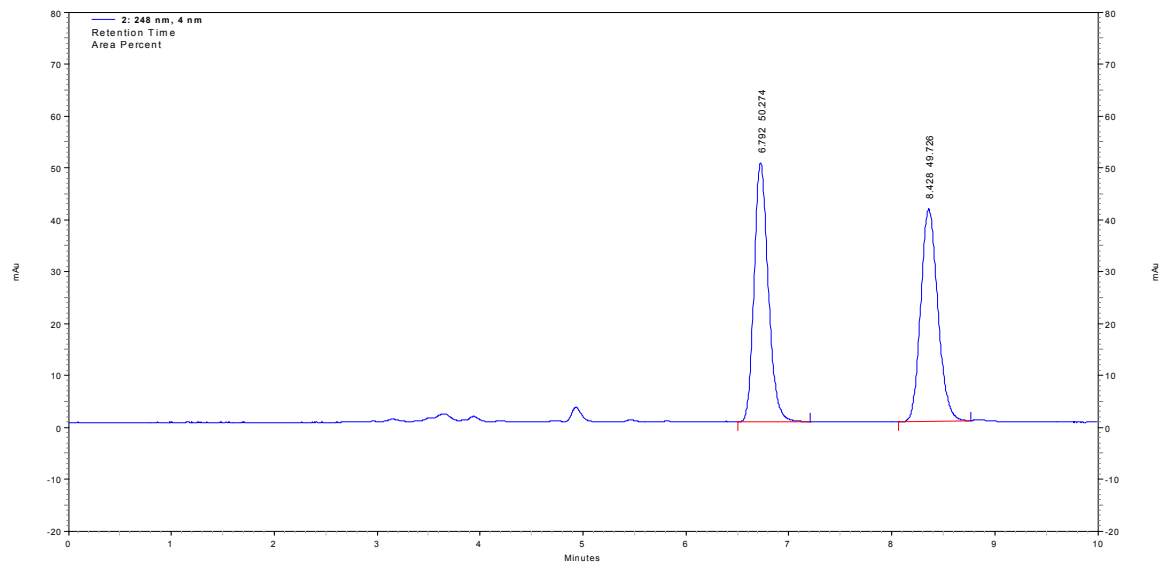
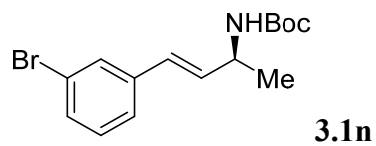
| 248 nm | |
|----------------|--------------|
| Retention Time | Area Percent |
| 5.864 | 8.717 |
| 6.956 | 91.283 |



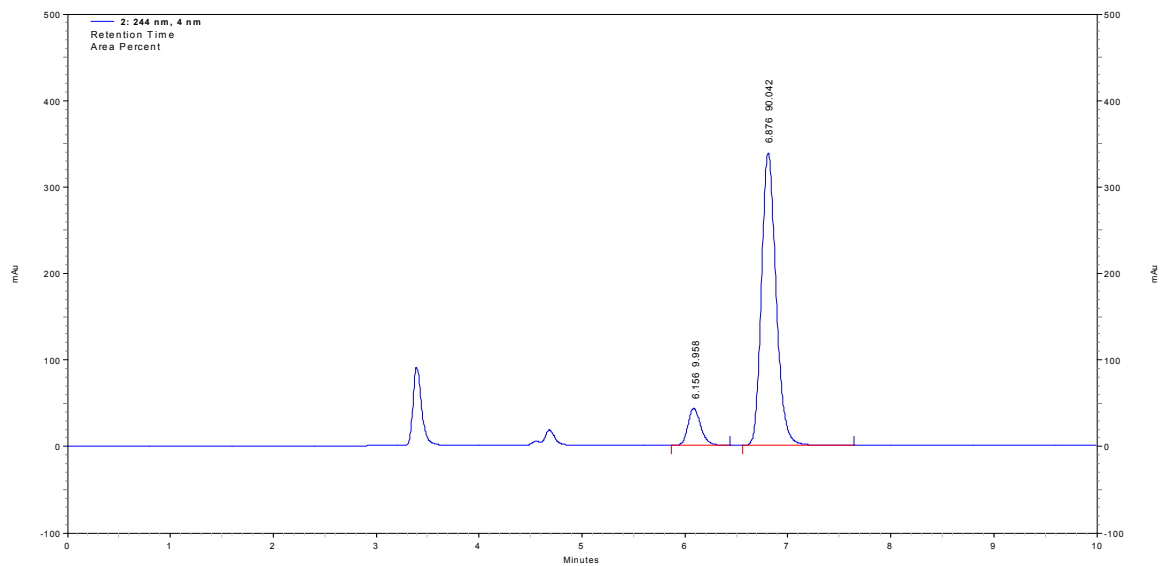
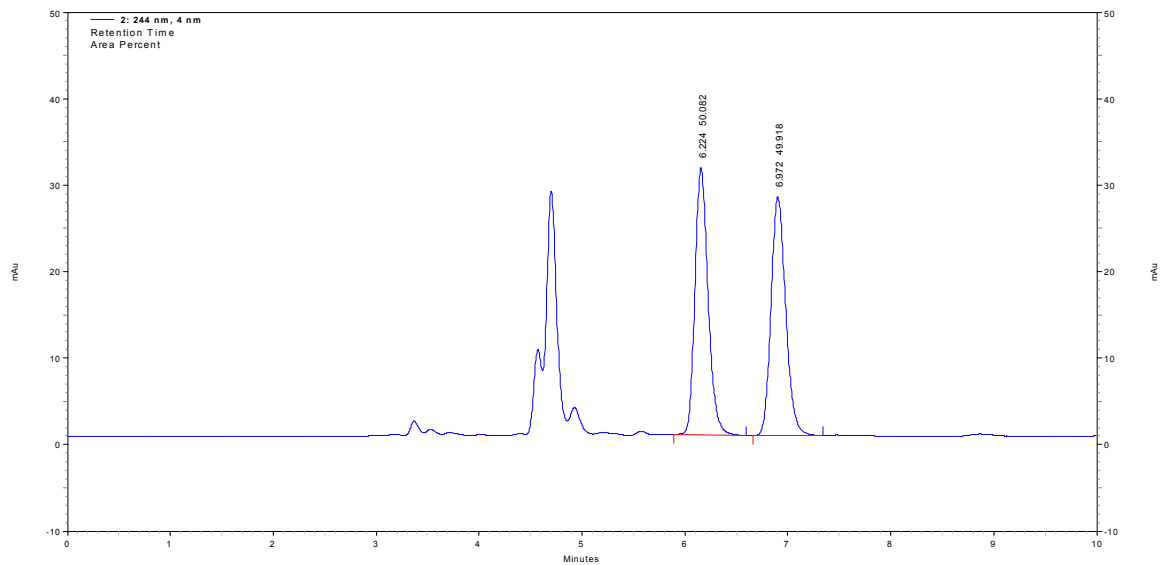
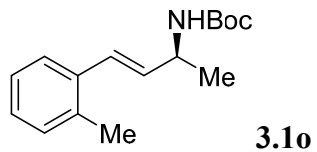
| 241 nm | |
|----------------|--------------|
| Retention Time | Area Percent |
| 9.104 | 14.018 |
| 13.552 | 85.982 |



| 248 nm | Retention Time | Area Percent |
|--------|----------------|--------------|
| | 9.040 | 11.080 |
| | 12.328 | 88.920 |



| 248 nm | Retention Time | Area Percent |
|--------|----------------|--------------|
| | 6.708 | 7.558 |
| | 8.268 | 92.442 |



244 nm

Retention Time

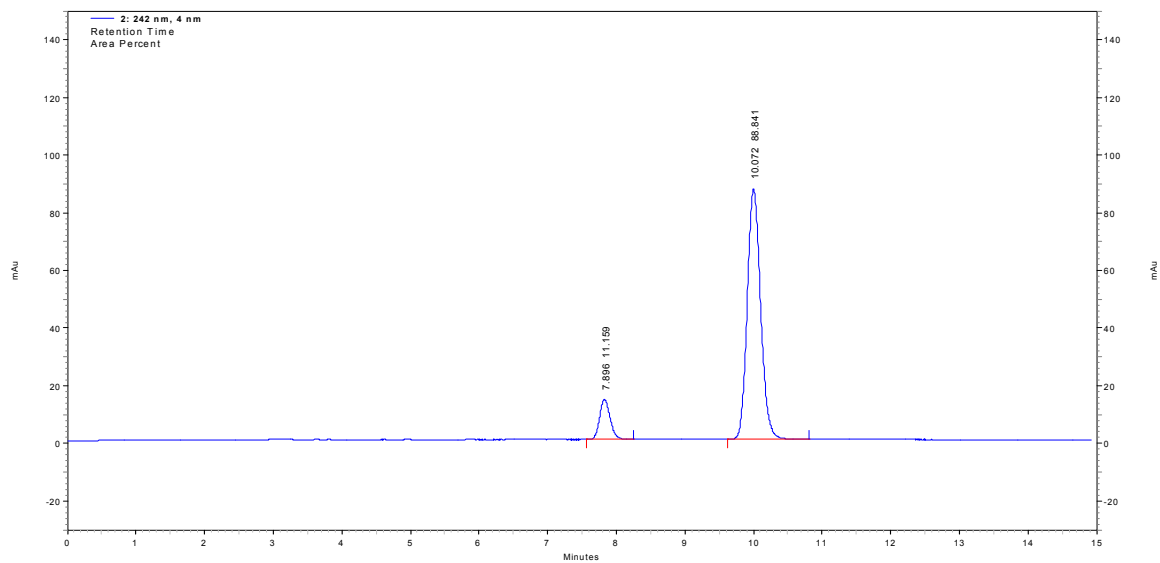
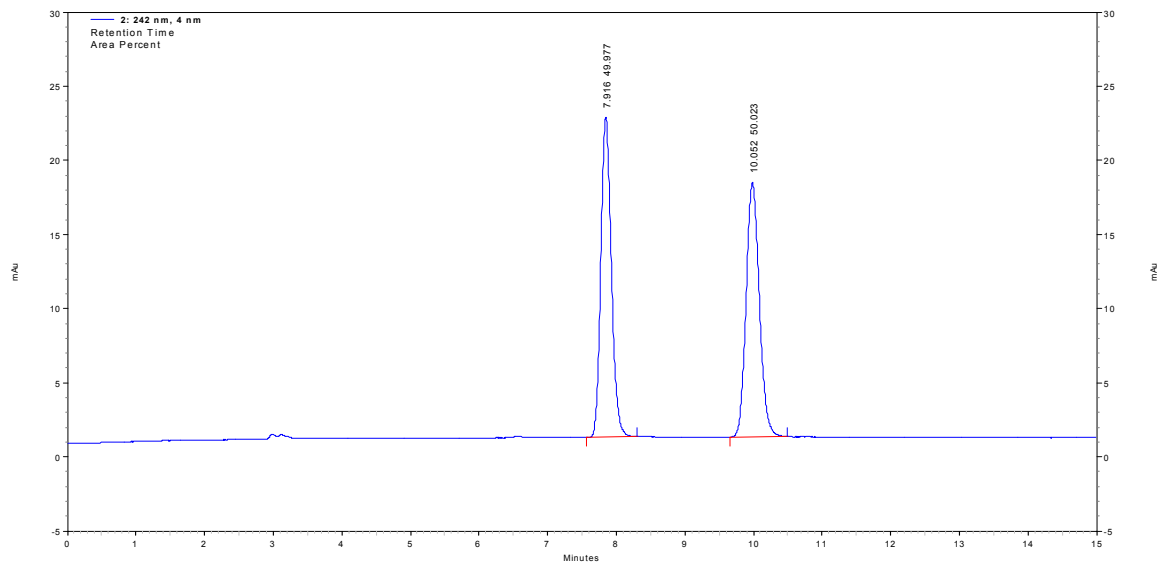
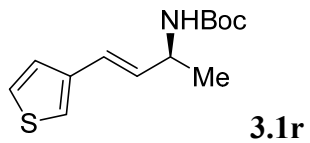
Area Percent

6.156

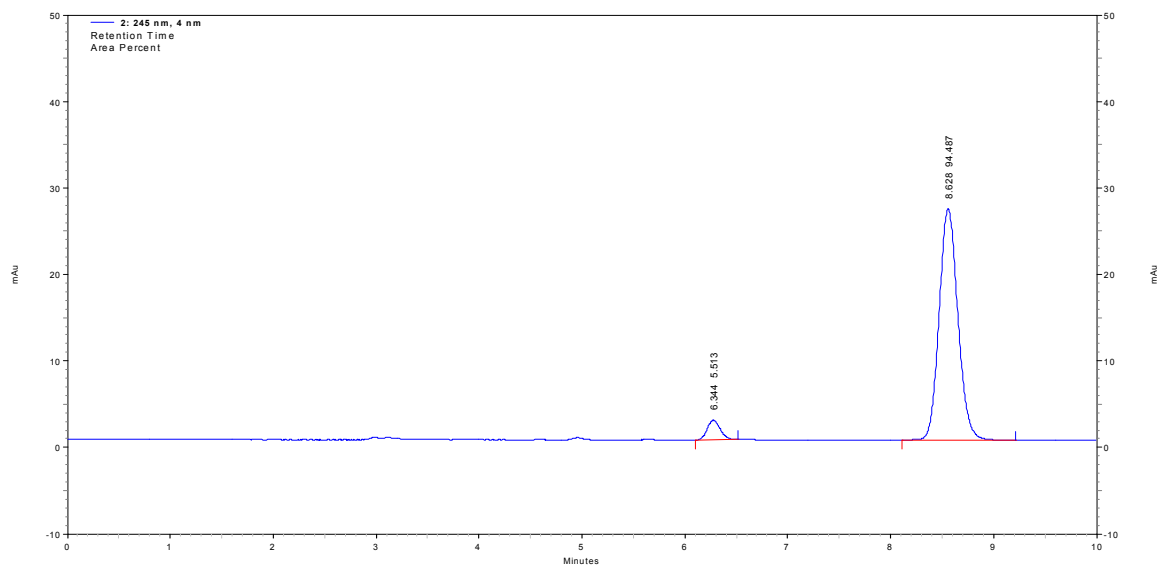
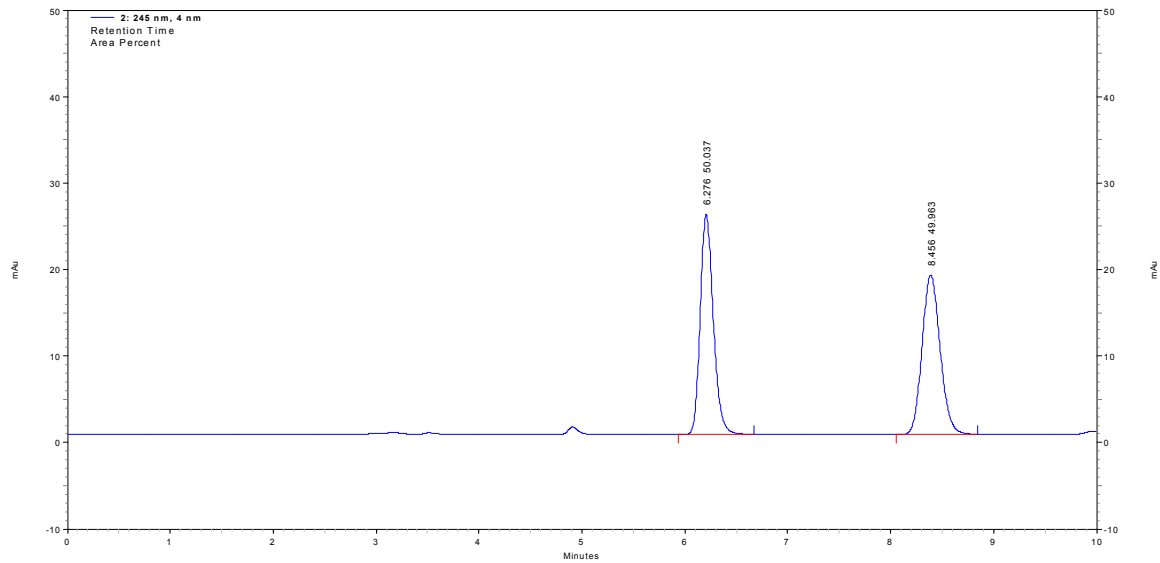
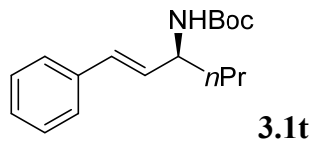
9.958

6.876

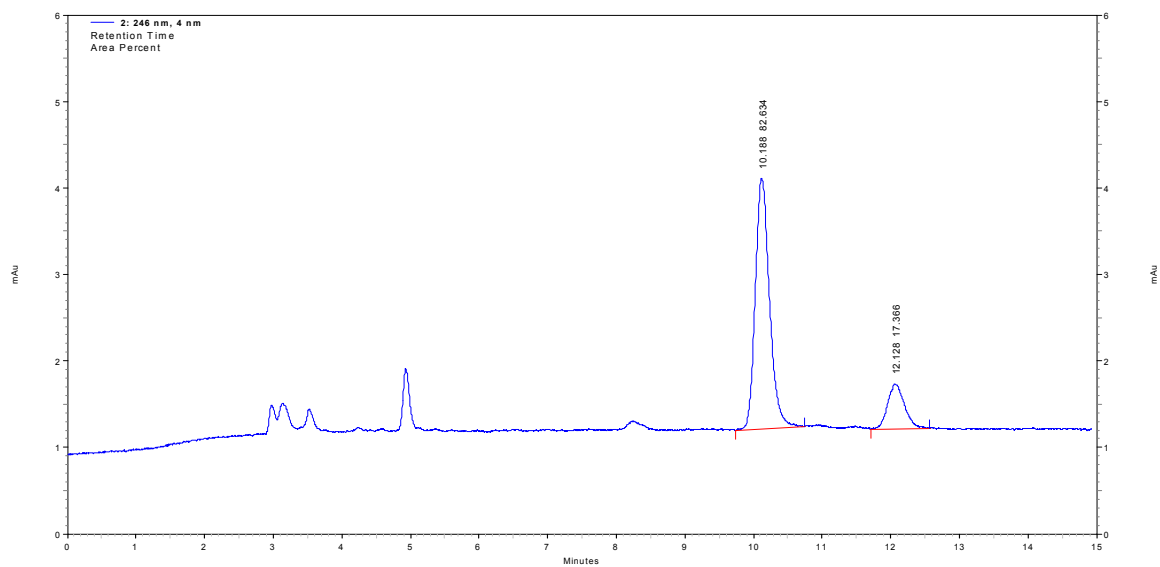
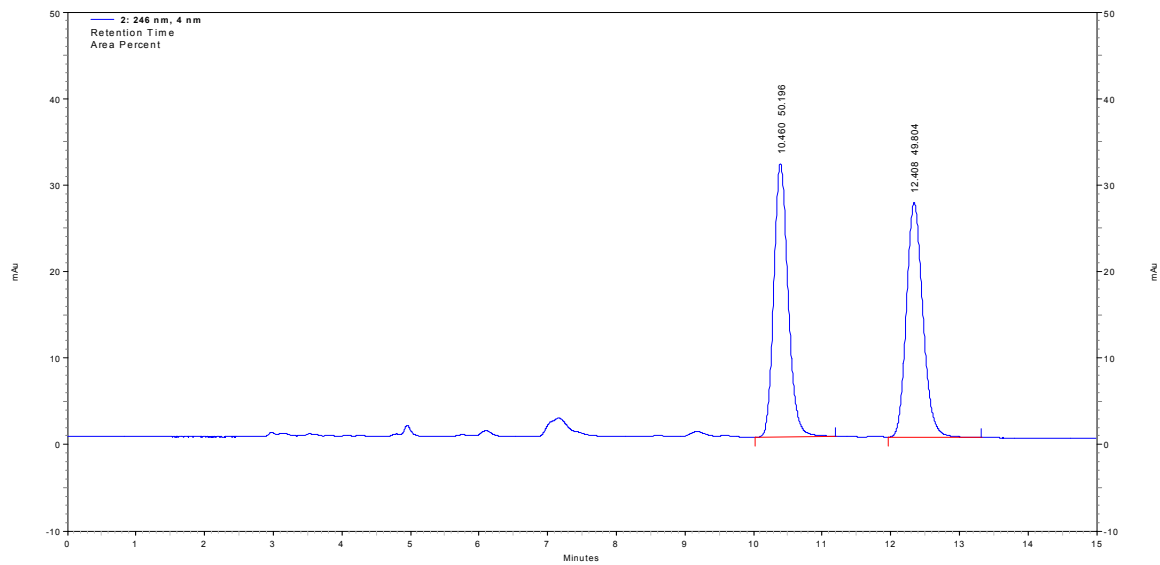
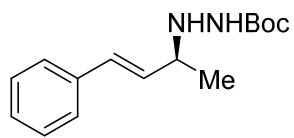
90.042



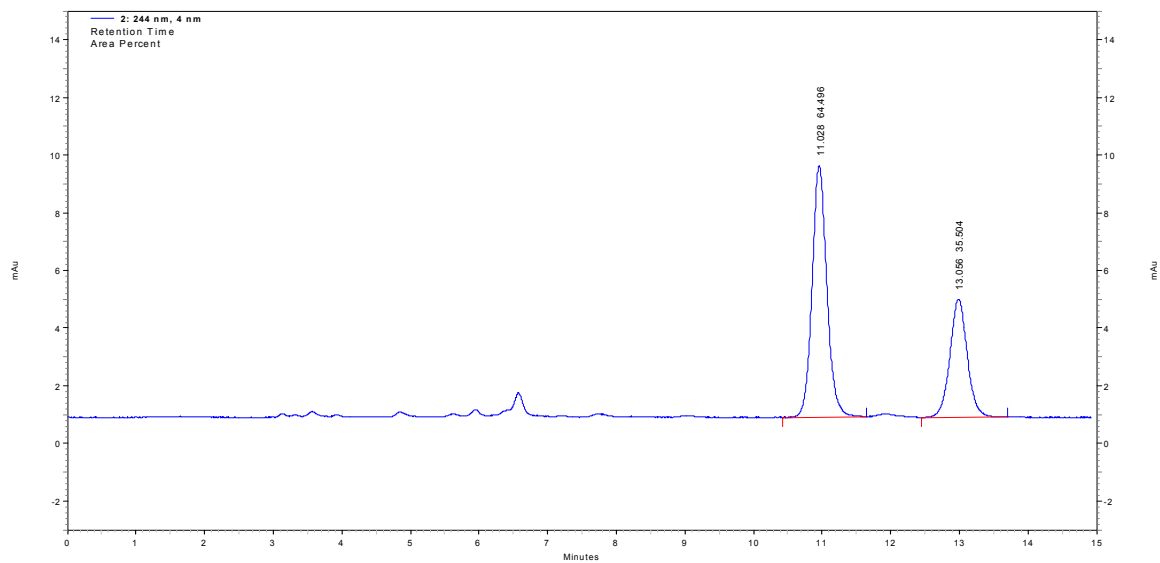
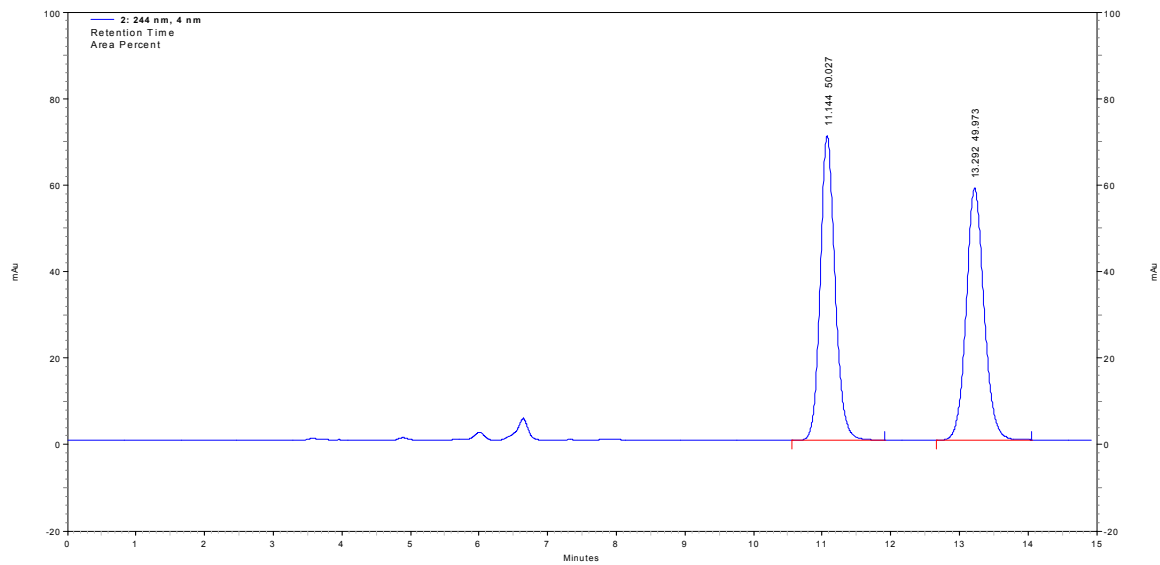
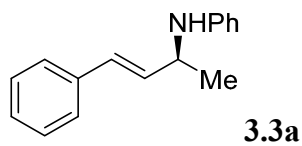
| 242 nm | |
|----------------|--------------|
| Retention Time | Area Percent |
| 7.896 | 11.159 |
| 10.072 | 88.841 |



| 245 nm | |
|----------------|--------------|
| Retention Time | Area Percent |
| 6.344 | 5.513 |
| 8.628 | 94.487 |



| Retention Time | Area Percent |
|----------------|--------------|
| 10.188 | 82.634 |
| 12.128 | 17.366 |



| 244 nm | |
|----------------|--------------|
| Retention Time | Area Percent |
| 11.028 | 64.496 |
| 13.056 | 35.504 |

Chapter 4. Enantioselective Hydroarylation and Cycloisomerization of Allenes:
Synthesis of Chiral Indenes and Cyclopentadienes

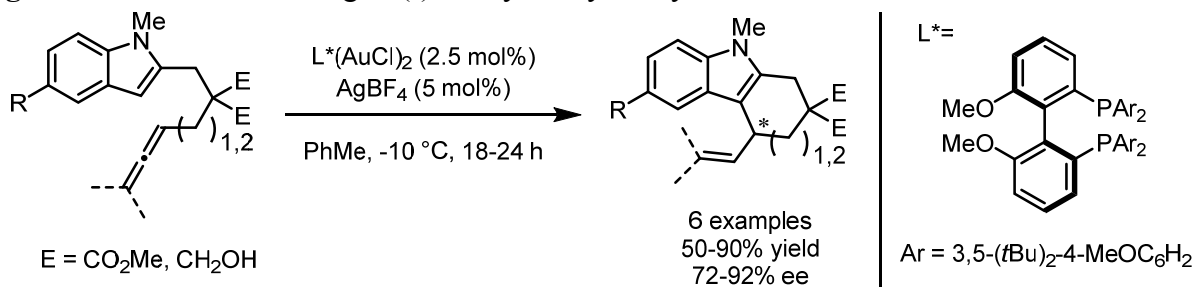
Introduction

Enantioselective Gold(I)-Catalyzed Hydroarylation

Intramolecular hydroarylation reactions are an effective method for generating a variety of polycyclic compounds, and numerous such gold(I)-catalyzed transformations have been reported.¹ A few asymmetric variants of this reaction have been developed, and they are summarized below. A related class of transformations, asymmetric tandem cycloisomerization-intermolecular hydroarylation, is not covered here.²⁻⁸

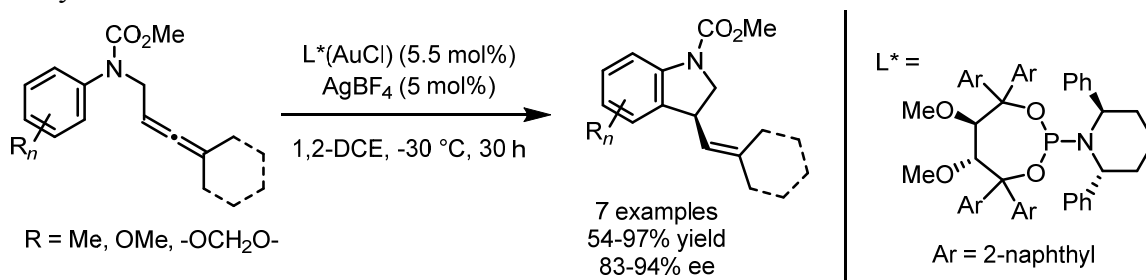
Widenhoefer and coworkers disclosed the 6-*exo-trig* hydroarylation of indole-tethered allenes to afford chiral tetrahydrocarbazole products.⁹ Under the optimized conditions, using a DTBM-MeOBIPHEP gold(I) complex, the reaction was applied successfully across a number of substrates, including one that furnished a seven-membered ring (Figure 4.1). However, the extension to substrates bearing existing chiral centers, such as those possessing 1,3-disubstituted allenes or a single E substituent, was not as effective, providing a mixture of stereoisomers in up to 60% ee.

Figure 4.1 Enantioselective gold(I)-catalyzed hydroarylation of indole-tethered allenes



Fürstner and colleagues reported the 5-*exo-trig* hydroarylation of allenes tethered to aniline carbamates, generating chiral indoline products.¹⁰ The authors applied a TADDOL-related gold(I) complex to achieve high levels of enantioselectivity across a number of electron-rich aromatic systems (Figure 4.2). Unexpectedly, the methyl carbamate protecting group was an important feature; tosyl-protected products were obtained in significantly lower levels of enantioselectivity (60-70% ee).

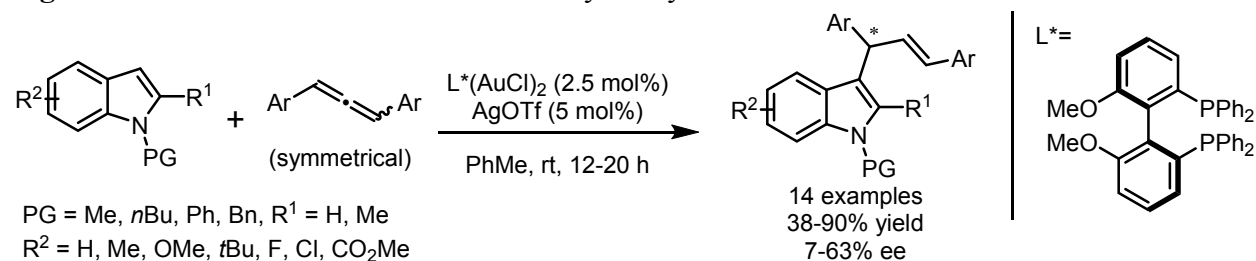
Figure 4.2 Enantioselective gold(I)-catalyzed synthesis of indolines by intramolecular hydroarylation of allenes



Che and coworkers reported the intermolecular hydroarylation of allenes with indoles.¹¹ The use of symmetrical 1,3-diaryllenes was necessary to circumvent regioselectivity issues, and

the application of MeOBIPHEP ligand (the most effective of those surveyed by the authors) afforded enantioselectivities that were only moderate, at best (Figure 4.3). DFT calculations suggested the reaction mechanism proceeded by allene coordination and outer-sphere nucleophilic attack at a single catalytic site, as opposed to dual activation of both nucleophile and electrophile involving both gold centers.

Figure 4.3 Intermolecular enantioselective hydroarylation of allenes with indoles



Several features are recurring in these examples. First, the presence of an indole or other nucleophilic aromatic residue is required for the observed Friedel-Crafts reactivity. Second, an allylic residue at the newly-formed chiral center is always present, arising from the distal, unreacted double bond of the allene. Third, in the two intramolecular examples, the mode of cyclization is consistently *exo*, forming either 5-, 6-, or 7-membered rings depending on the substrate connectivity.

Gold(I)-Catalyzed Synthesis of Indenes and Cyclopentadienes

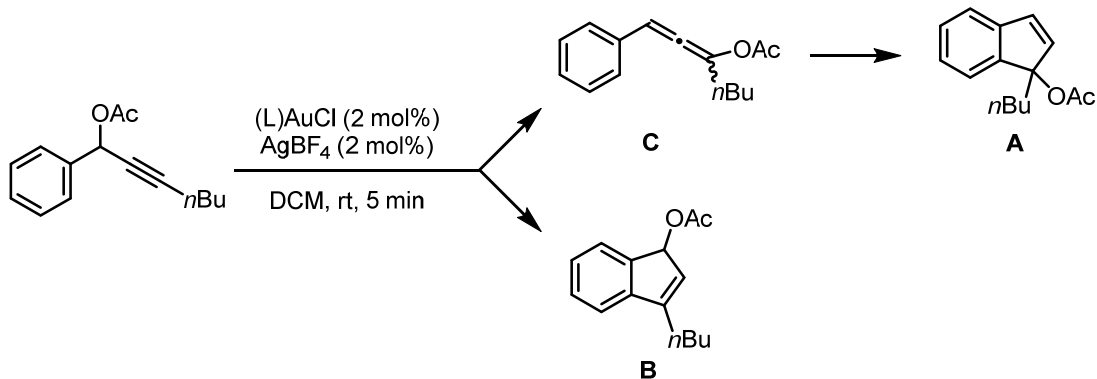
Indenes and cyclopentadienes are indispensable ligand structures for numerous metal complexes used in catalysis.^{12,13} The former are also important functional motifs due to their pharmacological properties.¹⁴ Gold catalysis has enabled their synthesis through a diversity of synthetic methods. In relatively few cases, however, have enantioselective versions of these transformations been disclosed.

Indenes

A number of the gold(I)-catalyzed syntheses of indenes proceed by the hydroarylation of unsaturated substrates (alkenes, allenes, alkynes) with pendant aryl residues.

Nolan and coworkers studied the formation of indenes from propargylic acetates.¹⁵ They identified two regioisomeric products of this reaction, corresponding to two divergent reaction pathways (Table 4.1). Indenes **A** were obtained from hydroarylation of allenyl ester intermediates **C**, which in turn arose from a [3,3]-rearrangement of the starting material. Conversely, indenes **B** were derived from a direct hydroarylation of the alkyne. The authors discovered that gold complexes displaying sterically large carbene ligands (entry 2) were selective for products obtained by the first tandem sequence, as opposed to those bearing phosphine ligands (entry 1), which gave a mixture of products from both pathways. A very similar silver-free protocol was reported later by the same group.¹⁶ Researchers in the research groups of Woodward¹⁷ and Liu¹⁸ have also reported related syntheses of indenes directly from allenyl ester starting materials.

Table 4.1 Two pathways for gold(I)-catalyzed formation of indenenes from propargylic acetates



| Entry ^a | Ligand | A | B | C |
|--------------------|------------------|----|----|---|
| 1 | PPh ₃ | 51 | 32 | 8 |
| 2 | IPr | 73 | 0 | 0 |

[a] All table entries are percent yield

Figure 4.4 Gold(I)-catalyzed synthesis of indenenes from 1,6-allenynes

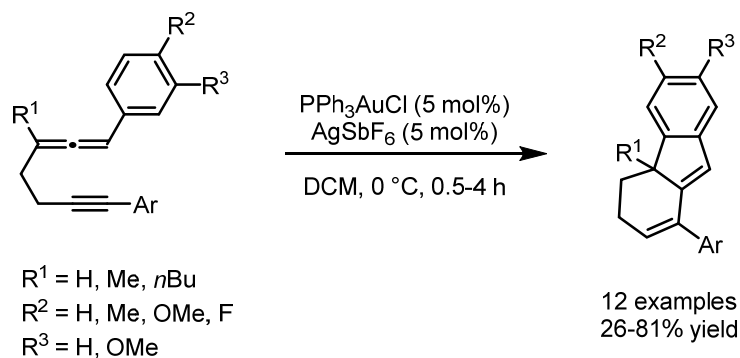
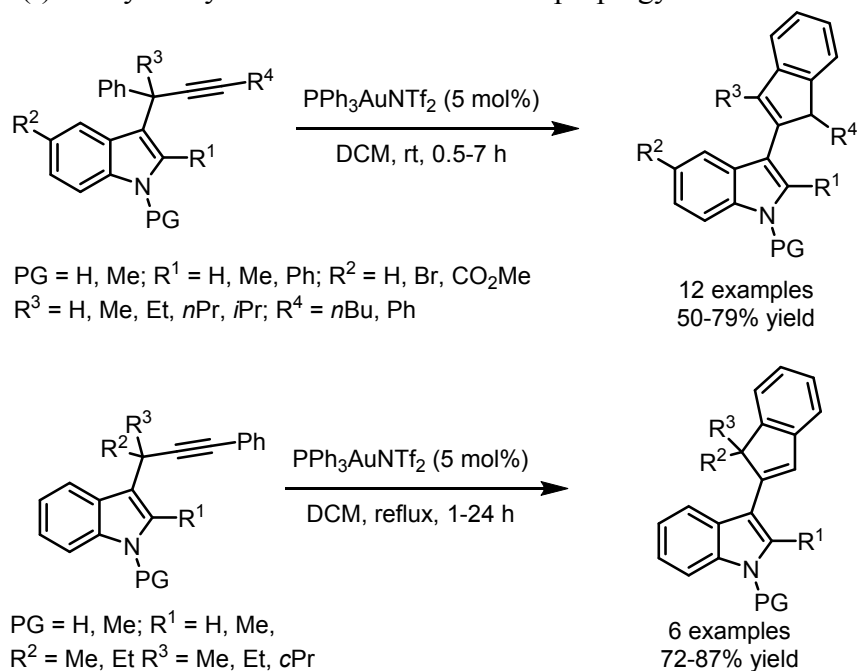


Figure 4.5 Gold(I)-catalyzed synthesis of indenenes from 3-propargylindoles



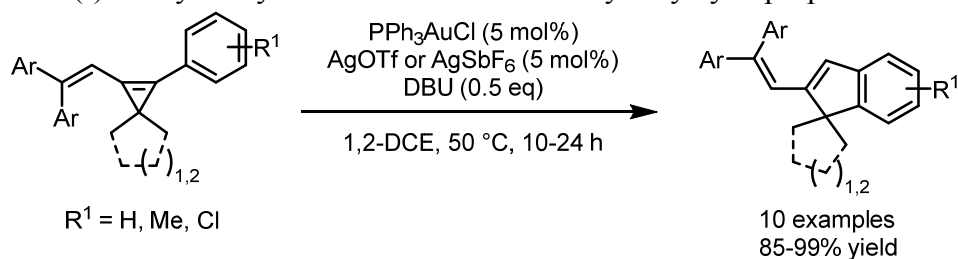
Liu and coworkers reported the synthesis of cyclohexene-fused indenenes (dihydrofluorenes) from 1,6-allenynes.¹⁹ The authors proposed that a 6-*endo-dig* cyclization forms a cationic cyclohexadiene intermediate which undergoes Nazarov cyclization to furnish the product upon protodeauration. Good yields were realized across a range of substrates (Figure 4.4).

Researchers in the Sanz group disclosed a synthesis of indenenes from 3-propargylindoles.²⁰ A 1,2-indole migration—intramolecular hydroarylation cascade enables the product formation. Two distinct substrate classes were shown to be competent in the reaction manifold (Figure 4.5). The methodology was later extended to the synthesis of structurally analogous indolyl-benzofulvenes.²¹

The reactivity of strained 3-membered rings has also been exploited in the gold(I)-catalyzed synthesis of indenenes.

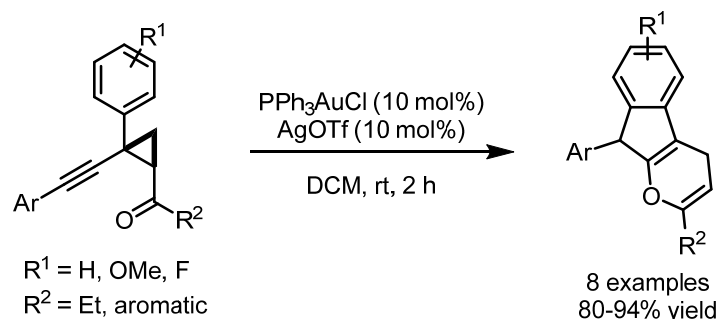
Zhu and Shi disclosed the cycloisomerization of arylvinylcyclopropanes to afford indenenes.²² The use of 1,8-diazabicyclo[5.4.0]undec-7-ene (DBU) as an additive enabled the reaction to proceed in a selective fashion, and a number of substrates were converted to the corresponding 2-vinyl indenenes in good yields (Figure 4.6). A similar reaction was later investigated by Lee and coworkers.^{23,24}

Figure 4.6 Gold(I)-catalyzed synthesis of indenenes from arylvinylcyclopropanes



Zhang and colleagues reported the synthesis of pyran-fused indenenes from aryl alkynyl cyclopropanes.²⁵ A variety of tricyclic products were obtained under the optimized reaction conditions (Figure 4.7). Furthermore, the same substrates were used in the formation of phenols under silver catalysis.

Figure 4.7 Gold(I)-catalyzed synthesis of indenenes from aryl alkynylcyclopropanes



A final strategy for the construction of indenes is the use of reactions which eliminate fragments of the starting material.

Echavarren and coworkers disclosed a retro-Buchner reaction of *ortho*-styrenylcycloheptatrienes affording 2-substituted indenes. Using a JohnPhos-gold(I) complex, the authors demonstrated moderate to good yields across a range of substrates (Figure 4.8). Mechanistically, the reaction proceeded through a gold(I)-carbenoid intermediate upon elimination of benzene, as illustrated in Figure 4.9.

Figure 4.8 Gold(I)-catalyzed synthesis of indenes from *ortho*-styrenylcycloheptatrienes

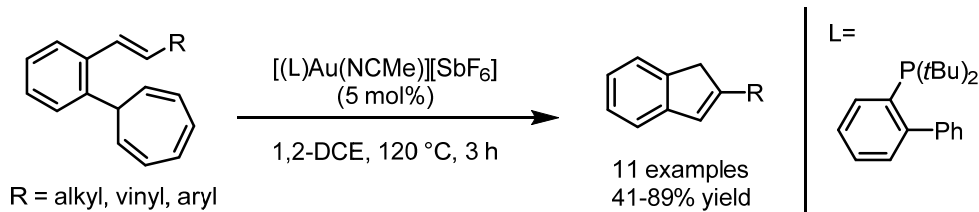
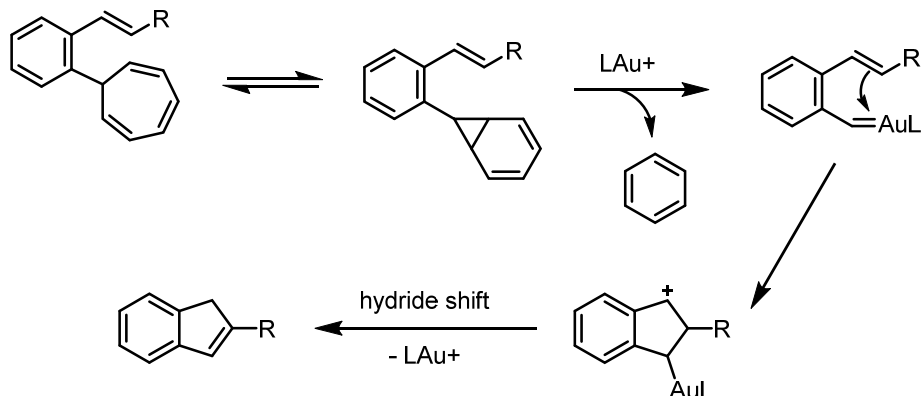


Figure 4.9 Proposed mechanism of the gold(I)-catalyzed retro-Buchner reaction



Researchers in the Hashmi laboratory identified a synthesis of indenes from diynes with extrusion of carbon monoxide.²⁶ Although the product yields were extremely variable, a variety of indenes, substituted at the 2, 5 and 6 positions, were accessible by this methodology (Figure 4.10). Through the appropriate carbon-13 and oxygen-18 isotopic labelling experiments, the authors demonstrated that the carbon and oxygen atoms of the carbon monoxide were derived from the substrate's terminal alkyne and the water additive, respectively. This supported a mechanistic proposal shown in Figure 4.11, involving a diaurated gold(I) vinylidene as a key intermediate.

Figure 4.10 Gold(I)-catalyzed synthesis of indenes from aryl *ortho*-diynes

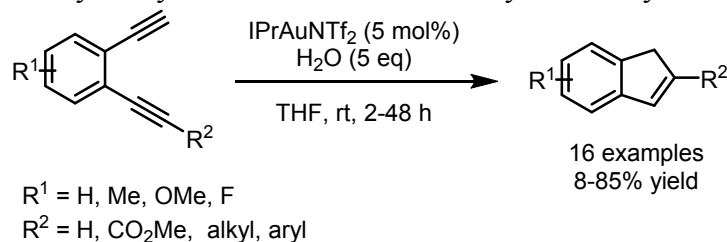
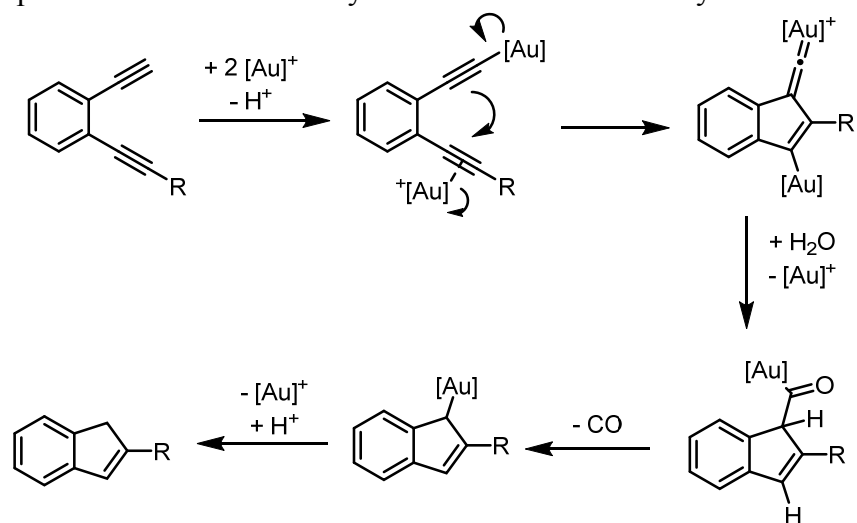
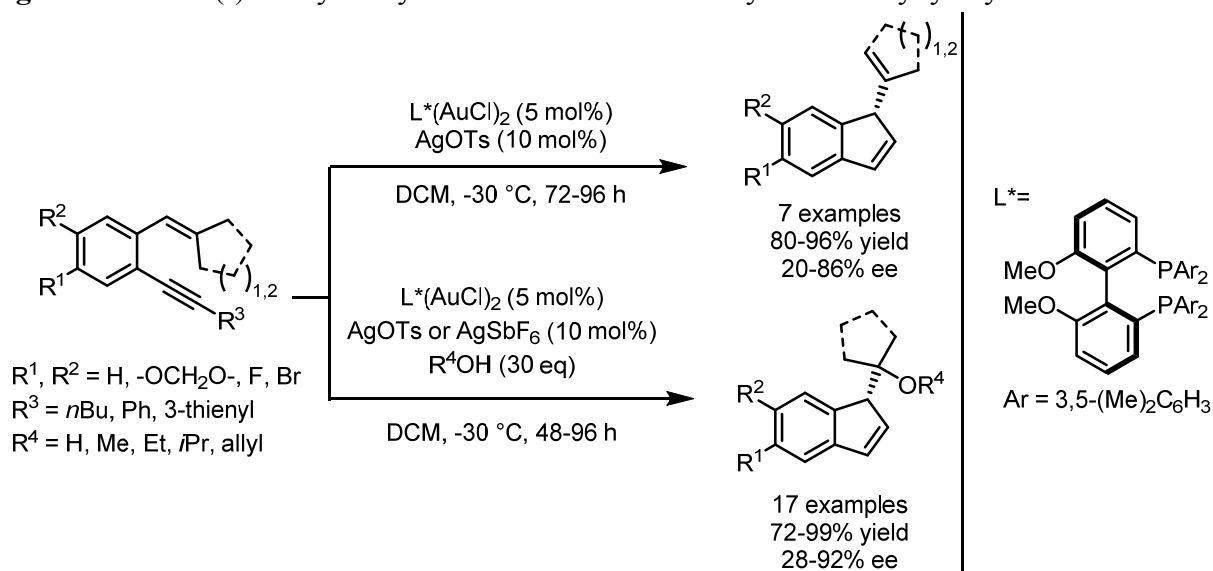


Figure 4.11 Proposed mechanism of the synthesis of indenenes from diynes



Lastly, only one gold(I)-catalyzed enantioselective approach to the synthesis of indenenes, from the Sanz group, has been reported to date.^{27,28} The use of *ortho*-alkynyl styrenes and the application of a DM-MeOBIPHEP gold(I) complex enables a 5-*endo-dig* cyclization to furnish desired chiral products (Figure 4.12).

Figure 4.12 Gold(I)-catalyzed synthesis of indenenes from aryl *ortho*-alkynyl styrenes



Cyclopentadienes

Relative to the synthesis of indenenes, there is a dearth of gold(I)-catalyzed reactions that furnish cyclopentadienes. Lee and Toste reported a Nazarov-like synthesis of cyclopentadienes from vinylallenes in 2007.²⁹ A variety of substituents on the alkene and allene moieties were tolerated in the basic reaction manifold (Figure 4.13a), and a tandem process involving ring expansion was also demonstrated (Figure 4.13b). Around the same time, Iwasawa and coworkers independently demonstrated a very similar reaction catalyzed by platinum, which also converted vinylallenes to cyclopentadienes.³⁰ More recently, this mode of reactivity has been recapitulated

by Helaja and colleagues, using enynamine substrates with gold(III) salt catalysts.³¹ They additionally reported moderate levels of point-to-center chirality transfer for several compounds in this transformation (Figure 4.14).³²

Figure 4.13 Gold(I)-catalyzed synthesis of cyclopentadienes from vinylallenes

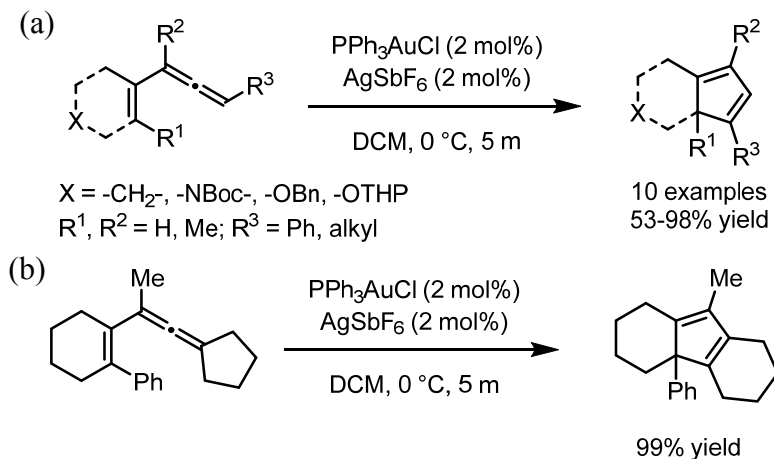
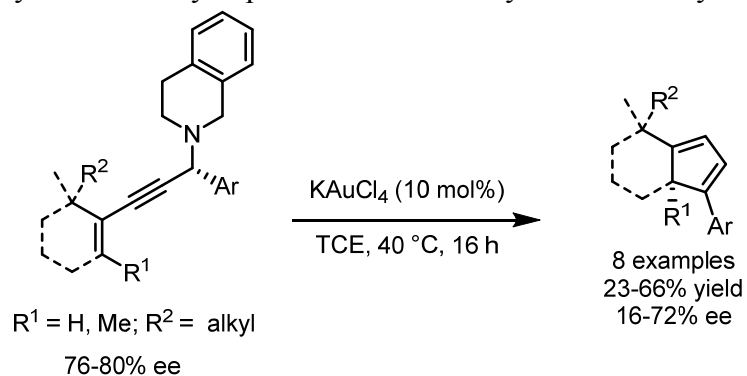
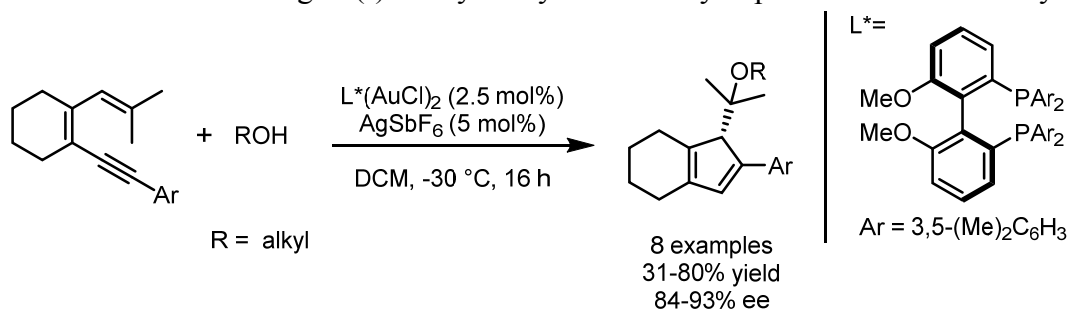


Figure 4.14 Chirality transfer to cyclopentadienes from enynamines catalyzed by gold(III)



The only enantioselective report of gold(I)-catalyzed synthesis of cyclopentadienes was disclosed by Sanz and coworkers.³³ The authors employed 1,3-dien-5-yne, which underwent tandem cyclization, alkyl migration, and alkoxy trapping to afford chiral cyclopentadiene products with variable yields but high ee's (Figure 4.15). These products were shown to further partake in a Diels-Alder reaction with a variety of dienophiles, which produced cycloadducts in a completely diastereoselective fashion with full retention of enantiomeric excess.

Figure 4.15 Enantioselective gold(I)-catalyzed synthesis of cyclopentadienes from dienynes



Results and Discussion

The initial forays into asymmetric hydroarylation were a consequence of investigations of the asymmetric hydroamination reaction (see Chapter 3). The hydroarylation of 2-naphthyl-allenes was a fortuitous discovery made in the course of exploring the substrate scope. When substrate **2.1p** was exposed to hydroamination conditions, significant formation of chiral 6,7-benzoindene product **4.1** was observed (Figure 4.16). Omitting the carbamate nucleophile and subjecting a closely related substrate (**4.2**) to the same conditions afforded increased yield of hydroarylation product **4.3** with promising levels of enantioselectivity (Figure 4.17). This substrate was carried through a series of optimization experiments.

Figure 4.16 Byproduct formation in asymmetric hydroamination of a 2-naphthylallene substrate

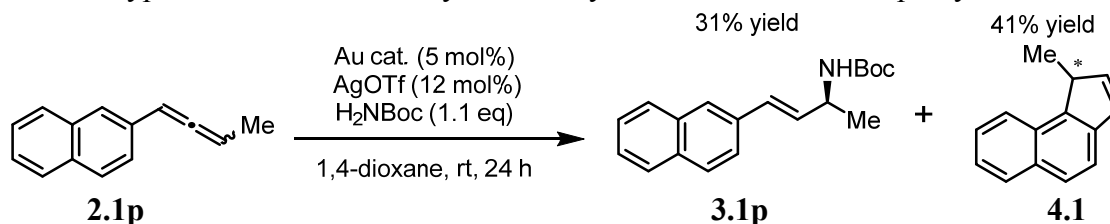
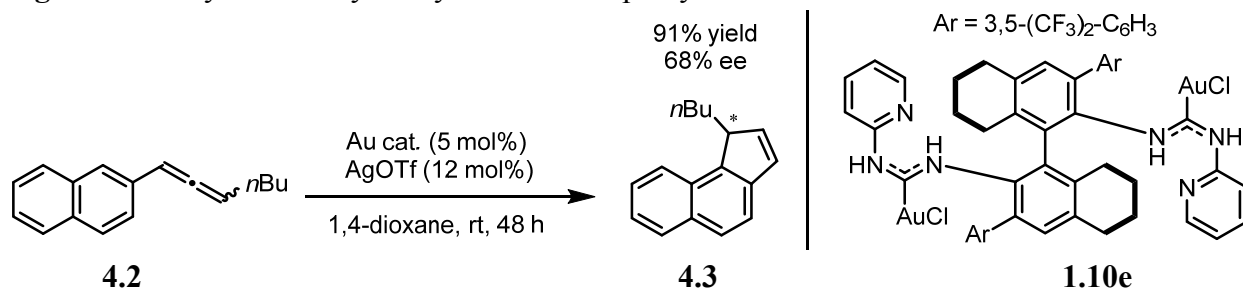
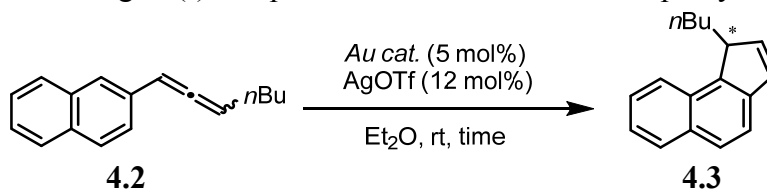


Figure 4.17 Asymmetric hydroarylation of 2-naphthylallene to form chiral benzoindene



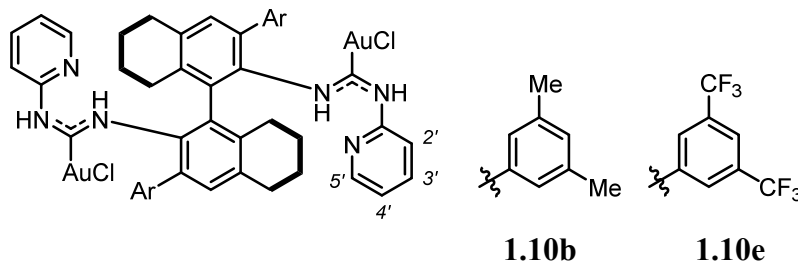
First, a number of chiral gold(I) complexes were tested in the reaction (Table 4.2). Axially chiral diphosphine gold(I) complexes were not competent catalysts for this reaction (entries 1 and 2). BINAM-derived ADC gold(I) complexes bearing 3,5-dimethylphenyl and 3,5-bis(trifluoromethyl)phenyl substituents were investigated next (entries 3-8). Introduction of a methoxy group in the 2' position on the pyridine ring led to increased selectivity, furnishing the product in 86% ee (entry 6). Interestingly, introducing the same methoxy group at the 4' position resulted in lower enantioselectivities but greater yields (entry 8). Using the most selective precatalyst **1.10k**, a survey of counterions was conducted (entries 9-12). Only with silver tetrafluoroborate was comparable selectivity observed, but the yield was much lower; thus silver triflate remained the optimal choice.

Table 4.2 Survey of chiral gold(I) complexes and counterions in 2-naphthylallene hydroarylation

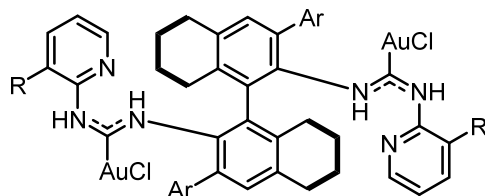


| Entry ^a | Precatalyst | Counterion | | Yield (%) ^b | ee (%) ^c |
|--------------------|--|----------------------|----------|------------------------|---------------------|
| | | Source | Time (h) | | |
| 1 | (<i>R</i>)-DM-MeOBIPHEP(AuCl) ₂ | AgOTf | 48 | 0 | n/d |
| 2 | (<i>R</i>)-BINAP(AuCl) ₂ | AgOTf | 48 | trace | n/d |
| 3 | 1.10b | AgOTf | 48 | 32 | 38 |
| 4 | 1.10e | AgOTf | 48 | 79 | 72 |
| 5 | 1.10i | AgOTf | 24 | 47 | 64 |
| 6 | 1.10k | AgOTf | 48 | 62 | 86 |
| 7 | 1.10m | AgOTf | 24 | 14 | 68 |
| 8 | 1.10o | AgOTf | 48 | 83 | 74 |
| 9 | 1.10k | AgNTf ₂ | 48 | 24 | 75 |
| 10 | 1.10k | AgBF ₄ | 48 | 16 | 87 |
| 11 | 1.10k | AgSbF ₆ | 48 | 45 | 74 |
| 12 | 1.10k | NaBARF ₂₄ | 48 | 8 | 15 |

[a] Conditions: 0.05 mmol **4.2**, 0.0025 mmol gold(I) precatalyst, 0.006 mmol silver/sodium salt, 1.0 mL of Et₂O (0.05 M), 24–48 hours at room temperature. [b] Determined by ¹H NMR with 1-fluoronaphthalene as an internal standard. [c] Determined by chiral HPLC.

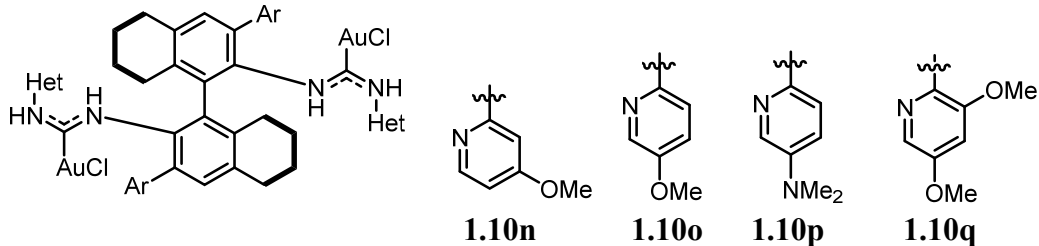


Ar = 3,5-(CF₃)₂C₆H₃



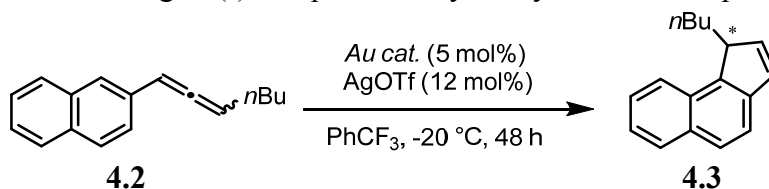
1.10i (R = OAc); **1.10j** (R = Me); **1.10k** (R = OMe); **1.10l** (R = OBn); **1.10m** (R = OCH₂tBu)

Ar = 3,5-(CF₃)₂C₆H₃



Further optimization of the reaction conditions revealed that running the reaction in trifluorotoluene solvent at decreased temperature led to a small increase in enantioselectivity (Table 4.3, entry 1). However, the low temperatures caused a decrease in the rate of reaction, and small quantities of starting material (which are inseparable from the product by column chromatography) remained in the crude reaction mixture. Leveraging the earlier observation that a 4' methoxy substituted catalyst provided higher yield, a catalyst displaying both 2' and 4' methoxy substituents (**1.10q**) was applied in the new conditions (entry 2). Gratifyingly, a small increase in both enantioselectivity and yield resulted, and most importantly, no traces of starting material were detected.

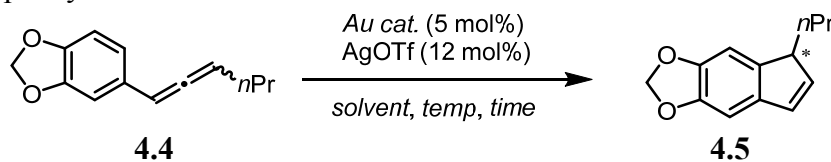
Table 4.3 Comparison of two gold(I) complexes in hydroarylation of 2-naphthylallene



| Entry ^a | Precatalyst | Yield (%) ^b | ee (%) ^c |
|--------------------|--------------|------------------------|---------------------|
| 1 | 1.10k | 82 | 88 |
| 2 | 1.10q | 85 | 93 |

[a] Conditions: 0.05 mmol **4.2**, 0.0025 mmol gold(I) precatalyst, 0.006 mmol silver triflate, 1.0 mL of PhCF₃ (0.05 M), 48 hours at -20 °C. [b] Determined by ¹H NMR with 1-fluoronaphthalene as an internal standard average of 4 runs. [c] Determined by chiral HPLC, average of 4 runs.

Table 4.4 Survey of chiral gold(I) complexes and solvents in hydroarylation of 3,4-methylenedioxyphenyl allene



| Entry ^a | Precatalyst | Solvent | Temp (°C) | Time (h) | Yield (%) ^b | ee (%) ^c |
|--------------------|--------------|-------------------|-----------|----------|------------------------|---------------------|
| 1 | 1.10b | Et ₂ O | rt | 0.5 | 37 | 46 |
| 2 | 1.10i | Et ₂ O | rt | 1 | 24 | 28 |
| 3 | 1.10k | Et ₂ O | rt | 0.5 | 49 | 68 |
| 4 | 1.10m | Et ₂ O | rt | 1 | 83 | 15 |
| 5 | 1.10q | Et ₂ O | rt | 0.5 | 54 | 68 |
| 6 | 1.10k | Et ₂ O | -20 | 14 | 20 | 55 |
| 7 | 1.10k | DCM | -20 | 14 | 36 | 59 |
| 8 | 1.10k | PhCF ₃ | -20 | 14 | 61 | 68 |

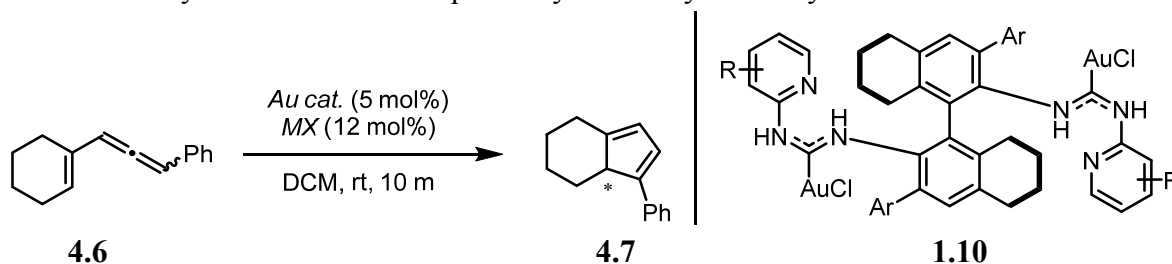
[a] Conditions: 0.05 mmol **4.2**, 0.0025 mmol gold(I) precatalyst, 0.006 mmol silver triflate, 1.0 mL of appropriate solvent (0.05 M), 0.5-14 hours at room temperature. [b] Determined by ¹H NMR with 1-fluoronaphthalene as an internal standard. [c] Determined by chiral HPLC.

Next, in order to extend the scope of the hydroarylation reaction, a substrate bearing an electron-rich aromatic ring (**4.4**) was investigated, and again a number of ADC gold(I) complexes were examined (Table 4.4). Although this new substrate exhibited markedly faster reactivity, the

observed selectivities were only moderate. The best ee's (68%) were again obtained with catalysts possessing 2'-methoxy substituents (entries 3 and 5). Disappointingly, the enantioselectivities could not be improved by running the reaction at low temperature (entries 6-8). Other electron-rich aryl rings were investigated, but in no cases were enantioselectivities over 70% ee observed.

Moving from the synthesis of chiral indenenes to the synthesis of chiral cyclopentadienes, I hoped to render enantioselective our group's earlier work on the cycloisomerization of vinylallenes.²⁹ In line with the authors' report, this reaction was exceedingly fast relative to the previous two, due to absence of aromaticity-breaking. Full consumption of starting material was observed within ten minutes (a conservative upper limit). An initial screen of counterions was undertaken with catalyst **1.10e**, revealing mostly poor enantioselectivities (Table 4.5, entries 1-5). However, the best performing counterion, tetrakis(3,5-trifluoromethyl)phenylborate, was selected for subsequent experiments with various ADC gold(I) complexes (entries 6-10). Once more, precatalyst **1.10k** was found to furnish the highest levels of enantioinduction (entry 7).

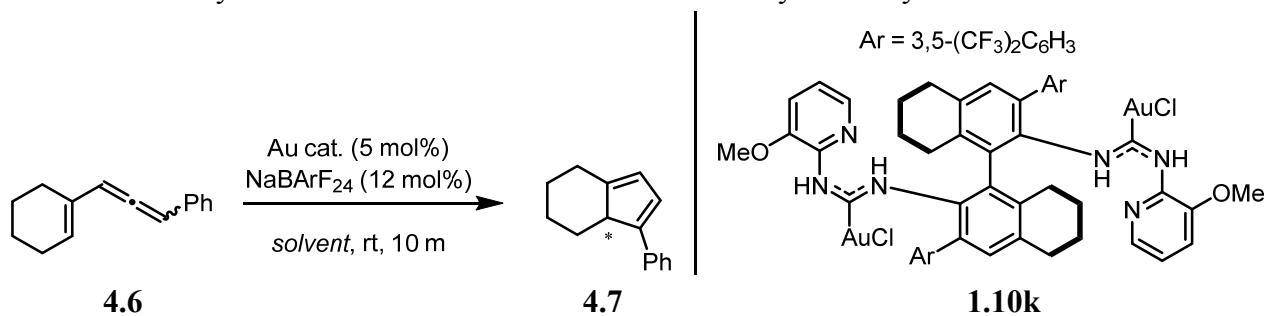
Table 4.5 Survey of counterions and precatalysts in vinylallene cycloisomerization



| Entry ^a | Precatalyst | Counterion | |
|--------------------|--------------|----------------------|---------------------|
| | | source | ee (%) ^b |
| 1 | 1.10e | AgOTf | 12 |
| 2 | 1.10e | AgNTf ₂ | -4 |
| 3 | 1.10e | AgBF ₄ | 14 |
| 4 | 1.10e | AgSbF ₆ | 14 |
| 5 | 1.10e | NaBArF ₂₄ | 20 |
| 6 | 1.10b | NaBArF ₂₄ | 7 |
| 7 | 1.10k | NaBArF ₂₄ | 49 |
| 8 | 1.10l | NaBArF ₂₄ | 20 |
| 9 | 1.10o | NaBArF ₂₄ | 17 |
| 10 | 1.10p | NaBArF ₂₄ | 4 |

[a] Conditions: 0.05 mmol **3.6**, 0.0025 mmol precatalyst **1.10**, 0.006 mmol silver/sodium salt, 1.0 mL of DCM (0.05 M), 10 minutes at room temperature. [b] Determined by chiral HPLC.

Several other factors were found to be important for reaction optimization. A study of reaction concentration revealed that dilution of the reaction mixture led to a decrease in ee (Table 4.6, entries 1-5). Next, a survey of solvents demonstrated that while chloroform gave the same enantioselectivity values as dichloromethane, other closely related chlorinated solvents were markedly worse (entries 6-9). Finally, running the reaction at cryogenic temperatures led to a small decrease in enantioselectivity (entry 10).

Table 4.6 Survey of concentration and solvent effects in vinylallene cycloisomerization

| Entry ^a | Solvent | Conc. (M) | ee (%) ^b |
|--------------------|-------------------|-----------|---------------------|
| 1 | DCM | 0.1 | 52 |
| 2 | DCM | 0.05 | 49 |
| 3 | DCM | 0.025 | 47 |
| 4 | DCM | 0.012 | 42 |
| 5 | DCM | 0.006 | 37 |
| 6 | CHCl ₃ | 0.1 | 52 |
| 7 | 1,2-DCE | 0.1 | 44 |
| 8 | 1,1,1-TCA | 0.1 | 35 |
| 9 | TCE | 0.1 | 30 |
| 10 ^c | DCM | 0.1 | 47 |

[a] Conditions: 0.05 mmol **3.6**, 0.0025 mmol precatalyst **1.10k**, 0.006 mmol NaBARF₂₄, 0.5-8.0 mL of solvent, 10 minutes at room temperature. [b] Determined by chiral HPLC. [c] Reaction run at -78 °C for 1 h.

In all the reactions presented, a chiral racemic allene substrate was converted to enantioenriched product. Additionally, unreacted starting material was found to be racemic. This implies two plausible mechanisms: a dynamic kinetic resolution with rapid interconversion of starting enantiomers, or a dynamic kinetic transformation which proceeds through an achiral intermediate. Due to the rapid racemization of chiral allenes by ADC gold(I) complexes demonstrated in Chapter 2, distinguishing between these two pathways has been difficult. Furthermore, the optimization of these transformations for enantioselectivity has also proved challenging. But the synthetic value of the target compounds justifies further exploration and investigation. Hopefully, the continued development of ADC gold(I) complexes will enable more efficient modes of enantioinduction in these reaction manifolds.

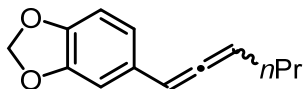
Experimental

General information

Unless otherwise noted, reagents were obtained from commercial sources and used without further purification. Anhydrous 1,4-dioxane was purchased from Sigma-Aldrich. All other solvents used are HPLC grade. TLC analysis of reaction mixtures was performed on Merck silica gel 60 F₂₅₄ TLC plates and visualized by ultraviolet light, iodine or potassium permanganate stain. Flash chromatography was carried out with ICN SiliTech 32-63 D 60 Å silica gel. ¹H and ¹³C NMR spectra were recorded with Bruker AV-500, DRX-500, or AV-600 spectrometers and were referenced to residual ¹H and ¹³C signals of the deuterated solvents, respectively (δ H 7.26, δ C 77.16 for chloroform-d and δ H 5.32, δ C 54.00 for dichloromethane-d₂). Enantioselectivity was determined by chiral HPLC using Daicel Chiralpak AD-H, AS-H, IB, OD-H, or Regis (R,R) WHELK-O1 columns (all 0.46 cm x 25 cm). Optical rotation was recorded on a Perkin Elmer Polarimeter 241 at the D line (1.0 dm path length, *c* = mg/mL). Generally, racemic samples were prepared in procedures modified from those reported by Toste and coworkers using IPrAuCl and AgOTf.²⁹ Mass spectral data were obtained via the Micro-Mass/Analytical Facility operated by the College of Chemistry, University of California, Berkeley using a Thermo LTQ-FT (ESI) instrument.

General procedure for preparation of allene substrates

Allene **4.4** was prepared in accordance with the procedure outlined in the Experimental section of Chapter 2.



4.4, 5-(hexa-1,2-dien-1-yl)benzo[d][1,3]dioxole

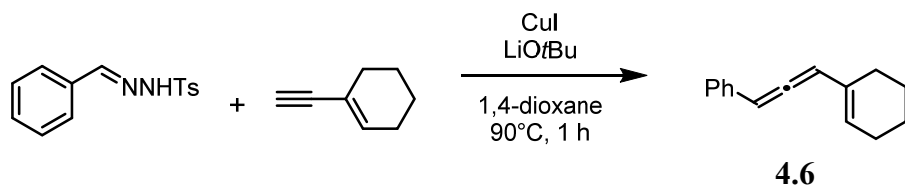
3.33 mmol scale, 57% yield (384 mg, 1.90 mmol)

¹H NMR (600 MHz, CDCl₃) δ 6.83 (d, *J* = 1.6 Hz, 1H), 6.78 – 6.66 (m, 2H), 6.06 (dq, *J* = 6.2, 3.1 Hz, 1H), 5.94 (s, 2H), 5.55 (q, *J* = 6.6 Hz, 1H), 2.09 (tdt, *J* = 10.3, 6.4, 2.3 Hz, 2H), 1.50 (hd, *J* = 7.4, 1.3 Hz, 2H), 0.97 (t, *J* = 7.4 Hz, 3H).

¹³C NMR (151 MHz, CDCl₃) δ 204.64, 148.11, 146.62, 129.39, 120.34, 108.41, 106.55, 101.08, 95.32, 94.50, 31.10, 22.53, 13.91.

HRMS (EI⁺): calcd. for [C₁₃H₁₄O₂]⁺: 202.0994, found: 202.0989.

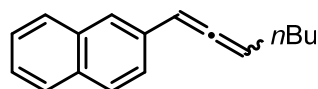
Allenes **4.2** and **4.6** were prepared in accordance with a procedure modified from the report of Wang and coworkers.³⁴



4.6, (3-(cyclohex-1-en-1-yl)propa-1,2-dien-1-yl)benzene

Under a nitrogen atmosphere, 1-ethynylcyclohexene (470 μ L, 423 mg, 4.0 mmol, 1.0 equiv) was added *via* syringe to a mixture of copper(I) iodide (154 mg, 0.81 mmol, 0.2 equiv), lithium *tert*-butoxide (1140 mg, 14.3 mmol, 3.6 equiv), and benzaldehyde tosylhydrazone (2390 mg, 8.7 mmol, 2.2 equiv) in 1,4-dioxane (40 mL). The solution was stirred at 90 $^{\circ}$ C for 1 h, and the progress of the reaction was monitored by TLC. Upon completion of the reaction, the mixture was cooled to room temperature and was filtered through a pad of silica gel and Celite, eluting with EtOAc and cyclohexane. The solvent was removed *in vacuo* to leave a crude mixture, which was purified by column chromatography on silica gel (eluting with hexanes) to afford vinylallene **4.6** as a colorless oil (362 mg, 1.84 mmol, 46% yield).

The spectral data are in agreement with those previously reported.³⁵



4.2, 2-(hepta-1,2-dien-1-yl)naphthalene

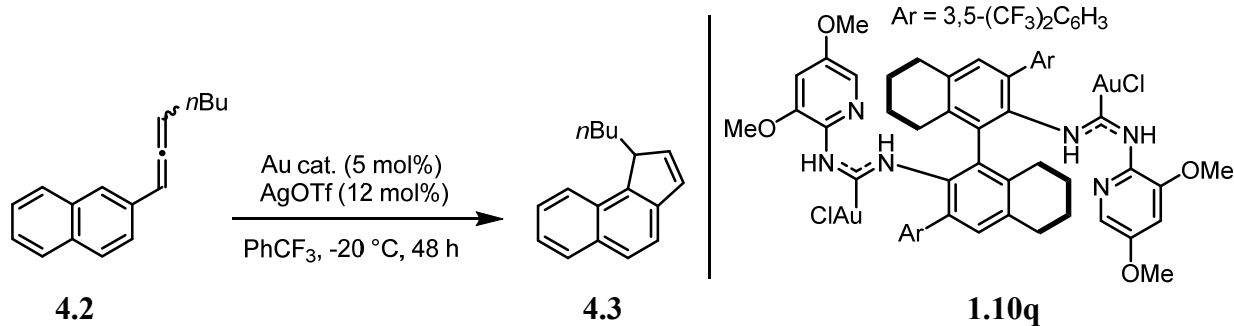
4.06 mmol scale, 18% yield (165 mg, 0.740 mmol)

^1H NMR (600 MHz, CDCl_3) δ 7.85 – 7.73 (m, 3H), 7.65 (s, 1H), 7.51 (dd, J = 8.5, 1.7 Hz, 1H), 7.48 – 7.38 (m, 2H), 6.31 (dt, J = 6.2, 3.1 Hz, 1H), 5.65 (q, J = 6.7 Hz, 1H), 2.19 (qd, J = 7.1, 3.0 Hz, 2H), 1.59 – 1.48 (m, 2H), 1.47 – 1.36 (m, 2H), 0.93 (t, J = 7.2 Hz, 3H).

^{13}C NMR (126 MHz, CDCl_3) δ 205.82, 133.84, 132.82, 132.62, 128.26, 127.83, 127.76, 126.27, 125.57, 125.31, 124.76, 95.50, 95.05, 31.43, 28.65, 22.43, 14.07.

HRMS (EI $^{+}$): calcd. for $[\text{C}_{17}\text{H}_{18}]^{+}$: 222.1409, found: 222.1412.

Procedure for gold(I)-catalyzed enantioselective hydroarylation



Precatalyst **1.10q** (3.7 mg, 0.0025 mmol, 0.05 equiv) and silver triflate (1.6 mg, 0.006 mmol, 0.12 equiv) were weighed in a dram vial and α,α,α -trifluorotoluene was added (0.25 mL). The heterogeneous mixture was sonicated for 5 min using a commercial ultrasonic cleaner, and then filtered through glass fiber into a second dram vial. Substrate **4.2** (11.1 mg, 0.05 mmol, 1.0 equiv.) was weighed in a third dram vial and α,α,α -trifluorotoluene was added (0.25 mL). Both vials were cooled to $-20\text{ }^{\circ}\text{C}$, and then the catalyst mixture was added to the reactant mixture *via* pipette (total volume 0.5 mL). The temperature was maintained for 48 h and then the solvent was removed *in vacuo*. The reaction mixture was diluted with hexane (~ 2 mL) and then passed through a short plug of silica gel to remove the catalyst, washing with hexanes. The solvent was then removed *in vacuo* and the crude reaction mixture was purified by flash column chromatography (hexanes, 4 mL Pasteur pipette column) to afford the product **4.3**.

4.3, 1-butyl-1H-cyclopenta[a]naphthalene

0.0500 mmol scale, 85% yield (9.4 mg, 0.0423)

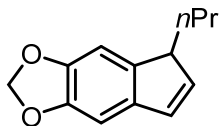
^1H NMR (600 MHz, CDCl_3) δ 8.02 (d, $J = 8.3$ Hz, 1H), 7.91 (d, $J = 8.2$ Hz, 1H), 7.78 (d, $J = 8.2$ Hz, 1H), 7.56 (d, $J = 8.2$ Hz, 1H), 7.52 (ddd, $J = 8.3, 6.8, 1.3$ Hz, 1H), 7.42 (dd, $J = 8.2, 6.8$ Hz, 1H), 6.94 (dt, $J = 5.3, 1.4$ Hz, 1H), 6.75 (dt, $J = 5.3, 1.4$ Hz, 1H), 4.05 – 3.81 (m, 1H), 2.54 – 2.19 (m, 1H), 1.57 (dp, $J = 14.7, 5.5, 5.0$ Hz, 1H), 1.48 – 1.20 (m, 4H), 0.92 – 0.86 (m, 3H).

^{13}C NMR (151 MHz, CDCl_3) δ 143.46, 141.77, 140.49, 132.08, 131.15, 129.74, 129.27, 127.55, 126.03, 124.31, 123.69, 120.68, 50.44, 32.24, 29.62, 23.17, 14.15.

HRMS (EI+): calcd. for $[\text{C}_{17}\text{H}_{18}]^+$: 222.1409, found: 222.1408.

HPLC: IB column, 100% hexanes, 1.00 mL/min, t_{R} = major: 16.9 min, minor: 31.1 min. 93% ee.

Indene **4.5** and cyclopentadiene **4.7** were prepared in an analogous fashion.



4.5, 5-propyl-5H-indeno[5,6-d][1,3]dioxole

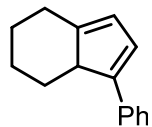
0.0500 mmol scale, 83% yield (8.4 mg, 0.0415 mmol)

^1H NMR (600 MHz, CDCl_3) δ 6.92 (s, 1H), 6.83 (s, 1H), 6.68 (dd, $J = 5.5, 1.9$ Hz, 1H), 6.46 (dd, $J = 5.6, 1.9$ Hz, 1H), 5.95 (s, 2H), 3.37 (td, $J = 5.6, 2.4$ Hz, 1H), 1.93 – 1.75 (m, 1H), 1.52 – 1.32 (m, 3H), 0.94 (t, $J = 7.1$ Hz, 3H).

^{13}C NMR (151 MHz, CDCl_3) δ 146.52, 145.79, 142.21, 138.50, 138.03, 130.41, 104.63, 102.09, 100.98, 50.30, 34.01, 20.84, 14.54.

HRMS (EI+): calcd. for $[C_{13}H_{14}O_2]^+$: 202.0994, found: 202.0990.

HPLC: OJ column, 100% hexanes, 1.00 mL/min, t_R = major: 5.5 min, minor: 6.2 min. 68% ee.



4.7, 3-phenyl-3a,5,6,7-tetrahydro-4H-indene

0.0500 mmol scale, 91% yield (8.9 mg, 0.045 mmol)

The spectral data are in agreement with those previously reported.³²

HPLC: IB column, 99.5:0.5 hexanes:isopropanol, 1.00 mL/min, t_R = major: 5.8 min, minor: 7.4 min. 52% ee.

References

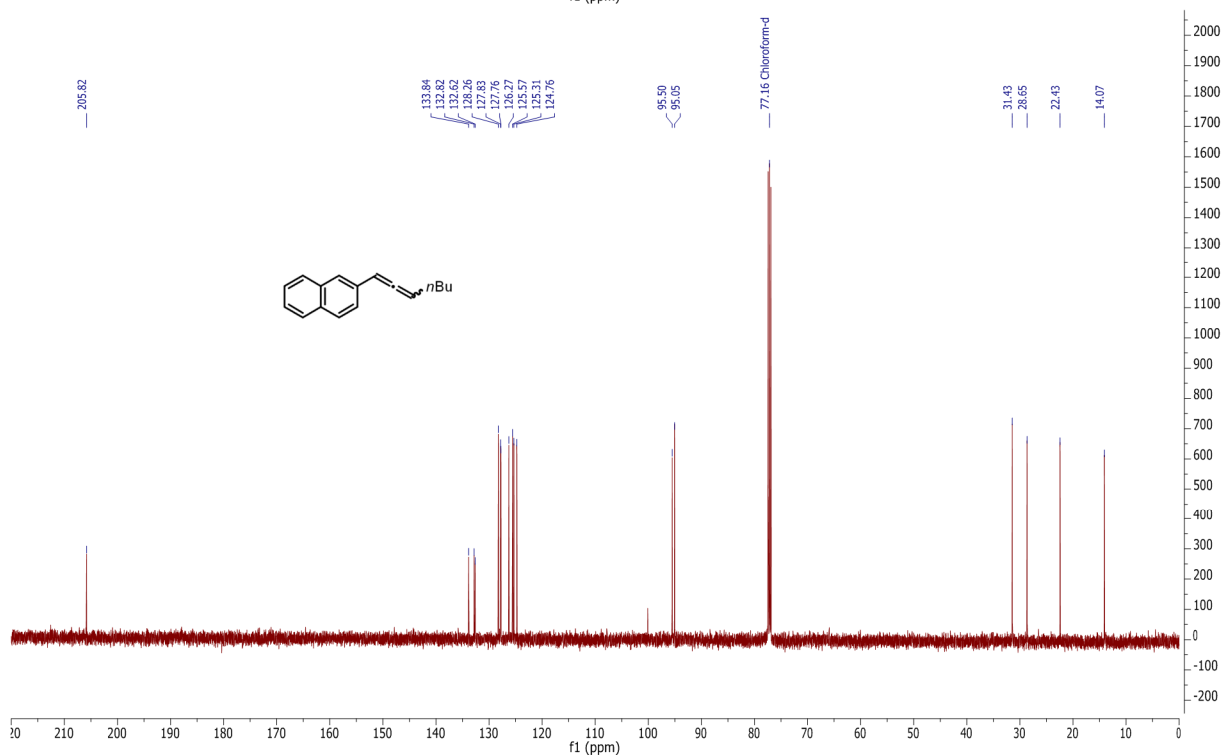
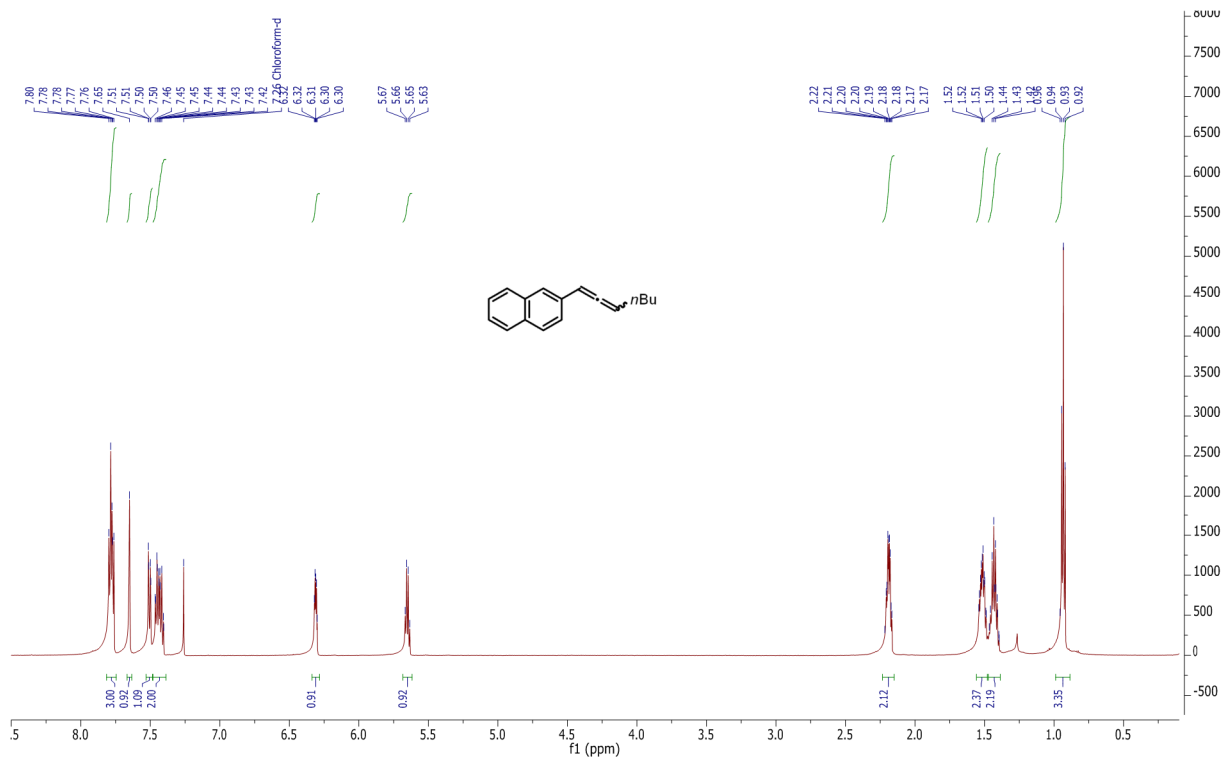
- (1) de Mendoza, P.; Echavarren, A. M. In *Modern Gold Catalyzed Synthesis*; Hashmi, A. S. K., Toste, F. D., Eds.; Wiley-VCH Verlag GmbH & Co. KGaA, 2012; pp 135–152.
- (2) Muñoz, M. P.; Adrio, J.; Carretero, J. C.; Echavarren, A. M. *Organometallics* **2005**, *24* (6), 1293.
- (3) Chao, C.-M.; Vitale, M. R.; Toullec, P. Y.; Genêt, J.-P.; Michelet, V. *Chem. – Eur. J.* **2009**, *15* (6), 1319.
- (4) Matsumoto, Y.; Selim, K. B.; Nakanishi, H.; Yamada, K.; Yamamoto, Y.; Tomioka, K. *Tetrahedron Lett.* **2010**, *51* (2), 404.
- (5) Andreiadis, E. S.; Vitale, M. R.; Mézailles, N.; Goff, X. L.; Floch, P. L.; Toullec, P. Y.; Michelet, V. *Dalton Trans.* **2010**, *39* (44), 10608.
- (6) Pradal, A.; Chao, C.-M.; Vitale, M. R.; Toullec, P. Y.; Michelet, V. *Tetrahedron* **2011**, *67* (24), 4371.
- (7) Wang, W.; Yang, J.; Wang, F.; Shi, M. *Organometallics* **2011**, *30* (14), 3859.
- (8) Yamada, K.; Matsumoto, Y.; Selim, K. B.; Yamamoto, Y.; Tomioka, K. *Tetrahedron* **2012**, *68* (22), 4159.
- (9) Liu, C.; Widenhoefer, R. A. *Org. Lett.* **2007**, *9* (10), 1935.
- (10) Teller, H.; Corbet, M.; Mantilli, L.; Gopakumar, G.; Goddard, R.; Thiel, W.; Fürstner, A. *J. Am. Chem. Soc.* **2012**, *134* (37), 15331.
- (11) Wang, M.-Z.; Zhou, C.-Y.; Guo, Z.; Wong, E. L.-M.; Wong, M.-K.; Che, C.-M. *Chem. – Asian J.* **2011**, *6* (3), 812.
- (12) Royo, B.; Peris, E. *Eur. J. Inorg. Chem.* **2012**, *2012* (9), 1309.
- (13) JohnJ Esteb. In *Stereoselective Polymerization with Single-Site Catalysts*; CRC Press, 2007; pp 83–99.
- (14) Gabriele, B.; Mancuso, R.; Veltri, L. *Chem. – Eur. J.* **2016**, *22* (15), 5056.
- (15) Marion, N.; Díez-González, S.; de Frémont, P.; Noble, A. R.; Nolan, S. P. *Angew. Chem. Int. Ed.* **2006**, *45* (22), 3647.
- (16) Nun, P.; Gaillard, S.; Poater, A.; Cavallo, L.; Nolan, S. P. *Org. Biomol. Chem.* **2010**, *9* (1), 101.
- (17) Asikainen, M.; Woodward, S. *Tetrahedron* **2012**, *68* (27–28), 5492.
- (18) Liu, Y.; Zhu, J.; Qian, J.; Xu, Z. *J. Org. Chem.* **2012**, *77* (12), 5411.
- (19) Lin, G.-Y.; Yang, C.-Y.; Liu, R.-S. *J. Org. Chem.* **2007**, *72* (18), 6753.
- (20) Sanz, R.; Miguel, D.; Rodríguez, F. *Angew. Chem. Int. Ed.* **2008**, *47* (38), 7354.
- (21) Álvarez, E.; Miguel, D.; García-García, P.; Fernández-Rodríguez, M.; Rodríguez, F.; Sanz, R. *Synthesis* **2012**, *44* (12), 1874.
- (22) Zhu, Z.-B.; Shi, M. *Chem. – Eur. J.* **2008**, *14* (33), 10219.
- (23) Bauer, J. T.; Hadfield, M. S.; Lee, A.-L. *Chem. Commun.* **2008**, No. 47, 6405.
- (24) Hadfield, M. S.; Häller, L. J. L.; Lee, A.-L.; Macgregor, S. A.; O'Neill, J. A. T.; Watson, A. M. *Org. Biomol. Chem.* **2012**, *10* (22), 4433.
- (25) Zhang, X.-M.; Tu, Y.-Q.; Jiang, Y.-J.; Zhang, Y.-Q.; Fan, C.-A.; Zhang, F.-M. *Chem. Commun.* **2009**, No. 31, 4726.
- (26) Bucher, J.; Stöber, T.; Rudolph, M.; Rominger, F.; Hashmi, A. S. K. *Angew. Chem. Int. Ed.* **2015**, *54* (5), 1666.
- (27) Martínez, A.; García-García, P.; Fernández-Rodríguez, M. A.; Rodríguez, F.; Sanz, R. *Angew. Chem. Int. Ed.* **2010**, *49* (27), 4633.

- (28) Sanjuán, A. M.; Rashid, M. A.; García-García, P.; Martínez-Cuezva, A.; Fernández-Rodríguez, M. A.; Rodríguez, F.; Sanz, R. *Chem. – Eur. J.* **2015**, *21* (7), 3042.
- (29) Lee, J. H.; Toste, F. D. *Angew. Chem. Int. Ed.* **2007**, *46* (6), 912.
- (30) Funami, H.; Kusama, H.; Iwasawa, N. *Angew. Chem. Int. Ed.* **2007**, *46* (6), 909.
- (31) Melchionna, M.; Nieger, M.; Helaja, J. *Chem. – Eur. J.* **2010**, *16* (28), 8262.
- (32) Wirtanen, T.; Muuronen, M.; Melchionna, M.; Patzschke, M.; Helaja, J. *J. Org. Chem.* **2014**, *79* (21), 10269.
- (33) Sanjuán, A. M.; García-García, P.; Fernández-Rodríguez, M. A.; Sanz, R. *Adv. Synth. Catal.* **2013**, *355* (10), 1955.
- (34) Hossain, M. L.; Ye, F.; Zhang, Y.; Wang, J. *J. Org. Chem.* **2013**, *78* (3), 1236.
- (35) Regás, D.; Ruiz, J. M.; Afonso, M. M.; Palenzuela, J. A. *J. Org. Chem.* **2006**, *71* (24), 9153.

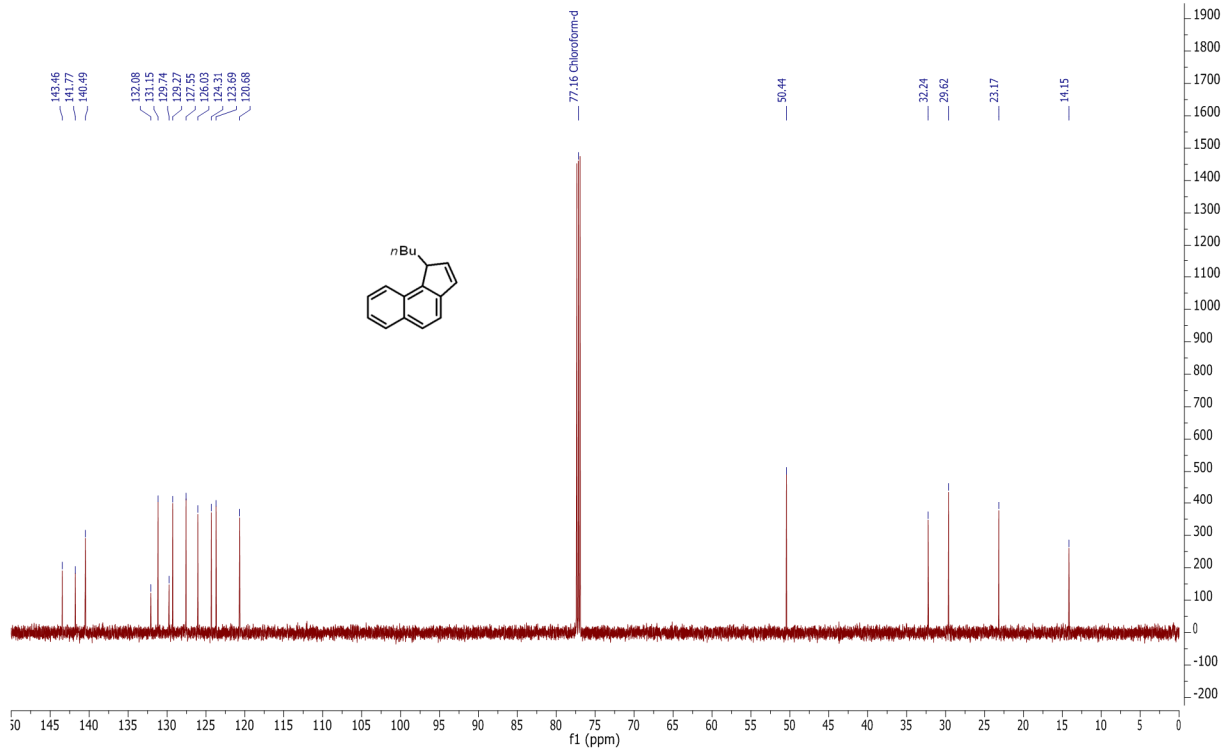
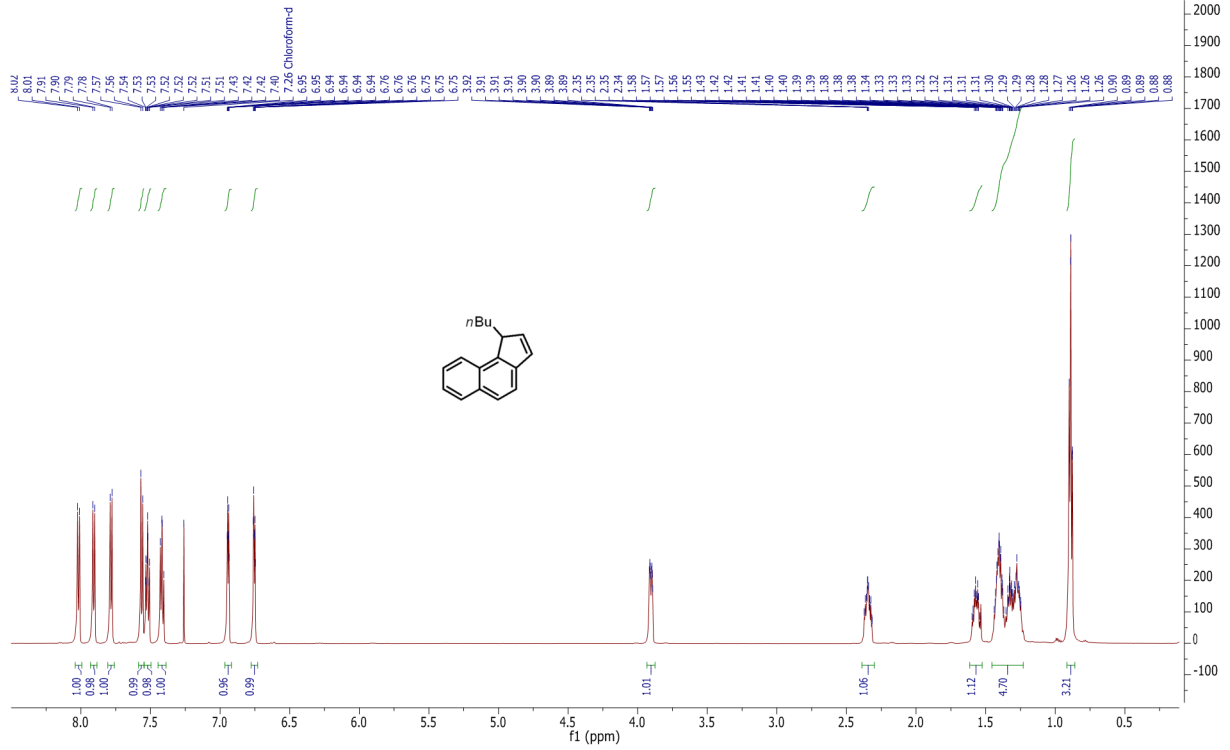
Appendix 1 - NMR Spectra

In some cases, unintegrated resonances in the 0-2 ppm region may appear. These correspond to trace quantities of residual solvents, including water, grease, and other aliphatic hydrocarbons.

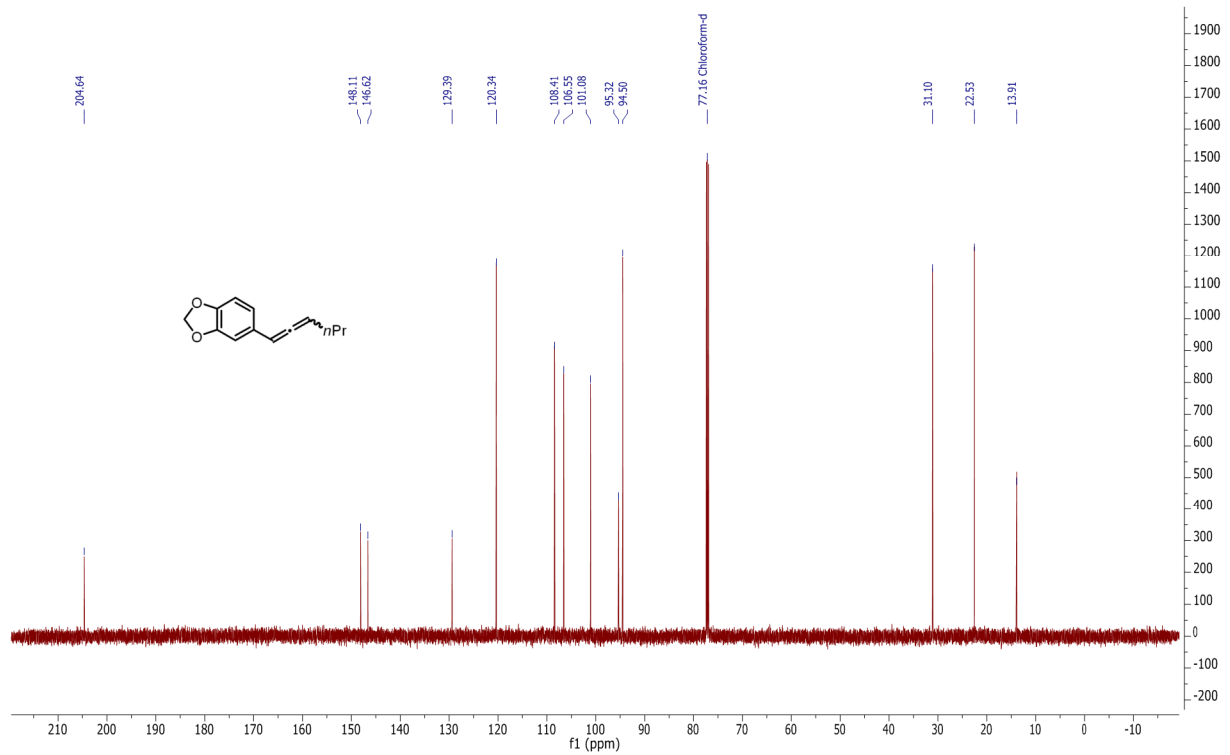
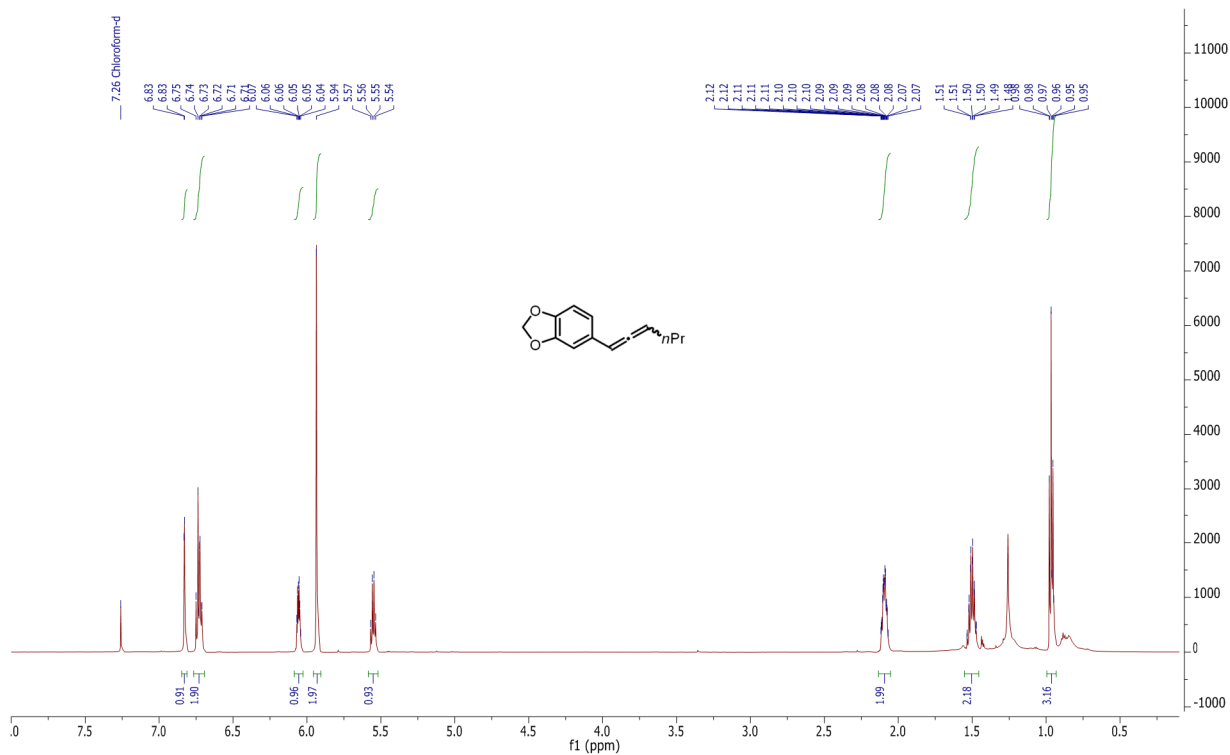
4.2



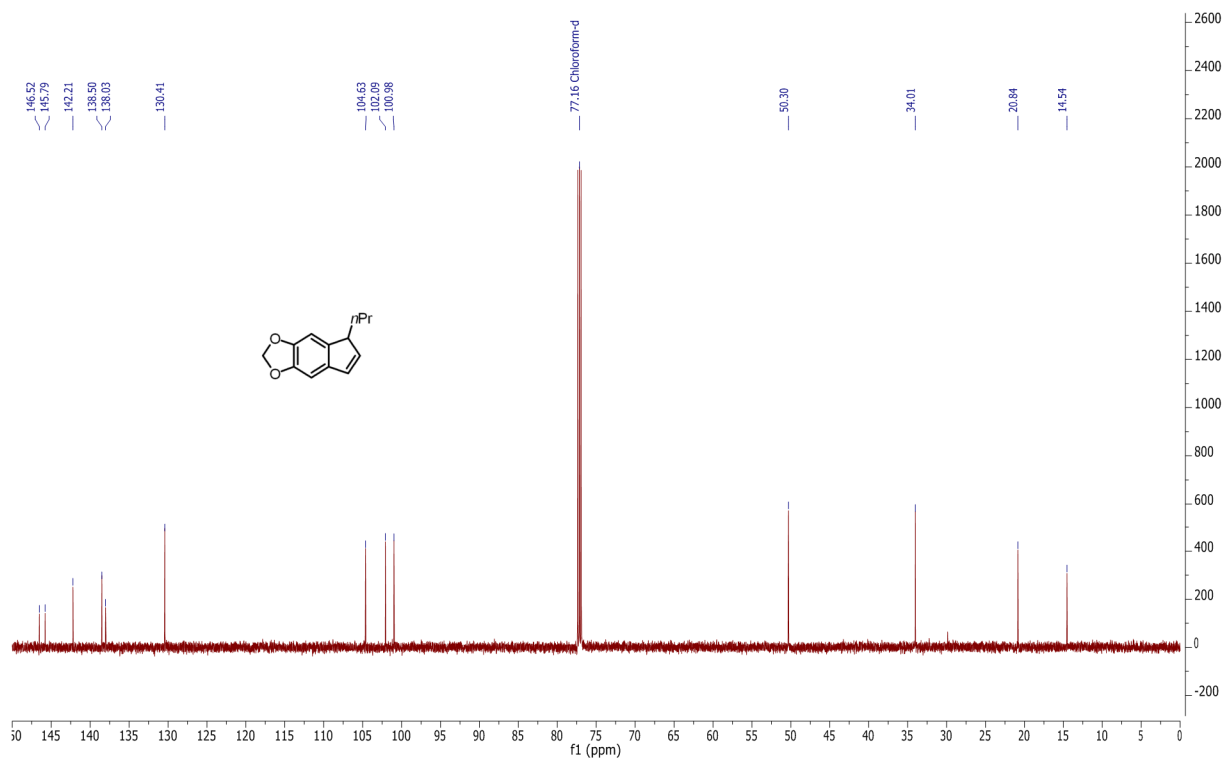
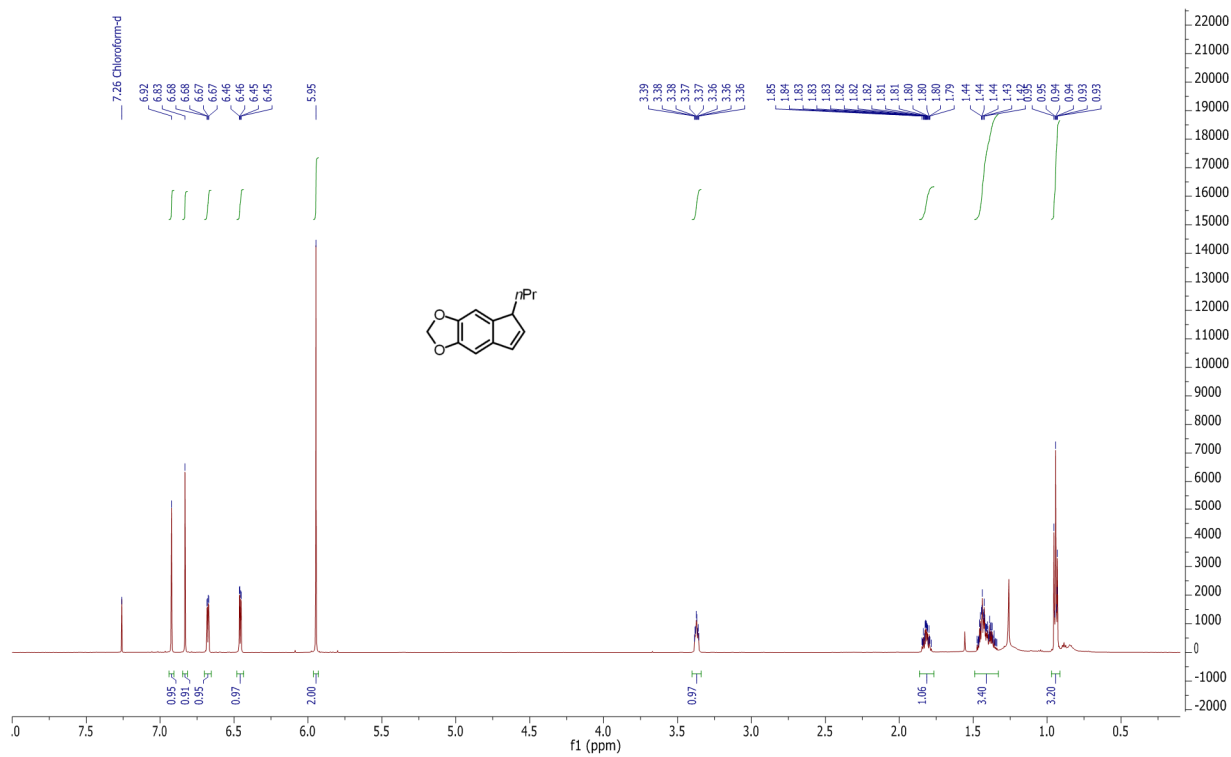
4.3



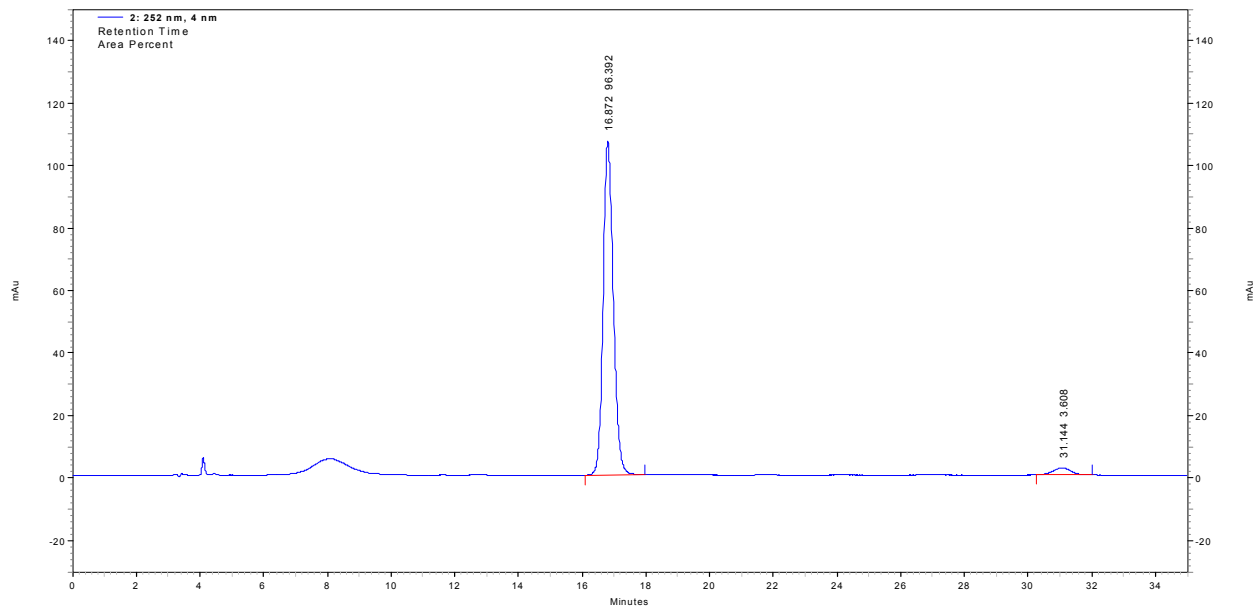
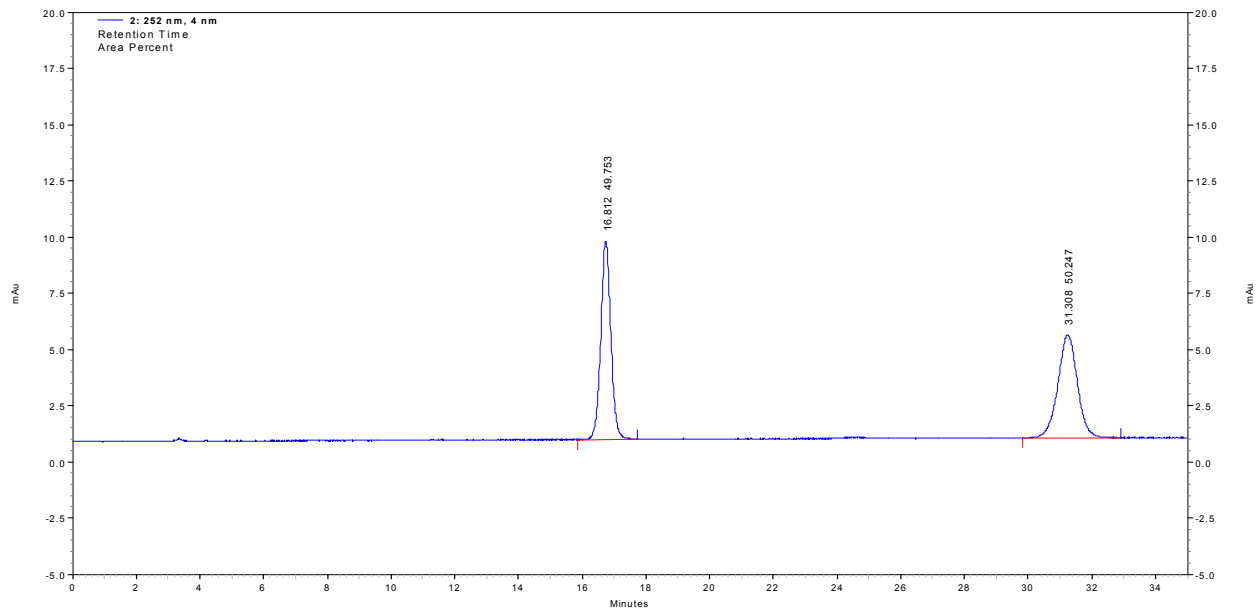
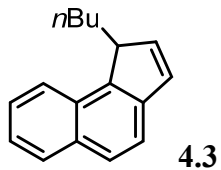
4.4



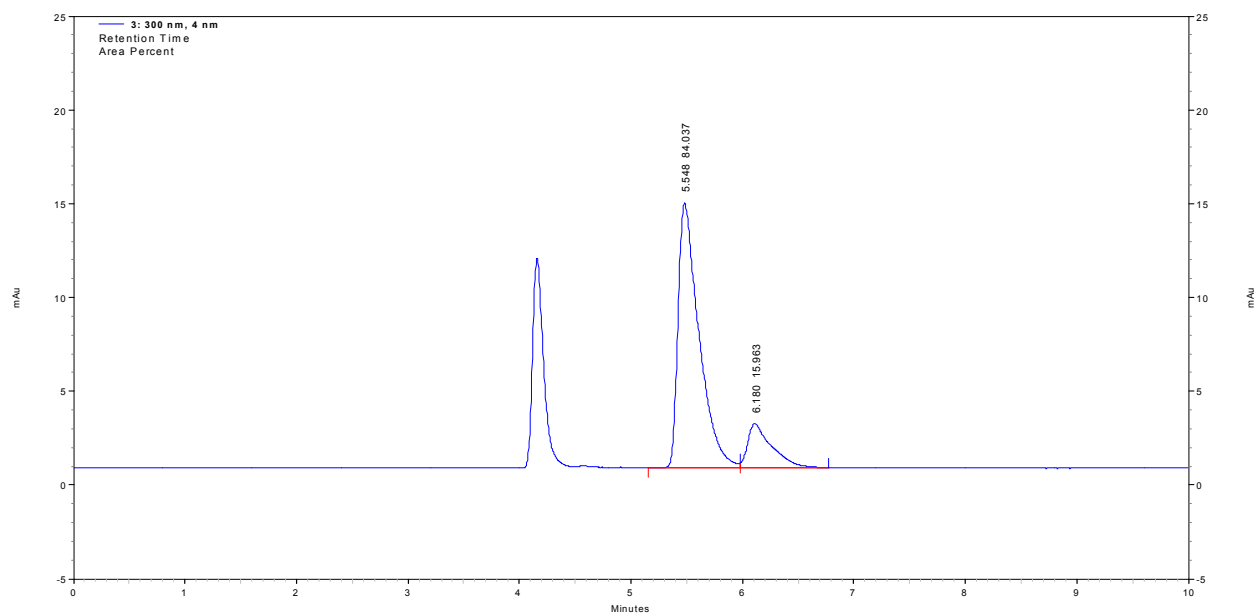
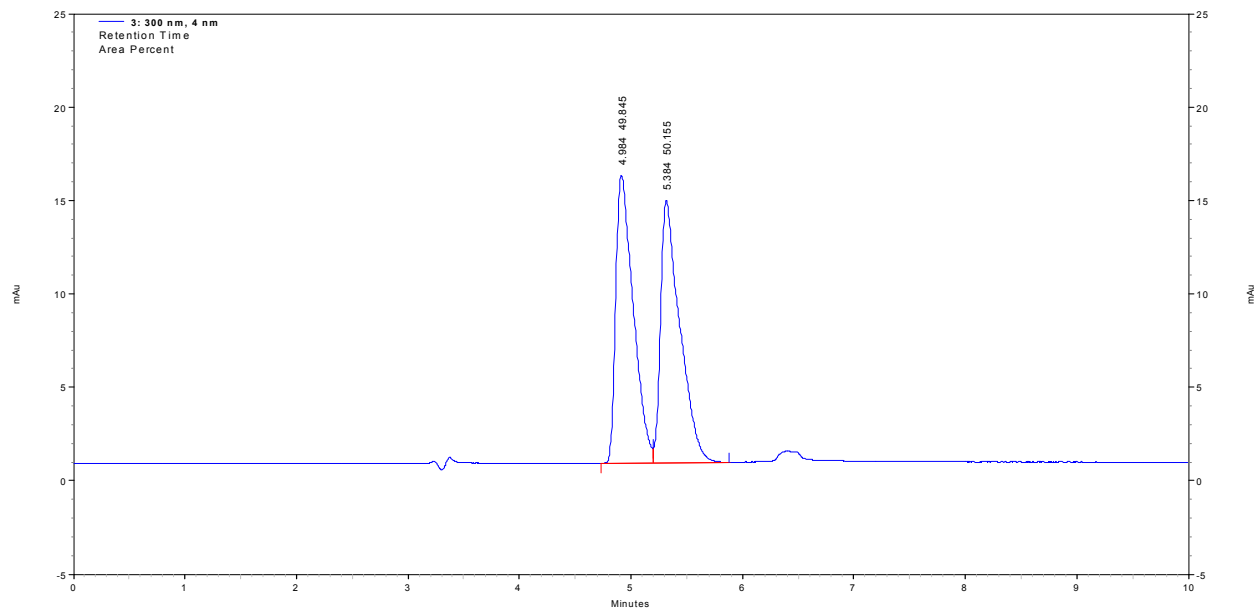
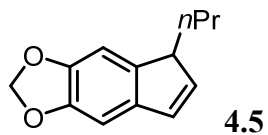
4.5



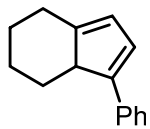
Appendix 2 - HPLC Traces



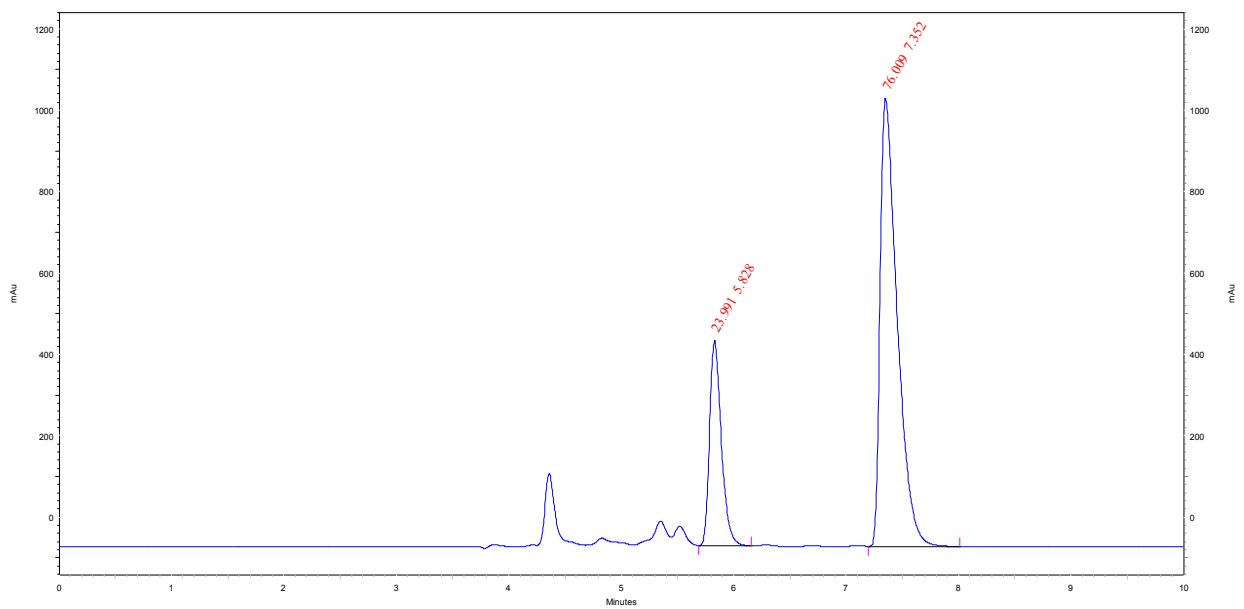
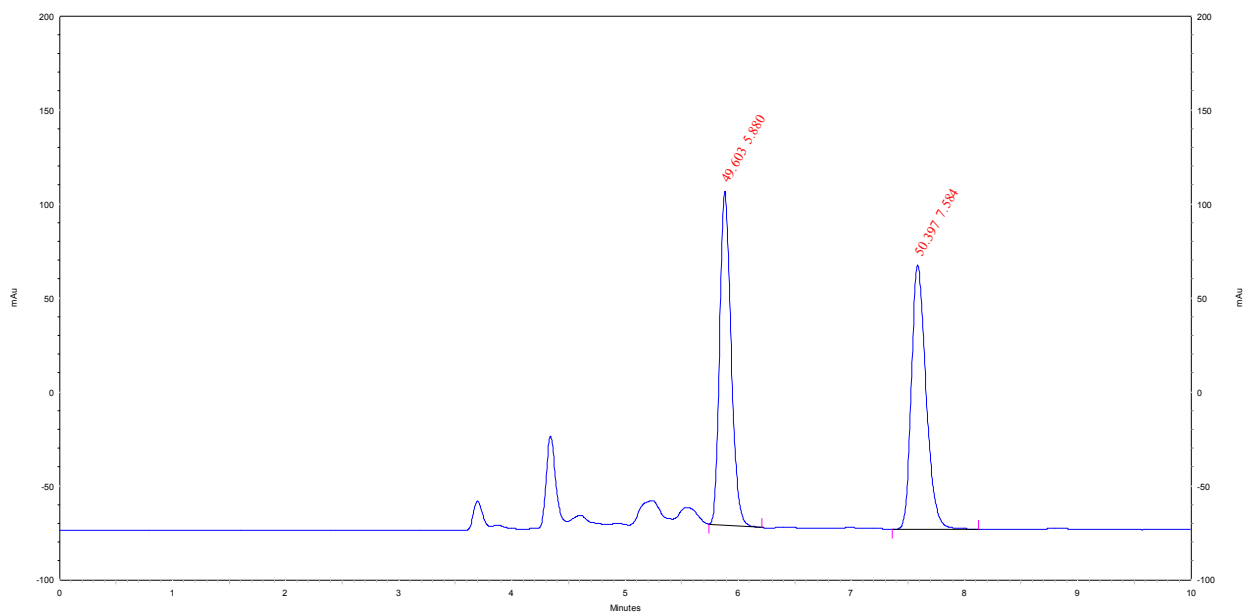
| Retention Time | Area Percent |
|----------------|--------------|
| 16.872 | 96.392 |
| 31.144 | 3.608 |



| 300 nm Retention Time | Area Percent |
|--------------------------|--------------|
| 5.548 | 84.037 |
| 6.180 | 15.963 |



4.7



220 nm

Retention Time Area Percent

5.828

23.991

7.352

76.009

Chapter 5. Enantioselective Tandem [3,3]-Rearrangement—[2+2] Cycloaddition

This work is currently being prepared for publication¹

¹ Dr. Christian N. Kuzniewski performed the initial reactions. Levi Pilapil prepared a number of substrates and performed racemic reactions. Zachary Niemeyer carries out all the computational work and reaction modelling. Dr. Suresh Pindi continues the synthesis of new catalysts and performs asymmetric reactions for model validation.

Introduction

Tandem reactions (also known as cascade or relay reactions) in which two or more distinct chemical transformations occur in one pot, are an efficient avenue for the rapid construction of chemical complexity, without the need for multiple work-up procedures or the isolation of reactive intermediates.¹ Gold-catalyzed tandem reactions have a rich history,² especially when used in the formation of carbo-, hetero-, or polycyclic compounds.^{3,4} Of particular import are the applications to indole- and indoline-containing scaffolds, which play an outsized role in medicinally relevant compounds,⁵ and several such examples are outlined below.

In 2005, Zhang reported the tandem [3,3]-rearrangement—[2+2] cycloaddition of indolyl propargyl acetates (Figure 5.1).⁶ The observed regiochemistry of the 2,3-indoline-fused cyclobutane products, as well as the intermediacy of an allenic ester, supported the envisioned tandem mechanism of the reaction illustrated in Figure 5.2.

Figure 5.1 Tandem [3,3]-rearrangement—[2+2] cycloaddition of indolyl propargyl acetates

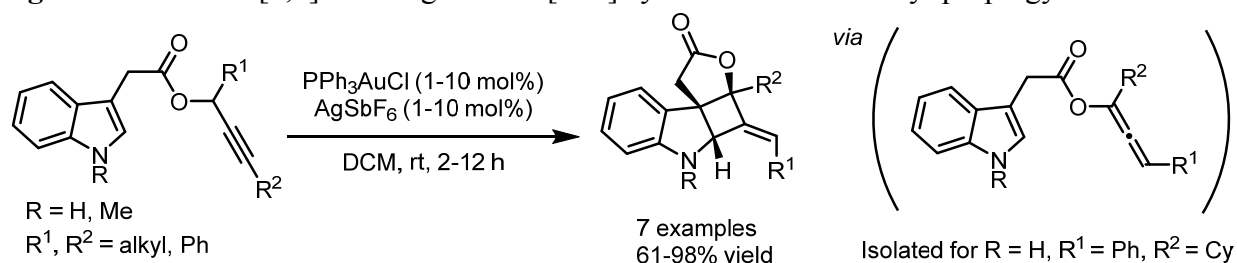
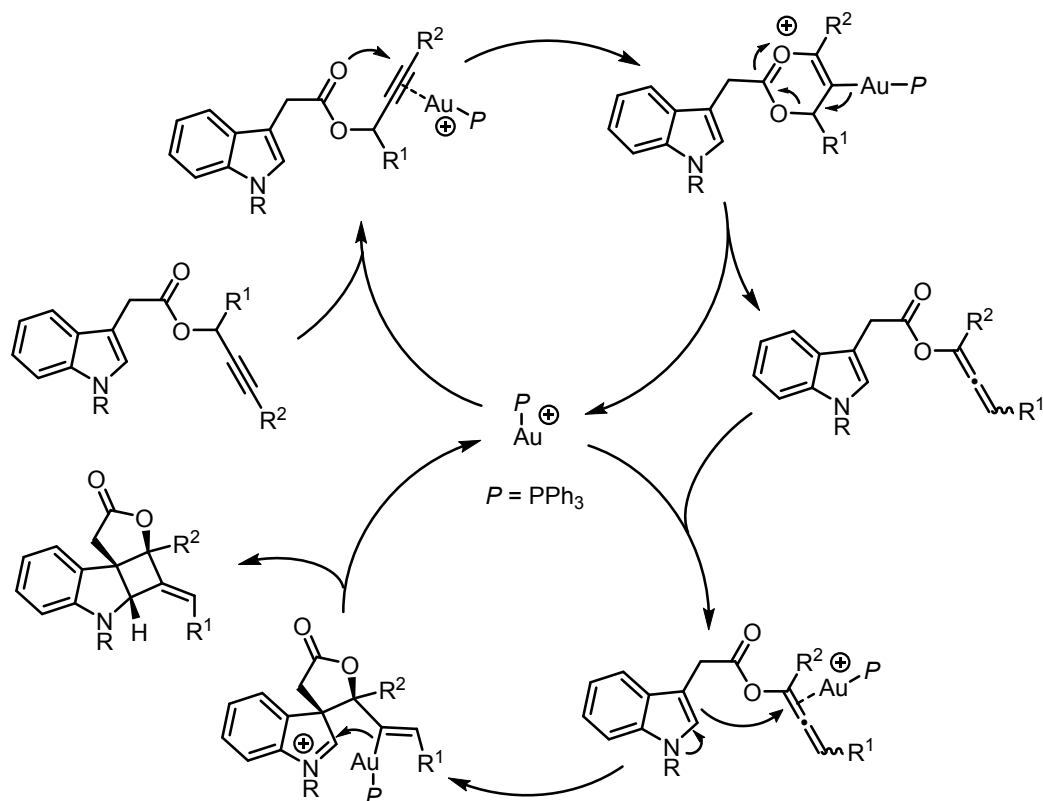


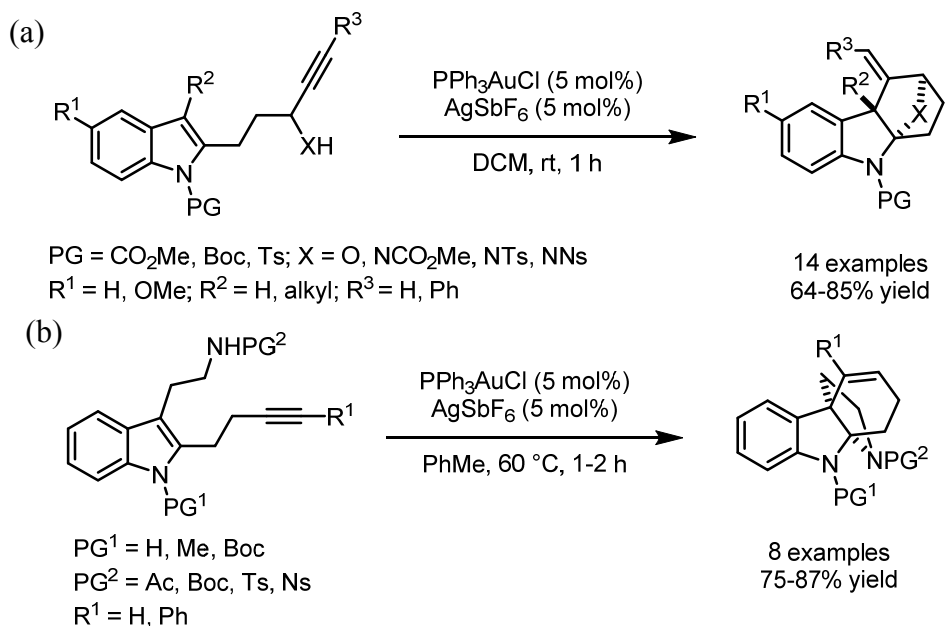
Figure 5.2 Proposed mechanism of tandem [3,3]-rearrangement—[2+2] cycloaddition



Activation of the alkyne by cationic gold(I) and subsequent [3,3]-rearrangement generates the allene intermediate. Gold(I) coordination to this allene sets up nucleophilic attack by the indole, generating a vinyl-gold complex which undergoes trapping of the iminium functional group, furnishing the 4-membered ring and regenerating the cationic catalytic species. Zhang and coworkers later showed that the same class of substrates displayed divergent reactivity when catalyzed by platinum, furnishing 2,3-indoline-fused cyclopentenes.⁷

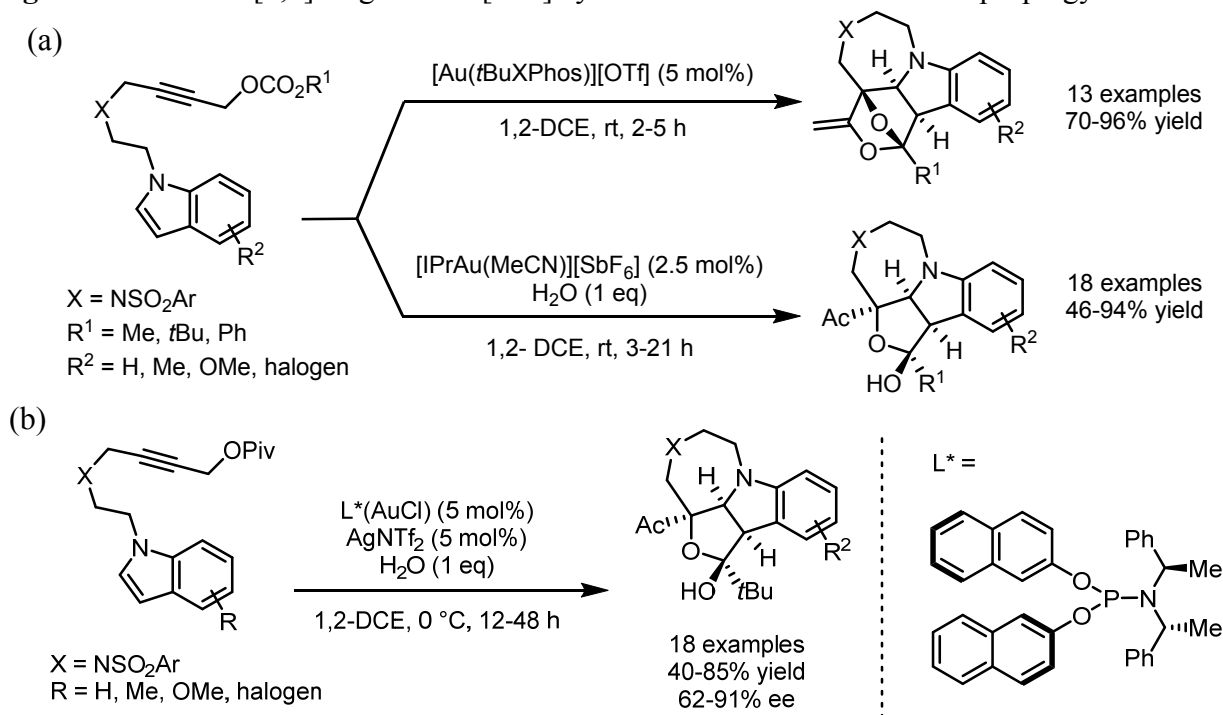
Several other gold(I)-catalyzed tandem strategies for the construction of polycyclic indoline-fused architectures have been disclosed. Wang and coworkers reported the formation of tetracyclic indolines from alkynylindoles with pendant heteroatom nucleophiles.⁸ Two classes of substrates were competent in the reaction manifold, reacting either to give 6-*endo-dig* cyclization products with bridging oxygen or nitrogen moieties (Figure 5.3a), or to form 6-*exo-dig* cyclization products with fused pyrrolidino- residues (Figure 5.3b). In the latter case, one of the compounds obtained was converted into a key intermediate from the total synthesis of Minfiensine, an akuammiline alkaloid.⁹ Researchers in the Wang lab later employed this methodology in the synthesis of novel aza-tricyclic indolines with interesting biological properties.¹⁰

Figure 5.3 Tandem cyclization—amination/alkoxylation of alkynylindoles



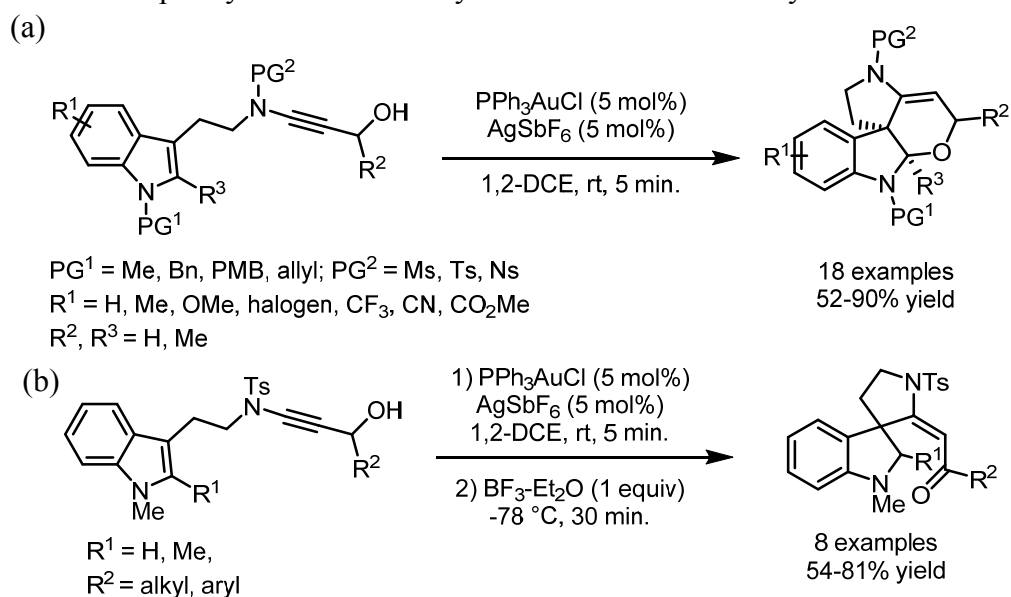
Shi and coworkers disclosed a synthesis of tetra- and pentacyclic indolines from indole-tethered propargylic ester substrates.¹¹ While reminiscent of the Zhang system, the mode of reactivity diverged due to the 1,2-migration of the ester and the different connectivity on the indole ring. The authors demonstrated good yields across a broad substrate scope in two closely related reactions, mainly differing in the presence or absence of water to open or leave closed the fifth ring system, respectively (Figure 5.4a). In addition, an enantioselective variant of the reaction was achieved through the application of a BINOL-derived chiral phosphoramidite ligand (Figure 5.4b).

Figure 5.4 Tandem [1,2]-migration—[3+2] cycloaddition of indole-tethered propargylic esters



Very recently, Yang and coworkers reported a synthesis of dihydropyran-fused pyrrolidinoindolines from indole-ynamide propargyl alcohols.¹² In addition to demonstrating good yields across a variety of substrates (Figure 5.5a), the authors obtained one tetracyclic product in 60% ee by using a MeOBIPHEP ligand. Furthermore, they showed that the pyran ring was opened with a Lewis acid in a second step (in one pot) revealing a spirocyclic product (Figure 5.5b).

Figure 5.5 Tandem spirocyclization—alkoxylation of indole-tethered ynamide alcohols



Results and Discussion

Motivated by our previous success in rendering enantioselective the tandem reaction of propargyl acetate substrates,¹³ and inspired by the dense functionalization of the indoline-fused cyclobutane products obtained from the seminal Zhang report,⁶ we sought to examine and optimize the asymmetric tandem [3,3]-rearrangement—[2+2] cycloaddition of indolyl propargyl acetates. Compound **5.1** was chosen as a model substrate due to its physical characteristics; it could be isolated as an easy-to-weigh powder, whereas most other derivatives were obtained as waxy solids or viscous oils.

Embarking on an exhaustive survey of ADC gold(I) complexes as catalysts for the reaction revealed several interesting and unexpected trends (Table 5.1). Modulating the electronics of 3,5-disubstituted aromatic groups (entries 1-5) revealed that the unsubstituted Ph analog (**1.10a**) gave the greatest ee value, albeit in the lowest yield. However, the steric influence of these aromatic groups appeared to be overriding, as revealed by the various bis(trifluoromethyl) derivatives (entries 5-8). Trifluoromethyl substitution in the 2,4 and 2,6 positions (**1.10f** and **1.10h**) gave much greater selectivity than that observed with the 3,5 pattern (**1.10e**), while 2,5 disubstitution (**1.10g**) provided an intermediate value.

Surprisingly, preserving the 3,5-bis(trifluoromethyl) aryl substitution and introducing pyridyl substituents at the 2' position (*ortho*- to the carbene nitrogen) induced a switch in the sense of enantioinduction (entries 9-12). The magnitude of this reversal appeared to track with the size of the substituent, and the greatest opposite ee values were obtained with a particularly bulky neopentoxy substituent (**1.10m**), implying a steric effect at this position. But, when 3' (*meta*-) and 4' (*para*-) pyridyl substituents were investigated (entries 13-15) the original sense of enantioinduction was restored, and even improved (compare entries 5, 13, and 15). A similar enantiodivergence and reversal was observed with catalysts bearing 3,5-dimethoxy aryl groups and 2' substituents (entries 19 and 20) versus a 4' substituent (entry 21). The presence of both 2' and 4' methoxy substituents (**1.10q**) demonstrated that the effect of *ortho*- substitution was overriding, but tempered by the presence of a *para*- substituent (compare entries 10, 14, and 16). The introduction of alternative heterocycles—pyrimidine and pyrazine—led to poor enantioselectivity, and in the latter case, significantly slowed the reaction (entries 17 and 18).

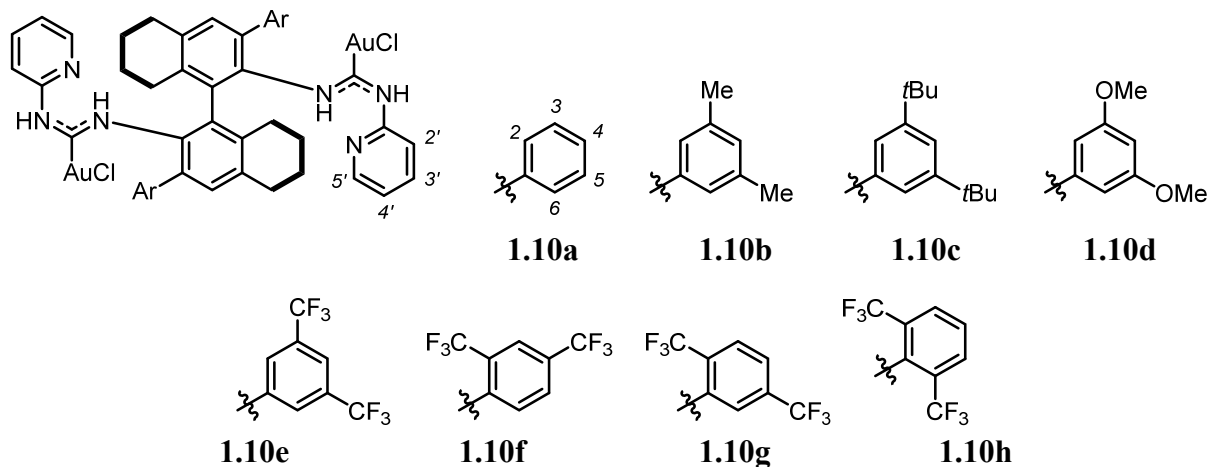
Table 5.1 Survey of ADC gold(I) complexes in tandem rearrangement—cycloaddition reaction



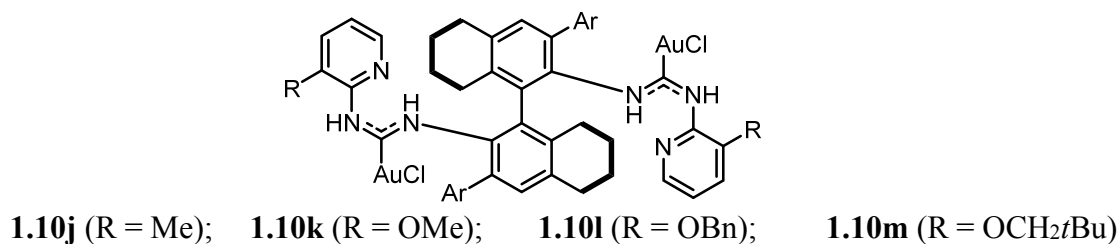
| Entry ^a | Precatalyst | Yield (%) ^b | ee (%) ^c |
|--------------------|--------------|------------------------|---------------------|
| 1 | 1.10a | 26 | 67 |
| 2 | 1.10b | 75 | 30 |
| 3 | 1.10c | 90 | 55 |
| 4 | 1.10d | 55 | 60 |

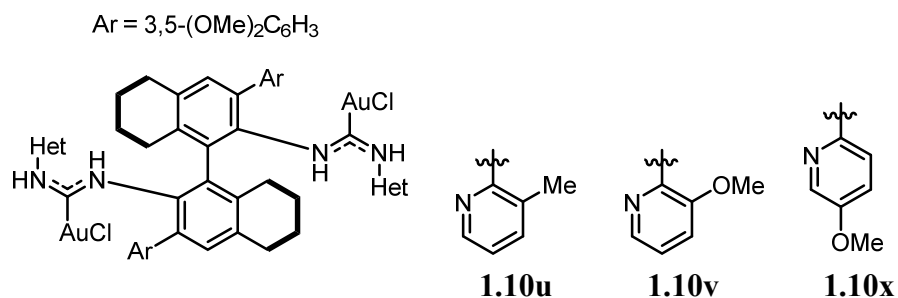
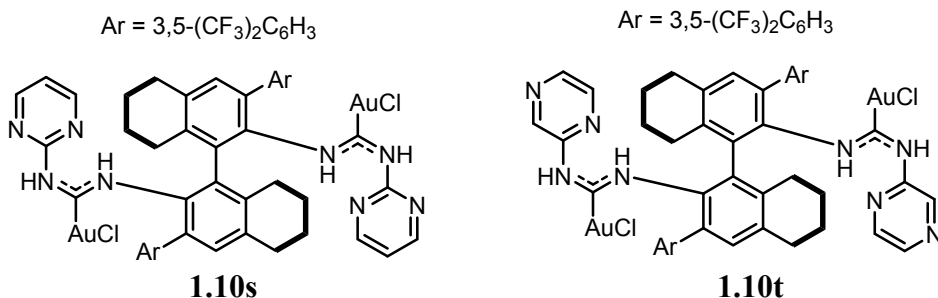
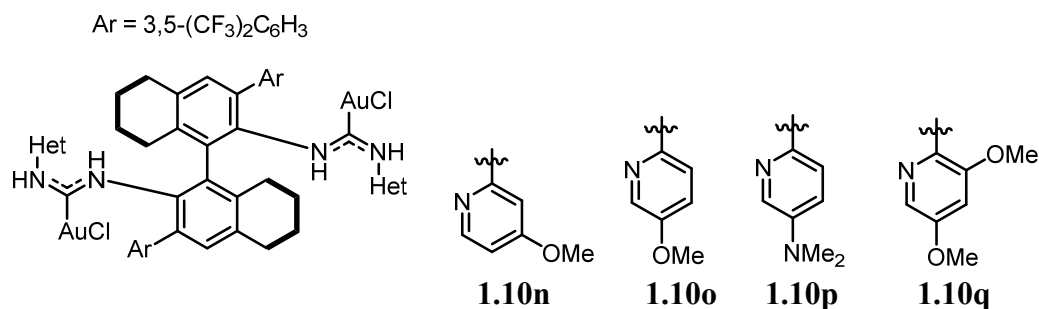
| Entry ^a | Precatalyst | Yield (%) ^b | ee (%) ^c |
|--------------------|--------------|------------------------|---------------------|
| 5 | 1.10e | 86 | 42 |
| 6 | 1.10f | 50 | 81 |
| 7 | 1.10g | 100 | 61 |
| 8 | 1.10h | 37 | 81 |
| 9 | 1.10j | 92 | -9 |
| 10 | 1.10k | 89 | -50 |
| 11 | 1.10l | 99 | -50 |
| 12 | 1.10m | 87 | -75 |
| 13 | 1.10n | 84 | 65 |
| 14 | 1.10o | 93 | 29 |
| 15 | 1.10p | 41 | 71 |
| 16 | 1.10q | 63 | -36 |
| 17 | 1.10s | 99 | -17 |
| 18 | 1.10t | trace | 12 |
| 19 | 1.10u | 89 | -16 |
| 20 | 1.10v | 37 | -29 |
| 21 | 1.10x | 61 | 42 |

a] Conditions: 0.05 mmol **5.1**, 0.0025 mmol gold(I) precatalyst, 0.006 mmol silver triflate, 1.0 mL of DCM (0.05 M), 3 hours at room temperature. [b] Determined by ¹H NMR with 1,3,5-trimethoxybenzene as an internal standard. [c] Determined by chiral HPLC.



Ar = 3,5-(CF₃)₂C₆H₃

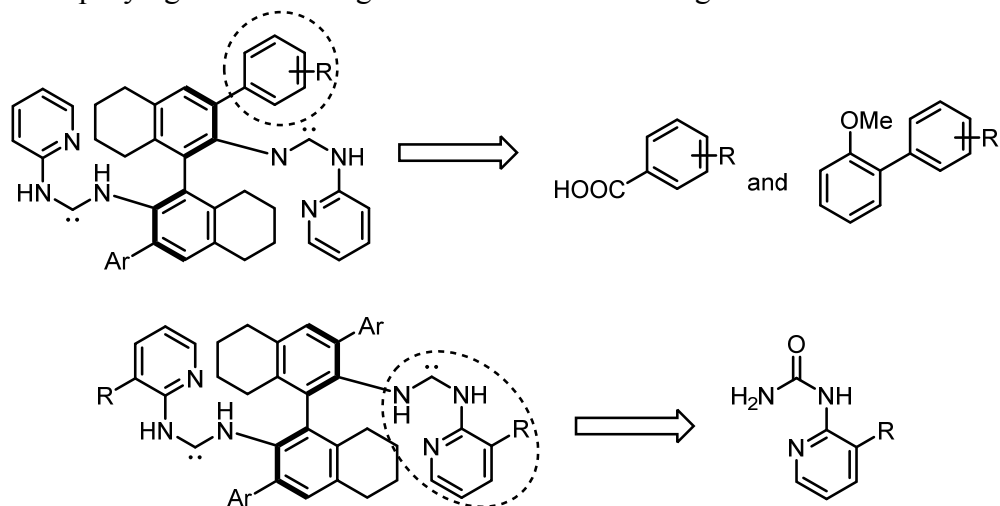




Eager to probe the cause of this unusual reversal of enantioselectivity, we have partnered with researchers in the Sigman group to analyze the reaction in a systematic manner. Sigman and coworkers published several studies in which they study enantioselective reactions by simplifying and assigning parameters to catalysts and substrates based on their steric and electronic properties, and then develop free-energy relationships to model the observed enantiomeric excesses and predict the effect of modifications to the system.^{14–18}

The parametrization strategy has focused on independently investigating the two domains of diversity in the BINAM-derived ADC gold(I) precatalysts. The aryl residues have been simplified to the corresponding carboxylic acids and 2'-methoxybiphenyls, while the pyridyl carbene fragments have been mapped onto the corresponding ureas (Figure 5.6). This approach allows for the assignment of the corresponding C=O stretching frequencies,¹⁹ dihedral angles, Sterimol distances²⁰ and Hammett values.²¹

Figure 5.6 Simplifying and modelling BINAM-derived ADC ligands



Initial studies have identified promising trends, and a model has been developed on the basis of this training set of precatalyst structures. Indeed, the correlation between the predicted and experimental selectivities is quite good, with a coefficient of determination (R-squared value) of 0.97. This work is still ongoing, and hopefully will lead to fruitful insights on the origins of selectivity, as well as the development of new ADC gold(I) catalysts. Additionally, we hope to further elaborate the model to include descriptors of the substrate structures in order to make predictions regarding the scope of the reaction.

Experimental

General information

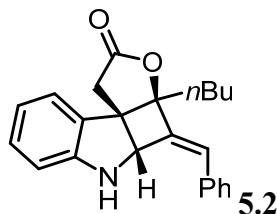
Unless otherwise noted, reagents were obtained from commercial sources and used without further purification. Dry dichloromethane was obtained by passage through activated alumina columns under argon. TLC analysis of reaction mixtures was performed on Merck silica gel 60 F₂₅₄ TLC plates and visualized by ultraviolet light, iodine or potassium permanganate stain. Flash chromatography was carried out with ICN SiliTech 32-63 D 60 Å silica gel. Enantioselectivity was determined by chiral HPLC using Daicel Chiralpak IC column (0.46 cm x 25 cm). A racemic sample was prepared in accordance with a procedure reported by Zhang.⁶

Substrate synthesis

The synthesis of indolyl propargyl acetate **5.1** has been described previously, and the spectral data are in agreement with those previously reported.⁶

Procedure for enantioselective gold(I)-catalyzed tandem reaction

The appropriate gold(I) precatalyst **1.10** (0.0025 mmol, 0.05 equiv) and silver triflate (1.6 mg, 0.006 mmol, 0.12 equiv) were weighed in a dram vial and DCM was added (1.0 mL). The heterogeneous mixture was sonicated for 5 min using a commercial ultrasonic cleaner, and then filtered through glass fiber into a second dram vial, which had been pre-weighed with substrate **5.1** (17.3 mg, 0.05 mmol, 1.0 equiv). The reaction vial was kept at room temperature for 3 h and then the reaction was quenched by addition of Et₃N (ca. 200 µL, 1.4 mmol). The reaction solvent was then removed *in vacuo* and the crude reaction mixture was re-dissolved in Et₂O and passed through a plug of silica gel to remove the catalyst. The solvent was again removed *in vacuo* and a solution of 1,3,5-trimethoxybenzene in CDCl₃ (1.0 mL, 0.03 M) was added *via* syringe for ¹H NMR analysis. A small portion of this sample was diluted with 85:15 hexanes:isopropanol and subjected to chiral HPLC analysis.



(E)-4-benzylidene-3a-butyl-3a,4,4a,5-tetrahydrofuro[3',2':2,3]cyclobuta[1,2-b]indol-2(1H)-one
0.050 mmol scale, 99% yield (17.1 mg, 0.0495 mmol)

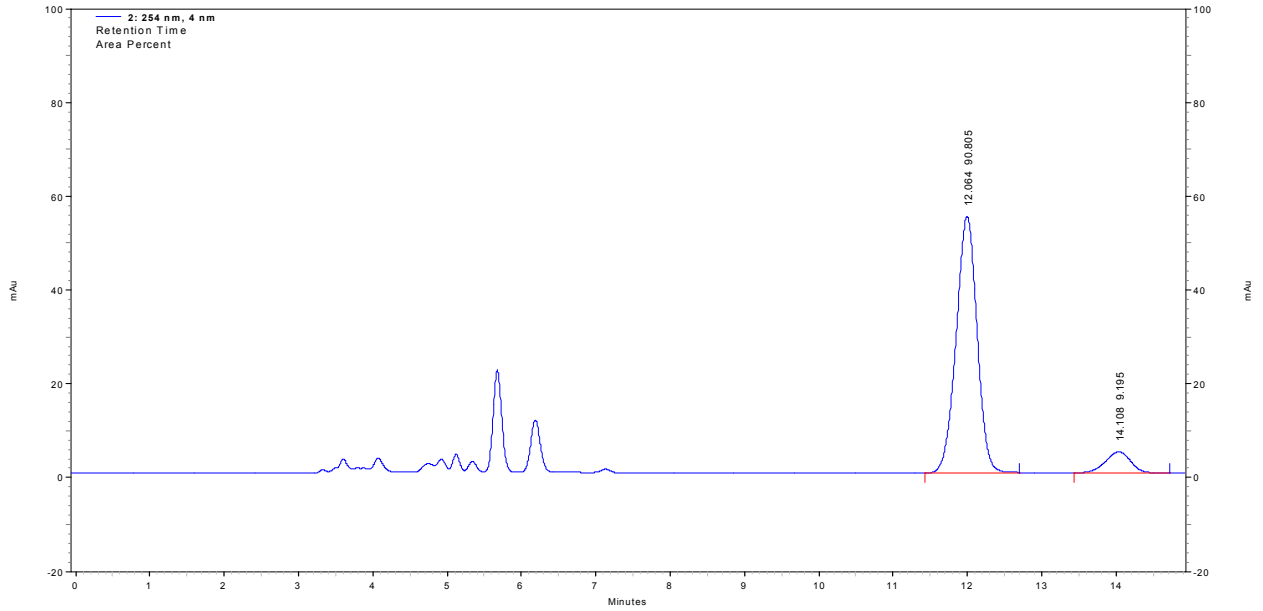
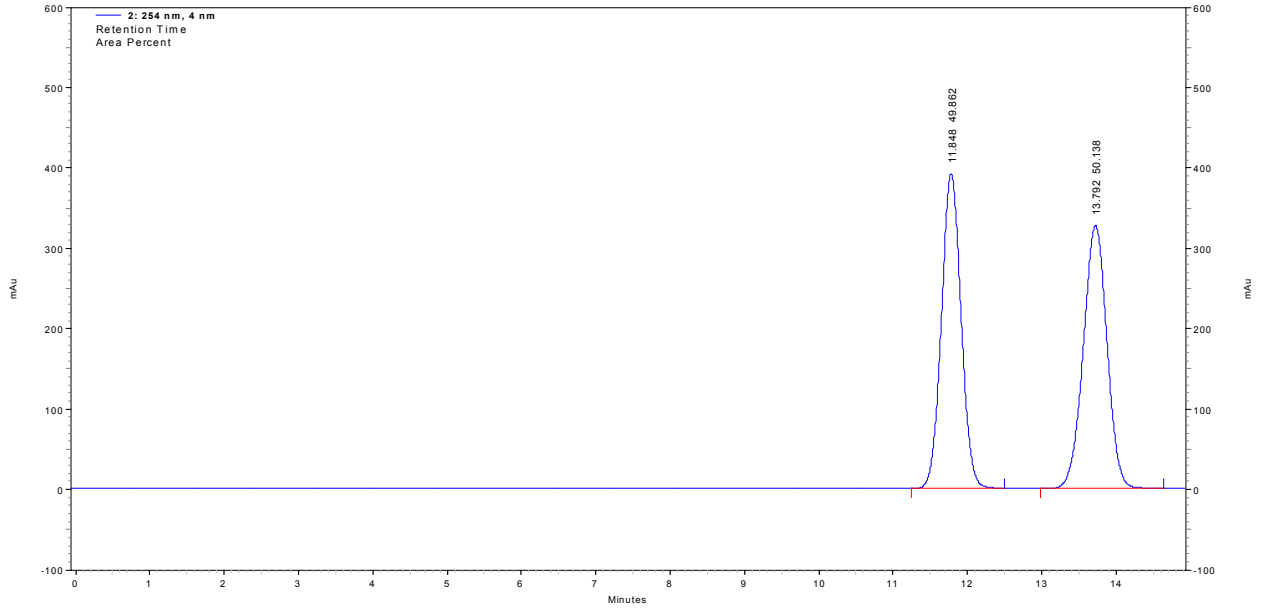
The spectral data are in agreement with those previously reported.⁶

HPLC: IC column, 85:15 hexanes:isopropanol, 1.00 mL/min, t_R = 12, 14 min. 81 to -75% ee.

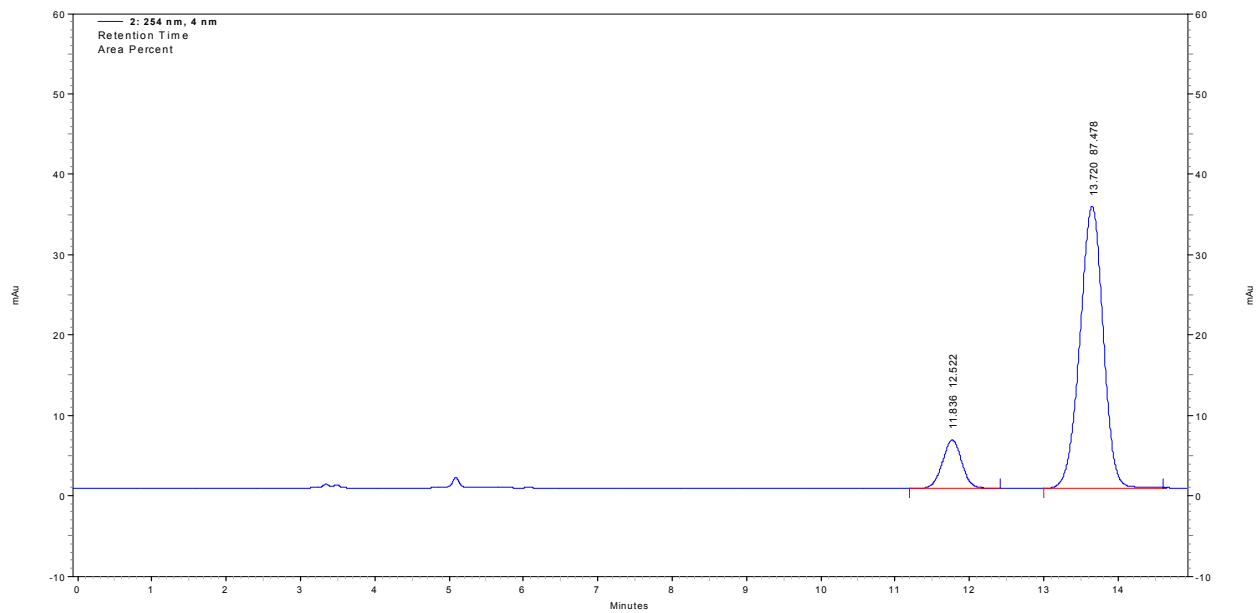
References

- (1) Pellissier, H. In *Enantioselective Multicatalysed Tandem Reactions*; Royal Society of Chemistry: Cambridge, 2014; pp v – xi.
- (2) Wang, Y.; Zhang, L. In *Catalytic Cascade Reactions*; Xu, P.-F., Wang, W., Eds.; John Wiley & Sons, Inc, 2013; pp 145–177.
- (3) Ohno, H. *Isr. J. Chem.* **2013**, *53* (11-12), 869.
- (4) Qian, D.; Zhang, J. *Chem. Rec.* **2014**, *14* (2), 280.
- (5) Wu, Y.-J. In *Heterocyclic Scaffolds II*; Gribble, G. W., Ed.; Topics in Heterocyclic Chemistry; Springer Berlin Heidelberg, 2010; pp 1–29.
- (6) Zhang, L. *J. Am. Chem. Soc.* **2005**, *127* (48), 16804.
- (7) Zhang, G.; Catalano, V. J.; Zhang, L. *J. Am. Chem. Soc.* **2007**, *129* (37), 11358.
- (8) Liu, Y.; Xu, W.; Wang, X. *Org. Lett.* **2010**, *12* (7), 1448.
- (9) Dounay, A. B.; Humphreys, P. G.; Overman, L. E.; Wroblewski, A. D. *J. Am. Chem. Soc.* **2008**, *130* (15), 5368.
- (10) Barbour, P. M.; Wang, W.; Chang, L.; Pickard, K. L.; Rais, R.; Slusher, B. S.; Wang, X. *Adv. Synth. Catal.* **2016**, n/a.
- (11) Yang, J.-M.; Li, P.-H.; Wei, Y.; Tang, X.-Y.; Shi, M. *Chem. Commun.* **2015**, *52* (2), 346.
- (12) Zheng, N.; Chang, Y.-Y.; Zhang, L.-J.; Gong, J.-X.; Yang, Z. *Chem. - Asian J.* **2016**, *11* (3), 418.
- (13) Wang, Y.-M.; Kuzniewski, C. N.; Rauniyar, V.; Hoong, C.; Toste, F. D. *J. Am. Chem. Soc.* **2011**, *133* (33), 12972.
- (14) Harper, K. C.; Sigman, M. S. *J. Org. Chem.* **2013**, *78* (7), 2813.
- (15) Harper, K. C.; Vilardi, S. C.; Sigman, M. S. *J. Am. Chem. Soc.* **2013**, *135* (7), 2482.
- (16) Milo, A.; Neel, A. J.; Toste, F. D.; Sigman, M. S. *Science* **2015**, *347* (6223), 737.
- (17) Zhang, C.; Santiago, C. B.; Crawford, J. M.; Sigman, M. S. *J. Am. Chem. Soc.* **2015**, *137* (50), 15668.
- (18) Neel, A. J.; Milo, A.; Sigman, M. S.; Toste, F. D. *J. Am. Chem. Soc.* **2016**, *138* (11), 3863.
- (19) Milo, A.; Bess, E. N.; Sigman, M. S. *Nature* **2014**, *507* (7491), 210.
- (20) Verloop, A.; Hoogenstraaten, W.; Tipker, J. *Med. Chem.* **1976**, *11* (7), 165.
- (21) Hammett, L. P. *J. Am. Chem. Soc.* **1937**, *59* (1), 96.
- (22) Kinder, R. E.; Zhang, Z.; Widenhofer, R. A. *Org. Lett.* **2008**, *10* (14), 3157.

Appendix 1 - HPLC Traces



| 254 nm | |
|----------------|--------------|
| Retention Time | Area Percent |
| 12.064 | 90.805 |
| 14.108 | 9.195 |



| 254 nm | |
|----------------|--------------|
| Retention Time | Area Percent |
| 11.836 | 12.522 |
| 13.720 | 87.478 |